

**Identification of Radioresistance Related Proteins
in Human Oral Cancer**

By

Mohd Yasser

[LIFE09201004023]

Tata Memorial Centre

Mumbai

*A thesis submitted to the
Board of Studies in Life Sciences
In partial fulfillment of requirements
for the Degree of*

DOCTOR OF PHILOSOPHY

Of

HOMI BHABHA NATIONAL INSTITUTE


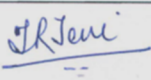

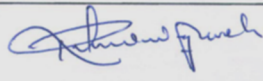
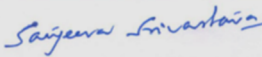
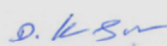


February, 2016

Homi Bhabha National Institute

Recommendations of the Viva Voce Committee

As members of the Viva Voce Committee, we certify that we have read the dissertation prepared by Mohd Yasser entitled "Identification of radioresistance related proteins in human oral cancer" and recommend that it may be accepted as fulfilling the thesis requirement for the award of Degree of Doctor of Philosophy.

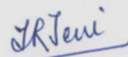
Chairman - Dr. Sorab N. Dalal		Date: 1/2/16
Research Guide - Dr. Tanuja Teni		Date: 1/2/2016
Member - Dr. Amit Dutt		Date: 1/2/2016
Member - Dr. Rukmini Govekar		Date: 01/02/16
Tech. Advisor - Dr. Sanjeeva Srivastava		Date: 2/2/16
External Examiner - Dr. D. Karunakaran		Date: 01-02-2016

Final approval and acceptance of this thesis is contingent upon the candidate's submission of the final copies of the thesis to HBNI.

I hereby certify that I have read this thesis prepared under my direction and recommend that it may be accepted as fulfilling the thesis requirement.

Date: 01-02-2016

Place: Navi Mumbai


Dr. Tanuja Teni
(Research Guide)

STATEMENT BY AUTHOR

This dissertation has been submitted in partial fulfillment of requirements for an advanced degree at Homi Bhabha National Institute (HBNI) and is deposited in the Library to be made available to borrowers under rules of the HBNI. Brief quotations from this dissertation are allowable without special permission, provided that accurate acknowledgement of source is made. Requests for permission for extended quotation from or reproduction of this manuscript in whole or in part may be granted by the Competent Authority of HBNI when in his or her judgment the proposed use of the material is in the interests of scholarship. In all other instances, however, permission must be obtained from the author.


Mohd Yasser

Date: 01-02-2016

Place: Navi Mumbai

DECLARATION

I, hereby declare that the investigation presented in the thesis has been carried out by me. The work is original and has not been submitted earlier as a whole or in part for a degree / diploma at this or any other Institution / University.


Mohd Yasser

Date: 01-02-2016

Place: Navi Mumbai

List of Publications arising from the thesis

Published:

1. Raman Spectroscopic Study of Radioresistant Oral Cancer Sublines Established by Fractionated Ionizing Radiation, **Mohd Yasser**, Rubina Shaikh, Murali Krishna Chilakapati, Tanuja Teni, PLoS ONE, 2014, Volume 9, Issue 5, doi:10.1371/journal.pone.0097777.

Under preparation-

1. Fractionated ionizing radiation induced radioresistance involves EMT like characteristics in oral cancer cells. **Mohd Yasser**, Siddharth Kamdar, Sagar Pawar, Tanuja Teni.

Conferences attended:

1. European Association for Cancer Research (EACR), Essen-Germany, February-2015.
2. Proteomics Society of India (PSI), IIT-Bombay, December- 2014.
3. Indian Society of Radiation Biology (ISRB), ACTREC, November-2012.
4. American Association for Cancer Research (AACR), Gurgaon, December-2011.

Others (Awards during the tenure):

1. Best Essay Award on “Draft human proteome map: where are the missing proteins?” at the 6th Annual meeting of Proteomics society of India, IIT-Bombay, December-2014.
2. Best Poster Award at Int. Conference on Radiation Biology, Mumbai, November-2012.
3. Best Essay Award on “Cancer Chemoprevention: Fact or Fiction”, at 30th Annual convention of Indian association for cancer research, IICB-Kolkata, February-2011.



Mohd Yasser

*Dedicated to
My Beloved
Parents*

ACKNOWLEDGEMENT

Thanks to Almighty Allah for uncountable blessings, good health and glory that flourished my thoughts and thrived my ambitions. I would like to express my special appreciation and thanks to my research guide Dr. Tanuja Teni for her constant encouragement & supervision, she has been a tremendous mentor for me. I am thankful to Dr. S.V. Chiplunkar (Director), Dr. Rajiv Sarin (Ex-Director) & Dr. Surekha Zingde (Ex-Deputy Director) for providing me the opportunity to carry out research in the premier cancer centre. I am indebted to UGC-India for funding my fellowship. I would like to thank my doctoral committee members; Dr. Sorab N. Dalal (Chairperson), Dr. M. Sheshadri (Ex-chairperson), Dr. Amit Dutt, Dr. Rukmini Govekar & Dr. Sanjeeva Srivastava (IIT-Bombay) for their useful comments & suggestions. I would also like to express my thanks to Dr. Murali Krishna Chilakapati & Miss Rubina for the Raman collaborative studies and Dr. Pritha Ray.

I would like to thank Common facility (Mr. Uday Dandekar), Radiation, Mass spectrometry (Mr. Shashi Dolas), Imaging (Jairaj, Tanuja, Vaishali), Flow cytometry (Rekha, Shyamal), Animal house (Dr. Arvind Ingle) & Administrative staff. I thank all the members of Teni lab; Mr. S. N Pawar (for his constant help in lab), Mr. Y.S Temkar (for teaching cell culture), Dr. V. Palve, Rupa, Prasad, Prajakta, Rajashree, Dhanashree, Abhay, Dipti & all the lab trainees.

A special thanks to my family, my grandfather (Late), grandmother for their blessings; my mother & father for supporting me in all my pursuits, I feel fortunate for being their son. My sister (Namrah), brother (Faisal), all my cousins and my loving wife (Bushra). I would also like to thank all my 2010 batch mates, who supported me to strive towards my goal. At the end, I would like to thank all those who have helped me during this work and I am unable to mention each of them due to space constraints.



Mohd Yasser

CONTENTS

	Page No.
SYNOPSIS	13-25
LIST OF ABBREVIATIONS	26-27
LIST OF FIGURES	28-31
LIST OF TABLES & FLOW CHARTS	32-34
CHAPTER 1: INTRODUCTION	35-38
CHAPTER 2: REVIEW OF LITERATURE	39-64
2.1 Oral cancer	40
2.2 Risk factors associated with oral cancer	42
2.3 Treatment Modalities for Oral Cancer	43
2.4 Bhabhatron II – Indigenously developed External Beam Radiotherapy machine	45
2.5 Ionizing radiation	46
2.6 Fractionated Radiotherapy	48
2.7 Clonogenic cell survival assay	48
2.8 Failure of Radiotherapy and Radioresistance	49
2.9 Establishment of Radioresistant sublines and its Global molecular profiling	50
2.10 Radioresistance related acquired features	51
2.10 a. Epithelial to Mesenchymal Transition (EMT)	51
2.10 b. Stem cell like characteristics	55
2.10 c. Potential of Raman Spectroscopy in characterizing established Radioresistant oral cancer cells	59
CHAPTER 3: AIMS & OBJECTIVES	65-66
CHAPTER 4: MATERIALS & METHODS	67-105

4.1 Materials	68-76
4.2 Methods	76-105
4.2.1 Cell Culture	76
4.2.2 Cell Irradiation	77
4.2.3 Establishment of Radioresistant sublines from Parental cell lines	78
4.2.4 Clonogenic cell survival assay	79
4.2.5 Soft agar assay	80
4.2.6 Two dimensional gel electrophoresis (2D)	80
4.2.7 PD Quest analysis of 2D gels	84
4.2.8 Mass Spectrometry for identification of differentially expressed protein spots	85
4.2.9 Protein extraction and quantification for 1D gels	87
4.2.10 Immunofluorescence	89
4.2.11 RNA extraction and cDNA synthesis	91
4.2.12 Quantitative Real time PCR	92
4.2.13 Cell morphology and F-Actin staining	94
4.2.14 siRNA transfection by Lipofectamine method	95
4.2.15 Cell migration assay	95
4.2.16 Cell invasion assay	95
4.2.17 Hanging drop assay	96
4.2.18 Spheroid formation assay	97
4.2.19 Flow cytometry for cell surface staining	97
4.2.20 Tumour formation in Immunocompromised mice	98
4.2.21 Raman Spectroscopy	98
4.2.22 cDNA Microarray	100
4.2.23 Schematic work-flow for Microarray analysis	104

4.2.24 Network Analysis for the differentially expressed genes	104
4.2.25 Statistical analysis	105
CHAPTER 5: RESULTS	106-177
5.1 To Generate Radioresistant sublines by Fractionated ionizing radiation from parental oral cancer cell lines and assess their radiosensitivity by clonogenic cell survival assay	107
5.1.1 Establishment of radioresistant sublines	107
5.1.2 Assessment of established radioresistance character in all the three sublines	107
5.1.3 Status of Radioresistance related proteins in established radioresistant sublines	110
5.2 To study the differential proteomic profile between parental oral cancer cell lines versus radioresistant sublines by 2-D gel electrophoresis and MALDI analysis	112
5.2.1 Differential proteomic profiling of parental and radioresistant cells by 2D	112
5.2.2 Analysis of 2D gels by PD-Quest gel analysis software	116
5.2.3 Identification of Differentially expressed proteins by MALDI-TOF/TOF	117
5.2.4 Schematic representation for the MALDI identified proteins	120
5.2.5 Differentially expressed proteins in each set of parental & radioresistant cells	120
5.2.6 Validation of MALDI identified proteins by western blotting	124
5.2.7 Common MALDI identified proteins in all 3 set of parental & radioresistant cells	125
5.2.8 Validation of common identified proteins by western blotting	126
5.2.9 Association Network among the common identified proteins (STRING v10)	127
5.3 To characterize the radioresistant sublines versus parental oral cancer cell lines by different parameters.	128
5.3.1 Study of EMT like characteristics in established radioresistant sublines	128
5.3.2 FIR leads to change in morphology of radioresistant cells, including increase in filopodia and decrease cell to cell adhesion	128

5.3.3 Assesment of EMT associated markers in the radioresistant cells	131
5.3.4 Status of EMT associated transcription factors in radioresistant cells	134
5.3.5 Radioresistant 70Gy-AW13516 cells exhibit increased migration and invasion	135
5.3.6 Radioresistant 70Gy-AW13516 cells show increase in cell motility associated ERM family protein Moesin	137
5.3.7 Increased co-expression of Moesin, with its cell surface receptor CD-44 at the migratory front of radioresistant 70Gy-AW13516 cells	138
5.3.8 siRNA mediated knockdown of Moesin in radioresistant 70Gy-AW13516 cells	140
5.3.9 Moesin knockdown leads to decrease in acquired migration and invasion of radioresistant 70Gy-AW13516 cells	141
5.3.10 Moesin knockdown leads to decrease in acquired radioresistant character of 70Gy-AW13516 cells	142
5.4 Study of Stem cell like characteristics in the established radioresistant sublines	143
5.4.1 Soft agar assay for the parental and radioresistant cells	143
5.4.2 3D Spheroid forming assay	145
5.4.3 Status of stem cell like markers in radioresistant cells	146
5.4.4 In-vivo tumorigenic potential of radioresistant cells	147
5.5 Raman spectroscopic study for the radioresistant sublines	150
5.5.1 Mean Raman spectra for the parental UPCI:SCC029B and radioresistant 50Gy- UPCI:SCC029B and 70Gy- UPCI:SCC029B sublines	150
5.5.2 Difference Raman spectra between the parental and radioresistant sublines of UPCI:SCC029B	152
5.5.3 Multivariate analysis	155
5.6 cDNA Microarray profile of parental and radioresistant cells	157
5.6.1 Differentially expressed genes for UPCI:SCC029B & 70Gy-UPCI:SCC029B cell	158

5.6.2 Differentially expressed genes for AW13516 & 70Gy-AW13516 cells	158
5.6.3 Validation of Microarray result by some randomly selected genes	159
5.6.4 Overlapping of proteomic and transcriptomic identities	160
5.6.5 Functional annotations for the DEGs with different curated databases	161
5.6.6 Reactome & Panther based functional annotations	162
5.6.7 KEGG pathway enrichment analysis	172
5.6.8 Gene Co-expression networks for the up and down regulated genes	175
CHAPTER 6: DISCUSSION	178-189
6.1 Advantage of fractionated radiotherapy	179
6.2 Establishment and validation of radioresistance sublines	180
6.3 Differential 2D profile of radioresistant cells	181
6.4 EMT associated changes in radioresistant cells	182
6.5 Acquisition of cancer stem like characteristics in radioresistant cells	184
6.6 Raman spectroscopy for the radioresistant cells	185
6.7 cDNA Microarray profile for the radioresistant cells	187
CHAPTER 7: SUMMARY & CONCLUSION	190-195
CHAPTER 8: REFERENCES	196-208
CHAPTER 9: APPENDIX	209-316
Appendix 1: Radiation schedule for the establishment of radioresistant sublines	210-213
Appendix 2: Agilent Bioanalyzer-2100 QC report of microarray analysis	214-215
Appendix 3: MS Spectra for the 102 identified proteins	216-227
Appendix4: Complete list of 102 identified proteins in standard format	228-251
Appendix 5: Up & Down regulated gene list from microarray (≥ 2 fold difference)	252-316
CHAPTER 10: PUBLICATION	317

Synopsis



Homi Bhabha National Institute

SYNOPSIS OF Ph.D. THESIS

- | | |
|--|--|
| 1. Name of the Student: | Mohd Yasser |
| 2. Name of the Constituent Institution: | ACTREC, Tata Memorial Centre,
Kharghar, Navi Mumbai – 410210 |
| 3. Enrolment No. : | LIFE09201004023 |
| 4. Title of the Thesis: | Identification of Radioresistance related
proteins in Human oral Cancer |
| 5. Board of Studies: | Life Sciences |

Introduction:

Oral cancer is one of the leading causes of death in developing countries (1). The countries of South Asian region including India are particularly affected with oral cancer and it ranks among top five cancers in these countries (2). One of the major causes associated with high prevalence of oral cancer in India is use of smokeless tobacco (3). Despite advancement in treatment modalities, five year survival rates for oral cancer patients have remained unchanged over past decades. Radiation therapy is an important component of oral cancer treatment and is given either alone or in combination with surgery & chemotherapy. But, sometimes radiotherapy associates with recurrence and treatment failure, as cancer cells became refractory to radiation and develop radioresistance. Several factors can contribute towards developing radioresistance in cancer cells. A relationship between radioresistance & expression of several genes namely Ras (4), Raf-1(5), Bcl-2 (6), Cox-2 (7) & PI-3K/Akt (8,9) has been reported. But, these findings have achieved a partial understanding of molecules associated with cellular radioresistance. Global molecular profiling may contribute to a better understanding of the mechanism involved in oral cancer treatment. Previous studies from our lab have demonstrated the altered expression of Bcl-2 family members and the over expression of anti-apoptotic splice variant of Mcl-1 in human oral cancers (10). Further, role of anti-apoptotic Mcl-1 in cellular radio & chemoresistance (11,12) was also demonstrated. Hence, in quest of predicting the clinical effectiveness of radiotherapy, we wanted to explore the differential molecular profiles of established radioresistant versus parental oral cancer cells. Aim of our study is to first establish radioresistant sublines by clinically admissible low dose fractionated ionizing radiation (FIR) & identify differentially

expressed proteins between radioresistant and parental cells. This might provide molecular clues associated with radioresistance in oral cancer.

Objectives of the study:

1. To generate radioresistant sublines by FIR from parental oral cancer cell lines and assess their radiosensitivity by clonogenic cell survival assay.
2. To study the differential proteomic profile between parental oral cancer cell lines versus radioresistant sublines by two-dimensional gel electrophoresis and identify the same by MALDI analysis.
3. To characterize the radioresistant sublines versus parental oral cancer cell lines by different parameters.

Results of the work done related to the project:

Objective 1: *To generate radioresistant sublines by FIR from parental oral cancer cell lines and assess their radiosensitivity by clonogenic cell survival assay.*

We have successfully established 3 radioresistant sublines namely 70Gy-AW13516, 70Gy-UPCI:SCC029B & 70Gy-AW8507 from their parental AW13516 (Tongue SCC), UPCI: SCC029B (Buccal SCC) & AW8507 (Tongue SCC) cell lines respectively. These radio-resistant sublines were developed by clinically admissible low dose FIR of 2Gy. Briefly, cells were irradiated by Cobalt-60 Gamma Irradiator (Bhabhatron-2, ACTREC) in 90mm culture plates at 60% confluency and allowed to grow till it reached 90% confluency. Cells were trypsinized, re-seeded in new culture plates and again irradiated. In this way a total dose of 70Gy was delivered in 35 fractions of 2Gy in a span of 4-5 months for generating each of the radioresistant subline. Parental cells were cultured simultaneously without giving any radiation treatment. Standard clonogenic cell survival

assay (13) was performed on the parental & radioresistant sublines and an increase in D_0 (dose at which 37% population survives) value was observed for all the established radioresistant sublines, that signifies their acquired radioresistant character. The observed D_0 values are AW13516 = 3.8Gy, 70Gy-AW13516 = 4.5 Gy; UPCI: SCC029B = 4.5Gy, 70Gy-UPCI:SCC029B = 5.6Gy; AW8507 = 5Gy, 70Gy-AW8507 = 5.5 Gy. Assay was performed 3 times in duplicates for parental & radioresistant sublines.

Expression of radioresistance related proteins like Mcl-1, Bcl-2, Bcl-xl, Cox-2, Beta-1 Integrin and Survivin were accessed in all the three radioresistant sublines. Increased expressions of these proteins were found in the radioresistant cells, compared to the parental cells. This signifies gain of radioresistant character in established cells due to multiple doses of FIR.

Objective 2: *To study the differential proteomic profile between parental oral cancer cell lines versus radioresistant sublines by two-dimensional gel electrophoresis and identify the same by MALDI analysis.*

Two-dimensional gel electrophoresis (2-D) was performed on protein lysates of AW13516/70Gy-AW13516, UPCI:SCC029B/70Gy-UPCI:SCC029B & AW8507/70Gy-AW8507 cells. Briefly, cells were lysed and protein concentration was determined by 2-D Quant kit and 600µg protein per sample was cleaned by 2-D Cleanup kit (G-Biosciences) and processed for first dimension protein focusing on 17cm, pH 3-10 IPG strip (Bio-Rad). The separation of proteins for second dimension was performed on Bio-Rad Xi Apparatus. Gels were stained with 0.1% CBB-R350 (GE). Each of the parental & radioresistant set of gels for all the 3 cell lines were run, fixed, stained and scanned (GS-800, calibrated densitometer, Bio-Rad) independently in 3 technical replicates. The scanned gels were analyzed on PD Quest 2-D gel analysis software (7.2.0, Bio-Rad) as per manufacturer's instructions. Briefly, all the gels of each set were converted into

match sets & filtered gel images were generated by the software. The spot detection wizard cross marked the spots in all the match set & normalized quantities of the identified spots were generated and compared.

For Mass Spectrometry (MS) acquisition, the differentially identified spots were excised and trypsin digested peptides were reconstituted in 0.1% TFA. Protein ID's were revealed by Swiss-Prot protein sequence database & identities of statistically significant proteins (Score>55) were further confirmed with MS-MS by choosing top 5 MS peaks using LIFT technology (Bruker). The identified protein was also confirmed with respect to its size and isoelectric point on the gels. The MS and MS-MS tolerance used for protein identification were 1.5 and 1 ppm respectively. The MALDI-TOF/TOF MS gave the identities for 102 protein spots across the three sets of parental and radioresistant gels with significant scores. Further, 25 differentially expressed spots in parental vs. 70Gy-AW13516, 32 in parental vs. 70Gy-UPCI:SCC029B and 22 in parental vs. 70Gy-AW8507 cells were found to be consistent among the 3 replicate sets of each parental and radioresistant gels. Among all the three sets, a total of 08 spots were found to be common differentially expressed. Some of the differentially expressed proteins like TCTP, PCNA, Moesin, Annexin-1, Vimentin, Keratin-8, HSP-70, Keratin-18 and Prohibitin were validated by western blotting. The transcript status of the 08 common identified proteins was checked by Real time PCR by 3 independently isolated RNA sets. Increase in transcript levels for common identified proteins was observed in the three sets of radioresistant cells. Antibody based validation for these common proteins are ongoing, that can be used to identify potential markers of cellular radioresistance.

Objective 3: *To characterize the radioresistant sublines versus parental oral cancer cell lines by different parameters.*

i) Raman spectroscopic study: Application of Raman spectroscopy (RS) for classification of different pathological conditions & cancer detection has been well reported in literature (14,15). In order to explore, radiation induced biochemical changes in established radioresistant sublines, we have performed RS analysis of radioresistant cells. Briefly, exponentially growing cells from 6 independent cultures of each of parental, 50Gy & 70Gy-UPCI:SCC029B cells were harvested and processed for spectra recording. 7 spectra were acquired from 3 replicates of each cell pellet by using fibre-optic Raman microprobe system (HE-785, Horiba-Jobin-Yvon, coupled with CCD) by adjusting microprobe on different points of the cell pellet. Thus, a total of approx 40 spectra/group were acquired for each parental, 50Gy & 70Gy cells & analysed by using PCA (principal component analysis, $p < 0.05$) algorithms implemented in MATLAB (Mathwork Inc). Mean & difference spectra were calculated for different cell populations and used for spectral comparison. The RS of parental UPCI:SCC029B, radioresistant 50Gy & 70Gy-UPCI:SCC029B cells gave a distinct Raman signature profile that indicate an overall differences in biomolecules like proteins, lipids and nucleic acids. Further, PCA provides 3 distinct clusters corresponds to radioresistant 50Gy, 70Gy & parental UPCI:SCC029B cells. This suggests an altered molecular profile acquired by radioresistant cells due to multiple doses of irradiation and can be clustered separately on the basis of these RS markers. The findings may provide RS as a potential non-invasive tool in predicting radiation response through spectral markers in oral cancer patients.

ii) EMT like characteristics: Failure of cancer therapy can be associated with EMT (Epithelial to Mesenchymal transition) reactivation that leads to metastatic progression of cancer cells by changing their adhesive properties and motility (16). Therefore, we have characterized UPCI:SCC029B/70Gy-UPCI:SCC029B & AW13516/70Gy-

AW13516 cells for EMT like changes. Expression of EMT markers were analysed by western blotting, immunofluorescence and Real time PCR. The cell junction proteins E-cadherin & Desmoplakin were found to be down regulated; whereas Vimentin and N-cadherin up regulated in radioresistant cells compared to parental cells. Also, EMT associated transcription factor Snail show significantly ($p<0.5$) increased transcript levels in the radioresistant cells. Both the radioresistant cells exhibited significant ($p<0.001$, 0.05) decrease in cell to cell adhesion (hanging drop assay) & an increase in number of filopodia (F-Actin staining, $p<0.001$) on cell surface compared to their parental cells. Further, we have found 70Gy-AW13516 cells to be more migratory ($p<0.01$) & invasive than their parental cells. Whereas, no significant increase in migratory & invasive behavior of 70Gy-UPCI:SCC029B was observed. To explore this increased migratory and invasive phenotype of 70Gy-AW13516 cells, we examined its 2D profile and found increased expression of an interesting cell motility associated protein Moesin (member of Ezrin/Radixin/Moesin family) in 70Gy-AW13516 cells. This was also validated by western blotting. Moesin functions as cross linker between actin filaments and plasma membrane & reported to be associated with cell motility (17). We have also found an increased association of Moesin with its reported cell surface receptor CD-44 at migratory front of 70Gy-AW13516 cells compared to its parental cells. These observations suggest that increased Moesin expression in radioresistant 70y-AW13516 cells might help it in acquiring increased migratory & invasive phenotype. Further, we have knocked down Moesin ($\approx 70\%$) in 70Gy-AW13516 cells by siRNA strategy & found significant ($p<0.05$) decrease in the migration & invasion of 70Gy-AW13516 cells. To check, whether Moesin knockdown leads to any effect on its acquired radioresistance. We performed clonogenic assay, post Moesin knockdown in these cells & found a significant ($p<0.001$) decrease in the

radioresistant character of 70Gy-AW13516 cells as compared to control siRNA treated cells. The D_0 value of 70Gy-AW13516 post Moesin knockdown was observed to be 4Gy, while it was 4.5Gy previously. These results signify the role of Moesin in migration, invasion & radioresistance of established radioresistant oral cancer cells.

iii) Stem cell like property and in-vivo xenograft in nude mice: Enrichment of stem cell like population in tumor undergoing radiotherapy may also be one of the associated factors behind the treatment failure (18). Thus, in order to gain an insight into the stem cell like properties of our established radioresistant sublines; we performed western blotting for stem cell markers on all the 3 sets. CD-44, CD-133, Oct-4 & Sox-2 were found to be upregulated in 70Gy-AW13516 cells; CD-44 & Nanog in 70Gy-UPCI:SCC029B cells; while Oct-4 & Nanog in 70Gy-AW8507 cells. Increased cell surface expression of CD-44 in both the radioresistant 70Gy-AW13516 & 70Gy-UPCI:SCC029B cells, while CD-133 in 70Gy-AW13516 were also determined by flow cytometry. Further, soft agar assay (both in size & colony no.) revealed a significant ($p < 0.001$ & 0.01) increase in anchorage independent growth for all three radioresistant cells compared to parental cells. Also, 70Gy-AW13516 & 70Gy-UPCI:SCC029B cells show increased 3-D spheroid formation as compared to its parental cells. Next, we have tested the *in-vivo* tumorigenic potential of our established radioresistant cells. Briefly, 5×10^6 cells (each parental & resistant) were injected subcutaneously into 5 Balb/c Nude or NOD/SCID mice/group & tumor volumes were observed for 3-4 months. Radioresistant 70Gy-AW13516 & 70Gy-AW8507 cells exhibit increased tumorigenicity in nude mice, while 70Gy-UPCI:SCC029B in NOD/SCID mice, but with late onset of tumors. These results suggest acquisition of stem cell like characteristics in the radioresistant cells.

iv) **Microarray analysis:** The cDNA microarray was performed on Affymetrix Gene chip-Human prim view array on parental & radioresistant sublines: UPCI:SCC029B/70Gy-UPCI :SCC029B & AW13516/70Gy-AW13516 (different oral sub sites i.e buccal & tongue). The raw data was analyzed by Gene Spring GX-12.5 software followed by differential gene expression clustering. A Moderate t-test was applied for assessing the statistically significant differentially expressed genes (DEG). The DEG list was processed for fold change analysis by taking fold change cut off ≥ 2 fold. Total 1378 genes were found to be upregulated and 1152 genes downregulated in UPCI:SCC029B/70Gy-UPCI:SCC029B set, while 1190 genes upregulated and 750 genes downregulated in AW13516/70Gy-AW13516 set. The microarray was performed with 2 technical duplicates for each set. The up/down regulated genes from both the sets were annotated by Gene Ontology (GO) enrichment analysis on basis of biological, cellular & molecular functions. For network analysis (with BioCos LS) of two sets; the raw data was normalized (RMA based) & Pearson correlation coefficient was calculated. This correlation is used to get relationships between genes & visualized by cytoscape software. Network data suggest pathways related to Integrin, Apoptosis, p38 MAPK, p53 & Toll receptor signalling as upregulated while Cadherin, Wnt signalling, Telomere maintenance & Membrane trafficking pathways as down regulated.

Acquisition of radioresistant character by the tumors undergoing radiotherapy is a challenging hurdle for its efficacy. In order to identify molecules that can be associated with radioresistance, we have established radioresistant sublines from parental oral cancer cell lines of different oral subsites by clinically admissible FIR. Identified differentially expressed molecules can be further studied & validated on radiotherapy failure oral tumor samples that will help in new biomarker identification.

References:

1. Jemal A, Bray F et al, Global cancer statistics, Cancer Journal for Clinicians, 2011, 61:2, 69-90.
2. International Agency for Research on Cancer, Globocan 2012, Fact Sheets by Population.
3. Gupta PC & Ray CS, Smokeless tobacco and health in India and South Asia, Respiriology, 2003, 8:4, 419-431.
4. McKenna WG, The RAS signal transduction pathway and its role in radiation sensitivity, Oncogene, 2003, 22:5866-75.
5. Kasid U, The Raf oncogene is associated with a radiation-resistant human laryngeal cancer, Science, 1987, 237:1039-41.
6. Ji-Yu Li, Yu-Yang Li et al, ABT-737 reverses the acquired radioresistance of breast cancer cells by targeting Bcl-2 and Bcl-xL, Journal of Experimental & Clinical Research, 2012, 31:102.
7. Lin F, Luo J, et al, Cox-2 promotes breast cancer cell radioresistance via p38 /MAPK-mediated cellular anti-apoptosis and invasiveness, Tumor Biology, 2013, 34:5, 2817-2826.
8. Gupta AK, Radiation sensitization of human cancer cells in vivo by inhibiting the activity of PI3K using LY294002, Int. J Radiat Oncol Biol Phys, 2003, 56:846-53.
9. Liang K, Targeting the phosphatidylinositol 3-kinase/Akt pathway for enhancing breast cancer cells to radiotherapy, Mol Cancer Ther, 2003, 2:353-60.
10. Mallick S, Patil R et al, Human oral cancers have altered expression of Bcl-2 family members and increased expression of the anti-apoptotic splice variant of Mcl-1, J Pathol 2009, 2398-407.
11. Palve V, Teni TR, Association of anti-apoptotic Mcl-1L isoform expression with radioresistance of oral squamous carcinoma cells, Radiation Oncology, 2012, 7:135-146.


12. Palve V, Mallick S et al, Overexpression of Mcl-1L splice variant is associated with poor prognosis and chemoresistance in oral cancers, *Plos One*,11(2014).
13. Franken AP, Clonogenic assay of cells in vitro, *Nature Protocols*,2006,1:2315-2319.
14. Krishna CM, Sockalingum GD et al. Micro-Raman spectroscopy for optical pathology of oral squamous cell carcinoma,*Appl Spectrosc*,2004,58(9):1128–1135.
15. Malini R, Venkatakrishna K et al, Discrimination of normal, inflammatory premalignant, and malignant oral tissue:a Raman spectroscopy study, *Biopolymers*,2006,81(3):179–193.
16. Thompson E.W, Newgreen D.F, Carcinoma Invasion and Metastasis: A Role for Epithelial-Mesenchymal Transition, *Cancer Research*,2005, 65;5991.
17. DeSouza1 L.V, Matta A et al. Role of moesin in hyaluronan induced cell migration in glioblastoma multiforme, *Molecular Cancer*,2013,12:74.
18. Han Lu, Shi S et al. Cancer stem cells: therapeutic implications and perspectives in cancer therapy, *Acta Pharmaceutica Sinica B*, 2013,3(2),65-75.

Publications in Referred Journal:**a. Published**

Raman spectroscopic study of radioresistant oral cancer sublines established by fractionated ionizing radiation, PloS One, 2014, **Mohd Yasser**, R. Shaikh, M.K Chilakapati, T. Teni.



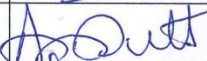
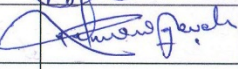

b. Communicated:

Fractionated ionizing radiation leads to radioresistance and EMT like characteristics in oral tumor derived cell lines. BBRC, **Mohd Yasser**, S. Kamdar, S. Pawar, T. Teni.


Signature of Student: 


Date: 30-03-2015

Doctoral Committee:

S. No.	Name	Designation	Signature	Date
1.	Dr. Sorab-Dalal	Chairman		30/3/15
2.	Dr. Tanuja Teni	Guide & Convener		30-3-15
3.	Dr. Amit Dutt	Member		30-3-15
4.	Dr. Rukmini Govekar	Member		30/03/15
5.	Dr. Sanjeeva Srivastava	Technical Adviser		31/3/15

Forwarded Through:


 Dr. S.V. Chiplunkar
 Director, ACTREC
 Chairperson,
 Academic & Training Program.


 Prof. K. Sharma
 Director, Academics
 T.M.C.

PROF. K. S. SHARMA
 DIRECTOR (ACADEMICS)
 TATA MEMORIAL CENTRE,
 PAREL, MUMBAI

LIST OF ABBREVIATIONS

APS	Ammonium persulfate
BME	β -Mercapto Ethanol
DAPI	4, 6-diamidino-2-phenylindole
DEPC	Diethyl pyro carbonate
DMSO	Dimethyl sulfoxide
DNA	Deoxyribonucleic acid
dNTP's	Deoxyribonucleotide mix
D/W	Distilled Water
ECL	Enhanced chemiluminescence
EDTA	Ethylene glycol tetra acetic acid
EtBr	Ethidium bromide
FBS	Fetal Bovine Serum
FIR	Fractionated Ionizing Radiation
FITC	Fluorescein isothiocyanate
GAPDH	Glyceraldehyde 3-phosphate dehydrogenase
H & E	Haematoxylin and eosin
HRP	Horse Radish Peroxidase
nt	Nucleotide
OD	Optical Density
OSCC	Oral Squamous cell carcinoma
PAGE	Polyacrylamide gel electrophoresis
PBS	Phosphate Buffered Saline
PCR	Polymerase chain reaction
PVDF	Polyvinylidene difluoride
qRT-PCR	Quantitative Real Time PCR
RNA	Ribonucleic Acid
RNase	Ribonuclease
RT	Room Temperature
RT-PCR	Reverse transcriptase PCR
SDS	Sodium dodecyl sulfate
siRNA	Small interfering RNA
TBST	Tris buffered saline with tween-20
TEMED	N-Tetramethylene diamine
WB	Western Blot
1D	One-dimensional polyacrylamide gel electrophoresis
2D	Two-dimensional polyacrylamide gel electrophoresis
ACN	Acetonitrile

Abbreviations

DTT	Dithiothreitol
cm	centimetre
gm	gram
IEF	Iso-Electric Focusing
IPG	Immobilized pH Gradient
kDa	kilo Dalton
MALDI	Matrix-assisted laser desorption ionization
mm	millimeter
mM	milli Molar
MS	Mass Spectrometry
Mw	Molecular Weight
µm	micrometer
pI	Isoelectric point
PMF	Peptide Mass Fingerprinting
TFA	Trifluoro-acetic acid
D	Down regulated
Gy	Gray
D0	Dose at which 37% population survives
EGF	Epidermal growth factor
FGF	Fibroblastic Growth factor
LIF	Leukemia inhibitory factor
L	Litre
Min	Minute
Hrs	Hours
Sec	Second
ppm	Parts per million
Da	Dalton
Conc	Concentration
ml	Milli litre
BPB	Bromophenol blue
PFA	Paraformaldehyde

LIST OF FIGURES

	Page No.
Figure 1: Treatment modalities in oral cancer	44
Figure 2: The Bhabhatron: an affordable solution for radiation therapy	45
Figure 3: Biological response of cancer cells to radiation treatment	47
Figure 4: Structure of ERM proteins, and their active and inactive states	52
Figure 5: ERM activation and signalling pathways	53
Figure 6: Radiation treatment and CSCs target	56
Figure 7: Fractionated radiotherapy and stem cells repopulation	57
Figure 8: Raman instrumentation for ex-vivo applications	61
Figure 9: Box whisker plot for the parental UPCI:SCC029B and radioresistant 70Gy- UPCI: SCC029B cells	102
Figure 10: Box whisker plot for parental AW13516 and radioresistant 70Gy-AW13516 cells	102
Figure 11: Log-linear clonogenic cell survival curves for parental AW13516 and radioresistant 70Gy-AW13516 cells	108
Figure 12: Log-linear clonogenic cell survival curves for parental UPCI:SCC029B and radioresistant 70Gy-UPCI:SCC029B cells	109
Figure 13: Log-linear clonogenic cell survival curves for parental AW8507 and radioresistant 70Gy-AW8507 cells	109
Figure 14: Expression of radioresistance related proteins in the established radioresistant sublines	110
Figure 15: Coomassie stained 2D gels for AW13516 & 70Gy- AW13516 cells	112

Figure 16: Technical replicate 2D gels for AW13516 & 70Gy- AW13516 cells	113
Figure 17: Coomassie stained 2D gels for UPCI:SCC029B & 70Gy-UPCI:SCC029B	114
Figure 18: Technical replicate 2D gels for UPCI:SCC029B & 70Gy-UPCI:SCC029B	114
Figure 19: Coomassie stained 2D gels for AW8507 & 70Gy-AW8507 cells	115
Figure 20: Technical replicate 2D gels for AW8507 & 70Gy-AW8507 cells	115
Figure 21: Representative filtered 2D gel image processed by PD-Quest	116
Figure 22: Validation for some of the 2-D identified proteins by western blotting	124
Figure 23: Western blots for common MALDI identified proteins from all the three set of parental and established radioresistant cells	126
Figure 24: The STRING network view for the common proteins	127
Figure 25: Morphology for the parental and radioresistant cells	129
Figure 26: F-Actin staining for the parental and radioresistant cells	130
Figure 27: Hanging drop assay for determining cell to cell contact	131
Figure 28: Western blot for EMT markers	132
Figure 29 Immunofluorescence study for EMT markers	133
Figure 30: Real time PCR quantitation for EMT associated transcription factors	134
Figure 31: Migration & Invasion assay for the parental AW13516 cells and radioresistant 70Gy-AW13516 cells	135
Figure 32: Migration & Invasion assay for the parental UPCI:SCC029B cells and radioresistant 70Gy-UPCI:SCC029B cells	136
Figure 33: Mass spectrometry based identification & validation of cell motility associated protein Moesin	137

Figure 34: Moesin co-expression with its cell surface receptor CD-44 at cell migratory front	139
Figure 35: siRNA mediated knock-down of Moesin in 70Gy-AW13516 cells	140
Figure 36: Migration and Transwell invasion assay post Moesin knock-down in 70Gy-AW13516 cells	141
Figure 37: Effect on the radioresistant phenotype of 70Gy-AW13516 cells, after Moesin knock-down	142
Figure 38: Soft agar assay for all the parental and radioresistant cells	144
Figure 39: Spheroid forming assay for all the parental and radioresistant cells	145
Figure 40: Stem cell like markers assessment in radioresistant cells by western blotting	146
Figure 41: Cell surface expression for CD- 44 by flow cytometry	147
Figure 42: Tumor formation ability of radioresistant 70Gy-AW13516 cells in BALB/c Nude mice	148
Figure 43: Tumor formation ability of radioresistant 70Gy-UPCI:SCC029B cells injected into BALB/c Nude and NOD-SCID mice	149
Figure 44: Mean Raman spectra of parental UPCI:SCC029B and radioresistant 50Gy & 70Gy-UPCI:SCC029B cells	151
Figure 45: Difference Raman spectra of parental UPCI:SCC029B and radioresistant 50Gy & 70Gy-UPCI:SCC029B cells	153
Figure 46: Clonogenic cell survival curve for parental, 50Gy & 70Gy-UPCI:SCC029B cells	154
Figure 47: PCA analysis for parental parental UPCI:SCC029B and radioresistant 50Gy & 70Gy-UPCI:SCC029B cells	156

Figure 48: Hcl clustering expression image for differentially expressed genes in parental and radioresistant AW13516 & UPCI:SCC029B cells	158
Figure 49: Microarray validation by real time PCR	159
Figure 50: Pie chart showing top up and down regulated pathways in UPCI:SCC029B & 70Gy-UPCI :SCC029B cells by Panther_pathway	163
Figure 51: Pie chart showing top up and down regulated pathways in UPCI:SCC029B & 70Gy-UPCI :SCC029B cells by Reactome _pathway	166
Figure 52: Pie chart showing top up and down regulated pathways in AW13516 & 70Gy- AW13516 cells by Panther _pathway	168
Figure 53: Pie chart showing top up and down regulated pathways in AW13516 & 70Gy- AW13516 cells by Reactome _pathway	170
Figure 54: Pie chart showing top up and down regulated pathways in UPCI:SCC029B & 70Gy-UPCI:SCC029B cells by KEGG analysis	172
Figure 55: Pie chart showing top up and down regulated pathways in AW13516 & 70Gy- AW13516 cells by KEGG analysis	174
Figure 56: Co-expression network for the differentially regulated genes in UPCI:SCC029B and 70Gy-UPCI:SCC029B cells.	176
Figure 57: Co-expression network for the differentially regulated genes in AW13516 and 70Gy-AW13516 cells.	177

LIST OF TABLES & FLOW CHARTS

	Page No.
Table 1: Antibodies used in the study	69
Table 2: Instruments used in the study	70
Table 3: 2D- Equilibration buffer 1 & 2 composition for 2D	72
Table 4: 2D Maxi- Gel Compositions	73
Table 5: List of cell lines used in the study	76
Table 6: Reagents used for protein estimation by 2D quant kit	81
Table 7: Standard table for 2D protein estimation	81
Table 8: Reagents used in 2D clean up kit	82
Table 9: Programme for protein focusing (17cm IPG strip)	83
Table 10: Protein estimation by Folin Lowry method	87
Table 11: Resolving gel composition (for 1D)	88
Table 12: Stacking gel composition (for 1D)	88
Table 13: List of antibodies used for western blotting & immunofluorescence	90
Table 14: Table for GAPDH-PCR	92
Table 15: GAPDH-PCR specification	92
Table 16: List of Primers with their sequences used in qRT-PCR	93
Table 17: List of 102 differentially expressed proteins identified by MALDI-TOF/TOF	118
Table 18: Differentially expressed proteins identified by MALDI analysis in AW13516 and 70Gy-AW13516 cells with their fold change values	121
Table 19: Differentially expressed proteins identified by MALDI analysis in UPCI:SCC029B and UPCI:70Gy-SCC029B cells with their fold change values	122
Table 20: Differentially expressed proteins identified by MALDI analysis in AW8507	123

and 70Gy-AW8507 with their fold change values

Table 21: List of common differentially expressed proteins identified in all the three set of parental and radioresistant cells with their fold change values	125
Table 22: Overlapped transcriptomic and proteomic identities	160
Table 23: List of up regulated pathways in UPCI:SCC029B & 70Gy-UPCI :SCC029B cells by Panther pathway analysis	163
Table 24: List of down regulated pathways in UPCI:SCC029B & 70Gy-UPCI:SCC029B cells by Panther pathway analysis	164
Table 25: List of up regulated pathways in UPCI:SCC029B & 70Gy-UPCI :SCC029B cells by reactome pathway analysis	166
Table 26: List of down regulated pathways in UPCI:SCC029B & 70Gy-UPCI: SCC029B cells by reactome pathway analysis	167
Table 27: List of up regulated pathways in AW13516 & 70Gy- AW13516 cells by Panther pathway analysis	169
Table 28: List of down regulated pathways in AW13516 & 70Gy- AW13516 cells by Panther pathway analysis	169
Table 29: List of up regulated pathways in AW13516 & 70Gy- AW13516 cells by Reactome pathway analysis	171
Table 30: List of down regulated pathways in AW13516 & 70Gy- AW13516 cells by Reactome pathway analysis	171
Table 31: List of up regulated pathways in UPCI:SCC029B & 70Gy-UPCI:SCC029B cells by KEGG pathway analysis	173
Table 32: List of down regulated pathways in UPCI:SCC029B & 70Gy-UPCI: SCC029B cells by KEGG pathway analysis	173

Table 33: List of up regulated pathways in AW13516 & 70Gy- AW13516 cells by KEGG pathway analysis	174
Table 34: List of down regulated pathways in AW13516 & 70Gy- AW13516 cells by KEGG pathway analysis	175

Flow Charts

Flow chart 1: Protocol used for establishing Radioresistant sublines	78
Flow chart 2: Schematic representation for the MALDI identified proteins	120

Chapter 1

Introduction

1. Introduction:

Oral cancer is the sixth most common cancer worldwide [1]. In India, extensive tobacco usage in various forms make it the leading type of cancer among males and third most common cancer in females [2,3]. In the last decade, developments in the field of oral cancer treatment have resulted only in a modest improvement in survival rate [4]. The treatment modalities of oral cancer are based on various factors including disease stage, access to the tumor site, age and physical status of patient. Although, surgery is choice of treatment in early stages; radiotherapy also holds an integral place either alone or as an adjuvant mode of treatment with chemotherapy [5,6].

Standard radiotherapy protocol for oral cancer involve daily exposure of 2Gy fractionated radiation dose for few weeks and in this way patients receive a cumulative dose of 50Gy to 70Gy during the course of fractionated radiotherapy [7,8]. Fractionated radiation kills fast dividing tumour cell population with decreased effects on surrounding normal tissues. This method provides time for normal cells to repopulate and recover while diminishing tumour cells that have aberrantly activated signalling pathways [9,10]. Such radiation therapy is the standard adjuvant treatment for oral cancer, but it often fails as the cancer cells become refractory to radiation and develops radioresistance [11]. The development of radioresistance is a major hurdle in the efficacy of radiotherapy in oral cancer patients and in order to make radiotherapy more effective, it is important to explore the phenotype of radioresistant oral cancer cells.

Previous studies from our lab have demonstrated, the altered expression of Bcl-2 family members and the over expression of anti-apoptotic splice variant of Mcl-1 in human oral cancers [12]. Further, the role of anti-apoptotic Mcl-1 in cellular radio & chemoresistance was also demonstrated [13,14]. Such anti-apoptotic molecules can be one of the factors

responsible for radioresistance, but development of radioresistance is a complex phenomenon, involving several proteins from different cellular processes. Therefore, global molecular profiling of radioresistant oral cancer cells would be of help in identifying radiation resistance related molecules and thus contribute to a better understanding of oral cancer treatment response.

Also, it has been observed that failure of cancer therapy has been associated with Epithelial to Mesenchymal transition (EMT) reactivation and enrichment of cancer stem cell like (CSCs) population within the tumors that are undergoing fractionated radiotherapy [15,16]. EMT is a complex order of events by which epithelial cells acquire mesenchymal traits by losing their polarity, cell-cell contact and reorganize their cytoskeleton [17]. The cells undergoing EMT acquire migratory properties to invade and metastasize due to loss of epithelial markers like E-cadherin, Desmoplakin and gain of mesenchymal markers such as Vimentin and N-cadherin [18,19]. Several reports suggest the role of these EMT markers in context to oral cancer [20,21] and expression of such EMT characteristics in chemoresistant model systems has been reported [22,23]; but its role in radioresistance and especially in context to oral cancers are largely unknown [24,25].

Similarly, studies have revealed that small heterogeneous population of cancer stem like cells within the tumor possess the property of self-renewal and differentiation [26]. Accelerated repopulation of tumor cells during or after radiotherapy treatments are among the well documented causes of treatment failure. Studies indicate that ionizing radiation can enhance the small population of cells expressing stem cell like markers [27]. These surviving stem cells like population may be responsible for resistance to cancer therapy [28] and are the focus of recent treatment modalities in oral cancer [29].

Further, the biomedical applications of Raman spectroscopy has already been investigated in pathological conditions and cancer detection [30]. The Raman related study with regard to radiation induced biochemical changes will be helpful in identifying distinct spectral signature profiles of the established radioresistant cells.

Therefore, in the present study we explored the differential profile and characterized the properties of radioresistant oral cancer cells. We first established oral radioresistant sublines from their parental cell lines of different oral subsites by treating with clinically admissible low dose fractionated ionizing radiation. These radioresistant sublines were generated by completing the course of radiotherapy that is generally given to the oral cancer patients during the course of their treatment. The proteomic and transcriptomic studies were carried out on the resulting radioresistant sublines in order to investigate their differential molecular profile. In addition, acquired radioresistance related properties like - EMT, cancer stem cells and Raman spectroscopic studies on these parental and established radioresistant cells were also carried out. The outcome of the study will help in understanding radiotherapy response leading to better treatment possibilities for oral cancer patients.

Chapter 2

Review of Literature

2.1 Oral cancer

Oral cancer is one of the most common cancers in India and accounts for 50–70% of total cancer associated mortality [31]. It is the sixth most common cancer worldwide but rank first among the male population in India [32]. India belongs to the region of high prevalence rate for oral cancer and accounts for one-third of its global burden in context to incidence and mortality [2,33]. Its high prevalence in India and South-East Asia is mainly due to habit of chewing tobacco and using tobacco related products [34]. Currently, it is seen as a major health threat in the Indian sub-continent and its seriousness can be understood by the fact that at least up to a quarter of the patients are found to be suffering from oral cancer, during a visit to a cancer treatment center in India [35].

Pathogenesis of oral cancer: Oral cancer is a multistep process of accumulating several genetic alterations and is preceded by pre-invasive stages like oral premalignant lesions, before developing into malignant carcinoma.

Oral Premalignant Lesions (OPMLs): They are morphologically altered tissues in which cancer is more likely to occur than in its apparently normal counterpart and in which its generalized state is associated with significantly increased risk of cancer [36]. Its rate of occurrence is about 2.5% of the general population and is an important target for cancer prevention [37].

The following are the main types of OPMLs:

a) Leukoplakia: According to World Health Organization (WHO), leukoplakia is defined as ‘a white patch or plaque that cannot be characterized, clinically or pathologically, as any other disease’ [36]. It is the most common premalignant lesion (~ 85%) and within a time span of 10-20 years, about four percent of the leukoplakia can transform into cancer [38].

Management of leukoplakia becomes a problem because of the involvement of multiple sites with often diffused margins and variable associated transformation risk characteristics [39].

b) Erythroplakia: These are red velvety plaques that represent epithelial atrophy and inflammation [38]. It can be found together with leukoplakia (erythro-leukoplakia) and predominately occurs in the floor of the mouth, soft palate, ventral tongue and tonsillar fauces. Oral erythroplakia has been identified as the one with the highest malignant transformation rates [40].

c) Oral Submucous Fibrosis (OSMF): Oral submucous fibrosis is mainly prevalent in South Asian populations including India and predominantly associated with the areca nut chewing; an ingredient of betel quid [41]. It is characterized by increased deposition of submucosal collagen and formation of fibrotic bands in the oral tissues, which increasingly limit mouth opening [42]. Presence of fibrous band is the most distinct feature and intermediate stage of OSMF and can transform into squamous cell carcinoma [43]. The rate of OSMF converting into malignancy is 4.5-7.6% [44] and the prevalence of leukoplakia is higher in submucous fibrosis patients (26%) while Erythroplakia are rarely associated with OSMF [45].

Oral squamous cell carcinoma (OSCC): OSCC encompass at least 90% of all oral malignancies [46,47] and constitute a major health problem in developing countries, where it represents as a leading cause of death. It is often preceded by a pre-invasive stage (discussed above) that may last for many years. The tumor progression in epithelia has been classified as normal, hyperplastic (non-dysplastic), dysplastic carcinoma *in-situ* and invasive carcinoma [48,49]. The tongue and the floor of the mouth are the main risk sites for the development of OSCC [50] whereas, other sites include tongue, alveolar mucosa, floor of mouth and lower lip [51]. Whereas, among Indian population, the gingiva and buccal mucosa are the common

sites for oral cancer development, due to habit of keeping the tobacco quid in the oral cavity [52].

2.2 Risk factors associated with oral cancer

The risk factors or possible causative agents that have been shown to be significantly associated with oral cancer includes - chemical factors like tobacco & alcohol, biological factors like viruses and dental hygiene. However, tobacco usage and neglect of overall oral health plays a major role in the increased prevalence of the oral cancer in the Indian subcontinent. Indeed, the age-adjusted incidence for oral cancer is highest in India, i.e. 15.7 per 100,000 and is predominantly due to use of tobacco [53].

The various risk factors associated with oral cancer are discussed below:

a) Tobacco: There are ample evidences suggesting that tobacco in various forms, including smoking, chewing and in betel quid have carcinogenic impact on oral cavity [54,55,56]. Smokeless tobacco products are the most commonly used form of tobacco in India [57], which is the second largest consumer of tobacco products in the world [58,59]. It is estimated that more than one-third (~35%) of Indian adults use tobacco in different forms [57]. However, there are great variations in prevalence of tobacco usage between the sex, urban-rural communities, and different socioeconomic & cultural groups in India and WHO predicts that by 2020 tobacco related deaths in India may exceed 1.5 million annually [60].

b) Alcohol: Association of alcohol with oral carcinogenesis has been reported to act both independently, as well as synergistically with smoking [61]. It is often difficult to separate the effect of alcohol with tobacco smoking and they both together exert an interactive and multiplicative effect on the risk of developing oral cancer [62,63]. Studies also suggest that alcohol may act as a solvent and facilitate the entry of carcinogens into the exposed cells, thus

altering its metabolism [64,65]. Also, acetaldehyde which is one of the alcohol metabolite has been identified as a tumor promoter [66].

c) Viruses: Human Papilloma Virus (HPV) and Herpes simplex virus (HSV) have been suggested to be associated with oral cancer [67]. HPV has been identified in approximately 23.5% of oral cancer cases and the most commonly detected HPV in OSCC is HPV-16, followed by HPV-18, HPV-31 and HPV-33[68]. Also, HSV-1 or ‘oral herpes’ that is commonly associated with sores around the mouth and lips has been suggested to be a causative agent of OSCC [69,70]. The direct association of these viruses in the development of OSCC is debatable. Moreover in this regard, a population based study show HSV-1 to enhance development of OSCC in HPV infected patients & individuals with history of cigarette smoking [71], that indicates the requirement of other risk factors also for the tumorigenic conversion.

c) Dental Hygiene and Related Factors: There is an inverse association between oral hygiene and incidence of oral cancer. Poor oral hygiene, prolonged irritation from sharp teeth and dental sepsis has been viewed for their possible role in the development of oral cancer [72].

2.3 Treatment Modalities for Oral Cancer

The selection of the treatment regimens in oral cancer depends mainly on the stage of the tumor, anatomical subsite involved in the tumor, lymph node status and patient’s age & general state of health [73]. Currently, the standard treatment modalities for oral cancer include Surgery, Radiotherapy (Brachytherapy and/or External beam radiotherapy), Chemotherapy or a combination of any these (Figure 1). Overall, Radiotherapy plays an important role in the management of oral cancer, either as a Neo-adjuvant therapy i.e

administered before surgery with an aim to shrink the tumor or as an Adjuvant therapy, administered after surgery to destroy tumor cells that may have been left behind.

Treatment Modalities in Oral Cancer

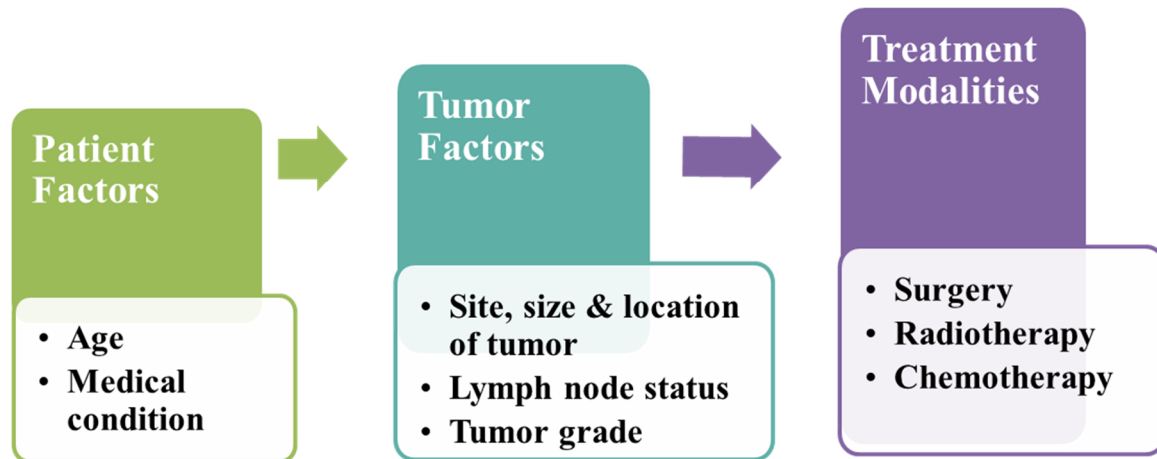


Figure 1: Radiation therapy is an integral part of oral cancer treatment, either as a single treatment modality or combined with surgery or chemotherapy.

Radiotherapy: In Radiotherapy, the radiation can be delivered to the tumor, mainly by two ways. **(i) Internal radiation or brachytherapy:** It is delivered from inside the body by radioactive sources, sealed in catheters or seeds directly into the tumor site [74]. It is highly conformal dose distribution to a small target area but its administration is not cost effective, requires expertise and mainly used for treating cancer at the internal body sites. This is used particularly in the routine treatment of gynecological and prostate malignancies as well as in situations where treatment is based on its short range of effects. **(ii) External beam radiotherapy (EBRT):** EBRT is delivered from outside the body by high energy rays (photons, protons or particle radiation) to the location of the tumor and is the most common approach in the clinical setting for treating cancer worldwide. In fact, in developing countries like India, EBRT is currently used as a potential inevitable component of modern cancer management and providing a possible cure for oral cancer patients [75].

2.4 Bhabhatron II – Indigenously developed External Beam Radiotherapy machine

Bhabhatron-II is an Isocentric, External beam radiation therapy machine of high specific activity with gamma source (Cobalt-60 radioisotope). It is developed by Bhabha Atomic Research Centre (BARC-India) & Panacea Biotech (India) and eight such machines are installed in various cancer hospitals in India, including Tata Memorial Centre [76](Figure 2).

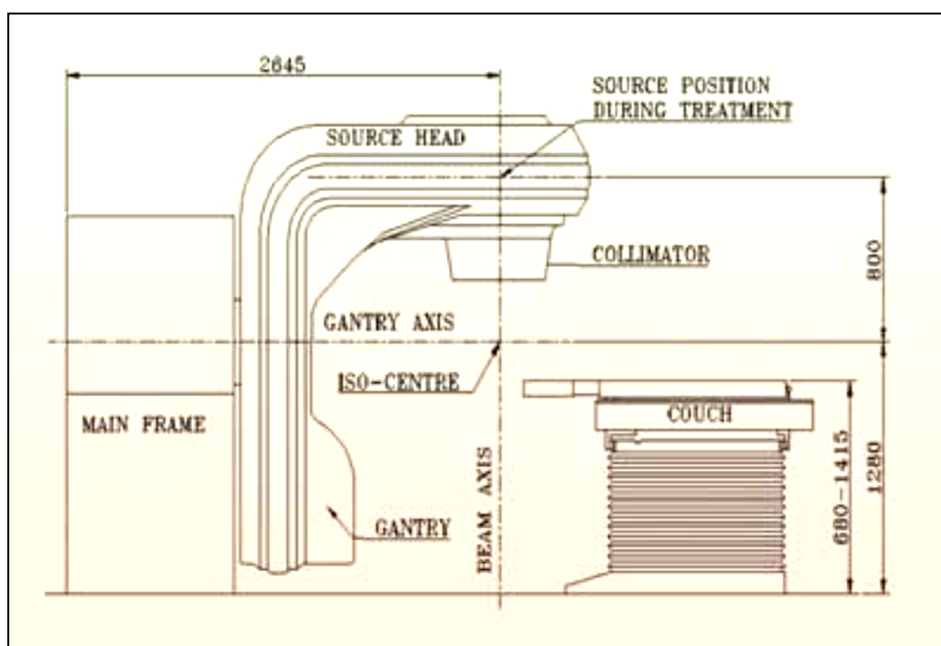


Figure 2: The Bhabhatron: an affordable solution for radiation therapy [76].

Bhabhatron II houses a cobalt-60 radioisotope and its Gantry can rotate around the patient on a horizontal axis by + 180 degree, thus allowing source positioning at any point on a circle of 80 cm radius. The collimator assembly controls the size and orientation of the Radiation beam. High energy Gamma rays emitted from the Source Head are directed to the cancer site to destroy cancerous cells and has a high capacity of 250 RMM (Roentgen per minute at one meter).

2.5 Ionizing radiation

Ionizing radiation (IR) is the radiation that carries enough energy to liberate electrons from atoms or molecules and thereby ionize them. Gamma rays are type of IR used in the radiotherapy for cancer patients via Cobalt-60 (Co-60) as source. Co-60 is used medically for radiation therapy, as an external source of radiation exposure and its radioisotope is produced from natural Cobalt-59 by the thermal neutron capture reaction.

Linear energy transfer (LET): For use in Radiobiology and radiation protection the physical quantity that is useful for defining the quality of an ionizing radiation beam is the linear energy transfer (LET) and the unit usually used for the LET is keV/ μm . A typical LET value for Cobalt-60 gamma rays is 0.3 keV/ μm and is considered as low LET (sparsely ionizing) radiations.

Ionizing radiation and cellular damage: Ionizing radiation causes cellular damage mainly in two ways – (i) Direct by inducing a variety of DNA lesions, including oxidized base damage, abasic sites, single-strand breaks (SSBs) and double-strand breaks (DSBs). These lesions, if unrepaired, ultimately result in cell death through mitotic catastrophe and apoptosis [77]. (ii) Indirect DNA damage & cell death by forming free radicals and ionization of oxygen molecules [78] (Figure 3). Radiotherapy in clinics is aimed to cause maximum killing of cancer cells while minimizing damage to surrounding normal tissue. The goal of radiation therapy is to deliver a precisely measured dose of ionizing radiation to a defined tumor area with as little damage as possible to surrounding healthy, non-cancerous tissue [79].

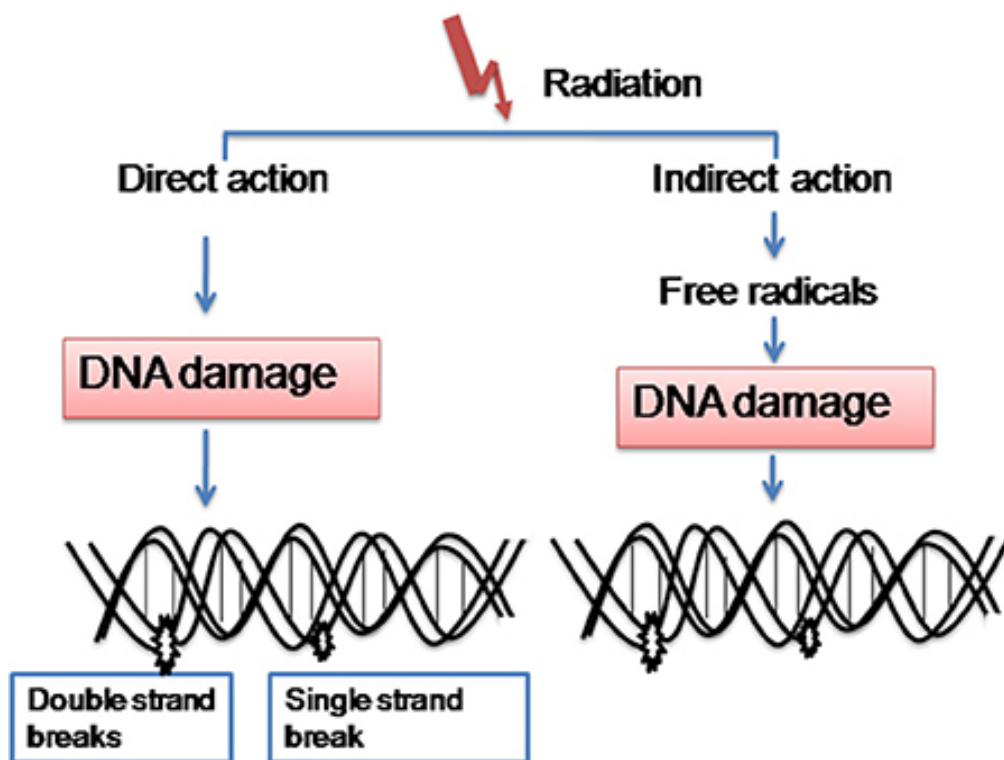


Figure 3: Biological response of cancer cells to radiation treatment [80]. Radiation mainly acts in two ways. (i) It induces direct ionization of the cellular molecules and causes damage. (ii) It acts indirectly by producing free radicals which are derived from the ionization or excitation of the water component of the cells.

However, patients undergoing radiation therapy can experience a range of serious side effects and therefore, sparing the normal tissue from additional damage by ionizing radiation may be overcome by dividing the total dose of radiation into clinically relevant fractionated doses [81]. This approach was found that to minimize the secondary effects of radiation in normal tissues and it is appropriate to divide the radiation dose required for elimination of cancer cells into a number of small fractions delivered at equal intervals [82,83]. Therefore, when tumor tissue receives doses in fractions delivered at defined interval it gives time to the surrounding normal tissue to recover from the side effects of radiation.

2.6 Fractionated Radiotherapy

In fractionated radiotherapy, radiation is given in fractions rather than as a single dose and thus allows time to normal cells for repair between each radiation sessions and protecting them from injury. Clinically admissible Fractionated Ionizing Radiation (FIR) used to treat various cancers is 1.8 to 2 Gray (Gy) per day, administered five days a week for five to seven weeks, depending on the particular clinical situation (Gray is a unit of measured absorbed radiation dose; equivalent to a deposition of energy of 1 Joule/kg) [7]. While this schedule allows relative intervals between doses of radiation that may allow normal cells to recover and regrow. Similarly, radiation therapy for treatment of OSCC is typically given in daily fractions of 2 Gy, 5 days a week and up to a total dose of 70 Gy over 7 weeks [84,85].

2.7 Clonogenic cell survival assay

Clonogenic assay or colony formation assay is an *in-vitro* cell survival assay based on the ability of a single cell to proliferate and thereby retain its reproductive ability to form a colony [86], this cell is then said to be clonogenic. The assay essentially tests every cell in the population for its ability to undergo ‘unlimited’ division and have played an essential role in radiobiology and widely used to determine cell reproductive death after treatment with ionizing radiation. Details about plating efficiency or percent cell survival after the dose of radiation treatment and based formulas are described in materials & methods section 4.2.4.

The relationship between the fractions of surviving colonies (i.e. the fraction of irradiated cells that maintain their reproductive integrity) and the absorbed dose is described by Cell Survival curve. Survival curve is graphically represented as function of radiation dose by plotting the surviving fraction on a logarithmic scale on the ordinate against different radiation doses on a linear scale on the abscissa. From these curves, D₀ values can be inferred, which is the dose required to reduce the cell surviving fraction to 37%. Thus, D₀

value is a mean of representing the relative radiosensitivity of the cell population i.e. more a cell population is radiosensitive, their D0 dose is less. Since, gamma rays are sparsely ionizing radiation; hence the cell survival curves generally show an initial slope followed by a shoulder region which then became nearly straight at higher doses.

2.8 Failure of Radiotherapy and Radioresistance

Accurate delivery of the IR dose has greatly improved over the past 2–3 decades, allowing more precise deposition of dose in the tumor while progressively reducing any unwanted dose to surrounding normal tissues [87]. Despite such technical improvements, and the fact that radiotherapy is one of the most effective forms of cancer treatment, many patients still suffer from locally recurrent disease during or after radiotherapy. Similarly, in OSCC patients such adaptive Radioresistant phenotype of such fraction of patients undergoing radiotherapy treatment, limit its efficacy and hence pose an obstruction towards successful treatment. Hence, Radioresistance is one of the main determinants of radiotherapy treatment outcome, but its prediction is difficult and remains a serious obstacle towards successful treatment in oral cancer [88].

Three main biological factors of tumors have been shown to affect outcome after radiotherapy: the extent of hypoxia [89], the ability of the surviving cells to repopulate within a treatment time of 6–7 weeks [90,91] and the intrinsic radioresistance of the tumor cells [92]. Convincing evidence of a role for each of these factors in clinical radiotherapy has accumulated from many studies and relationship between radioresistance and expression of several related markers like Hypoxia inducible factors [93], Ras [94], Raf-1 [95], Bcl-2 [96] and Survivin [97] has been reported in different cancer types. Also, in oral malignancies including OSCCs, Cox-2 [98], 14-3-3 sigma protein [99], DNA-dependent protein kinase [100], p-53 [101] and NF-kappa B [102] are reported to be associated with radioresistance.

But, our understanding for radioresistance at molecular level and especially in oral cancer is limited.

Since, Radioresistance is a relatively wide phenomenon and may involve direct and indirect intervention of molecules belonging to different classes like DNA repair pathways, stress related pathways, chromatin modification and cytoskeleton proteins etc. Therefore, identification of a wider group of molecules associated with clinical radioresistance will be needed and it will help in uncovering the multi-dimensional property of cellular radioresistance. Knowledge of more such molecules will lead to the development of strategies to overcome or modulate them in order to increase ionizing radiation-induced killing of tumor cells.

2.9 Establishment of Radioresistant sublines and its Global molecular profiling

Reports suggest, that the mechanism of radioresistance involves multiple molecules and interactions [87,88]. For assessing such interactions, global profiling of molecules associated with radioresistance needs to be explored. In the similar line, there have been studies on the identification of radioresistance related genes using microarray techniques in Esophageal cancer [103], Pancreatic cancer [104], Cervical cancer [105], Lung cancer [106,107], Head and neck cancer [20,108] and Oral cancer [11]. These studies have identified genes and genetic alterations related to radioresistance in different cancer types including establishing radioresistant cell lines. But most of these studies have used radioresistant cancer cell lines induced under dosed radiation with little regard for clinically administered radiation dose.

In addition, reports regarding global proteomic profiling related to radioresistance with clinical setting are limited. Since, there is an urgent need for finding molecules related to radioresistance in oral cancer and its determinant will help in improving the prognosis of oral cancer patients. Therefore, identifying differentially expressed protein molecules between

parental and radioresistant oral cancer cells, established by clinically admissible ionizing radiation, may provide of potential radioresistance related markers that may be helpful in clinical settings to improve the efficacy of radiotherapy for oral cancer.

2.10 Radioresistance related acquired features

Acquisition of the following features in the cancer cells due to the effect of multiple doses of fractionated ionizing radiation may also be associated with the radioresistant phenotype:

2.10 a. Epithelial to Mesenchymal Transition (EMT)

Malignant transformation in many carcinomas is associated with the loss of Epithelial differentiation and gain of a Mesenchymal phenotype; a process known as EMT [109]. OSCC can also spread by local and distant metastasis and thus creates a challenge for the development of successful clinical approaches to radiotherapy. EMT is a complex order of events by which epithelial cells acquire Mesenchymal traits by losing their polarity, cell-cell contact and reorganizing their cytoskeleton [17]. The cells undergoing EMT acquire migratory properties to invade and metastasize due to loss of epithelial markers like E-cadherin, Desmoplakin and gain of Mesenchymal markers such as Vimentin and N-cadherin [18,19]. E-cadherin is a calcium-dependent trans-membrane glycoprotein that is expressed in most epithelial cells, and functions in establishing cell polarity and maintaining normal tissue structure [110]. The loss of E-cadherin expression together with the upregulation of Vimentin expression is known to be a marker of EMT changes in epithelial cells [111]. Vimentin is a type-III intermediate filament protein that is normally found in Mesenchymal cells, though it is sometimes expressed in migratory epithelial cells, such as during embryogenesis and wound healing [110]. Its expression in oral epithelial cells has been pathologically associated with tumor invasion and metastasis [110,112,113]. Desmosomes are cell-cell adhesion junctions and their role is to maintain tissue integrity and structure by providing mechanical

strength [114]. N-cadherin (Neural cadherin) is another adhesion molecule and is reported to be associated with invasive potential in cancer [115].

Several reports suggest the role of these EMT markers in context to oral cancer [20,21,116] along with the transcriptional regulators snail, slug and twist [117,118,119]. Also, expression of EMT characteristics by virtue of above mentioned EMT markers and regulators in chemoresistance [22,23] and radioresistance of different tumor types are reported [24,25,120], but their role in context to radioresistance of oral cancer is limited.

ERM family of proteins: ERM (Ezrin, Radixin and Moesin) are three highly homologous protein members of the FERM (4.1-band ERM) superfamily [121] (Figure 4). They are essential for linking the actin cytoskeleton to the cell membrane and are key organizers of specialized membrane domains [122]. Their function as cytoskeletal linkers places them at the center of an elaborate regulatory network of many cellular processes, such as migration & adhesion [123] and cancer cell invasion & metastasis [124]. There is also evidence that the ERM proteins are important for cell to cell and cell-matrix contacts, potentially through interactions with Cadherin complexes and Integrin proteins [125] as well as for the reorganization of the cytoskeleton [126].

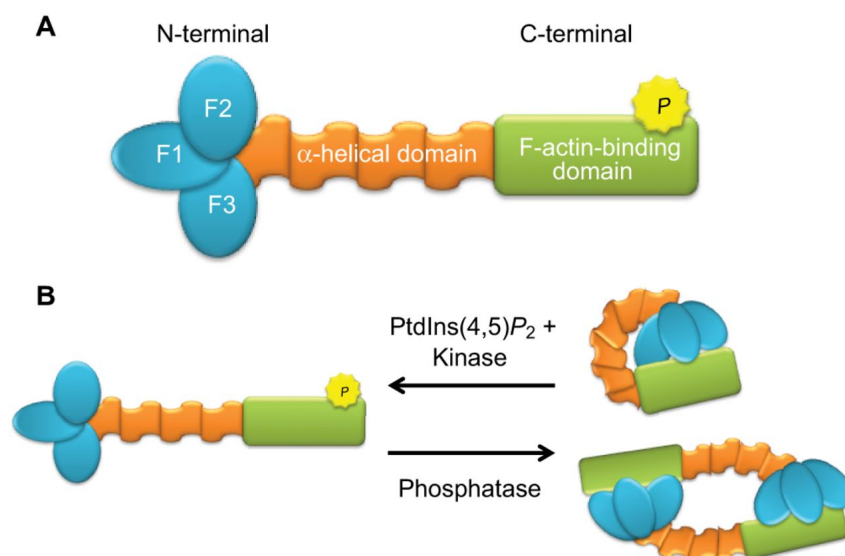


Figure 4: Structure of ERM proteins, and their active and inactive states [127]. (A) ERM proteins have F actin binding, C terminal domain and the FERM containing N terminal domain and separated by a third alpha-helical domain. (B) ERM activation/inactivation: ERM proteins C-terminal domain binds with the FERM domain of either, same molecule through self-association or with another ERM molecule, to form a homo- or heterodimer.

This intramolecular interaction leads to head–tail interaction and the consequent masking of both the membrane and actin binding sites, resulting in inactivation of the proteins.

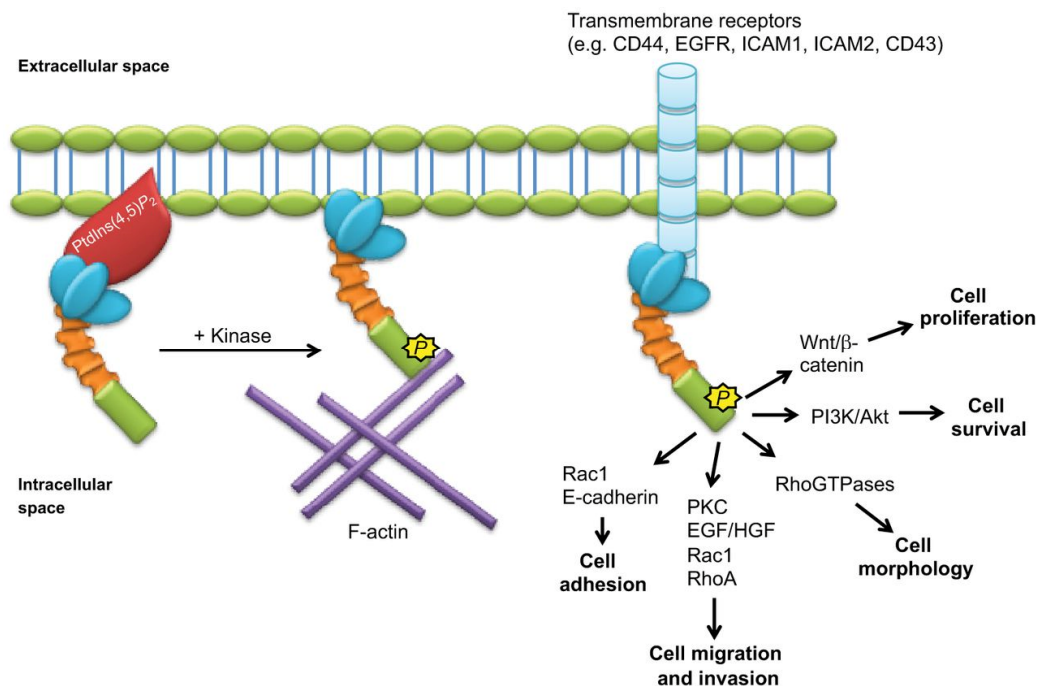


Figure 5: ERM activation and signalling pathways [127]. The ERM proteins will remain in inactive conformation until FERM domain binds to phosphatidylinositol (4,5)-bisphosphate [PtdIns(4,5)P₂] located at cell membrane and the conserved threonine residues -T567, T564 and T558 for Ezrin, Radixin & Moesin respectively become phosphorylated. This activation results in directly linking the actin cytoskeleton to the plasma membrane through positively charged F3 lobe of the FERM domain, which has been proposed to have a high affinity for negatively charged phospholipids within the plasma membrane.

ERM proteins have been suggested to influence tumor progression, as it can modulate the activity of the Ras superfamily of small GTPases, including the Ras and Rho subgroups [128,129] (Figure 5). Recently, the role of these three ERM proteins in tumor progression has become the focus of attention; in order to determine the exact molecular roles these proteins play during cancer progression [127].

Role of Moesin in Cancer progression & EMT: Moesin shares ~78% amino acid sequence identity with other ERM member proteins- Ezrin and Radixin. It acts as linking protein of the sub-membranous cytoskeleton and plays a key role in the control of cell morphology, adhesion and motility via actin filament remodeling [130]. Moesin has been correlated to cancer progression and its expression pattern has been linked to increased tumor size, as well as mode of invasion and differentiation in OSCC [131]. It is reported to relocate from the plasma membrane to the cytoplasm in tumor cells that have a higher incidence of lymph node metastasis [132]. Recently, Zhu et al. demonstrated a correlation between the high expression of Moesin in high-grade glioblastoma tumors without any significant change in the expression levels of other ERM proteins i.e Ezrin & Radixin [133]. Further, Moesin is reported to be essential for EMT in the human mammary cell line, whereas Ezrin and Radixin were not. It was also observed that after stimulation with TGF- β , Moesin was observed to relocate from cell-cell adhesions to filopodia and large membrane protrusions [113]. Further, the integral membrane proteins such as CD-44, CD-43, Intercellular adhesion molecules (ICAM) and actin are identified as ligands of Moesin [134,135]. The elevated Moesin expression and its co-localization with CD-44 at membrane extensions have also been observed in established glioblastoma cell lines [133]. In context to Moesin association with CD-44, it has been shown that during EMT, CD-44 is most abundant at dorsal protrusions to promote cell-substrate adhesion and this localization is drastically reduced when Moesin is depleted [130]. Therefore, these studies suggest that, Moesin has a role in

promoting EMT by affecting the reorganization of the actin cytoskeleton, including its co-localization with CD-44.

2.10 b. Stem cell like characteristics

Recent studies reveal that cancer stem-like cells (CSCs) properties could contribute to tumor heterogeneity, metastasis and radioresistance in a variety of cancers, including OSCC [28,136]. According to American association for cancer research workshop on cancer stem cells, CSCs are defined as heterogeneous cell population within the tumors that possess the property of self-renewal and differentiation [137]. The ability of self-renewal, differentiation and regeneration of CSCs possess significant resistance to current treatment modalities [138,139]. Literature has suggested that current therapies might fail because of this small, surviving CSC population that may also be responsible for tumorigenesis and resistance to cancer therapy [140].

Radiation biology has always attributed CSCs a central place for therapeutic response. Radiobiological mechanisms related to cancer stem cells, including experimental and clinical studies provide evidence that cancer stem cell content and the intrinsic radiosensitivity of cancer stem cells affect the radio-curability of a cancer. One key issue in cancer research and treatment during the past decade has been whether the persistent growth of malignant tumors is driven by substantial proportions of tumor cells or exclusively by rare subpopulations, termed as CSCs (Figure 6). This question has been at the heart of radiation oncologists and radiation biologists for decades.

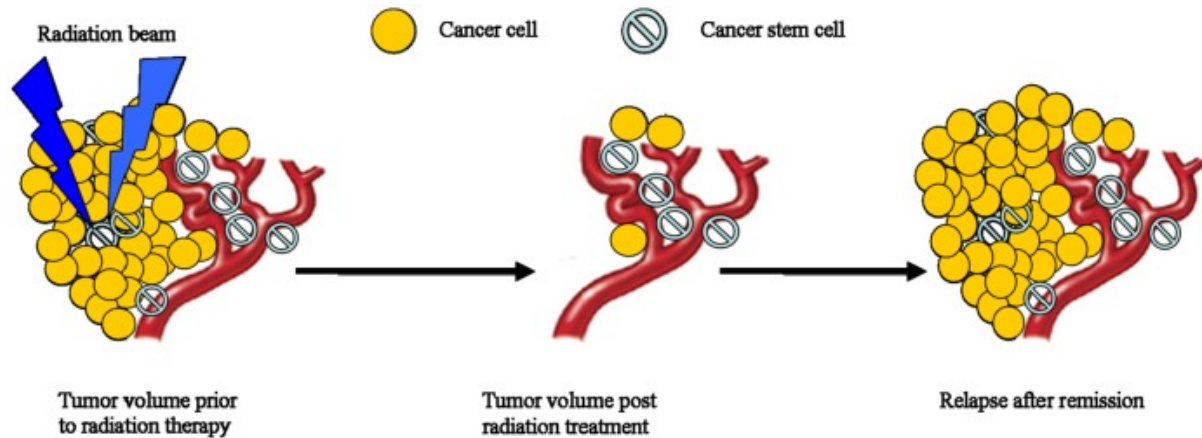


Figure 6: Radiation treatment and CSCs target. The conventional radiation treatment may target mainly the bulk of the tumor rather than the cancer stem cells (CSCs) in the perivascular niche [141]. The CSCs that remain after radiation therapy can differentiate and subsequently form a new tumor.

Therefore, by assuming that CSCs are randomly distributed in the bulk of tumor and to make radiotherapy more effective, the current standard treatment plans will be needed with an aim to deliver a homogenous dose over the tumor bed, in order to effectively remove any of these CSCs like population. Tumor radioresistance is thought to be caused by CSCs, which harbor preferential activation of the DNA damage response (DDR), efficient DNA repair machinery and resistance to apoptosis [141,142]. Also, accelerated repopulation of tumor cells during or after radiotherapy treatments are well documented causes of treatment failure and studies show that irradiation enriches the fraction of cells expressing CSC markers [143]. For example, radioresistant esophageal carcinoma cells established through fractionated irradiation exhibit enhanced CSC properties and tumorigenic ability, approximately 40-times higher than that of radiosensitive cells [22]. In another study, Zhang et al. reported that several of the putative stem cell markers such as β -catenin, Oct3/4 and β -integrin were significantly increased in two radioresistant esophageal cell lines [23]. Also, repopulation of stem cells during the treatment period and recovery from radiation damage between fractions,

have been shown to increase tumor resistance against fractionated radiotherapy [90] (Figure 7).

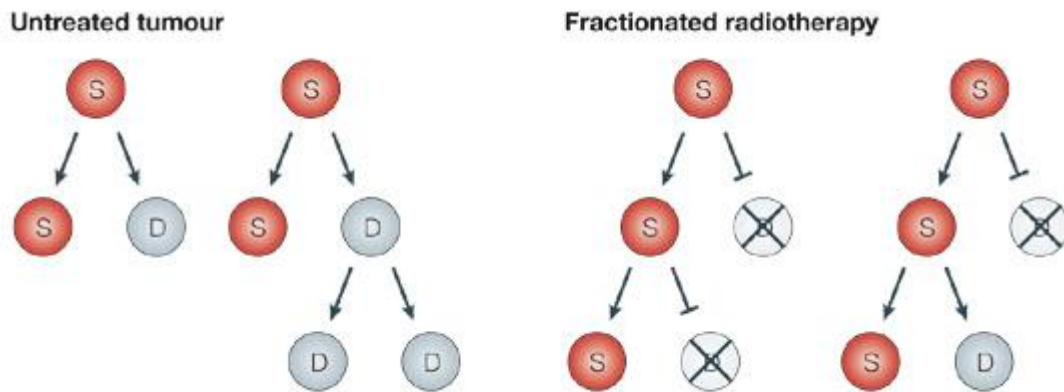


Figure 7: Fractionated radiotherapy and stem cells repopulation. After fractionated radiotherapy, the relative production of tumour stem (S) cells is increased compared with the production of terminally differentiated (D) cells [90].

Radiotherapy are given in multiple doses, which is spaced out to allow the recovery of normal tissues between treatments. However, surviving cancer cells also proliferate during the intervals between treatments and this process of repopulation is an important cause of treatment failure. Therefore, targeting CSCs is likely to be the key to cure cancer and thus increase the efficacy of treatment modalities.

Markers associated with CSCs: Following are some of the well-studied markers for characterizing cancer stem cell like properties-

(i) **Oct-4:** Also known as Oct-3, Oct-3/4 is a member of the POU (Pit-Oct-Unc) family of transcription factors, known to be expressed in both embryonic and adult stem cells [144] and is an important marker of CSCs [145]. Oct-4 is particularly involved in both controlling the maintenance of embryonic stem (ES) cell pluripotency and proliferation potential [144].

Reports suggest that, differentiated somatic cells can be reprogrammed to a pluripotent state by the overexpression of defined transcription factors (Oct-4/Sox-2/Klf-4/c-Myc or Oct-4/Sox-2/Nanog/Lin-28) [146] and among these transcription factors, Oct-4 plays a key role in both maintaining and re-establishing pluripotency.

(ii) Sox-2: is a high mobility group domain-containing transcription factor, involved in the maintenance of pluripotency and self-renewal in undifferentiated stem cells [147]. It expressed in various types of embryonic and adult stem cells [148]. Sox-2 together with Oct-4 and Nanog, act as master regulators of pluripotency [149]. Recent data suggest that Sox-2 is one of four major factors to reprogram adult fibroblasts into induced pluripotent stem cells (iPS) [150]. Sox-2 was shown to correlate with proliferative activity [151], anchorage-dependent growth [152], drug resistance [153] and metastasis [154] of cancer cells.

(iii) Nanog: Nanog is a homeodomain-containing transcription factor along with Oct-4 and Sox-2. It is a part of the key set of transcription factors that are involved in the maintenance of pluripotency and self-renewal in undifferentiated ES cells [145]. In oral squamous cell carcinoma, higher expression of Nanog, along with Oct-4, was associated with advanced cancer stage and shorter patient survival rate [155].

(iv) CD-44: It is a trans-membrane glycoprotein and a major adhesion molecule for the extracellular matrix that binds primarily to the extracellular glycosaminoglycan hyaluronan [156]. CD-44 is one of the most frequently observed CSC markers in solid tumors [157] and it is often combined with other cell surface markers to isolate CSCs. In a recent report, it was demonstrated that CD44+ cells along with other marker (SSEA-4) are novel phenotypes of oral CSCs having characteristics of self-renewal, high tumorigenicity, and relatively

increased drug resistance in oral cancer [158]. CD-44 is also, thought to be involved in tumour progression and metastasis through its role as a regulator of growth, survival, differentiation, and migration [159].

(v) **CD-133:** is also a trans-membrane glycoprotein and has been identified as a putative CSC marker in a variety of human cancers, including oral cancer [160]. CD-133 expression has been detected in cancer stem cells of head neck including OSCC [161,162,163]. CD-133 is consistently used for enrichment for CSCs and studies have suggested that CD133+ cells isolated from squamous cell carcinoma cell lines, display increased clonogenicity, EMT phenotype, tumour sphere formation, self-renewal, proliferation, multilinear differentiation and tumorigenicity [164,165].

2.10 c. Potential of Raman Spectroscopy in characterizing established Radioresistant oral cancer cells

Biomedical application of optical spectroscopic techniques like Fluorescence, Fourier transfer infra-red (FTIR), Diffused reflectance and Raman spectroscopy (RS) for classification of different pathological conditions and cancer detection has been widely reported [30,166,167,168]. Among these techniques, RS has added advantages like it is label free, sensitive to biochemical variations, applicable to *in-vitro* and *in-vivo* conditions, has minimum interference from water and provides molecular fingerprints [169,170,171]. Recent studies have demonstrated the efficacy of RS in classifying healthy, premalignant and malignant lesions of oral submucosa [172,173], classification of the normal and abnormal exfoliated cells [174] and in the prediction of tumor response towards concurrent chemoradiotherapy in cervical cancers [175]. Also, studies demonstrate the potential of RS in

identifying early transformation changes in oral buccal mucosa [176], its feasibility in detecting asthma and determining treatment response through serum in asthma patients [177], in classifying normal and oral cancer serum [178] and in identifying multidrug resistance phenotype in human leukemia [179] and uterine sarcoma cell lines [180].

We therefore carried out RS studies in order to explore the molecular fingerprints of our established radioresistant cells. The RS studies related to radiation induced biochemical changes in prostate, lung and breast cancer cell lines irradiated with radiation doses between 15 and 50Gy are reported [181,182]. However, these studies were carried out at single doses of radiation that aimed to investigate the *in-vitro* radiation response on human cancer cell lines. On the other hand, our aim was to develop *in-vitro* radioresistant character in the cell lines over a period of time and then explore the feasibility of Raman spectroscopy to categorize the acquired trait from its parental untreated cells. This study will help in investigating the utility of RS in acquired radioresistant oral cancer sublines established from parental oral cell line by clinically administered fractionated ionizing radiation.

Raman spectroscopy overview: RS is a spectroscopic technique that is used to observe rotational, vibrational and other low-frequency modes in a system [183]. It is commonly used to provide molecular fingerprint by which chemically altered profile can be identified. It is based on Raman Effect, named after its discoverer, the Indian physicist Sir C.V. Raman, who first observed it in 1928 on the basis of inelastic scattering of light. He won the Nobel Prize in Physics in 1930 for this discovery, accomplished using filtered sunlight as a monochromatic source of photons, a colored filter as a monochromator and the human eye as detector [184,185].

Raman effect & Raman shift: The Raman Effect arises when a photon, incident on a molecule, interacts with the electric dipole of the molecule. In classical terms, this interaction

can be viewed as a perturbation of the molecule's electric field. Most of the photons are elastically scattered i.e. with same energy as the incident photons. However, a small fraction of photons (approximately 1 in 10^7) are scattered at optical frequencies different from and usually lower than the frequency of the incident photons. The process leading to this inelastic scatter is termed as Raman Effect. The energy difference between the initial and final vibrational levels are known as Raman shift and represented in wavenumber (cm^{-1}).

Raman Instrumentation: A typical Raman system consists of four major components: an excitation source, filters, spectrograph and detector. A sample (placed on the sample stage) is illuminated with a laser beam in the ultraviolet (UV), visible or near-infrared (NIR) region. Scattered light is collected, filtered and sent through a spectrograph to generate Raman spectrum. Schematic representation of a typical Raman instrument is shown in Figure 8.

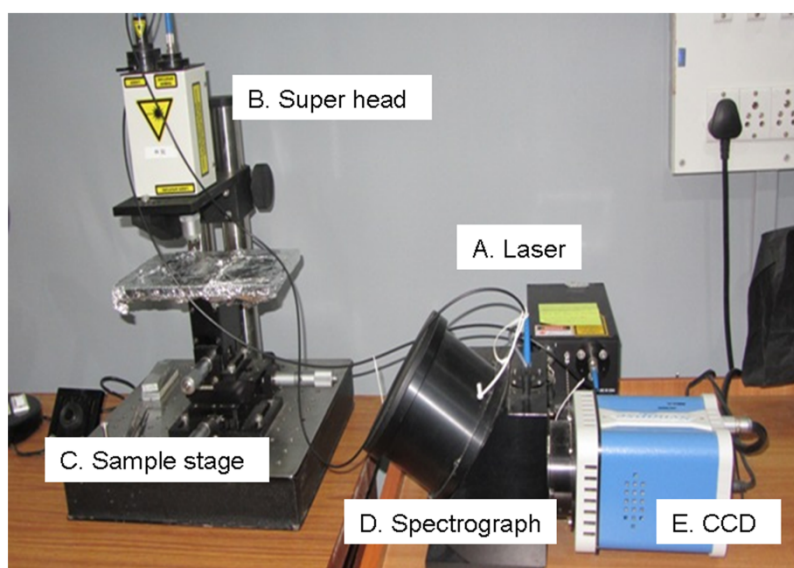


Figure 8: Raman instrumentation for ex-vivo applications at ACTREC-TMC. (A) Laser: excitation source, $\lambda 785$ nm, (B) Superhead: optical assembly that couples excitation and detection elements, (C) Sample stage: assembly to place ex-vivo samples (D) Spectrograph (E) CCD.

(i) Excitation Source (LASER): A laser system is made up of lasing medium (atom, molecule or ion), a resonant cavity and an excitation source (electrical, radiation or others). The excitation source takes the atoms or ions of the lasing medium to a higher energy state. Transition from this state to a lower state gives the laser radiation.

(ii) Filters: These are used to filter out the background signals. The filters used in delivery path can block unwanted emission from the laser that would otherwise swamp the Raman spectrum.

(iii) Spectrograph: The main function of the spectrograph is to disperse the light from an object into its component wavelengths. It consists of, a collimating element which may be a lens or a mirror to obtain parallel rays; a dispersing element, usually a grating which spreads the light intensity in space as a function of wavelength, such that it leave the grating at slightly different angles depending on the wavelength and a focusing element to form an image of the entrance slit at the detector of focal plane.

(iv) Detector: A CCD (charge coupled device) detector is an array of photosensitive elements or pixels arranged in horizontal rows and vertical columns, fabricated on a monolithic silicon chip. It helps in recording the intensity of the Raman signal at each wavelength. Quantum efficiencies close to 90% can be achieved from the visible to the near-IR wavelength range by using CCD technology.

Statistical tools for Raman Spectroscopy: (i) Multivariate analysis- The multivariate analysis (MVA) is based on the statistical principle of multivariate statistics, which involves observation and analysis of more than one statistical outcome variable at a time. Data generated from Raman experiments consist of multiple variables (wave-numbers) for a number of observations. If there are 'n' variables (or Raman bands) each object may be said to reside at a unique position in an abstract entity referred to as n-dimensional hyperspace. The underlying theme of multivariate analysis (MVA) is simplification or dimensionality

reduction. This can occur in one of two ways; either using an unsupervised or a supervised learning algorithms. In general, unsupervised methods such as principal component analysis (PCA) are used to assess the ‘natural’ differences and similarities between spectra. This method is employed to discover structure in the data and can be used to ‘cluster’ samples into groups by producing scatter plots. In contrast, the supervised methods - like linear discriminant analysis (LDA) is ‘calibrated’ with some known existing parameters of the sample. A prior knowledge is used in the construction of the LDA model followed by validation of model with test data or cross validation [186,187,188].

(ii) Principal Component Analysis (PCA): PCA is one of the most widely used unsupervised multivariate methods for data compression and over-viewing. Main function of PCA is to identify trends, pattern and outliers in the data set [189,190]. It decomposes a set of spectra into their most common variations (factors) and produces small set of well-defined numbers (scores) for each sample that represent the amount of variation present in the spectrum.

(iii) Linear Discriminant Analysis (LDA): It is a supervised classification method, as the categories to which objects are to be classified is known before the model is created. The objective of LDA is to determine the best fit parameters for classification of samples as well prediction of unknown samples [191].

Biomedical applications of Raman Spectroscopy: Raman spectroscopy has been used for several years to characterize mineralized structures in living organisms, notably bone and teeth [192]. It is a topic of continuous research in biomedicine and in recent years, there has been a remarkable increase in the application of RS to the field of medicine. This has come out of the awareness that RS is non-invasive, vibrational spectroscopic technique capable of

providing details on the chemical composition, molecular structure and molecular interactions in cells and tissues. Since, there are several Raman active biological molecules in tissue that give distinctive peaks in the spectrum, thus giving structural and environmental information about the tissue. The changes in tissue that occur as a result of a disease yield a characteristic Raman spectrum that can be used for diagnosis. Thus, everything from precancerous tissues to benign abnormalities can in principle be differentiated and detected. As a disease leads to changes in the molecular composition of affected tissues, these changes should be reflected in the spectra. The wealth of information provided by Raman spectra provides wide applicability, ranging from quantitative determination of the chemical composition of tissues or analyte concentrations in blood to real-time *in vivo* tissue classification [193,194,195,196,197,198]. Furthermore, if the spectral changes are specific enough for a particular disease state, they can in principle be used as phenotypic markers of the disease.

In the field of cancer biology, RS has been studied extensively for cancer tissue diagnosis on Skin [199], Brain [200], Intestinal [201], Esophagus [202], Breast [203], Bladder & Prostate [204], Cervix [205], Lung [206] and Oral cancer [173,176]. Nevertheless, RS could bring faster and more reliable diagnosis for cancerous changes in human tissue. It offers disease classification from biochemical composition and thus enables not only early diagnosis, but also provides an insight into the involved disease process. Although, respective *in-vivo* tests have to be done together to fully evaluate the usefulness of Raman spectroscopy.

Chapter 3

Aims & Objectives

The objectives of the study are as follows:

1. To generate radioresistant sublines by FIR from parental oral cancer cell lines and assess their radiosensitivity by clonogenic cell survival assay.
2. To study the differential proteomic profile between parental oral cancer cell lines versus radioresistant sublines by two-dimensional gel electrophoresis and identify the same by MALDI analysis.
3. To characterize the radioresistant sublines versus parental oral cancer cell lines by different parameters.
 - a) Study of EMT like characteristics.
 - b) Stem cell like & in vivo tumorigenic potential.
 - c) Raman spectroscopic study.
 - d) Microarray analysis.

Chapter 4

Materials & Methods

4.1 Materials

The following chemicals/ reagents/ kit/ enzymes were obtained from-

Sigma: Paraformaldehyde, Sodium Orthovanadate, Acrylamide, β -mercapethanol, Bovine Serum Albumin, EDTA, Glycine, N-N Methylene Bis-Acrylamide, Sodium Dodecyl Sulphate, Tween-20, Triton X-100, Tris, Trypsin, TEMED, CHAPS, DTT, Iodo-Acetamide, Thiourea, Bromophenol Blue, Coomassie brilliant blue, Di-amino benzidine, DMSO, DEPC, Ethidium Bromide, EDTA, FBS, Fast green, 8-Hydroxyquinoline, Oligonucleotides, Proteinase K, Insulin, Glutaraldehyde, TRIzol, Tri-fluoro acetic acid, Low melting agarose, Insulin, Erythrosine B, Ponceau stain, DAPI, Tri-Sodium citrate, Crystal Violet. **Qualigens:** Boric acid, Disodium hydrogen hydrophosphate, $MgCl_2$, NaOH pellets, Sodium dihydrogen orthophosphate, Tri-sodium citric acid, Glacial acetic acid, Glycine, Xylene, DPX Mountant. **SISCO Research Laboratories:** Chloroform, Folin Ciocalteu reagent, Isopropanol, Isoamyl alcohol, Methanol, Molecular biology grade ethanol, Phenol, Sodium chloride, Sodium acetate, Trichloro acetic acid.

MBI Fermentas: First strand cDNA kit, 6X loading dye, 25mM $MgCl_2$, Protein ladder, 10X PCR buffer, Taq polymerase, Proteo-block protease Inhibitor, Proteo-jet Mammalian cell lysis reagent. **Gibco:** Fetal Bovine Serum, DMEM, IMDM, Ampicillin. **Invitrogen:** Lipofectamine-3000. **USB:** Urea, Ammonium persulfate. **Bio Rad:** Mineral oil, IPG strips, Bio-lyte (Ampholite). **Roche:** dNTPs, Protease inhibitors, Taq polymerase. **Amersham Lifesciences:** Enhanced Chemiluminescence Kit. **Merck Millipore:** PVDF membrane. **SD Fine:** Acetonitrile (spectroscopy grade). **Nunc and BD-Falcon:** Tissue culture petridish and flasks. **Axygen and Tarson:** Disposable tips and DNase, RNase free eppendorf tubes. **MP Biomedicals:** Epidermal growth factor, Fibroblastic Growth factor, Leukemia inhibitory factor. **Ambion:** Moesin siRNA, Control/Non-target siRNA. **BD Biosciences:** Cell culture

inserts, culture plates with notch, BD Matrigel matrix. **G Biosciences:** NI Protein Assay (2D quantification kit), Perfect- FOCUS (2D clean up kit). **GE Healthcare:** PlusOne Coomssie tablets PhastGel Blue R-350, Whatman filter paper. **Thermo Scientific:** Super signal West Femto. **Life Technologies:** Alexa Fluor-488 phalloidin. **Kodak:** Developing films. **Vector labs (USA):** Vectashield (anti-fade mounting medium).

The water used for the preparation of all solutions and reagents was obtained from MilliQ water plant (Millipore).

Table 1: Antibodies used in the study.

Antibody	Clone	Company & Catalogue
Prohibitin	Rabbit polyclonal	Abcam, ab-2996
TCTP	Rabbit polyclonal	Santa Cruz, sc-30124
Vimentin	Mouse monoclonal	Sigma, V 6630
Moesin	Rabbit polyclonal	Cell Signaling, 3150 BC
CD-44 (156-3C11)	Mouse monoclonal	Cell Signaling, 3570 BC
CD-133	Rabbit polyclonal	Biorbyt, orb-18124
Oct-4	Rabbit polyclonal	Imgenex, IMG-6030A
Sox-2	Rabbit polyclonal	Imgenex, IMG-6467A
Nanog	Rabbit polyclonal	Imgenex, IMG-5798A
Nestin	Rabbit polyclonal	Imgenex, IMG-6492A
Keratin-8	Mouse monoclonal	Sigma, C 5301
Keratin-18	Mouse monoclonal	Sigma, C 8541
HSP-70	Rabbit polyclonal	Santa Cruz , sc-25837
PCNA	Mouse monoclonal	Santa Cruz, sc-25280
E-cadherin	Mouse monoclonal	BD Biosciences, BD-610182
EGFR	Mouse monoclonal	Sigma, E-3138
Desmoplakin-1/2	Rabbit polyclonal	Abcam, ab-71690
N-cadherin	Mouse monoclonal	BD Biosciences, BD-610920
Beta-1 integrin	Mouse monoclonal	Santa Cruz Biotech, sc-59827
Survivin	Rabbit polyclonal	Santa Cruz Biotech, sc-10811
Cox-2	Goat polyclonal	Santa Cruz Biotech, sc-1747
Mcl-1	Rabbit polyclonal	Santa Cruz Biotech, sc-20679
BCl-2	Rabbit polyclonal	Santa Cruz Biotech, sc-492
Bcl-xl	Rabbit monoclonal	Cell Signaling, 2764S

NF- κ B	Rabbit polyclonal	Santa Cruz Biotech, sc-109
α -Tubulin	Mouse monoclonal	Imgenex, IMG-80196
GRp-94	Rat monoclonal	Pierce, MA3-016
GRp-78	Mouse monoclonal	BD Biosciences, 610978
Annexin 1	Mouse monoclonal	BD Biosciences, 610066
HSP-A8	Rabbit polyclonal	Pierce, PA5-24624
HSPA1B	Mouse monoclonal	Abcam, ab-55288
STIP-1	Rabbit polyclonal	Pierce, PA5-21473
PDI A3	Rabbit polyclonal	Pierce, PA5-29810
Annexin-A2	Mouse monoclonal	Zymed laboratories, 03-4400
PK-M2	Rabbit polyclonal	Pierce, PA5-13980
PGP	Rabbit polyclonal	Pierce, PA5-26852
β -Catenin	Rabbit monoclonal	Cell Signaling, 8480-BC
β -actin	Rabbit polyclonal	Santa Cruz Biotech, sc-1616
Alexa Fluor-568	Goat anti-rabbit	Invitrogen, 11011
Alexa Fluor-488	Goat anti-rabbit	Invitrogen, 11008
Alexa Fluor-488	Goat anti-mouse	Invitrogen, 11059
Anti-Rabbit IgG	Secondary antibody	Santa Cruz Biotech, sc-2004
Anti-Mouse IgG	Secondary antibody	Santa Cruz Biotech, sc-2005
Anti-Goat IgG	Secondary antibody	Santa Cruz Biotech, sc-2020
Anti-Rat IgG	Secondary antibody	Sigma, A 8438

Table 2: Instruments used in the study.

Instrument	Model	Company
Spectrophotometer	UV-160 A, UV-240 U-2001 Biophotometer, 6131	Shimadzu, Japan Hitachi, Japan Eppendorf, Germany
Spectro-fluorophotometer	RF-1501	Shimadzu, Japan
High speed centrifuge	Rota 4-R, Superspin R -V FA	Plasto Crafts, India
Table top ultracentrifuge	Optima MAX-XP	Beckman Coulter, USA
Microfuge	G Fuge	Genetix Biotech, India
Speedvac concentrator	SVC 1000, AES 1000	Savant, USA
Inverted microscope	Axiovert-200M	Zeiss, Germany
Upright microscope	Axio Imager Z1 Eclipse 50i	Zeiss, Germany Nikon, Japan
Confocal microscope	LSM 510 Meta TCS SP8 STED	Zeiss, Germany Lieca, Germany

X-ray film developing machine	Optimax	Pro-Tec, Germany
pH meter	Orion	Thermo scientific,
Vertical electrophoresis assembly	Mini-PROTEAN Tetra Cell, PROTEAN II xi Cell	Bio-Rad, USA
Electroblot transfer assembly	Technoblot Trans - Blot Cell	Techno Source, India Bio-Rad, USA
Power packs	EPS-301	Amersham, UK
Orbital Shaker	OS-200	Bench top Lab systems, India
IEF	PROTEAN IEF Cell	Bio Rad, USA
Flow cytometer	FACS Calibur	Becton Dickinson, USA
MALDI Instrument	Ultra Flex-2	Bruker, Germany
ELISA reader	Spectra Max 190	Molecular Devices, USA
Calibrated Gel densitometer	GS-800	Bio-Rad, USA
Real Time PCR machine	Quant Studio 12K Flex	Applied Biosystems, USA

Reagents for Mass spectrometry

All the plastic ware used for mass spectrometry were un-autoclaved to minimise the chances of plastic polymer contamination in the MALDI samples.

Coomassie staining: Dissolve 1 tablet of PhastGel Blue R-350 in 80 ml deionized water + 120 ml methanol, stir and filter (0.2% stock solution). For 0.1% working solution, mix 1:1 with 20% acetic acid in deionized water.

Destaining and washing of coomassie stained gel pieces: Destaining solution - 10 ml acetic acid + 90 ml deionized water in a un-autoclaved T-50 tube. Washing solution-50 mM NH_4HCO_3 / Acetonitrile (v/v) i.e dissolve 40 mg NH_4HCO_3 in 10 ml deionized water in a un-autoclaved T-50 tube.

Trypsin for in-gel digestion: Working concentration (10 ng/ μl)- 20 μg Trypsin (proteomic grade) powder was dissolved in 2 ml of 25 mM Ammonium bicarbonate to make a 10 ng/ μl solution of Trypsin and kept in 100 μl aliquots at -80 °C for further use.

Extraction buffer for extracting peptides from gel pieces: 50% Acetonitrile & 5% Tri-fluoro acetic acid (TFA, proteomics grade)- 500 µl of 100% Acetonitrile, 450 µl of deionized water and 50 µl of TFA were mixed.

Peptides reconstitution buffer: 50% Acetonitrile & 0.1% TFA- 500 µl of 100% acetonitrile, 499 µl of deionized water and 1 µl of TFA were mixed.

Matrix for loading of peptides on to the MALDI plate: Saturated solution of α -Cyano Hydroxy Cinnamic acid (CHCA) (Brucker-201344, approx. 20 mg/ml) in 50 % Acetonitrile and 0.1 % TFA.

Reagents for 2D sample buffer (Cell lysis buffer): 8 M Urea (480 mg/ml), 2 M Thiourea (152 mg/ml), 2% CHAPS (200 µl from the stock solution made of 10% CHAPS in deionized water) and 1% DTT (100 µl from the stock solution made of 10% DTT in deionized water) were dissolved in deionized water to the final volume of 1 ml.

Equilibration buffer I: 6 M Urea, 0.375 M Tris (pH 8.8), 2% SDS, 20% Glycerol, 2% DTT.

Equilibration buffer II: 6 M Urea, 0.375 M Tris (pH 8.8), 2% SDS, 20% Glycerol, 2.5% Iodoacetamide.

Table 3: 2D- Equilibration buffer 1 & 2.

Constituent's	Equilibration buffer I (For 5 ml)	Equilibration buffer II (For 5 ml)
Urea	1.8 gm	1.8 gm
1M Tris pH 8.8	1.875 ml	1.875 ml
SDS	0.1 gm	0.1 gm
Glycerol	1ml	1 ml
DTT	0.1 gm	-
Iodoacetamide	-	0.125 gm

The above mentioned components were added into the T-50 tube (final volume by D/W).

Rehydration buffer: 8 M Urea (480 mg/ml), 2 M Thiourea (152 mg/ml), 2% CHAPS (200 μ l from the stock solution made of 10% CHAPS in deionized water) and 1% DTT (100 μ l from the stock solution of 10% DTT in deionized water), 2 μ l Ampholite and 2 μ l of 0.1% Bromophenol Blue (BPB) were dissolved in deionized water to make final volume upto 1 ml.

IPG strips: pH 3 to 10, 17 cm.

Table 4: 2D Maxi-Gel Compositions.

Components	Stacking Gel (5%, 10 ml)	Resolving Gel (12%, 60 ml)
De ionized water	6.8 ml	19.8 ml
Acrylamide solution (30%, Acrylamide:Bis acrylamide=29:1)	1.7 ml	24 ml
Tris (1.5M,pH 8.8)	-	15 ml
Tris (1 M,pH 6.8)	1.25 ml	-
SDS (10%)	0.1 ml	0.6 ml
APS (10%)	0.1 ml	0.6 ml
TEMED	0.008 ml	0.048 ml

Electrophoresis buffer (5X): 0.125 M Tris, 0.96 M Glycine and 0.5 % SDS-15.1 gm Tris, 72.06 gm glycine and 5 gm SDS were dissolved in 1000 ml deionized water. To make final volume (working 1X) add 200ml of 5X in 800 ml of deionized water (1 litre).

Transfer buffer: Tris base 9 g + Glycine 39.5 g (Mix well) then add Methanol-600 ml and make volume with deionized water up to 3 litre.

Stripping buffer: (100ml) - 1.63 gm (w/v) of 100 mM beta mercaptoethanol, 10 ml of 20% stock of SDS, 6.23 ml of 1M stock of Tris (pH-6.7) & make up volume with deionized water.

Immunoblotting: Tris buffered saline (TBS, 10X):24.2 g Tris, 80 g NaCl, dissolve in 900 ml deionized water then adjust pH 7.6 and make final volume to 1 litre. For a 1X solution, mix 1

part of the 10X solution with 9 parts deionized water. The final molar concentrations of the 1X solution are 20 mM Tris and 150 mM NaCl. Tris buffered saline with Tween (TBST)-TBS + 0.1 % Tween 20. Fast green (0.1%) - 0.1% fast green in 100 ml of destainer; Ponceau S Staining Solution- 0.1% (w/v) Ponceau S in 5% (v/v) acetic acid.

Protein loading dye (3X): 1.9 ml of 1M Tris pH 6.8, 3 ml Glycerol, 6 ml of 10% SDS, 0.006 BPB, 0.15 ml β -mercaptoethanol (BME) and make final volume to 10 ml. The final molar concentration of 1X solution are 0.063M Tris, 10% Glycerol, 2% SDS, 0.02% BPB and 5% of BME.

RNA isolation and c-DNA synthesis: Double autoclaved DEPC water (0.1%), TRIzol reagent, Chloroform, Isopropanol, ethanol (70%). For 10 X Phosphate buffer - 0.2 M Sodium dihydrogen orthophosphate (Monobasic) - 15.6 gm in 500 ml & 0.2 M Disodium hydrogen orthophosphate (dibasic) - 14.2 gm in 500 ml were made separately. For preparing 10X buffer, 117 ml of 0.2 M of monobasic salt and 183 ml of dibasic salt was added and volume made upto 900 ml with DEPC treated water and autoclaved. Revert Aid First strand cDNA synthesis, 5X reaction buffer, 10 mM dNTP mix, random hexamer primer, oligo dT primer, sterile DEPC treated water and PCR reagents.

Quantitative Real time PCR: RNase free water (0.1% DEPC treated), SYBR green master mix, gene specific primers.

siRNA transfection: Lipofectamine method - control / nontargeting siRNA, gene specific siRNA, DMEM without serum, Lipofectamine-3000 transfection reagent, DMEM with 10% FBS without antibiotic.

Wound healing and Invasion: Wound Healing - 6 well culture plates, 0.2% FBS containing media and time lapse inverted microscope. Invasion - BD Matrigel matrix, Cell culture insert

(8 µm pore size), Culture plates with notch, DMEM with 0.1% FBS. H & E staining: 4% PFA (paraformaldehyde) in 1X PBS, Hematoxylin, 70% & 90% alcohol, Eosin, Xylene and DPX Mountant.

3D spheroid: EGF (10 ng/ml), FGF (10 ng/ml), LIF (10 ng/ml), Insulin (20 ng/ml), ultra-low attachment 12 well flat bottom culture plates, 1% Agarose for coating the wells (in sterile 1X PBS), media filter 0.2 micron.

Mice experiment: BALB/c nude and NOD SCID mice.

Protein extraction and quantification: Cell pellets, Proteojet Mammalian cell lysis reagent, Proteoblock protease Inhibitor, BSA 1 mg/ml. Folin Lowry reagents - CTC reagent (20% Na_2CO_3 , 0.2% $\text{CuSO}_4 \cdot 5\text{H}_2\text{O}$, 0.2% $\text{KNaC}_4\text{H}_4\text{O}_6 \cdot 4\text{H}_2\text{O}$), take these in 2:1:1 composition to prepare CTC stock solution (light sensitive). CTC working solution (CTC stock solution, 0.8N NaOH, 10% SDS in D/W), take these components in 1:1:1:1 composition. Folin reagent working (1:5 diluted with D/W).

Mammalian cell culture

DMEM (Dulbecco's Modified Eagle Medium) - Powdered medium was dissolved in 800 ml autoclaved D/W, supplemented further with 3.024 gm sodium bicarbonate (NaHCO_3) and volume made up to 1 L. The medium was filtered through 0.2 micron filter and stored at 4°C. IMDM (Iscoe's Modified Dulbecco's Medium) was prepared similarly as mentioned above. Antibiotic for regular cultures (for 10 ml stock) - Combination of 0.2 ml of Amphotericin B (2.5 mg/ml), 2.5 ml of Penicillin (50000 units/ml), 0.4 ml of Streptomycin (100000 units/ml), volume was made up to 10 ml with 6.9 ml distilled water. The antibiotic solution was stored at 4°C. Fetal bovine serum (FBS) - Serum dispensed in 50 ml sterile bottles and was stored at -20°C. Complete medium - IMDM or DMEM supplemented with 10% FBS and 1% of

antibiotics. Freezing medium - FBS was supplemented with 10% DMSO (anti-freeze agent) and stored at -20 °C. Phosphate buffered saline (PBS) - NaCl-8.0 g, KCl-0.2 g, KH₂PO₄-0.2 g, Na₂HPO₄ -1.5 g, Phenol red indicator (0.01%), pH was adjusted to 7.4 and sterilized by autoclaving. Phenol Red Solution: 0.1 g phenol red powder was dissolved in 100 ml D/W, autoclaved and stored at 4° C. Trypsin–EDTA - 0.25 g Trypsin, 0.58 g NaHCO₃, Phenol Red (0.01%), 1.0 g EDTA Sodium salt, 1.0 g D-glucose, 0.4 g KCl, 8.0 g NaCl. Erythrosin B (0.4 %): 40 mg Erythrosin B in 10 ml 1X-PBS.

Soft agar and Invasion

Soft agar: lower layer, 2% low melting point (LMP) agarose in autoclaved distilled water, 35mm culture plates, complete medium. Invasion: Invasion chambers, BD matrigel, 12 well culture plates with notch.

4.2 METHODS

4.2.1 Cell Culture

The different cell lines that are used in this study (described in the table below) were cultured under standard conditions in their respective medium supplemented with 10% FBS, in a humidified incubator containing 5% CO₂ at 37° C.

Table 5: List of cell lines used in the study.

Cell line	Origin	Culture medium	Reference
AW13516	Tongue SCC	DMEM	[207]
AW8507	Tongue SCC	IMDM	
UPCI:SCC029B	Buccal Mucosa	DMEM	[208]
HCT116	Colorectal Carcinoma	DMEM	[209]

Cell passaging/counting/freeze down and revival: For passaging the cells, briefly the medium was removed and adhered cells were washed with PBS (pH-7.2) and 1 ml trypsin/EDTA solution was added followed by incubation at 37°C, until cells detached from the surface. Detached cells were then re-suspended in 1 ml complete medium and spun down at 1200 rpm for 5 min, washed once with medium, counted using hemocytometer and seeded as per requirement. Cell count was taken in Neubauer's hemocytometer using Erythrosin B. The cell suspension was diluted in complete media and 10 µl of this suspension was mixed with Erythrosin B in the ratio of 1:1 and loaded onto the hemocytometer, placed under microscope. Dead cells can be distinguished as they take up the dye and appear pink. All the cells in the four WBC chambers were counted to give total count. Cells per ml = the average count per chamber x the dilution factor x 10^4 . During the establishment of radioresistant cell lines, the cells at different radiation stages were freezed down and similarly revived as per the requirement. For freezing, the 70-80% confluent cultures were trypsinised and harvested as above. Cells were washed twice with 1X PBS and freezing media was added to the cells at a final concentration of 1×10^6 cells/ml. The freezing vials were suspended in a cylinder with liquid nitrogen vapours and cooled gradually before being stored in liquid nitrogen. Reviving Cell cultures - The stored vials in liquid Nitrogen container were thawed at 37°C in a water bath & the cell suspension was transferred gently to a tube containing complete media. The cell pellet was obtained by spinning the cell suspension and subsequently, the cell pellet was washed with 1X PBS for the removal of freezing media and suspended in 1 ml of complete medium. The cell suspension was mixed gently with a Pasteur pipette to remove any clumps and finally plated in a culture plate or flask.

4.2.2 Cell Irradiation

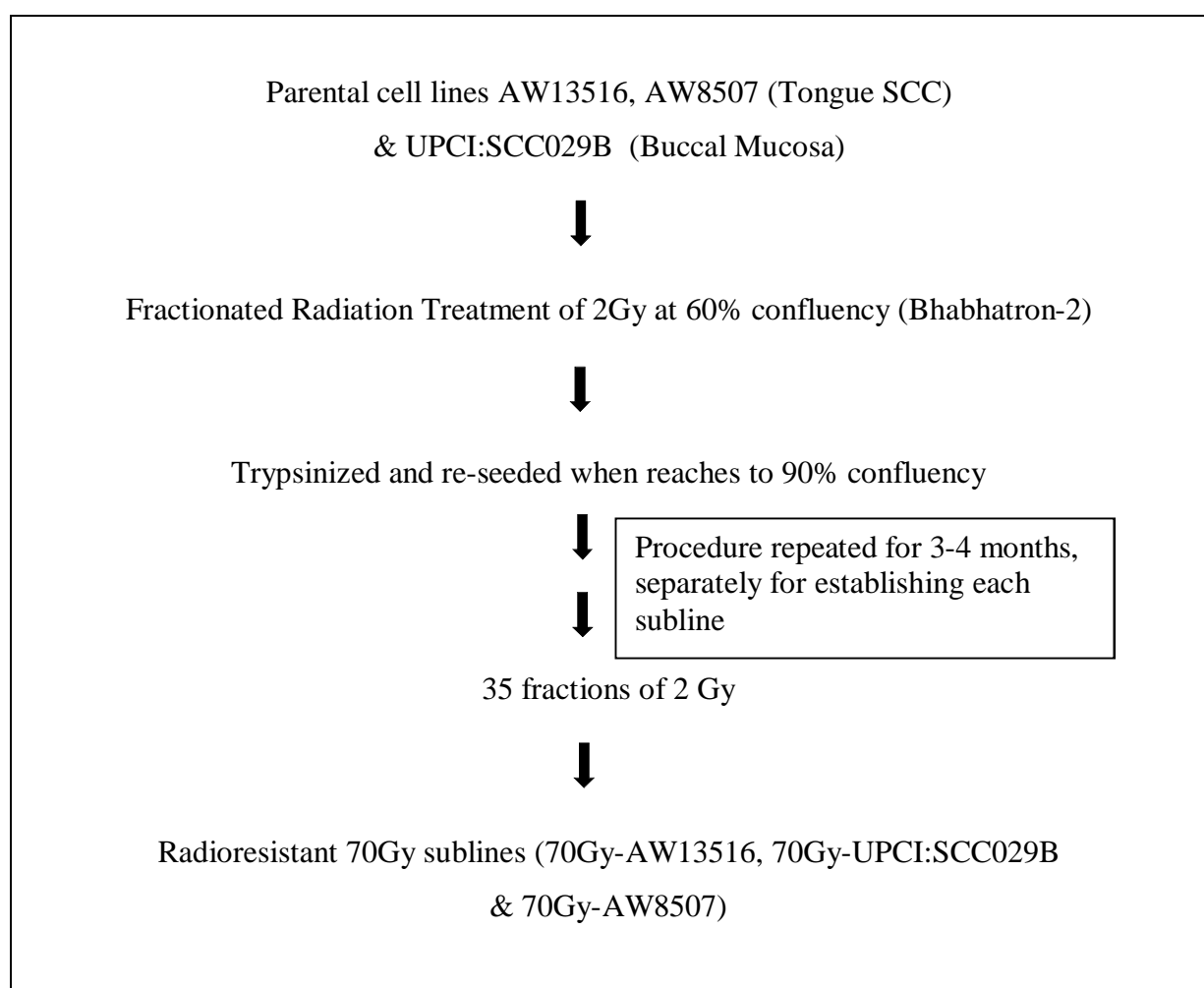
The cells were irradiated by Bhabhatron-2 (indigenously developed by Bhabha Atomic Research Centre (BARC) and Panacea Medical Technologies Pvt. Ltd.- India, (Figure 2) with

Co-60 as a source of gamma ionizing radiation [76]. Bhabhatron-2 is successfully used in radiotherapy treatment of patients. The same machine which is used for the radiotherapy treatment to the patients is used for irradiating cancer cells in the culture plates by a calibrated and standardized setup for cell culture. For cell culture radiation, $30 \times 30 \text{ cm}^2$ field size was taken, SSD = 80 cm (source to specimen distance) i.e the distance of radiation source of 80 cm was used to irradiate the cells with depth $d = 0.5 \text{ cm}$.

4.2.3 Establishment of Radioresistant sublines from Parental cell lines

The three radioresistant sublines were established from their respective parental cell lines of different oral sub sites. The protocol used for the establishment of radioresistant sublines are as follows:

Flow chart 1: Protocol used for establishing radioresistant sublines.



4.2.4 Clonogenic Cell Survival Assay

The standard clonogenic assay was performed as described earlier [86]. Briefly, each of the parental and radioresistant cells were harvested, counted and known number of cells were seeded in duplicates in 100 mm culture plates. The cells were kept in incubator for 8-10 hours for adherence to the plates and radiated with different doses of IR (0, 2, 4, 6 and 8 Gy) using ^{60}Co - γ radiator along with untreated control. After radiation, cells were incubated up to 14 days and observed to form colonies. The colonies were fixed with absolute ethanol and stained with 0.1% crystal violet for 20 min on slow rocker, rinsed and air-dried. The numbers of colonies (≥ 50 cells) were counted using a microscope. Colonies consisting of 50 or more cells were counted as clonogenic survivors. The percent plating efficiency, D_0 value (radiation dose at which 37% population survives) and surviving fraction at a given radiation dose were calculated on the basis of survival of non-irradiated cells as described below:

Formula used for calculating plating efficiency & cell surviving fractions: Plating efficiency (PE) is the ratio of the number of colonies to the number of cells seeded - $PE = (\text{no. of colonies in the control plate} / \text{no. of cells seeded}) \times 100\%$. Surviving fraction is the numbers of colonies formed after radiation treatment and expressed in terms of PE: $SF = \text{no. of colonies formed after radiation treatment} / \text{no. of cells seeded} \times PE$. The readings of clonogenic survival for each of the parental cell lines and radioresistant sublines were plotted on logarithmic scale. Three independent experiments were performed, each time in duplicates with parental and radioresistant sublines and cell survival curve was plotted after calculating surviving fraction at each dose. Further, student t-test and/or One-way ANOVA statistical analysis was performed to find the significant difference in cell survival at different doses of ionizing radiation.

4.2.5 Soft agar assay

Soft agar assay was performed to test the anchorage independent growth of the cells. Briefly, 35 mm culture plates were coated with a basal layer made up from 1:1 dilution of 2% low melting point agarose (LMP) and complete medium (2X). The plates were kept in culture hood for 30 minutes in order to set the basal layer. Upper layer (4 ml) was prepared with 2 ml of 1X medium, 800 μ l each of 2X medium, 2% LMP agarose and 4000 cells in 400 μ l volume. 1 ml of upper was plated onto the basal layer and kept for 30 minutes in culture hood, so that it solidifies. The plates were then incubated for 15 days at 37°C in a 5% CO₂ incubator and fed with complete medium on alternate days. The colonies were photographed using inverted microscope (Axiovert-200M, Zeiss) while colony size was measured by AxioVision (4.7, Zeiss). The assay was done independently thrice in triplicates.

4.2.6 Two dimensional gel electrophoresis (2D)

Preparation of cell lysate for 2D gel Electrophoresis: For 2D analysis, approximately 3.5×10^6 cells were lysed in 200-250 μ l of lysis buffer (sample buffer) and mixed by gentle pipetting. The mixture was then centrifuged at 55,000 rpm for 1 hour at 4° C in the Optima MAX-XP ultracentrifuge. The supernatant was collected and stored at -80° C.

Protein estimation by 2D quantification kit: Concentration of the protein in the lysate was estimated by the 2D quant kit (NI protein assay, G Biosciences). The NI protein assay is a highly sensitive colorimetric assay that is suitable for determining protein concentration in 2D sample buffer containing detergents (urea, thiourea) and reducing agents (DTT). The protein estimation is based on mixing protein sample with an alkaline solution containing a known concentration of copper salt, the copper ions bind to the peptide backbone and the assay measures the unbound copper ions. The color density in the assay is inversely

proportional to the amount of protein present in the sample. Therefore, blank reading need not to be subtracted from the sample reading as absorbance will decrease as protein concentration increases.

Table 6: Reagents used for protein estimation by 2D quant kit.

Description	Volume used per sample
UPPA I (Universal Precipitating Agent I)	500 µl
UPPA II (Universal Precipitating Agent II)	500 µl
Copper Solution (Reagent I)	100 µl
Reagent II (for 10 ml)	900 µl Colour reagent A + 100 µl Colour reagent B

Table 7: Standard table for 2D protein estimation.

Tube no. (in duplicates)	1	2	3	4	5	6
BSA protein Std (2mg/ml) µl	Blank	4	8	12	20	25
BSA protein in µg	0	8	16	24	40	50
Unknown protein sample (µl)	2 µl, 5 µl and 10 µl unknown protein samples were taken.					

Protein sample clean up by 2D cleanup kit: Briefly, 600 µg protein samples were processed for clean up by Perfect-FOCUS kit (G Biosciences) to make the samples free from agents like- ionic detergents, salts, lipids, charged polysaccharides and nucleic acids that can interfere with protein focusing. Prior to protein samples processed for Iso-electric focusing (IEF), the sample should ideally free from agents that known to interfere with the net protein charge. Therefore, the kit is based on quantitative precipitation and concentration of protein

solutions using Universal protein precipitating agent (UPPA). The cleaned protein sample is processed for the next step after solubilizing in rehydration buffer.

Table 8: Reagents used in 2D clean up kit.

Description	Volume used per sample (600 µg protein)
UPPA I (Universal Precipitating Agent I)	450 µl
UPPA II (Universal Precipitating Agent II)	450 µl
Focus wash	60 µl
Distilled water	30 µl
Orgosol Buffer (chilled)	1 ml
SEED	5 µl

Protein Rehydration and Focusing on IPG strip: For 2D, 17 cm (pH- 3 to 10) immobilized pH gradient (IPG) strips were rehydrated with 300 µl of rehydration buffer. The rehydration buffer containing the protein sample (600 µg) was dispensed along the length of the rehydration tray and the IPG strip was placed on the sample in the rehydration tray (gel side facing down) and incubated for 20 min at RT. After the incubation, 2 ml of mineral oil was overlaid on each of the IPG strips to prevent evaporation during the process of rehydration. The IPG strips were rehydrated overnight (14-16 hrs) at RT. After overnight rehydration, IPG strips were carefully removed from the rehydration tray and excess mineral oil was drained out by placing the tip of the IPG strip on a tissue paper. Small paper wicks were cut from Whatman filter paper and placed on both ends of electrodes in the Protean IEF focusing tray (gel side facing down) and were wet with 8 µl of deionized water. After removing air bubbles beneath the IPG strips, the IEF focusing tray was placed in the Protean IEF cell (Bio Rad) and the proteins were focused using the following program. Temperature was set at 20°C and the maximum current was set at 50 µA/strip.

Table 9: Programme for protein focusing (17cm IPG strip)

Step	Start voltage	End voltage	Time	Final volt-hours	
1	0 V	250 V	20 minutes	-	Linear
2	250 V	10000 V	2 hour 30 minutes	-	Linear
3	10000 V	10000 V	-	40000 V-h	Rapid

Gel Equilibration and second dimension protein separation: After the IEF run is over, the IPG strip was placed in the rehydration tray with the gel side up and briefly 2.5 ml equilibration buffer-1 was put over it and placed on a slow rocker for 10 minutes. Similar, washing was done with equilibration buffer-2. The reduction and alkylation of proteins was done during washing in the equilibration buffers. The IPG strip is now ready for second dimension run. Separation in the second dimension was carried out in the PROTEAN II Xi Cell (Bio-rad) apparatus with IPG strip placed horizontally over the 12% SDS polyacrylamide gel and sealed with 1% agarose containing bromophenol blue (BPB) to track the gel run. Second dimension separation was carried out at a constant voltage of 100 V. The reference dye (BPB) was allowed to run out and then the instrument was then switched off. Two-dimensional electrophoresis of the proteins was done essentially according to Laemmli [210].

2D Gel fixation and staining: After the second dimension run, the gels were fixed in 50% methanol (made in D/W) overnight and followed by coomassie staining. Briefly, the PhastGel Blue R coomassie stain tablets were dissolved in 120 ml methanol + 80 ml D/W and filtered to make 0.2% staining solution (stock). For 0.1% working solution, 1 part of stock was added to 1 part of 20% acetic acid in D/W. The gels were kept for staining in 0.1% coomassie solution for about 16-18 hours at RT.

Gel Destaining and Scanning: To remove the excess background stain and clear visualization of protein spots, the stained gels were destained in 10% acetic acid and 50% methanol made in D/W. The gels were destained by several changes of this destaining solution and the gel images were scanned on the calibrated densitometer GS-800 (Bio-Rad) in an auto scale mode. One set of parental and radioresistant cell lysate was run, stained and acquired simultaneously and similarly each of these sets was run in three technical replicates.

4.2.7 PD Quest analysis of 2D gels

The scanned 2D gels were analyzed on PD Quest 2D gel analysis software (Bio-Rad) as per the manufacturer's instructions that are described below:

Creating Match sets and Master gel: Each of the parental and radioresistant set of gels in three technical replicates were converted into Match Set, which is PD Quest mechanism for comparing and analyzing the protein spots in an experiment. Match set contain copies of the Gaussian and Filtered images, as well as the original scan of the gels in an experiment. Based on the best average spot quality of a constituent gel of a match set, the software automatically chooses the Master gel. The Master gel is a synthetic image that contains the spot data from all the gels in the Match Set and all spot comparisons and analysis are coordinated through the Master gel. This creation of a Match Set will help in making quantitative and qualitative spot comparisons across gels.

Filtering and Normalization of gels: Filtering of the constituent gels of the Match Set was done automatically by the software and it removes the small noise features in the gel image. After filtering, the Match Set proceeded for normalization by the software. For normalization, a total quantity in valid spots method was selected. In this normalization method, the raw

quantity of each spot in a member gel is divided by the total quantity of all the spots in that gel that have been included in the Master gel.

Spot detection parameter wizard: After normalization, the Match Set is ready for automatic spot detection. First, the faint spot and faintest spot in the gel scan was chosen, this will set the sensitivity and minimum peak value parameters. Next, a box was drawn around the largest spot cluster on the gel image; this sets the radius of the background subtraction and the streak removal. Vertical and horizontal streak removal checkboxes were selected to remove streaks in the gel images.

Automated spot detection and matching: After completing the spot detection wizard settings the software proceeded for spot detection and matching in the Match Set. After a while, spot crosshairs mark the center of the spots in each constituent gel of Match Set in accordance with the Master gel. The spots that were marked in green in any of the Match set gel are the ones that are present on the Master gel also and the spots that were cross marked with red are the ones that are not present on the Master gel. These spots can be manually added to the Master gel at the specified position.

Spot Quantity: The spot detection and matching in the end gave three separate images; the original Raw gel scan which remains unchanged, the Filtered image - which is a copy of the original scan that has been filtered and processed and the Gaussian image - which is a synthetic image containing the Gaussian spots. All quantitation and other analysis are performed on the Gaussian image by the software. After the spot matching process, the quantities of the spots were displayed. Spot Quantity is basically, the total intensity of a defined spot in a normalized gel image and it is simply the sum of the intensities of the pixels.

4.2.8 Mass Spectrometry for the Identification of Differentially Expressed Protein Spots

The differentially identified protein spots were picked from the coomassie stained 2D gels by puncturing gel with an un-autoclaved tip (front portion cut accordingly with the scissor) fitted with the pipette and stored in destaining solution at 4° C. In order to identify these spot by MALDI-TOF/TOF by using Ultraflex II (Bruker), the gel plugs were processed for trypsin digestion, according to Shevchenko et.al [211]. After destaining of gel pieces by 2-3 washes of destainer and distilled water on a slow vortex, the gel pieces were put in 100 µl of gel shrinking solution (100% Acetonitrile) for 5 minutes at RT. The acetonitrile (ACN) was removed by drying in a speed vacuum. The proteins in the plugs were then trypsinized overnight at 37°C with 10 ng/µl trypsin in 25 mM ammonium bicarbonate (10 µl/plug) and the peptides were recovered by extraction with 40 µl of 50% ACN and 5% TFA (2 to 3 times). Tryptic protein digests were reconstituted in a solvent containing 10% ACN and 0.1% TFA, before subjecting them to mass spectrometry analysis.

Mass spectrometer instrument and calibration: The reconstituted peptides were mixed in equal volume with the matrix (2 µl each) and loaded onto 384 spot plate of MALDI-TOF/TOF. Mass calibration was carried out using peptide mixture of five known peptides, spanning mass range of 757-3147 m/z and error was kept to less than 10 ppm. Accelerating voltage of 25 kV was applied to the first TOF tube. The MS data was acquired in an automated manner using a solid state NdYAG laser at 337 nm. The resulting MS data was analysed using Flex analysis-3.0 (Bruker Daltonik, Germany) software and was acquired using Biotoools software (Bruker Daltonik, Germany). Five most intense peaks for protein identity obtained in MS analysis were subjected to MS/MS. The MS peak list and MS/MS ions of the chosen peptides were searched against SwissProt database, using MASCOT search engine for protein ID with precursor tolerance of 100-200 ppm for MS and fragment tolerance of 1 Da for MS/MS analysis.

4.2.9 Protein extraction and quantification for 1D gels

Cells were harvested from culture plates by trypsinization and cell pellets were washed twice with 1X PBS to remove traces of medium. Whole cell lysate was prepared by solubilizing the cell pellets in Proteo JET mammalian cell lysis reagent containing 1% protease inhibitor (Proteoblock, Fermentas). Briefly, the cells were mixed and spun at 15,000 rpm for 15 min at 4° C. The debris at the bottom was discarded and clear lysate was collected in a fresh tube & total protein was estimated.

Determination of Protein concentration by Folin Lowry Method: Protein estimation was done using Folin Lowry Method [212]. Briefly, BSA standards from 1 mg/ml stock were taken (as described in the table no. 10 below) and unknown protein samples were diluted approximately in the range of standards. 500 µl of Folin reagent was added to the above standards and unknown protein samples. The absorbance on spectrophotometer was measured at 750 nm and concentration of protein in unknown samples was determined according to the standard curve.

Table 10: Protein estimation by Folin Lowry method

BSA (1mg/ml) µl	D/W µl	CTC (working) µl		Folin reagent (1:5 diluted) µl	
Blank	1000	1000	<i>Kept at RT in dark for 10 Minute</i>	500	<i>Kept at RT for 20 Minute & OD was taken at 750 nm</i>
5	995	1000		500	
10	990	1000		500	
15	985	1000		500	
20	980	1000		500	
25	975	1000		500	
30	970	1000		500	
Unknown (1 µl)	999	1000		500	
Unknown (2 µl)	998	1000		500	

SDS-Polyacrylamide gel electrophoresis (PAGE): SDS-PAGE was performed to resolve the protein, the gels are formed by cross linking monomeric acrylamide with N, N'-methylene Bis-Acrylamide and pore size is controlled by modulating the concentrations of acrylamide and Bis-Acrylamide while preparing a gel. The size of these pores decreases as the Bis-Acrylamide: acrylamide ratio increases, therefore resolving gels of different percentage (8% to 15%) were used to properly resolve proteins of different molecular weights.

Table 11: Resolving gel composition (for 1D)

Components (for 10 ml)	8%	10%	12%	15%
De ionized water	4.6 ml	4 ml	3.3 ml	2.3 ml
Acrylamide solution (30%, Acrylamide:Bis-acrylamide=29:1)	2.7 ml	3.3 ml	4 ml	5 ml
Tris (1.5M, pH 8.8)	2.5 ml	2.5 ml	2.5 ml	2.5 ml
SDS (10%)	0.1 ml	0.1 ml	0.1 ml	0.1 ml
APS (10%)	0.1 ml	0.1 ml	0.1 ml	0.1 ml
TEMED	0.008 ml	0.008 ml	0.008 ml	0.008 ml

Table 12: Stacking gel composition (for 1D).

Components (for 10 ml)	Gel (5%)
De ionized water	6.8 ml
Acrylamide solution (30%)	1.7 ml
Tris (1 M, pH 6.8)	1.25 ml
SDS (10%)	0.1 ml
APS (10%)	0.1 ml
TEMED	0.008 ml

The protein samples were mixed with 3X gel loading dye, to a final concentration of 1X, denatured by keeping on a float in boiling water bath (100°C) for 5 min and were then loaded into the wells of polyacrylamide gel and electrophoresed at a constant current of 25 mA for 2-

3 h at room temperature. Pre-stained protein ladder was also run simultaneously in the gel along with protein samples, so as to determine the mobility and molecular weights of the various proteins in the gel.

Transfer of proteins on PVDF membrane: Proteins that were separated by SDS-PAGE were electro-transferred onto an adsorbent Polyvinylidene difluoride (PVDF) membrane to allow binding of specific antibodies. Briefly, wet electro-blotting was carried at 20 V overnight or 80 V for 4 hrs. Transfer of proteins was visualized using Ponceau-S or Fast green and destained by washing with distilled water or destainer respectively. Subsequently, the membrane blot was incubated in blocking solution (5% skimmed milk or 3% BSA made in 1X TBS) for 1 hr at RT on a slow rocker. The blots were then incubated with appropriate concentration of primary antibodies (diluted in 2.5% milk or 1 % BSA in 1X TBST) overnight at 4°C or 1 hr at RT on slow rocker. The blots were then washed six times (10 min each) with 1X TBST followed by incubation with horseradish peroxidase (HRP) conjugated secondary antibody for 1 hr at RT on the rocker. The blots were then washed and developed using ECL chemi-luminescence reagent (Amersham, USA) according to the manufacturer's protocol. The X-ray films were developed on the automated developing machine.

4.2.10 Immunofluorescence

To detect the localization of proteins in the cell, immunofluorescence study was performed. Cells were grown on sterile glass cover slips for 48 hrs till they reached 60-70% of confluency and washed twice with PBS. The cells were fixed and permeabilized either with 4% paraformaldehyde for 15 minutes at 37°C and 0.7% Triton-X or with chilled methanol in -20°C followed by 0.3% Triton-X in chilled absolute methanol (exactly for 90 sec) or with chilled methanol. Cells were blocked with either 5% BSA or 3% BSA in PBS for 1 hour at

RT. After 2-3 washes of PBS, the coverslip were incubated with desired dilution of respective primary antibody overnight at 4°C. Further, cells were washed 3-4 times with 1X PBS before incubating with Alexa-conjugated secondary antibody for 1hr in dark. After washing the cells on the coverslips again, it was counter stained with DAPI (0.5µg/ml in PBS) for 20 min at room temperature and mounted with Vecta-shield antiquescenting mounting medium (Vector laboratories). The cells were imaged with 510 META Confocal microscope (Zeiss, Germany) and/or with TCS SP8 STED (Leica, Germany).

Table 13: List of antibodies used for western blotting & immunofluorescence.

Antibody	Dilution for WB	Dilution for IF
Prohibitin	1:1000	-
TCTP	1:2000	-
Vimentin	1:5000	1:200
Moesin	1:1000	1:50
CD-44	1:1000	1:50
CD-133	1:1000	-
OCT-4	1:100	-
Sox-2	1:200	-
Nanog	1:250	-
Nestin	1:100	-
Keratin-8	1:8000	-
Keratin-18	1:8000	-
HSP-70	1:300	-
PCNA	1:500	-
E-cadherin	1:1000	1:200
EGFR	1:2000	-
Desmoplakin-1/2	1:500	1:200
N-cadherin	1:500	1:50
Beta-1 integrin	1:3000	-
Survivin	1:1000	-
Cox-2	1:500	-
Mcl-1	1:1000	-
BCl-2	1:500	-
Bcl-xl	1:1000	-

NF kB	1:500	-
α -Tubulin	1:8000	-
GRp-94	1:1000	-
GRp-78	1:3000	-
Annexin-1	1:3000	-
HSP-A8	1:1000	-
HSPA1B	1:1000	-
STIP-1	1:1000	-
PDI A3 (Erp 57)	1:1000	-
Annexin-A2	1:1000	-
PK-M2	1:1000	-
PGP	1:200	-
Beta Catenin	1:1000	1:100
β -actin	1:3000	-
Alexa Fluor-568	-	1:1000
Alexa Fluor-488	-	1:1000
Alexa Fluor-488	-	1:1000
Anti-Rabbit IgG	1:2500	-
Anti-Mouse IgG	1:3000	-
Anti-Goat IgG	1:2000	-
Anti-Rat IgG	1:1000	-

Densitometric analysis of blots: Densitometry was performed using Image J (NIH, USA) software by inverting and subtracting the background of the blot and calculating the mean intensity of each band by selecting the largest band area. Similarly, the intensity of the respective loading controls from the same blot was determined to get normalized relative values. Data presented as mean \pm SD of 3 independent samples in each group.

4.2.11 RNA extraction and cDNA synthesis

RNA was isolated by TRIZOL reagent (Sigma) and cDNA synthesis was performed by using the Revert Aid first strand cDNA synthesis kit (Fermentas) according to the manufacturer's instruction. Briefly, 1 μ g of RNA and 1 μ l of random hexamer/oligo dT primer and DEPC water in a volume of 12 μ l were incubated at 65° C for 5 minutes. After the denaturation of

RNA, the following reagents were added to it with specified volume. 5X reaction buffer-4 µl, 10mM dNTPs mix-2µl, Reverse Transcriptase enzyme-1µl, RiboLock RNase Inhibitor-1 µl. The mixture was incubated at 25°C for 5 min followed by 42°C for 1 hr. The reaction was stopped by heating at 70°C for 5 min. The efficiency of cDNA synthesis was assessed by GAPDH-PCR. The products were resolved on 2% agarose gel containing ethidium bromide and quantitated using Gel-doc system (UVP, UK).

Table 14: Table for GAPDH-PCR.

Component	Stock Conc.	Working Conc.	Amount added (25 µl reaction)
PCR Buffer	10 X	1 X	2.5 µl
dNTPs	2 mM	0.2 mM	2.5 µl
Mgcl ₂	50 mM	1.5 mM	0.75 µl
Forward primer	100 ng/ µl	100 ng/ µl	1 µl
Reverse primer	100 ng/ µl	100 ng/ µl	1 µl
Taq polymerase	5 units	1 unit	0.2 µl
cDNA	-	-	1 µl (100-200 ng)
Distilled water	-	-	16.05 µl

Table 15: GAPDH- PCR specification.

Gene	Primer sequence	Conditions (°C - Min/Sec)	Product size (bp)
GAPDH	F-CAAGGTCATCCATGACAACTTTG R- GTCCACCACCCTGTTGCTGTAG	94-1 52-1 72-1 } 30 cycles	496

4.2.12 Quantitative Real time PCR

Real-time quantitative PCR was done by using SYBR green chemistry on Quant studio instrument (Applied Biosystems). The standard curve was generated for each primer pair and genes of interest were assigned a relative expression value by the software from this standard curve using the Cycle threshold (Ct) and the comparative Ct method ($2^{-\Delta\Delta C_t}$) of relative

quantification was used to analyze gene expression among samples as described earlier [213].

All expression values were normalized against HPRT house-keeping gene and amplifications were done three times in duplicate with a NTC (Non template control) each time.

Table 16: List of Primers with their sequences used in qRT-PCR.

Gene	Primer Sequence	Product length	Reference
Snail	F: 5'-TAGCGAGTGGTTCTTCTGCG-3' R: 5'-AGGGCTG CTGGAAGGTAAAC-3'	164	Self- designed by NCBI/ Primer- BLAST
Slug	F: 5'- AGACCCCATGCCATTGAAG-3' R: 5'-GGCCAG CCCAGAAAAAGTTG-3'	79	
Twist	F: 5'-AGCTGAGCAAGATTGACACCC-3' R:5'-GCAG CTTGCCATCTTGGAGT3'	101	
HPRT	F: 5'-GAACCAGGTTATGACCTTGA-3' R: 5'- GAG ATCATCTCCACCAATTA-3.'	327	
HIF1A	F 5' GTGGTGGTTACTCAGCACTT 3' R 5' CTCCGACATTGGGAGCTCAT 3'	154	
BECN1	F 5' GTCGCTGAAGACAGAGCGAT3' R 5' GTCACCCAAGTCCGGTCTAC3'	94	
IL8	F 5' TCAGAGACAGCAGAGCACAC3' R 5' GGCAAACTGCACCTTCACA3'	159	
NOTCH2	F 5' AGAATCAGCCCTGCCAGAAT 3' R 5' GATTTCATACCCCGAGTGCC 3'	91	
PARVA	F 5' AGGAGGGAATGAACGCCATC3' R 5' ATCCACCATTGTTTCGCACCT 3'	104	
Nibrin	F 5' GCAGAAATTGGATTGGCGGT3' R 5' AAGGCTTGGTCCTGGAGTTG3'	105	
SIRT1	F 5' TCCTACTGGCCTGAGGTTG 3' R 5' AAAAGAGCGAATCCACTGGCA3'	143	
E-CAD	F 5'GTGAACACCTACAATGCCGC 3' R 5' GGAAACTCTCTCGGTCCAGC 3'	139	
GRP 94	F - CCGCCTTCCTTGTAGCAGAT R – TTGTCGTTCCCCGTCCTAGA	138	
STIP1	F- TGAGAAAGGGTGTGCGGT R- GGCTGTTAGGTTCTGAATGTTCC	142	
PDI A3	F- TGCTGGGCACAACTCAACT R- CATCACGCGAGAACTCCTCC	161	
HSP A8	F- GTCTATTGGCCGGGGAAGC	185	

	R- ACATGGTTGCTGGGGTGTAG		
PGP	F- TCATCACCAACAACAGCAGC R- AGTAGGCCGTGCCGAAGA	117	
PKM 2	F- GAGGCCTCCTTCAAGTGCTG R- GACGAGCTGTCTGGGGATTC	133	
HSPA-1A	F: TAACCCCATCATCAGCGGAC R: AGCTCCAAAACAAAACAGCAA	154	
HSPA-1B	F: TGTGTAACCCCATCATCAGCG R: GGAAAACAGCAGCAAAGTCC	194	

4.2.13 Cell morphology and F-Actin staining

Morphological changes observed during fractionated ionizing radiation were photographed using the inverted microscope (Axiovert-200M, Zeiss) coupled with digital camera. Representative images of parental and radioresistant cells were processed by using AxioVision software (4.7, Zeiss). To investigate the distribution of filamentous actin (F-actin) in cells, phalloidin staining was used. Briefly, cells were grown on coverslips in mono layers, fixed with 4% paraformaldehyde (in 1X PBS) for 15 minutes and permeabilized with 0.7% Triton-X (in 1X PBS for 15 minutes at 37°C). A high affinity filamentous actin (F-Actin) probe Alexa Fluor-488 phalloidin was diluted 1:20 (in 1X PBS) and incubated with cells on coverslips for 30 minutes at room temperature in dark. After incubation, the coverslips were washed two times with 1X PBS for 10 minutes. DAPI (1:20 diluted in 1X PBS) staining was done for approximately 1 minute and coverslips were then mounted in vectashield on a clean glass slide and examined with LSM-510 Meta confocal system. Each of the parental and radioresistant cells were grown in duplicates on coverslips and random images for 50 cells were acquired. In this way, the staining was performed three times independently and 50 cells were analysed each time from all the cell population types for slender cytoplasmic projection (filopodia) counting.

4.2.14 siRNA transfection by Lipofectamine method

Moesin knockdown was achieved using silencer select validated siRNA of moesin (s-8986, 4390826) along with a control siRNA (4390843) from Ambion (Life Technologies). The siRNA duplexes were transfected using Lipofectamine-3000 (Invitrogen) according to the manufacturer's instructions. Medium was changed after 17 hours of transfection and 72 hours after post transfection, cells were assessed for knockdown by western blotting. The specific silencing of Moesin protein was confirmed in three independent experiments.

4.2.15 Cell Migration Assay

The parental and radioresistant cells were grown in 6-well culture plates till they acquire 70% confluency, followed by serum starvation for 16 hours to inhibit proliferation. Three linear scratches was made per well and observed for time lapse on inverted microscope, fitted with movable stage maintained at 37°C, 5% CO₂. Similarly for Moesin siRNA transfection, cells were transfected and after 17 hours of transfection, allowed to grow for further 32 hours. Cells were then serum starved for 16 hours and scratches were made and observed for time lapse. All assays were performed independently thrice in duplicates and images were taken every 5 min for 20 hour using an AxioCam MRm camera. The migration measurements were done by Image-J software (NIH) and percent migration was calculated by using the formula: % wound closure = $(0^{\text{th}} \text{ area} - \text{time point area} / 0^{\text{th}} \text{ area}) \times 100$.

4.2.16 Cell Invasion Assay

The BD Matrigel was thawed for 12 hours on ice and diluted 1:10 in incomplete medium inside the culture hood. 100 µl of diluted matrix was put into culture inserts resting on the notch plates and allowed to set for 5-6 hours inside the incubator. Then, 0.2×10^6 cells in 0.1% FBS were placed in the invasion chambers (8 µm pore size) and the lower chamber was

filled with 0.6 ml of complete media. The cells were allowed to invade for 16 hours in standard cell culture conditions. Similarly, invasion assay was done for Moesin siRNA transfected cells. For staining, the inserts were removed from the notch plates and 1X PBS wash was given, before putting the insert into 4% PFA for 15 minutes to fix the invaded cells on the lower part of invasion column. The un-invaded cells from the upper part of the inserts were swabbed by a cotton plug. The filter of invasion column were carefully cut from the periphery by a surgical blade and processed for H&E staining followed by mounting on glass slides. For quantification of invasiveness, five random fields were used and data obtained from three separate experiments were shown as their mean values.

Hematoxylin and Eosin staining for Invaded cells: The lower round circle that was cut from the invasion column was held with a fine forceps and dipped into the hematoxylin solution for exactly 1 minute. Followed by dipping in tap water twice and in distilled water once to wash the excess stain. The circle was then placed in 70% alcohol, 95% alcohol (2 minutes each), Eosin (1 minute) and in absolute alcohol to remove excess eosin stain. The invasion circle was rinsed and dipped in Xylene (2 minutes) and finally placed over a drop of DPX mountant, placed on a clean glass slide, with the cell invaded side facing down. The invasion circle was sealed slowly to avoid any bubble with the coverslip and pictures of invaded cells were taken on the upright microscope from five random fields for each circle.

4.2.17 Hanging Drop Assay

Hanging drop assay was performed to measure the cell adhesion [214]. About 2×10^4 cells were suspended in a 35 μ l drop of complete medium from the lid of 24-well culture plate for 16 hr in the cell culture incubator. The corresponding wells were filled with sterile 1X PBS to maintain humidity. After the incubation, the drops were pipetted 5 times with a standard 200

μl tip, fixed with 3% glutaraldehyde and aliquots were spread on coverslips. Images of 5 random fields from 3 independent suspensions were taken with a plan-Neofluar lens (numerical aperture 0.3) on an upright Axio Imager Z1 microscope for each sample. The area of cell clusters was determined using the AxioVision software (release 4.5, Zeiss).

4.2.18 Spheroid formation assay

The spheroid formation assay was originally established as an *in-vitro* culture system that enriches for mammalian stem cells of the central nervous system [215]. It is currently used as an assay to enrich the cells with stem cell like characteristics. Briefly, 2×10^3 cells for each of the parental and radioresistant were seeded in ultra-low attachment 12 well plates. The wells were supplemented with spheroid media without FBS and containing EGF, FGF, LIF and Insulin (compositions are described in materials section) and allowed to form 3D spheroids in non-adherent condition. 100 μl of spheroid media was added after every 2 days and plates were kept in incubator under 5% CO₂ for 14-16 days. The images of spheroids were captured on Inverted microscope. The assay was done thrice in duplicate for each of the parental and radioresistant cells.

4.2.19 Flow cytometry for cell surface staining

The cells were grown for 48 hours, harvested by trypsinization and 1×10^6 cells were fixed (1% PFA) and incubated with anti CD-44 antibody (1:100) for 45 minutes. After incubation with primary antibodies, cells were washed with FACS buffer (1% FBS, 0.02% sodium azide) and incubated with Alexa-488 Anti-mouse-IgG secondary antibody for 45 minutes. Cells were analysed with FACS Calibur and Mean fluorescence intensity was measured by using Cell Quest software (BD) in arbitrary units Msiy.

4.2.20 Tumour formation in Immunocompromised mice

Tumour formation in Nude or SCID mice was performed as described previously [216]. Five animals per group were used for injecting parental and radioresistant cells. All protocols for the animal studies were reviewed and approved by the Institutional Animal Ethics Committee (IAEC) constituted under the guidelines of the Committee for the Purpose of Control and Supervision of Experiments on Animals (CPCSEA), Government of India (project approval id: 13/2014). For each animal 5×10^6 cells in 100 μ l sterile 1X-PBS were injected subcutaneously into the dorsal flank of 5 to 6 week old Nude or SCID mice. The tumor formation was observed for 3-4 months and the ellipsoid volume formula $\frac{1}{2} \times L \times W \times H$ was used to calculate the tumor volume [217].

4.2.21 Raman Spectroscopy

Sample preparation and spectral acquisition: Parental and radioresistant cells were cultured in 100 mm culture plates and exponentially growing cells (3×10^6 cells) from 6 independent cultures of each of the parental, 50Gy and 70Gy cells were harvested and phosphate buffer saline (PBS) wash was given to the cell pellets prior to spectra recording. Approximately 7 spectra were acquired from each cell pellet by using fiber-optic Raman microprobe system as described earlier [177]. Thus a total of 40 spectra per group were acquired for each of the parental and radioresistant cells. The Raman system utilized in this study consists of a diode laser (Process Instruments) of 785 nm wavelength as excitation source and a high efficiency (HE-785, Horiba-Jobin- Yvon, France) spectrograph coupled with a CCD (Synapse, Horiba-Jobin-Yvon, France) as detection element. Optical filtering, sample preparation and spectral acquisition of unwanted noise including Rayleigh signals were accomplished through ‘Superhead’ auxiliary component of the system. Superhead

coupled with a 40X microscopic objective (Nikon, NA 0.65) was used to deliver laser light as well as to collect Raman signals. The spectrograph has no movable parts, had fixed 950 gr/mm grating and spectral resolution as per manufacturer's specification was $\sim 4 \text{ cm}^{-1}$. Estimated laser spot size at the cell pellet sample was 5–10 μm . Spectra were integrated for 6 seconds and averaged over 3 accumulations. Typical laser power at the specimen was 40±0.05 mW.

Spectral pre-processing and data analysis: Raman spectra were pre-processed by correcting charged couple device (CCD) response from a National Institute of Standards and Technology (NIST) certified standard reference material 2241 (SRM 2241) followed by subtraction of background signals from optical elements and CaF_2 window. To remove interference of the slow moving background, first derivatives of spectra (Savitzky - Golay method) were used for data analysis [218,219]. Then spectra were interpolated in the 900–1800 cm^{-1} range and vector normalized. Analysis of the pre-processed spectra was carried out using PCA (principal component analysis) algorithms implemented in MATLAB (Mathwork Inc.) based in-house software [220]. PCA is unsupervised data overview tool used to look at the differences and similarities among the spectra. This method reveals outliers, groups and trends in the data. It describes data variance by identifying a new set of orthogonal features, these are known as loads of factor or principal components (PCs) ($p < 0.05$). Principal components are linear combinations of original data variables. As the present study is an exploratory study therefore we have carried out PCA method of analysis, also this method was used in different *in-vitro* studies on cell lines [179,180]. Mean and difference spectra were calculated for different cell populations and used for spectral comparison. The mean spectra were computed from the background subtracted spectra prior to derivatization by averaging Y-axis variations and keeping the X-axis constant for each class. The baseline

correction was performed by fitting a 5th order polynomial function. These baseline corrected spectra were used for spectral comparisons across all groups. The difference spectra were generated by subtracting the mean spectra of radioresistant cells with parental cells.

4.2.22 cDNA Microarray

The cDNA microarray was performed by using Affymetrix Gene chip-Human prim view array (I-life discoveries, Gurgaon-India) and raw data was analyzed by Gene spring GX-12.5 software followed by differential gene expression clustering. A Moderate t-test was applied for assessing the statistically significant differentially expressed genes (DEGs) and the DEG list was processed for fold change analysis by taking fold change cut off ≥ 2 fold. The microarray was performed with two technical replicates for each of the parental and radioresistant set of cells. The up and down regulated genes from both the sets were annotated by three different curated databases i.e Panther [221], Reactome [222] and KEGG [223] enrichment analysis for functional annotations and significant pathway study.

Sequence of events in Microarray analysis: The total number of probe sets detected in the microarray experiment was 49,395. Further, the probe sets that have low intensity were excluded and only intensity that has a value between 20 to 100 percentiles in normalized data is included. After this analysis, only 43,307 probe sets remain in UPCI:SCC029B set; while 46,000 probe sets left in AW13516 set. The baseline transformation was performed by taking median of all the probe sets and the transformation has been shifted from 20% to 75% of raw intensity data in Gene Spring tool on the basis of the median values.

Data pre-processing and Normalization: All the original microarray data (.CEL files) for the Parental and Radioresistant group was preprocessed using RMA (Robust Multichip Average) algorithm [224] that consists of three steps: Background adjustment, Quantile normalization and summarization, that were done by selecting RMA algorithm in Gene spring Gx12.5 software. Genes of low intensity information content in each data set were filtered as follows: the probes of intensities less than the 10.0 percentile in the raw data were excluded from the analysis and average of intensity values over the replicates experiment set has been taken. The control probes are included while performing normalization. Baseline to median for all samples was performed by calculating median of the log summarized values for each probe from all the samples and subtracted from each samples [225].

Raw signal values & normalization: The term 'raw' signal values refer to the linear data after thresholding and summarization that was performed by computing the geometric mean. The normalized values were generated after log transformation and normalization.

Differential gene expression & fold change analysis: A moderate t-test method was applied for assessing the statistically significant differentially expressed genes with the p-value cut off 0.05. The fold change analysis was used to identify genes with expression ratios between the treatment (radioresistant) and control (parental) groups that are outside of the cutoff or threshold.

Box whisker plot: The Box whisker plot represents the visualization summary of the normalized microarray data. The box whisker plots for both the groups (parental and radioresistant UPCI:SCC029B & AW13516) were created from normalized intensity values

of all the probes. In the figure 9 & 10, the box whisker plot shows the median in the middle of the box, the 25th quartile (lower) and the 75th quartile (upper).

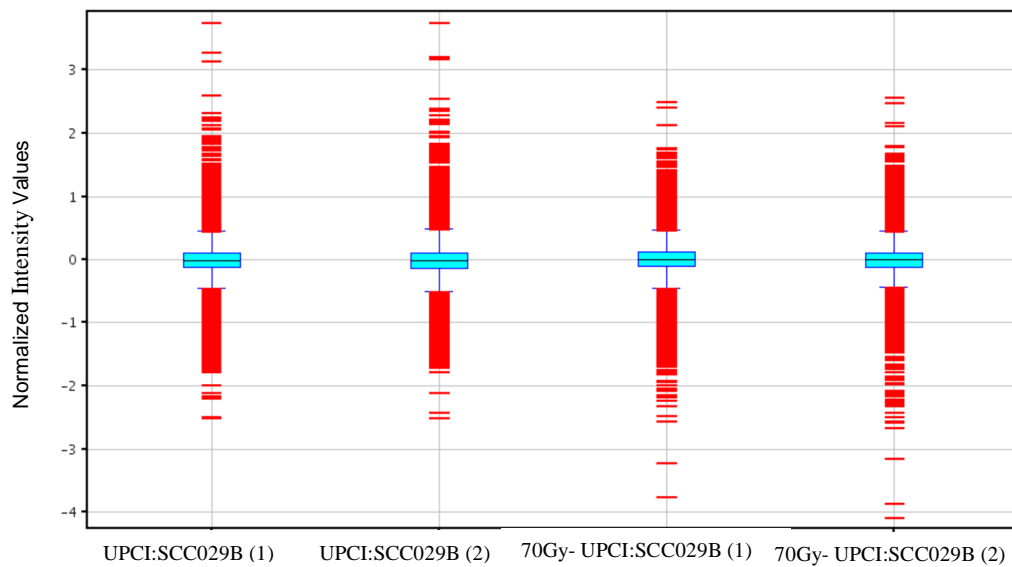


Figure 9: Box whisker plot for the Parental UPCI:SCC029B and Radioresistant 70Gy-UPCI:SCC029B cells in two technical replicates. Plot represent that the replicate experiment has a similar type of expression pattern.

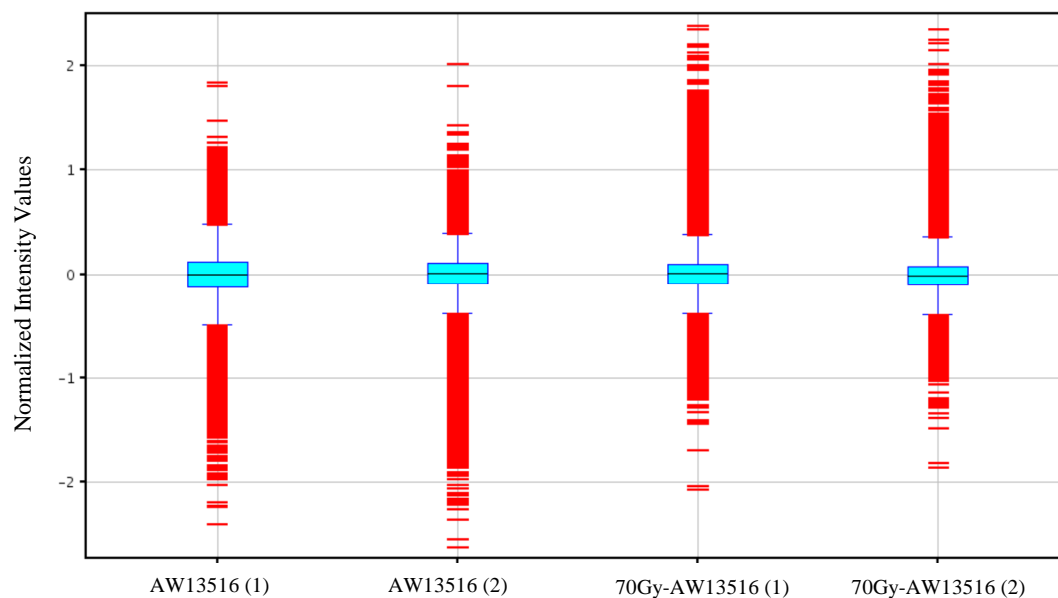
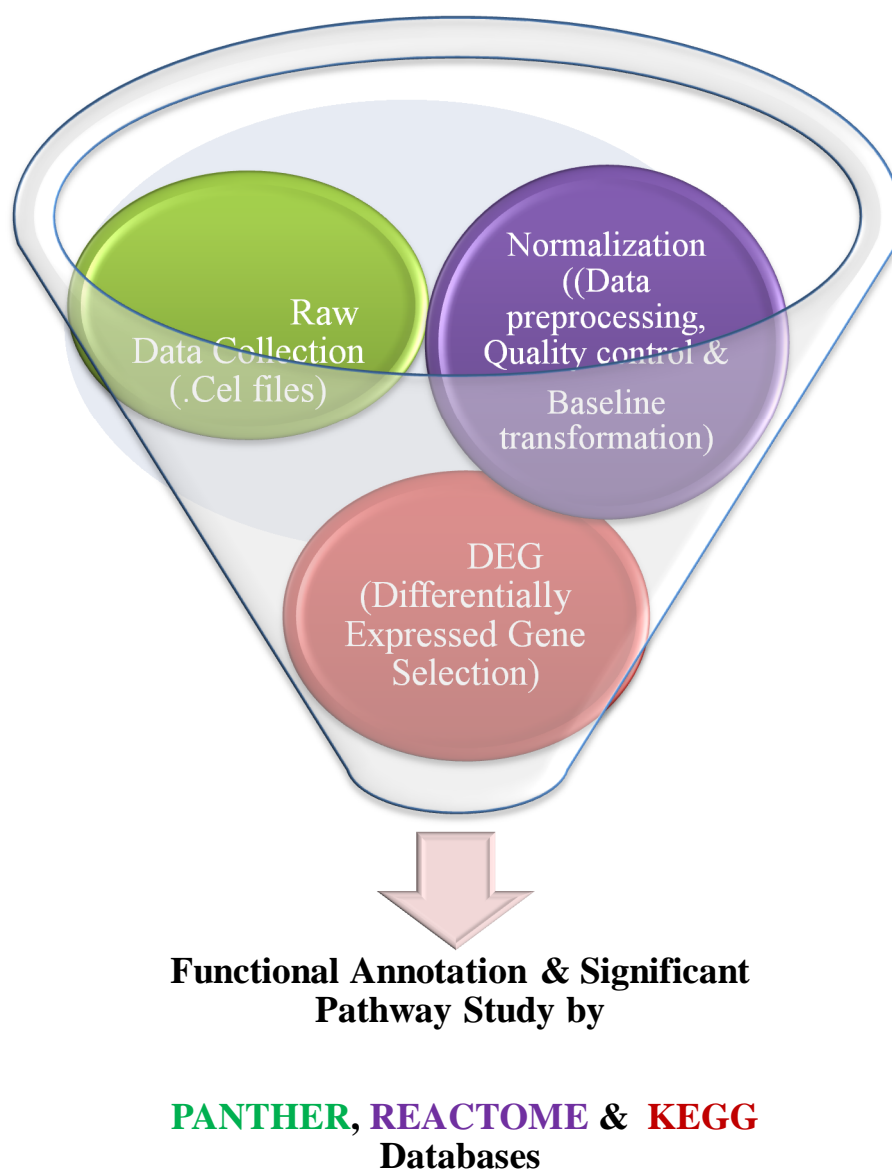


Figure 10: Box whisker plot for Parental AW13516 and Radioresistant 70Gy-AW13516 cells in two technical replicates. The data is RMA Normalized and aligns well with the baseline to median.

Hierarchical Clustering (HCL): Hierarchical clustering is one of the simplest and widely used unsupervised clustering techniques for the analysis of gene expression data [226]. The method follows an agglomerative approach, where the most similar expression profiles are joined together to form a group. These profiles are further joined in a tree structure, until all data forms a single group. The dendrogram is the most intuitive view of the results of this clustering method and linkage rule is important parameter, which control the order of merging entities and sub-clusters in the dendrogram. After two most similar entities (clusters) are clubbed together, this group is treated as a single entity.

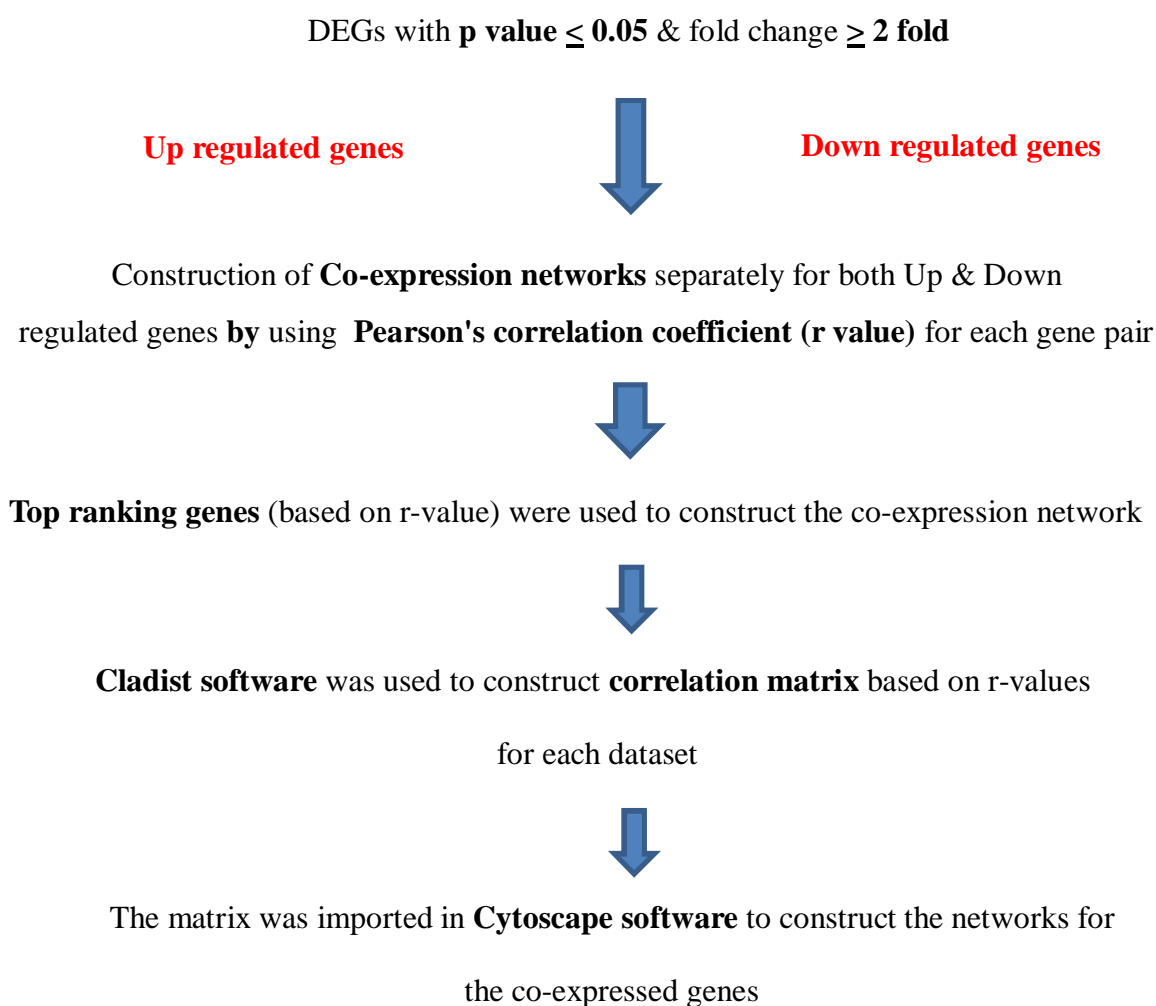
In the current work, HCL (average linkage) has been performed to explore the co-expression or co-regulation of genes in two groups. Only the genes expressed more than two fold change were processed for the cluster analysis and the HCL expression image represents in the form of dendrogram. The expression image tree further characterizes on the basis of color. The red color shows over expression, blue color- under expression and yellow color- normal expression of genes in respective radioresistant cells as compared to parental cells. In condition tree, the experiment having similar type of expression (replicates) profile are clustered adjacent in the tree and also, the genes having similar type of expression profile are clustered adjacent or at same tree node.

4.2.23 Schematic work flow for Microarray analysis:



4.2.24 Network Analysis for the differentially expressed genes

In order to understand the metabolic pathways that may be associated with the cellular radioresistance, the functional network analysis was carried out with the differentially expressed genes identified in the microarray experiment. The computational part of this work is carried out by Biocos life sciences Pvt. Ltd (Bangalore). The work flow for generating the network is as follows:



4.2.25 Statistical Analysis

The data were statistically analysed by student's t-test and one-way ANOVA, using Graph pad prism 5 software (version 5.01) and represented as mean values independently from three experiments with \pm standard deviation. A p value of less than 0.05 was considered statistically significant. The statistical analysis used for Raman spectral processing and microarray are described under their respective sections.

Chapter 5

RESULTS

5.1 To Generate Radioresistant sublines by Fractionated ionizing radiation from parental oral cancer cell lines and assess their Radiosensitivity by clonogenic cell survival assay

5.1.1 Establishment of Radioresistant sublines

Three Radioresistant sublines namely 70Gy-AW13516, 70Gy-UPCI:SCC029B & 70Gy-AW8507 were successfully established from their parental AW13516 (Tongue SCC), UPCI:SCC029B (Buccal SCC) & AW8507 (Tongue SCC) cell lines of different oral sub sites. Each of these radioresistant sublines were developed by clinically admissible, low dose fractionated ionizing radiation (FIR) of 2Gy i.e 70Gy radiation was delivered in 35 fractions of 2Gy in a span of 3-4 months (the resulting radioresistant sublines were named as 70Gy-AW13516/UPCI:SCC029B/AW8507). The parental cells were cultured simultaneously without giving any radiation treatment. The method for establishing these radioresistant sub lines was described in section 4.2.3, while the Radiation schedule for the establishment of radioresistant sublines is detailed in appendix 1.

5.1.2 Assessment of established Radioresistant character in all the three sublines

After the establishment, the radioresistant characters of all the radioresistant sublines were assessed by standard clonogenic cell survival assay [86] (material and method section 4.2.4) by treating them with increasing doses of ionizing radiation along with their respective parental cells. The dose response curve for the parental and radioresistant cells were plotted from the surviving colonies and D_0 values were calculated (Figure 11, 12 & 13). The D_0 value is the dose at which 37% cell population survives and is used for comparing the cell radiosensitivity in clonogenic survival assay. An increase in D_0 value was observed for all

the established radioresistant sublines compared to their parental cell lines, this signifies their acquired radioresistant character.

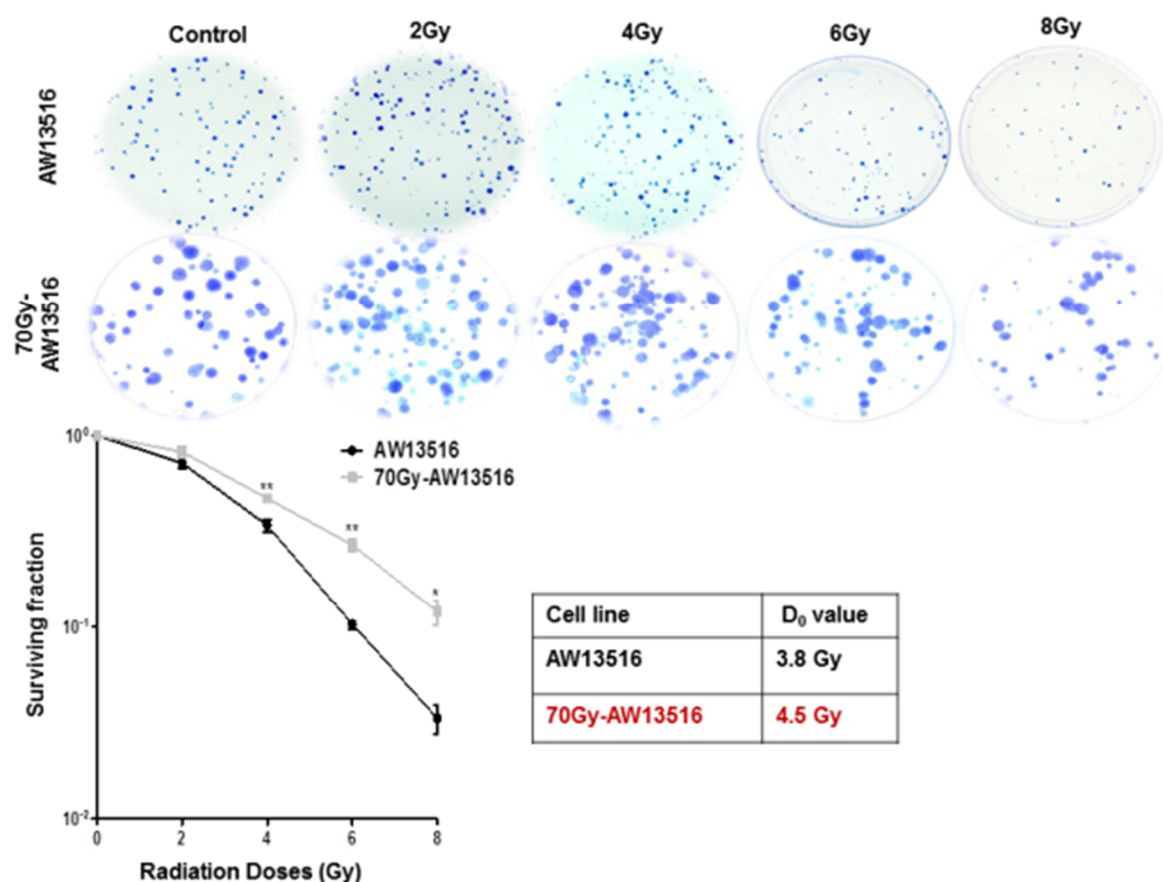


Figure 11: Log-linear clonogenic cell survival curve for AW13516 parental cells and radioresistant 70Gy-AW13516 cells with the calculated D_0 values. Data is represented as percentage survival of cells with mean (\pm SD) of three independent experiments. Student t-test was performed on surviving fractions at the given doses (p, 0.05 & 0.01).

The calculated D_0 values from the respective dose response curve were as follows: Parental AW13516 = 3.8Gy, Radioresistant 70Gy-AW13516 = 4.5Gy (Figure 11); Parental UPCI:SCC029B = 4.5Gy, Radioresistant 70Gy-UPCI:SCC029B = 5.6Gy (Figure 12) and Parental AW8507 = 5Gy, Radioresistant 70Gy-AW8507 = 5.5Gy (Figure 13).

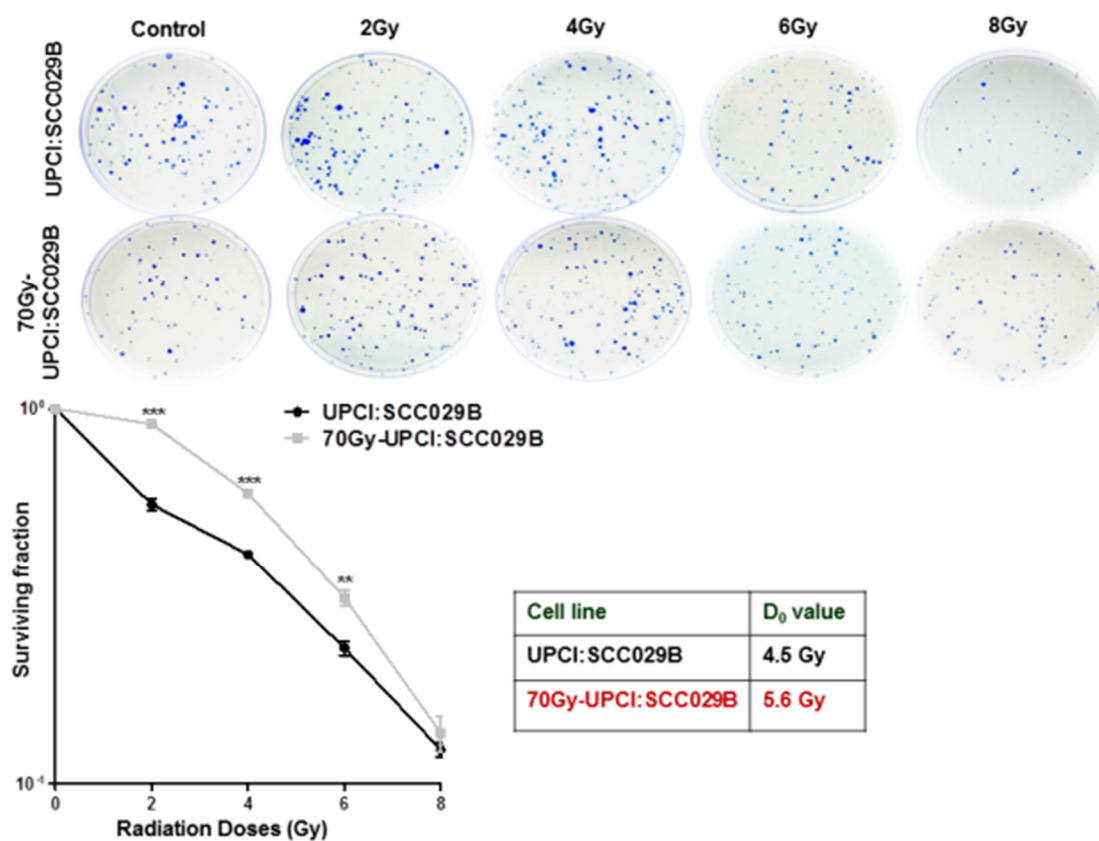


Figure 12: Cell survival curve for UPCI:SCC029B parental cells and 70Gy-UPCI:SCC029B radioresistant cells.

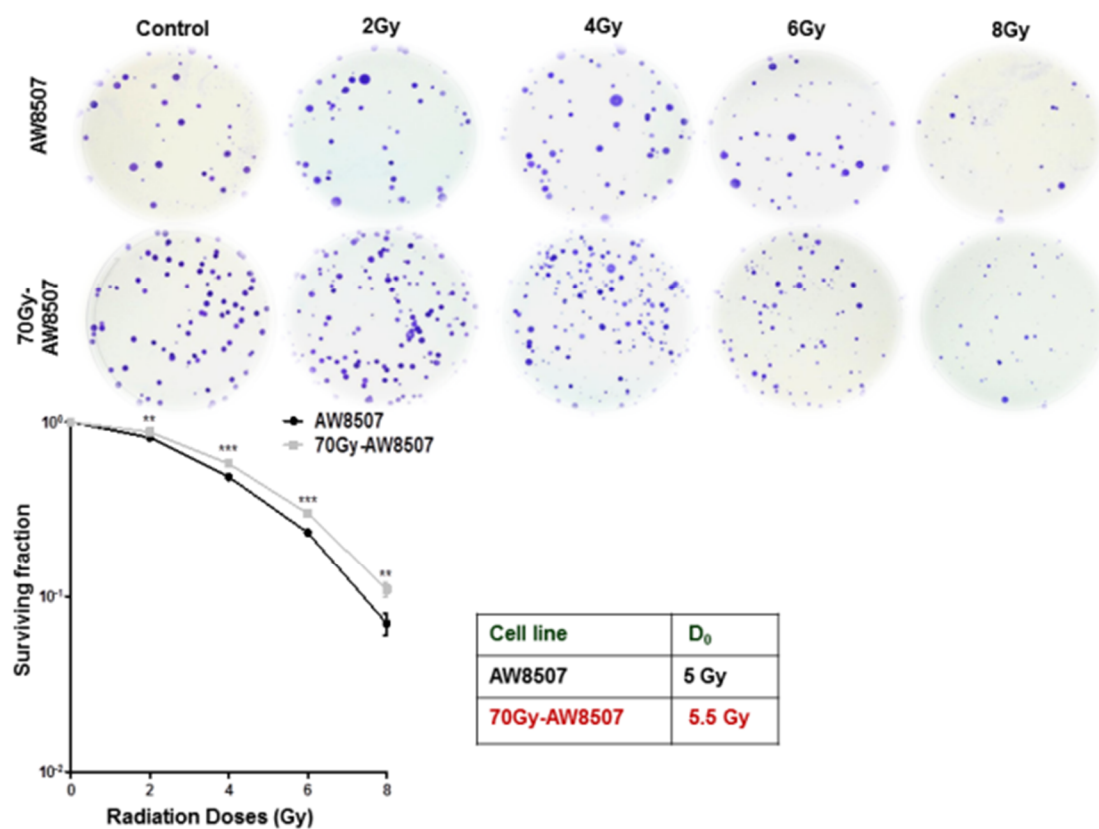


Figure 13: Cell survival curve for AW8507 parental cells and radioresistant 70Gy-AW8507 cells. Data is represented as percentage survival of cells with mean (\pm SD) of three independent experiments (p, 0.01 & 0.001).

The assay was performed independently three times in duplicates for each of the parental & radioresistant cells. The formula for calculating surviving fractions at 2, 4, 6 and 8 Gy of IR doses and D_0 values were described in section 4.2.4.

5.1.3 Status of Radioresistance related proteins in Established radioresistant sublines

The status for some of the known radioresistance related proteins like Mcl-1 (Myeloid cell leukemia-1), Bcl-2 (B cell lymphoma-2), Bcl-xl (B cell lymphoma extra-large), Cox-2 (Cyclooxygenase-2), Beta-1 Integrin, NF-kB and Survivin were accessed by western blotting in all the three radioresistant sublines with respect to their parental cell lines.

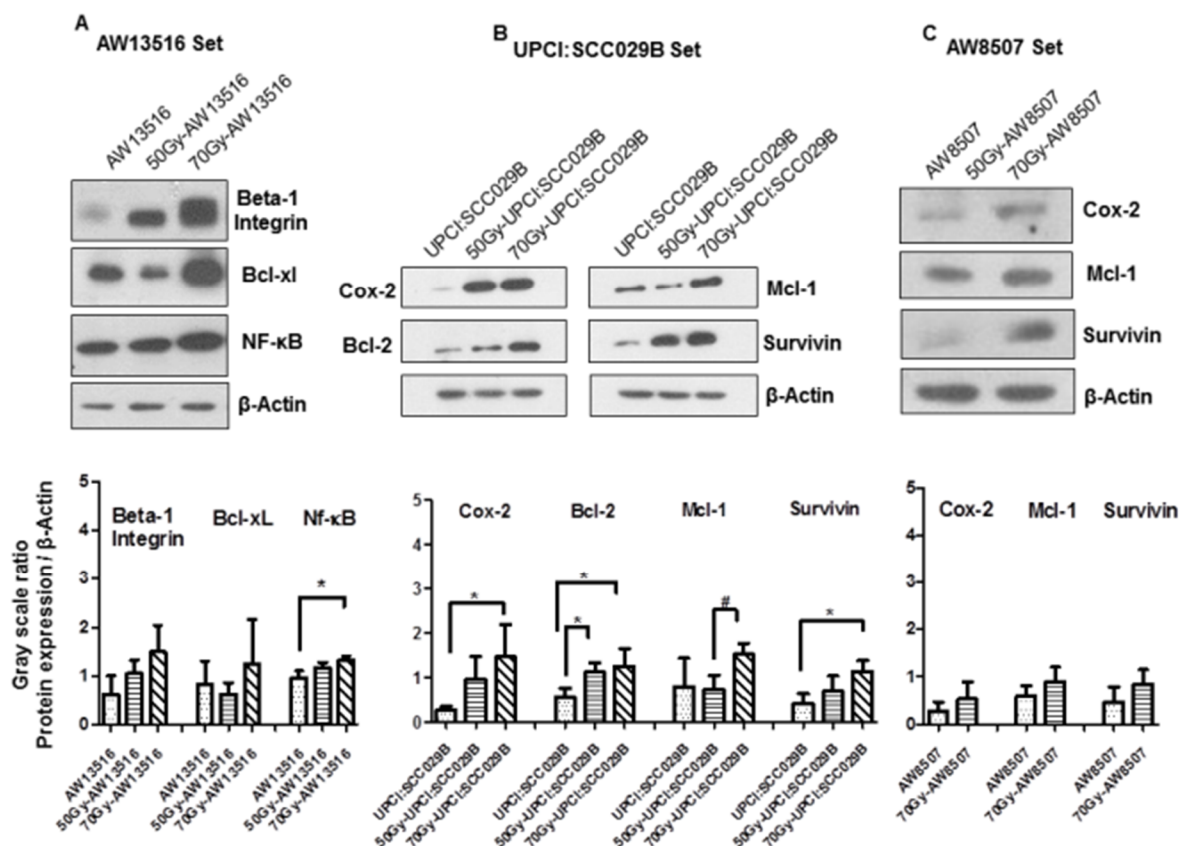


Figure 14: Expression of radioresistance related proteins in the established radioresistant sublines. Western blotting for Cox-2, Bcl-2, Bcl-xl, Mcl-1, Beta-1 Integrin, NfκB and Survivin. (A) AW13516 set (B) UPCI:SCC029B set (C) AW8507 set. β-Actin is used as loading control. Densitometry analysis of western blots from three separate experiments are represented below; bars represent- mean \pm s.d. * Represent protein expression compared to parental cell line, while # represent protein expression compared between 50Gy-UPCI:SCC029B and 70Gy-UPCI:SCC029B sublines (p,0.05).

These proteins are reported to be linked with radioresistance related studies in different cancer types (discussed in section 2.8). Expression of these proteins were assessed in all the three radioresistant sublines and depicted in Figure 14. The 50Gy-AW13516 and 50Gy-UPCI:SCC029B are the intermediate radioresistant cells (that receives 25 fractions of 2Gy). Since, the radiotherapy protocols for oral cancer treatment consist of a total 50Gy to 70Gy radiation dose by fractionated radiation of 2Gy. Therefore, status of some of these proteins was also accessed in 50Gy radioresistant sublines.

As illustrated in Figure 14, the protein levels of the respective radioresistance related proteins were found to be upregulated in radioresistant sublines (except Bcl-xl & Mcl-1 in 50Gy-AW13516 and 50Gy-UPCI:SCC029B) compared to the parental cell lines. The reason could be that Bcl-xl, Mcl-1 are the anti-apoptotic members of Bcl-2 protein family and plays a central part in control of apoptosis [227], the relative equilibrium between the pro- & anti-apoptotic proteins may influence the susceptibility of cells to apoptosis. Also, both these proteins have a short half-life due to its rapid turnover through ubiquitination [228,229]. Our result possibly implies, since the level of both these proteins were further upregulated in final 70Gy radioresistant cells. Thus, possibly the other proteins mentioned in the respective figure may contribute to the increased survival for radioresistant cells at early stages of acquired

radioresistance development while Bcl-xl and Mcl-1 may have a role in later stages, as development of radioresistance is a complex phenomenon and cannot be associated with a single protein.

5.2 To study the differential proteomic profile between Parental oral cancer cell lines versus Radioresistant sublines by 2-D gel electrophoresis and identify the same by MALDI analysis

5.2.1 Differential Proteomic profiling of Parental and Radioresistant cells by Two-dimensional Gel electrophoresis (2D)

After establishing the radioresistant sublines, their proteomic profiling was carried out by 2D gel electrophoresis.

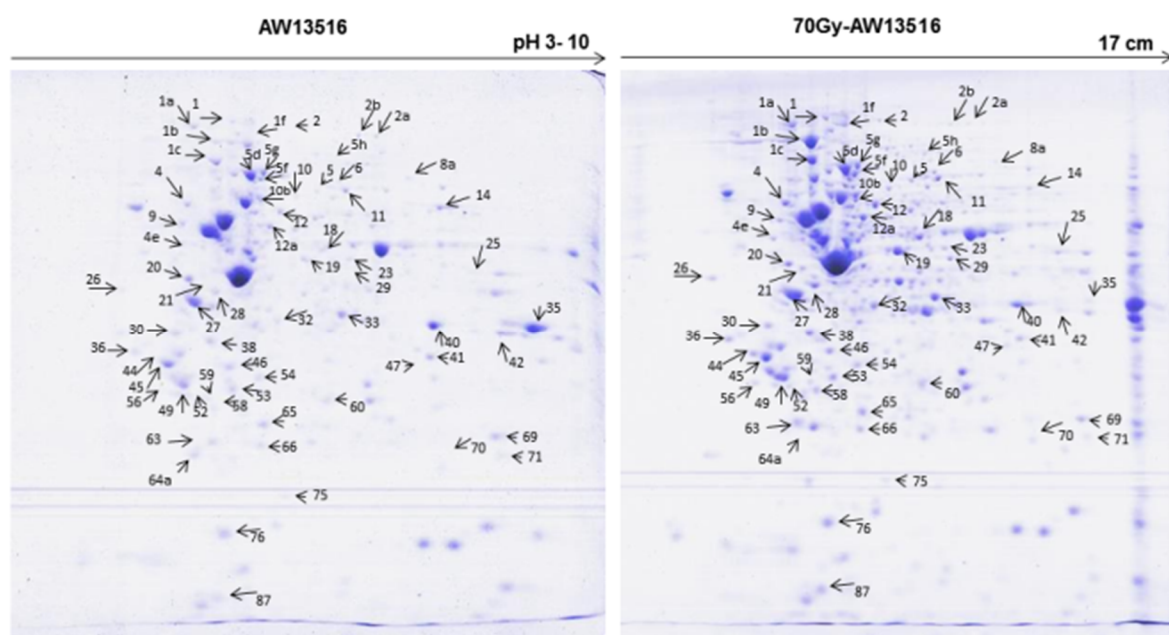


Figure 15: Representative coomassie stained 2D gels for parental AW13516 & radioresistant 70Gy-AW13516 cells. Run on a 17 cm, pH 3–10 IPG strip with a 12% SDS-PAGE in the second dimension.

Briefly 600 µg of protein for each of the parental and radioresistant cells were focused on a 17 cm, pH 3-10 IPG strip, followed by separation in second dimension. The protein spots were fixed and visualized by coomassie staining.

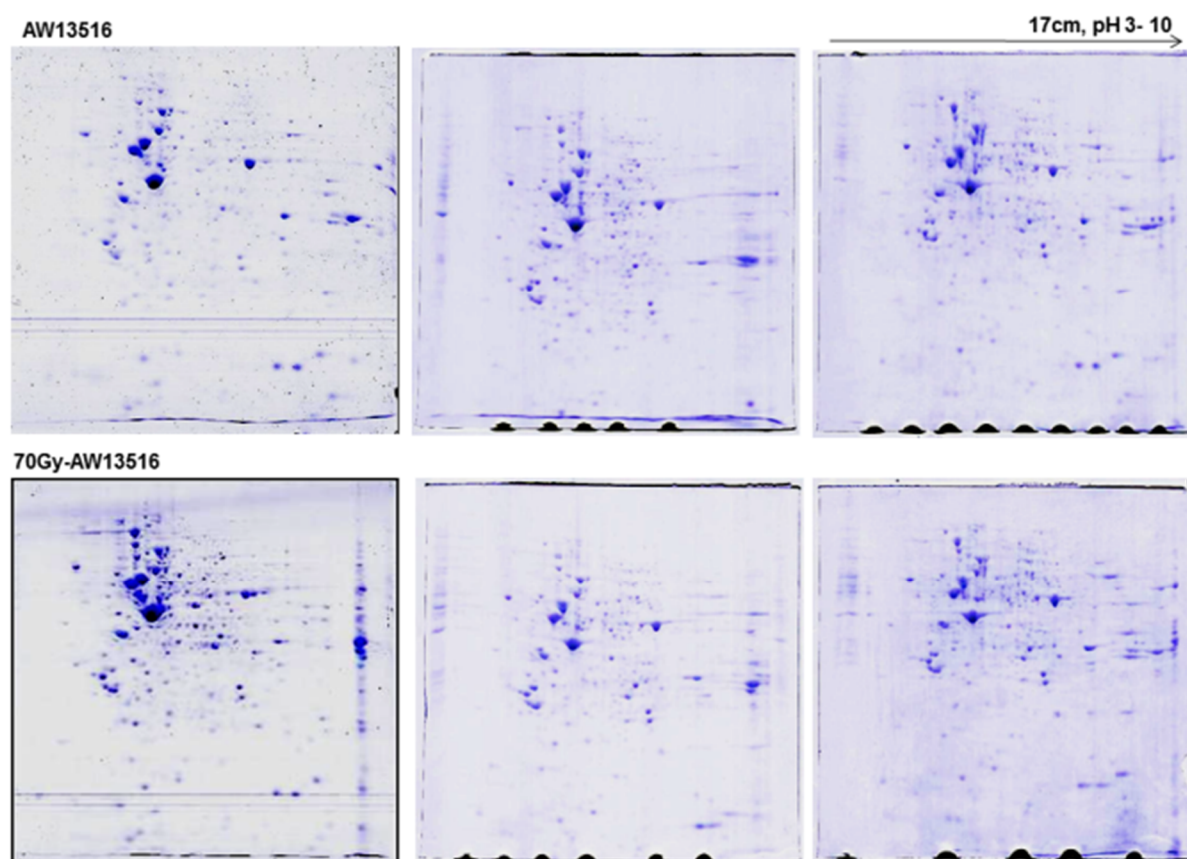


Figure 16: Technical replicate 2D gels for parental AW13516 & radioresistant 70Gy-AW13516. Each set of parental and radioresistant gels were run simultaneously with 17cm, pH 3-10 IPG strip.

Figures 15, 17 & 19 are representing coomassie stained 2D gels for the three parental and the established radioresistant cells and Figure 16, 18 & 20 are representing technical replicate gels for each of them. The 2D gels for each set of parental and radioresistant cells were run, fixed and stained in three technical replicates. The protein lysate preparation, quantification, cleaning, IEF focusing and process of 2D gel electrophoresis are described in section 4.2.6.

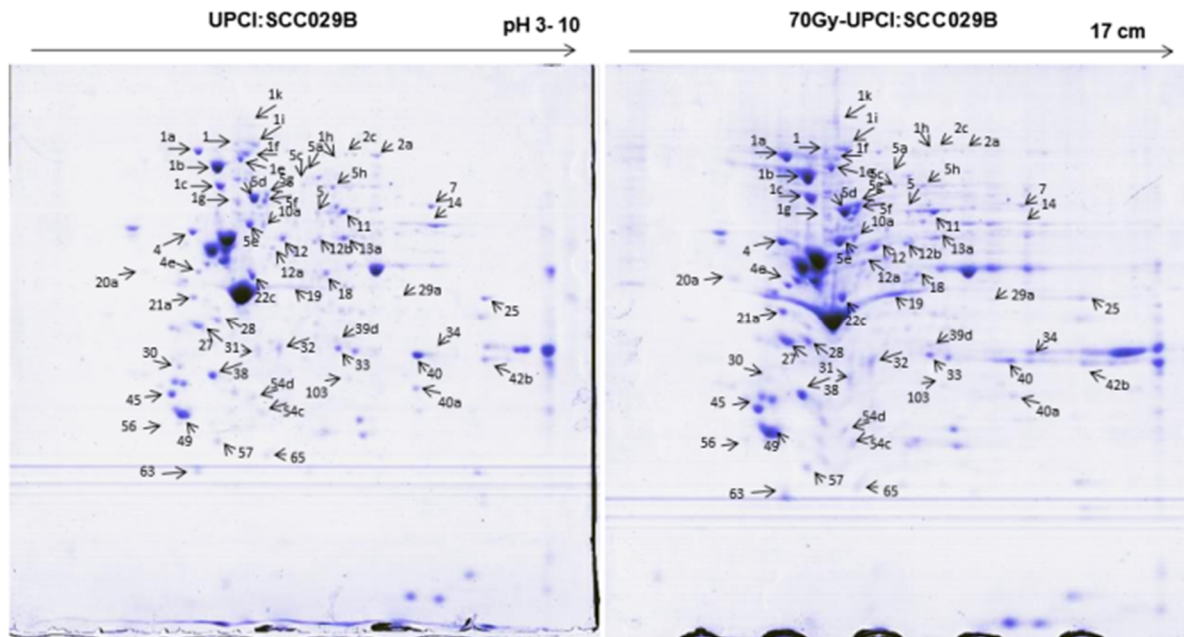


Figure 17: Coomassie stained 2D gels for parental UPCI:SCC029B & radioresistant 70Gy-UPCI:SCC029B cells.

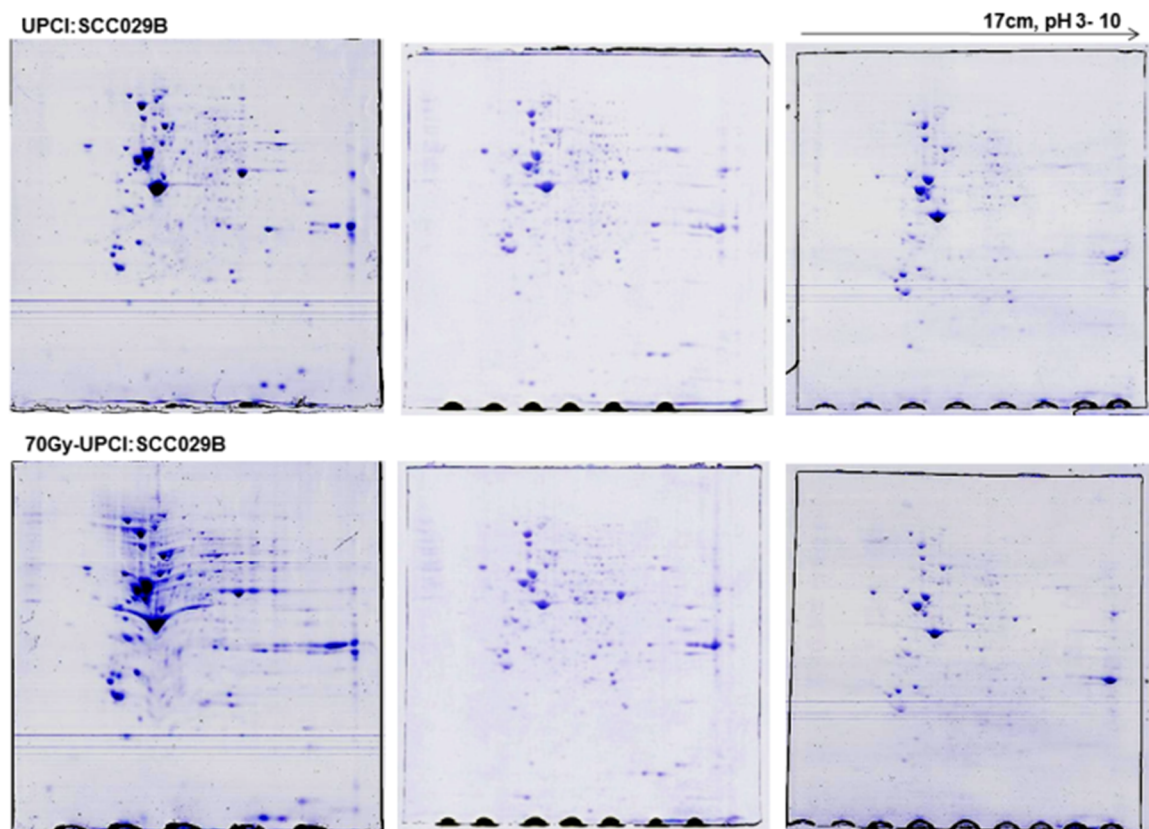


Figure 18: Technical replicate gels for UPCI:SCC029B & 70Gy-UPCI:SCC029B. The gels were run on a 17 cm, pH 3–10 IPG strip on Bio Rad Xi apparatus.

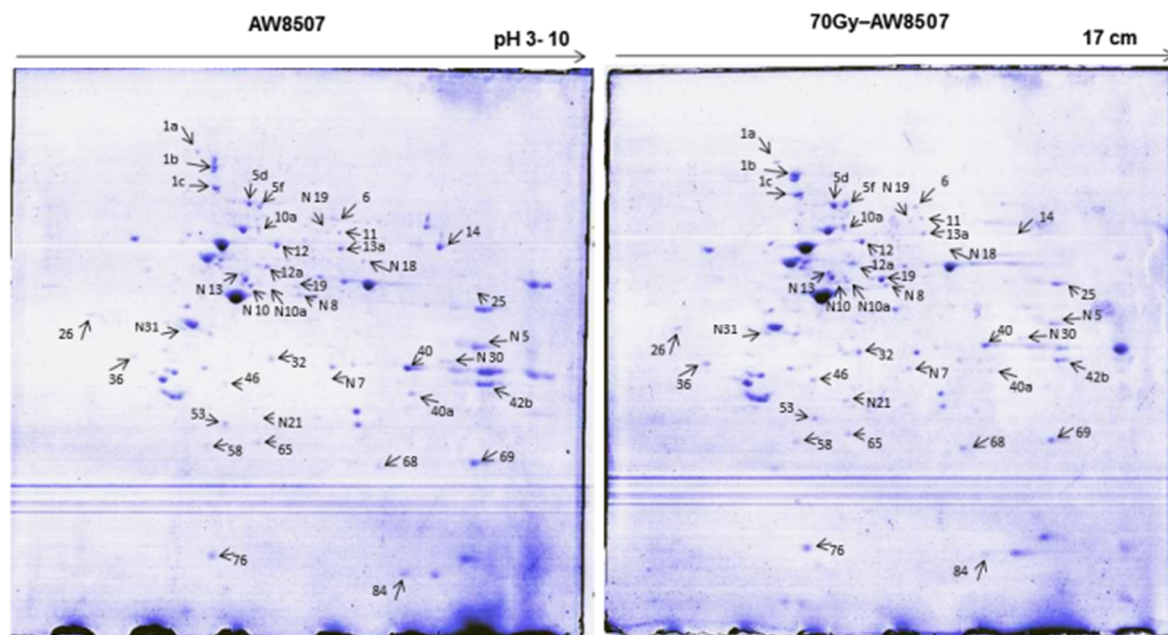


Figure 19: Coomassie stained 2D gels for the third set of parental AW8507 & radioresistant 70Gy-AW8507 cells.

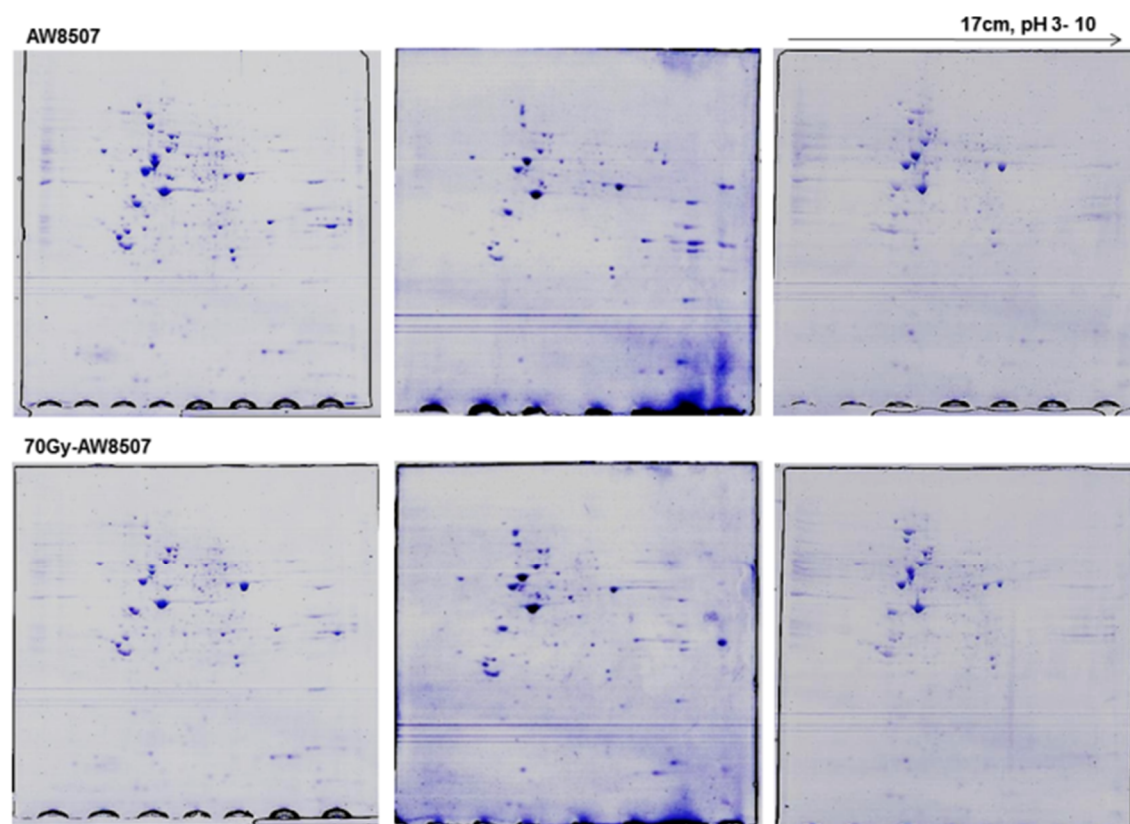


Figure 20: Technical replicate 2D gels for AW8507 & 70Gy-AW8507 cells.

5.2.2 Analysis of 2D Gels by PD-Quest Gel analysis software

All the 18 gels of 2D in technical replicates for the three set of parental and radioresistant cells (6 gel per set of parental & radioresistant) were scanned on GS-800 calibrated gel densitometer on auto-scale mode and proceed for the analysis. On these technical replicates of each set, standard analysis was carried out by PD Quest 2D gel analysis software (Bio-Rad) as per manufacturer's instructions.

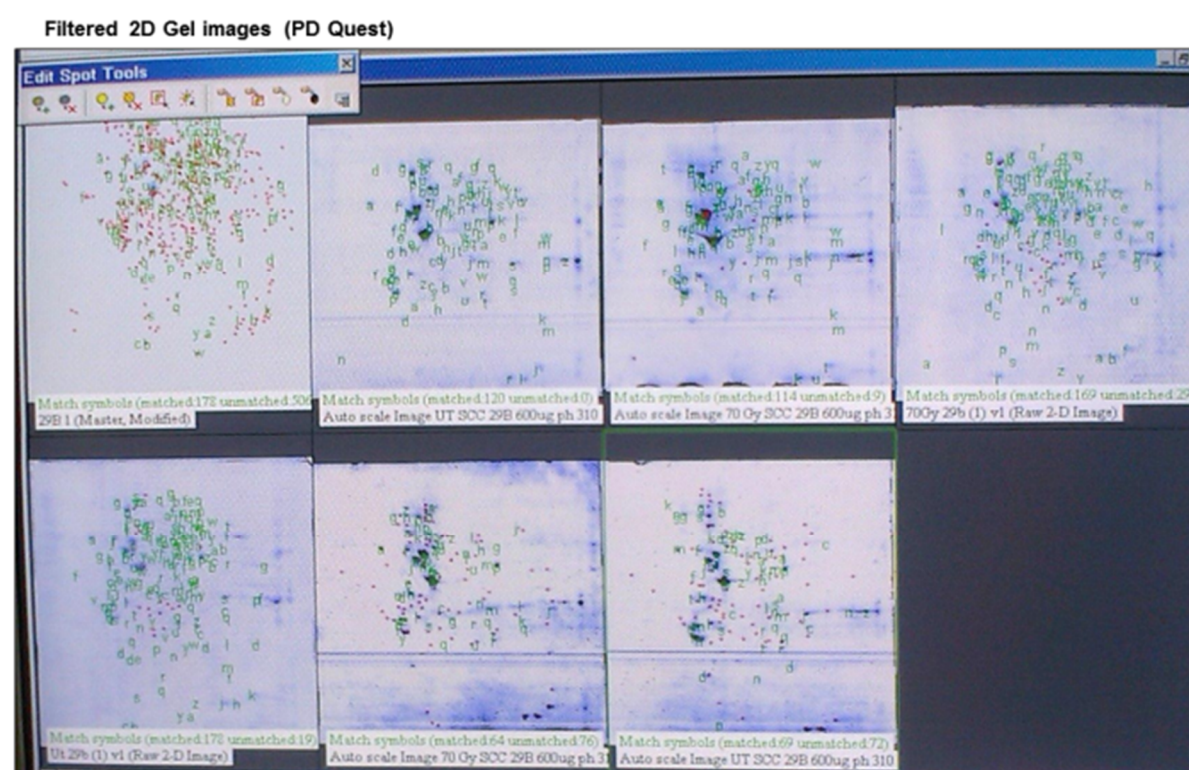


Figure 21: Representative filtered 2D gel image processed by PD-Quest. The parental and radioresistant gels of all the three established sublines were analysed by the same approach (as described above) and the normalized quantities of the spots were assessed.

Separately, the parental and radioresistant set of gels were grouped and Match Sets were created. Gels were then normalized by selecting the normalization by total quantity in valid

spots method in the software. After the normalization, the automatic spot detection and matching wizard of the software were initiated and after selecting a small, faint and large protein spot in the constituent gel of the match set; the software convert each member gel of the match set into three images i.e original scanned image, filtered image (gel image cleared out of streaks) and Gaussian image (hypothetical image made by the software for selecting and quantitating gel spots). Figure 21, show the representative filtered 2D gel image with cross marked spots identified by the software. The software then automatically select the Master Gel among the constituent gel of the Match Set and cross mark the identified spots in all the gels of the Match Set. After reviewing and adding the left out spots to the master gel, the normalized quantities of spots were displayed in each member gel of the Match Set for quantification.

5.2.3 Identification of Differentially expressed proteins by MALDI-TOF/TOF

The differentially expressed spots were excised from the gels and processed for Mass spectrometry based identification. Trypsin digestion of protein in gel plugs, extraction and reconstitution for MALDI analysis is described in section 4.2.8. Table 17, enlisted the 102 differentially expressed proteins identified by MALDI-TOF/TOF with their MS and MS/MS scores. The complete catalogue for these 102 proteins in standard format, including protein accession number, molecular weight, PI, intensity coverage, sequence coverage, searched peaks, matched peaks, tolerance (MS-MS/MS) and peptides identified are described in appendix 4, whereas MS spectra of all the identified proteins are represented in appendix 3.

Table 17: List of 102 differentially expressed proteins identified by MALDI-TOF/TOF with their MS and MS/MS scores (MS score ≥ 55 is significant as determined by the software).

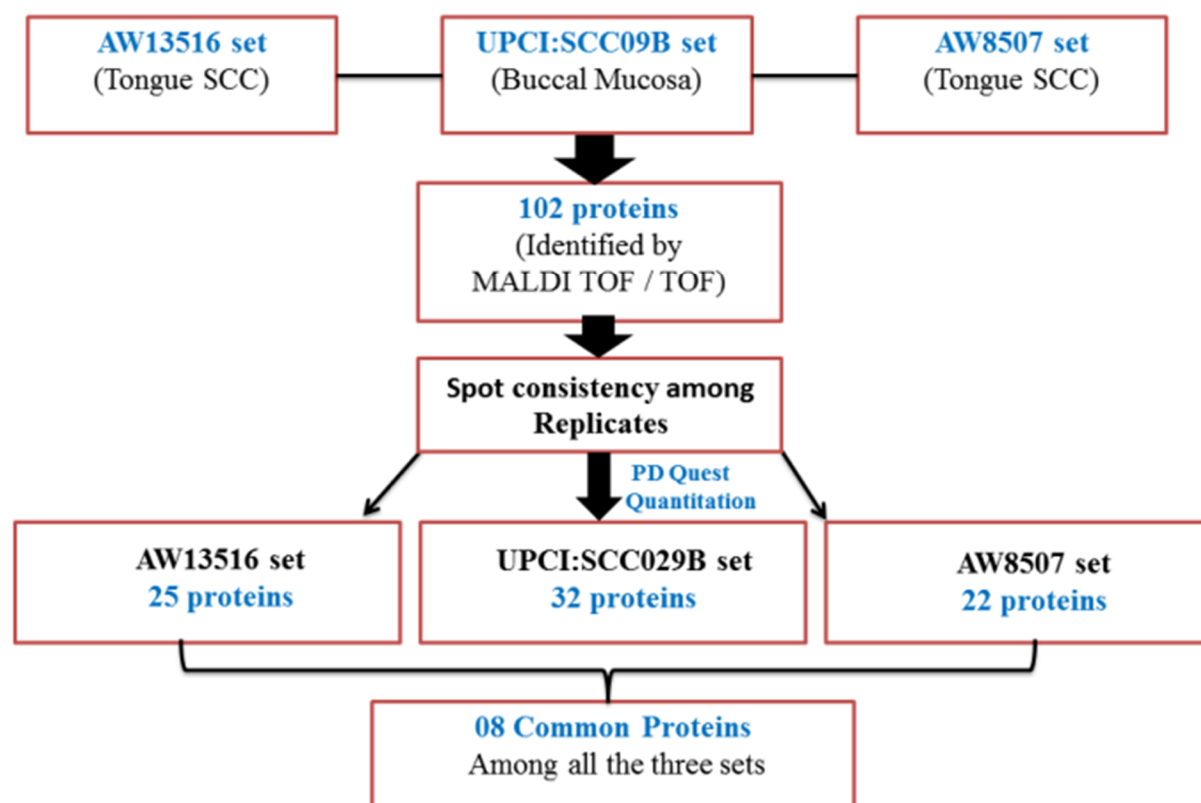
Spot	Protein name	Score MS / MS-MS	Spot	Protein name	Score MS / MS-MS
39d	Heterogeneous nuclear ribonucleo protein H3	161/144	22c	Eukaryotic initiation factor 4A-I	173/267
84	Peptidyl prolyl cis-trans isomerase A	59/69	32	Phosphatidylinositol transfer protein beta isoform	32.4/39.2
57	Rho GDP-dissociation inhibitor 1	46/28	54d	Proteasome activator complex subunit 2	58.6/98.7
34	Pyrroline-5-carboxylate reductase 3	39.3/49.2	2a	Elongation factor 2	71.3/217
56	Eukaryotic translation initiation factor 6	58.5/225	7	Transketolase	123/118
20	40S ribosomal protein SA	105/136	35	Glyceraldehyde-3-phosphate dehydrogenase	55.5/65.1
69	Peroxiredoxin-1	104/246	52	Ubiquitin carboxyl-terminal hydrolase isozyme L3	93/105
33	Annexin A1	185/309	56	Eukaryotic translation initiation factor 6	62.3/69.2
2	Neutral alpha-glucosidase AB	77/77	59	Calpain small subunit 1	148/164
75	Nucleoside diphosphate kinase A	154/189	60	Peroxiredoxin-6	107/127
9	Histone-binding protein RBBP4	77.6/102	47	Proteasome subunit alpha type-4	60.8/112
41	Guanine nucleotide-binding protein subunit beta-2-like 1	159/234	66	Peroxiredoxin-2	60.1/60.1
71	Transgelin-2	90.7/123	5a	Mitochondrial inner membrane protein	63.8/74.4
53	Ran specific GTPase activating protein	60/60	5c	Glycine-tRNA ligase	76.3/69.3
1	Heat shock 70 kDa protein 4	172 / 279	5g	Stress-70 protein mitochondrial	170 / 335
1k	Hypoxia up-regulated protein 1	66.5/84.6	5h	Moesin	74 / 134
1a	Endoplasmic reticulum chaperone	114 / 483	6	WD repeat containing protein 1	191 / 254
1b	Heat shock protein 90 Alpha	158 / 489	8a	Far upstream element binding protein-1	72 / 74
1c	GRP78	200 / 658	10	TCP-1 subunit alpha	119 / 123
1e	TERA	210 / 258	10a	TCP-1 subunit epsilon	70/101
1f	Alpha Actinin 4	204 / 302	10b	TCP-1 subunit theta	161 / 258
1i	Alanine-tRNA ligase	65 / 64	11	Stress induced phosphoprotein-1	135 / 181
1g	Plastin-2	151 / 125	12	PDI-A3	132 / 226
40	Annexin A2	231/268	12a	Keratin, type 2 cytoskeletal 8	146 / 256

Results

2c	Cytoplasmic aconitate hydratase	188 / 193	14	Pyruvate kinase isozyme M1/M2	254 / 295
4	Protein disulfide isomerase	125 / 302	18	EF-1 Gamma	85 / 180
4e	Vimentin	278 / 472	20a	Calumenin	79 / 69
5	TCP-1 gamma	100 / 116	21	Spermine synthase	76 / 93
5e	HSP 60	96 / 334	23	Elongation factor Tu, mitochondrial	106 / 150
5f	Heat shock 70kDa protein 1A/1B	65 / 115	25	Phospho glycerate kinase 1	90 / 86
27	Nucleophosmin	50 / 196	30	PCNA	116 / 115
28	STRAP	72 / 83	38	Annexin A5	124 / 140
12b	T-complex protein 1 subunit beta	135/152	26	SET Protein	90/85
65	Glutathione S-transferase P	80.9/151	5d	Heat Shock Cognate 71kDa Protein	158/241
29a	26S protease regulatory subunit 10B	95.4/123	19	Phosphoglycolate phosphatase	56/41
31	F-actin-capping protein subunit alpha-1	70.6/85.1	36	Complement Component 1Q sub component binding protein, Mitochondrial	66/123
40a	GNBP subunit beta-2-like 1	68 / 81	58	Rho GDP dissociation Inhibitor 1	58/58
42	HnRp A2/B1	69 / 74	76	Eukaryotic Translation initiation Factor 5A-1	74.5/77.7
44	CdK2 interacting protein	28 / 60	N 10	K 18	81/70
45	14-3-3 protein epsilon	87 / 156	13a	G6PD	264/312
49	14-3-3 protein beta/alpha	132 / 194	N 18	Fascin	262/282
54	Prohibitin	201 / 262	N 30	Aldo Keto reductase family 1 member C 1	101/96
64a	ATP synthase subunit d, mitochondrial	64 / 65	42 b	L-lactate Dehydrogenase A chain	100/90
63	TCTP	60 / 56	N 19	Ran binding Protein 3	67/64
70	PEB protein-1	69 / 83	N 5	Fructose biphosphate aldolase A	112/102
87	Galectin-1	117 / 184	N 13	HnRp F	90/113
103	S-formyl glutathione hydrolase	134 / 159	N 7	Proteasome subunit Alpha Type 1	50/45
N 8	Adenosyl Homocysteinase	95/110	46	Chloride Intra Cellular Channel protein 1	101/138
N 31	Hepatoma derived growth factor	40/39	1h	Src substrate cortactin	89.4/284
N 21	Casein Kinase 2 subunit Beta	60/60	N 10a	Cytochrome bc1 Complex subunit 1	70.5/73.3
21a	40S ribosomal protein SA	170/196	68	GTP binding nuclear protein RAN	58/57

5.2.4 Schematic representation for the MALDI identified proteins

In total, 102 proteins were identified by MALDI-TOF/TOF in the three set of parental and radioresistant cells of different oral subsites. These proteins were further reviewed on the basis of their corresponding 2D spot consistencies among their respective replicate gels for each set and are shown schematically in the following Flow chart 2.



Flow chart 2: Schematic representation for the MALDI identified proteins in all the three set of parental and radioresistant cells.

5.2.5 Differentially expressed proteins in each parental and radioresistant set of cells

As mentioned in the Flow chart 2, the differentially expressed proteins were reviewed for each set of the parental and radioresistant cells and only those proteins whose corresponding spot show consistency among their technical replicates were included. These proteins were

categorically represented with their corresponding fold change values, determined by PD Quest in Tables 18, 19 & 20.

Table 18: Differentially expressed proteins identified by MALDI analysis in AW13516 / 70Gy-AW13516 with their MS/MS-MS score, Mw/ pI, Sequence Coverage (%) and fold change values. (D) Symbolize down regulated proteins. **Note:** the list is without 08 common proteins.

Spot	Protein name	Score MS/MS-MS	Mw / pI	Sequence Coverage (%)	Fold change (by PD Quest)
1b	HSP 90 alpha	158 / 489	85.005 / 4.8	34	2.0
6	WDP-1	191 / 254	66.83 / 6.2	64.2	2.64
8a	FUBP-1	72 / 74	67.689 / 7.8	22.7	1.83 (D)
10	TCP-1 Alpha	119 / 123	60.818 / 5.7	36.9	2.46
21	Spermine synthase	76 / 93	41.697 / 4.7	51.6	3.45
23	EF Tu	106 / 150	49.85 / 7.9	41.2	1.83
42	HnRp A2/B1	69 / 74	37.46 / 9.3	35.7	1.20
54	Prohibitin	201 / 262	29.842 / 5.5	69.1	1.88
87	Galectin-1	117 / 184	15 / 5.2	63.7	1.24
44	CdK2 IP	28 / 60	24.47 / 5.9	27.8	2.36
5h	Moesin	74 / 134	67.8 / 6	14	1.8
1g	Plastin-2	151 / 125	70.814 / 5.2	34.8	2.30
25	PGK-1	90 / 86	44.98 / 9.2	45.6	10.88
2a	EF-2	71.3 / 217	96.246 / 6.4	10.8	1.59
70	PEB-1	69 / 83	21.157 / 7.8	45.5	1.44
26	SET protein	90 / 108	33.4 / 4.1	29.7	1.22
10b	TCP-1 Theta	161 / 258	60.152 / 5.3	41.2	1.15

Table 19: Differentially expressed proteins identified by MALDI analysis in UPCI:SCC029B /UPCI:70Gy-SCC029B with their fold change values. (D) Symbolize down regulated proteins. **Note:** the list is without 08 common proteins.

Spot	Protein name	Score MS/MS-MS	Mw / pI	Sequence Coverage (%)	Fold change (by PD Quest)
1e	Transitional,ER ATPase	210 / 258	89.9 / 5	44.8	1.83
1i	Alanine-tRNA ligase	65 / 64	107.5 / 5.2	15	1.40
1k	Hypoxia URP 1	66 / 84	111.4 / 5	22.9	1.08
29a	26S protease 10B	95 / 123	44.4 / 7.8	36.2	1.40
54d	Proteasome act subunit 2	58 / 98	27.5 / 5.4	21.3	1.95
31	FACP Alpha 1	70 / 85	33 / 5.4	42.7	1.72
33	Annexin A1	75 / 156	38.9 / 6.7	27.5	1.09
2c	Cytoplasmic aconitate	188 / 193	98.849 / 6.2	34	1.87 (D)
103	S-formyl GH	134 / 159	31.955 / 6.6	52.5	1.27 (D)
56	ETI 6	58 / 225	27 / 4.4	44.1	1.34
57	Rho GDP- inhibitor 1	40 / 38	23.2 / 6.4	24.3	1.10
1h	Src cortactin	89 / 284	61.7 / 5.1	19.8	1.87
1g	Plastin-2	151 / 125	70.814 / 5.2	34.8	1.71 (D)
12b	TCP1 Beta	135 / 152	57.7 / 6	44.5	1.28
20a	Calumenin	79 / 69	37.197 / 4.3	27	3.46
7	Transketolase	123 / 118	68.5 / 8.5	19.6	1.52 (D)
5c	Glycine-tRNA ligase	76 / 69	83.8 / 6.7	14.5	1.04 (D)
5a	Mito Inner Membrane Pro	63 / 74	84 / 6.1	18.9	1.09
5e	HSP 60	96 / 334	61.187 / 5.6	38.2	1.69
21a	40S ribosomal protein SA	170 / 196	32.94 / 4.6	44.7	1.18
22c	EIF 4A-I	173 / 267	46.3 / 5.2	52.7	1.60

2a	EF 2	71.3 / 217	96.246 / 6.4	10.8	1.75 (D)
39d	HNRP H3	161 / 144	36.9 / 6.4	63.9	3.11 (D)
34	Pyrroline-5-carboxylate reductase 3	39 / 49	29.1 / 8.1	13.9	2.10

Table 20: Differentially expressed proteins identified by MALDI analysis in AW8507 / 70Gy-AW8507 with their fold change values. (D) Symbolize down regulated proteins. **Note:** the list is without 08 common proteins.

Spot	Protein name	Score MS/MS-MS	Mw / pI	Sequence Coverage (%)	Fold change (by PD Quest)
68	RAN GTP	57 / 58	24.5 / 7.8	34.7	1.02
84	Peptidyl cis-trans Isom A	68 / 101	18.2 / 9	44.2	1.42 (D)
69	Peroxiredoxin 1	74 / 74.5	22.3 / 9.2	43.7	1.01 (D)
N18	Fascin	262 / 282	55.1 / 7	66.1	3.09 (D)
N13	HnRp F	89 / 113	45.9 / 5.3	36.9	1.23
N19	RBP 3	66 / 64	60.5 / 4.6	19	1.74
N7	Proteasome α Type 1	50 / 45	29.8 / 6.2	30	1.85
6	WDP 1	191 / 254	66.83 / 6.2	64.2	1.82
N30	Aldo Keto reductase C 1	101 / 95	37.2 / 9	54.8	2.27 (D)
N8	Adenosyl Homocysteinase	94 / 110	48.2 / 5.9	29.9	1.30
N10a	Cytochrome bc1 subunit 1	70 / 73	53.2 / 5.9	41.7	1.58
N21	Casein Kinase 2 Beta	60 / 60	25.2 / 5.2	38.6	1.82
N5	Fructose biphosphate A	112 / 102	39.8 / 9.2	49.2	1.16 (D)
N31	HDGF (Hepatoma derived growth factor)	39 / 39	26.8 / 4.6	33.8	1.72

In summary, the two-dimensional gel electrophoresis followed by PD Quest Analysis revealed 102 differentially identified proteins among the 3 sets of parental and radioresistant

cells. Among them, on the basis of their corresponding spot consistency among replicate gels; 25 differentially expressed proteins were found in parental vs. 70Gy-AW13516, 32 in parental vs. 70Gy-UPCI:SCC029B and 22 in parental vs. 70Gy-AW8507 cells.

5.2.6 Validation of MALDI identified proteins by western blotting

In the next step, some of the MALDI identified proteins were validated by western blotting performed on the protein lysate of parental and radioresistant cells.

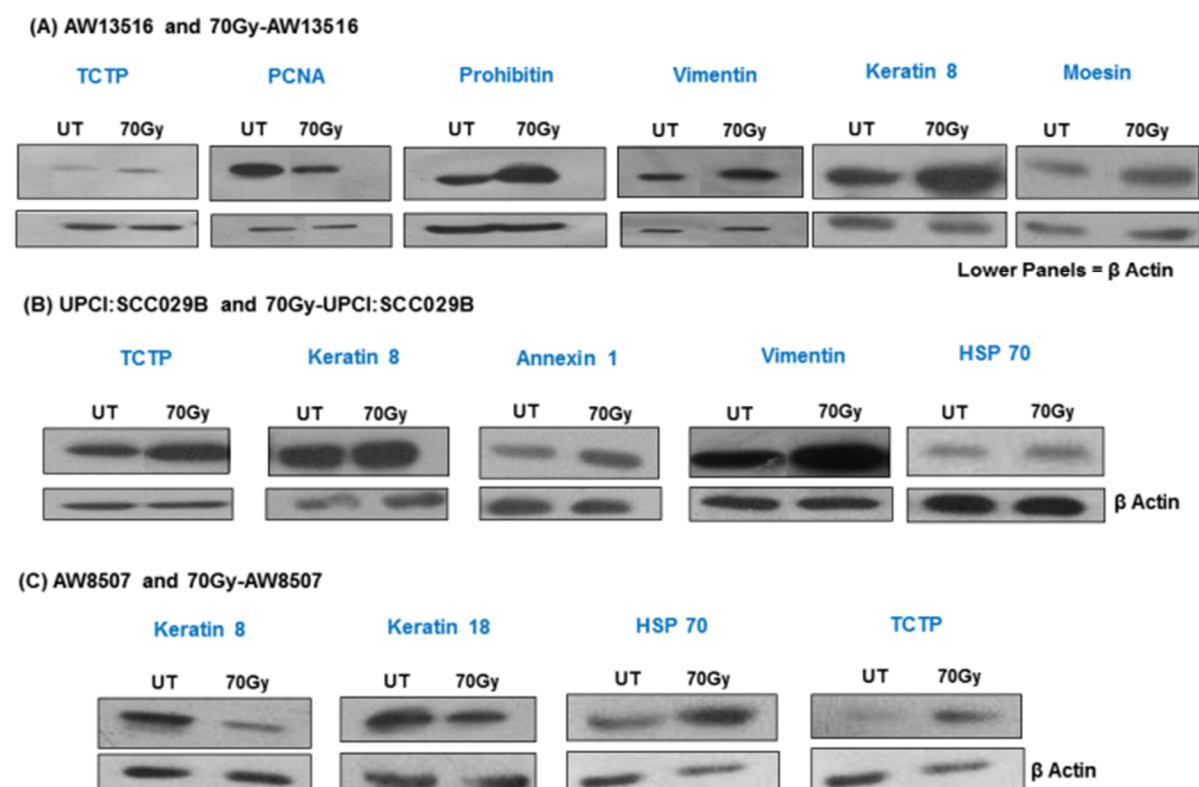


Figure 22: Validation for some of the 2-D identified proteins by western blotting. (A) AW13516 / 70Gy-AW13516 (B) SCC029B / 70Gy-UPCI:SCC029B (C) AW8507 / 70Gy-AW8507. The corresponding spot from 2D gel is shown in the lower panel of each set. β-Actin was used as loading control.

The Figure 22 illustrate western blots for TCTP, PCNA, Prohibitin, Vimentin, Keratin 8, Keratin 18, Moesin, Annexin 1 and HSP 70. The similar expression pattern revealed by western blotting for some of the 2D identified proteins thus signifies its validity.

5.2.7 Common MALDI identified proteins in all the three set of parental & radioresistant cells

Following proteins are found to be common differentially regulated among the three set of parental and radioresistant cells. These eight common proteins are enlisted with their fold change values in the following Table 21 with their known or proposed functions.

Table 21: List of common differentially expressed proteins identified in all the three set of parental and radioresistant cells with their fold change values. (D)= down regulated protein.

Spot	Protein name	Score MS/MS-MS	Mw / pI	Sequence Coverage (MS)	Fold change a) AW13516 set b) UPCI:SCC029B set c) AW8507 set	Known / Proposed Function
5d	HSP A8	158/241	71 / 5.2	41.8%	a)1.36 b)1.5 c) 2.13	Protein folding
19	PGP	56.6/41	34.4 / 5.8	27.4%	a)2.44 b)3.4 c)3.37	Phosphatase activity
1c	GRP 78	200 / 658	72.40 / 4.9	28.1%	a)1.7 b)1.41 c)1.3	ER homeostasis, Oncogenic survival
1a	GRP 94	114 / 483	92.696 / 4.6	24.7%	a)1.65 b)1.8 c)1.37	Processing & protein transport
12	PDI A3	132 / 226	57.145 / 5.9	35.2 %	a)1.4 b)1.6 c) 1.32	ER stress signalling (UPR)
14	PKI M1/M2	254 / 295	58.470 / 7.9	62.5%	a)3.5 b)3.24 c)1.43 (D)	Glycolytic enzyme
11	STIP 1	135 / 181	63.2 / 6.4	29.1%	a)2.26 b)1.55 c)1.9	Adapter protein for HSP-70 & 90
5f	HSC 70kDa 1A/1B	65 / 115	70.294 / 5.4	14.7%	a)1.7 b)1.4 c) 1.7	Protein stabilisation & folding

5.2.8 Validation of common identified proteins by western blotting

The MALDI identified common proteins from all the three set of parental and radioresistant cells were validated by western blotting. Figure 23 illustrates the western blots for STIP 1, PKI M 2, PGP, HSPA1B (HSC 70kDa 1A/1B), ERP57 (PDI A3), GRP 94 and HSPA 8 proteins. The GRP 78 protein does not show any difference in the protein levels in any of these three radioresistant cells compared to their respective parental cells.

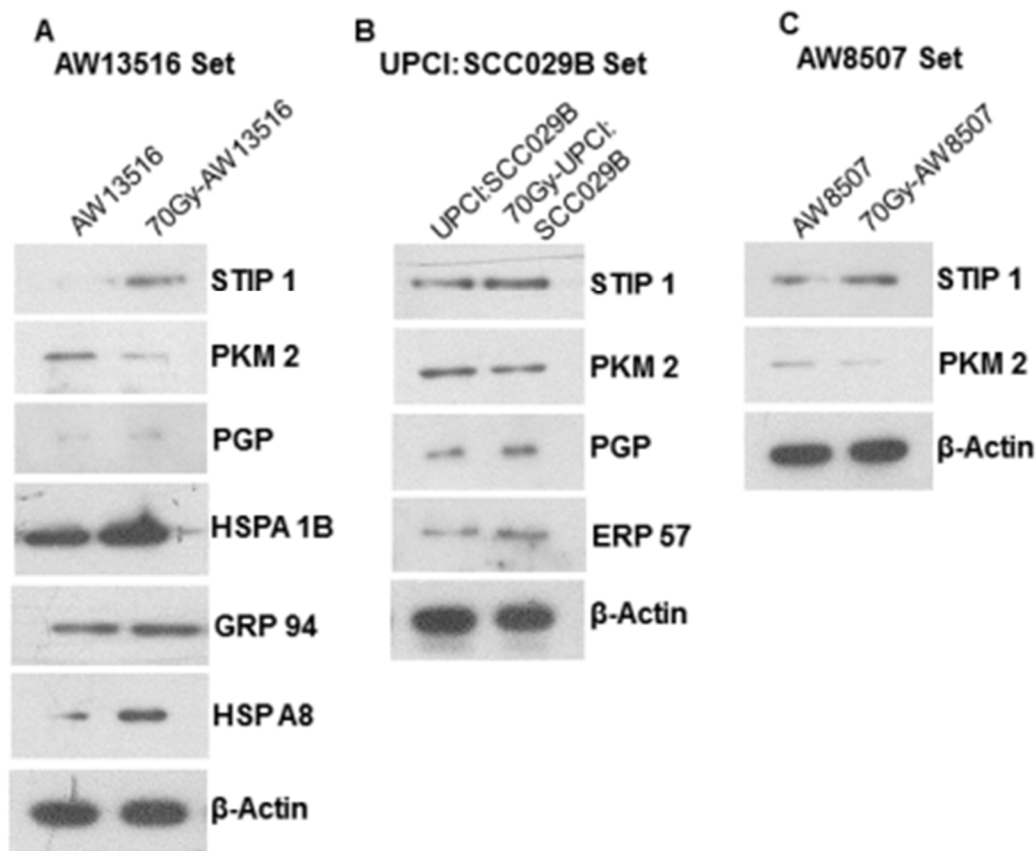


Figure 23: Western blots for common MALDI identified proteins from all the three set of parental and established radioresistant cells. (A) AW13516 & 70Gy-AW13516 (B) UPCI:SCC029B & 70Gy-UPCI:SCC029B (C) AW8507 & 70Gy-AW8507 cells. β actin is used as loading control.

As shown in the above Figure 23, the up & down regulated expression of STIP 1 and PKM 2 in all the three radioresistant set of cells (compared to their parental cells) are found to be

validated by western blotting. Similarly, expression of STIP 1, PKM 2 & PGP in 70Gy-AW13516 & 70Gy-UPCI:SCC029B cells (A & B). While expression of 06 out of 08 common proteins were found to be validated in 70Gy-AW13516 cells (A) and expression of PDI A3 (ERP 57) only in 70Gy-UPCI:SCC029B cells (B).

5.2.9 Association network among the common identified proteins (STRING v10)

The functional protein association networks between the common identified proteins from the three set of parental and radioresistant cells were exhibited by STRING (version 10) database, meant for predicting protein interactions [230].

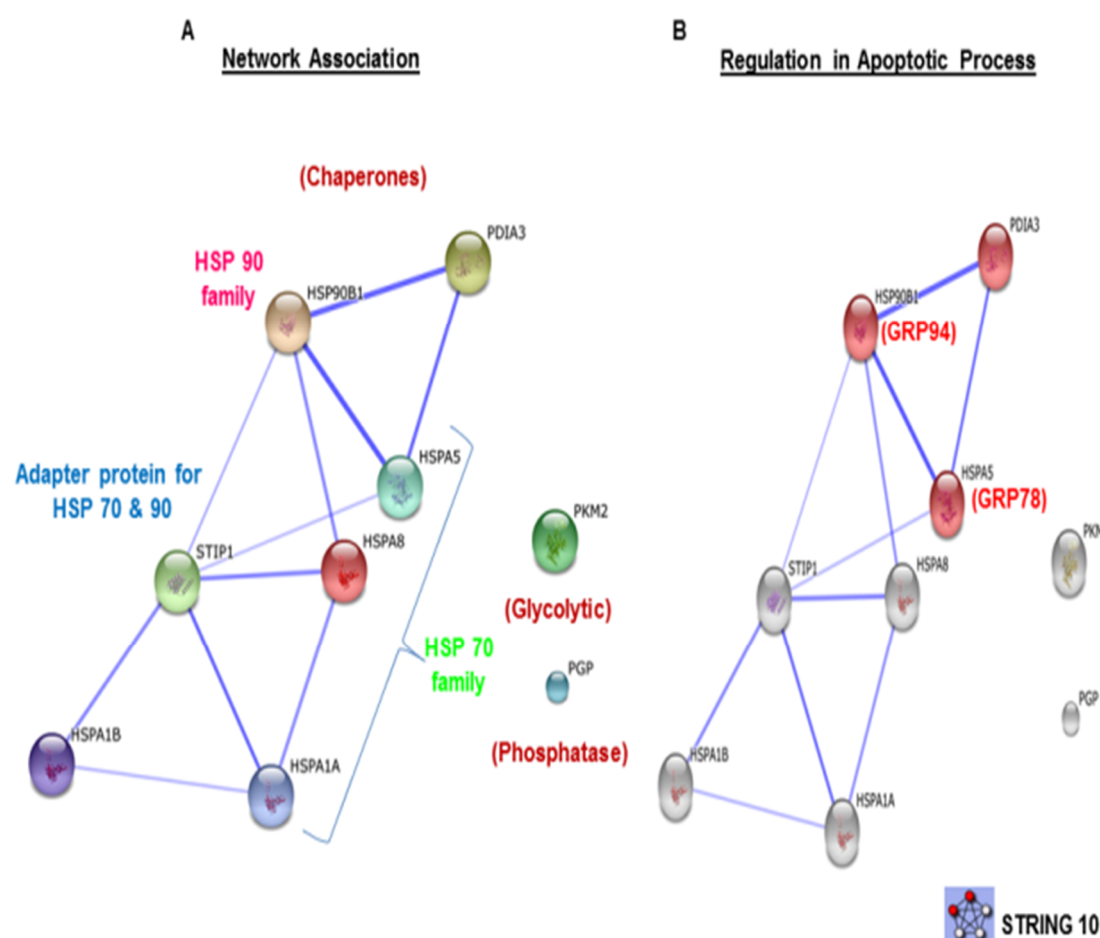


Figure 24: The STRING network view for the common proteins. (A) Network association (B) Regulation in apoptotic process. Lines between the proteins indicate the type of interaction, while the protein nodes which are enlarged indicate the availability of 3D protein

structure information. Note: HSC 70kDa 1A/1B is represented as separate HSC 70kDa 1A & HSC 70kDa 1B.

STRING classifies HSP A5 (GRP 78), HSP A8, HSPA 1A/ 1B as HSP 70 family members and HSP90 B1 (GRP 94) as HSP 90 family member, while STIP 1 as an adapter protein for these two family members (Figure 24, A). Therefore, signifies the role of STIP 1 in coordination of HSP- 70 & 90 family member proteins. In addition, STRING network also represent HSP A5, HSP 90B1 and PDI A3 as effective candidates in the regulation of apoptotic process (Figure 24, B) among all the identified common proteins. The anti-apoptotic regulation can be a beneficiary factor for the acquisition of radioresistance feature. The PKI M2 & PGP represented as the glycolytic and phosphatase protein respectively.

5.3 To characterize the Radioresistant sublines versus Parental oral cancer cell lines by different parameters.

5.3.1 Study of EMT like characteristics in established Radioresistant sublines

The acquisition of Epithelial to Mesenchymal transition characteristics (EMT) were studied in two radioresistant sublines i.e 70Gy-AW13516 and 70Gy-UPCI:SCC029B that were established from its parental AW13516 & UPCI:SCC029B cell lines. These two radioresistant cell lines were chosen for studying EMT like features as it belongs to two different oral subsite i.e tongue and buccal mucosa respectively.

5.3.2 FIR leads to change in morphology of Radioresistant cells, including increase in filopodia and decrease cell to cell adhesion

It was observed that the radioresistant 70Gy-AW13516 and 70Gy-UPCI:SCC029B cells exhibit altered characteristics including decrease in compact growth pattern and elongated morphology (Figure 25) with fine elongations at the cell surface (Figure 25 B, 40X).

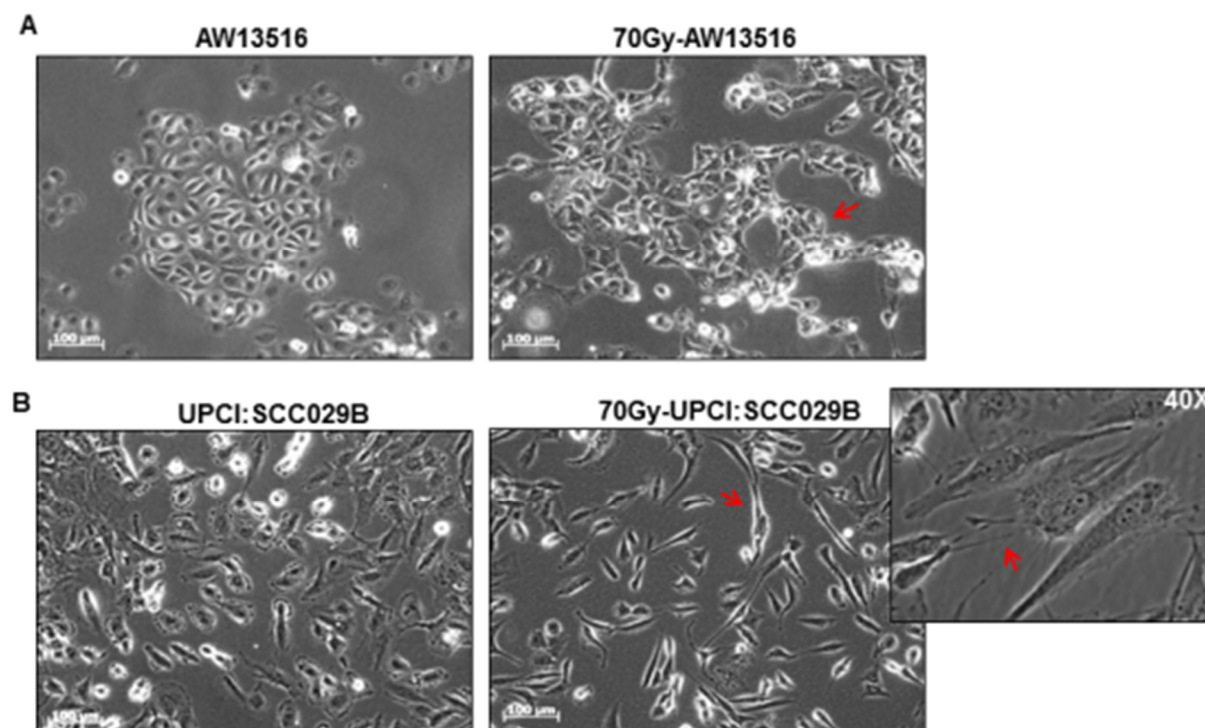


Figure 25: Morphology for the parental and radioresistant cells. (A) Parental AW13516 cells and radioresistant 70Gy-AW13516 cells. (B) parental UPCI:SCC029B cells and radioresistant 70Gy-UPCI:SCC029B cells. Scale bars: 100 μ m.

To study these changes; F-Actin staining (Filamentous actin, to get an insight into their actin reorganization) and Hanging drop assay (to explore cell to contact) was performed on both of these parental and radioresistant cells. F-Actin staining show significant increase (Figure 26) in the number of filopodia (long, slender and actin rich cellular protrusions proposed to have role as sensory and exploratory organelles [231]) in both the 70Gy-AW13516 and 70Gy-UPCI:SCC029B cells (p 0.05 & 0.001) in comparison to their parental cells. Similarly, Figure 27 signifies less cell to cell contact (p 0.01 & 0.05) in both the radioresistant cells in

comparison to their parental cells; as revealed by hanging drop assay. The gain of these morphological changes in radioresistant sublines, hint towards its altered characteristic due to long term fractionated radiation treatment and EMT may one such feature acquired in them.

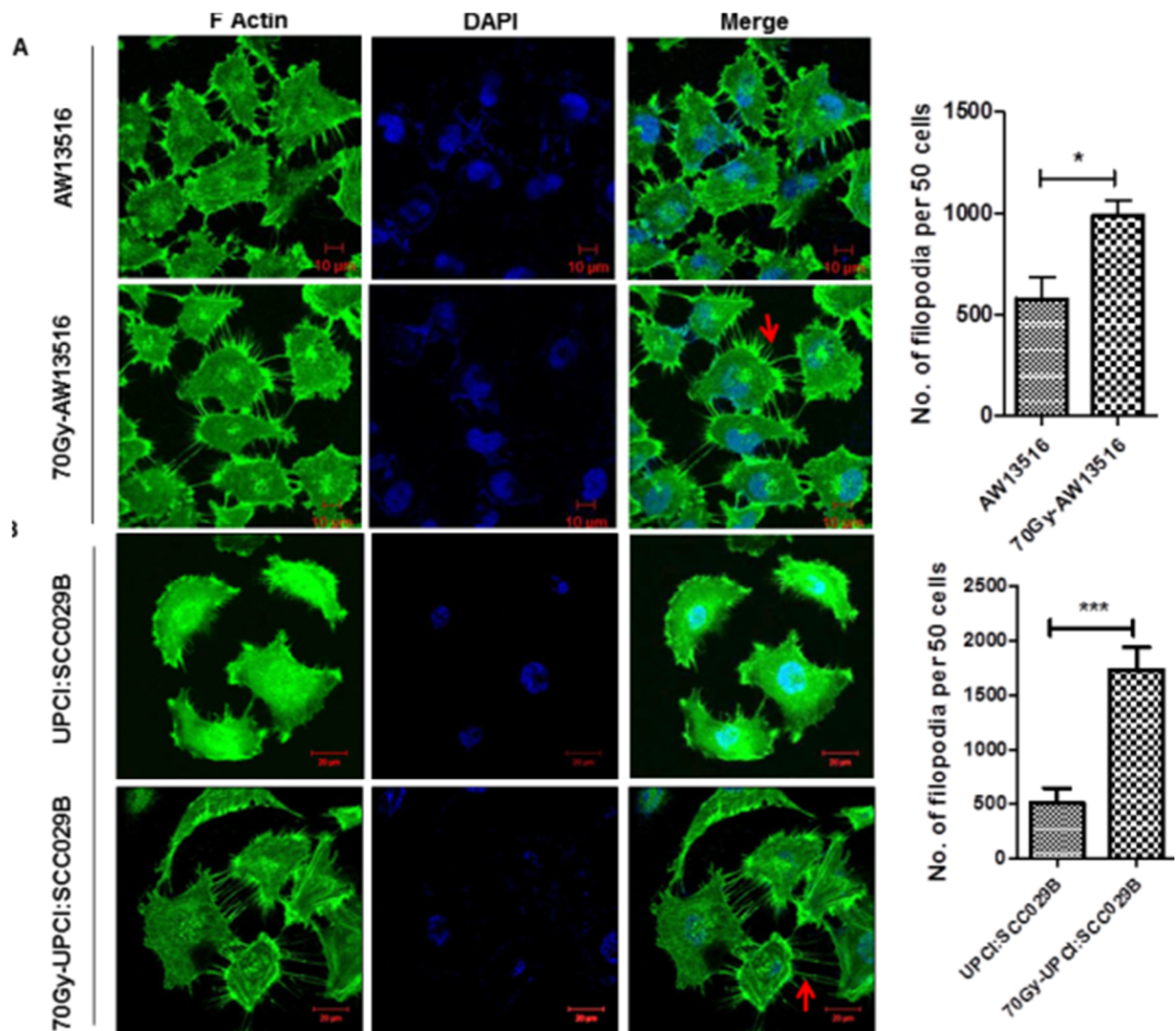


Figure 26: F-Actin staining for the parental and radioresistant cells (A) AW13516 and 70Gy-AW13516 cells (B) UPCI:SCC029B and 70Gy-UPCI:SCC029B cells. Confocal images of filamentous actin, stained with Alexa Fluor-488 phalloidin. Cells were counter stained with DAPI, scale bars: 10 μ m, arrow indicates filopodia as fine cell surface extensions. Analysis

based on 50 cells per population with mean and standard deviation of three independent experiments plotted at the right side (p 0.05, 0.001).

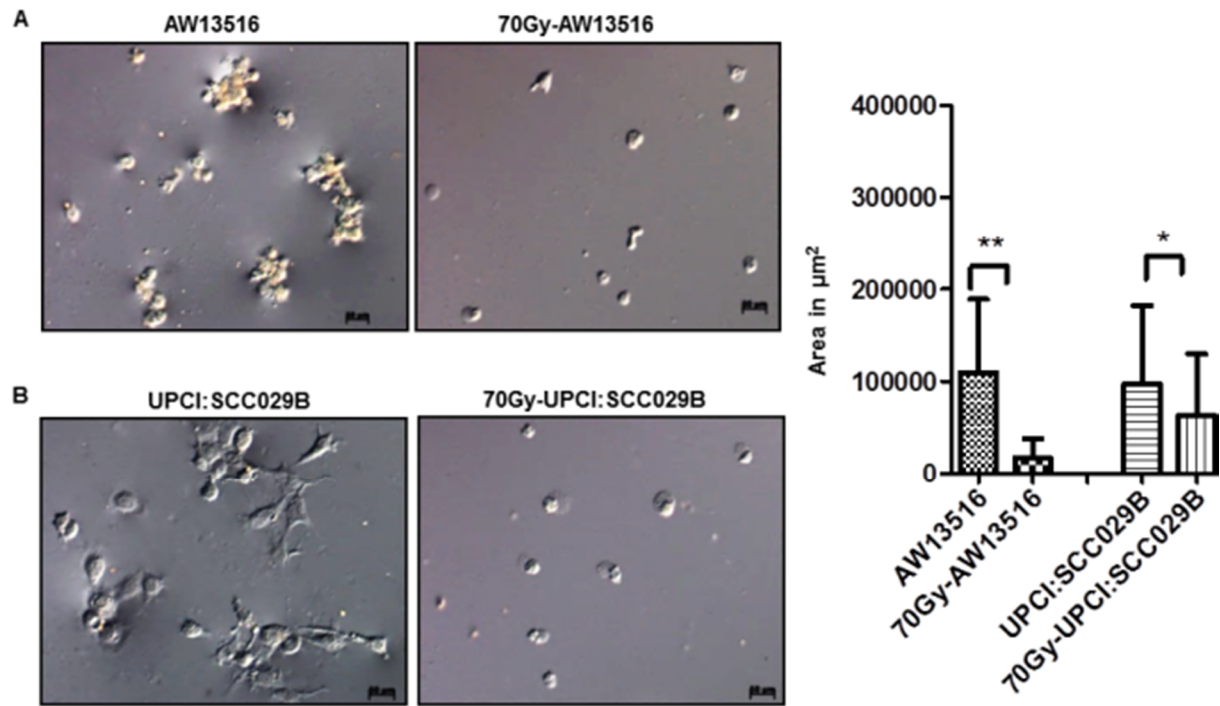


Figure 27: Hanging drop assay for determining cell to cell contact. In panel A & B both the radioresistant cells show significant decrease in cell- cell adhesion compared to their parental cells, Scale bars: 50 μm . Results are from three independent experiments with mean and standard deviation.

5.3.3 Assessment of EMT associated markers in the Radioresistant cells

To investigate the EMT like changes in these cells, the expression of EMT associated markers were assessed by western blotting and immunofluorescence. Figure 28 represent upregulation of mesenchymal markers like Vimentin and N-cadherin while down regulation of epithelial marker like E-cadherin and cell junction protein Desmoplakin in both the radioresistant cells; except for E-cadherin in 70Gy-AW13516 cells as levels of E-cadherin

were not detected in its parental AW13516 cells. The reason could be that may be E-cadherin is already absent in the oral tumor from which parental AW13516 cell line was initially established. Loss of epithelial markers can also be inferred from the reduced cell to cell adhesion property of both the radioresistant cells that have been shown in the upper panel.

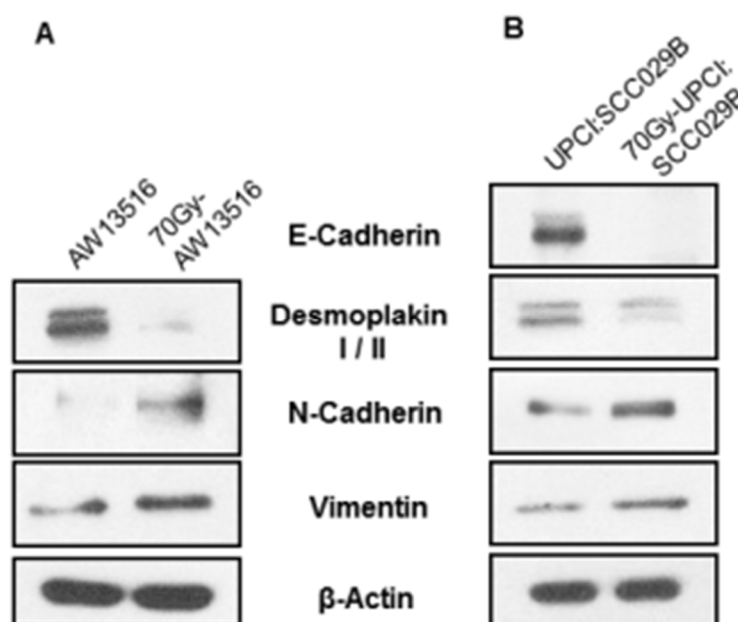


Figure 28: Western blot for EMT markers (A) Parental AW13516 & radioresistant 70Gy-AW13516 cells (B) Parental UPCI:SCC029B & radioresistant 70Gy-UPCI:SCC029B cells. Levels of E-cadherin were not detected in parental AW13516 cells. β -Actin is used as loading control.

These results were also assessed by fluorescence microscopy to specifically assess the cellular localization of these proteins. Figure 29 (A & B), represents both the parental and radioresistant cells staining with EMT markers mentioned in upper section. The immunofluorescence study also confirms the upregulation of mesenchymal markers (Vimentin & N-cadherin) and downregulation of E-cadherin and Desmoplakin in the respective

radioresistant cells. Figure 29 (C) represent cell surface Desmoplakin staining in HCT 116 cells that is taken as positive control for desmo staining, as our parental cells show more cytoplasmic staining instead of cell surface for the same.

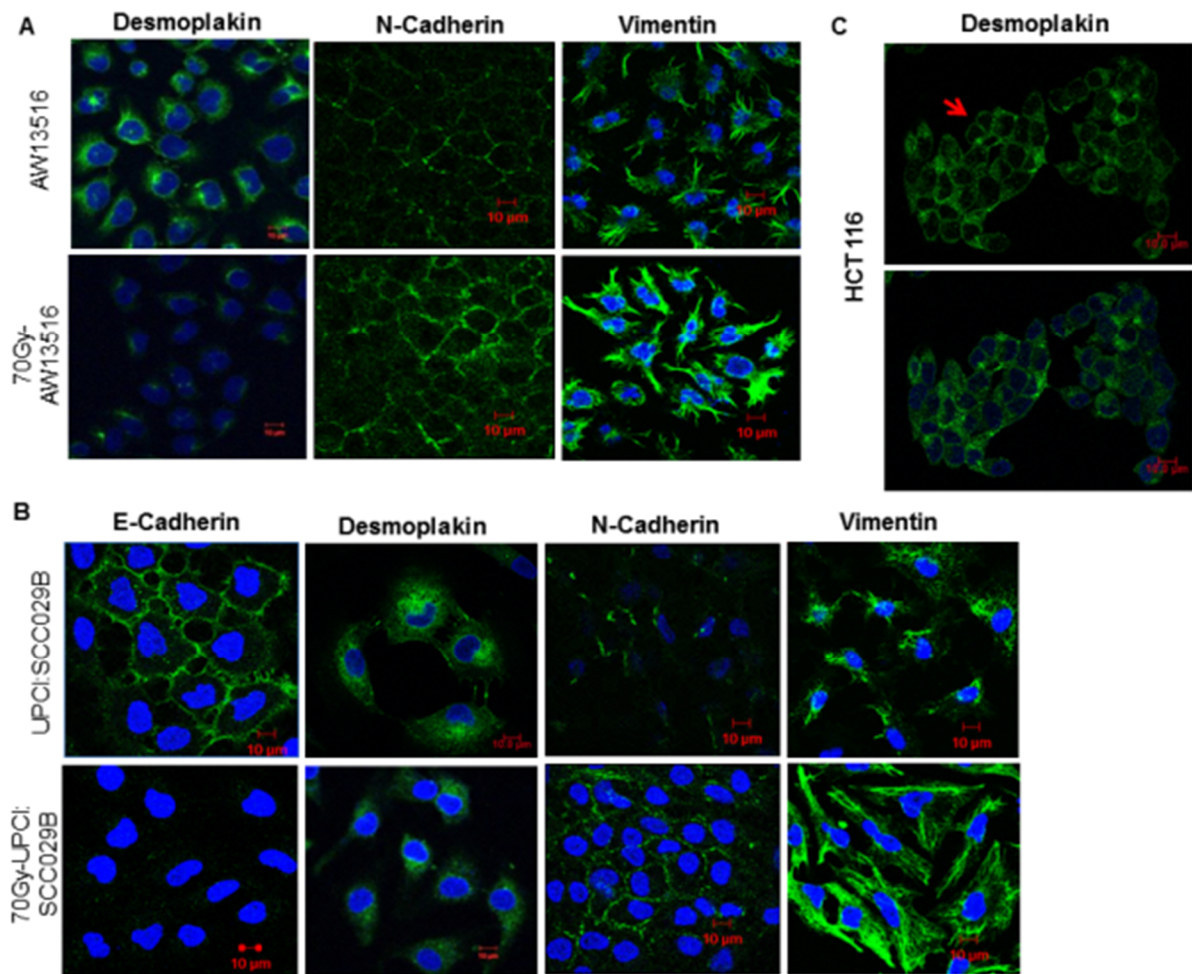


Figure 29 Immunofluorescence study for EMT associated markers. (A) Immunofluorescence staining for EMT markers in AW13516 & 70Gy-AW13516 cells (B) UPCI:SCC029B & 70Gy-UPCI: SCC029B cells. (C) Positive control for Desmoplakin staining in HCT-116 cells. Scale bars: 10μm.

5.3.4 Status of EMT associated transcription factors in Radioresistant cells

Next, we performed SYBR based Real time PCR quantification for some of the known EMT associated transcription factors. As shown in Figure 30, Snail ($p<0.05$) and Twist are upregulated in both the radioresistant cells while Slug only in 70Gy-AW13516 cells compared to their parental cells. Upregulation of these transcription factors suggests their possible role in the acquisition of radiation induced EMT properties in these cells.

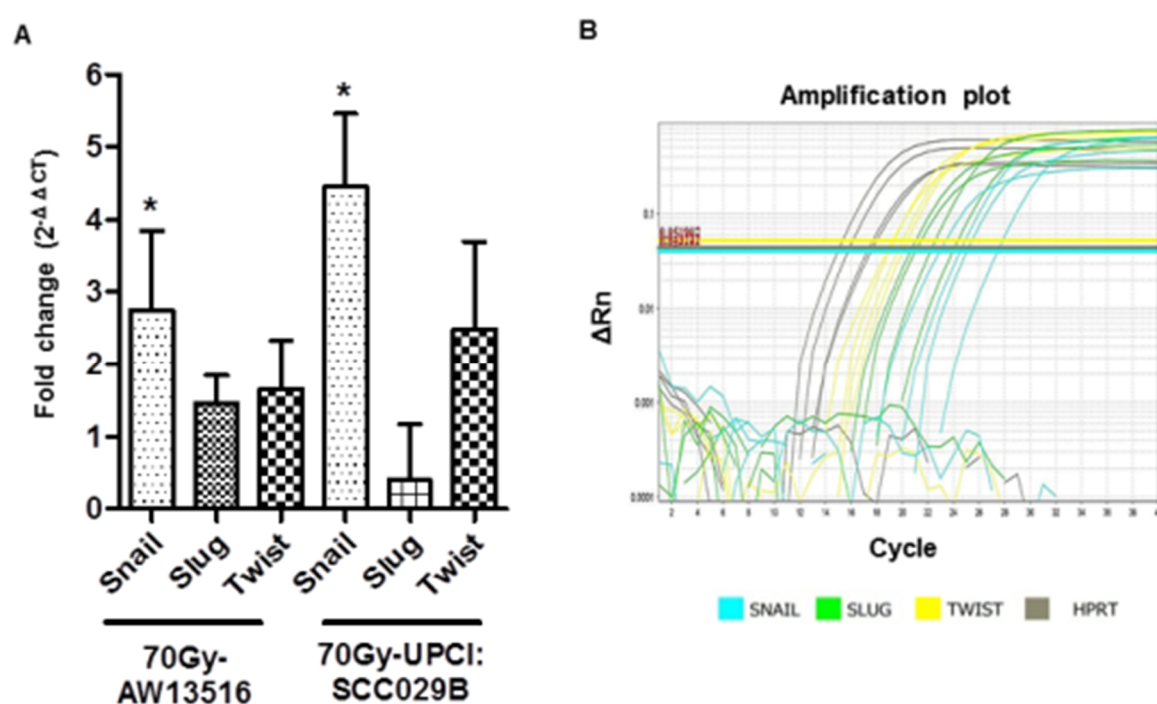


Figure 30: Real time PCR quantitation for EMT associated transcription factors, showing fold change levels for the snail, slug and twist in both the parental & radioresistant cells. (A) AW13516 & 70Gy-AW13516 (B) UPCI:SCC029B & 70Gy-UPCI:SCC029B. HPRT used as internal control ($p<0.05$). Results are from three independent experiments with mean and standard deviation.

5.3.5 Radioresistant 70Gy-AW13516 cells exhibit increased Migration and Invasion

We next wanted to determine whether the attainment of these EMT traits (change in cellular morphology, increase in filopodia, reduced cell-cell adhesion, expression of EMT associated markers & transcription factors) in the radioresistant cells leads to any change in their migratory and invasive character. Therefore, we have carried out migration and transwell invasion assay with these cells.

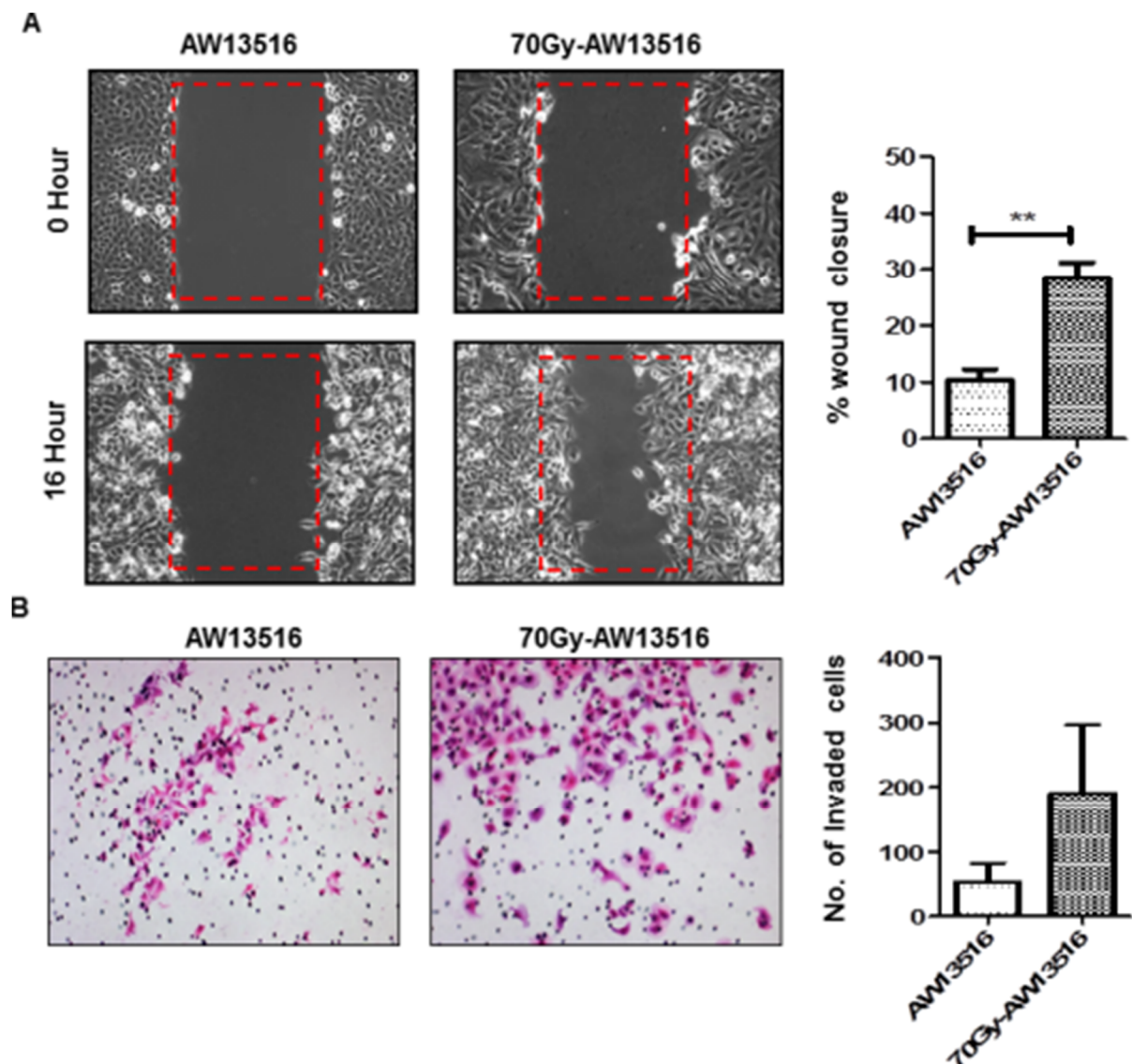


Figure 31: Migration & Transwell invasion assay for the parental AW13516 cells and radioresistant 70Gy-AW13516 cells. Data is from three independent experiments. $p, 0.01$.

As shown in Figure 31, the 70Gy-AW13516 cells exhibit increase in both wound closure (p 0.01, ~3 fold) and invasiveness (~2 fold) as compared to its parental cells. However, no increase in the migratory and invasive behavior of 70Gy-UPCI:SCC029B cells was observed in comparison to their parental cells Figure 32, instead they exhibit a decreasing pattern in both migration and invasion.

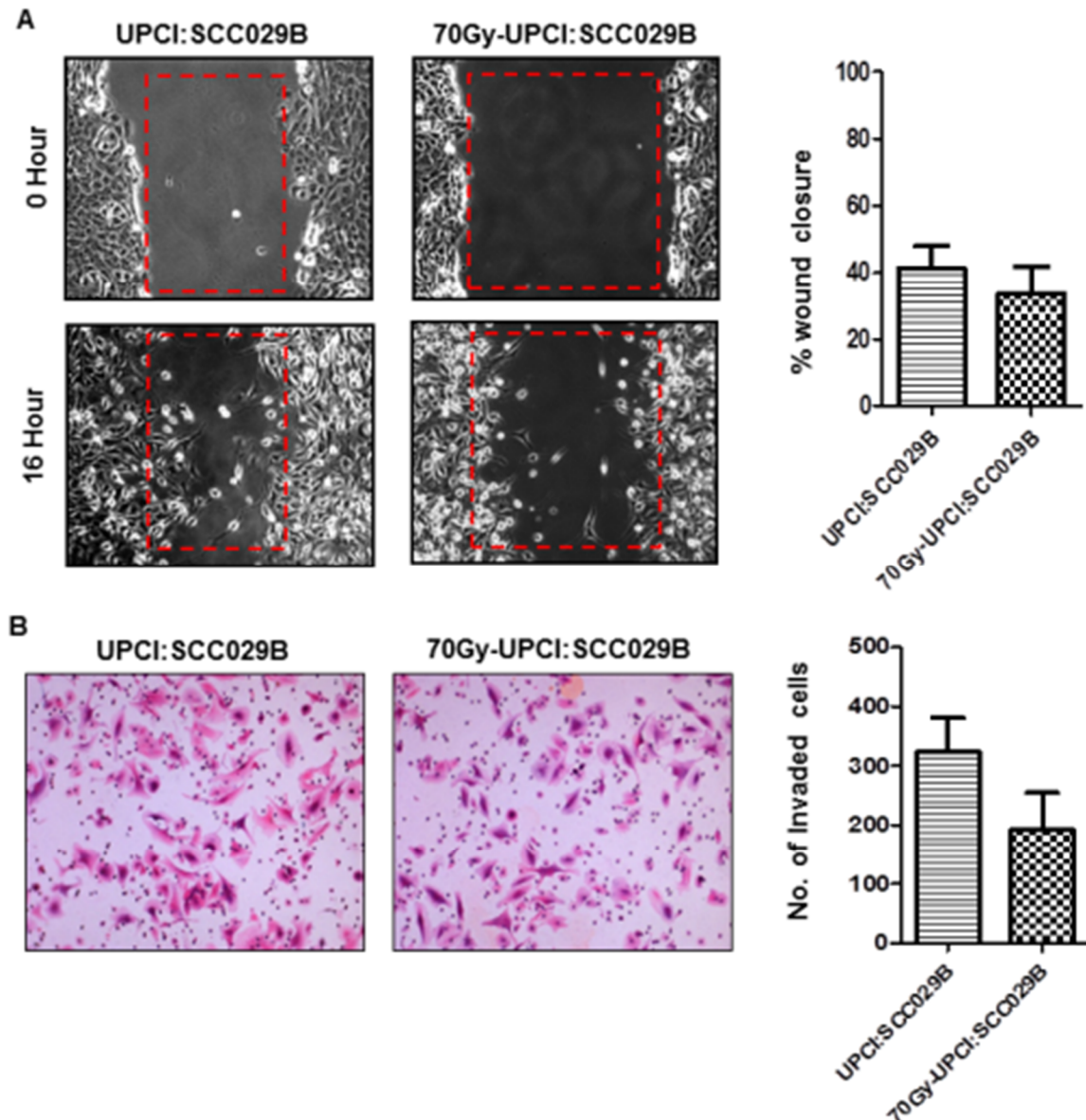


Figure 32: Migration & Invasion assay for the parental UPCI:SCC029B cells and radioresistant 70Gy-UPCI:SCC029B cells.

These results indicate that only radioresistant 70Gy-AW13516 cells have acquired increased migratory and invasive trait and not the 70Gy-UPCI:SCC029B cells due to fractionated

radiation. This could be due to the possibility of different molecular profiles has attained in these two set of radioresistant cells of different oral subsites.

5.3.6 Radioresistant 70Gy-AW13516 cells show increase in cell motility associated ERM family protein Moesin

To understand the reason behind the increased migratory and invasive behaviour of radioresistant 70Gy-AW13516 cells, its 2D proteomic profile was analysed, to find the differentially expressed proteins related to cell motility & invasiveness.

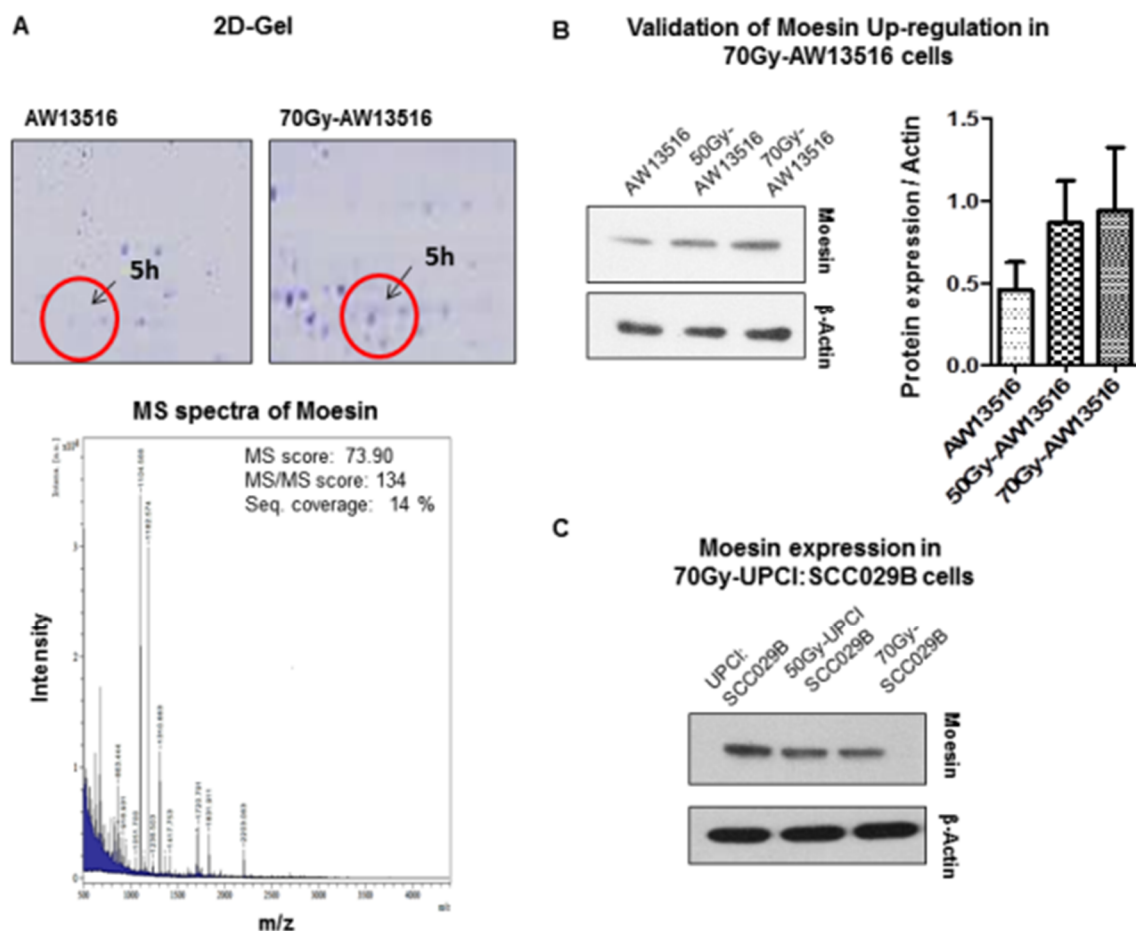


Figure 33: Mass spectrometry based identification & validation of cell motility associated protein Moesin. (A) 2D-gel showing differentially expressed Moesin protein spot in 70Gy-AW13516 cells with MS spectra for Moesin protein (B) Validation of increased Moesin

expression in 70Gy-AW13516 cells by western blotting (C) Moesin expression in 70Gy-UPCI:SCC029B cells. The 50Gy are the intermediate radioresistant sublines

Among the differentially identified proteins, an ERM (Ezrin, Radixin, Moesin) member protein- Moesin was found to be upregulated in its 2D profile. (Figure 33-A). The Moesin upregulation was also validated by western blotting in 70Gy-AW13516 cells (Figure 33-B). Figure 33-C shows western blot for Moesin in 70Gy-UPCI:SCC029B cells, where a relative decrease in their expression pattern from the parental cells is seen which coincides with its decreased migratory & invasive behaviour as discussed in the upper section. Moesin protein is reported to be associated with cell migration, by acting as a cross linker between actin filaments and plasma membrane. Therefore, we want to determine the relationship between Moesin and the increased migratory and invasive characteristic of 70Gy-AW13516 cells. The other ERM proteins i.e Ezrin and Radixin were not detected in our 2D result.

5.3.7 Increased co-expression of Moesin, with its cell surface receptor CD-44 at the migratory front of Radioresistant 70Gy-AW13516 cells

Activated ERM proteins connect the actin cytoskeleton to the transmembrane receptors, that includes CD-44, Intercellular adhesion molecule (ICAM-1, 2), CD-43 or EGFR. Binding to these receptors leads to activation of different pathways including cell proliferation, survival, morphology, adhesion and cell migration and invasion (section 2.10 a). Also, among these transmembrane receptors; the association of ERM family protein Moesin & CD-44 is reported to be linked with cell cytoskeletal organization & cell polarity [232] as well as in membrane protrusions [133]. Therefore, to assess the possible role of Moesin in the acquired migratory and invasive property of 70Gy-AW13516 cells, co-expression of Moesin with its cell surface receptor CD-44 was assessed in a wound healing experiment. The parental and

radioresistant 70Gy-AW13516 cells were grown on coverslips till it became ~70% confluent, followed by serum starvation. After it, linear scratches were made on the cover slips and allowed to migrate under standard culture conditions for about 10 hours. The cells were then fixed and co-stained with anti-Moesin, CD-44 antibodies and cell migratory fronts were observed under confocal microscope.

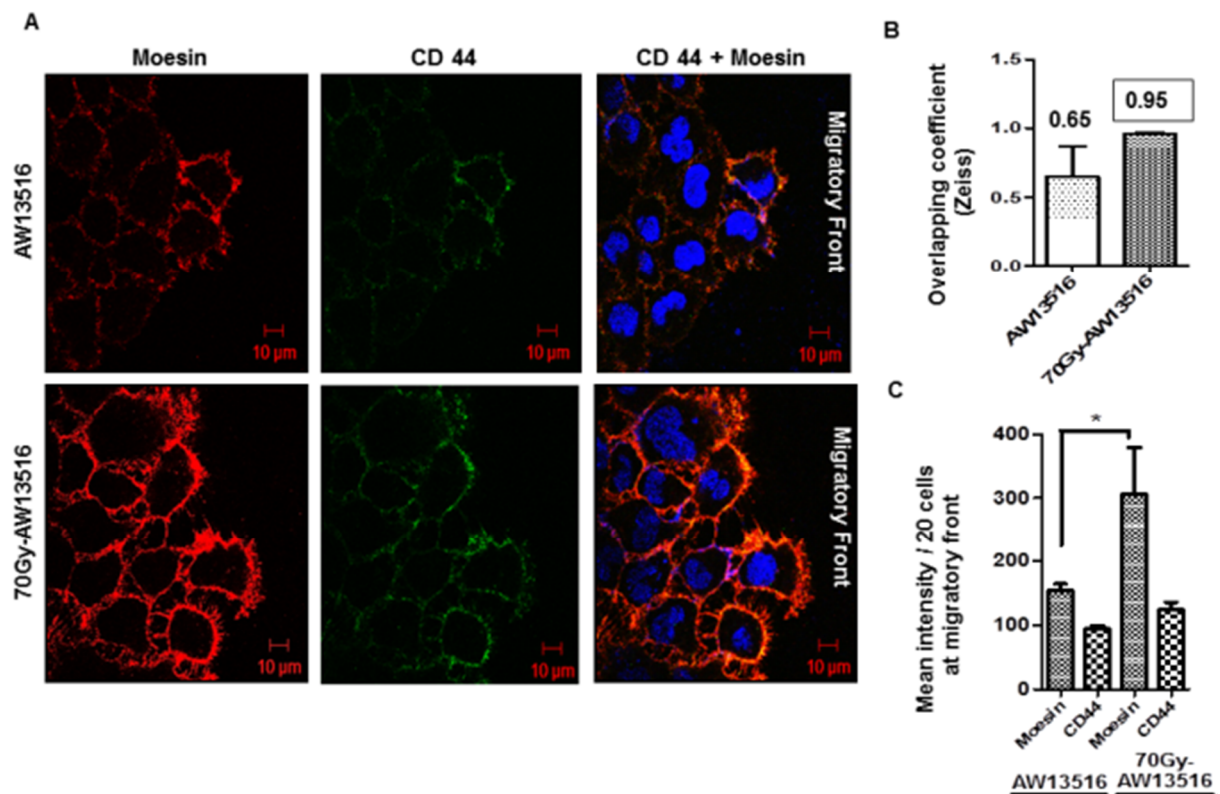


Figure 34: Moesin co-expression with its cell surface receptor CD-44 at cell migratory front. (A) Confocal microscopy, representing increased co-expression of Moesin-CD44 at migratory fronts of 70Gy-AW13516 cells (B) with overlapping coefficient (Ziess) close to 1 for 70Gy-AW13516 cells (C) Mean fluorescence intensity (\pm s.d) of Moesin and CD-44 expression per 20 cells at the migratory edges of 70Gy-AW13516 cells ($p < 0.05$). Scale bars: 10 μ m.

Figure 34-A represent increased co-expression of CD-44 and Moesin at migratory fronts of 70Gy-AW13516 cells with overlapping coefficient close to 1 (Figure 34-B), while Figure 34-

C represents a significant ($p < 0.05$) increase in mean intensity of Moesin expression in 70Gy-AW13516 cells at the migratory edges. These results signify that Moesin-CD44 interaction contributes towards the increased migration of radioresistant 70Gy-AW13516 cells.

5.3.8 siRNA mediated knockdown of Moesin in Radioresistant 70Gy-AW13516 cells

Further, in order to determine more about the role of Moesin protein in the acquired migratory behaviour of 70Gy-AW13516 cells. We have carried out siRNA mediated knockdown of Moesin protein in these cells.

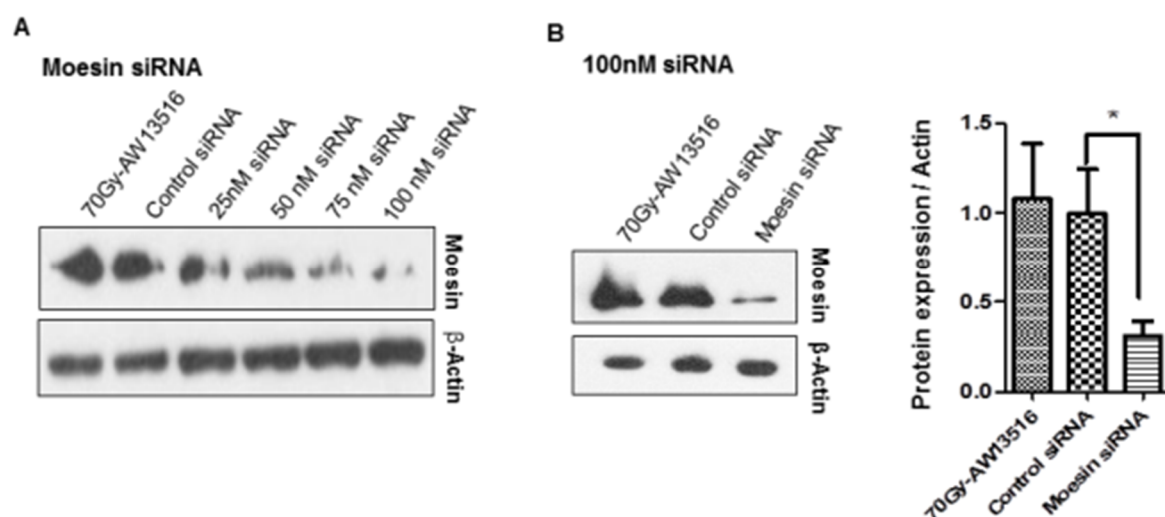


Figure 35: siRNA mediated knock-down of Moesin in 70Gy-AW13516 cells. (A) Moesin western blot after treating cells with increasing concentration of Moesin siRNA (B) Western blot showing effective (~70%, $p < 0.05$) knockdown for Moesin protein along with the non-targeted control siRNA (both the siRNA with 100nM concn.) β -actin is used as loading control.

Figure 35-A, represent 100nM siRNA concentration as effective dose for the knockdown of Moesin protein and Figure 35-B show significant knockdown ($p < 0.05$, ~70%) of Moesin protein, compared to the negative control and no-treatment 70Gy-AW13516 cells (100nM concentration was used for both control and Moesin siRNA).

5.3.9 Moesin Knockdown leads to decrease in acquired Migration and Invasion of Radioresistant 70Gy-AW13516 cells

The Migration and Invasion assay were performed after Moesin knockdown in radioresistant 70Gy-AW13516 cells.

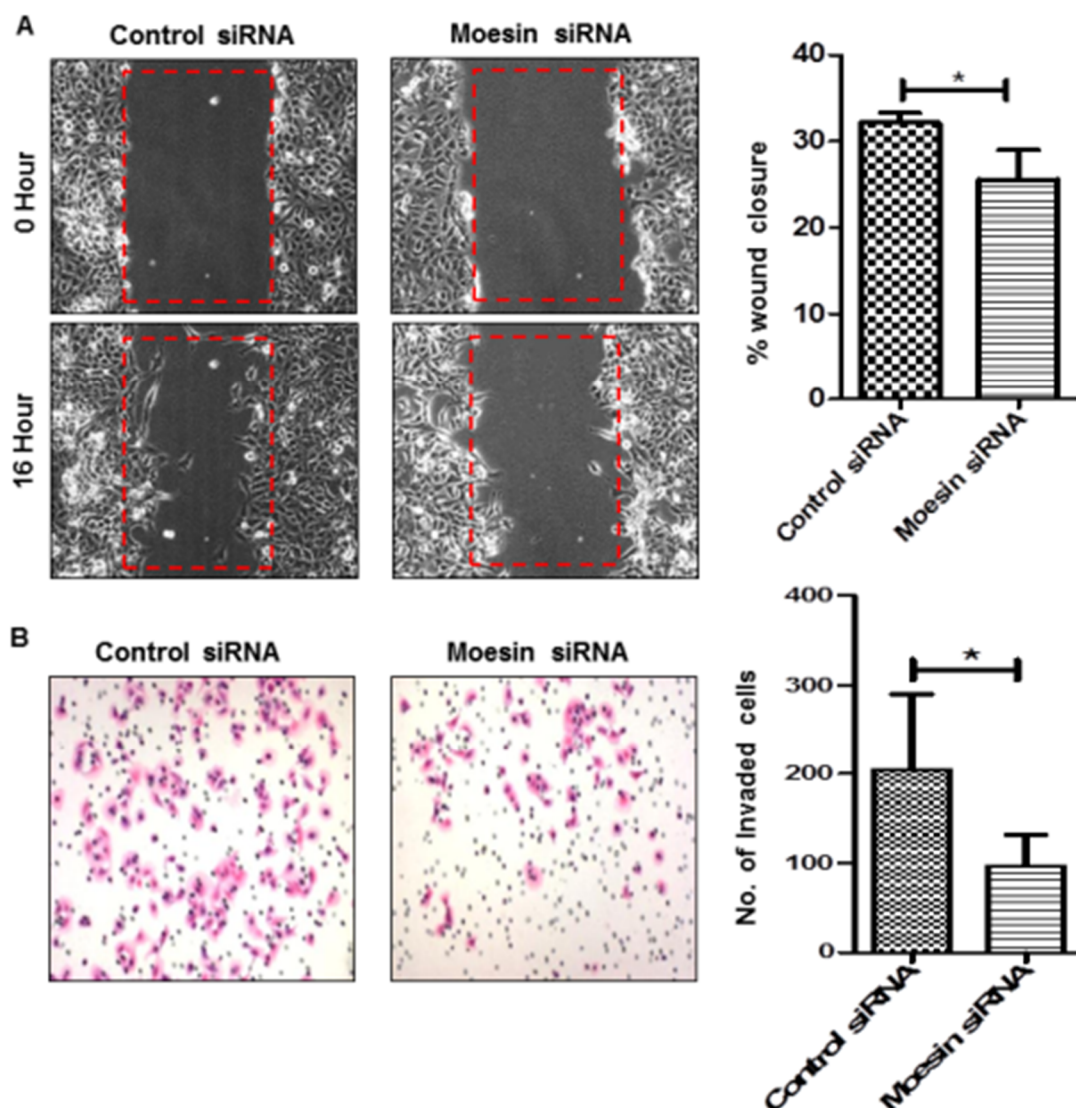


Figure 36: Migration and Transwell invasion assay post Moesin knock-down in 70Gy-AW13516 cells. (A & B) Decreased wound healing and invasiveness of 70Gy-AW13516 cells post Moesin knockdown ($p < 0.05$).

Post Moesin knockdown, a significant ($p < 0.05$) decrease in both the migration and invasion (Figure 36 A & B) of 70Gy-AW13516 cells was observed, compared to the negative control siRNA treated cells. These results suggest the role of cytoskeleton organizing protein Moesin in the acquired radioresistant cells.

5.3.10 Moesin Knockdown leads to decrease in acquired Radioresistant character of 70Gy-AW13516 cells

Next, we wanted to examine whether Moesin knockdown has any effect on the acquired radioresistant character of 70Gy-AW13516 cells.

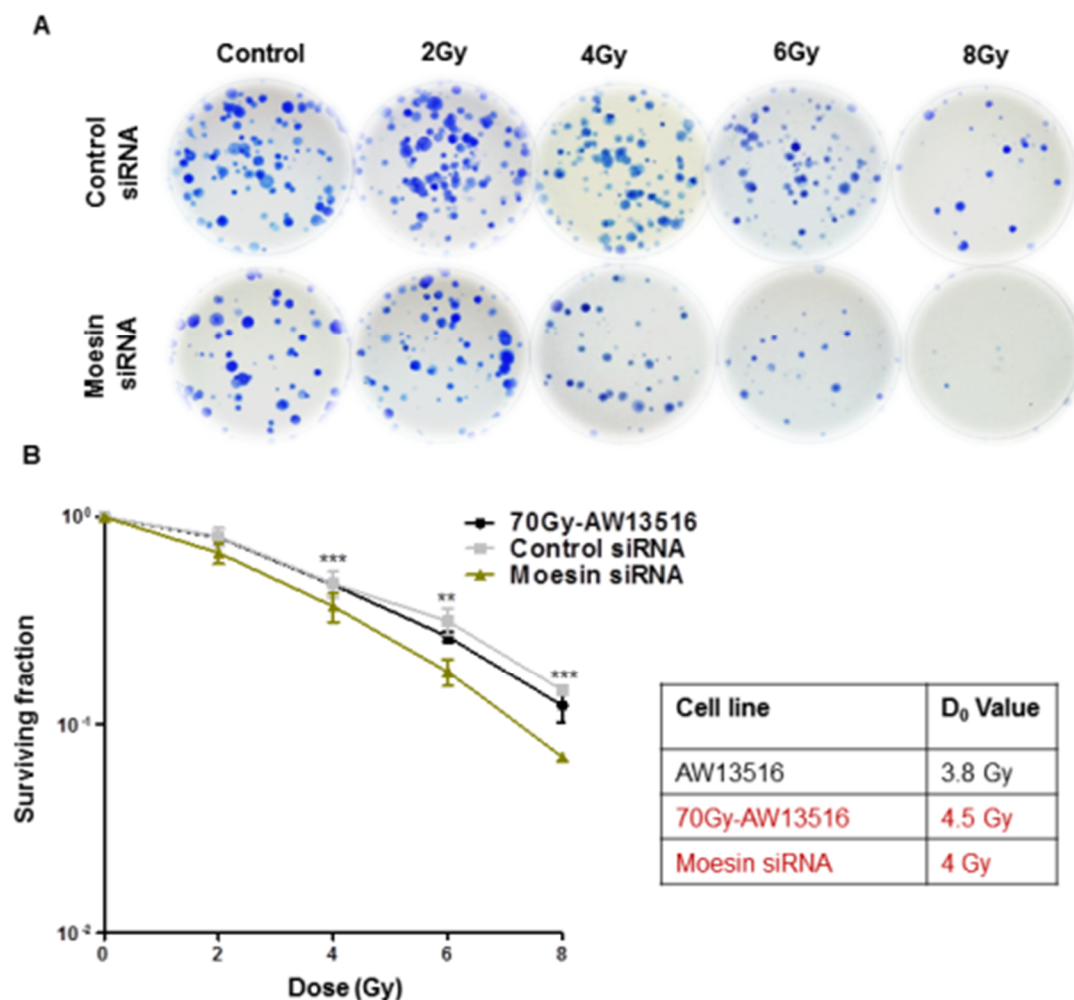


Figure 37: Effect on the radioresistant phenotype of 70Gy-AW13516 cells, after Moesin knock-down (A) Clonogenic cell survival assay for 70Gy-AW13516 cells post Moesin

knockdown, colonies > 50 cells were considered as clonogenic survivor. (B) Cell survival curve based on the surviving colonies. Data represented as percentage survival of no-treatment and treated with control siRNA and Moesin siRNA 70Gy-AW13516 cells. One-way ANOVA statistical analysis was performed on surviving fractions at the given doses from three independent experiments ($p < 0.01$, 0.001).

Since upregulation of Moesin was observed in the radioresistant background and it was detected in its differential 2D gel profile. Therefore, clonogenic cell survival assay was also performed post Moesin knockdown in 70Gy-AW13516 cells. As shown in Figure 37-A & B, a decrease in the survival of radioresistant 70Gy-AW13516 cells was observed, after treatment with Moesin siRNA. The D_0 value post Moesin knockdown was observed as 4Gy in comparison to the earlier D_0 dose of 4.5Gy for the radioresistant 70Gy-AW13516 cells. These observations together suggest the role of Moesin protein in the increased migratory, invasive and radioresistant character of radioresistant oral cancer cells, established by clinically admissible fractionated ionizing radiation.

5.4 Study of Stem cell like characteristics in the established Radioresistant sublines

Acquisition of stem cell like characteristics were studied in all the three established radioresistant sublines by assessing their anchorage independent growth properties, status for stem cell like markers, ability to form 3D spheroids and *in-vivo* tumorigenic potential.

5.4.1 Soft agar assay for the Parental and Radioresistant cells

For assessing anchorage independent growth and thus transforming potential of the radioresistant cells, their ability to form colonies on soft agar were analysed.

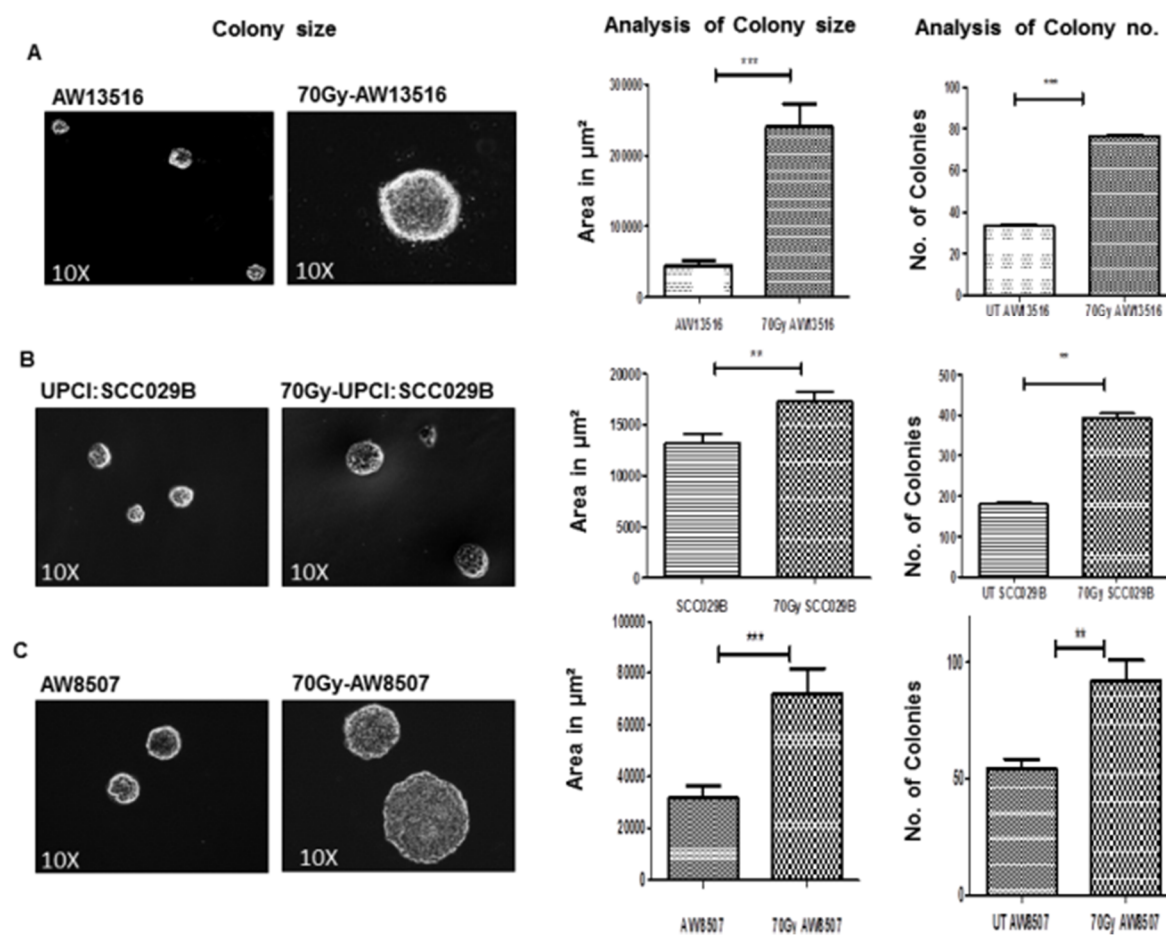


Figure 38: Soft agar assay for all the parental and radioresistant cells. (A) AW13516 and 70Gy-AW13516 cells (B) UPCI:SCC029B and 70Gy-UPCI:SCC029B cells and (C) AW8507 and 70Gy-AW8507 cells. Results are from three independent experiments with mean and standard deviation (p 0.01, 0.001).

As shown in Figure 38, a significant increase in both size and number of colonies on soft agar was observed for all the three radioresistant cells, compared to their non-irradiated parental cells. The result signifies the attainment of anchorage independent growth properties in all the established radioresistant cells. This can be the first step towards its possible attainment of stem cell like character but 3D spheroid assay will clarify more as it is used specifically for characterizing the stem cells.

5.4.2 3D Spheroid forming assay

The spheroid forming assay has been widely used as an *in-vitro* assay to identify stem cells based on their capacity of self-renewal and differentiation at the single cell level [233].

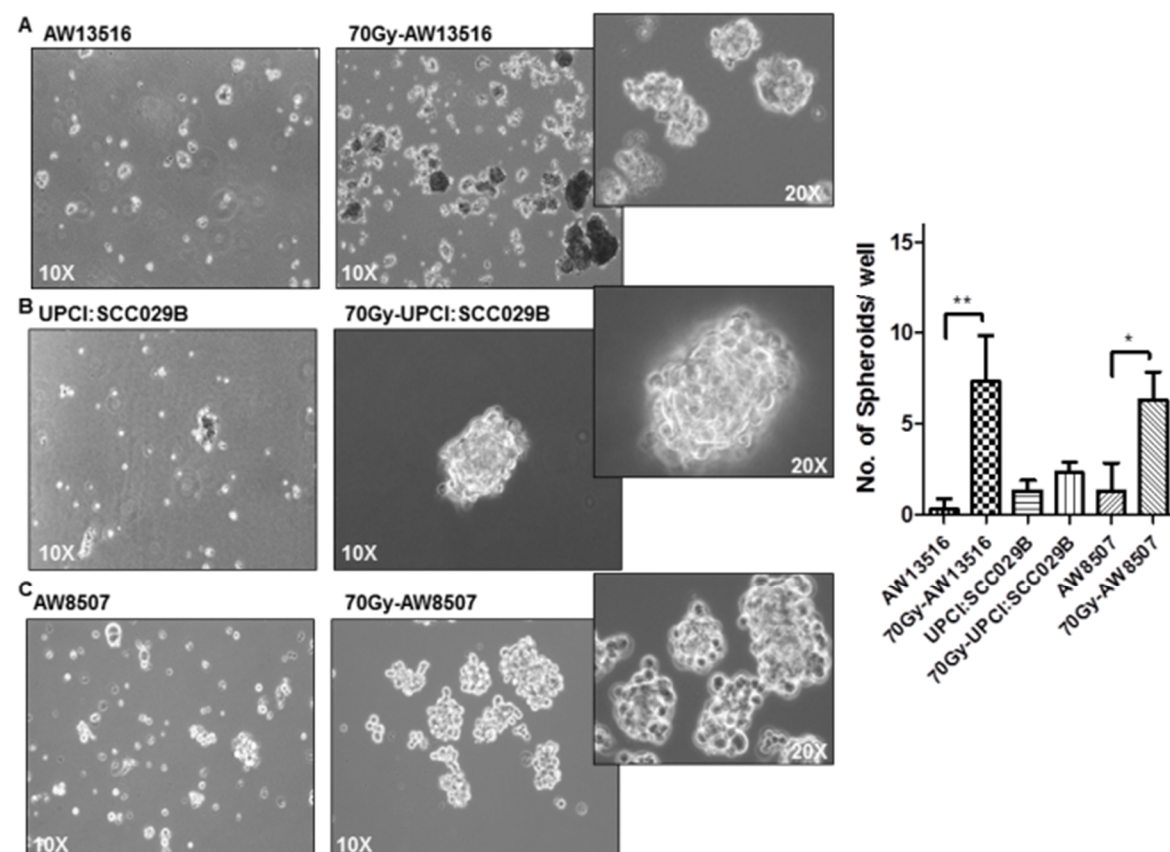


Figure 39: Spheroid forming assay for all the parental and radioresistant cells. (A) AW13516 and 70Gy-AW13516 cells (B) UPCI:SCC029B and 70Gy-UPCI:SCC029B cells (C) AW8507 and 70Gy-AW8507 cells. Bar graph showing number of spheroids in each of the parental & radioresistant set of cells, values are from three experiments done in duplicates (p 0.05, 0.01). Cells were grown in ultra-low attachment, without FBS and supplemented with EGF, FGF, Insulin & LIF (10 ng/ μ l) for about 2 weeks. Supplements were added after every two days and images were captured on inverted microscope.

The ability of our established radioresistant cells to form three dimensional spheroids in a growth factor enriched medium was examined and depicted in Figure 39. This sphere

forming property of sub-population within the radioresistant cells suggest the enrichment of stem cell like characteristics in these radioresistant cells and it also supports the Kummermerhr and Trott model [143] (discussed in section 2.10 b).

5.4.3 Status of Stem cell like markers in Radioresistant cells

In order to gain insight into the stem cell like features acquired by the radioresistant cells, the status of some stem cell markers like Oct-4, Sox-2, Nanog, CD-44 and CD-133 was assessed in all the three parental and radioresistant sublines (Figure 40).

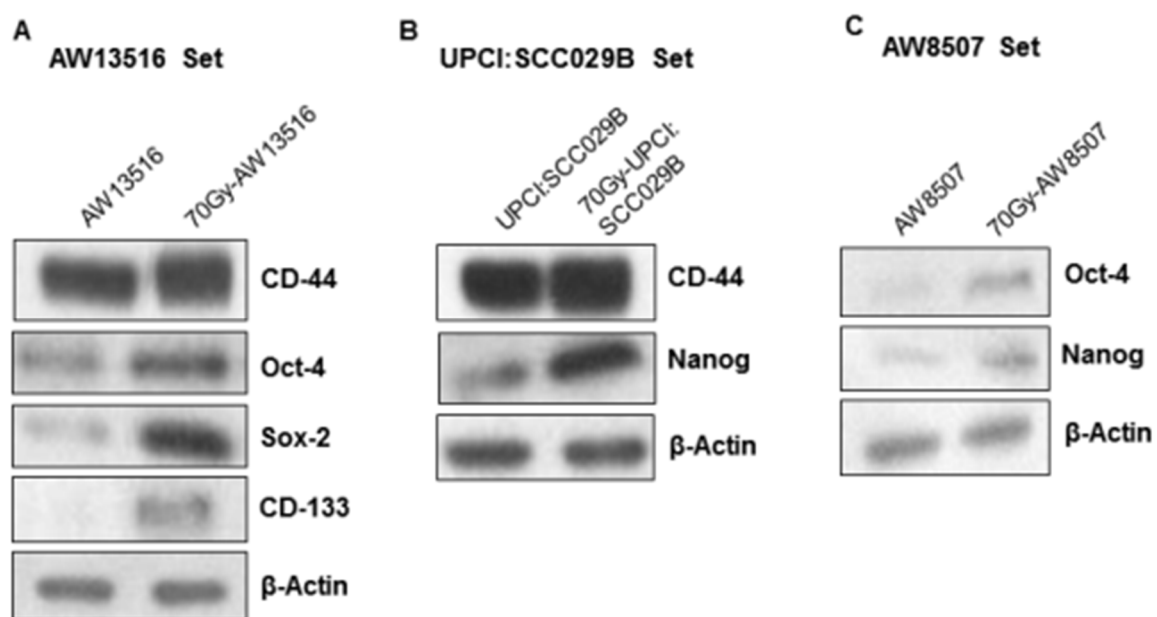


Figure 40: Stem cell like markers assessment in radioresistant cells by western blotting. (A) AW13516 & 70Gy-AW13516 (B) UPCI:SCC029B & 70Gy-UPCI:SCC029B (C) AW8507 & 70Gy-AW8507 cells, β -Actin is used as loading control.

The cell surface expression of CD-44 was also assessed by flow cytometry in AW13516 and UPCI:SCC029B cells (Figure 41).

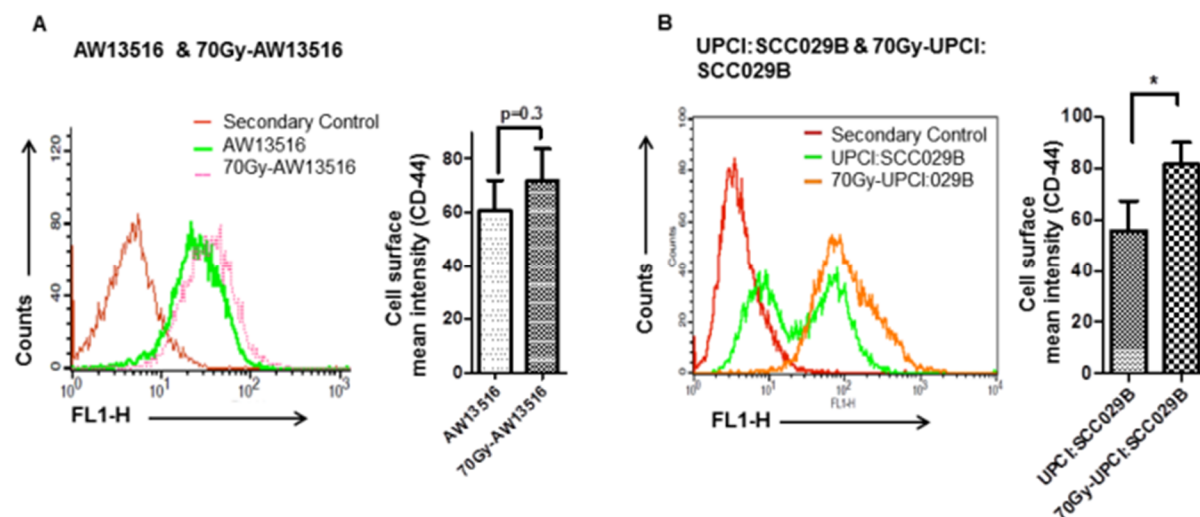


Figure 41: Cell surface expression for CD- 44 by flow cytometry (A) Mean intensity for CD- 44 in AW13516/70Gy-AW13516 cells (p 0.05) (B) Mean intensity for CD-44 in UPCI:SCC029B/70Gy-UPCI:SCC029B cells.

5.4.4 *In-vivo* Tumorigenic potential of Radioresistant cells

Further, as a gold standard for checking the stemness; the radioresistant cells were injected into the immunocompromised mice along with their parental cells and their tumorigenic potential was observed. As shown in Figure 42, the radioresistant 70Gy-AW13516 are found to be tumorigenic in BALB/c nude mice and tumor formation was observed in all the five animals (Figure 42-A), while the parental AW13516 cells are non tumorigenic and failed to form tumors in none of the animals (n=5). Similarly, the 70Gy-AW8507 cells are found to be more tumorigenic (Figure 42-B) compared to its parental AW8507 cells. The parental AW8507 cells were able to form tumors in nude mice, but tumors were smaller in size from the 70Gy-AW13516 mice tumors and they start regressing after 4th or 6th week of injection.

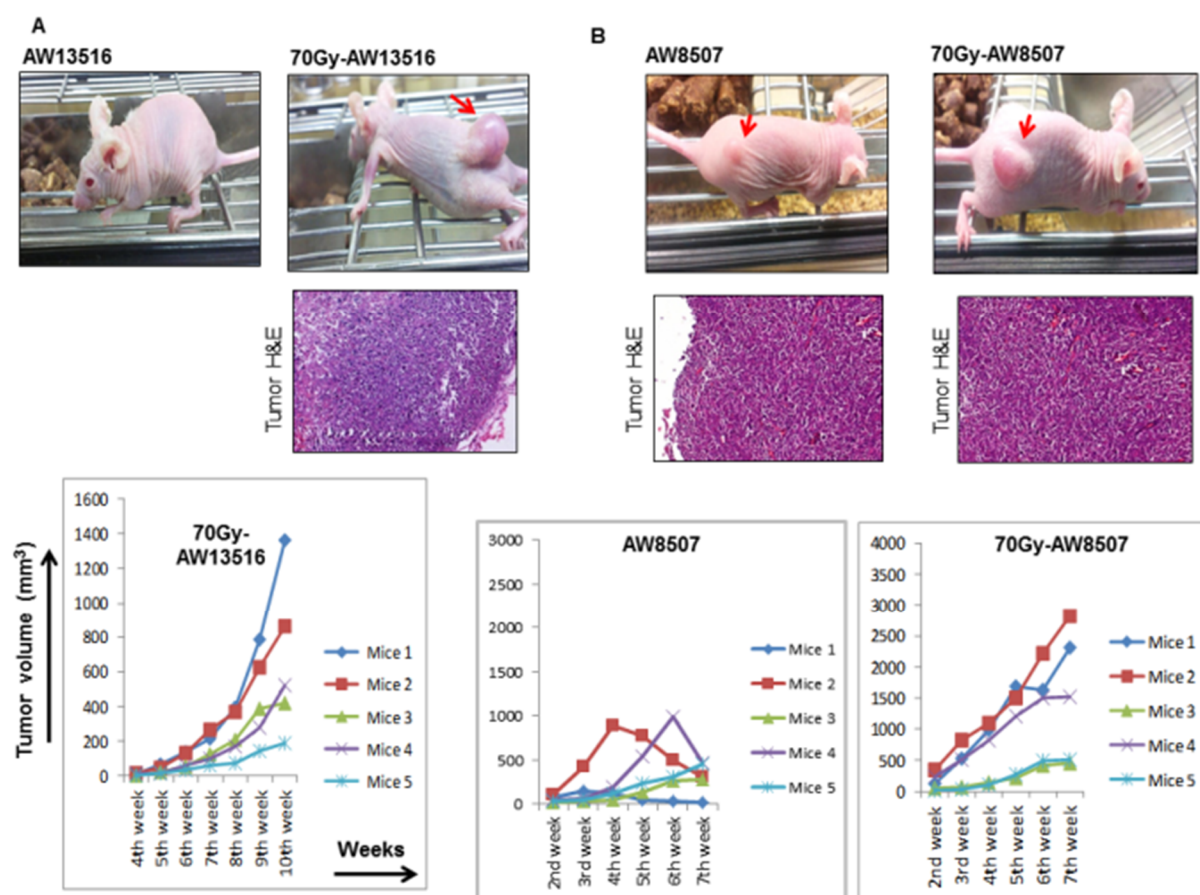


Figure 42: Cells injected into BALB/c Nude mice. 5×10^6 parental and radioresistant cells were injected into the dorsal flank of mice ($n = 5$ per group) and weekly tumor measurement were taken. (A) Tumor formation by AW13516 & 70Gy-AW13516 cells. (B) AW8507 & 70Gy-AW8507. The H & E staining of the tumors are also shown under the respective set of mice.

The third set of radioresistant cells (70Gy-UPCI:SCC029B) however failed to form tumors in Nude mice, even after 3-4 months of observation. Whereas, its parental UPCI:SCC029B cells formed fluid filled out growth that start oozing out after few weeks of injection (Figure 43-A). Therefore, this third set of radioresistant cells (UPCI:SCC029B & 70Gy-UPCI:SCC029B) were tested in another strain of mice i.e NOD-SCID mice. As shown in Figure 43-B, the parental UPCI:SCC029B cells formed similar fluid filled bulging's but

when it was dissected, a small solid mass of tumor was observed (confirmed by H & E), suggesting their ability to form tumor along with fluid filled bulges which may be the property of this cell line. On the other hand, radioresistant 70Gy-UPCI:SCC029B cells formed solid tumors (Figure 43-B), but the onset of the tumors was very late (starts appearing after ~ 3 months & very slow growing). Due to this property of late onset tumors in the third set and also time constraints, this was not tested in more number of animals.

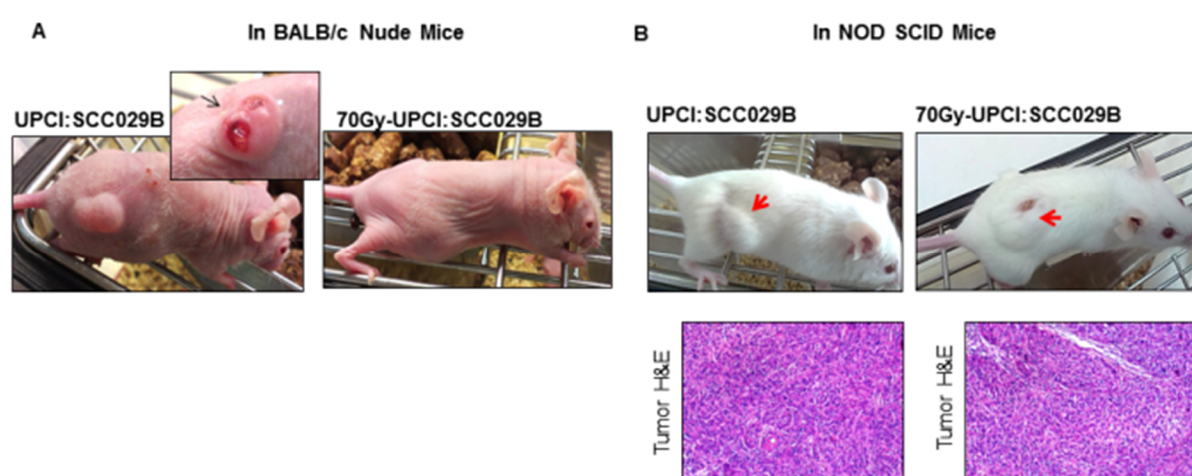


Figure 43: Cells injected into BALB/c Nude and NOD-SCID mice. 5×10^6 parental and radioresistant cells were injected into the dorsal flank of mice ($n = 5$ per group) and weekly tumor measurement were taken. (A) Fluid filled bulge formation by UPCI:SCC029B cells (arrow indicates fluid discharge, after few weeks), while 70Gy-UPCI: SCC029B cells show no growth in BALB/c Nude (B) Tumor formation by UPCI:SCC029B & 70Gy-UPCI:SCC029B cells in NOD-SCID mice. The H & E staining of the tumors is also shown in the respective set of mice.

5.5 Raman spectroscopic study for the Radioresistant sublines

Taking the emerging advantage of Raman spectroscopy (RS) in the field of biomedicine, we have performed RS study to gain insight into the Raman profile for our established radioresistant sublines. The importance of RS in context to biomedical applications and various cancer studies (both *in-vivo* & *in-vitro*) has been described in section 2.10 c. The Raman spectra for the parental and established radioresistant cancer cells of UPCI:SCC029B set, that belongs to oral buccal subsite were recorded from its cell pellets and we attempted to identify their differential Raman spectral signature profile. The identification of the unique Raman spectral features of buccal radioresistant cancer cells will help in further studies related to Raman spectroscopy based classification of oral buccal cancer patient response to radiation treatment. As incidence of oral buccal cancer cases is high in Indian population, due to habit of placing tobacco inside the buccal cavity and it is also an accessible site for examination with Raman molecular probes.

5.5.1 Mean Raman spectra for the Parental UPCI:SCC029B and Radioresistant 50Gy- UPCI:SCC029B and 70Gy- UPCI:SCC029B sublines

The mean normalized spectra for parental UPCI:SCC029B cell line, radioresistant 50Gy and 70Gy-UPCI:SCC029B sublines were computed and depicted in Figure 44. The 50Gy and 70Gy are two radioresistant sublines, established from parental UPCI:SCC029B cells by 25 and 35 fractions of 2Gy radiation doses (as described earlier). Since, oral cancer patients receive 50Gy to 70Gy radiations during a course of radiotherapy regime; these two populations were included in the study along with its parental cells.

Mean spectrum has been used as a representative spectrum for the respective population in the spectral analysis.

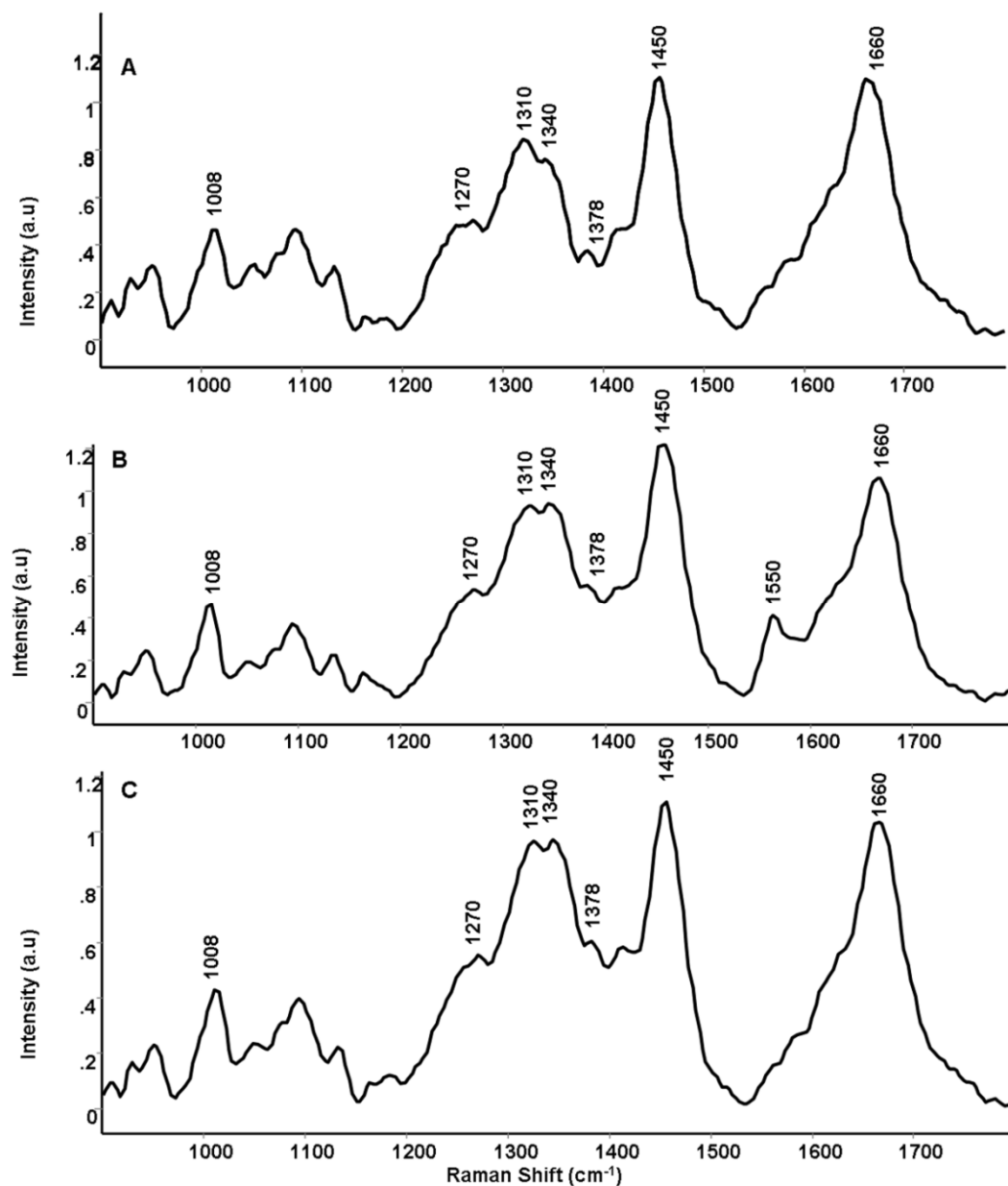


Figure 44: Mean Raman spectra of parental and radioresistant sublines (A) Parental UPCI:SCC029B cell line (B) Radioresistant 50Gy-UPCI:SCC029B subline (C) Radioresistant 70Gy-UPCI:SCC029B subline.

As, illustrated in Figure 44, the spectral features of parental and radioresistant sublines of UPCI:SCC029B cells were dominated by bands around 1008 (assigned to - phenylalanine), 1270 (amide III), 1450 (δ CH₂) and 1660 (amide I) cm⁻¹ and may be attributed to cellular proteins. Whereas, bands at 1310 (CH₃/CH₂) twisting or bending modes of lipid), 1340 (ring structure of adenine) and 1378 cm⁻¹ (ring breathing modes of nucleic acid) suggest presence of cellular nucleic acid and lipids. The Mean spectra for 50Gy-UPCI:SCC029B cells (Figure 44-B) show shift around 1310, 1450 and 1660 cm⁻¹; while a prominent peak was observed at 1550 cm⁻¹ (tryptophan). Similarly, in the Mean spectra of radioresistant 70Gy-UPCI:SCC029B cells (Figure 44-C) intensity related variations at 1270, 1310, 1340 and 1660 cm⁻¹ whereas a shift at 1450 cm⁻¹ were observed. Thus, it can be observed that, overall differences in the form of shifts in Raman bands and intensity variations were observed in the average spectra of both the 50Gy and 70Gy groups.

5.5.2 Difference Raman spectra between the parental and radioresistant sublines of UPCI:SCC029B

In order to bring out spectral differences among the groups, the ‘difference spectra’ were calculated from the Mean spectra. The ‘difference spectra’ provide a more clear illustration for the differences among various groups. As shown in Figure 45, the ‘difference spectra’ were computed for 50Gy-UPCI:SCC029B and 70Gy- UPCI:SCC029B cells by subtracting them from parental UPCI: SCC029B cell spectra (Figure 45- A & B) and between the two radioresistant cell spectra (Figure 45- C). The ‘difference spectrum’ (50Gy - parental) exhibited positive peaks at 1008, 1340, 1378, 1450, 1550, 1664 cm⁻¹ and negative peaks at 1240 and 1310 cm⁻¹; suggesting changes in proteins and nucleic acids, possibly due to altered cell signaling cascades caused by fractionated irradiation. The noticeable change at 1550 cm⁻¹ in 50Gy cells is indicative of freely accessible tryptophan possibly as a result of protein

folding/ misfolding by activated chaperones due to radiation stress. Similarly, in difference spectrum (70Gy - parental) positive peaks were observed at 1340 and 1378 cm^{-1} which is associated with DNA, whereas negative peak were observed at 1240, 1450 and 1650 cm^{-1} associated with protein change.

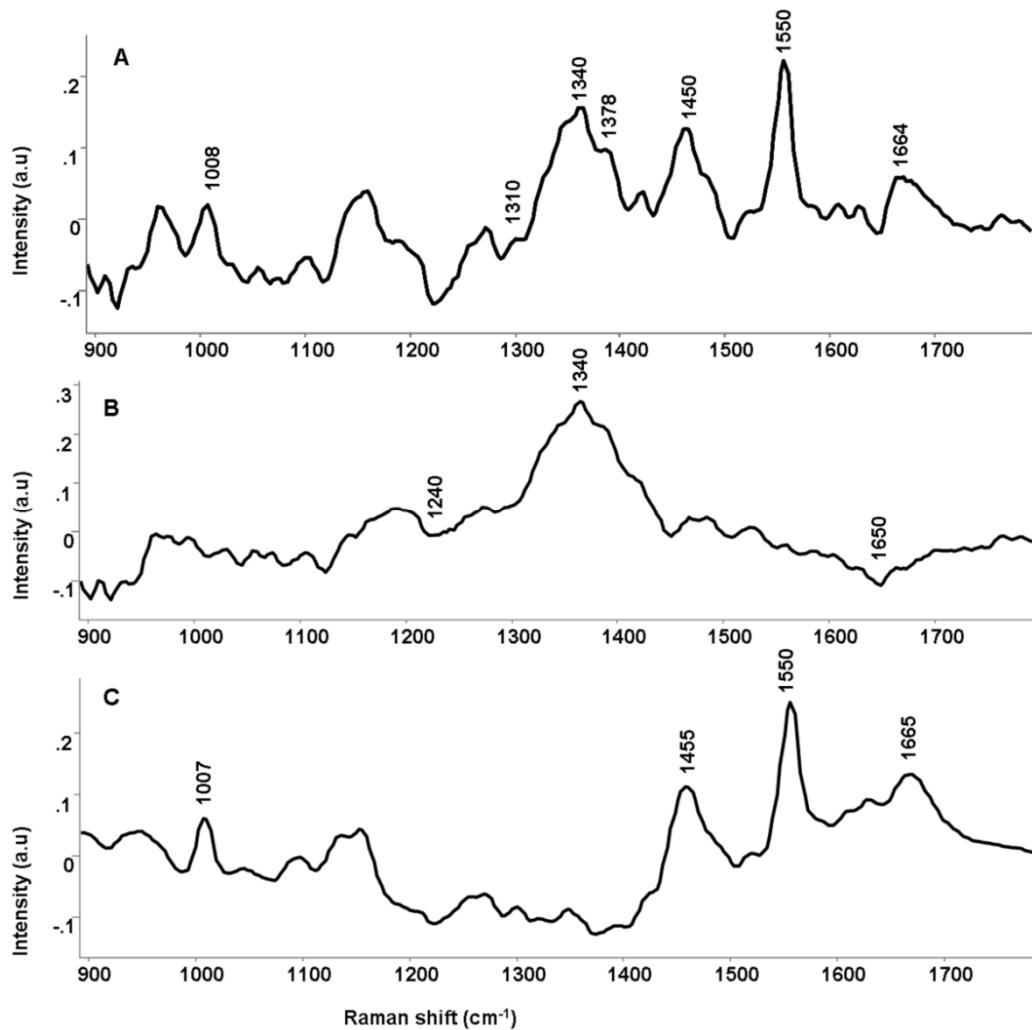


Figure 45: Difference Raman spectra of parental and radioresistant sublines. (A) Radioresistant 50Gy-UPCI: SCC029B subline – parental UPCI:SCC029B cell line (B) Radioresistant 70Gy-UPCI:SCC029B subline – parental UPCI:SCC029B cell line (C) 50Gy-UPCI:SCC029B subline – 70Gy-UPCI:SCC029B subline.

As shown by the clonogenic assay below (Figure 46), both the 50Gy-UPCI:SCC029B and 70Gy-UPCI:SCC029B cells have acquired radioresistant character as compared to parental cells. Also, 70Gy cells are relatively more radioresistant than 50Gy cells and exhibit distinct difference spectra, which may be due to different properties acquired by them.

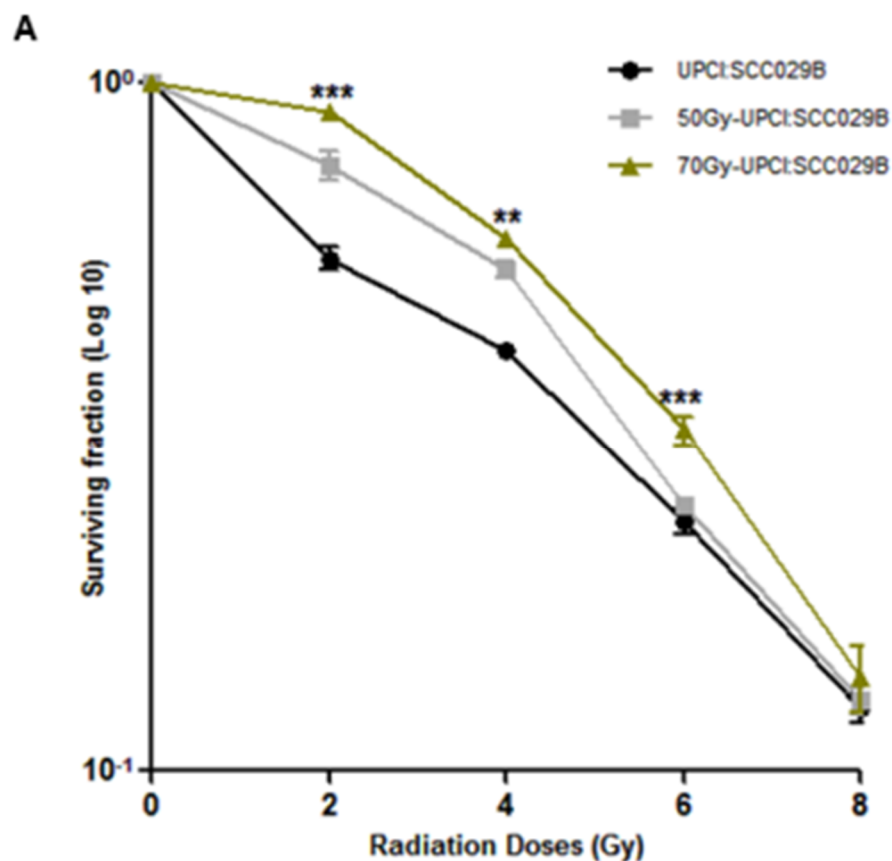


Figure 46: Clonogenic cell survival curve parental, 50Gy & 70Gy cells. (A) UPCI:SCC029B parental cells, 50Gy-UPCI:SCC029B intermediate radioresistant cells and 70Gy-UPCI:SCC029B final radioresistant cells. Data is represented as percentage survival of cells with mean (\pm SD) of three independent experiments. One-way ANOVA statistical analysis was performed on surviving fractions at the given doses, $p, 0.01$ & 0.001 .

Moreover, the (50Gy-70Gy) difference spectrum showed positive peaks at 1008, 1450, 1550 and 1664 cm^{-1} all related to proteins while DNA related negative peak was observed at 1378 cm^{-1} . The presence of prominent positive tryptophan peak (1550 cm^{-1}) in 50Gy radioresistant subline hints towards the enriched tryptophan moieties that may have anti-oxidative property because of the indolic group which serves as hydrogen radical donor [234]. Since, ionizing radiations can induce reactive oxygen species (ROS) production that can cause endogenous attack on the deoxyribosyl backbone of DNA [235,236]. To counteract the effects of ROS, cells have several antioxidant factors that can scavenge ROS and protect against radiation induced damage [237]. The distinct tryptophan residue peak in 50Gy radioresistant cells might correlate with such factors that are rich in these residue types and shields the cell against oxidative stress. The upregulation of these factors have also been reported in the context of radioresistance [238,239,240]. Moreover, the recorded spectrum may result in an average and representative spectrum of the given cell line that reflects an overall information of the cell status; because in a cell pellet, the probing beam encounters a stack of cells and scattering can be expected from different organelles like nucleus, mitochondria and other cellular compartments.

5.5.3 Multivariate analysis

As mentioned above, PCA was used to explore the feasibility of classification among radioresistant 50Gy and 70Gy sublines from the parental cell line. PCA is a frequently used method for data compression and visualization to observe the pattern in the data. It is a mathematical analysis by which the features in the whole data set of thousands of points are resolved into a few significant eigenvectors that can express the entire data set with their scores for each spectrum. This can provide imperative clues on biochemical variations among different groups, in our case different classes of macromolecules. Further, the profiles of

principal components also known as factor loadings can provide vital clues on biochemical variations among different classes. Loading of factors 1, 2 and 3 that lead to demarcation among groups are presented in Figure 47- A.

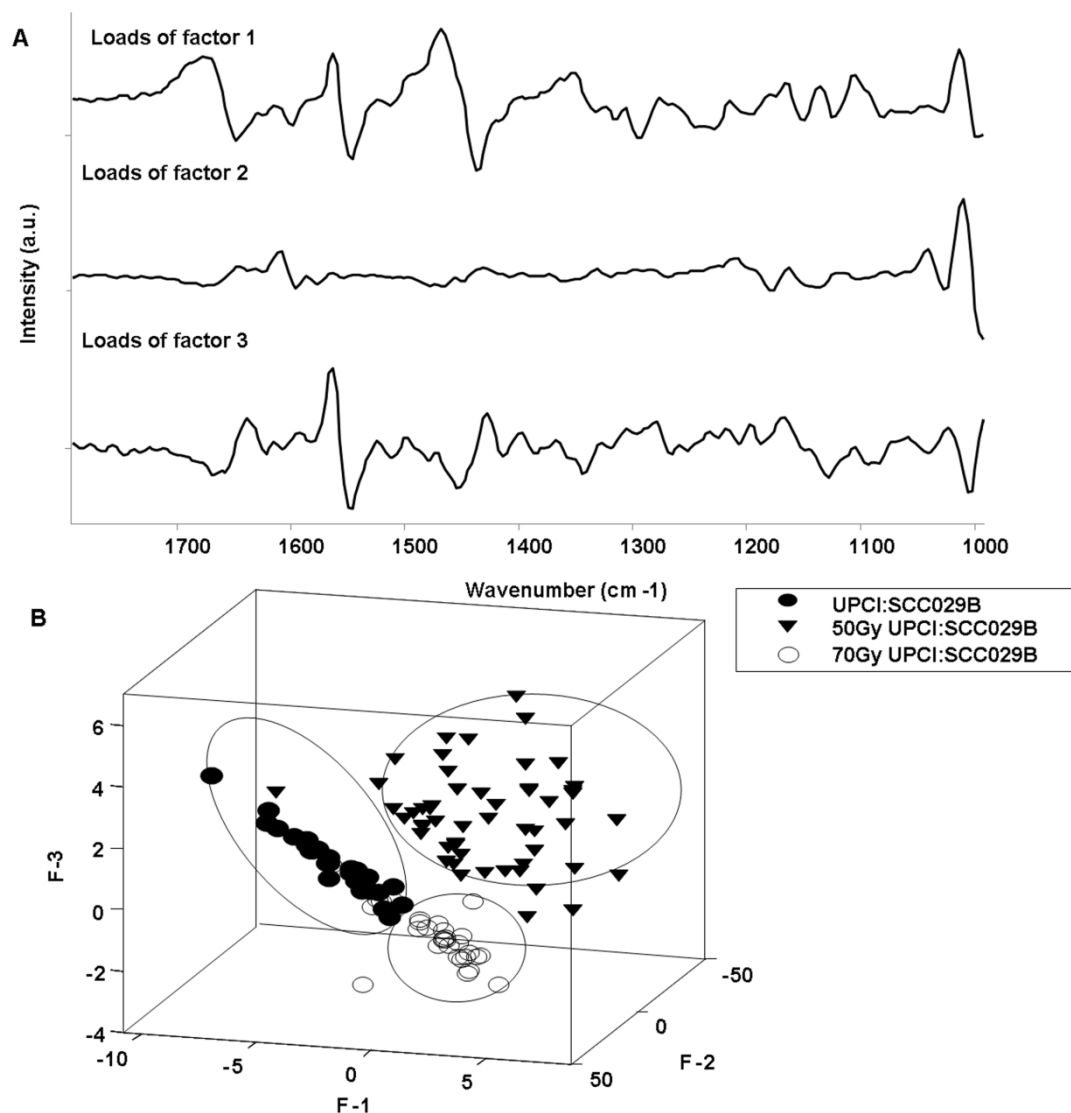


Figure 47: PCA analysis for parental and radioresistant sublines. (A) Loads of factor 1, 2 and 3 (B) 3-D scatter plot for parental UPCI:SCC029B cell line, radioresistant 50Gy-UPCI:SCC029B and 70Gy-UPCI:SCC029B sublines.

Conforming spectral variability as suggested by difference spectra; the loading plots also indicate differences in DNA content, amino acids and protein profiles of parental and radioresistant groups. For visual discrimination, we project each of the spectra in the newly formed coordinate space of selected PCs. First three significant discriminating PCs were selected for three-dimensional visualization of the data. Three clusters belonging to parental UPCI:SCC029B cells and radioresistant 50Gy- UPCI:SCC029B, 70Gy-UPCI:SCC029B cells were observed (Figure 47- B). While 50Gy-UPCI: SCC029B cells formed a separate cluster and a slight overlap between the clusters of 70Gy-UPCI:SCC029B and parental cells was observed. These patterns of observed clustering may be due to overall different biochemical profile acquired by the cell types. Taking in view that PCA will reveal an overall change including the various cellular profiles; it indicates that radioresistant cells have acquired an altered molecular profile different from its parental cells with subtle variations.

5.6 cDNA Microarray profile of Parental and Radioresistant cells

In order to examine the transcriptomic profile of the radioresistant cells, cDNA microarray was performed on the two sets of parental and established radioresistant sublines i.e UPCI:SCC029B/70Gy-UPCI:SCC029B and AW13516/70Gy-AW13516, which belongs to two different oral subsites (i.e Buccal Mucosa & Tongue). Figure 48 represent the clustering expression images for differentially expressed genes of both sets. The array details and brief procedure for the same has been described in section 4.2.22. The microarray was done in duplicates for both the sets of parental and radioresistant cells and the RNA quality and QC report is briefed in appendix 2.

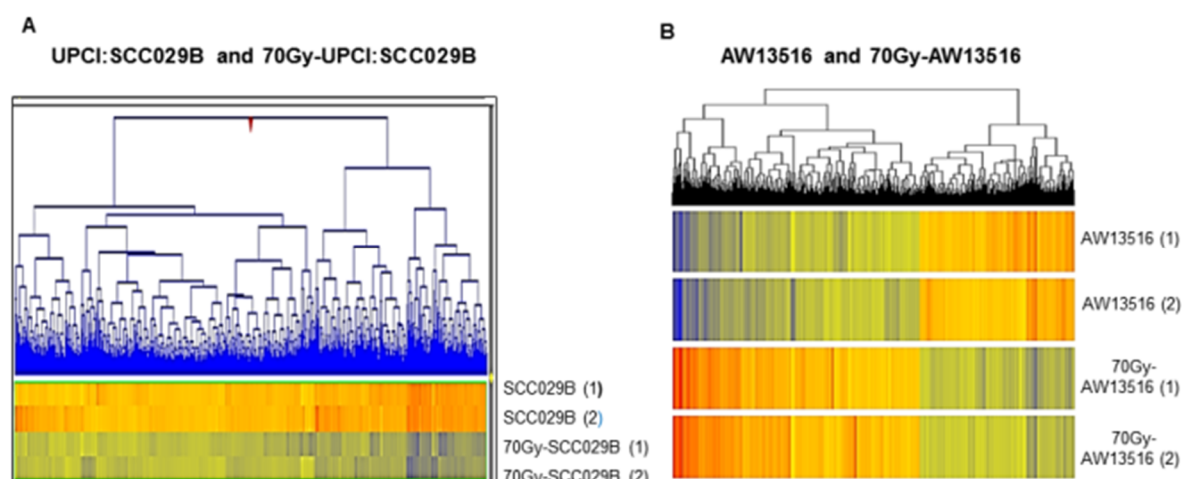


Figure 48: Hcl clustering expression image for differentially expressed genes. (A) parental UPCI:SCC029B and radioresistant 70Gy-UPCI:SCC029B (B) parental AW13516 and radioresistant 70Gy-AW13516. Replicate experiment of parental & radioresistant cells are clustered in the same clusters and displayed similar type of expression profile. Red color shows over-expressed genes (>2.0) & Blue color shows under-expressed genes (<2.0). The Hcl heat map image has been generated on the basis of \log_2 normalized intensity values for significant genes, $p \leq 0.05$.

5.6.1 Differentially expressed genes for UPCI:SCC029B & 70Gy-UPCI: SCC029B cells

In UPCI:SCC029B/70Gy-UPCI:SCC029B set; among the 23,312 DEGs with $p < 0.05$, a total of 2530 genes demonstrate ≥ 2 fold expression. Among these 2530 genes; 1378 genes were found to be upregulated and 1152 were down regulated.

5.6.2 Differentially expressed genes for AW13516 & 70Gy-AW13516 cells

Among the 12,092 DEGs with $p < 0.05$ in AW13516 / 70Gy-AW13516 set, a total of 1940 genes demonstrate ≥ 2 fold expression. Among these 1940 genes; 1190 genes were found to be upregulated and 750 were down regulated.

The complete list of differentially expressed genes (DEGs) in the microarray experiment for both the sets with fold change ≥ 2 and $p \leq 0.05$ were enlisted in appendix 5.

5.6.3 Validation of Microarray result by some randomly selected genes

The microarray result was validated by analyzing few randomly selected genes by Real time PCR using cDNA of UPCI:SCC029B and 70Gy-UPCI:SCC029B cells. As mentioned in Figure 49, the fold change values deduced by real time PCR (by $2^{-\Delta\Delta CT}$ method [213]) for NOTCH 2, HIF 1 α , IL 8, BECN 1, NIBRIN, PARVA and STRAP were found to be similar with the fold change values determined by the microarray experiment.

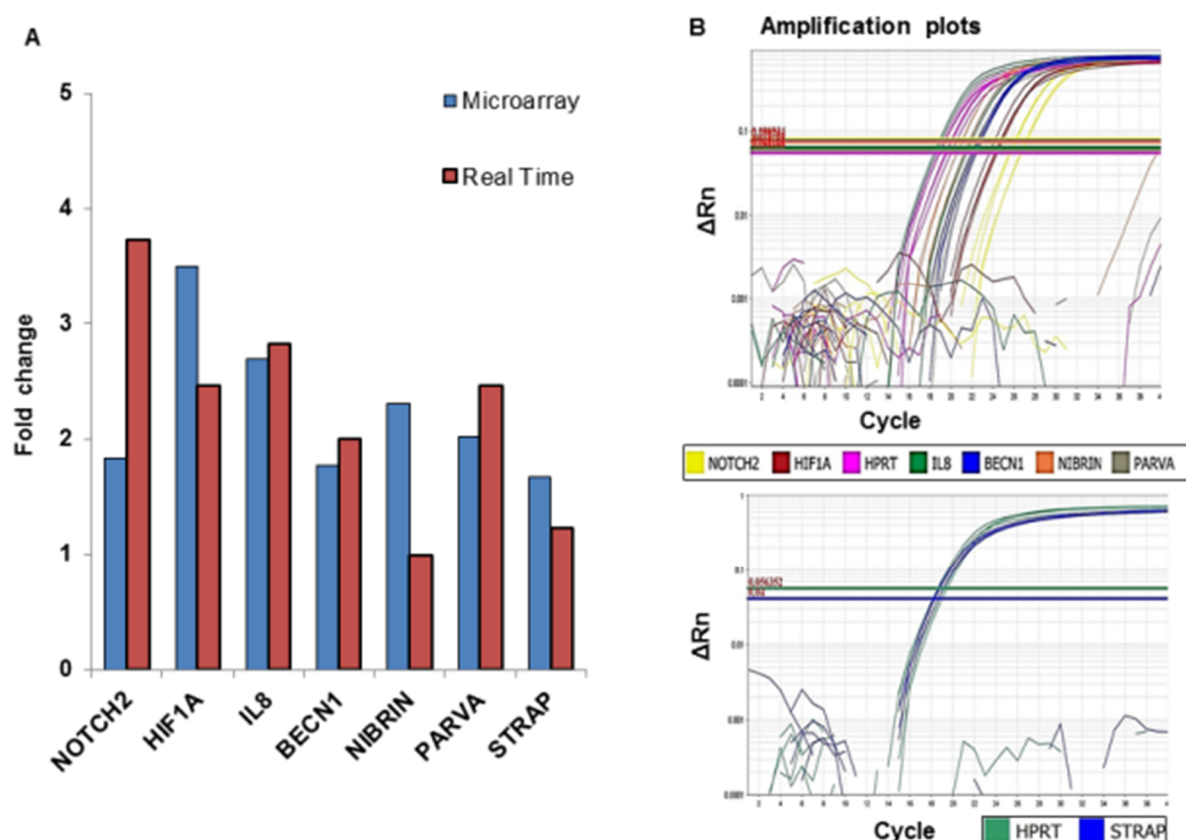


Figure 49: Microarray validation by real time PCR using the cDNA of UPCI:SCC029B and 70Gy-UPCI: SCC029B cells. (A) Graph shows comparison of microarray and real time PCR fold change values for some of these randomly selected genes, HPRT was used as internal

control and $2^{-\Delta\Delta CT}$ method applied for calculating fold change values. Note: The microarray fold change values represented here are the raw fold change values and not the log 2 fold changes.

5.6.4 Overlapping of Proteomic and Transcriptomic identities

Next, the differential proteomic (from 2D) and transcriptomic profile (cDNA microarray) of both the parental & radioresistant cells were compared and overlapping identities were obtained.

Table 22: Overlapped transcriptomic and proteomic id's in UPCI:SCC029B /70Gy-UPCI:SCC029B and AW13516 / 70Gy-AW13516 cells.

UPCI:SCC029B & 70Gy- UPCI:SCC029B set * <u>24 identities out of 32 Proteomic Identities</u>	AW13516 & 70Gy-AW13516 set * <u>13 identities out of 25 Proteomic Identities</u> ** <u>(D) = Down regulated</u>
Heat Shock Cognate 71kDa Protein (HSPA8)	Heat Shock Cognate 71kDa Protein (HSPA8)
Phosphoglycolate phosphatase	Phosphoglycolate phosphatase
Heat shock 70kDa protein 1A/1B	GRP 78 (HSPA5)
Endoplasmic (GRP 94)	Endoplasmic (GRP 94)
Protein disulfide Iso. family A3	Heat shock 70kDa protein 1A/1B
Stress induced phospho-protein 1	PKI M1/M2 (PKM) (D)
GRP 78 (HSPA5)	FUBP 1 (D)
Transketolase (D)	Plastin-2 (LCP1)
Mito Inner Membrane Pro (IMMT)	Eukaryotic elongation factor Tu (D)
Elongation Factor 2	Spermin synthase (SRM)
Cortactin (CTTN) (D)	Moesin
Rho GDP Dissoc. Inhibitor 1	TCP 1 Theta
Pyrroline 5 Carboxylate reductase 3	Phospho glycerate kinase 1

(PYCRL)		
Annexin A1		
Alanine-tRNA ligase (AARS)		
Plastin-2 (LCP1) (D)		
HSP60 (HSPD1)		
Cytoplasmic aconitate (ACO1)		
Eukaryotic translation initiation factor 2		
Hypoxia Upregulated 1		
TCP 1 Beta		
Calumenin		
40S ribosomal protein SA		
F Actin Capping Protein Alpha (CAPZA1)		

In UPCI:SCC029B & 70Gy-UPCI:SCC029B set, 24 identities out of its 32 proteomic id's were found to be differentially regulated at transcript level (Table 22, left pannel) and 07 were transcripts of the 08 common proteomic identities. Similarly, in AW13516 & 70Gy-AW13516 set, 13 identities were found to be differentially regulated at transcript level, from its 25 proteomic id's (given in section 5.2.5) obtained from the 2D result. These are enlisted in the following Table 22- right panel. Among these 13 identities, 06 were the transcripts of the 08 common proteomic identities. Thus, the 2D identified proteins are also showing differential expression at the transcript level, for both the sets of parental and radioresistant cells.

5.6.5 Functional annotations for the DEGs with different curated databases

To interpret the biological functions of the differentially expressed genes (DEGs), we have performed advanced analysis of microarray data with different curated database like,

PANTHER (Protein Analysis Through Evolutionary Relationships), REACTOME and KEGG (Kyoto Encyclopedia of Genes and Genomes).

Panther is a comprehensive open source software system for inferring the functions of genes based on their evolutionary relationships with an emphasis on signaling [221]. Reactome is also an open source, curated and peer-reviewed pathway database of human pathways and processes [222]. While, KEGG pathway database is a recognized and comprehensive database including all kinds of biochemistry pathways [223]. In the KEGG database resource are viewed as perturbed states of the molecular system and contains pathway maps for the molecular systems in both normal and diseased states.

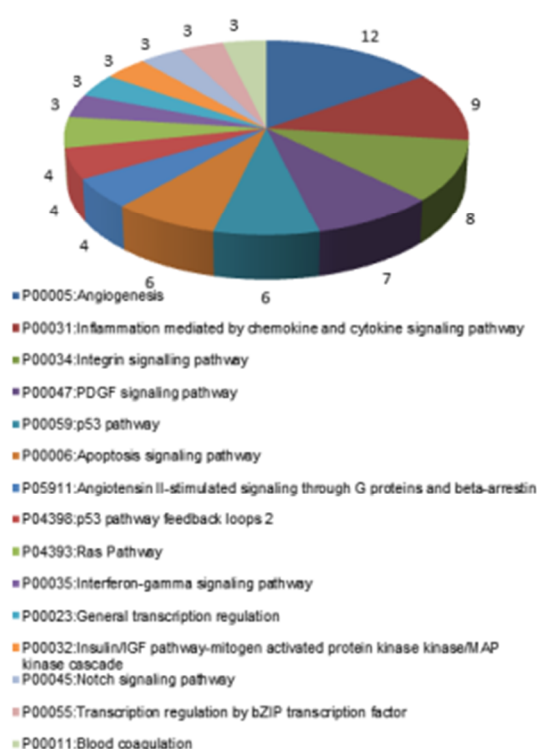
5.6.6 Reactome & Panther based functional annotations

The functional annotations based on Reactome & Panther databases was performed for the significant DEGs having fold change ≥ 3.0 values for the sets. These DEGs were carried out for batch annotation and protein term enrichment analysis to highlight the most relevant associated proteins by using DAVID functional annotation tool. The protein annotations for the mapped genes were performed using INTERPRO database in DAVID, which is based on enrichment analytic algorithm with annotation content coverage. This protein domain analysis helped in identifying the functional annotation for the up and down regulated genes.

For UPCI:SCC029B & 70Gy-UPCI:SCC029B set:

The pie charts in Figure 50, represents top up & down regulated pathways respectively for the genes showing ≥ 3 fold change difference, analysed by PANTHER in parental UPCI:SCC029B & radioresistant 70Gy-UPCI:SCC029B cells. The description of the genes involved in each of these pathways is enlisted in Table 23 and 24.

Top Fifteen Up Regulated Pathways (Panther_Pathway)



Top Fifteen Down Regulated Pathways (Panther_Pathway)

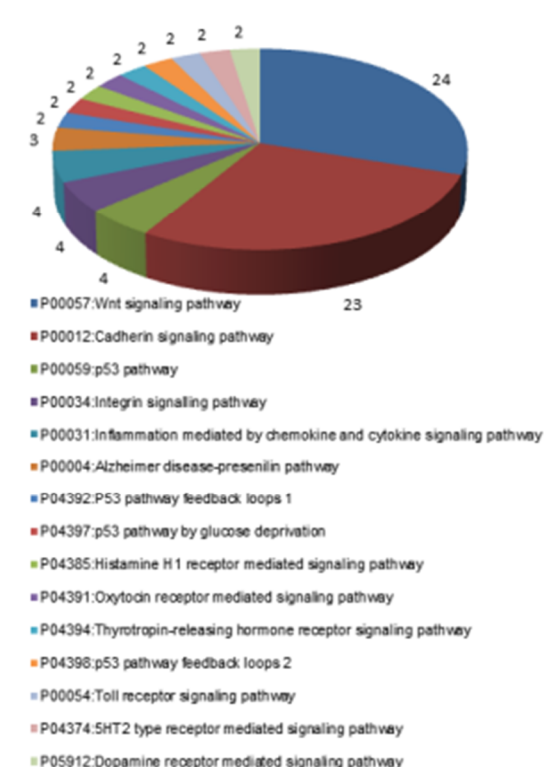


Figure 50: Pie charts illustrate top up and down regulated pathways in UPCI:SCC029B & 70Gy-UPCI :SCC029B cells by PANTHER_PATHWAY (Genes ≥ 3.0 fold change). Numbers in the pie chart represent the genes matched with the pathway.

Table 23: List of up regulated pathways in UPCI:SCC029B & 70Gy-UPCI :SCC029B cells by Panther pathway analysis (genes ≥ 3.0 fold change).

Term	Count	%	p value	Genes
P00005:Angiogenesis	12	4.270463	0.012768	WNT5A, FOS, HIF1A, F3, RHOA, JAK1, RHOB, PDGFC, BIRC5, CRK, EPHA3, AKT2
P00031:Inflammation mediated by chemokine and cytokine signaling pathway	9	3.202847	0.421518	PTGS2, IL8, ITGA6, RHOA, NFKBIA, JAK1, RHOB, IFNGR1, AKT2
P00034:Integrin signalling pathway	8	2.846975	0.250843	RND3, COL4A2, ITGA6, ITGAV, RHOA, RHOB, RAP1B, COL1A1
P00047:PDGF signaling pathway	7	2.491103	0.248328	FOS, ELF1, RHOA, ELK1, JAK1, RHOB, AKT2

P00059:p53 pathway	6	2.135231	0.148183	SIAH1, CCNG1, GADD45B, THBS1, IGFBP3, AKT2
P00006:Apoptosis signaling pathway	6	2.135231	0.183014	FOS, ATF3, TM6IM6, NFKBIA, HSPA5, AKT2
P05911:Angiotensin II-stimulated signaling through G proteins and beta-arrestin	4	1.423488	0.121068	EGR1, RHOA, ELK1, RHOB
P04398:p53 pathway feedback loops 2	4	1.423488	0.176496	SIAH1, RB1, CCNG1, AKT2
P04393:Ras Pathway	4	1.423488	0.353939	RHOA, ELK1, RHOB, AKT2
P00035:Interferon-gamma signaling pathway	3	1.067616	0.180341	SOCS2, JAK1, IFNGR1
P00023:General transcription regulation	3	1.067616	0.223451	POLR2E, TAF9B, POLR2C
P00032:Insulin/IGF pathway-mitogen activated protein kinase kinase/MAP kinase cascade	3	1.067616	0.302445	FOS, INS-IGF2, ELK1
P00045:Notch signaling pathway	3	1.067616	0.328644	HES1, ADAM10, PSEN1
P00055:Transcription regulation by bZIP transcription factor	3	1.067616	0.354592	POLR2E, TAF9B, POLR2C
P00011:Blood coagulation	3	1.067616	0.371706	F3, SERPINA1, PLAUI

Table 24: List of down regulated pathways in UPCI:SCC029B & 70Gy-UPCI :SCC029B cells by Panther pathway analysis (genes ≥ 3.0 fold change).

Term	Count	%	p value	Genes
P00057:Wnt signaling pathway	24	10.30043	8.66E-10	PCDHGA9, PCDHGA8, PCDHGC5, PCDHGA7, PCDHGC4, PCDHGA6, CDH1, PCDHGC3, PCDHGA5, PCDHGA4, CDH3, PCDHGA3, PCDHGA2, PCDHGA1, PCDHGB1, FAT2, PLCB1, PCDHGA12, PCDHGA10, TCF7, PCDHGA11, PCDHGB7, PCDHGB6, PCDHGB3, PCDHGB2, PCDHGB5, PCDHGB4
P00012:Cadherin signaling pathway	23	9.871245	1.10E-15	PCDHGA9, PCDHGA8, PCDHGC5, PCDHGA7, PCDHGC4, PCDHGA6, CDH1, PCDHGC3, PCDHGA5, PCDHGA4, CDH3, PCDHGA3, PCDHGA2, PCDHGA1, PCDHGB1, FAT2, PCDHGA12, TCF7, PCDHGA10, PCDHGA11, PCDHGB7, PCDHGB6, PCDHGB3, PCDHGB2, PCDHGB5, PCDHGB4

P00059:p53 pathway	4	1.716738	0.35108	TMEM47, SERPINB5, TP63, MDM4
P00034:Integrin signalling pathway	4	1.716738	0.75043	COL17A1, LAMA3, ITGAX, ITGB6
P00031:Inflammation mediated by chemokine and cytokine signaling pathway	4	1.716738	0.914187	RGS4, PLCG2, PLCB1, DCLK1
P00004:Alzheimer disease-presenilin pathway	3	1.287554	0.68117	TCF7, CDH1, CDH3
P04392:P53 pathway feedback loops 1	2	0.858369	0.116374	TP63, MDM4
P04397:p53 pathway by glucose deprivation	2	0.858369	0.391486	TP63, PRKAA2
P04385:Histamine H1 receptor mediated signaling pathway	2	0.858369	0.526198	PLCG2, PLCB1
P04391:Oxytocin receptor mediated signaling pathway	2	0.858369	0.65094	PLCG2, PLCB1
P04394:Thyrotropin-releasing hormone receptor signaling pathway	2	0.858369	0.657177	PLCG2, PLCB1
P04398:p53 pathway feedback loops 2	2	0.858369	0.669327	TP63, MDM4
P00054:Toll receptor signaling pathway	2	0.858369	0.681054	LY96, TLR2
P04374:5HT2 type receptor mediated signaling pathway	2	0.858369	0.703298	PLCG2, PLCB1
P05912:Dopamine receptor mediated signaling pathway	2	0.858369	0.789836	FRMD4B, EPB41L4B

*Count = No. of genes that map to this particular annotation data category. % = Share of genes compared to the total genes for the particular data category. p value represented here is for the particular pathway.

Similarly, pie chart representing the top up and down regulated pathways for the parental UPCI:SCC029B & radioresistant 70Gy-UPCI:SCC029B cells analysed by REACTOME is represented in Figure 51, while the corresponding gene list involved in each of these pathways are shown in Table 25 & 26.

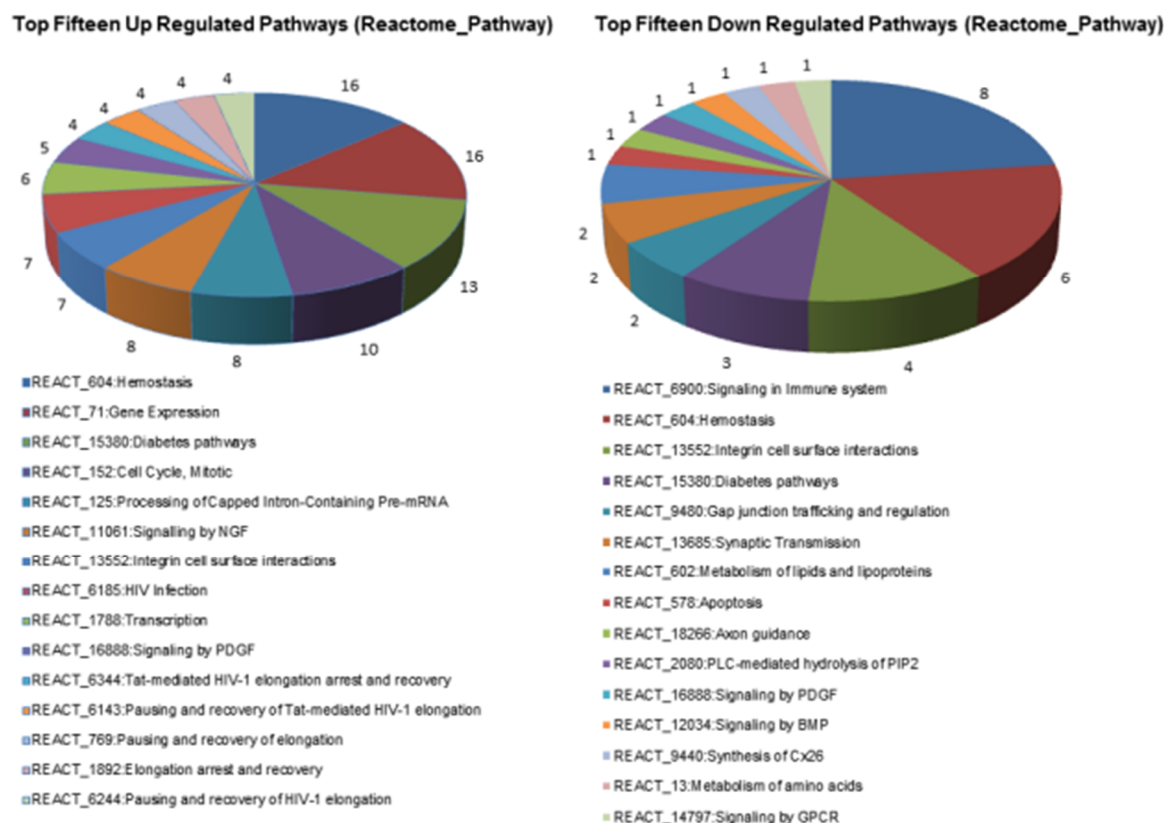


Figure 51: Pie chart showing top up and down regulated pathways in UPCI:SCC029B & 70Gy-UPCI:SCC029B cells by REACTOME_PATHWAY (Genes ≥ 3.0 fold change).

Table 25: List of up regulated pathways in UPCI:SCC029B & 70Gy-UPCI:SCC029B cells by Reactome pathway analysis (genes ≥ 3.0 fold change).

Term	Count	%	p value	Genes
REACT_604:Hemostasis	16	5.69395	0.001345	SLC3A2, SPARC, TGFB2, CALU, SLC16A1, ITGA6, PPIA, F3, ITGAV, RAP1B, SERPINA1, COL1A1, HSPA5, THBS1, CRK, PLA2
REACT_71:Gene Expression	16	5.69395	0.046704	POLR2E, TH1L, RPL15, RNPS1, EEF2, CCNC, QARS, NXF1, HNRNPA1, POLR2C, EIF2B1, PAPOLA, EIF4E, METTL3, EEF1G, TCEA1
REACT_15380:Diabetes pathways	13	4.626335	0.080422	UQCRC1, INS-IGF2, ALDOC, PGAM1, IGF2, COX7A2L, DNAJB9, ATF3, RAP1B, HSPA5, ATP5A1, IGFBP3, SERP1, IGFBP5
REACT_152:Cell Cycle, Mitotic	10	3.558719	0.441342	RAD21, MCM7, NDEL1, NEK2, PSMD2, BIRC5, CDC20, RB1, CDC16, TFDP1

REACT_125:Processing of Capped Intron-Containing Pre-mRNA	8	2.846975	0.028057	PAPOLA, POLR2E, EIF4E, METTL3, RNPS1, NXF1, POLR2C, HNRNPA1
REACT_11061:Signalling by NGF	8	2.846975	0.197213	PSEN1, RHOA, NFKBIA, ELK1, RICTOR, CLTC, CRK, AKT2
REACT_13552:Integrin cell surface interactions	7	2.491103	0.021276	COL4A2, ITGA6, ITGAV, RAP1B, COL1A1, THBS1, CRK
REACT_6185:HIV Infection	7	2.491103	0.380511	POLR2E, PPIA, TH1L, PSMD2, TCEA1, POLR2C, AP2M1
REACT_1788:Transcription	6	2.135231	0.280357	PAPOLA, POLR2E, TH1L, RNPS1, TCEA1, POLR2C
REACT_16888:Signaling by PDGF	5	1.779359	0.093588	COL4A2, PDGFC, COL1A1, THBS1, CRK
REACT_6344:Tat-mediated HIV-1 elongation arrest and recovery	4	1.423488	0.046029	POLR2E, TH1L, TCEA1, POLR2C
REACT_6143:Pausing and recovery of Tat-mediated HIV-1 elongation	4	1.423488	0.046029	POLR2E, TH1L, TCEA1, POLR2C
REACT_769:Pausing and recovery of elongation	4	1.423488	0.049991	POLR2E, TH1L, TCEA1, POLR2C
REACT_1892:Elongation arrest and recovery	4	1.423488	0.049991	POLR2E, TH1L, TCEA1, POLR2C
REACT_6244:Pausing and recovery of HIV-1 elongation	4	1.423488	0.049991	POLR2E, TH1L, TCEA1, POLR2C

Table 26: List of down regulated pathways in UPCI:SCC029B & 70Gy-UPCI :SCC029B cells by Reactome pathway analysis (genes ≥ 3.0 fold change).

Term	Count	%	p value	Genes
REACT_6900:Signaling in Immune system	8	3.433476	0.004512	ITGAX, LY96, TLR2, CDH1, PROS1, SIRPA, HLA-DRA, HLA-F
REACT_604:Hemostasis	6	2.575107	0.030093	CD36, ITGAX, PLCG2, PLCB1, PROS1, SIRPA
REACT_13552:Integrin cell surface interactions	4	1.716738	0.022864	ITGAX, ITGB6, CDH1, SPP1
REACT_15380:Diabetes pathways	3	1.287554	0.654494	KCNS3, CPE, PLCB1
REACT_9480:Gap junction trafficking and regulation	2	0.858369	0.206596	GJB6, GJB2
REACT_13685:Synaptic Transmission	2	0.858369	0.467211	GLUL, MDM2
REACT_602:Metabolism of lipids and lipoproteins	2	0.858369	0.692192	CH25H, HSD11B1
REACT_578:Apoptosis	1	0.429185	1	CDH1
REACT_18266:Axon guidance	1	0.429185	1	PRNP
REACT_2080:PLC-mediated hydrolysis of PIP2	1	0.429185	1	PLCG2
REACT_16888:Signaling by PDGF	1	0.429185	1	SPP1
REACT_12034:Signaling	1	0.429185	1	CHRD1

by BMP				
REACT_9440:Synthesis of Cx26	1	0.429185	1	GJB2
REACT_13:Metabolism of amino acids	1	0.429185	1	GLUL
REACT_14797:Signaling by GPCR	1	0.429185	1	CXCR7

For AW13516 & 70Gy-AW13516 set:

Figure 52, represents the pie chart of the top up and down regulated pathways for the parental AW13516 and radioresistant 70Gy-AW13516 cells, analysed by PANTHER. The corresponding list of genes involved in each of these pathways is shown in Table 27 & 28.

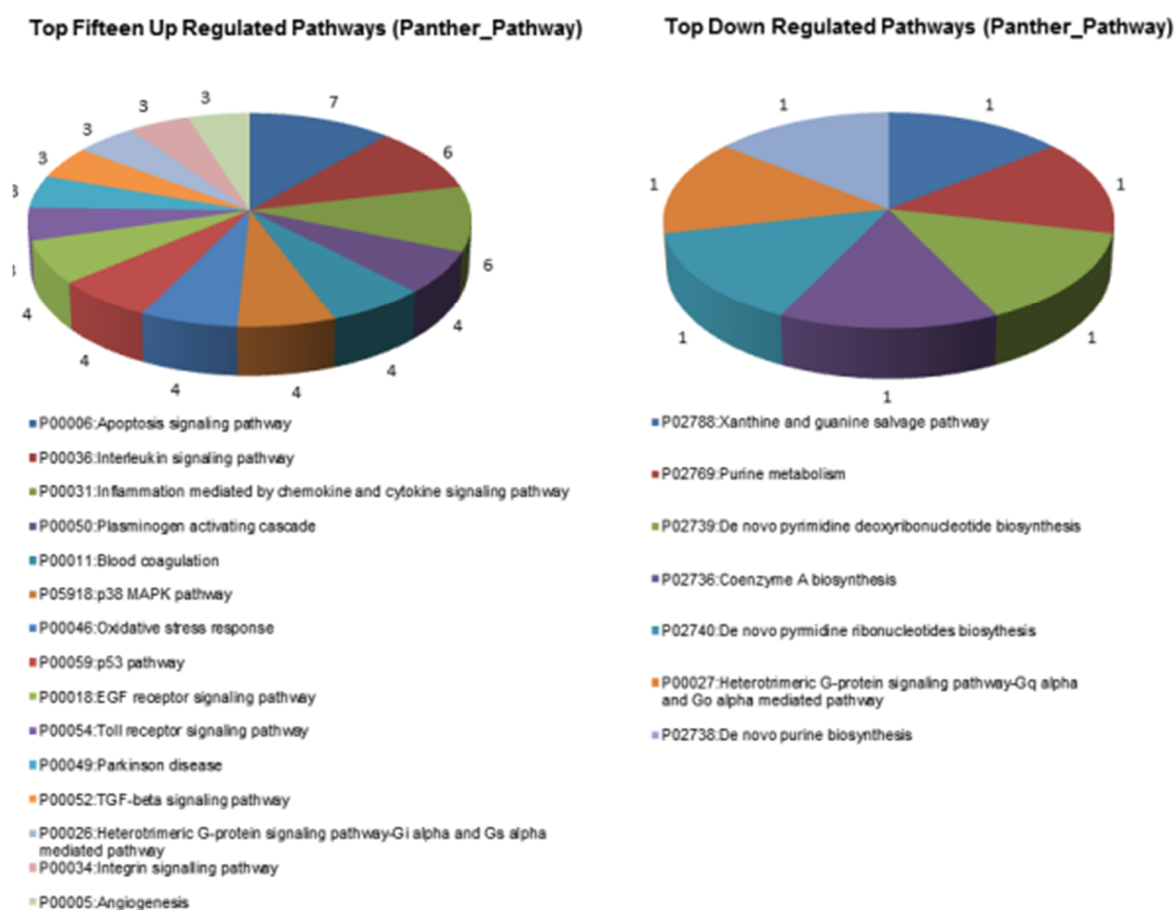


Figure 52: Pie chart showing top up and down regulated pathways in AW13516 & 70Gy-AW13516 cells by PANTHER_PATHWAY (Genes ≥ 3.0 fold change).

Table 27: List of up regulated pathways in AW13516 & 70Gy- AW13516 cells by Panther pathway analysis (genes ≥ 3.0 fold change).

Term	Count	%	p value	Genes
P00006:Apoptosis signaling pathway	8	3.910615	0.011619	FOS, ATF3, TNF, HSPA6, HSPA7, HSPA5, BIRC3, HSPA8
P00036:Interleukin signaling pathway	6	3.351955	0.210774	FOS, IL6, IL23A, C21ORF7, IL8, IL1A
P00031:Inflammation mediated by chemokine and cytokine signaling pathway	6	3.351955	0.488931	PLA2G4A, C21ORF7, PTGS2, IL8, CCL20, RGS3
P00050:Plasminogen activating cascade	4	2.234637	0.004008	SERPINE1, SERPINB2, MMP3, PLAU
P00011:Blood coagulation	4	2.234637	0.048456	SERPINE1, SERPINB2, SERPINA1, PLAU
P05918:p38 MAPK pathway	4	2.234637	0.048456	C21ORF7, DUSP1, DUSP10, GADD45A
P00046:Oxidative stress response	4	2.234637	0.07016	DUSP5, PLA2G4A, DUSP1, DUSP10
P00059:p53 pathway	4	2.234637	0.269342	SERPINE1, GADD45B, GADD45A, ATM
P00018:EGF receptor signaling pathway	4	2.234637	0.357287	EREG, TGFA, ATM, SPRY4
P00054:Toll receptor signaling pathway	3	1.675978	0.250379	C21ORF7, PTGS2, TNFAIP3
P00049:Parkinson disease	3	1.675978	0.458371	HSPA6, HSPA7, HSPA5, HSPA8
P00052:TGF-beta signaling pathway	3	1.675978	0.68025	FOS, C21ORF7, GDF15
P00026:Heterotrimeric G-protein signaling pathway-Gi alpha and Gs alpha mediated pathway	3	1.675978	0.745235	ADRB2, RGS2, RGS3
P00034:Integrin signalling pathway	3	1.675978	0.853948	RND3, LAMB3, RND1
P00005:Angiogenesis	3	1.675978	0.859356	PTPRJ, FOS, PLA2G4A

Table 28: List of down regulated pathways in AW13516 & 70Gy- AW13516 cells by Panther pathway analysis (genes ≥ 3.0 fold change).

Term	Count	%	p value	Genes
P02788:Xanthine and guanine salvage pathway	1	5.555556	1	GDA
P02769:Purine metabolism	1	5.555556	1	GDA
P02739:De novo pyrimidine deoxyribonucleotide biosynthesis	1	5.555556	1	DSCAM
P02736:Coenzyme A biosynthesis	1	5.555556	1	PANK1
P02740:De novo pyrimidine ribonucleotides	1	5.555556	1	DSCAM

biosynthesis				
P00027:Heterotrimeric G-protein signaling Pathway -Gq alpha and Go alpha mediated pathway	1	5.555556	1	SIPA1L2
P02738:De novo purine biosynthesis	1	5.555556	1	DSCAM

Similarly, The list of the top up or down regulated pathways for the parental AW13516 & radioresistant 70Gy- AW13516 cells, analysed by REACTOME is represented in Figure 53 and the corresponding genes identified in each of these pathways is shown in the Table 29 & 30.

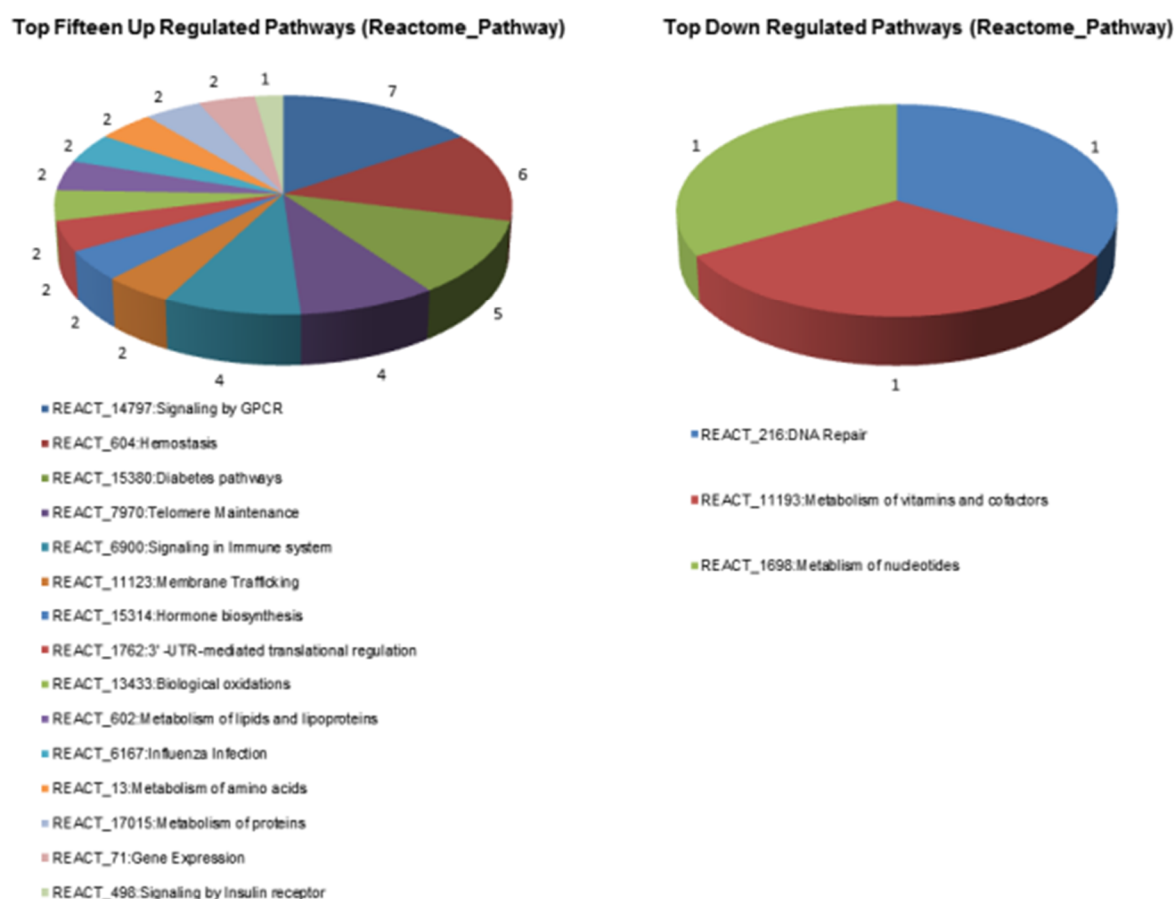


Figure 53: Pie chart showing top up and down regulated pathways in AW13516 & 70Gy- AW13516 cells by REACTOME _PATHWAY (Genes ≥ 3.0 fold change).

Table 29: List of up regulated pathways in AW13516 & 70Gy- AW13516 cells by Reactome pathway analysis (genes ≥ 3.0 fold change).

Term	Count	%	p value	Genes
REACT_14797:Signaling by GPCR	7	3.910615	0.757969	CXCL1, ADRB2, IL8, CCL20, CXCL3, CXCL2, GABBR1
REACT_604:Hemostasis	6	3.351955	0.128402	SERPINE1, SERPINB2, SERPINA1, HSPA5, PLA2, SRGN
REACT_15380:Diabetes pathways	5	2.793296	0.416061	HERPUD1, ATF3, INS-IGF2, IGF2, HSPA5, DDIT3
REACT_7970:Telomere Maintenance	4	2.234637	0.025487	HIST1H2AB, HIST2H2AA3, HIST2H2AA4, HIST1H2BD, HIST2H2BE, HIST1H2AE
REACT_6900:Signaling in Immune system	4	2.234637	0.649918	ICAM1, C3, CFB, HLA-B
REACT_11123:Membrane Trafficking	2	1.117318	0.378809	SEC24A, HSPA8
REACT_15314:Hormone biosynthesis	2	1.117318	0.453844	PTGS2, HSD11B1
REACT_1762:3' -UTR-mediated translational regulation	2	1.117318	0.718294	RPS18, RPL28
REACT_13433:Biological oxidations	2	1.117318	0.743953	PTGS2, SULT1C2
REACT_602:Metabolism of lipids and lipoproteins	2	1.117318	0.829821	ABCC3, HSD11B1
REACT_6167:Influenza Infection	2	1.117318	0.843632	RPS18, RPL28
REACT_13:Metabolism of amino acids	2	1.117318	0.854596	SAT1, KYNU
REACT_17015:Metabolism of proteins	2	1.117318	0.924879	RPS18, RPL28
REACT_71:Gene Expression	2	1.117318	0.985942	RPS18, RPL28
REACT_498:Signaling by Insulin receptor	1	0.558659	1	INS-IGF2, IGF2

Table 30: List of down regulated pathways in AW13516 & 70Gy- AW13516 cells by Reactome pathway analysis (genes ≥ 3.0 fold change).

Term	Count	%	p value	Genes
REACT_216:DNA Repair	1	5.555556	1	ERCC4
REACT_11193:Metabolism of vitamins and cofactors	1	5.555556	1	PANK1
REACT_1698:Metabolism of nucleotides	1	5.555556	1	GDA

The significantly expressed, top up and down regulated pathways from Panther & Reactome analysis for both of these sets are discussed in section 6.7, in the discussion chapter.

5.6.7 KEGG pathway enrichment analysis

The KEGG pathway analysis was performed by using KEGG Pathway Mapper with selection of species *Homo sapiens*.

For UPCI:SCC029B & 70Gy-UPCI:SCC029B set:

The pie charts in Figure 54 are showing the top up and down regulated KEGG enriched pathways for the parental UPCI:SCC029B & radioresistant 70Gy-UPCI:SCC029B cells. The matched genes for each of these pathways were enlisted in Table 31 & 32.

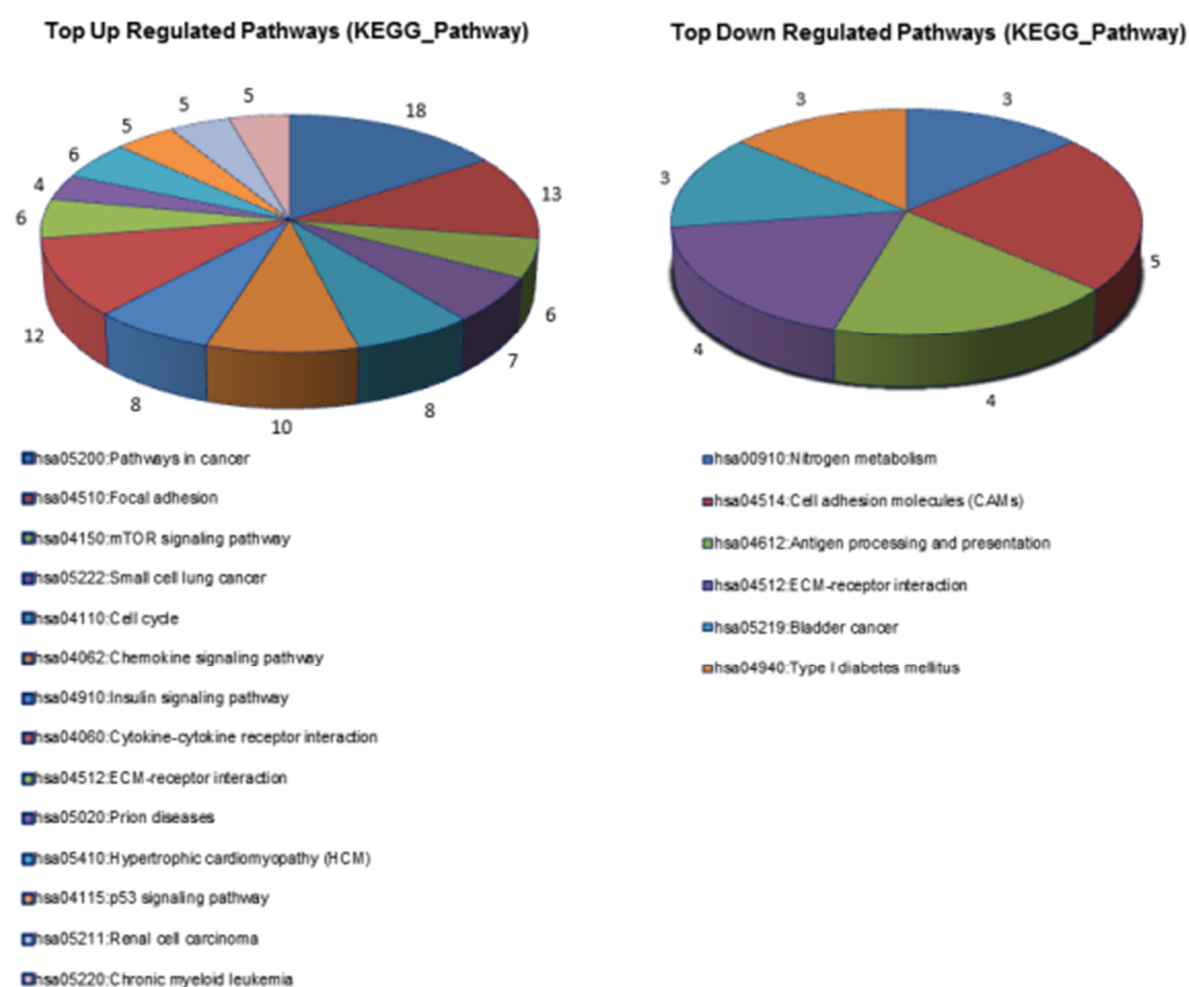


Figure 54: Pie chart showing top up and down regulated pathways in UPCI:SCC029B & 70Gy-UPCI:SCC029B cells by KEGG analysis (Genes ≥ 3.0 fold change).

Table 31: List of up regulated pathways in UPCI:SCC029B & 70Gy-UPCI:SCC029B cells by KEGG pathway analysis (genes ≥ 3.0 fold change).

Term	Count	%	p value	Genes
hsa05200:Pathways in cancer	18	6.405694	0.001335	WNT5A, COL4A2, IL8, PTGS2, NFKBIA, BIRC5, RB1, FZD6, TGFB2, TPM3, FOS, HIF1A, ITGA6, ITGAV, RHOA, JAK1, CRK, AKT2
hsa04510:Focal adhesion	13	4.626335	0.002236	ACTB, COL4A2, ELK1, PPP1CB, ITGA6, ITGAV, RHOA, PDGFC, RAP1B, COL1A1, THBS1, CRK, AKT2
hsa04150:mTOR signaling pathway	6	2.135231	0.00673	HIF1A, EIF4E, IGF2, PRKAA1, RICTOR, AKT2
hsa05222:Small cell lung cancer	7	2.491103	0.012833	COL4A2, PTGS2, ITGA6, ITGAV, NFKBIA, RB1, AKT2
hsa04110:Cell cycle	8	2.846975	0.025429	RAD21, MCM7, CDC20, RB1, CDC16, GADD45B, TFDPI, TGFB2
hsa04062:Chemokine signaling pathway	10	3.558719	0.028875	CXCL1, IL8, CXCL3, CXCL2, RHOA, NFKBIA, RAP1B, CXCL6, CRK, AKT2
hsa04910:Insulin signaling pathway	8	2.846975	0.036591	EIF4E, SOCS2, INS-IGF2, ELK1, IGF2, PRKAA1, CRK, PPP1CB, AKT2
hsa04060:Cytokine-cytokine receptor interaction	12	4.270463	0.039664	CXCL1, INHBA, TNFRSF21, TNFRSF11B, IL8, CXCL3, CXCL2, PDGFC, CXCL6, IFNGR1, IL11, TGFB2
hsa04512:ECM-receptor interaction	6	2.135231	0.044693	COL4A2, CD44, ITGA6, ITGAV, COL1A1, THBS1
hsa05020:Prion diseases	4	1.423488	0.04654	EGR1, ELK1, STIP1, HSPA5
hsa05410:Hypertrophic cardiomyopathy (HCM)	6	2.135231	0.046639	ACTB, ITGA6, ITGAV, PRKAA1, TGFB2, TPM3
hsa04115:p53 signaling pathway	5	1.779359	0.07224	SIAH1, CCNG1, GADD45B, THBS1, IGFBP3
hsa05211:Renal cell carcinoma	5	1.779359	0.078572	HIF1A, RAP1B, CRK, TGFB2, AKT2
hsa05220:Chronic myeloid leukemia	5	1.779359	0.095568	NFKBIA, RB1, CRK, TGFB2, AKT2

Table 32: List of down regulated pathways in UPCI:SCC029B & 70Gy-UPCI:SCC029B cells by KEGG pathway analysis (genes ≥ 3.0 fold change).

Term	Count	%	p value	Genes
hsa00910:Nitrogen metabolism	3	1.287554	0.025132	GLUL, CA12, CA2
hsa04514:Cell adhesion molecules (CAMs)	5	2.145923	0.053502	CDH1, CDH3, PDCD1LG2, HLA-DRA, HLA-F
hsa04612:Antigen processing & presentation	4	1.716738	0.059998	CTSB, CD74, HLA-DRA, HLA-F
hsa04512:ECM-receptor interaction	4	1.716738	0.061759	CD36, LAMA3, ITGB6, SPPI
hsa05219:Bladder cancer	3	1.287554	0.075139	MDM2, CDH1, DAPK1
hsa04940:Type I diabetes mellitus	3	1.287554	0.075139	CPE, HLA-DRA, HLA-F

For AW13516 & 70Gy- AW13516 set:

Similarly, the list of the top up and down regulated pathways for the parental AW13516 & radioresistant 70Gy- AW13516 cells, analysed by KEGG is represented in Figure 55 and the list of identified genes in each of these pathways in Table 33 & 34.

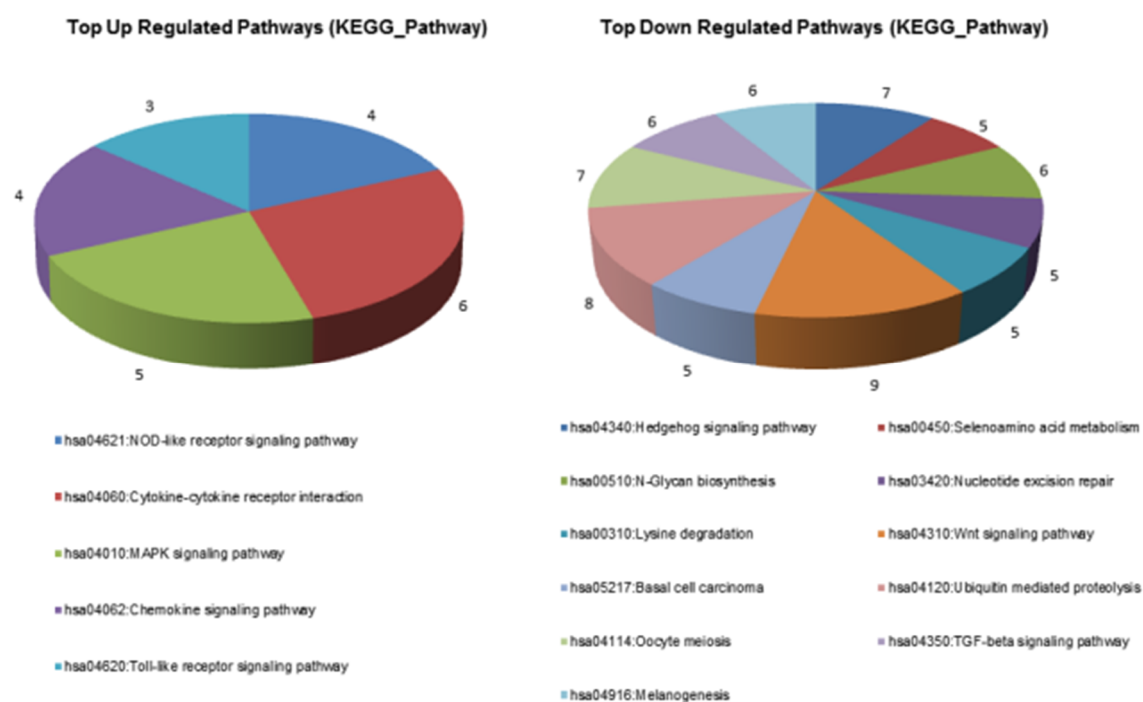


Figure 55: Pie chart showing top up and down regulated pathways in AW13516 & 70Gy- AW13516 cells by KEGG analysis (Genes ≥ 3.0 fold change).

Table 33: List of up regulated pathways in AW13516 & 70Gy- AW13516 cells by KEGG pathway analysis (genes ≥ 3.0 fold change).

Term	Count	%	p value	Genes
hsa04621:NOD-like receptor signaling pathway	4	10.52632	0.001236	IL8, CXCL2, IL1B, TNFAIP3
hsa04060:Cytokine-cytokine receptor interaction	6	15.78947	0.00172	CSF2, IL8, CCL20, CXCL3, CXCL2, IL1B
hsa04010:MAPK signaling pathway	5	13.15789	0.012679	FOS, DUSP10, HSPA6, IL1B, HSPA7, DDIT3
hsa04062:Chemokine signaling pathway	4	10.52632	0.026576	IL8, CCL20, CXCL3, CXCL2
hsa04620:Toll-like receptor signaling pathway	3	7.894737	0.048612	FOS, IL8, IL1B

Table 34: List of down regulated pathways in AW13516 & 70Gy- AW13516 cells by KEGG pathway analysis (genes ≥ 3.0 fold change).

Term	Count	%	p value	Genes
hsa04340:Hedgehog signaling pathway	7	1.375246	0.001586	BTRC, RAB23, PTCH1, GAS1, GLI2, GLI3, PRKX
hsa00450:Selenoamino acid metabolism	5	0.982318	0.002608	SEPHS2, SEPHS1, MAT2A, SCLY, LCMT2
hsa00510:N-Glycan biosynthesis	6	1.178782	0.003682	MGAT2, ALG10B, ALG2, ALG6, ALG10, UTP14C
hsa03420:Nucleotide excision repair	5	0.982318	0.017298	ERCC6, CUL4A, POLE2, ERCC4, GTF2H1
hsa00310:Lysine degradation	5	0.982318	0.017298	SETD1B, SETMAR, ACAT2, NSD1, SUV420H1
hsa04310:Wnt signaling pathway	9	1.768173	0.021335	PPP2R1B, EP300, VANGL1, BTRC, CREBBP, RAC1, AXIN2, PRKX, APC
hsa05217:Basal cell carcinoma	5	0.982318	0.035945	PTCH1, AXIN2, GLI2, GLI3, APC
hsa04120:Ubiquitin mediated proteolysis	8	1.571709	0.036183	UBE3B, CUL4A, BTRC, TRIM32, SMURF2, ANAPC7, CDC27, UBE2Q1
hsa04114:Oocyte meiosis	7	1.375246	0.038926	PPP2R1B, ADCY9, BTRC, CALM3, ANAPC7, CDC27, CALM2, PRKX, CALM1
hsa04350:TGF-beta signaling pathway	6	1.178782	0.047692	PPP2R1B, EP300, CREBBP, BMPR2, SMURF2, TFDP1
hsa04916:Melanogenesis	6	1.178782	0.074736	EP300, ADCY9, CREB1, CREBBP, CALM3, CALM2, PRKX, CALM1

5.6.8 Gene Co-expression networks for the up and down regulated genes in UPCI:SCC029B/ 70Gy-UPCI:SCC029B and AW13516 / 70Gy-AW13516 cells

The gene co-expression networks for both the parental and radioresistant set of cells were made (as described in the materials and methods section 4.2.24) in order to understand the network association between the metabolic pathways in the established radioresistant cells. The up and down regulated networks from each set of the radioresistant cells are shown in Figure 56 & 57. The colour of the nodes in the network represent the significance while the size of nodes represent the number of genes involved in that particular pathway. The up and down networks is represented by different colours (blue and black respectively).

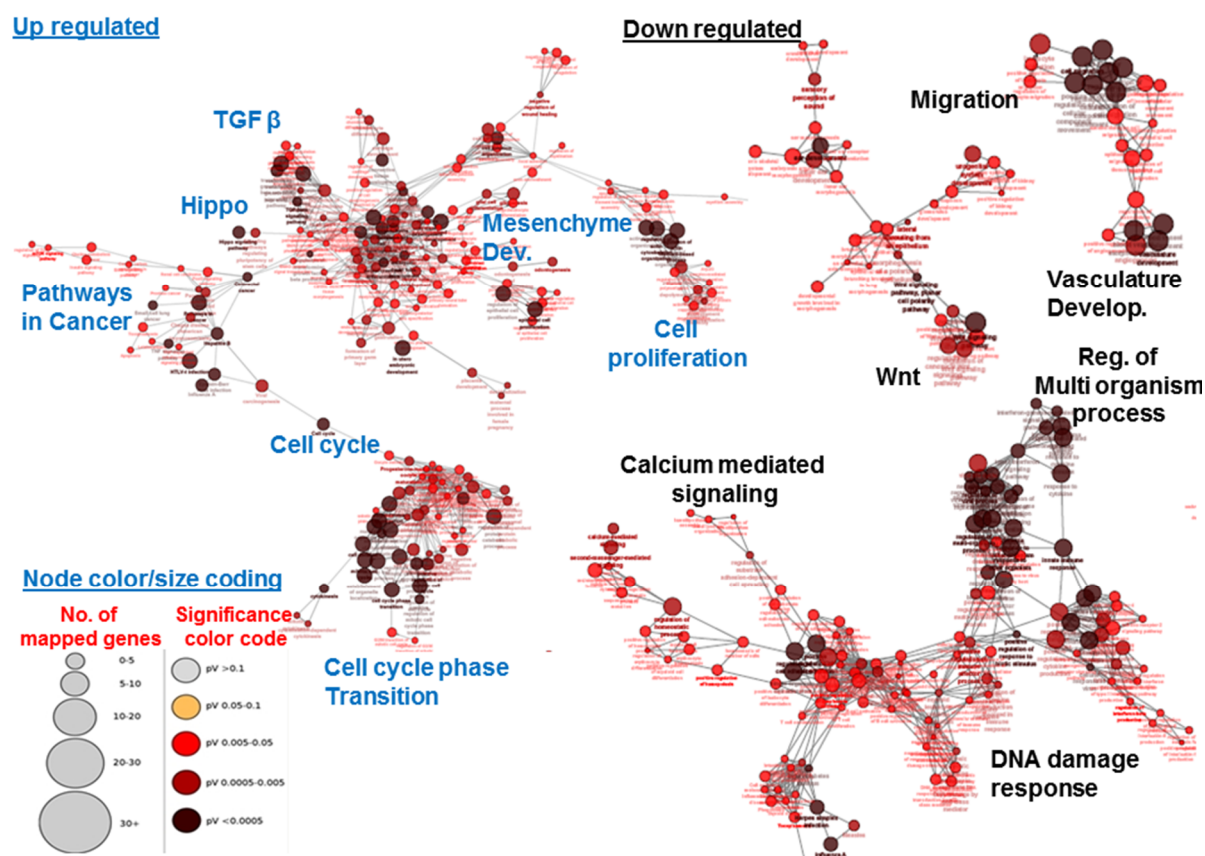


Figure 56: Co-expression network for the differentially regulated genes in UPCI:SCC029B and 70Gy-UPCI:SCC029B cells. (Genes ≥ 2.0 fold change, $p \leq 0.05$ used for constructing the networks).

The pathways related to TGF-Beta, Hippo signaling, Mesenchymal development, Pathways in cancer, Cell cycle, Cellular proliferation and Cell cycle phase transition are identified as significantly upregulated while networks associated with Migration (we have shown in EMT part that these cells are less migratory), Vasculature development, Wnt signaling, Calcium mediated signaling, Regulation of multiorganism process and DNA damage response as down regulated in the co-expression network of 70Gy-UPCI:SCC029B cells compared to its parental cells.

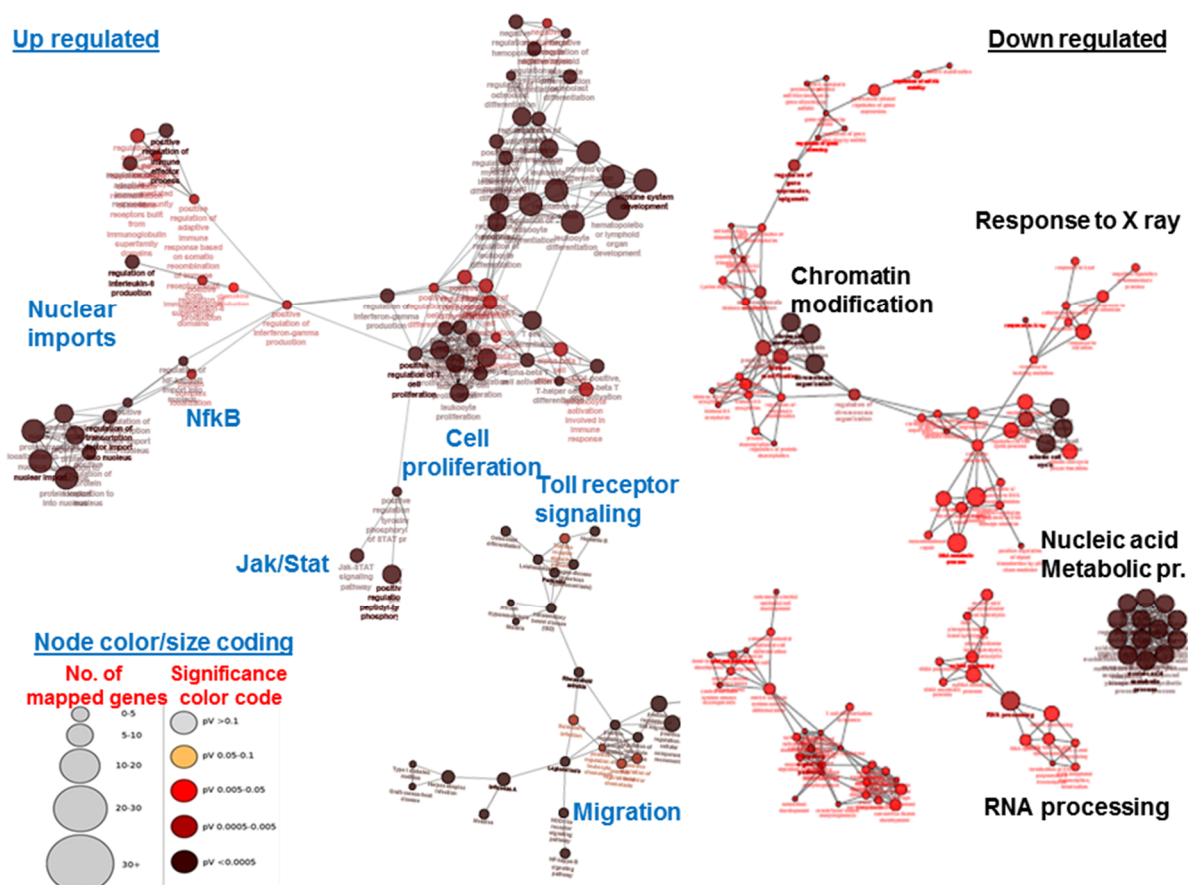


Figure 57: Co-expression network for the differentially regulated genes in AW13516 and 70Gy-AW13516 cells. (genes ≥ 2.0 fold change, $p \leq 0.05$ used for constructing the networks).

As mentioned in the Figure 57, the pathways related to Nuclear import, Nf-Kappa B signaling, Cellular proliferation, Jak/Stat kinase pathways, Toll receptor signaling, Cellular proliferation and migration (these radioresistant 70Gy-AW13516 cells are found to be more migratory and invasive as shown in the EMT part of this study) as significantly up regulated. While, pathways related to Response to X-rays, chromatin modification, Nucleic acid metabolic processes and RNA processing as significantly downregulated in the radioresistant 70Gy-AW13516 cells compared to its parental AW13516 cells.

Chapter 6

Discussion

Discussion

Radiation therapy has been in clinical use for over a millennium [241]. The era of radiation treatment began at the turn of last century with Roentgen's discovery of X-rays and Pierre and Marie Curie's discovery of radium. While, the modern era of radiation therapy began in 1950's with the introduction of cobalt teletherapy, which utilized synthetic radium. Radiotherapy is one of the main pillar of cancer treatment used either alone or with surgery & chemotherapy and is used to treat approximately 50% of all cancer patients [242]. However, despite modern radiation techniques & advanced multimodal treatments; tumors often develop adaptive response and become more resistant, aggressive & invasive, limiting the progression of treatment [243]. Some of the physical tumor associated factors like site, size of the tumor and duration of the disease are possibly associated with clinical radioresistance. Also, acquired radioresistance to fractionated gamma radiations is a recurrent event in medical setting and certain malignancies respond well to the small doses of radiation originally, but during the time course of treatment they became radioresistant. Therefore, radioresistance is a multifactorial process that cannot be associated with a single factor and rather involves multiple changes occurring at the molecular level.

6.1 Advantage of Fractionated Radiotherapy

The dose of irradiation that can be given to the tumor is determined by the radiosensitivity of surrounding normal tissues as well as intrinsic sensitivity/resistance of tumors [244]. In radiotherapy, fractionated treatment regimens have been established and standard fractionation is defined as single doses of 1.8Gy to 2Gy, once daily, 5 days per week. The radiotherapy protocol thus, usually consists of 50Gy to 70Gy in fractions of 2Gy radiation, five times a week for few months. Fractionation in radiotherapy was introduced as a means to

limit side effects when giving therapeutic radiation doses [245]. The principal rationale for fractionation is based on the fact that recovery after radiation is better in normal tissue than in tumors. Fractionated radiotherapy may reoxygenate and thereby radiosensitize the irradiated tumor during therapy time as increased oxygenation then reverses hypoxic radioresistance of the tumor and improves the therapeutic outcome of radiotherapy [246,247]. Also, fractionated radiotherapy can re-distribute the cell cycle of the tumor cells in more sensitive phases and thus minimize repopulation of the tumor during therapy [248].

Hence, we have carried out our study to understand the radioresistance related changes in human oral cancer cells of different oral subsites that were established by clinically admissible fractionated ionizing radiation. The step wise discussion for the outcome of the study is as follows:

6.2 Establishment and validation of radioresistance sublines

The three radioresistant sublines were established from its parental oral cancer cell lines of tongue and buccal mucosa subsites. These are the common oral cancer sites occurred among Indian population due to usage of smokeless tobacco products. Further, patients with oral tongue and buccal sites tumors are also treated with curative radiotherapy, during their treatment regimen. Also, all the three radioresistant sublines were established by clinically relevant 2Gy fractionated ionizing radiation doses, completing the course of 70Gy in 35 fractions that is generally followed in standard oral cancer treatment. The established radioresistant character of the sublines was assessed by clonogenic cell survival assay (increase in D_0 values) and increased expression for some of the reported radioresistance related molecules. Therefore, our established radioresistant sublines provide a good *in-vitro* platform to study the changes associated with clinical radioresistance.

6.3 Differential 2D profile of radioresistant cells

The proteomic profiling by two-dimensional gel electrophoresis followed by MALDI/TOF-TOF analysis on all the three sets of parental and radioresistant cells has identified in total 102_differentially expressed proteins with significant MS and MS/MS scores. The identified proteins belong to different cellular processes and involve functionality majorly associated with DNA repair, chromatin modification, cellular stress related, glycolytic pathway, cell cytoskeleton, glycoproteins, cell signaling, mitochondrial and apoptosis related proteins. On the basis of their consistency among the technical replicates, the identified proteins were further classified to each set respectively. The identification of these proteins related to wide array of functions, support the fact that radioresistance is a multidimensional phenomenon and may involve proteins from various cellular pathways. Some of the mass spectrometry based identified proteins were also validated by western blotting and the proteins that were identified in our work are also found to be matched with some of the reports related to profiling of radioresistant cells in other cancers [221,249,250,251].

Further, from our 2D & MALDI result, 08 proteins were found to be common differentially regulated among the three sets of parental and radioresistant cells and majority of these proteins were molecular chaperones. Earlier it was known that chaperones work exclusively to assist proteins in correct folding and are directly related to the stress related pathways. But, increasing reports suggest the multidimensional role of chaperones in different pathways, ranging from apoptotic, stress response and radioresistance pathways [252,253,254]. On validating these common proteins by more specific western blotting, 06 proteins were found to be validated in radioresistant 70Gy-AW13516 cells, 04 proteins in 70Gy-UPCI:SCC029B cells and 02 proteins in 70Gy-AW8507 cells. Altogether, two proteins i.e. STIP-1 and PKM 2 were found to be validated as common up & down regulated proteins in all the three set of

cells and STIP-1, PKM 2 & PGP in two set of radioresistant cells. Our result suggests that these three common proteins can be further studied for their role in radioresistance in oral cancer. As regarding STIP 1, the increasing evidence suggest that this HSP70 and 90 organizing protein facilitates the function of oncoproteins [255]; down regulation of PKM 2 which is known as major glycolytic enzyme hint towards hypoxic condition, which is one the determinant of radioresistance and the multiple role of PKM 2 in cancer cells are still not very well understood [256,257]; while PGP is a phosphatase with broad substrate specificity and has been also identified in the panel of protein markers in lung cancer [258].

All of these common 2D identified proteins were tested on the protein lysate of all the three set of cells, but every protein failed to show validation by western technique. The reason could be either due to difference in 2D spot intensity across its technical replicates or presence of more than one protein in a single 2D spot, where only the dominant protein can be identified by MALDI [259]. Apart from this, the other 2D identified proteins from each set of established radioresistant cells could also be associated with the cellular radioresistance and can be the targets for the future studies; provided with the prior validation of the 2D result.

6.4 EMT associated changes in radioresistant cells

The role of EMT has been well investigated in tumor invasion, metastasis, chemotherapy resistance and cancer stem cells [258,260,261], while the emerging evidence suggests that EMT plays an important role in cancer radioresistance [262,263]. Radioresistant cancer cells demonstrated epithelial-mesenchymal transition (EMT), which was believed to be linked with adaptation to hypoxia, enhanced DNA repair ability and activated growth factor pathways [264,265,266]. Association of EMT with the poor radiotherapy response and

disease management [267,268] is reported, but its role in radioresistance acquirement during the radiotherapy of oral cancer remains unclear. Therefore, in our present study, we have investigated the EMT like characteristics in two of the acquired radioresistant sublines. We hypothesized that during radioresistance, ionizing radiation can induce EMT like changes which may be one of the factors associated with their resistant phenotype. We have observed that these radioresistant cells exhibited elongated morphology, fine cell surface extensions (filopodia) as compared to their parental cells. The radioresistant cells show decrease in epithelial markers like E-cadherin, cell junction protein Desmoplakin and upregulation of mesenchymal markers like N-cadherin and Vimentin. Also, both of the radioresistant cells represent decrease in their cell to cell contact compared to the parental cells. Next, migratory and invasive properties of both the radioresistant cells were examined and found that only radioresistant 70Gy-AW13516 cells and not 70Gy-UPCI:SCC029B cells have acquired increased migration and invasion as compared to their parental cells. The possible reason for this may be due to induction of different molecular pathways in these cells of differing oral subsites, by the multiple fractions of radiation.

Next, to investigate the increased migratory and invasive phenotype of 70Gy-AW13516 cells, we reanalysed its 2D profile in the search of differentially expressed proteins related to cellular motility and invasiveness. We found an interesting cell motility associated ERM family member protein Moesin to be upregulated in 70Gy-AW13516 cells compared to its parental cells. Earlier studies suggest a role for Moesin in context to migration and glioma progression marker [133,269] and in organizing the cell cortex [270]. We have also found an increased Moesin co-expression with its cell surface receptor CD-44 at the leading migratory edges of 70Gy-AW13516 cells. Moreover, to affirm the role of Moesin protein in these acquired radioresistant properties of 70Gy-AW13516 cells, we transiently knocked down Moesin protein in these cells and found that the radioresistant 70Gy-AW13516 cells were

less migratory, invasive and more radiosensitive in comparison to the control siRNA treated 70Gy-AW13516 cells.

These results affirm the role of cell cytoskeleton associated Moesin protein in acquired migratory, invasive and radioresistant character of oral cancer cells. To the best of our knowledge, we have reported for the first time the role of Moesin in the acquired radioresistance character of an *in-vitro* established radiation resistant oral cancer cells. The future studies related to the downstream effector molecules of Moesin will help in elucidating the cellular radioresistance pathway related to Moesin.

6.5 Acquisition of Cancer stem like characteristics in radioresistant cells

Literature suggest that, a newly emerged plausible explanation for tumor radioresistance is the existence of a subpopulation of cancer stem cells (CSCs) that are intrinsically more resistant to multiple clinical therapies [271]. A direct implication of the CSC hypothesis is that cell populations with different properties co-exist within the same tumor and CSCs have the ability to create the cellular heterogeneity. Also, literature suggests that these CSCs subpopulation may increase within the tumors, during the course of fractionated radiotherapy [143]. Therefore, in the present study, we also characterized the established radioresistant cells for CSCs like properties.

Significant increase in the soft agar colonies was observed in all the resistant cells, compared to their parental cells. Soft agar assay is a method to evaluate the anchorage independent growth property of cells and increase in colonies (both in number and size) of radioresistant cells, implies its altered transforming potential. Further, in context to stem cells; the preferred method for the enrichment of CSCs is to cultivate the cancer cells in serum free medium, supplemented with growth factors, as absence of serum allows maintenance of an

undifferentiated stem cell status and the addition of growth factors has been reported to induce the proliferation of CSC [155,272]. Therefore, cultured all our parental and radioresistant cells in serum free media supplemented with EGF, bFGF, Insulin and LIF growth factors and found that, a small population of radioresistant cells was able to form increased 3D spheroids in comparison to their parental cells. However, we have not carried out, the further cultivation of these spheroids in second and third passages to check the spheroid forming potential of the enriched cells in later passages. In addition to above observation these radioresistant cells also exhibit increased expression for some of the well-studied stem cell markers compared to their parental cells; these includes CD-44, CD-133, Oct-4, Sox-2 and Nanog. Further, as a gold standard to check the tumorigenic potential of the established radioresistant cells, these were injected into immunocompetent mice along with their parental cells. The results suggest that all the three radioresistant cells are more tumorigenic compared to their parental cells.

Therefore, the Kummermehr & Trott model regarding repopulation of stem cells during radiotherapy [143] is found to be supportive from our study as well. These observations will help in further perspective that the cells that survive radiation may enriched for more stem cell like features and these can be the causative factor for resistant to radiation therapy.

6.6 Raman spectroscopy for the radioresistant cells

Raman spectroscopic studies related to radiation induced biochemical changes in prostate, lung and breast cancer cell lines irradiated with radiation doses between 15Gy and 50Gy are reported [181,182]. These studies were carried out at single doses of radiation that aimed to investigate the *in-vitro* radiation response on human cancer cell lines. On the other hand, we have carried out the present study by taking advantage of continuous low dose fractionated

irradiation that is routinely used as standard radiotherapy protocol in clinics for oral cancer treatment. Our aim was to explore the feasibility of Raman spectroscopy to categorize the acquired trait in radioresistant oral cancer cells (different from its parental untreated cells) that were established by clinically implementable 2Gy fractionated radiation dose. For the same, we have chosen radioresistant cells at two different stages i.e 50Gy and 70Gy of UPCI:SCC029B cells of oral buccal mucosa origin. The rationale behind selecting these two populations is that 50Gy and 70Gy are the end points of the standard radiation protocol given to oral cancer patients and buccal mucosa is quite an accessible site in patients for molecular Raman probe. To the best of our knowledge, we are first to report the utility of RS in acquired radioresistant oral cancer sublines established from parental oral cancer cell line by clinically administered fractionated ionizing radiation.

The Raman spectra of parental UPCI:SCC029B, 50Gy-UPCI:SCC029B and 70Gy-UPCI:SCC029B cells were acquired and spectral features indicate possible differences in biomolecules like proteins, lipids and nucleic acids. Alterations in DNA content of these cells may be because of numerous genetic insults occurring through multiple fractions of radiation by FIR and change in lipids may be predominantly due to the altered morphology of these cells. Further, Principal component analysis (PCA) provided three clusters corresponding to radioresistant 50Gy-UPCI:SCC029B, 70Gy-UPCI:SCC029B sublines and parental UPCI:SCC029B cell line with minor overlap, which suggest altered molecular profile acquired by the radioresistant cells due to multiple doses of irradiation. The findings of this study support the potential of Raman spectroscopy in prediction of radioresistance and possibly contribute to better prognosis of oral cancer.

Taken together, the results of our work are quite promising and suggest the feasibility of RS as a potential non-invasive tool for oral cancer patients in predicting radiation response

through spectral markers. It may improve the patient survival rates by virtue of optical diagnosis to categorize them in radiosensitive and radioresistant types, thereby help in selecting better treatment regimens.

6.7 cDNA Microarray profile for the radioresistant cells

The cDNA Microarray study on two of the established radioresistant sublines of different oral sites (tongue and buccal mucosa) namely 70Gy-AW13516 and 70Gy-UPCI:SCC029B with their respective parental cells revealed significant number of up and down regulated genes in both the sets. This was carried out, in order to reveal changes occurring at the transcript levels in radioresistant cells due to multiple doses of clinically administered fractionated doses. The genes that exhibited greater than and equal to three fold difference in radioresistant cells as compared to their parental cells were further analysed for their functional annotations. For the same each of the parental and radioresistant set of cells were analysed by three different curated databases i.e. Panther, Reactome and KEGG.

Briefly, for the UPCI:SCC029B & 70Gy-UPCI:SCC029B set- the Panther pathway analysis identified Angiogenesis pathway (P00005, p value 0.012768) as significantly upregulated pathway containing 12 genes that are matched from its microarray data. Similarly, two pathways i.e. Wnt signaling pathway (P00057, p 8.66E-10) and Cadherin signaling pathway (P00012, p 1.10E-15) are found to be significantly down regulated with 24 & 23 gene counts. Some of these angiogenesis pathway associated genes that are matched with our result has already reported in radioresistance related studies, like HIF 1A [273], JAK 1 [274], AKT 2 [275]. Therefore, identified genes of this pathway can be used as potential members for mapping other novel peripheral genes that can be related to radioresistance. The down regulation for one of the constituent gene identified in Wnt & Cadherin signaling pathway i.e

CDH1 (E cadherin) has already been validated in the EMT study above. Therefore, taking this as the validators for these two pathways, the other genes need to be validated and assessed in further studies.

In the Reactome pathway analysis; REACT_604: Hemostasis (p 0.001345), REACT_71: Gene Expression (p 0.046704), REACT_125: Processing of Capped Intron-Containing Pre-mRNA (p 0.028057), REACT_13552: Integrin cell surface interactions (p 0.021276), REACT_1892: Elongation arrest and recovery (p 0.049991) are some of the significantly upregulated pathways, while REACT_6900: Signaling in Immune system (p 0.004512) as significantly down regulated pathway that may be associated with cellular radioresistance.

In KEGG enrichment analysis, where diseases are viewed as perturbed states of the molecular system and represented as disease pathway maps in the KEGG pathway database (hsa); hsa05200: Pathways in cancer (p 0.001335), hsa04510: Focal adhesion (p 0.002236), hsa04150: mTOR signaling pathway (p 0.00673), hsa04110: Cell cycle (p 0.025429), hsa04062: Chemokine signaling pathway (p 0.028875), hsa04910: Insulin signaling pathway (p 0.036591), hsa04060: Cytokine-cytokine receptor interaction (p 0.039664) and hsa04512 : ECM-receptor interaction (p 0.044693) were found to be significantly upregulated pathways. While, hsa04514: Cell adhesion molecules (p 0.053502) as significantly down regulated pathway.

For AW13516 & 70Gy-AW13516 set; the Panther pathway analysis has identified P00006: Apoptosis signaling pathway (p 0.011619) as upregulated, wherein some of the matched genes like FOS [276], TNF [277] and HSPA8 [278] are well studied in different cancer processes. Also, P00050: Plasminogen activating cascade (p 0.004008), P05918: p38 MAPK pathway (p 0.048456) are other the significantly upregulated and promising pathways that

can be related to radioresistance. The Reactome pathway analysis has identified REACT_7970: Telomere Maintenance (p 0.025487) as a significantly upregulated pathway.

Further, the KEGG enrichment has identified; hsa04621: NOD-like receptor signaling pathway (p 0.001236), hsa04060: Cytokine-cytokine receptor interaction (p 0.00172), hsa04010: MAPK signaling pathway (p 0.012679), hsa04062: Chemokine signaling pathway (p 0.026576), hsa04620: Toll-like receptor signaling pathway (p 0.048612) as significantly upregulated. While, hsa04340: Hedgehog signaling pathway (p 0.001586), hsa00510: N-Glycan biosynthesis (p 0.003682), hsa03420: Nucleotide excision repair (p 0.017298), hsa04310: Wnt signaling pathway (p 0.021335), hsa04120: Ubiquitin mediated proteolysis (p 0.036183) and hsa04350: TGF-beta signaling pathway (p 0.047692) are among the top significantly down regulated pathways, that are likely to be associated with acquired radioresistant phenotype of these cells and may provide important clues related to clinical radioresistance. Also, from the network analysis in both the set of established radioresistant set of cells, the cluster of networks identified as up and down regulated will help in the identification of important molecular targets associated with the radioresistance. The network analysis is not complete and currently ongoing in the laboratory.

Understanding radioresistance in cancer cells is important for developing therapeutic strategies. In our present work, we showed that low dose fractionated ionizing radiation can induce radioresistance in oral cancer cells of different oral subsites. We observed that radioresistant character is also accompanied with EMT & CSCs like features. These acquired phenotypes lead to an array of differentially expressed molecules that we identify in our 2D and microarray results. These molecules may provide potential targets responsible for radioresistance and help in enhancing the efficacy of radiotherapy.

Chapter 7

Summary & Conclusion

The main findings of the study are as follows –

- We have successfully established, three radioresistant sublines from their parental oral cancer cell lines of different oral subsites i.e. two tongue and one buccal mucosa cell line.
- These radioresistant sublines show increased D_0 values compared to their parental cells and expressed some of the reported radioresistance related markers that validate its acquired radioresistance character and make them a prospective in-vitro podium for studying acquired radioresistance related molecular changes.
- To the best of our knowledge, this is the **first such study from India** regarding the establishment of radioresistant sublines by clinically admissible low dose fractionated ionizing radiation.
- The differential proteomic profiling of these radioresistant cells compared to their respective parental cells by two dimensional gel electrophoresis followed by mass spectrometry analysis has identified 102 differentially expressed proteins.
- Expression of some of the mass spectrometry based identified proteins was validated by western blotting.
- The standard PD quest analysis on the three technical replicates for each of the parental and radioresistant set of cells provided groups of differentially expressed proteins in all the sets that belong to different cellular functions; affirming the probable role of distinct pathways related to radioresistance.
- Further, a total of 08 proteins were found to be common among all the three parental and radioresistant set of cells. On validating the same by western blotting, it was found that STIP 1 and PKM 2 are common up & down regulated in all the three set of cells; thus are worthy of further analysis.

- Also, among these eight common proteins; STIP 1, PKM 2 and PGP expression were validated by western blotting in two of the radioresistant set of cells that belong to different oral subsites. The expression of six proteins (out of eight) was found to be validated in one of the established radioresistant set of cells; thus implying their possible association with cellular radioresistance.
- Apart from this, there are array of proteins that does not came as common among all the three set of parental and radioresistant cells (may be due to dissimilar response of these different set of cells towards radiation), but they can also be the prospective molecules for further investigations.
- Two of the established radioresistant cells exhibit elongated morphology, less cell to cell contact, increased filopodia on cell surface and markers associated with epithelial to mesenchymal transition; suggesting the acquisition of EMT phenotype in the radioresistant cells.
- One of the established tongue radioresistant cells show increased migratory and invasive behaviour compared to its parental cell. Further, from its differential 2D profile; an actin binding- ERM family member protein Moesin was found to be up regulated, which is further validated by western blotting.
- Increased co-expression of Moesin with its cell surface receptor CD44 was also found at the leading migratory edges of these radioresistant cells that hint towards its role in the acquired migratory and invasive behaviour of these cells.
- siRNA mediated knock down of Moesin protein in these radioresistant cells resulted in its decreased migration and invasion, thus associating the role of Moesin protein with the acquired migratory and invasive property.

- Further, Moesin knockdown also results in the reduction of the acquired radioresistance character of these cells compared to the control siRNA treated cells. To the best of our knowledge, this is the **first such study** showing the role of Moesin with the cellular radioresistance and therefore makes it one of the target proteins for further studies.
- All the radioresistant cells exhibited increase in soft agar colonies (both in area and number of colonies) and suggest the acquisition of anchorage independent growth property in these cells.
- These radioresistant cells also exhibit increased ability to form 3D spheroids compared to their respective parental cells. Spheroid forming potential is one of the properties that are reported to be associated with stem cell features.
- All the established radioresistant cells exhibit increased expression of stem cell associated markers. Therefore, these observations i.e. anchorage independent growth, spheroid formation & stem cell markers together suggest the enrichment of stem cell like properties in them, post multiple doses of fractionated ionizing radiation.
- Finally, these radioresistant cells also show increased tumorigenic potential in immuno-compromised mice compared to their respective parental cells. This is the gold standard method to test the stemness and thus suggests the enrichment of cancer stem cell like features in these established radioresistant cells.
- Distinct Raman spectral profile for two of the established radioresistant sublines of buccal mucosa origin suggest the feasibility of Raman spectroscopy as a potential non-invasive tool for predicting radiation response through spectral markers in oral cancer patients.

- To the best of our knowledge, the Raman spectroscopic study is the **first report** that represents the utility of Raman spectroscopy in acquired radioresistant oral cancer sublines, established from parental oral cancer cell lines by clinically administered fractionated ionizing radiation. As, other reported studies were related to radiation induced biochemical changes in cancer cell lines at single doses of radiation only.
- The cDNA microarray profile of two of the established radioresistant sublines (tongue & buccal oral subsites) gave 1190 and 1378 as significantly up regulated while 750 and 1152 as down regulated genes with > 2 fold change respectively.
- The microarray result validated by real time PCR; done independently on the cDNA of parental and radioresistant cells for some of the randomly selected differentially expressed genes.
- To interpret the biological functions of the differentially expressed genes; the functional annotation of the same was carried out by three different curated databases i.e. Panther, Reactome & KEGG for both the parental and radioresistant set of cells.
- Panther analysis revealed pathways related to Angiogenesis, Apoptosis signalling, Plasminogen activating cascade & p38 MAPK pathways as significantly up regulated while Wnt signalling, cadherin signalling as significantly down regulated pathway in radioresistant cells.
- Reactome analysis identify; Hemostasis, Integrin cell surface interactions, Telomere Maintenance as significantly up regulated, while Signaling in Immune system pathways as significantly down regulated in the radioresistant cells compared to the parental cells.
- The KEGG enrichment analysis revealed; Pathways in cancer, Focal adhesion, mTOR signalling, Cell cycle, Chemokine signaling, Insulin signaling and ECM-receptor interaction,

Cytokine-cytokine receptor interaction and Toll-like receptor signaling pathways as significantly upregulated. Whereas, Cell adhesion molecules, Hedgehog signalling, Nucleotide excision repair, Ubiquitin mediated proteolysis and TGF-beta signaling pathways as the significantly down regulated pathways.

- This integrated analysis from three different databases on two different set of established radioresistant set of cells may help in understanding the underlying molecular differences between parental and radioresistant oral cancer cells.

In conclusion, our findings indicate that clinically admissible fractionated ionizing radiation induced different in-vitro characteristics will help in understanding radioresistance in oral cancer. The identified molecules both at proteomic & transcriptomic levels and spectral profiles may have important therapeutic implications in the treatment of oral cancer.

Chapter 8

References

- [1] T. Sasahira, T. Kirita, H. Kuniyasu, Update of molecular pathobiology in oral cancer: a review, *International journal of clinical oncology* 19 (2014) 431-436.
- [2] R. Dikshit, P.C. Gupta, C. Ramasundarahettige, V. Gajalakshmi, L. Aleksandrowicz, R. Badwe, R. Kumar, S. Roy, W. Suraweera, F. Bray, Cancer mortality in India: a nationally representative survey, *The Lancet* 379 (2012) 1807-1816.
- [3] R. Rajendran, *Shafer's textbook of oral pathology*, Elsevier India, 2009.
- [4] J.P. Shah, B. Singh, Keynote comment: why the lack of progress for oral cancer?, *The lancet oncology* 7 (2006) 356-357.
- [5] A. Bessell, A.M. Glenney, S. Furness, J.E. Clarkson, R. Oliver, D.I. Conway, M. Macluskey, S. Pavitt, P. Sloan, H.V. Worthington, Interventions for the treatment of oral and oropharyngeal cancers: surgical treatment, *The Cochrane Library* (2011).
- [6] S.H. Huang, Oral cancer: Current role of radiotherapy and chemotherapy, *Medicina oral, patologia oral y cirugía bucal* 18 (2013) e233.
- [7] M. John-Aryankalayil, S.T. Palayoor, D. Cerna, C.B. Simone, M.T. Falduto, S.R. Magnuson, C.N. Coleman, Fractionated radiation therapy can induce a molecular profile for therapeutic targeting, *Radiation research* 174 (2010) 446-458.
- [8] M.M. Carrillo, I.T. Martín, I.M. Lara, J.M.R. de Almodóvar Rivera, R.D.M. Ávila, Selective use of postoperative neck radiotherapy in oral cavity and oropharynx cancer: a prospective clinical study, *Radiation Oncology* 8 (2013) 103.
- [9] B. Bucci, S. Misiti, A. Cannizzaro, R. Marchese, G.H. Raza, R. Miceli, A. Stigliano, D. Amendola, O. Monti, M. Biancolella, Fractionated ionizing radiation exposure induces apoptosis through caspase-3 activation and reactive oxygen species generation, *Anticancer research* 26 (2006) 4549-4557.
- [10] R. Fenton, D. Longo, Cancer cell biology and angiogenesis, *Harrisons principles of internal medicine* 16 (2005) 453.
- [11] T. Ishigami, K. Uzawa, M. Higo, H. Nomura, K. Saito, Y. Kato, D. Nakashima, M. Shiiba, H. Bukawa, H. Yokoe, Genes and molecular pathways related to radioresistance of oral squamous cell carcinoma cells, *International journal of cancer* 120 (2007) 2262-2270.
- [12] S. Mallick, R. Patil, R. Gyanchandani, S. Pawar, V. Palve, S. Kannan, K. Pathak, M. Choudhary, T. Teni, Human oral cancers have altered expression of Bcl-2 family members and increased expression of the anti-apoptotic splice variant of Mcl-1, *The Journal of pathology* 217 (2009) 398-407.
- [13] V.C. Palve, T.R. Teni, Association of anti-apoptotic Mcl-1L isoform expression with radioresistance of oral squamous carcinoma cells, *Radiation Oncology* 7 (2012) 1-11.
- [14] V. Palve, S. Mallick, G. Ghaisas, S. Kannan, T. Teni, Overexpression of Mcl-1L Splice Variant Is Associated with Poor Prognosis and Chemoresistance in Oral Cancers, (2014).
- [15] E.W. Thompson, D.F. Newgreen, Carcinoma invasion and metastasis: a role for epithelial-mesenchymal transition?, *Cancer research* 65 (2005) 5991-5995.
- [16] L. Han, S. Shi, T. Gong, Z. Zhang, X. Sun, Cancer stem cells: therapeutic implications and perspectives in cancer therapy, *Acta Pharmaceutica Sinica B* 3 (2013) 65-75.
- [17] G. Berx, E. Raspé, G. Christofori, J.P. Thiery, J.P. Sleeman, Pre-EMTing metastasis? Recapitulation of morphogenetic processes in cancer, *Clinical & experimental metastasis* 24 (2007) 587-597.
- [18] J.P. Thiery, Epithelial-mesenchymal transitions in tumour progression, *Nature Reviews Cancer* 2 (2002) 442-454.
- [19] J. Yang, R.A. Weinberg, Epithelial-mesenchymal transition: at the crossroads of development and tumor metastasis, *Developmental cell* 14 (2008) 818-829.
- [20] S.W. Pyo, M. Hashimoto, Y.S. Kim, C.H. Kim, S.H. Lee, K.R. Johnson, M.J. Wheelock, J.U. Park, Expression of E-cadherin, P-cadherin and N-cadherin in oral squamous cell carcinoma: correlation with the clinicopathologic features and patient outcome, *Journal of Cranio-Maxillofacial Surgery* 35 (2007) 1-9.
- [21] S. Krisanaprakornkit, A. Iamaroon, Epithelial-mesenchymal transition in oral squamous cell carcinoma, *ISRN oncology* 2012 (2012).
- [22] X. Chen, S. Lingala, S. Khoobyari, J. Nolte, M.A. Zern, J. Wu, Epithelial mesenchymal transition and hedgehog signaling activation are associated with chemoresistance and invasion of hepatoma subpopulations, *Journal of hepatology* 55 (2011) 838-845.
- [23] W.-L. Zhuo, Y. Wang, X.-L. Zhuo, Y.-S. Zhang, Z.-T. Chen, Short interfering RNA directed against TWIST, a novel zinc finger transcription factor, increases A549 cell sensitivity to cisplatin via MAPK/mitochondrial pathway, *Biochemical and biophysical research communications* 369 (2008) 1098-1102.
- [24] J. Theys, B. Jutten, R. Habets, K. Paesmans, A.J. Groot, P. Lambin, B.G. Wouters, G. Lammering, M. Vooijs, E-Cadherin loss associated with EMT promotes radioresistance in human tumor cells, *Radiotherapy and oncology* 99 (2011) 392-397.

- [25] J.-W. Jung, S.-Y. Hwang, J.-S. Hwang, E.-S. Oh, S. Park, I.-O. Han, Ionising radiation induces changes associated with epithelial-mesenchymal transdifferentiation and increased cell motility of A549 lung epithelial cells, *European Journal of Cancer* 43 (2007) 1214-1224.
- [26] A.K. Templeton, S. Miyamoto, A. Babu, A. Munshi, R. Ramesh, Cancer stem cells: progress and challenges in lung cancer, *Stem Cell Investigation* 1 (2014) 9.
- [27] P.C. Hermann, S.L. Huber, T. Herrler, A. Aicher, J.W. Ellwart, M. Guba, C.J. Bruns, C. Heeschen, Distinct populations of cancer stem cells determine tumor growth and metastatic activity in human pancreatic cancer, *Cell stem cell* 1 (2007) 313-323.
- [28] J.E. Visvader, G.J. Lindeman, Cancer stem cells in solid tumours: accumulating evidence and unresolved questions, *Nature Reviews Cancer* 8 (2008) 755-768.
- [29] G. Sridharan, The Concept of Cancer Stem Cell in Oral Squamous Cell Carcinoma, *Journal of Tumor* 2 (2014) 257-260.
- [30] K. Venkatakrishna, J. Kurien, K.M. Pai, M. Valiathan, N.N. Kumar, C. Murali Krishna, G. Ullas, V. Kartha, Optical pathology of oral tissue: a Raman spectroscopy diagnostic method, *Current science* 80 (2001) 665-669.
- [31] H. Ram, J. Sarkar, H. Kumar, R. Konwar, M. Bhatt, S. Mohammad, Oral cancer: risk factors and molecular pathogenesis, *Journal of maxillofacial and oral surgery* 10 (2011) 132-137.
- [32] W.H. Organization, GLOBOCAN 2012: Estimated cancer incidence, mortality and prevalence worldwide in 2012, Lyon, France: International Agency for Research on Cancer.[Links] (2014).
- [33] S. Subramanian, R. Sankaranarayanan, B. Bapat, T. Somanathan, G. Thomas, B. Mathew, J. Vinoda, K. Ramadas, Cost-effectiveness of oral cancer screening: results from a cluster randomized controlled trial in India, *Bulletin of the World Health Organization* 87 (2009) 200-206.
- [34] U. Nair, H. Bartsch, J. Nair, Alert for an epidemic of oral cancer due to use of the betel quid substitutes gutkha and pan masala: a review of agents and causative mechanisms, *Mutagenesis* 19 (2004) 251-262.
- [35] S. Warnakulasuriya, Global epidemiology of oral and oropharyngeal cancer, *Oral oncology* 45 (2009) 309-316.
- [36] W.H. Organization, Report of a meeting of investigators on the histological definition of precancerous lesions, Geneva: World Health Organization 731 (1973).
- [37] S. Carnelio, G.S. Rodrigues, R. Shenoy, D. Fernandes, A brief review of common oral premalignant lesions with emphasis on their management and cancer prevention, *Indian Journal of Surgery* 73 (2011) 256-261.
- [38] I. Krammer, R. Lucas, J. Pindborg, Definition of leukoplakia and related lesion: An aid to study on oral cancer, *Oral Surg Oral Med Oral Path Journal* 46 (1978) 518-539.
- [39] M. Gorsky, F.L. Ms, Oral leukoplakia and malignant transformation. A follow-up study of 257 patients, *Cancer* 53 (1984) 563-568.
- [40] A. Villa, C. Villa, S. Abati, Oral cancer and oral erythroplakia: an update and implication for clinicians, *Australian dental journal* 56 (2011) 253-256.
- [41] M. Ajit Auluck, M.P. Rosin, B. Lewei Zhang, K. Sumanth, Oral submucous fibrosis, a clinically benign but potentially malignant disease: report of 3 cases and review of the literature, *JCDA* 74 (2008) 735-740.
- [42] C.B. More, S. Das, H. Patel, C. Adalja, V. Kamatchi, R. Venkatesh, Proposed clinical classification for oral submucous fibrosis, *Oral oncology* 48 (2012) 200-202.
- [43] D. Daftary, P. Murti, R. Bhonsle, P. Gupta, F. Mehta, J. Pindborg, Oral precancerous lesions and conditions of tropical interest, *Oral diseases in the tropics* (1993) 402-424.
- [44] S. Pundir, S. Saxena, P. Aggrawal, Oral submucous fibrosis a disease with malignant potential-Report of two Cases, *J Clin Exp Dent* 2 (2010) 215-218.
- [45] C. More, K. Thakkar, Oral submucous fibrosis-An insight, *J Pearldent* 1 (2010).
- [46] S.W. Beenken, M.M. Urist, Head and neck tumors, *Current surgical diagnosis and treatment* 3 (2003) 282-297.
- [47] J. Coleman, M. Sultan, Tumors of the head and neck, *Principles of surgery*. 7th ed. New York: McGraw-Hill (1999) 601-665.
- [48] F. Meyskens Jr, Biology and intervention of the premalignant process, *Cancer Bull* 43 (1991) 475-480.
- [49] A.L. Carvalho, J. Pintos, N.F. Schlecht, B.V. Oliveira, A.S. Fava, M.P. Curado, L.P. Kowalski, E.L. Franco, Predictive factors for diagnosis of advanced-stage squamous cell carcinoma of the head and neck, *Archives of Otolaryngology-Head & Neck Surgery* 128 (2002) 313-318.
- [50] G.F. Funk, L.H. Karnell, R.A. Robinson, W.K. Zhen, D.K. Trask, H.T. Hoffman, Presentation, treatment, and outcome of oral cavity cancer: a National Cancer Data Base report, *Head & neck* 24 (2002) 165-180.
- [51] B.W. Neville, T.A. Day, Oral cancer and precancerous lesions, *CA: a cancer journal for clinicians* 52 (2002) 195-215.

- [52] K. Warnakulasuriya, R. Ralhan, Clinical, pathological, cellular and molecular lesions caused by oral smokeless tobacco—a review, *Journal of oral pathology & medicine* 36 (2007) 63-77.
- [53] Z.U. Khan, An Overview of Oral Cancer in Indian Subcontinent and Recommendations to Decrease its Incidence, (2012).
- [54] P. Balaram, H. Sridhar, T. Rajkumar, S. Vaccarella, R. Herrero, A. Nandakumar, K. Ravichandran, K. Ramdas, R. Sankaranarayanan, V. Gajalakshmi, Oral cancer in southern India: The influence of smoking, drinking, paan-chewing and oral hygiene, *International journal of cancer* 98 (2002) 440-445.
- [55] T. Teni, S. Pawar, V. Sanghvi, D. Saranath, Expression of bcl-2 and bax in chewing tobacco-induced oral cancers and oral lesions from India, *Pathology Oncology Research* 8 (2002) 109-114.
- [56] P. Boffetta, S. Hecht, N. Gray, P. Gupta, K. Straif, Smokeless tobacco and cancer, *The lancet oncology* 9 (2008) 667-675.
- [57] G. Bhawna, Burden of Smoked and Smokeless Tobacco Consumption in India-Results from the Global adult Tobacco Survey India (GATS-India)-2009-2010, *Asian Pacific Journal of Cancer Prevention* 14 (2013) 3323-3329.
- [58] W.H. Organization, WHO report on the global tobacco epidemic, 2008: the MPOWER package, (2008).
- [59] R. Shimkhada, J.W. Peabody, Tobacco control in India, *Bulletin of the World Health Organization* 81 (2003) 48-52.
- [60] C.J. Murray, A.D. Lopez, Global mortality, disability, and the contribution of risk factors: Global Burden of Disease Study, *The Lancet* 349 (1997) 1436-1442.
- [61] I.A.f.R.o. Cancer, Alcohol drinking (IARC Monographs on the Evaluation of Carcinogenic Risks to Humans, Vol. 44), Lyon, France: International Agency for Research on Cancer (IARCPress) (1988).
- [62] W.J. Blot, J.K. McLaughlin, D.M. Winn, D.F. Austin, R.S. Greenberg, S. Preston-Martin, L. Bernstein, J.B. Schoenberg, A. Stemhagen, J.F. Fraumeni, Smoking and drinking in relation to oral and pharyngeal cancer, *Cancer research* 48 (1988) 3282-3287.
- [63] F. Lewin, S.E. Norell, H. Johansson, P. Gustavsson, J. Wennerberg, A. Biörklund, L.E. Rutqvist, Smoking tobacco, oral snuff, and alcohol in the etiology of squamous cell carcinoma of the head and neck, *Cancer* 82 (1998) 1367-1375.
- [64] E.L. Wynder, I.J. Bross, R.M. Feldman, A study of the etiological factors in cancer of the mouth, *Cancer* 10 (1957) 1300-1323.
- [65] G. McCoy, A biochemical approach to the etiology of alcohol related cancers of the head and neck, *The Laryngoscope* 88 (1978) 59-62.
- [66] L.C. Harty, N.E. Caporaso, R.B. Hayes, D.M. Winn, E. Bravo-Otero, W.J. Blot, D.V. Kleinman, L.M. Brown, H.K. Armenian, J.F. Fraumeni Jr, Alcohol dehydrogenase 3 genotype and risk of oral cavity and pharyngeal cancers, *Journal of the National Cancer Institute* 89 (1997) 1698-1705.
- [67] P.K. Ha, J.A. Califano, The role of human papillomavirus in oral carcinogenesis, *Critical Reviews in Oral Biology & Medicine* 15 (2004) 188-196.
- [68] A.R. Kreimer, G.M. Clifford, P. Boyle, S. Franceschi, Human papillomavirus types in head and neck squamous cell carcinomas worldwide: a systematic review, *Cancer Epidemiology Biomarkers & Prevention* 14 (2005) 467-475.
- [69] E. Schildt, M. Eriksson, L. Hardell, A. Magnuson, Oral infections and dental factors in relation to oral cancer: a Swedish case-control study, *European Journal of Cancer Prevention* 7 (1998) 201-206.
- [70] K.H. Kassim, T.D. Daley, Herpes simplex virus type 1 proteins in human oral squamous cell carcinoma, *Oral surgery, oral medicine, oral pathology* 65 (1988) 445-448.
- [71] J.R. Starr, J.R. Daling, E.D. Fitzgibbons, M.M. Madeleine, R. Ashley, D.A. Galloway, S.M. Schwartz, Serologic evidence of herpes simplex virus 1 infection and oropharyngeal cancer risk, *Cancer research* 61 (2001) 8459-8464.
- [72] P. Wahi, U. Kehar, B. Lahiri, Factors influencing oral and oropharyngeal cancers in India, *British journal of cancer* 19 (1965) 642.
- [73] T.A. Day, B.K. Davis, M.B. Gillespie, J.K. Joe, M. Kibbey, B. Martin-Harris, B. Neville, S.G. Reed, M.S. Richardson, S. Rosenzweig, Oral cancer treatment, *Current treatment options in oncology* 4 (2003) 27-41.
- [74] M. Nishio, T. Sakurai, Y. Kagami, N. Narimatsu, [Brachytherapy of cancer], *Gan to kagaku ryoho. Cancer & chemotherapy* 14 (1987) 1519-1530.
- [75] C.E. Palme, P.J. Gullane, R.W. Gilbert, Current treatment options in squamous cell carcinoma of the oral cavity, *Surgical oncology clinics of North America* 13 (2004) 47-70.
- [76] D. Kar, K. Jayarajan, S. Sharma, M. Singh, G. Subrahmanyam, The Bhabhatron: an affordable solution for radiation therapy, *Biomed Imaging Intervention J* 4 (2008) e50-12.
- [77] P. Jeggo, M.F. Lavin, Cellular radiosensitivity: how much better do we understand it?, *International journal of radiation biology* 85 (2009) 1061-1081.

- [78] G. Steel, The dose rate effect: brachytherapy and targeted radiotherapy, *Basic Clinical Radiobiology*, 3rd edition. Hodder Arnold, London, UK (2002) 192-204.
- [79] N. Burnet, R. Wurm, J. Nyman, J. Peacock, Normal tissue radiosensitivity—How important is it?, *Clinical oncology* 8 (1996) 25-34.
- [80] R. Baskar, J. Dai, N. Wenlong, R. Yeo, K.-W. Yeoh, Biological response of cancer cells to radiation treatment, *Frontiers in Molecular Biosciences* 1 (2014).
- [81] J.F. Fowler, M.J. Lindstrom, Loss of local control with prolongation in radiotherapy, *International Journal of Radiation Oncology* Biology* Physics* 23 (1992) 457-467.
- [82] M. Baumann, C. Petersen, TCP and NTCP: a basic introduction, *Rays* 30 (2004) 99-104.
- [83] H.R. Withers, H.D. Thames, Dose fractionation and volume effects in normal tissues and tumors, *American journal of clinical oncology* 11 (1988) 313-329.
- [84] J. Bourhis, J. Overgaard, H. Audry, K.K. Ang, M. Saunders, J. Bernier, J.-C. Horiot, A. Le Maître, T.F. Pajak, M.G. Poulsen, Hyperfractionated or accelerated radiotherapy in head and neck cancer: a meta-analysis, *The Lancet* 368 (2006) 843-854.
- [85] M. Řezáčová, G. Rudolfová, A. Tichý, A. Bačíková, D. Mutná, R. Havelek, J. Vávrová, K. Odrážka, E. Lukášová, S. Kozubek, Accumulation of DNA damage and cell death after fractionated irradiation, *Radiation research* 175 (2011) 708-718.
- [86] N.A. Franken, H.M. Rodermond, J. Stap, J. Haveman, C. Van Bree, Clonogenic assay of cells in vitro, *Nature protocols* 1 (2006) 2315-2319.
- [87] S. Bhide, C. Nutting, Recent advances in radiotherapy, *BMC medicine* 8 (2010) 25.
- [88] A.C. Begg, F.A. Stewart, C. Vens, Strategies to improve radiotherapy with targeted drugs, *Nature Reviews Cancer* 11 (2011) 239-253.
- [89] M. Nordsmark, S.M. Bentzen, V. Rudat, D. Brizel, E. Lartigau, P. Stadler, A. Becker, M. Adam, M. Molls, J. Dunst, Prognostic value of tumor oxygenation in 397 head and neck tumors after primary radiation therapy. An international multi-center study, *Radiotherapy and Oncology* 77 (2005) 18-24.
- [90] J.J. Kim, I.F. Tannock, Repopulation of cancer cells during therapy: an important cause of treatment failure, *Nature Reviews Cancer* 5 (2005) 516-525.
- [91] H. Withers, J. Taylor, B. Maciejewski, The hazard of accelerated tumor clonogen repopulation during radiotherapy, *Acta Oncologica* 27 (1988) 131-146.
- [92] C. West, S.E. Davidson, S.A. Roberts, R.D. Hunter, Intrinsic radiosensitivity and prediction of patient response to radiotherapy for carcinoma of the cervix, *British journal of cancer* 68 (1993) 819.
- [93] J. Zhao, F. Du, Y. Luo, G. Shen, F. Zheng, B. Xu, The emerging role of hypoxia-inducible factor-2 involved in chemo/radioresistance in solid tumors, *Cancer treatment reviews* (2015).
- [94] M.D. Sklar, The ras oncogenes increase the intrinsic resistance of NIH 3T3 cells to ionizing radiation, *Science* 239 (1988) 645-647.
- [95] U. Kasid, A. Pfeifer, R. Weichselbaum, A. Dritschilo, G. Mark, The raf oncogene is associated with a radiation-resistant human laryngeal cancer, *Science* 237 (1987) 1039-1041.
- [96] S. Kitada, S. Krajewski, T. Miyashita, M. Krajewska, J.C. Reed, Gamma-radiation induces upregulation of Bax protein and apoptosis in radiosensitive cells in vivo, *Oncogene* 12 (1996) 187-192.
- [97] K. Asanuma, R. Moriai, T. Yajima, A. Yagihashi, M. Yamada, D. Kobayashi, N. Watanabe, Survivin as a radioresistance factor in pancreatic cancer, *Cancer Science* 91 (2000) 1204-1209.
- [98] N. Terakado, S. Shintani, J. Yano, L. Chunnan, M. Mihara, K.-i. Nakashiro, H. Hamakawa, Overexpression of cyclooxygenase-2 is associated with radioresistance in oral squamous cell carcinoma, *Oral oncology* 40 (2004) 383-389.
- [99] D. Uchida, N. Begum, A. Almofti, H. Kawamata, H. Yoshida, M. Sato, Frequent downregulation of 14-3-3 σ protein and hypermethylation of 14-3-3 σ gene in salivary gland adenoid cystic carcinoma, *British journal of cancer* 91 (2004) 1131-1138.
- [100] S. Shintani, M. Mihara, C. Li, Y. Nakahara, S. Hino, K.i. Nakashiro, H. Hamakawa, Up-regulation of DNA-dependent protein kinase correlates with radiation resistance in oral squamous cell carcinoma, *Cancer science* 94 (2003) 894-900.
- [101] Y. Yamazaki, I. Chiba, A. Hirai, K.-i. Notani, H. Kashiwazaki, K. Tei, Y. Totsuka, T. Iizuka, T. Kohgo, H. Fukuda, Radioresistance in Oral Squamous Cell Carcinoma With p 53 DNA Contact Mutation, *American journal of clinical oncology* 26 (2003) e124-e129.
- [102] T. Tamatani, M. Azuma, Y. Ashida, K. Motegi, R. Takashima, K. Harada, S.i. Kawaguchi, M. Sato, Enhanced radiosensitization and chemosensitization in NF- κ B-suppressed human oral cancer cells via the inhibition of γ -irradiation-and 5-FU-induced production of IL-6 and IL-8, *International journal of cancer* 108 (2004) 912-921.
- [103] K. Fukuda, C. Sakakura, K. Miyagawa, Y. Kuriu, S. Kin, Y. Nakase, A. Hagiwara, S. Mitsufuji, Y. Okazaki, Y. Hayashizaki, Differential gene expression profiles of radioresistant oesophageal cancer

- cell lines established by continuous fractionated irradiation, *British journal of cancer* 91 (2004) 1543-1550.
- [104] K. Ogawa, T. Utsunomiya, K. Mimori, F. Tanaka, N. Haraguchi, H. Inoue, S. Murayama, M. Mori, Differential gene expression profiles of radioresistant pancreatic cancer cell lines established by fractionated irradiation, *International journal of oncology* 28 (2006) 705-713.
 - [105] O. Kitahara, T. Katagiri, T. Tsunoda, Y. Harima, Y. Nakamura, Classification of sensitivity or resistance of cervical cancers to ionizing radiation according to expression profiles of 62 genes selected by cDNA microarray analysis, *Neoplasia* 4 (2002) 295-303.
 - [106] W.-F. Guo, R.-X. Lin, J. Huang, Z. Zhou, J. Yang, G.-Z. Guo, S.-Q. Wang, Identification of differentially expressed genes contributing to radioresistance in lung cancer cells using microarray analysis, *Radiation research* 164 (2005) 27-35.
 - [107] B. Hellman, D. Brodin, M. Andersson, K. Dahlman-Wright, U. Isacson, D. Brattstrom, M. Bergqvist, Radiation-induced DNA-damage and gene expression profiles in human lung cancer cells with different radiosensitivity, *Exp Oncol* 27 (2005) 102-107.
 - [108] E. Hanna, D.C. Shrieve, V. Ratanatharathorn, X. Xia, R. Breau, J. Suen, S. Li, A novel alternative approach for prediction of radiation response of squamous cell carcinoma of head and neck, *Cancer research* 61 (2001) 2376-2380.
 - [109] J.J. Christiansen, A.K. Rajasekaran, Reassessing epithelial to mesenchymal transition as a prerequisite for carcinoma invasion and metastasis, *Cancer research* 66 (2006) 8319-8326.
 - [110] L.-K. Liu, X.-Y. Jiang, X.-X. Zhou, D.-M. Wang, X.-L. Song, H.-B. Jiang, Upregulation of vimentin and aberrant expression of E-cadherin/ β -catenin complex in oral squamous cell carcinomas: correlation with the clinicopathological features and patient outcome, *Modern Pathology* 23 (2010) 213-224.
 - [111] J.M. Lee, S. Dedhar, R. Kalluri, E.W. Thompson, The epithelial-mesenchymal transition: new insights in signaling, development, and disease, *The Journal of cell biology* 172 (2006) 973-981.
 - [112] M. Mandal, J.N. Myers, S.M. Lippman, F.M. Johnson, M.D. Williams, S. Rayala, K. Ohshiro, D.I. Rosenthal, R.S. Weber, G.E. Gallick, Epithelial to mesenchymal transition in head and neck squamous carcinoma, *Cancer* 112 (2008) 2088-2100.
 - [113] M.M. Nijkamp, P.N. Span, I.J. Hoogsteen, A.J. van der Kogel, J.H. Kaanders, J. Bussink, Expression of E-cadherin and vimentin correlates with metastasis formation in head and neck squamous cell carcinoma patients, *Radiotherapy and Oncology* 99 (2011) 344-348.
 - [114] M. Gurjar, K. Raychaudhuri, S.N. Dalal, Loss of the desmosomal plaque protein plakophilin 3 does not induce the epithelial mesenchymal transition.
 - [115] S. Nakajima, R. Doi, E. Toyoda, S. Tsuji, M. Wada, M. Koizumi, S.S. Tulachan, D. Ito, K. Kami, T. Mori, N-cadherin expression and epithelial-mesenchymal transition in pancreatic carcinoma, *Clinical Cancer Research* 10 (2004) 4125-4133.
 - [116] N. Tanaka, T. Odajima, K. Ogi, T. Ikeda, M. Satoh, Expression of E-cadherin, α -catenin, and β -catenin in the process of lymph node metastasis in oral squamous cell carcinoma, *British journal of cancer* 89 (2003) 557-563.
 - [117] L.-F. Zhu, Y. Hu, C.-C. Yang, X.-H. Xu, T.-Y. Ning, Z.-L. Wang, J.-H. Ye, L.-K. Liu, Snail overexpression induces an epithelial to mesenchymal transition and cancer stem cell-like properties in SCC9 cells, *Laboratory investigation* 92 (2012) 744-752.
 - [118] M.J. Joseph, S. Dangi-Garimella, M.A. Shields, M.E. Diamond, L. Sun, J.E. Koblinski, H.G. Munshi, Slug is a downstream mediator of transforming growth factor- β 1-induced matrix metalloproteinase-9 expression and invasion of oral cancer cells, *Journal of cellular biochemistry* 108 (2009) 726-736.
 - [119] S.D. Silva, M.A. Alaoui-Jamali, F.A. Soares, D.M. Carraro, H.P. Brentani, M. Hier, S.R. Rogatto, L.P. Kowalski, TWIST1 is a molecular marker for a poor prognosis in oral cancer and represents a potential therapeutic target, *Cancer* 120 (2014) 352-362.
 - [120] E. He, F. Pan, G. Li, J. Li, Fractionated Ionizing Radiation Promotes Epithelial-Mesenchymal Transition in Human Esophageal Cancer Cells through PTEN Deficiency-Mediated Akt Activation, *PloS one* 10 (2015).
 - [121] N. Sato, N. Funayama, A. Nagafuchi, S. Yonemura, S. Tsukita, A gene family consisting of ezrin, radixin and moesin. Its specific localization at actin filament/plasma membrane association sites, *Journal of cell science* 103 (1992) 131-143.
 - [122] M. Baumgartner, A.L. Sillman, E.M. Blackwood, J. Srivastava, N. Madson, J.W. Schilling, J.H. Wright, D.L. Barber, The Nck-interacting kinase phosphorylates ERM proteins for formation of lamellipodium by growth factors, *Proceedings of the National Academy of Sciences* 103 (2006) 13391-13396.
 - [123] M. Arpin, D. Chirivino, A. Naba, I. Zwaenepoel, Emerging role for ERM proteins in cell adhesion and migration, *Cell adhesion & migration* 5 (2011) 199-206.
 - [124] B. Fiévet, D. Louvard, M. Arpin, ERM proteins in epithelial cell organization and functions, *Biochimica et Biophysica Acta (BBA)-Molecular Cell Research* 1773 (2007) 653-660.

- [125] Y. Jung, J.H. McCarty, Band 4.1 proteins regulate integrin-dependent cell spreading, *Biochemical and biophysical research communications* 426 (2012) 578-584.
- [126] N.V. Belkina, Y. Liu, J.-J. Hao, H. Karasuyama, S. Shaw, LOK is a major ERM kinase in resting lymphocytes and regulates cytoskeletal rearrangement through ERM phosphorylation, *Proceedings of the National Academy of Sciences* 106 (2009) 4707-4712.
- [127] J. Clucas, F. Valderrama, ERM proteins in cancer progression, *Journal of cell science* 127 (2014) 267-275.
- [128] T. Sperka, K.J. Geißler, U. Merkel, I. Scholl, I. Rubio, P. Herrlich, H.L. Morrison, Activation of Ras requires the ERM-dependent link of actin to the plasma membrane, *PloS one* 6 (2011) e27511.
- [129] K. Takahashi, T. Sasaki, A. Mammoto, K. Takaishi, T. Kameyama, S. Tsukita, S. Tsukita, Y. Takai, Direct interaction of the Rho GDP dissociation inhibitor with ezrin/radixin/moesin initiates the activation of the Rho small G protein, *Journal of Biological Chemistry* 272 (1997) 23371-23375.
- [130] J. Haynes, J. Srivastava, N. Madson, T. Wittmann, D.L. Barber, Dynamic actin remodeling during epithelial-mesenchymal transition depends on increased moesin expression, *Molecular biology of the cell* 22 (2011) 4750-4764.
- [131] H. Kobayashi, J. Sagara, H. Kurita, M. Morifuji, M. Ohishi, K. Kurashina, S.i. Taniguchi, Clinical significance of cellular distribution of moesin in patients with oral squamous cell carcinoma, *Clinical cancer research* 10 (2004) 572-580.
- [132] H. Kobayashi, J. Sagara, J. Masumoto, H. Kurita, K. Kurashina, S. Taniguchi, Shifts in cellular localization of moesin in normal oral epithelium, oral epithelial dysplasia, verrucous carcinoma and oral squamous cell carcinoma, *Journal of oral pathology & medicine* 32 (2003) 344-349.
- [133] X. Zhu, F.C. Morales, N.K. Agarwal, T. Dogruluk, M. Gagea, M.-M. Georgescu, Moesin is a glioma progression marker that induces proliferation and Wnt/ β -catenin pathway activation via interaction with CD44, *Cancer research* 73 (2013) 1142-1155.
- [134] S. Tsukita, K. Oishi, N. Sato, J. Sagara, A. Kawai, ERM family members as molecular linkers between the cell surface glycoprotein CD44 and actin-based cytoskeletons, *The Journal of cell biology* 126 (1994) 391-401.
- [135] S. Yonemura, M. Hirao, Y. Doi, N. Takahashi, T. Kondo, S. Tsukita, S. Tsukita, Ezrin/radixin/moesin (ERM) proteins bind to a positively charged amino acid cluster in the juxta-membrane cytoplasmic domain of CD44, CD43, and ICAM-2, *The Journal of cell biology* 140 (1998) 885-895.
- [136] P. Dalerba, R.W. Cho, M.F. Clarke, Cancer stem cells: models and concepts, *Annu. Rev. Med.* 58 (2007) 267-284.
- [137] M.F. Clarke, J.E. Dick, P.B. Dirks, C.J. Eaves, C.H. Jamieson, D.L. Jones, J. Visvader, I.L. Weissman, G.M. Wahl, Cancer stem cells—perspectives on current status and future directions: AACR Workshop on cancer stem cells, *Cancer research* 66 (2006) 9339-9344.
- [138] O. Al-Assar, R.J. Muschel, T.S. Manton, W.G. McKenna, T.B. Brunner, Radiation response of cancer stem-like cells from established human cell lines after sorting for surface markers, *International Journal of Radiation Oncology* Biology* Physics* 75 (2009) 1216-1225.
- [139] S.P. Hong, J. Wen, S. Bang, S. Park, S.Y. Song, CD44-positive cells are responsible for gemcitabine resistance in pancreatic cancer cells, *International Journal of Cancer* 125 (2009) 2323-2331.
- [140] M. Diehn, M.F. Clarke, Cancer stem cells and radiotherapy: new insights into tumor radioresistance, *Journal of the National Cancer Institute* 98 (2006) 1755-1757.
- [141] G.H. Nguyen, M.M. Murph, J.Y. Chang, Cancer stem cell radioresistance and enrichment: where frontline radiation therapy may fail in lung and esophageal cancers, *Cancers* 3 (2011) 1232-1252.
- [142] M. Baumann, M. Krause, R. Hill, Exploring the role of cancer stem cells in radioresistance, *Nature Reviews Cancer* 8 (2008) 545-554.
- [143] K.-R. Trott, The mechanisms of acceleration of repopulation in squamous epithelia during daily irradiation, *Acta Oncologica* 38 (1999) 153-157.
- [144] P.A. Campbell, C. Perez-Iratxeta, M.A. Andrade-Navarro, M.A. Rudnicki, Oct4 targets regulatory nodes to modulate stem cell function, *PLoS One* 2 (2007) e553.
- [145] T. Hu, S. Liu, D.R. Breiter, F. Wang, Y. Tang, S. Sun, Octamer 4 small interfering RNA results in cancer stem cell-like cell apoptosis, *Cancer research* 68 (2008) 6533-6540.
- [146] K. Takahashi, S. Yamanaka, Induction of pluripotent stem cells from mouse embryonic and adult fibroblast cultures by defined factors, *cell* 126 (2006) 663-676.
- [147] M.-Y. Chou, F.-W. Hu, C.-H. Yu, C.-C. Yu, Sox2 expression involvement in the oncogenicity and radiochemoresistance of oral cancer stem cells, *Oral oncology* 51 (2015) 31-39.
- [148] A. Sarkar, K. Hochedlinger, The sox family of transcription factors: versatile regulators of stem and progenitor cell fate, *Cell stem cell* 12 (2013) 15-30.

- [149] X. Chen, H. Xu, P. Yuan, F. Fang, M. Huss, V.B. Vega, E. Wong, Y.L. Orlov, W. Zhang, J. Jiang, Integration of external signaling pathways with the core transcriptional network in embryonic stem cells, *cell* 133 (2008) 1106-1117.
- [150] K. Takahashi, K. Tanabe, M. Ohnuki, M. Narita, T. Ichisaka, K. Tomoda, S. Yamanaka, Induction of pluripotent stem cells from adult human fibroblasts by defined factors, *cell* 131 (2007) 861-872.
- [151] M. Herreros-Villanueva, J. Zhang, A. Koenig, E. Abel, T. Smyrk, W. Bamlet, A.A. de Narvajias, T. Gomez, D. Simeone, L. Bujanda, SOX2 promotes dedifferentiation and imparts stem cell-like features to pancreatic cancer cells, *Oncogenesis* 2 (2013) e61.
- [152] J. Ji, P.-S. Zheng, Expression of Sox2 in human cervical carcinogenesis, *Human pathology* 41 (2010) 1438-1447.
- [153] M. Piva, G. Domenici, O. Iriondo, M. Rábano, B.M. Simoes, V. Comaills, I. Barredo, J.A. López-Ruiz, I. Zabalza, R. Kypka, Sox2 promotes tamoxifen resistance in breast cancer cells, *EMBO molecular medicine* 6 (2014) 66-79.
- [154] X. Ye, F. Wu, C. Wu, P. Wang, K. Jung, K. Gopal, Y. Ma, L. Li, R. Lai, β -Catenin, a Sox2 binding partner, regulates the DNA binding and transcriptional activity of Sox2 in breast cancer cells, *Cellular signalling* 26 (2014) 492-501.
- [155] S.-H. Chiou, C.-C. Yu, C.-Y. Huang, S.-C. Lin, C.-J. Liu, T.-H. Tsai, S.-H. Chou, C.-S. Chien, H.-H. Ku, J.-F. Lo, Positive correlations of Oct-4 and Nanog in oral cancer stem-like cells and high-grade oral squamous cell carcinoma, *Clinical Cancer Research* 14 (2008) 4085-4095.
- [156] H. Ponta, L. Sherman, P.A. Herrlich, CD44: from adhesion molecules to signalling regulators, *Nature reviews Molecular cell biology* 4 (2003) 33-45.
- [157] M. Zöller, CD44: can a cancer-initiating cell profit from an abundantly expressed molecule?, *Nature Reviews Cancer* 11 (2011) 254-267.
- [158] Z. Noto, T. Yoshida, M. Okabe, C. Koike, M. Fathy, H. Tsuno, K. Tomihara, N. Arai, M. Noguchi, T. Nikaido, CD44 and SSEA-4 positive cells in an oral cancer cell line HSC-4 possess cancer stem-like cell characteristics, *Oral oncology* 49 (2013) 787-795.
- [159] K. Chikamatsu, G. Takahashi, K. Sakakura, S. Ferrone, K. Masuyama, Immunoregulatory properties of CD44+ cancer stem-like cells in squamous cell carcinoma of the head and neck, *Head & neck* 33 (2011) 208-215.
- [160] Y. Wu, P.Y. Wu, CD133 as a marker for cancer stem cells: progresses and concerns, *Stem cells and development* 18 (2009) 1127-1134.
- [161] L. Pang, G. Bergkvist, A. Cervantes-Arias, D. Yool, R. Muirhead, D. Argyle, Identification of tumour initiating cells in feline head and neck squamous cell carcinoma and evidence for gefitinib induced epithelial to mesenchymal transition, *The Veterinary Journal* 193 (2012) 46-52.
- [162] Q. Zhang, S. Shi, Y. Yen, J. Brown, J.Q. Ta, A.D. Le, A subpopulation of CD133+ cancer stem-like cells characterized in human oral squamous cell carcinoma confer resistance to chemotherapy, *Cancer letters* 289 (2010) 151-160.
- [163] O. Felthaus, T. Ettl, M. Gosau, O. Driemel, G. Brockhoff, A. Reck, K. Zeitler, M. Hautmann, T. Reichert, G. Schmalz, Cancer stem cell-like cells from a single cell of oral squamous carcinoma cell lines, *Biochemical and biophysical research communications* 407 (2011) 28-33.
- [164] X.D. Wei, L. Zhou, L. Cheng, J. Tian, J.J. Jiang, J. MacCallum, In vivo investigation of CD133 as a putative marker of cancer stem cells in Hep-2 cell line, *Head & neck* 31 (2009) 94-101.
- [165] Y. Sun, J. Han, Y. Lu, X. Yang, M. Fan, Biological characteristics of a cell subpopulation in tongue squamous cell carcinoma, *Oral diseases* 18 (2012) 169-177.
- [166] D. De Veld, M. Witjes, H. Sterenborg, J. Roodenburg, The status of in vivo autofluorescence spectroscopy and imaging for oral oncology, *Oral oncology* 41 (2005) 117-131.
- [167] J.G. Wu, Y.Z. Xu, C.W. Sun, R.D. Soloway, D.F. Xu, Q.G. Wu, K.H. Sun, S.F. Weng, G.X. Xu, Distinguishing malignant from normal oral tissues using FTIR fiber-optic techniques, *Biopolymers* 62 (2001) 185-192.
- [168] D. Ferreira, P.J. Coutinho, E. Castanheira, J. Correia, G. Minas, Fluorescence and diffuse reflectance spectroscopy for early cancer detection using a new strategy towards the development of a miniaturized system, *Engineering in Medicine and Biology Society (EMBC), 2010 Annual International Conference of the IEEE, IEEE, 2010*, pp. 1210-1213.
- [169] C.M. Krishna, G. Sockalingum, J. Kurien, L. Rao, L. Venteo, M. Pluot, M. Manfait, V. Kartha, Micro-Raman spectroscopy for optical pathology of oral squamous cell carcinoma, *Applied spectroscopy* 58 (2004) 1128-1135.
- [170] R. Malini, K. Venkatakrishna, J. Kurien, K. M. Pai, L. Rao, V. Kartha, C.M. Krishna, Discrimination of normal, inflammatory, premalignant, and malignant oral tissue: a Raman spectroscopy study, *Biopolymers* 81 (2006) 179-193.

- [171] A. Nijssen, S. Koljenović, T.C.B. Schut, P.J. Caspers, G.J. Puppels, Towards oncological application of Raman spectroscopy, *Journal of biophotonics* 2 (2009) 29-36.
- [172] S. Singh, A. Deshmukh, P. Chaturvedi, C.M. Krishna, Raman spectroscopy in head and neck cancers: Toward oncological applications, *Journal of cancer research and therapeutics* 8 (2012) 126.
- [173] S. Singh, A. Deshmukh, P. Chaturvedi, C.M. Krishna, In vivo Raman spectroscopic identification of premalignant lesions in oral buccal mucosa, *Journal of biomedical optics* 17 (2012) 1050021-1050029.
- [174] S. Rubina, M. Amita, R. Bharat, C.M. Krishna, Raman spectroscopic study on classification of cervical cell specimens, *Vibrational Spectroscopy* 68 (2013) 115-121.
- [175] S. Rubina, M. Vidyasagar, C. Murali Krishna, Raman spectroscopic study on prediction of treatment response in cervical cancers, *Journal of Innovative Optical Health Sciences* 6 (2013) 1350014.
- [176] S. Singh, A. Sahu, A. Deshmukh, P. Chaturvedi, C.M. Krishna, In vivo Raman spectroscopy of oral buccal mucosa: a study on malignancy associated changes (MAC)/cancer field effects (CFE), *Analyst* 138 (2013) 4175-4182.
- [177] A. Sahu, K. Dalal, S. Naglot, P. Aggarwal, C.M. Krishna, Serum based diagnosis of asthma using Raman spectroscopy: an early phase pilot study, (2013).
- [178] A. Sahu, S. Sawant, H. Mamgain, C.M. Krishna, Raman spectroscopy of serum: an exploratory study for detection of oral cancers, *Analyst* 138 (2013) 4161-4174.
- [179] C.M. Krishna, G. Kegelaer, I. Adt, S. Rubin, V.B. Kartha, M. Manfait, G.D. Sockalingum, Combined Fourier transform infrared and Raman spectroscopic approach for identification of multidrug resistance phenotype in cancer cell lines, *Biopolymers* 82 (2006) 462-470.
- [180] C.M. Krishna, G. Kegelaer, I. Adt, S. Rubin, V. Kartha, M. Manfait, G. Sockalingum, Characterisation of uterine sarcoma cell lines exhibiting MDR phenotype by vibrational spectroscopy, *Biochimica et Biophysica Acta (BBA)-General Subjects* 1726 (2005) 160-167.
- [181] Q. Matthews, A. Brolo, J. Lum, X. Duan, A. Jirasek, Raman spectroscopy of single human tumour cells exposed to ionizing radiation in vitro, *Physics in medicine and biology* 56 (2011) 19.
- [182] Q. Matthews, A. Jirasek, J. Lum, A. Brolo, Biochemical signatures of in vitro radiation response in human lung, breast and prostate tumour cells observed with Raman spectroscopy, *Physics in medicine and biology* 56 (2011) 6839.
- [183] D. Gardiner, P. Graves, H. Bowley, *Practical Raman spectroscopy*. 1989, Springer-Verlag.
- [184] C.V. Raman, A new radiation, *Indian Journal of physics* 2 (1928) 387-398.
- [185] C.V. Raman, K.S. Krishnan, A new type of secondary radiation, *Nature* 121 (1928) 501-502.
- [186] C. Chatfield, A.J. Collins, *Introduction to multivariate analysis*, Springer, 2013.
- [187] B.F. Manly, *Multivariate statistical methods: a primer*, CRC Press, 2004.
- [188] D.I. Ellis, R. Goodacre, Metabolic fingerprinting in disease diagnosis: biomedical applications of infrared and Raman spectroscopy, *Analyst* 131 (2006) 875-885.
- [189] K. Polat, S. Güneş, Principles component analysis, fuzzy weighting pre-processing and artificial immune recognition system based diagnostic system for diagnosis of lung cancer, *Expert Systems with Applications* 34 (2008) 214-221.
- [190] L. Wang, B. Mizaikoff, Application of multivariate data-analysis techniques to biomedical diagnostics based on mid-infrared spectroscopy, *Analytical and bioanalytical chemistry* 391 (2008) 1641-1654.
- [191] J. Friedman, T. Hastie, R. Tibshirani, *The elements of statistical learning*, Springer series in statistics Springer, Berlin, 2001.
- [192] A.L. Boskey, R. Mendelsohn, Infrared spectroscopic characterization of mineralized tissues, *Vibrational Spectroscopy* 38 (2005) 107-114.
- [193] G.V. Nogueira, L. Silveira, A.A. Martin, R.A. Za, M.T. Pacheco, M.C. Chavantes, C.A. Pasqualucci, Raman spectroscopy study of atherosclerosis in human carotid artery, *Journal of biomedical optics* 10 (2005) 031117-0311177.
- [194] P. Chen, A. Shen, W. Zhao, S.-J. Baek, H. Yuan, J. Hu, Raman signature from brain hippocampus could aid Alzheimer's disease diagnosis, *Applied optics* 48 (2009) 4743-4748.
- [195] H.M. Schipper, C.S. Kwok, S.M. Rosendahl, D. Bandilla, O. Maes, C. Melmed, D. Rabinovitch, D.H. Burns, Spectroscopy of human plasma for diagnosis of idiopathic Parkinson's disease, (2008).
- [196] J.R. Maher, M. Takahata, H.A. Awad, A.J. Berger, Raman spectroscopy detects deterioration in biomechanical properties of bone in a glucocorticoid-treated mouse model of rheumatoid arthritis, *Journal of biomedical optics* 16 (2011) 087012-087012-087016.
- [197] N.C. Dingari, I. Barman, G.P. Singh, J.W. Kang, R.R. Dasari, M.S. Feld, Investigation of the specificity of Raman spectroscopy in non-invasive blood glucose measurements, *Analytical and bioanalytical chemistry* 400 (2011) 2871-2880.
- [198] M. Gniadecka, O.F. Nielsen, D.H. Christensen, H.C. Wulf, Structure of water, proteins, and lipids in intact human skin, hair, and nail, *Journal of investigative dermatology* 110 (1998) 393-398.

- [199] M. Gniadecka, P.A. Philipsen, S. Sigurdsson, S. Wessel, O.F. Nielsen, D.H. Christensen, J. Hercogova, K. Rossen, H.K. Thomsen, R. Gniadecki, Melanoma diagnosis by Raman spectroscopy and neural networks: structure alterations in proteins and lipids in intact cancer tissue, *Journal of investigative dermatology* 122 (2004) 443-449.
- [200] C. Krafft, S.B. Sobottka, G. Schackert, R. Salzer, Near infrared Raman spectroscopic mapping of native brain tissue and intracranial tumors, *Analyst* 130 (2005) 1070-1077.
- [201] A. Molckovsky, L.-M.W.K. Song, M.G. Shim, N.E. Marcon, B.C. Wilson, Diagnostic potential of near-infrared Raman spectroscopy in the colon: differentiating adenomatous from hyperplastic polyps, *Gastrointestinal endoscopy* 57 (2003) 396-402.
- [202] C. Kendall, N. Stone, N. Shepherd, K. Geboes, B. Warren, R. Bennett, H. Barr, Raman spectroscopy, a potential tool for the objective identification and classification of neoplasia in Barrett's oesophagus, *The Journal of pathology* 200 (2003) 602-609.
- [203] J. Smith, C. Kendall, A. Sammon, J. Christie-Brown, N. Stone, Raman spectral mapping in the assessment of axillary lymph nodes in breast cancer, *Technology in Cancer Research & Treatment* 2 (2003) 327-331.
- [204] P. Crow, A. Molckovsky, N. Stone, J. Uff, B. Wilson, L.-M. Wongkeesong, Assessment of fiberoptic near-infrared Raman spectroscopy for diagnosis of bladder and prostate cancer, *Urology* 65 (2005) 1126-1130.
- [205] R. Richards-Kortum, Rapid Communication Development of a Fiber Optic Probe to Measure NIR Raman Spectra of Cervical Tissue In Vivo, *Photochemistry and photobiology* 68 (1998) 427-431.
- [206] Z. Huang, A. McWilliams, H. Lui, D.I. McLean, S. Lam, H. Zeng, Near-infrared Raman spectroscopy for optical diagnosis of lung cancer, *International journal of cancer* 107 (2003) 1047-1052.
- [207] R.J. Tatake, N. Rajaram, R. Damle, B. Balsara, A. Bhisey, S.G. Gangal, Establishment and characterization of four new squamous cell carcinoma cell lines derived from oral tumors, *Journal of cancer research and clinical oncology* 116 (1990) 179-186.
- [208] C.L. Martin, S.C. Reshmi, T. Ried, W. Gottberg, J.W. Wilson, J.K. Reddy, P. Khanna, J.T. Johnson, E.N. Myers, S.M. Gollin, Chromosomal imbalances in oral squamous cell carcinoma: examination of 31 cell lines and review of the literature, *Oral oncology* 44 (2008) 369-382.
- [209] T.A. Chan, H. Hermeking, C. Lengauer, K.W. Kinzler, B. Vogelstein, 14-3-3 σ is required to prevent mitotic catastrophe after DNA damage, *Nature* 401 (1999) 616-620.
- [210] U.K. Laemmli, Cleavage of structural proteins during the assembly of the head of bacteriophage T4, *Nature* 227 (1970) 680-685.
- [211] A. Shevchenko, H. Tomas, J. Havli, J.V. Olsen, M. Mann, In-gel digestion for mass spectrometric characterization of proteins and proteomes, *Nature protocols* 1 (2006) 2856-2860.
- [212] O.H. Lowry, N.J. Rosebrough, A.L. Farr, R.J. Randall, Protein measurement with the Folin phenol reagent, *J biol Chem* 193 (1951) 265-275.
- [213] T. Schmittgen, K. Livak, Analyzing real-time PCR data by the comparative C (T) method *Nat Protoc* 3 (6): 1101-1108, Find this article online (2008).
- [214] M. Elbert, D. Cohen, A. Misch, PAR1b promotes cell-cell adhesion and inhibits Dishevelled-mediated transformation of Madin-Darby canine kidney cells, *Molecular biology of the cell* 17 (2006) 3345-3355.
- [215] J.B. Jensen, M. Parmar, Strengths and limitations of the neurosphere culture system, *Molecular neurobiology* 34 (2006) 153-161.
- [216] U. Raul, S. Sawant, P. Dange, R. Kalraiya, A. Ingle, M. Vaidya, Implications of cytokeratin 8/18 filament formation in stratified epithelial cells: induction of transformed phenotype, *International journal of cancer* 111 (2004) 662-668.
- [217] H. Alam, S.T. Kundu, S.N. Dalal, M.M. Vaidya, Loss of keratins 8 and 18 leads to alterations in $\alpha 6\beta 4$ -integrin-mediated signalling and decreased neoplastic progression in an oral-tumour-derived cell line, *Journal of cell science* 124 (2011) 2096-2106.
- [218] A. Nijssen, K. Maquelin, L.F. Santos, P.J. Caspers, T.C.B. Schut, J.C. den Hollander, M.H. Neumann, G.J. Puppels, Discriminating basal cell carcinoma from perilesional skin using high wave-number Raman spectroscopy, *Journal of biomedical optics* 12 (2007) 034004-034004-034007.
- [219] S. Koljenović, T.C.B. Schut, J.M. Kros, H.J. van den Berge, G.J. Puppels, Discriminating vital tumor from necrotic tissue in human glioblastoma tissue samples by Raman spectroscopy, *Laboratory Investigation* 82 (2002) 1265-1277.
- [220] A. Ghanate, S. Kothiwale, S. Singh, D. Bertrand, C.M. Krishna, Comparative evaluation of spectroscopic models using different multivariate statistical tools in a multicancer scenario, *Journal of biomedical optics* 16 (2011) 025003-025003-025009.

- [221] D.S. Kim, Y.P. Choi, S. Kang, M.Q. Gao, B. Kim, H.R. Park, Y.D. Choi, J.B. Lim, H.J. Na, H.K. Kim, Panel of candidate biomarkers for renal cell carcinoma, *Journal of proteome research* 9 (2010) 3710-3719.
- [222] D. Croft, G. O'Kelly, G. Wu, R. Haw, M. Gillespie, L. Matthews, M. Caudy, P. Garapati, G. Gopinath, B. Jassal, Reactome: a database of reactions, pathways and biological processes, *Nucleic acids research* (2010) gkq1018.
- [223] M. Kanehisa, S. Goto, M. Furumichi, M. Tanabe, M. Hirakawa, KEGG for representation and analysis of molecular networks involving diseases and drugs, *Nucleic acids research* 38 (2010) D355-D360.
- [224] B.M. Bolstad, R.A. Irizarry, M. Åstrand, T.P. Speed, A comparison of normalization methods for high density oligonucleotide array data based on variance and bias, *Bioinformatics* 19 (2003) 185-193.
- [225] D. Holder, R.F. Raubertas, V.B. Pikounis, V. Svetnik, K. Soper, Statistical analysis of high density oligonucleotide arrays: a SAFER approach, *GeneLogic Workshop on Low Level Analysis of Affymetrix GeneChip Data*, 2001.
- [226] M.B. Eisen, P.T. Spellman, P.O. Brown, D. Botstein, Cluster analysis and display of genome-wide expression patterns, *Proceedings of the National Academy of Sciences* 95 (1998) 14863-14868.
- [227] A. Okaro, A. Deery, R. Hutchins, B. Davidson, The expression of antiapoptotic proteins Bcl-2, Bcl-XL, and Mcl-1 in benign, dysplastic, and malignant biliary epithelium, *Journal of clinical pathology* 54 (2001) 927-932.
- [228] G. Packham, E.L. White, C.M. Eischen, H. Yang, E. Parganas, J.N. Ihle, D.A. Grillot, G.P. Zambetti, G. Nuñez, J.L. Cleveland, Selective regulation of Bcl-XL by a Jak kinase-dependent pathway is bypassed in murine hematopoietic malignancies, *Genes & development* 12 (1998) 2475-2487.
- [229] B. Wang, M. Xie, R. Li, T. Owonikoko, S. Ramalingam, F. Khuri, W. Curran, Y. Wang, X. Deng, Role of Ku70 in deubiquitination of Mcl-1 and suppression of apoptosis, *Cell Death & Differentiation* 21 (2014) 1160-1169.
- [230] D. Szklarczyk, A. Franceschini, S. Wyder, K. Forslund, D. Heller, J. Huerta-Cepas, M. Simonovic, A. Roth, A. Santos, K.P. Tsafou, STRING v10: protein-protein interaction networks, integrated over the tree of life, *Nucleic acids research* (2014) gku1003.
- [231] C. Yang, T. Svitkina, Filopodia initiation: focus on the Arp2/3 complex and formins, *Cell adhesion & migration* 5 (2011) 402-408.
- [232] H. Nakamura, M. Yamada, M. Fukae, H. Ozawa, The localization of CD44 and moesin in osteoclasts after calcitonin administration in mouse tibiae, *Journal of bone and mineral metabolism* 15 (1997) 184-192.
- [233] M. Vinci, S. Gowan, F. Boxall, L. Patterson, M. Zimmermann, C. Lomas, M. Mendiola, D. Hardisson, S.A. Eccles, Advances in establishment and analysis of three-dimensional tumor spheroid-based functional assays for target validation and drug evaluation, *BMC biology* 10 (2012) 29.
- [234] B. Moosmann, C. Behl, Cytoprotective antioxidant function of tyrosine and tryptophan residues in transmembrane proteins, *European Journal of Biochemistry* 267 (2000) 5687-5692.
- [235] T. Yamamori, H. Yasui, M. Yamazumi, Y. Wada, Y. Nakamura, H. Nakamura, O. Inanami, Ionizing radiation induces mitochondrial reactive oxygen species production accompanied by upregulation of mitochondrial electron transport chain function and mitochondrial content under control of the cell cycle checkpoint, *Free Radical Biology and Medicine* 53 (2012) 260-270.
- [236] M. Valko, M. Izakovic, M. Mazur, C.J. Rhodes, J. Telser, Role of oxygen radicals in DNA damage and cancer incidence, *Molecular and cellular biochemistry* 266 (2004) 37-56.
- [237] J. Sun, Y. Chen, M. Li, Z. Ge, Role of antioxidant enzymes on ionizing radiation resistance, *Free Radical Biology and Medicine* 24 (1998) 586-593.
- [238] H. Yasuda, Solid tumor physiology and hypoxia-induced chemo/radio-resistance: novel strategy for cancer therapy: nitric oxide donor as a therapeutic enhancer, *Nitric Oxide* 19 (2008) 205-216.
- [239] J.D. Chapman, E.L. Engelhardt, C.C. Stobbe, R.F. Schneider, G.E. Hanks, Measuring hypoxia and predicting tumor radioresistance with nuclear medicine assays, *Radiotherapy and oncology* 46 (1998) 229-237.
- [240] H.-C. Lee, D.-W. Kim, K.-Y. Jung, I.-C. Park, M.-J. Park, M.-S. Kim, S.-H. Woo, C.-H. Rhee, H. Yoo, S.-H. Lee, Increased expression of antioxidant enzymes in radioresistant variant from U251 human glioblastoma cell line, *International journal of molecular medicine* 13 (2004) 883-887.
- [241] S. Rosenberg, R. DePinho, R. Weinberg, Devita, Hellman, and Rosenberg's Cancer: principles and practice of oncology, Philadelphia: Lippincott Williams and Wilkins, 2008.
- [242] M. Toulany, H.P. Rodemann, Potential of Akt mediated DNA repair in radioresistance of solid tumors overexpressing erbB-PI3K-Akt pathway, *Translational Cancer Research* 2 (2013) 190-202.
- [243] K.M. Ahmed, J.J. Li, ATM-NF- κ B connection as a target for tumor radiosensitization, *Current cancer drug targets* 7 (2007) 335.

- [244] B. Jones, R.G. Dale, A.M. Gaya, Linear quadratic modeling of increased late normal-tissue effects in special clinical situations, *International Journal of Radiation Oncology* Biology* Physics* 64 (2006) 948-953.
- [245] J. Bernier, E.J. Hall, A. Giaccia, Radiation oncology: a century of achievements, *Nature Reviews Cancer* 4 (2004) 737-747.
- [246] C.-A. Maftei, C. Bayer, K. Shi, S.T. Astner, P. Vaupel, Changes in the fraction of total hypoxia and hypoxia subtypes in human squamous cell carcinomas upon fractionated irradiation: evaluation using pattern recognition in microcirculatory supply units, *Radiotherapy and Oncology* 101 (2011) 209-216.
- [247] T. Narita, H. Aoyama, K. Hirata, S. Onodera, T. Shiga, H. Kobayashi, J. Murata, S. Terasaka, S. Tanaka, K. Houkin, Reoxygenation of glioblastoma multiforme treated with fractionated radiotherapy concomitant with temozolomide: changes defined by 18F-fluoromisonidazole positron emission tomography: two case reports, *Japanese journal of clinical oncology* (2011) hyr181.
- [248] T.M. Pawlik, K. Keyomarsi, Role of cell cycle in mediating sensitivity to radiotherapy, *International Journal of Radiation Oncology* Biology* Physics* 59 (2004) 928-942.
- [249] J.T.-C. Chang, S.-H. Chan, C.-Y. Lin, T.-Y. Lin, H.-M. Wang, C.-T. Liao, T.-H. Wang, L.-Y. Lee, A.-J. Cheng, Differentially expressed genes in radioresistant nasopharyngeal cancer cells: gp96 and GDF15, *Molecular cancer therapeutics* 6 (2007) 2271-2279.
- [250] L. Smith, O. Qutob, M.B. Watson, A.W. Beavis, D. Potts, K.J. Welham, V. Garimella, M.J. Lind, P.J. Drew, L. Cawkwell, Proteomic identification of putative biomarkers of radiotherapy resistance: a possible role for the 26S proteasome?, *Neoplasia* 11 (2009) 1194-1207.
- [251] X.-P. Feng, H. Yi, M.-Y. Li, X.-H. Li, B. Yi, P.-F. Zhang, C. Li, F. Peng, C.-E. Tang, J.-L. Li, Identification of biomarkers for predicting nasopharyngeal carcinoma response to radiotherapy by proteomics, *Cancer research* 70 (2010) 3450-3462.
- [252] T.-Y. Lin, J.T.-C. Chang, H.-M. Wang, S.-H. Chan, C.-C. Chiu, C.-Y. Lin, K.-H. Fan, C.-T. Liao, I.-H. Chen, T.Z. Liu, Proteomics of the radioresistant phenotype in head-and-neck cancer: Gp96 as a novel prediction marker and sensitizing target for radiotherapy, *International Journal of Radiation Oncology* Biology* Physics* 78 (2010) 246-256.
- [253] W.-Y. Kim, S.H. Oh, J.-K. Woo, W.K. Hong, H.-Y. Lee, Targeting heat shock protein 90 overrides the resistance of lung cancer cells by blocking radiation-induced stabilization of hypoxia-inducible factor-1 α , *Cancer research* 69 (2009) 1624-1632.
- [254] B. Zhang, J.-Q. Qu, L. Xiao, H. Yi, P.-F. Zhang, M.-Y. Li, R. Hu, X.-X. Wan, Q.-Y. He, J.-H. Li, Identification of heat shock protein 27 as a radioresistance-related protein in nasopharyngeal carcinoma cells, *Journal of cancer research and clinical oncology* 138 (2012) 2117-2125.
- [255] J. Trepel, M. Mollapour, G. Giaccone, L. Neckers, Targeting the dynamic HSP90 complex in cancer, *Nature Reviews Cancer* 10 (2010) 537-549.
- [256] W. Luo, G.L. Semenza, Emerging roles of PKM2 in cell metabolism and cancer progression, *Trends in Endocrinology & Metabolism* 23 (2012) 560-566.
- [257] S. Wu, H. Le, Dual roles of PKM2 in cancer metabolism, *Acta biochimica et biophysica Sinica* 45 (2013) 27-35.
- [258] Y.Z. Liu, Y.Y. Jiang, B.S. Wang, J.J. Hao, L. Shang, T.T. Zhang, J. Cao, X. Xu, Q.M. Zhan, M.R. Wang, A panel of protein markers for the early detection of lung cancer with bronchial brushing specimens, *Cancer cytopathology* 122 (2014) 833-841.
- [259] B. Thiede, C.J. Koehler, M. Strozynski, A. Treumann, R. Stein, U. Zimny-Arndt, M. Schmid, P.R. Jungblut, High resolution quantitative proteomics of HeLa cells protein species using stable isotope labeling with amino acids in cell culture (SILAC), two-dimensional gel electrophoresis (2DE) and nano-liquid chromatography coupled to an LTQ-OrbitrapMass spectrometer, *Molecular & Cellular Proteomics* 12 (2013) 529-538.
- [260] Y. Shintani, A. Okimura, K. Sato, T. Nakagiri, Y. Kadota, M. Inoue, N. Sawabata, M. Minami, N. Ikeda, K. Kawahara, Epithelial to mesenchymal transition is a determinant of sensitivity to chemoradiotherapy in non-small cell lung cancer, *The Annals of thoracic surgery* 92 (2011) 1794-1804.
- [261] A.-P. Morel, M. Lièvre, C. Thomas, G. Hinkal, S. Ansieau, A. Puisieux, Generation of breast cancer stem cells through epithelial-mesenchymal transition, *PloS one* 3 (2008) e2888.
- [262] D.T. Marie-Egyptienne, I. Lohse, R.P. Hill, Cancer stem cells, the epithelial to mesenchymal transition (EMT) and radioresistance: potential role of hypoxia, *Cancer letters* 341 (2013) 63-72.
- [263] N. Tiwari, A. Gheldof, M. Tatari, G. Christofori, EMT as the ultimate survival mechanism of cancer cells, *Seminars in cancer biology*, Elsevier, 2012, pp. 194-207.
- [264] P. Zhang, Y. Wei, L. Wang, B.G. Debeb, Y. Yuan, J. Zhang, J. Yuan, M. Wang, D. Chen, Y. Sun, ATM-mediated stabilization of ZEB1 promotes DNA damage response and radioresistance through CHK1, *Nature cell biology* (2014).

- [265] N. Chiba, V. Comaills, B. Shiotani, F. Takahashi, T. Shimada, K. Tajima, D. Winokur, T. Hayashida, H. Willers, E. Brachtel, Homeobox B9 induces epithelial-to-mesenchymal transition-associated radioresistance by accelerating DNA damage responses, *Proceedings of the National Academy of Sciences* 109 (2012) 2760-2765.
- [266] E. Kim, H. Youn, T. Kwon, B. Son, J. Kang, H.J. Yang, K.M. Seong, W. Kim, B. Youn, PAK1 Tyrosine Phosphorylation Is Required to Induce Epithelial–Mesenchymal Transition and Radioresistance in Lung Cancer Cells, *Cancer research* 74 (2014) 5520-5531.
- [267] A.C. Begg, Predicting recurrence after radiotherapy in head and neck cancer, *Seminars in radiation oncology*, Elsevier, 2012, pp. 108-118.
- [268] N. Vig, I.C. Mackenzie, A. Biddle, Phenotypic plasticity and epithelial-to-mesenchymal transition in the behaviour and therapeutic response of oral squamous cell carcinoma, *Journal of Oral Pathology & Medicine* (2015).
- [269] L.V. DeSouza, A. Matta, Z. Karim, J. Mukherjee, X.S. Wang, O. Krakovska, G. Zadeh, A. Guha, K. Siu, Role of moesin in hyaluronan induced cell migration in glioblastoma multiforme, *Molecular cancer* 12 (2013) 1-13.
- [270] A.L. Neisch, R.G. Fehon, Ezrin, radixin and moesin: key regulators of membrane–cortex interactions and signaling, *Current opinion in cell biology* 23 (2011) 377-382.
- [271] K. Rycaj, D.G. Tang, Cancer stem cells and radioresistance, *International journal of radiation biology* 90 (2014) 615-621.
- [272] A. Okamoto, K. Chikamatsu, K. Sakakura, K. Hatsushika, G. Takahashi, K. Masuyama, Expansion and characterization of cancer stem-like cells in squamous cell carcinoma of the head and neck, *Oral oncology* 45 (2009) 633-639.
- [273] H. Harada, S. Kizaka-Kondoh, G. Li, S. Itasaka, K. Shibuya, M. Inoue, M. Hiraoka, Significance of HIF-1-active cells in angiogenesis and radioresistance, *Oncogene* 26 (2007) 7508-7516.
- [274] I. Skvortsova, S. Skvortsov, T. Stasyk, U. Raju, B.-A. Popper, B. Schiestl, E. von Guggenberg, A. Neher, G.K. Bonn, L.A. Huber, Intracellular signaling pathways regulating radioresistance of human prostate carcinoma cells, *Proteomics* 8 (2008) 4521-4533.
- [275] T. Ettl, S. Viale-Bouroncle, M.G. Hautmann, M. Gosau, O. Kölbl, T.E. Reichert, C. Morsczeck, AKT and MET signalling mediates antiapoptotic radioresistance in head neck cancer cell lines, *Oral oncology* 51 (2015) 158-163.
- [276] S. Mahner, C. Baasch, J. Schwarz, S. Hein, L. Wölber, F. Jänicke, K. Milde-Langosch, C-Fos expression is a molecular predictor of progression and survival in epithelial ovarian carcinoma, *British journal of cancer* 99 (2008) 1269-1275.
- [277] H. Wajant, The role of TNF in cancer, *Death Receptors and Cognate Ligands in Cancer*, Springer, 2009, pp. 1-15.
- [278] F. Zagouri, T.N. Sergentanis, M. Gazouli, A. Tsigginou, C. Dimitrakakis, I. Papaspyrou, E. Eleutherakis-Papaiakevou, D. Chrysikos, G. Theodoropoulos, G.C. Zografos, HSP90, HSPA8, HIF-1 alpha and HSP70-2 polymorphisms in breast cancer: a case–control study, *Molecular biology reports* 39 (2012) 10873-10879.

Chapter 9

Appendix

Appendix 1: Radiation schedule for the establishment of radioresistant sublines.

- Time for dose has been increased as $t \frac{1}{2}$ of Cobalt-60 increases (decays over time).
- Parental cells were passaged simultaneously without giving any radiation treatment.

(i) For establishing 70Gy-AW13516 subline:

S. No	Date of irradiation	Dose (Gy)	Time (Minutes)	Established sublines	Total Dose in fraction
AW13516 (Parental)					
1	12-3-2011	2 Gy	1.67	2 Gy-AW13516	2 Gy
2	14-3-2011	2 Gy	”	4 Gy-AW13516	4 Gy
3	17-3-2011	2 Gy	”	6 Gy-AW13516	6 Gy
4	19-3-2011	2 Gy	”	8 Gy-AW13516	8 Gy
5	21-3-2011	2 Gy	”	10 Gy-AW13516	10 Gy
6	24-3-2011	2 Gy	”	12 Gy-AW13516	12 Gy
7	26-3-2011	2 Gy	1.68	14 Gy-AW13516	14 Gy
8	29-3-2011	2 Gy	”	16 Gy-AW13516	16 Gy
9	31-3-2011	2 Gy	”	18 Gy-AW13516	18 Gy
10	2-4-2011	2 Gy	”	20 Gy-AW13516	20 Gy
11	5-4-2011	2 Gy	”	22 Gy-AW13516	22 Gy
12	7-4-2011	2 Gy	”	24 Gy-AW13516	24 Gy
13	9-4-2011	2 Gy	”	26 Gy-AW13516	26 Gy
14	11-4-2011	2 Gy	1.69	28 Gy-AW13516	28 Gy
15	15-4-2011	2 Gy	”	30 Gy-AW13516	30 Gy
16	18-4-2011	2 Gy	”	32 Gy-AW13516	32 Gy
17	21-4-2011	2 Gy	”	34 Gy-AW13516	34 Gy
18	23-4-2011	2 Gy	”	36 Gy-AW13516	36 Gy
19	25-4-2011	2 Gy	”	38 Gy-AW13516	38 Gy
20	28-4-2011	2 Gy	”	40 Gy-AW13516	40 Gy
21	2-5-2011	2 Gy	”	42 Gy-AW13516	42 Gy
22	4-5-2011	2 Gy	”	44 Gy-AW13516	44 Gy
23	7-5-2011	2 Gy	1.73	46 Gy-AW13516	46 Gy
24	10-5-2011	2 Gy	”	48 Gy-AW13516	48 Gy

25	13-5-2011	2 Gy	”	50 Gy-AW13516	50 Gy
26	16-5-2011	2 Gy	”	52 Gy-AW13516	52 Gy
27	19-5-2011	2 Gy	”	54 Gy-AW13516	54 Gy
28	23-5-2011	2 Gy	”	56 Gy-AW13516	56 Gy
29	27-5-2011	2 Gy	”	58 Gy-AW13516	58 Gy
30	30-5-2011	2 Gy	1.74	60 Gy-AW13516	60 Gy
31	3-6-2011	2 Gy	”	62 Gy-AW13516	62 Gy
32	7-6-2011	2 Gy	”	64 Gy-AW13516	64 Gy
33	11-6-2011	2 Gy	”	66 Gy-AW13516	66 Gy
34	14-6-2011	2 Gy	”	68 Gy-AW13516	68 Gy
35	17-6-2011	2 Gy	”	70 Gy-AW13516	70 Gy

(ii) For establishing 70Gy-UPCI:SCC029B subline:

S. No	Date of irradiation	Dose (Gy)	Time (Minutes)	Established sublines	Total Dose in fraction
UPCI:SCC029B (Parental)					
1	16-1-2012	2 Gy	1.85	2 Gy-SCC029B	2 Gy
2	19-1-2012	2 Gy	”	4 Gy-SCC029B	4 Gy
3	21-1-2012	2 Gy	”	6 Gy-SCC029B	6 Gy
4	24-1-2012	2 Gy	”	8 Gy-SCC029B	8 Gy
5	27-1-2012	2 Gy	”	10 Gy-SCC029B	10 Gy
6	30-1-2012	2 Gy	1.86	12 Gy-SCC029B	12 Gy
7	1-2-2012	2 Gy	”	14 Gy-SCC029B	14 Gy
8	3-2-2012	2 Gy	”	16 Gy- SCC029B	16 Gy
9	6-2-2012	2 Gy	”	18 Gy- SCC029B	18 Gy
10	10-2-2012	2 Gy	”	20 Gy- SCC029B	20 Gy
11	13-2-2012	2 Gy	1.87	22 Gy- SCC029B	22 Gy
12	16-2-2012	2 Gy	”	24 Gy- SCC029B	24 Gy
13	18-2-2012	2 Gy	”	26 Gy- SCC029B	26 Gy
14	21-2-2012	2 Gy	”	28 Gy- SCC029B	28 Gy
15	25-2-2012	2 Gy	”	30 Gy- SCC029B	30 Gy
16	28-2-2012	2 Gy	”	32 Gy- SCC029B	32 Gy
17	2-3-2012	2 Gy	”	34 Gy- SCC029B	34 Gy
18	5-3-2012	2 Gy	1.88	36 Gy- SCC029B	36 Gy
19	7-3-2012	2 Gy	”	38 Gy- SCC029B	38 Gy
20	10-3-2012	2 Gy	”	40 Gy- SCC029B	40 Gy

21	13-3-2012	2 Gy	”	42 Gy- SCC029B	42 Gy
22	15-3-2012	2 Gy	”	44 Gy- SCC029B	44 Gy
23	19-3-2012	2 Gy	”	46 Gy- SCC029B	46 Gy
24	21-3-2012	2 Gy	1.89	48 Gy- SCC029B	48 Gy
25	24-3-2012	2 Gy	”	50 Gy- SCC029B	50 Gy
26	27-3-2012	2 Gy	”	52 Gy- SCC029B	52 Gy
27	29-3-2012	2 Gy	”	54 Gy- SCC029B	54 Gy
28	2-4-2012	2 Gy	”	56 Gy- SCC029B	56 Gy
29	4-4-2012	2 Gy	”	58 Gy- SCC029B	58 Gy
30	7-4-2012	2 Gy	”	60 Gy- SCC029B	60 Gy
31	9-4-2012	2 Gy	1.90	62 Gy- SCC029B	62 Gy
32	12-4-2012	2 Gy	”	64 Gy- SCC029B	64 Gy
33	17-4-2012	2 Gy	”	66 Gy- SCC029B	66 Gy
34	19-4-2012	2 Gy	”	68 Gy- SCC029B	68 Gy
35	21-4-2012	2 Gy	”	70 Gy- SCC029B	70 Gy

(iii) For establishing 70Gy-AW8507 subline:

S. No	Date of irradiation	Dose (Gy)	Time (Minutes)	Established sublines	Total Dose in fraction
AW8507 (Parental)					
1	22-3-2013	2 Gy	2.19	2 Gy-AW8507	2 Gy
2	26-3-2013	2 Gy	”	4 Gy-AW8507	4 Gy
3	29-3-2013	2 Gy	”	6 Gy- AW8507	6 Gy
4	2-4-2013	2 Gy	”	8 Gy-AW8507	8 Gy
5	5-4-2013	2 Gy	”	10 Gy-AW8507	10 Gy
6	8-4-2013	2 Gy	”	12 Gy-AW8507	12 Gy
7	12-4-2013	2 Gy	”	14 Gy-AW8507	14 Gy
8	15-4-2013	2 Gy	2.20	16 Gy-AW8507	16 Gy
9	17-4-2013	2 Gy	”	18 Gy-AW8507	18 Gy
10	20-4-2013	2 Gy	”	20 Gy-AW8507	20 Gy
11	24-4-2013	2 Gy	”	22 Gy-AW8507	22 Gy
12	27-4-2013	2 Gy	”	24 Gy-AW8507	24 Gy
13	30-4-2013	2 Gy	2.21	26 Gy-AW8507	26 Gy
14	4-5-2013	2 Gy	”	28 Gy-AW8507	28 Gy
15	7-5-2013	2 Gy	”	30 Gy-AW8507	30 Gy
16	11-5-2013	2 Gy	”	32 Gy-AW8507	32 Gy

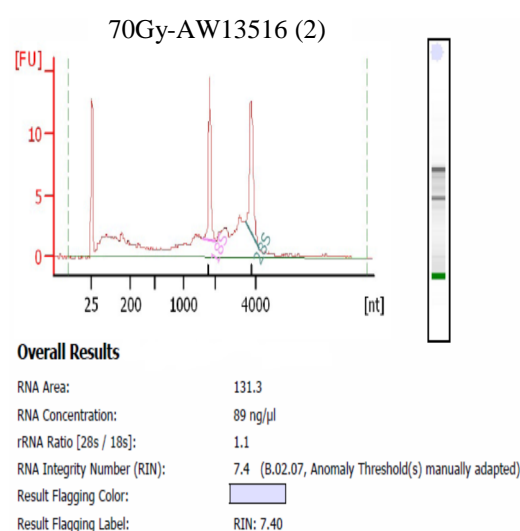
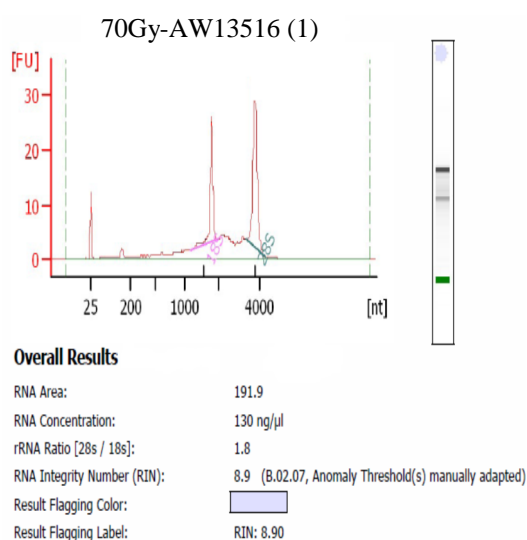
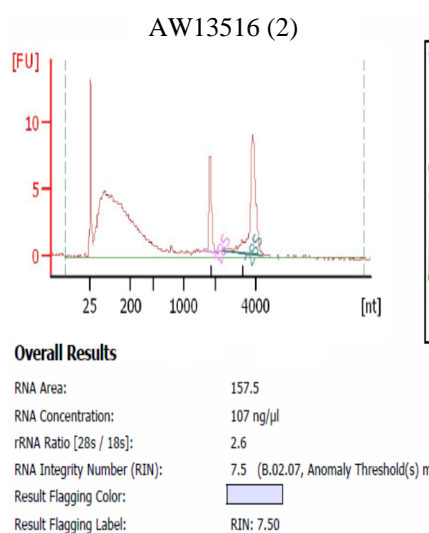
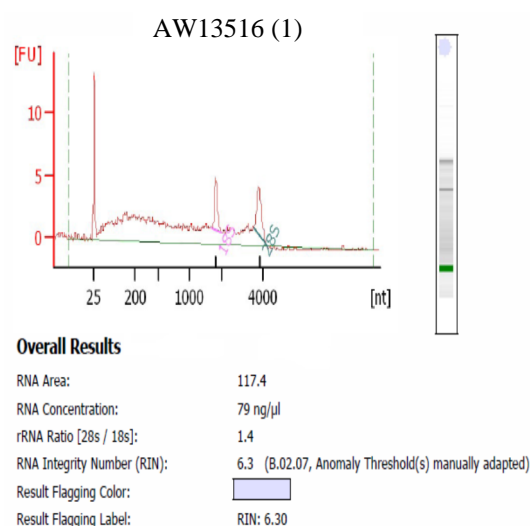
17	15-5-2013	2 Gy	”	34 Gy-AW8507	34 Gy
18	18-5-2013	2 Gy	”	36 Gy-AW8507	36 Gy
19	21-5-2013	2 Gy	”	38 Gy-AW8507	38 Gy
20	24-5-2013	2 Gy	2.22	40 Gy-AW8507	40 Gy
21	27-5-2013	2 Gy	”	42 Gy-AW8507	42 Gy
22	30-5-2013	2 Gy	”	44 Gy-AW8507	44 Gy
23	3-6-2013	2 Gy	”	46 Gy-AW8507	46 Gy
24	6-6-2013	2 Gy	”	48 Gy-AW8507	48 Gy
25	8-6-2013	2 Gy	”	50 Gy-AW8507	50 Gy
26	12-6-2013	2 Gy	2.23	52 Gy-AW8507	52 Gy
27	14-6-2013	2 Gy	”	54 Gy-AW8507	54 Gy
28	17-6-2013	2 Gy	”	56 Gy-AW8507	56 Gy
29	19-6-2013	2 Gy	”	58 Gy-AW8507	58 Gy
30	21-6-2013	2 Gy	”	60 Gy-AW8507	60 Gy
31	24-6-2013	2 Gy	”	62 Gy-AW8507	62 Gy
32	26-6-2013	2 Gy	”	64 Gy-AW8507	64 Gy
33	28-6-2013	2 Gy	”	66 Gy-AW8507	66 Gy
34	1-7-2013	2 Gy	2.25	68 Gy-AW8507	68 Gy
35	3-7-2013	2 Gy	”	70 Gy-AW8507	70 Gy

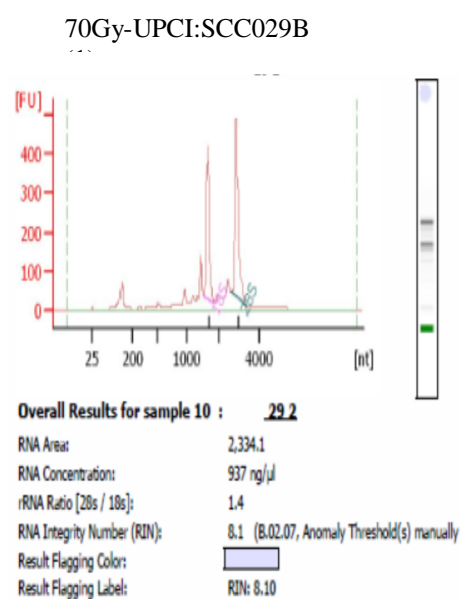
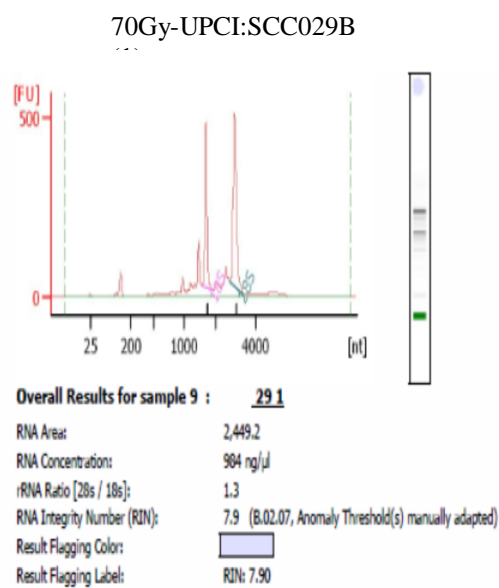
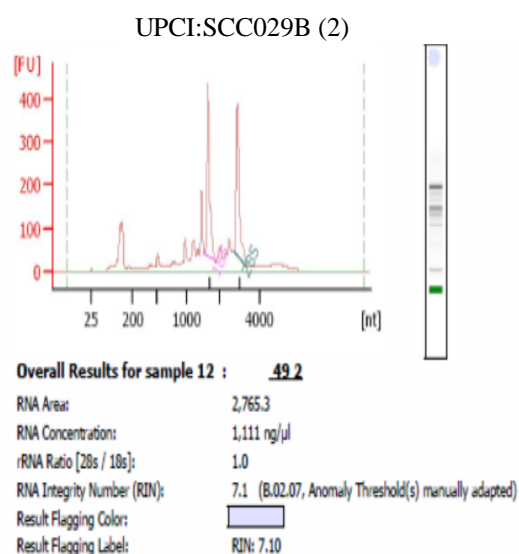
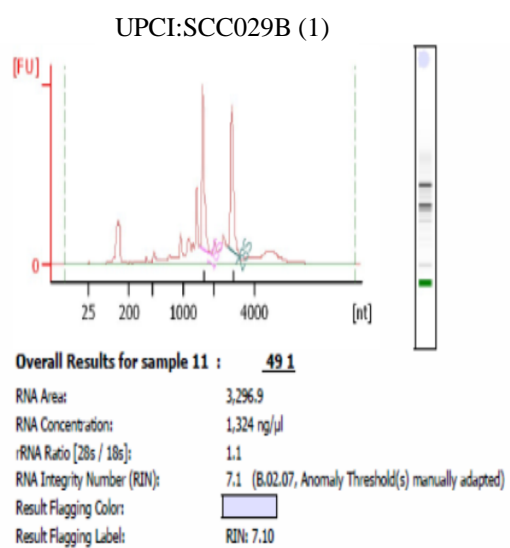
Appendix 2: Agilent Bioanalyzer-2100 QC report of microarray analysis

S.No	Sample I.D	Conc. ng/ul	RIN value	rRNA ratio
1	AW13516 (1)	79	6.3	1.4
2	AW13516 (2)	107	7.5	2.6
3	70Gy-AW13516 (1)	130	8.9	1.8
4	70Gy-AW13516 (2)	89	7.4	1.1
5	UPCI:SCC029B (1)	1,324	7.1	1.1
6	UPCI:SCC029B (2)	1,111	7.1	1
7	70Gy-UPCI:SCC029B (1)	984	7.9	1.3
8	70Gy-UPCI:SCC029B (2)	937	8.1	1.4

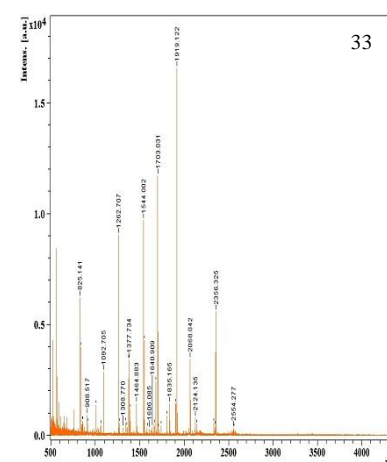
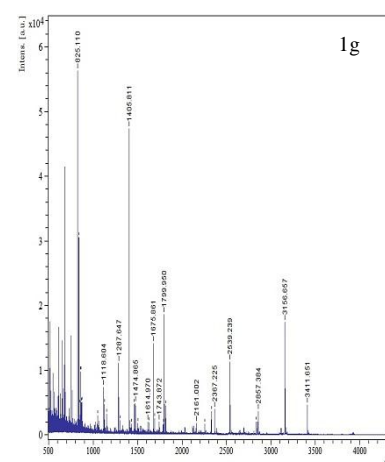
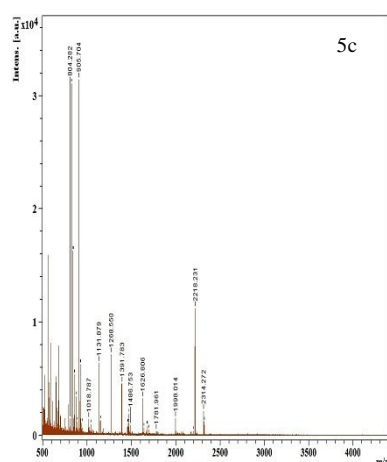
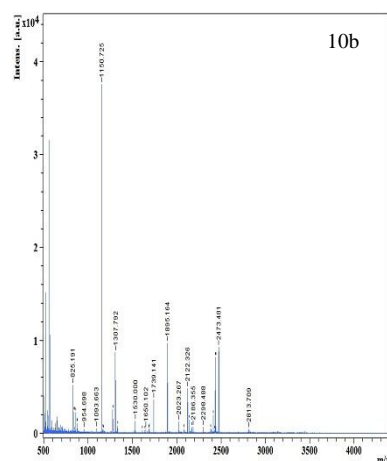
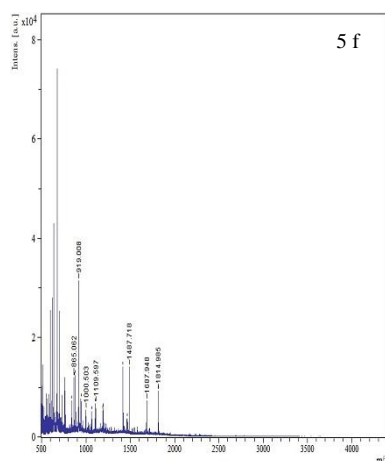
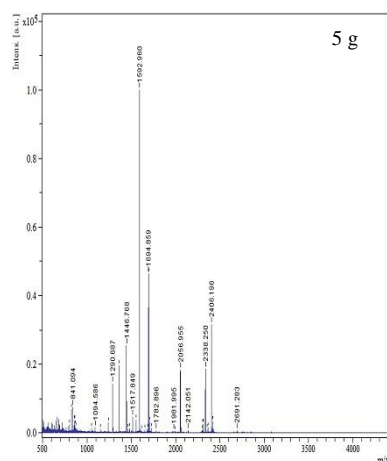
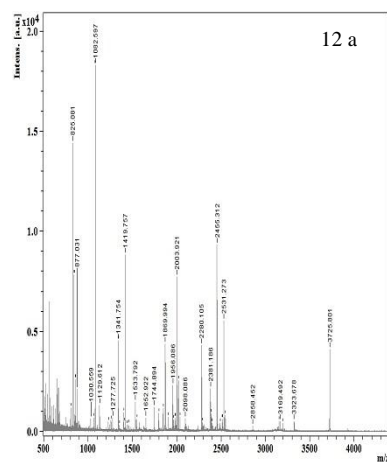
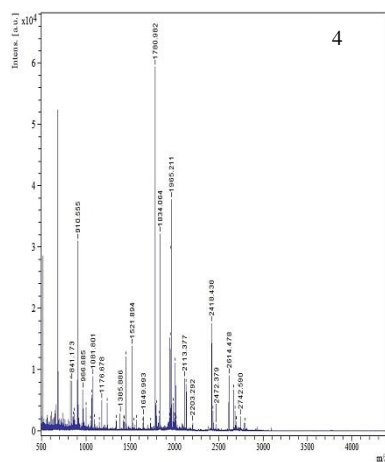
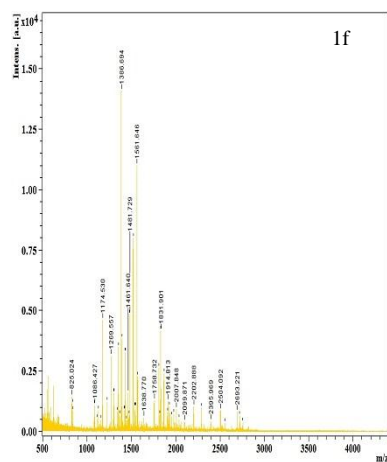
***RIN=RNA Integrity Number, rRNA ratio= 18s and 28s ribosomal RNA ratio.**

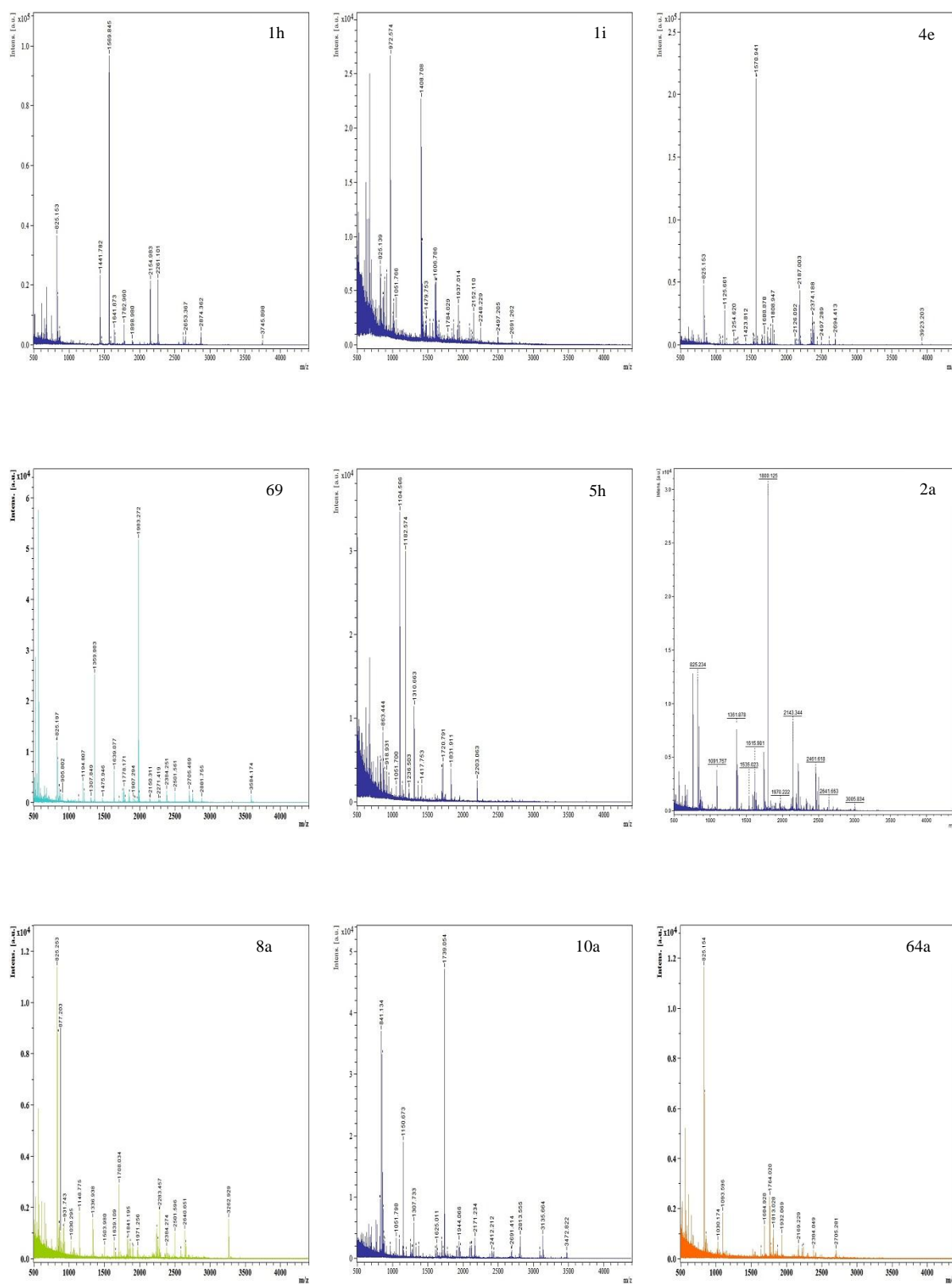
- All the samples are showing RIN value above 6. RNA above RIN value 5.0 is considered as good RNA for Microarray experiment.

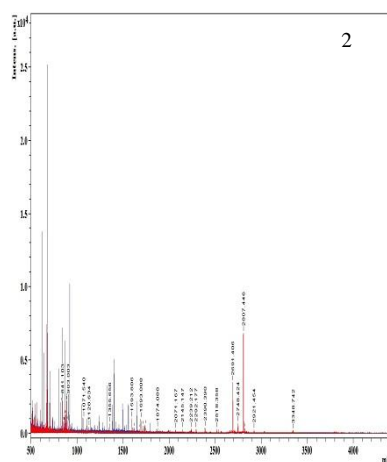
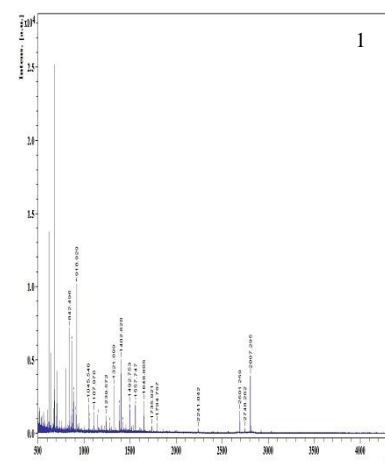
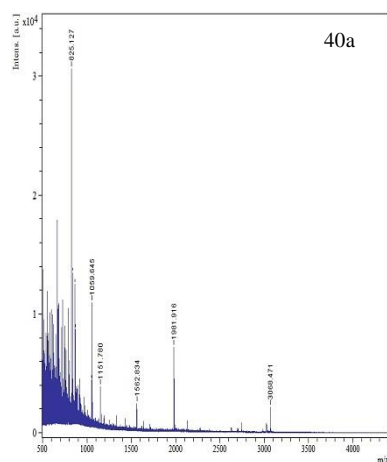
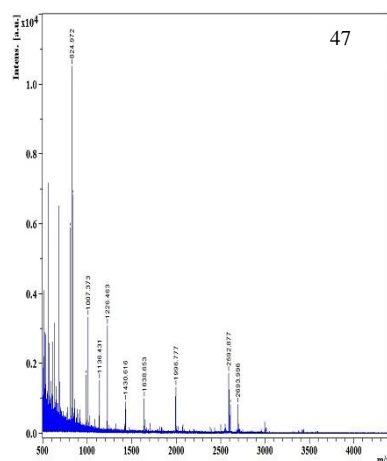
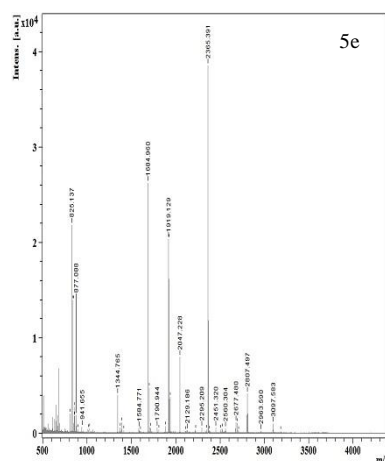
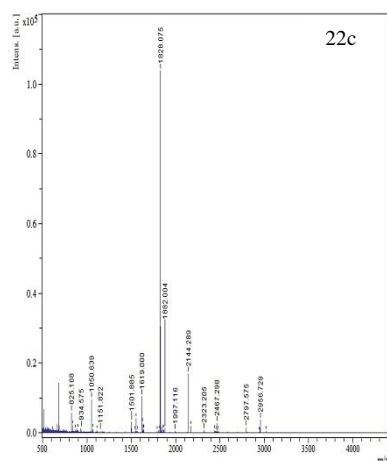
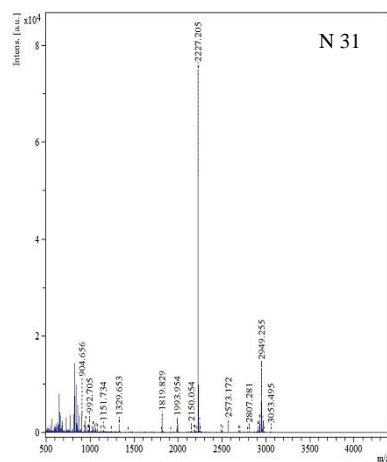
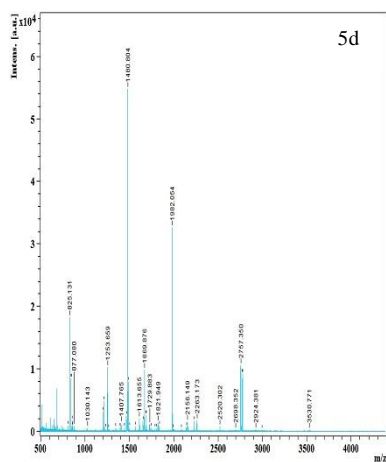
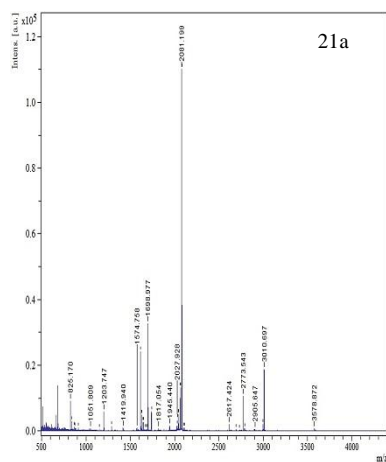


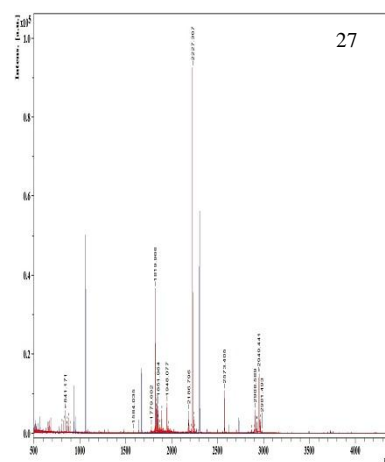
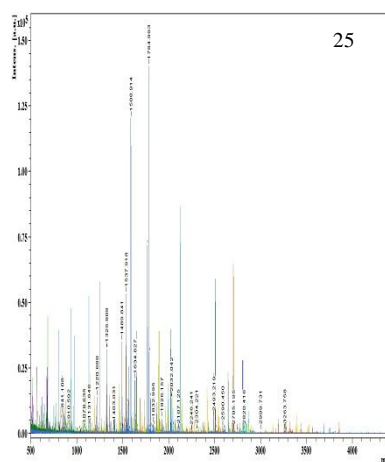
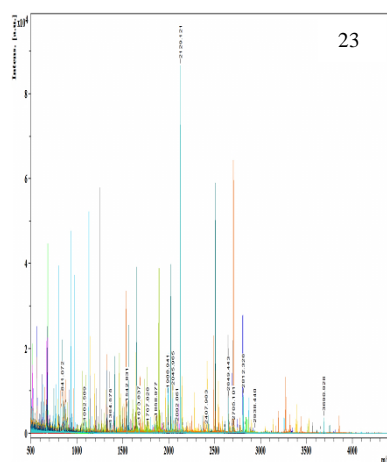
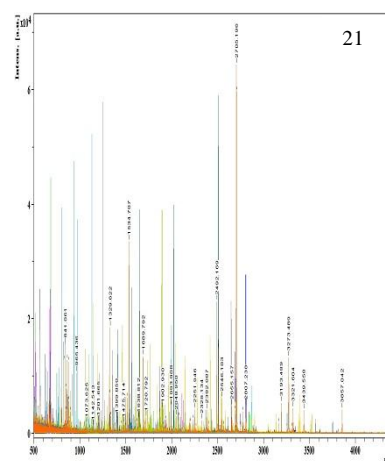
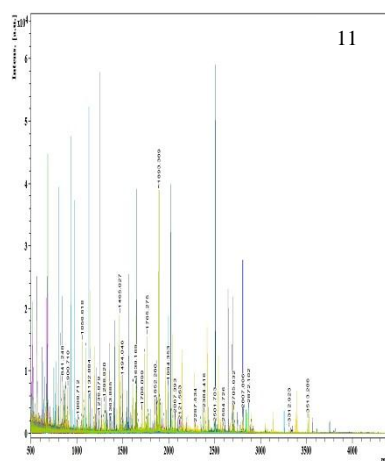
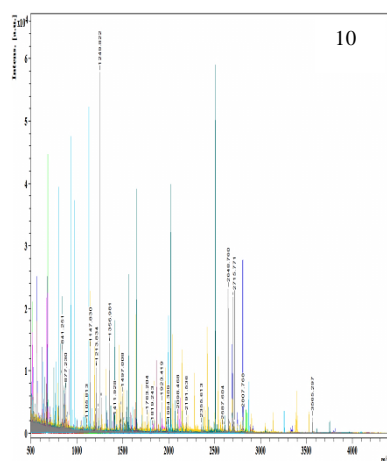
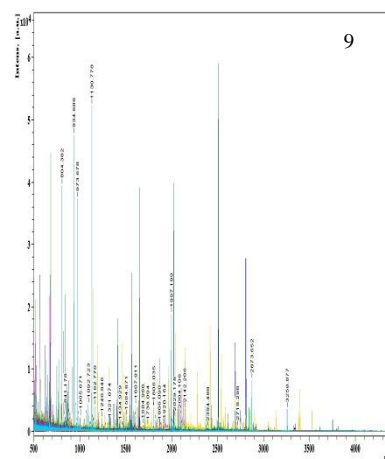
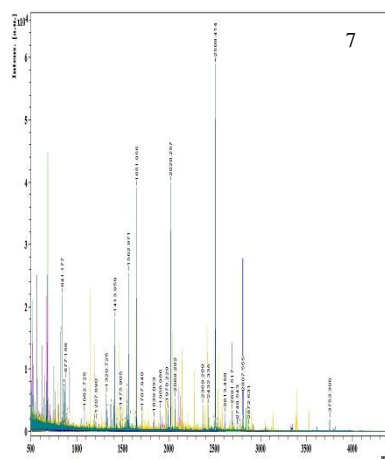
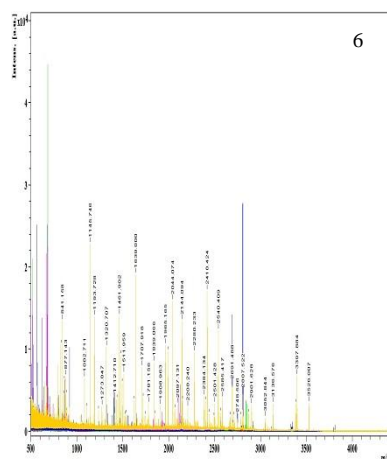


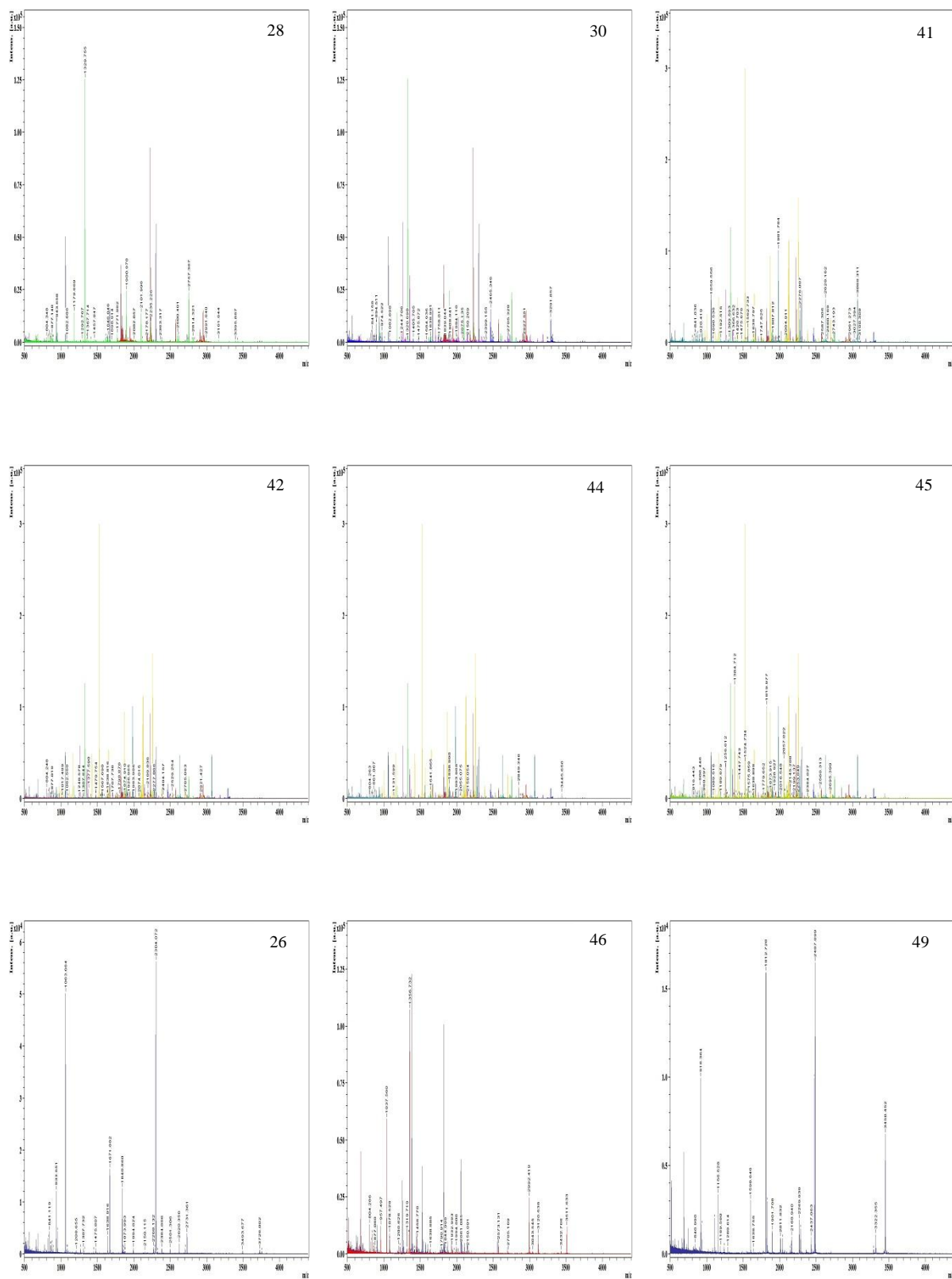


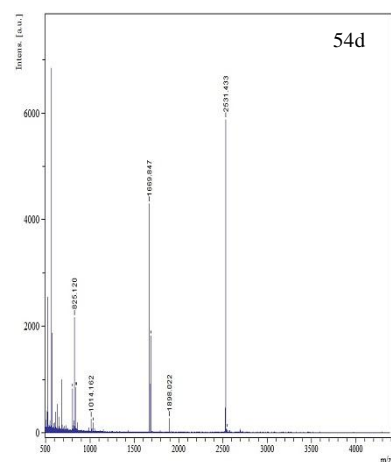
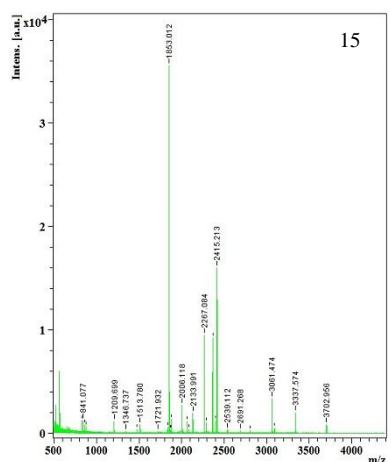
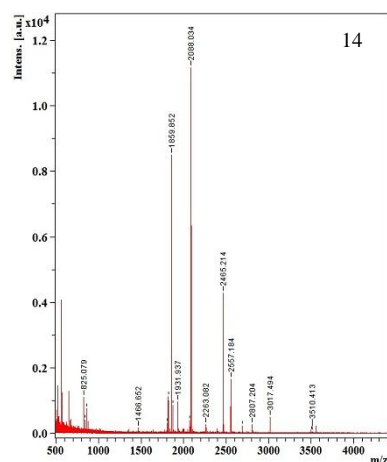
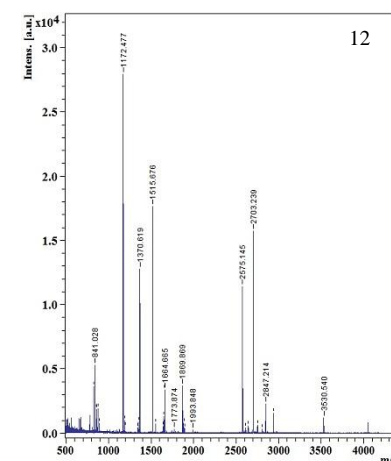
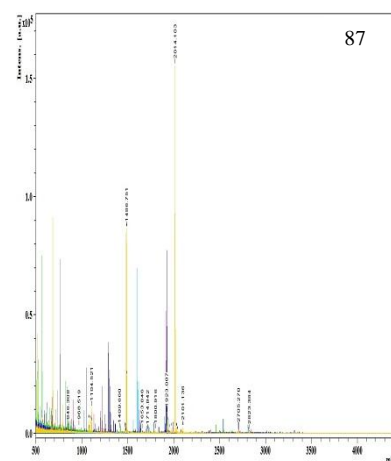
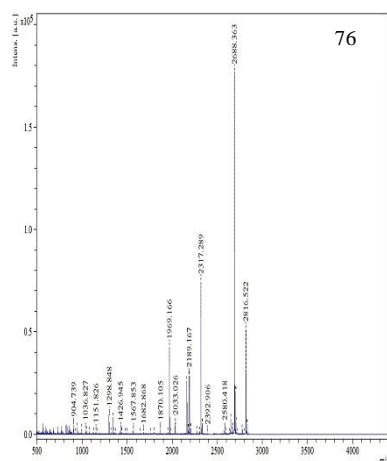
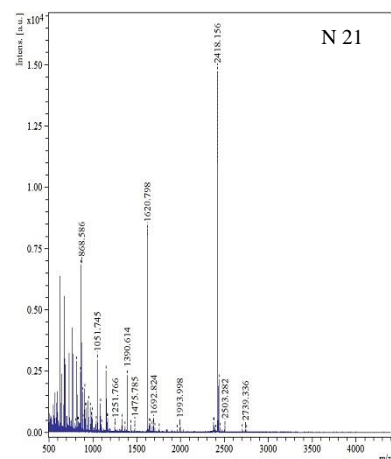
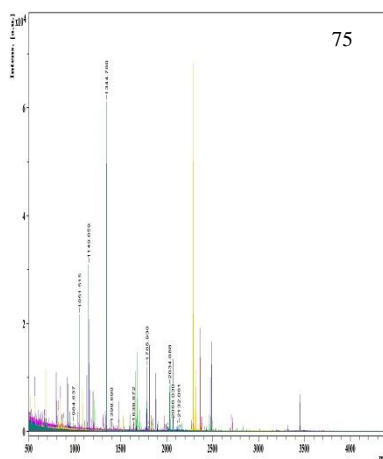
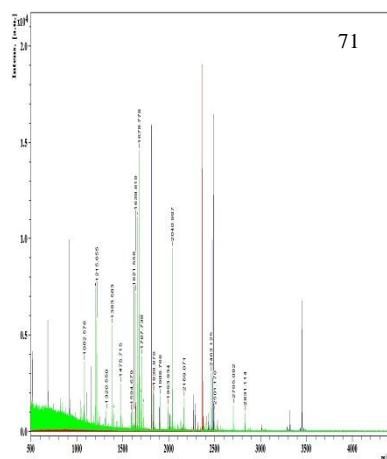


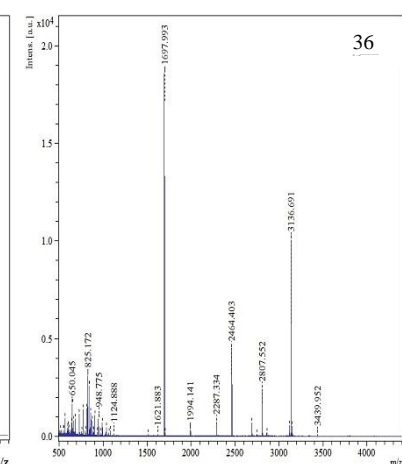
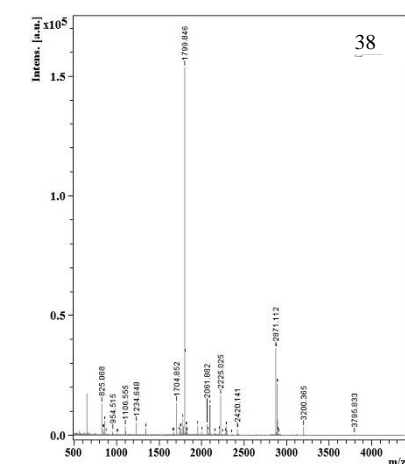
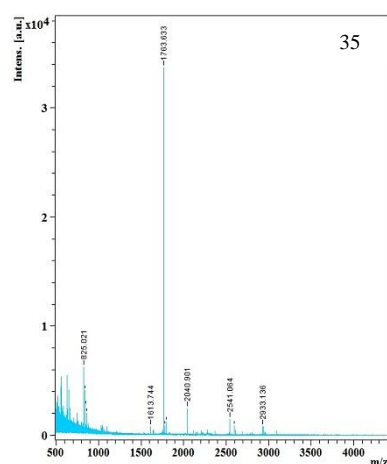
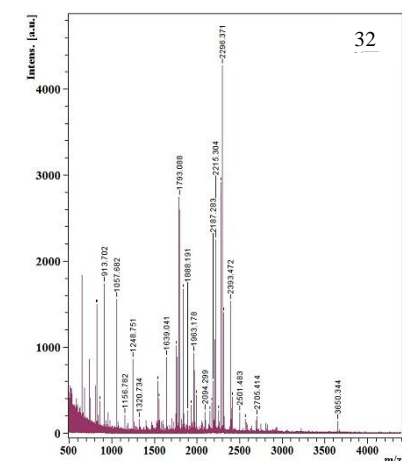
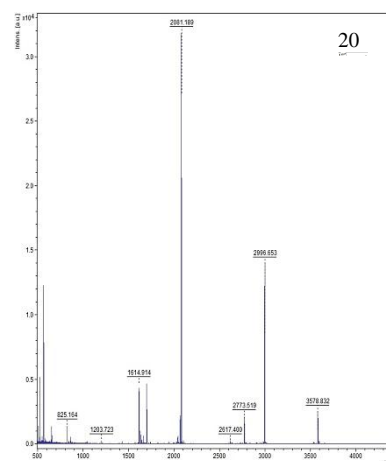
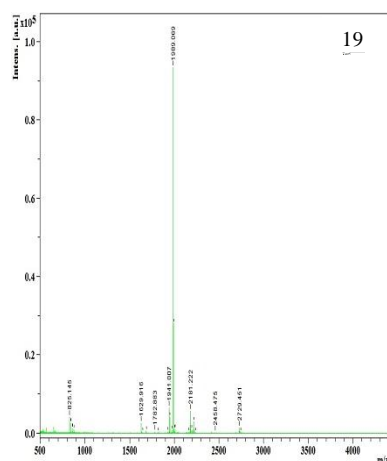
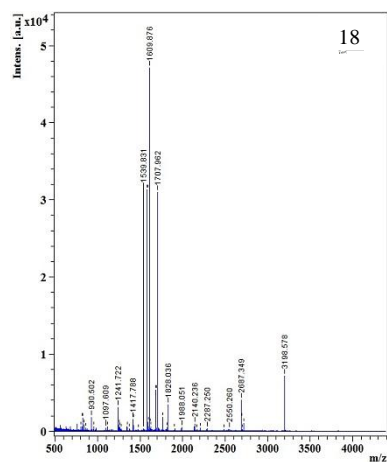
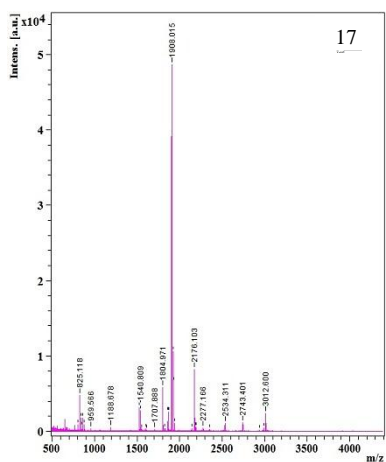
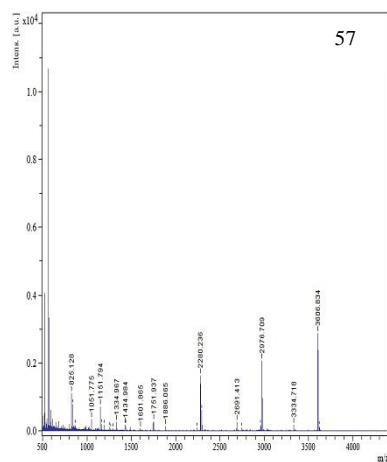


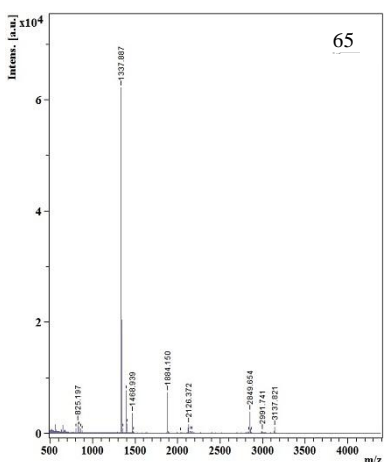
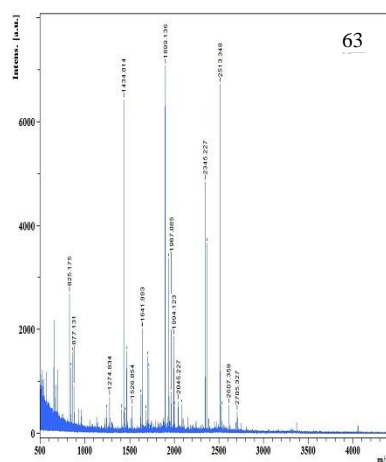
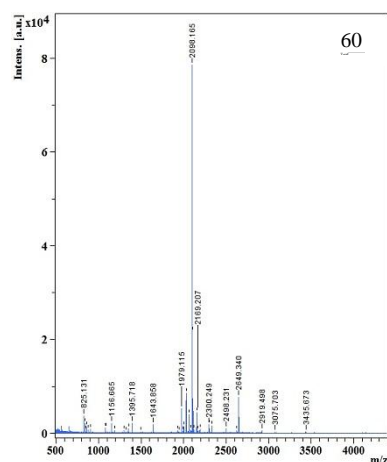
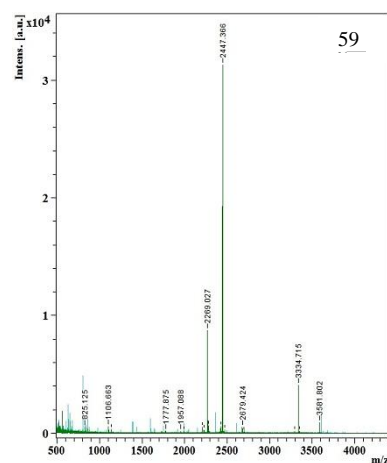
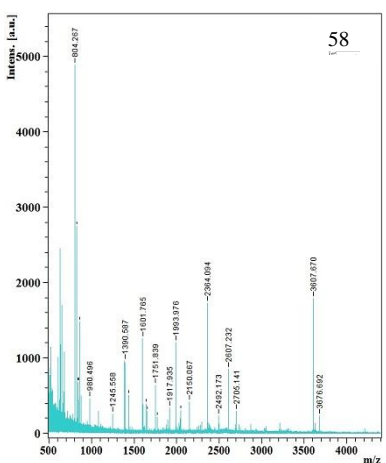
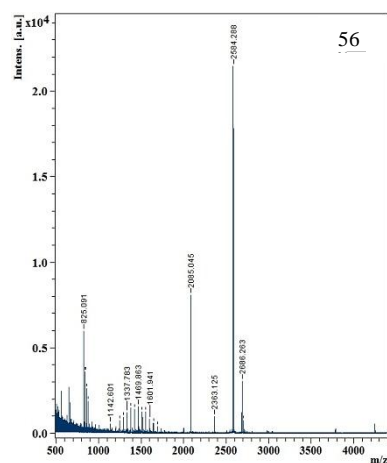
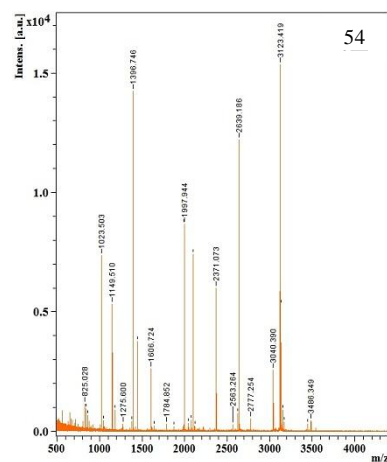
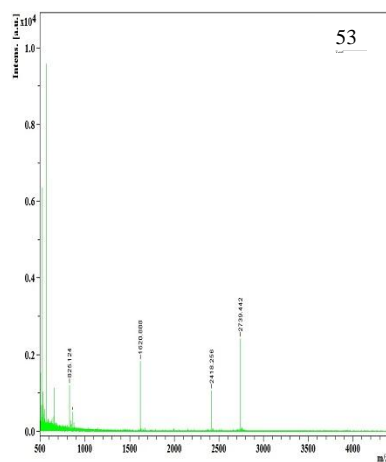
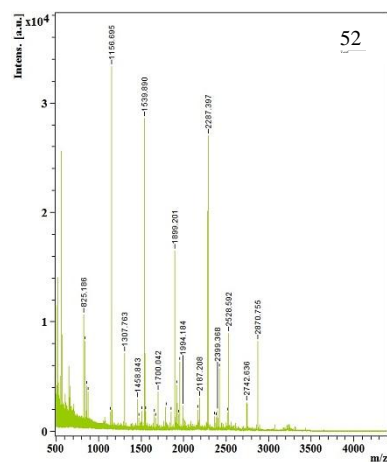


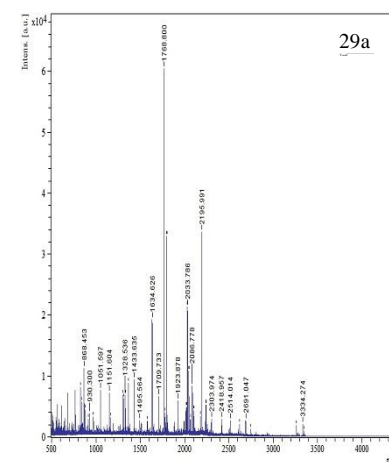
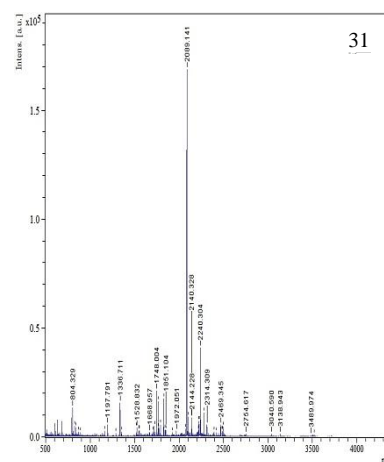
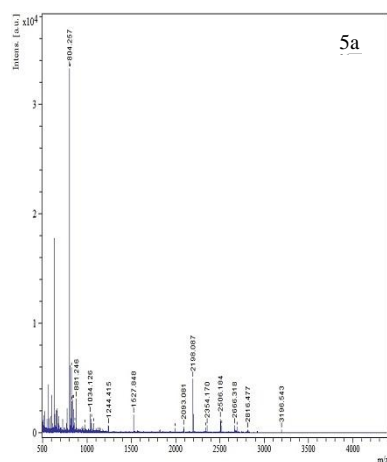
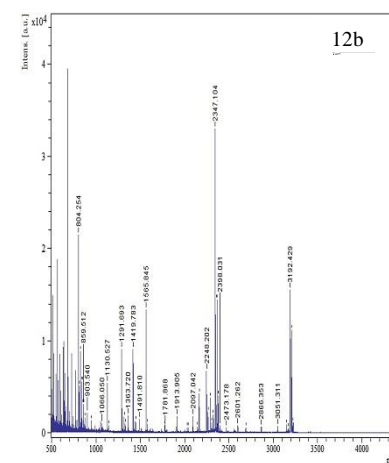
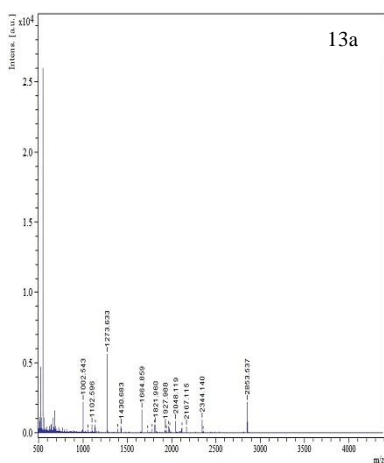
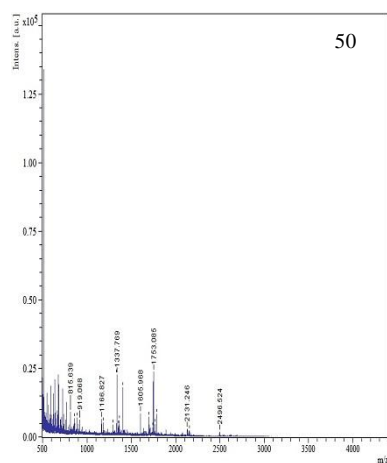
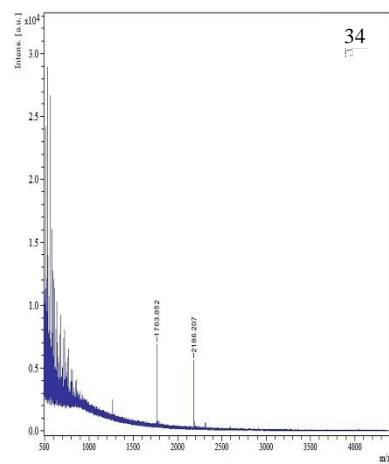
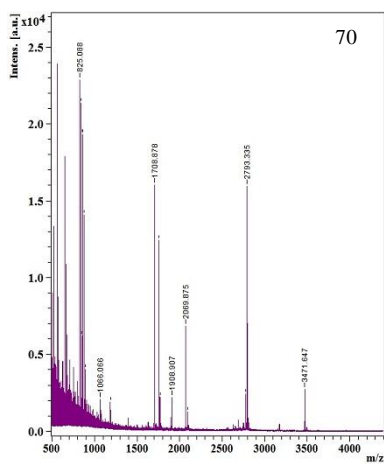
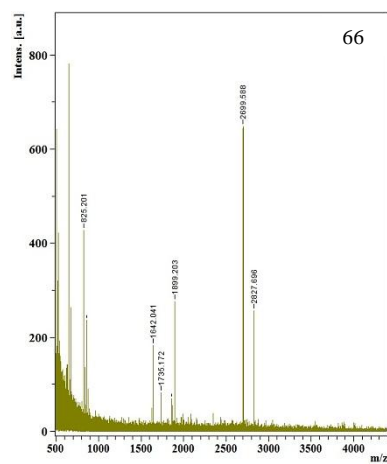


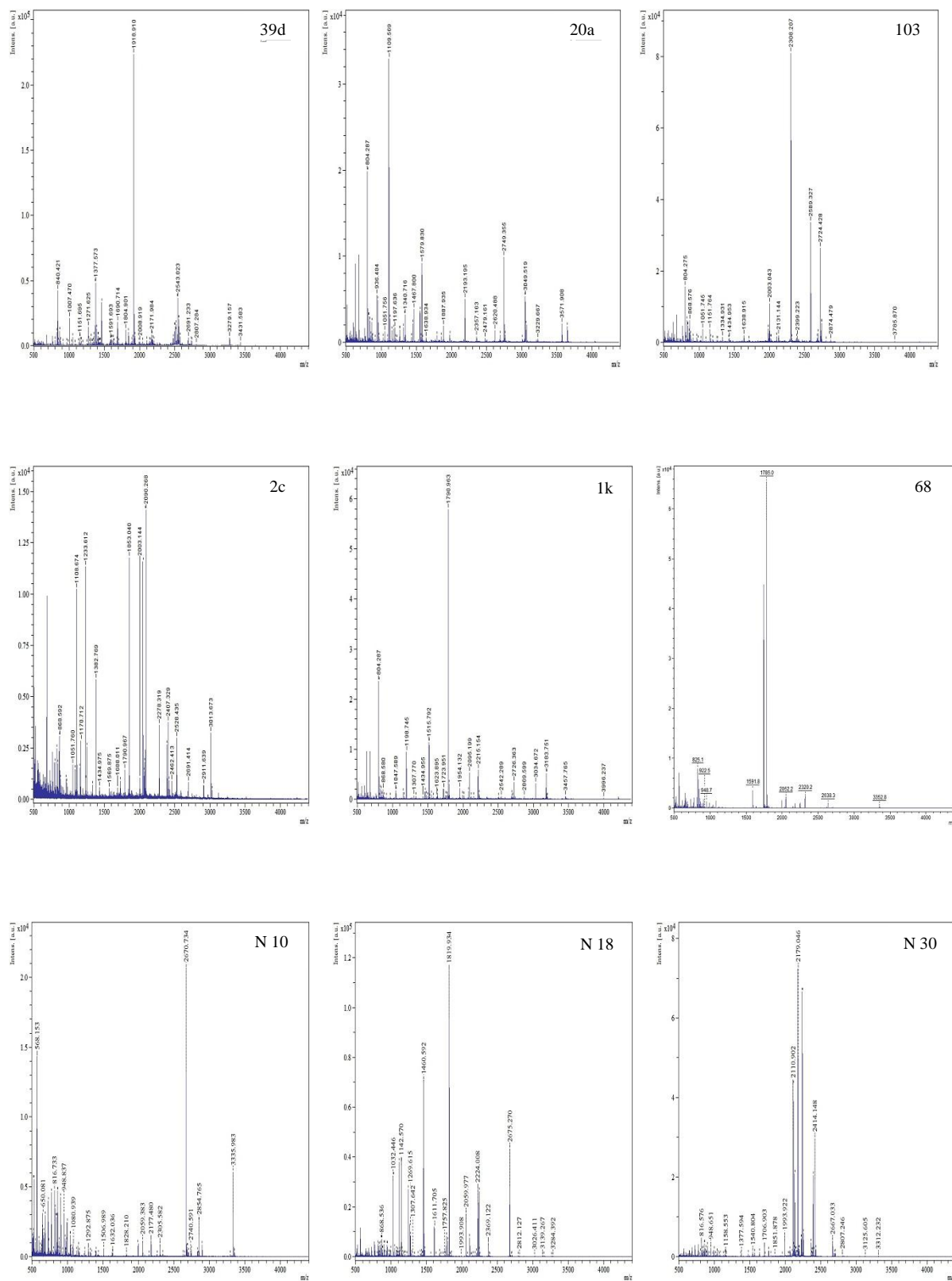


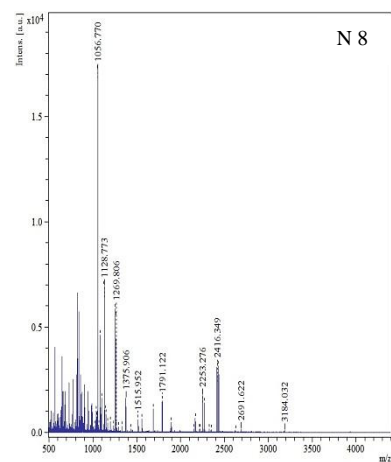
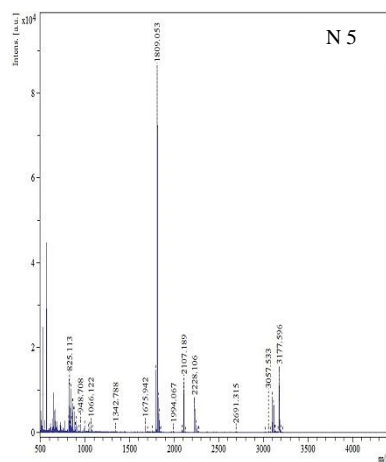
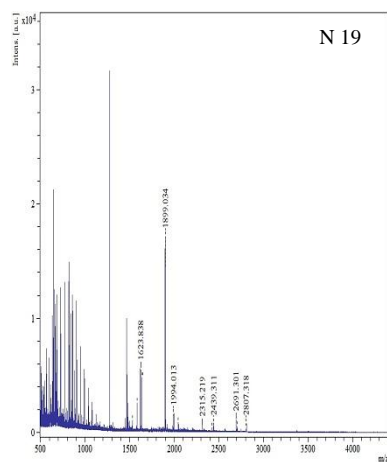












Appendix4: Complete list of 102 identified proteins in standard format

Spot No.	Protein name	Protein ID	Accession No.	MS						MS/MS				
				Total Score	Mass (kDa)	PI	IC %	SC %	Searched Peaks	Matched Peaks	Tolerance/ppm	Peptides Identified	Score	Tolerance (Da)
39d	Heterogeneous nuclear ribonucleoprotein H3	HNRH3_HUMAN	Q9UFU4	161	36.9	6.4	57.1	63.9	82	21	100	-YIEIFR -GFYDPPRR -STGEAFVQFASK -ATENDIANFFSPLNPIR -GMGGHG YGGAGD ASSGFH GGHFVHMR	144	1.5
84	Peptidyl prolyl cis-trans isomerase A	PPIA_HUMAN	P62937	59	18.2	9	31.9	32.1	10	4	100	-GFGYKGS SCFHR -VKEGMNIVEAMER -IIPGFMCQGGDFT R -SIYGEKFEDENFILK	69	1.5
57	Rho GDP-dissociation inhibitor 1	GDIR1_HUMAN	P52565	46	23.2	6.4	23.5	18.1	26	6	100	-IDKTDY MVGSY GPR -AEEYEFLTPVEEAPK	38.3	1.5
34	Pyrroline-5-carboxylate reductase 3	P5CR3_HUMAN	Q53H96	39	29.1	8.1	100	13.9	2	2	100	-AGKVEAQHILASAP TDR -MGMPSSLAHRIAA QTLLGTAK	49	1.5
56	Eukaryotic translation initiation factor 6	IF6_HUMAN	P56537	58.5	27	4.4	47.0	46.1	23	6	200	-NSLPDTVQIR -ASFENNCEIGCF AK -HGLLVPNNTTDQ ELQH IR -LNEAQPS TIATSM RDSLIDSLT -TSIEDQDELSSLL QVPLVAGTVNR	225	1

20	40S ribosomal protein SA	RSSA_HUMAN	Q86VC0	105	32.9	4.6	88.0	39.7	24	10	200	- GAHSVG LMWWM LAR - FTPGTFT NQIQAA FR - FTPGTFT NQIQAA FREPR - FLAAGT HLGGTN LDFQME QYIYKR - ADHQPL TEASYV NLPTIAL CNTDSPL R	136	1
69	Peroxiredoxin-1	PRDX1_HUMAN	Q06830	104	22.3	9.2	62.4	61.3	37	9	200	- SVDETLR - QITVNDL PVGR - GLFIIDD KGILR - QGGLGP MNIPLV SDPK - TIAQDY GVLKAD EGISFR	246	1
33	Annexin A1	ANXA1_HUMAN	P04083	185	38.9	6.7	50.9	66.2	42	20	200	- TPAQFD ADELR - GVDEATI IDILTKR - GTDVNV FNTILTT R - GLGTDE DTLIEIL ASR - GGPGSA VSPYPTF NPSSDV AALHK	309	1
2	Neutral alpha-glucosidase AB	GANAB_HUMAN	Q14697	77	107.2	5.7	21.7	18.0	34	13	200	- YFTWDP SR - DAQHYG GWEHR - WYQMG AYQPFFR - KPGINVA SDWSIH LR - LSFQHDP ETSVLV LR	77	1
75	Nucleoside diphosphate kinase A	NDKA_HUMAN	P15531	154	17.3	5.8	98.9	61.2	14	11	200	- GDFCIQV GR - DRPFAG LVK - TFIAIKP	189	1

Appendix

												DGVQR - VMLGET NPADSK P GTIR - EHYVDL KDRPFFA GLVK		
9	Histone-binding protein RBBP4	RBBP4_HUMAN	Q09028	77.6	47.91	4.6	56.8	23.3	52	9	200	- LMIWDT R - TVALWD LR - RLNVWD LSK - HPSKPDP SGECNP DLR - IGEEQSP EDAEDG P PELLFIH GGHTAK	102	1
41	Guanine nucleotide-binding protein subunit beta-2-like 1	GBLP_HUMAN	Q6FH47	159	35.51	8.9	70.6	65	50	15	200	- VWQVTI GTR - LTRDET NYGIPQR - YTVQDE SHSEWV SCVR - HLYTLD GGDIINA L CFSPNR - AEPPQCT SLAWSA DGQTLF AGYTDN L VR	234	1
71	Transgelin-2	TAGL2_HUMAN	P37802	90.7	22.54	9.3	36.0	47.2	26	10	200	- NVIGLQ MGTNR - TLMNLG GLAVAR - GASQAG MTGYG M PR - QMEQIS QFLQAA ER - DVGRPQ PGRENF Q NWLK	123	1
53	Ran specific GTPase activating protein	RANG_HUMAN	P43487	60	23.46	5.1	71.6	28.4	5	3	200	- FASENDL PEWKER - ICANHVI TPMMEL KPNAGS DR - AWVWN THADFA D ECPKPEL	60	1

Appendix

												LAIR		
22c	Eukaryotic initiation factor 4A-I	IF4A1_HUMAN	P60842	173	46.3	5.2	81.0	52.7	38	19	100	- VFDMLNRR - MFVLDEADEMLSR - LQMEAPHIIVGTPGR - GIYAYGF EKP SAIQQR - GIDVQQVSLV INIDLPTNR	267	1.5
32	L-lactate dehydrogenase B chain	LDHB_HUMAN	P07195	32.4	36.9	5.7	38.7	25.4	36	9	200	- IVVVTA GVR - FRYLMAEK - EVHKMV VESA YEVIK - GMYGIE NEVF LSLPCIL NAR - GMYGIE NEVF LSLPCIL NAR	39.2	1
54d	Proteasome activator complex subunit 2	PSME2_HUMAN	Q9UL46	58.6	27.5	5.4	39.2	21.3	13	3	100	- QNLFQEAEEFLYR - ILYLNQL LQED SLNVAD LTSLR	98.7	1.5
2a	Elongation factor 2	EF2_HUMAN	P13639	71.3	96.246	6.4	53.8	31.2	56	20	200	-KDEQER - ALLELQLEPE ELYQTF QR - LMEPIYL VEIQ CPEQVV GGIYG VLNR	217	1.5
7	Transketolase	TKT_HUMAN	P29401	123	68.5	8.5	62.9	36.6	46	15	200	- VLDPFTIKPLDR - MFGIDR DAIA QAVR - TVPFCST FAAF FTR - ILATPPQ EDAP	118	1

Appendix

												SVDIANI R - TSRPENAI IYN NNEDFQ VGQ AK		
35	Glycerol dehyde- 3- phospha te dehydro genase	G3P_H UMAN	P0440 6	55.5	36.2	9.3	70.1	24.8	12	5	200	- LISWYD NEFG YSNR - LVINGNP ITIFQ ERDPSK - VIHDNFG IVE GLMTTV HAITATQ K - VIISAPSA DAP MFVMGV NHEKYD NSLK	65.1	1
52	Ubiquiti n carboxyl - terminal hydrolas e isozyme L3	UCHL 3_HU MAN	P1537 4	93	26.33	4.7	50.6	46.1	34	10	200	- YLENYD AIR - FMERDP DELR - FLEESVS MSP EER - WLPLEA NPEV TNQFLK - KPFPINH GETS DETLLED AIEVCKK	105	1
56	Eukaryo tic translati on initiatio n factor 6	IF6_H UMAN	P5653 7	62.3	27	4.4	47	46.1	23	6	200	- NSLPDTV QIR - ASFENN CEIG CFAK - HGLLVP NNTT DQELQHI R - LNEAQPS TIAT SMRDSLI DSL - TSIEDQD ELSS LLQVPL VAGTVN R	69.2	1
59	Calpain small subunit 1	CPNS1 _HUM AN	P0463 2	148	28.46	4.9	96.1	65.3	19	12	200	- YLWNNI KR - YSDESG NMD FDNFISC LVR - YSDESG NMD FDNFISC LVR - ILGGVIS	164	1

Appendix

												AISE AAQYN PEPPPPR - SGTICSS ELPG AFEAAAG FHLNEH LYNMIIR		
60	Peroxi- redoxin-6	PRDX6 _HUMAN	P3004 1	107	25.13	6	69.2	42.4	40	10	200	- DFTPVCT TEL GR - FHDFLG DSWG ILFSHPR - PGGLLL GDVA PNFEANT TVGR - IRFHDFL GDS WGILFSH PR - DINAYN CEEP TEKLPFP IIDDR	127	1
47	Proteas- ome subunit alpha type-4	PSA4_ HUMAN	P2578 9	60.8	29.75	8.7	25.4	29.9	13	6	200	- TTIFSPE GR - LLDEVFF SEK - LSAEKV EIAT LTR - LNEDMA CSV AGITSDA NVL TNE LR - YLLQYQ EPIP CEQLVT ALCD IK	112	1
66	Peroxi- redoxin-2	PRDX2 _HUMAN	P3211 9	60.1	22.04	5.6	39.5	21.2	8	4	200	- EGGLGP LNIPL LADVTR - KEGGLG PLNI PLLADV TR - LGCEVL GVS DSQFTHL AWINTP R - LGCEVL GVS DSQFTHL AWINTP RK	60.1	1
5a	Mitocho- ndrial inner membra- ne protein	IMMT_ HUMAN	Q7Z3 X1	63.8	84	6.1	11.1	18.9	30	8	100	- VVSQYH ELV VQAR - LSQEQV DNFT LDINTAY AR - RLSQEQ	74.4	1.5

Appendix

												VDNF TLDINTA YAR - ANCSDN EFTQ ALTAaip PESL TR - GMSVSD LAD KLSTDD LNSLIAH AHR		
5c	Glycine- tRNA ligase	SYG_ HUMA N	P4125 0	76.3	83.8	6.7	19.3	18.7	34	12	200	- QQGDLV RK - SCYDLSC HAR - LPFAAA QIGN SFR - TSYGWIE IVG CADR - TLYVEE VVPN VIEPSFG LGR	69.3	1
1	Heat shock 70 kDa protein 4	HSP74 _HUM AN	P3493 2	172	95.12	5	40.5	19.3	28	14	200	- SVLEQT KLK - VLATAF DTTL GGR - NAVEEY VYE MR - FVSEDD RNSF TLK - SVMDAT QIAG LNCLR	279	1
1k	Hypoxia up- regulate d protein 1	HYOU 1_HU MAN	Q9Y4 L1	66.5	111.4	5	23.5	22.9	57	15	100	- FPEHELT FDP QR - DAVVYPI LVE FTR - MMALDR EVQ YLLNK - VAIVKPG VPM EIVLNKE SR - YSHDFN FHIN YGD LGF LGPEDLR	84.6	1.5
1a	Endopla smin	ENPL_ HUMA N	P1462 5	114	92.69	4.6	33.6	24.7	31	17	200	- AYGDRIE R - GLFDEY GSK - FAFQAE VNR - SII.FVPTS	483	1

Appendix

												APR - FQSSHHP TDIT SLDQYV ER		
1b	Heat shock protein 90 Alpha	HS90A _HUM AN	P0790 0	158	85.00 5 / 4.8	4.8	54.5	34	43	22	200	- RAPFDLF ENR - HFSVEG QLEFR - HSQFIGY PITL FVEKER - HNDDEQ YAW ESSAGGS FTVR - VFIMDN CEELI PEYLNFI R	489	1
1c	78 kDa glucose- regulate d protein	GRP78 _HUM AN	P1102 1	200	72.4	4.9	75.8	28.1	29	16	200	- AKFEEL NMDL FR - ITPSYVA FTPE GER - VTHAVV TVP AYFNDA QR - DNHLLG TFDL TGIPPAP R - IEIESFYE GED FSETLTR	658	1
1e	Transiti onal endopla smic reticulu m ATPase	TERA_ HUMA N	P5507 2	210	89.9	5	29.1	37.1	48	17	200	- WALSQS NPSA LR - KYEMFA QTL QQSR - EMVELP LRHP ALFK - AHVIVM AAT NRPN SID PAL RR - ETVVEV PQV TWEDIG GLEDVK R	258	1
1f	Alpha Actinin 4	ACTN 4_HU MAN	O4370 7	204	105.2 4	5.2	70.9	34.5	57	27	200	- EGLLLW CQR - VGWEQL LTTI AR - TIPWLED RVP QK -	302	1

Appendix

												KTFTAW CNS HLR - ELPPDQA EYC IAR		
li	Alanine- tRNA ligase cytoplas mic	SYAC_ HUMA N	P4958 8	65	107.5	5.2	50.3	15.0	39	11	100	-FIDFFKR	64	1.5
lg	Plastin- 2	PLSL_ HUMA N	P1379 6	151	70.81 4	5.2	51.3	34.8	36	18	100	- LNLAFIA NLF NR - FSLVGIG GQD LNEG NR - VNDDIIV NWV NETLR	125	1.5
40	Annexin A2	ANXA 2_HU MAN	P0735 5	231	38.80	8.5	69.2	46	38	17	100	- WISIMTE R - QDIAFAY QR - SYSPYD MLES IR - GVDEVTI VNI LTNR - SYSPYD MLES IRK	268	1.5
2c	Cytopla smic aconitat e hydratas e	ACOC_ HUM AN	P2139 9	188	98.84 9	6.2	77.0	34.0	40	23	100	- YGRLPFS IR - WGSQAF HN MR - FVEFFGP GVA QLSIADR - VILQDFT GVP AVVDFA AMR - IIPPGSGII HQP NLEYLA R	193	1.5
4	Protein disulfide isomera se	PDIA1 _HUM AN	P0723 7	125	57.47	4.6	52.7	38.2	52	16	100	- YKPESEE LTA ER - VDATEE SDLA QQYGVR - ILFIFIDS DHT DNQR - HNQLPL VIEFT EQTAPK - KPHLMS QELP EDWDKQ	302	1

Appendix

4e	Vimentin	VIME_HUMAN	Q8N850	278	53.67	4.9	74.5	68.0	48	27	100	PVK - FANYIDKVR - ISLPLPNFSSLNLR - FADLSEANR - NNDALR - EMEENFAVE - AANYQDTIGR - SYVTTSTRTY - SLGSALRPSTSR	472	1.5
5	TCP-1 gamma	TCPG_HUMAN	P49368	100	61.06	6.1	48.3	21.3	21	9	200	- AVAQALEVI - PR - TAVETAVLLLR - AMTGVEQWPYR - GISDLAQHYLMR - VEKIPGGIIED - SCVLR	116	1
5e	60 kDa heat shock protein, mitochondrial	CH60_HUMAN	P10809	96	61.187	5.6	65.6	45.4	45	20	200	- AAVEEGI - VLG - GGCALLR - ISSIQSIVPALE - IANAHR - TLNDELEIIEG - MKFDR - KISSIQSIVPAL - EIANAHR - KPLVIIAEDV - DGEALSTLVLR - NR	334	1
5f	Heat shock 70kDa protein 1A/1B	HSP71_HUMAN	P08107	65	70.29	5.4	28.5	14.7	25	8	100	- LLQDFFNGR - LVNHFVEEFKR - TTPSYVAFDTER - IINEPTAAIA - YGLDR - NQVALNPQN - TVFDAKR	115	1.5

Appendix

27	Nucleop hosmin	NPM_ HUMA N	Q8WT W5	50	32.72	4.5	62.7	21.8	37	7	200	- MTDQEA IQD LWQWR - MTDQEA IQD LWQWR - MTDQEA IQD LWQWR K - MSVQPT VSLG GFEITPP VVLR - MSVQPT VSLG GFEITPP VVLR	196	1
28	Serine- threonin e kinase receptor - associat ed protein	STRAP _HUM AN	Q9Y3 F4	72	38.75	4.8	22	43.4	45	9	200	- GHFGPIH CVR - QGDTGD WIG TFLGHK - VWDAVS GDE LMTLAH K - FSPDGEL YAS GSEDGT LR - YDYNNG EELE SYKGHF GPIHCVR	83	1
5g	Stress- 70 protein mitocho ndrial	GRP75 _HUM AN	Q9UC 56	170	73.91	5.8	85.1	32.8	45	20	100	- AQFEGIV TDL IR - SDIGEV LVG GMTR - LLGQFTL IGIP PAPR - NAVITVP AYF NDSQR - AMQDAE VSK SDIGEV LVGGMT R	335	1.5
5h	Moesin	MOES _HUM AN	P2603 8	74	67.8	6	75.4	14	20	9	200	- IGFPWSE IR - APDFVF YAPR - KAPDFV FYA PR - TQEQLA LEM AELTAR - ILALCM GN HELYMR	134	1.5

Appendix

6	WD repeat containing protein 1	WDR1_HUMAN	O75083	191	66.83	6.2	42.8	64.2	63	24	200	- DHLLSVSLSG YINYLDR - LATGSD DNC AAFFEGP PFK - MTVDES GQLI SCSMDD TVR - NIDNPAL ADI YTEHAH QVVVAK	254	1
8a	Far upstream element binding protein-1	FUBP1_HUMAN	Q96AE4	72	67.689	7.8	24.2	22.7	32	12	200	- FAVGIVIGR - GTPQQID YAR - IGGNEGID VPI PR - SVMTEE YKV PDGMVG FIIGR - IQQESGCKIQI APDSGG LPER	74	1
10	TCP-1 subunit alpha	TCPA_HUMAN	P17987	119	60.818	5.7	36.3	36.9	43	16	200	- EQLAIAEFAR - YFVEAG AMAVR - GANDFMC DEMER - YINENLIVNTDEL G RDCLINAK - SVVPPGG GAVEAAL SIYLENY ATSMGSR	123	1
10a	TCP-1 subunit epsilon	TCPE_HUMAN	P48643	70	60.08	5.3	29.5	25.1	44	10	100	- AVTIFIR - IADGYE QAAR - GVIVDK DFSHPQM PK - WVGGP EIELIAIAT GGR - VVNSCH RQMAEIA VNAVLT VADMER	101	1.5
10b	TCP-1 subunit theta	TCPQ_HUMAN	P50990	161	60.152	5.3	85.0	41.2	36	19	200	- FAEAFEAI PR - HFSGLEE AVYR	258	1

Appendix

												- IGLSVSE VIEGYEI ACR - LFVTND AATILRE L EVQHPA AK - LIAQACV SIFPDSG HFNVNDNI R		
11	Stress induced phospho protein-1	STIP1_HUMAN	P31948	135	63.22	6.4	18.9	29.1	71	14	200	- AAALF LNRFEI AK - FMNPFN MPNLY QK - AMADPE VQQIMSD PAMR - ALDLDS CKEAD GYQR - AMADPE VQQIMSD PAMR	181	1
12	PDI-A3	PDIA3_HUMAN	P30101	132	57.14	5.9	79.1	34.7	34	13	200	- FVMQEE FSR - ELSDFIS YLQR - FLQDYF DGNLKR - TFSHEL DFGLET A GEIPVVA IR - KTFSHEL SDFGLES TAGEIPV VAIR	226	1
12a	Keratin, type 2 cytoskeletal 8	K2C8_HUMAN	Q6GMY0	146	53.7	5.4	49	54.9	57	23	200	- FASFIDK VR - LQAEIEG LKGQR - LEGLTDE INFLR - SNMDNM FESYINNLRR - SNMDNM FESYINNLRR	256	1
14	Pyruvate kinase isozyme M1/M2	KPYM_HUMAN	Q9WB5	254	58.47	9	88.4	29.0	20	10	200	- RFDEILE ASDGIM V AR - FGVEQD VDMVFAS FIR - EAEAAIY	295	1

Appendix

												HLQLFEE LRR - TATESFA SDPILYR PVAVAL DTK - GIFPVLC KDPVQE AWAEDV DLR		
18	Elongati on factor 1- gamma	EF1G_ HUMA N	P2664 1	85	50.42	6.3	59	15.3	11	6	100	- STFVLDE FKR - ALIAAQ YSGAQV R - WFLTCIN QPQFR - EYFSWE GAFQHV GK - VLSAPPH FHFGQT NR	180	1.5
20a	Calume nin	CALU_ HUMA N	O4385 2	79	37.19 7	4.3	42.7	27	58	10	100	- EQFVEFR - WIYEDV ER - TEREQFV EFR - WIYEDV ERQWK - TFDQLTP EESKER	69	1.5
21	Spermin e synthase	SPSY_ HUMA N	P5278 8	76	41.69 7	4.7	38.7	51.6	61	11	200	-RLPPIVR - YWPTAD GR - GGAIDR YWPTAD GR - QFGNILI LSGDVN L AESDLA YTR - YFTQGN CVNLTE A LSLYEEQ LGR	93	1
23	Elongati on factor Tu, mitocho ndrial	EFTU_ HUMA N	P4941 1	106	49.85	7.9	60.7	41.2	43	14	200	- LLDAVD TYIPVP AR - ELAMPG EDLKFN L ILR - ADAVQD SEMVEL VELEIR - DLEKPFL LPVEAV YSVPGR - NMITGT APLDGCI LVVAAN DGPMPQ	150	1

Appendix

												TR		
25	Phospho glycerat e kinase 1	PGK1_ HUMA N	P0055 8	90	44.98	9.2	19.4	45.6	59	14	200	- AEPAKIE AFR - LGDVYV NDAFGT AHR - ALES PER PFLAILG GAK - VDFNVP MKNNQI T NNQR - TGQATV ASGIPAG WMGLD CGPESSK	86	1
30	Prolifera ting cell nuclear antigen	PCNA_ HUMA N	P1200 4	116	29.09	4.4	43.7	64	55	16	200	- MPSGEF AR - YLNFFTK - SEGFDY R - LMDLDV EQLGIPE QEYSCV VK	115	1
38	Annexin A5	ANXA 5_HU MAN	P0875 8	124	35.97	4.8	69.9	54.4	48	15	200	- SEIDLFNI RK - GLGTDE ESILTLL T SR - WGTDEE KFITIFG TR - GTVTDFP GFDERA DAETLR - QVYEEE YGSSLED DVVGDT SGYYQR	140	1
12b	T- complex protein 1 subunit beta	TCPB_ HUMA N	P7837 1	135	57.7	6	45.7	44.5	54	19	100	- LIEEVM GEDK - KIHPQTII AGWR - MLPTIIA DNAGYD SADLVA QLR - TVYGGG CSEMLM AHAVTQ LANR - QLIYNYP EQLFGA AGVMAI EHADFA GVER	152	1.5
65	Glutathi one S- transfera se P	GSTP1 _HUM AN	P0921 1	80.9	23.56	5.3	83.1	47.6	21	8	200	- PPYTVV YFPVR - MPPYTV VYFPVR -	151	1

												FQDGD LTYQSN TILR - ALPGQL KPFETLL S QNQGGK - TLGLYG KDQQEA ALVDMV NDGVED LR		
29a	26S protease regulatory subunit 10B	PRS10 _HUMAN	P62333	95.4	44.4	7.8	32.2	36.2	51	14	100	- EVIELPL TNPELFQR - TLMELL NQMDGF DTLHR - TLMELL NQMDGF DTLHR - DHQPCII FMDEIDA IGGR - ELREVIE LPLTNPE LFQR	123	1.5
31	F-actin- capping protein subunit alpha-1	CAZAL_HUMAN	P52907	70.6	33	5.4	43.9	42.7	51	8	100	- ISFKFDHLR - LLLNNDNLLR - EASDPQP EEADGGLKSWR - FITHAPP GEFNEVF NDVR - TIDGQQT IIACIESH QFQPK	85.1	1.5
40a	Guanine nucleotide- binding protein subunit beta-2- like 1	GBLP_HUMAN	Q6FH47	68	35.51	8.9	24.7	26.5	11	5	100	- VWQVTIGTR - LTRDET NYGIPQR - FVGHTK DVLS VAFSSD NR - YTVQDE SHS EWVSCVR - AEPPQCT SLA WSADGQ TLFAGY TDNLVR	81	1.5

42	Heterogeneous nuclear ribonucleoproteins A2/B1	ROA2_HUMAN	P22626	69	37.46	9.3	27.1	35.7	55	11	200	- GGGGNF GPG PGSNFR - LFIGGLS FETT EESLR - RGFGFV TFDD HDPVDK - NMGGPY GGG NYGPGG SGGSGG YGGR - NMGGPY GGG NYGPGG SGGSGG YGGR	74	1
44	Cyclin-dependent kinase 2-interacting protein	CINP_HUMAN	Q9BW66	28	24.47	5.9	16.1	27.8	19	3	200	- ISLLNKD KIEL DSSSPAS K - ENEEKV CLEY NEELEK - MEKLSS TTKG ICELENY HYGEES K	60	1
45	14-3-3 protein epsilon	1433E_HUMAN	Q7M4R4	87	29.32	4.5	66.8	44.7	52	15	200	- MKGDYH R - YLAEFA TGN DR - YLAEFA TGND RK - VAGMDV ELT VEER - AASDIA MTL PPTHPIR	156	1
49	14-3-3 protein beta/alpha	1433B_HUMAN	P31946	132	28.17	4.6	72.1	50.8	26	13	200	- MKGDYF R - AVTEQG HELS NEER - LAEQAE RYD DMAAA MK - LAEQAE RYD DMAAA MK - AVTEQG HELS NEERNL LSVA YK	194	1
54	Prohibin	PHB_HUMAN	P35232	201	29.842	5.5	91.5	69.1	34	16	200	- AVIFDRF R - LFRPVAS	262	1

Appendix

												QLPR - AAELIAN SLA TAGDGLI ELR - IFTSIGED YDE RVLPSIT TEILK - GVQDIV VGEG THFLIPW VQKPIIF DCR		
64a	ATP synthase subunit d, mitocho ndrial	ATP5H _HUM AN	O7594 7	64	18.53	5.1	20.3	38.5	18	5	200	- SWNETL TSR - KYPYWP HQPI ENL - AIASSLK SWN ETLTSR - TIDWVA FAEII PQNQK - LAALPE NPPA IDWAYY K	65	1
63	Translat ionally controll ed tumour protein	TCTP_ HUMA N	P1369 3	60	19.69	4.7	7.6	42.4	30	5	100	- GKLEEQ RPER - EDGVTP YMIF FK - IREIADG LCLE VEGK - DLISHDE MFSD IYK - NYQFFIG ENM NPDGMV ALLDYR	56	1
70	PEB protein- 1	PEBP1 _HUM AN	P3008 6	69	21.15 7	7.8	33.3	45.5	18	6	200	- YVWLVI EQD RPLK - YREWHH FLV VNMK - YREWHH FLV VNMK - APVAGT CYQ AEWDDY VPK - YVWLVI EQD RPLKCD EPILS NR	83	1
87	Galectin -1	LEG1_ HUMA N	P0938 2	117	15	5.2	46.4	63.7	36	9	200	- LPDGYEF K - DGGAW GTE	184	1

Appendix

												QR - LPDGYEF KFP NR - DSNNLC LHFN PR - ACGLVA SNLN LKPGECL R		
103	S- formyl glutathi one hydrolas e	ESTD_ HUMA N	P1076 8	134	31.95 5	6.6	65.9	52.5	47	13	100	- MSIFGHS MGG HGALICA LK - MSIFGHS MGG HGALICA LK - SGYHQS ASEH GLVVIAP DTS PR - LQEGYD HSYY FIATFITD HIR - MYSYVT EELP QLINANF PVPDQR	159	1.5
N8	Adenos yl Homocy steinase	SAHH_ HUM AN	P2352 6	95	48.2	5.9	56.1	30	44	12	150	- YPQLLP GIR - VADIGL AAW GR - SKFDNL YGCR - KALDIAE NEM PGLMR - QAQYLG MSC DGPFPK DHYRY	110	1
N31	Hepato ma derived growth factor	HDGF_ HUM AN	P5185 8	<u>40</u>	26.8	4.6	5.7	34	50	6	150	- GYPHWP AR - MKGYPH WP AR - EYKCGD LVF AK - GFSEGL WEIE NNPTVK - YQVFFF GTHE TAFLGPK	39	1
N21	Casein Kinase 2 subunit Beta	CSK2B_ HUM AN	P6787 0	60	25.2	5.2	7.9	38.6	51	7	100	- RPNQF VPR - YQQGDF GYC PR -	60	1

												YILTNRG IAQ MLEK - LYCPKC MDV YTPK - RPNQF VPRL YGFK		
N10a	Cytochrome bc1 Complex subunit 1, mitochondrial	QCR1_HUMAN	P31930	70.5	53.2	5.9	2.2	33.8	75	12	150	- RIPLAEW ESR - NNGAGY FLE HLAFK - NALVSH LDGT TPVCEDI GR - HLGGIP WTYA EDAVPT LTPCR - NILRNAL VSH LDGTTTP VCEDIGR	73.3	1
26	SET Protein	SET_HUMAN	Q01105	90	33.4	4.1	75.7	29.7	39	10	200	- QPFFQKR - LRQPFFQK - VEVTEFE DIK SGYR - IDFYFDE NPYF ENK - SGYRIDFYFD ENPYFENK	85	1
5d	Heat Shock Cognate 71kDa Protein	HSP7C_HUMAN	P11142	158	71.08	5.2	72.1	41.8	48	23	200	- FEELNA DLFR - ARFEELN ADLFR - TTPSYVA FTD TER - HWPFMV VND AGRPK - TVTNAV VTV PAYFND SQR	241	1
19	Phosphoglycolate phosphatase	PGP_HUMAN	A6NDG6	56	34.44	5.8	9.1	27.4	27	5	200	- AVEMAA QRQ ADIIGKPSR - FIAGTGC LVR AVEMAA QR - FIFDCVS QEYG INPER -	41	1

Appendix

												YLQQPG CLLV GTNMDN R - LGFGGP AGPG ASLEVFG TAY CTALYL R		
36	Comple ment Compon ent 1Q sub compon ent binding protein, Mitocho ndrial	C1QBP _HUM AN	Q0702 1	66	31.7	4.6	43	60.6	54	8	150	- AFVDFLS DEI KEER - VEEQEPE LTST PNFVVE VIK - ITVTFNI NNSIP PTFDGEE EPSQGQ K - DTNYTL NTDS LDWALY DHLMDF LADR - ALVLDC HYPE DEVGQE DEAESDI FSIR	123	1
58	Rho GDP dissociat ion Inhibitor 1	GDIR1 _HUM AN	P5256 5	58	23.24	4.9	19.9	34.8	24	6	200	- YIQHTYR - IDKTDY MVG SYGPR - AEEYEFL TPV EEAPK - SIQEIQEL DKD DESLR - FTDDDK TDHL SWEWNL TIK	58	1
76	Eukaryo tic Translat ion initiatio n Factor 5A-1	EIF5A 1_HU MAN	P6324 1	74.5	17	4.9	17.4	43	63	8	150	- VHLVGI DIFT GK - EDLRLPE GDL GK - YEDICPS THN MDVPNI K - KYEDICP STH NMDVPN IK - YEDICPS THN MDVPNI KR	77.7	1
N10	Keratin, type I cytoskel etal 18	K1C18 _HUM AN	P0578 3	81	48.02	5.2	17.7	44.9	86	13	150	- IIEDLRA QIFA NTVDNA R -	70	1

Appendix

												YALQME QLNG ILLHLES ELAQ TR - SLGSVQ APSY GARPVSS AASVYA GAGGSG SR - GGMGSG GLA TGIAGGL AGMGGI QNEKET MQSLND R		
13a	Glucose -6- phospha te 1- dehydro genase	G6PD_ HUMA N	P1141 3	264	59.67	6.4	81.6	44.5	24	16	100	- WDGVPF ILR - GGYFDE FGIIR - DGLLPE NTFI VGYAR - KPGMFF NPPE SELDLTY GNR	312	1.5
N18	Fascin	FSCN1 _HUM AN	Q1665 8	262	55.1	7	77.4	66.1	100	30	100	- GEHGFIG CR - WSLQSE AHR - FLIVAHD DGR - NASCYF DIE WR - LVARPEP ATG YTLEFR	282	1
N30	Aldo Keto reductas e family 1 member C 1	AK1C1 _HUM AN	Q048 28	101	37.2	9	49.2	54.8	85	14	100	- HIDSAHL YNN EEQVGL AIR	96	1
42b	L- lactate Dehydro genase A chain	LDHA_ HUM AN	P0033 8	100	36.95	9.3	51.2	43.4	32	14	100	- LVIITAG AR - RVHPVS TMIK - GEMMDL QH SLFLR - LKGEMM DLQ HGSLFLR - LKGEMM DLQ HGSLFLR	90	1.5
N19	Ran binding Protein 3	RANB P3_HU MAN	Q9H6 Z4	67	60.5	4.6	41.8	19	14	6	100	- NESSNAS EEE ACEK - LNDMAS TDD GTLOSR	64	1

Appendix

												- ESLAESA AAY TKATAR - EQQRSV LRPA VLQAPQ PK - MADLAN EEK PAIAPPV FVF QK		
N5	Fructose bisphos phate aldolase A	ALDO A_HU MAN	P0407 5	112	39.8	9.2	51.2	49.2	54	13	100	- CPLLKP WALT FSYGR - FSHEEIA MAT VTALRR - IGEHTPS ALAI MENANV LAR - YTPSGQ AGA AASESLF VSNHAY - QLLLTA DDR VNPCIGG VILFHET LYQK	102	1
N13	Heterog eneous nuclear ribonucl eoprotei n F	HNRP F_HU MAN	P5259 7	90	45.9	5.3	37.2	36.9	54	9	100	- DLSYCLS GM YDHR - ITGEAFV QFA SQELAE K - FMSVQR PGPY DRPGTA R - ATENDIY NFFS PLNPVR - YGDSEFT VQS TTGHCV HMR	113	1
N7	Proteaso me subunit Alpha Type 1	PSA1_ HUMA N	P2578 6	54.5	29.8	6.2	4.9	30	48	6	100	- FVFDRPL PVSR - NQYDND VTV WSPQGR - ILHVDN HIGIS IAGLTAD AR - KILHVD NHIGI SIAGLTA DAR - QECLDS RFVF DRPLPVS R	45	1

Appendix

46	Chloride Intra Cellular Channel protein 1	CLIC1_HUMAN	O00299	101	27.24	4.9	76.3	61.8	38	13	200	- YLSNAYAR - GFTIPEAFR - IGNCPFQSR - YRGFTIPEAFR - VLDNYLTSPL - PEEVDET - SAEDEGVSR	138	1
1h	Src substrate cortactin	SRC8_HUMAN	Q14247	89.4	61.7	5.1	62.1	19.8	19	8	100	- YGLFPA NYVE LR - YGLFPA NYVE LRQ - LRENVF QEHQ TLK - GPVSGTE PEP - VYSMEA ADYR - FGVQMD RVD - QSAVGFEYQ GK	284	1.5
21a	40S ribosomal protein SA	RSSA_HUMAN	Q86VC0	170	32.94	4.6	78.1	44.7	42	13	100	- FAAATG ATP I AGR - GAHSVGLM - WWMLAR - FTPGTFT NQI QAAFR - FTPGTFT NQI QAAFRE PR - FLAAGT HLGG - TNLDFQ MEQYIKR	196	1.5
68	GTP binding nuclear protein RAN	RAN_HUMAN	Q9CS P3	58	24.5	7.8	44.4	34.7	55	6	150	- SNYNFE KPFL WLAR - YVATLG VEV - HPLVFHTNR - KYVATLGVE - VHPLVF HTNR - DGYIQAQCA - IIMFDVTSR	57	1

Annex 5: Up & Down regulated gene list (≥ 2 fold, $p \leq 0.05$) for UPCI:SCC029B/70Gy-UPCI:SCC029B

Upregulated			Downregulated		
Gene Symbol	Log FC	p Value	Gene Symbol	Log FC	p Value
IL8	5.033893885	7.43E-09	KRT6A	-7.523657625	1.96E-09
IL8	4.908269503	1.04E-08	CHI3L1	-6.332563689	2.08E-09
ACTB	4.253484685	1.53E-08	KRT6B	-5.149859183	7.03E-09
HIF1A	3.429180372	3.58E-08	CCND2	-4.482794526	1.64E-08
STARD7	3.563957068	3.68E-08	S100A9	-4.430168911	1.81E-08
CAPZA1	3.277297701	4.82E-08	GJB6	-4.351619857	1.84E-08
ATP5A1	3.000061208	6.71E-08	TMEM255A	-4.337972444	2.29E-08
CAPZA1	3.105249898	9.01E-08	DST	-3.588271499	3.22E-08
FDCSP	3.412639102	9.81E-08	ANO1	-4.702853005	3.73E-08
COPS7A	2.733520323	1.15E-07	MAP2	-3.53791361	6.16E-08
DDX3X	2.970882509	1.17E-07	HS6ST2	-3.524134911	7.30E-08
CCT2	2.680644191	1.19E-07	HLA-DRA	-3.435032764	8.75E-08
IGF2 /// INS-IGF2	3.274442325	1.26E-07	MIR205HG	-3.224766172	9.65E-08
STIP1	2.682918413	1.32E-07	RNF128	-3.999586038	1.07E-07
TCEA1	2.84946264	1.60E-07	---	-2.862531868	1.09E-07
KRT8	2.610204564	1.65E-07	EMB /// EMBP1	-2.668082431	1.22E-07
ALDH1A3	3.224649571	1.76E-07	KCNS3	-4.051153469	1.23E-07
ATP5A1	2.885561349	1.78E-07	KRT6A /// KRT6B /// KRT6C	-2.785530315	1.26E-07
MIR21 /// VMP1	2.542143291	1.90E-07	DPP4	-2.731413261	1.36E-07
HSPA5	2.520514181	1.90E-07	FGFBP1	-3.011657522	1.44E-07
ARL6IP1	2.5858792	1.95E-07	CLCA2	-4.774959727	1.52E-07
DNAJB9	2.58160323	1.95E-07	LINC00273	-2.5500932	1.58E-07
MSMO1	2.39314865	1.97E-07	DDR2	-2.444432018	1.79E-07
TRA2A	2.53416332	2.22E-07	IL24	-2.664845156	1.87E-07
DIO2	2.292042172	2.44E-07	FLRT3	-3.689703287	1.89E-07
ATF3	2.639143943	2.51E-07	SEL1L3	-2.412405657	1.93E-07
GYG1	2.572546749	2.51E-07	KRT6A	-4.408217033	2.17E-07
SCOC	3.028982802	2.54E-07	RGS4	-2.450754245	2.17E-07
GOLPH3	2.316926122	2.59E-07	COL17A1	-3.667283117	2.56E-07
UQCRC1	2.66297767	2.69E-07	TP63	-3.327717675	2.91E-07
RALY	2.361414216	2.69E-07	GBP5	-2.421222767	2.92E-07
KRT8	2.263606849	2.76E-07	CSAG2 /// CSAG3 /// LOC101060231	-2.218551746	3.09E-07
PSPC1	2.829641274	2.78E-07	RGS4	-2.38576283	3.25E-07
PTGS2	2.347315271	2.84E-07	OLFML2B	-2.222813238	3.27E-07
EIF4E	2.452952849	2.95E-07	RGS4	-2.532719086	3.30E-07
POLR2C	2.456455075	3.07E-07	MAP1B	-2.160737689	3.35E-07
SIAH1	2.338742226	3.09E-07	CA2	-2.734939029	3.61E-07
SCOC	2.550355909	3.27E-07	NUPR1	-2.819286274	3.82E-07
IL11	2.254299598	3.34E-07	HRK	-2.122974844	3.84E-07
COTL1	2.201301603	3.40E-07	RSAD2	-2.389813044	3.92E-07
THBS1	2.575759287	3.42E-07	ABCC9	-2.373893455	3.97E-07

Appendix

ADM	2.401445019	3.45E-07	PHACTR2	-2.177460606	4.22E-07
KRT8	2.148751791	3.61E-07	DYNLRB2	-2.431416687	4.23E-07
EIF4E	2.51041126	3.66E-07	PROM2	-2.79614206	4.30E-07
FOS	2.170939695	3.66E-07	MME	-2.501923476	4.57E-07
ARFIP2	2.298070765	3.70E-07	HTN3	-2.326807466	4.63E-07
ADAM9	2.239795514	3.78E-07	ESRP1	-2.710162959	4.88E-07
CSGALNACT1	2.352878788	3.85E-07	CXCR7	-2.185468081	5.08E-07
RNPS1	2.089925721	3.90E-07	MMP10	-3.323146699	5.31E-07
KRT8	2.506653305	3.96E-07	LY75	-2.249293299	5.49E-07
IGFBP5	2.659257195	4.14E-07	HLA-F	-1.962988381	5.57E-07
CXCL1	2.362092044	4.14E-07	C1orf115	-1.89327662	6.06E-07
PDIA4	2.365659555	4.41E-07	CPED1	-2.059421973	6.14E-07
NAP1L4	2.023269373	4.44E-07	MCOLN3	-2.018479471	6.18E-07
KRT8	2.493295425	4.46E-07	SUN3	-2.01738215	6.29E-07
NEK2	2.202871993	4.48E-07	TACSTD2	-1.899354099	6.39E-07
HIF1A	2.110916467	4.49E-07	CHRD1	-2.728583731	6.68E-07
INHBA	2.400049815	4.65E-07	LY96	-2.035334068	6.81E-07
HIF1A	2.032590985	4.93E-07	EMB	-2.611262292	6.92E-07
PPIF	2.359639162	4.94E-07	ASAH1	-1.863060869	7.00E-07
CSN1S1	2.138027524	5.02E-07	CMPK2	-2.615607348	7.03E-07
ACTB	1.961371602	5.17E-07	GIMAP2	-1.941952203	7.06E-07
TGFB2	1.97813964	5.18E-07	ITGB6	-3.44502196	7.21E-07
OLA1	2.144305749	5.23E-07	ENPP2	-2.13562241	7.22E-07
SEC23A	2.053676954	5.41E-07	HSD11B1	-1.827303976	7.27E-07
SLC3A2	2.441455201	5.55E-07	GPM6A	-1.882916508	7.46E-07
ANXA5	1.933926406	5.68E-07	PRUNE2	-1.864586774	7.64E-07
DUSP1	2.635603389	5.74E-07	S100A14	-3.585659991	7.66E-07
EID1	2.058334727	6.01E-07	PHACTR2	-1.948123457	7.93E-07
DIO2	2.874001779	6.03E-07	OLFML2B	-1.863841801	7.96E-07
PTGS2	2.405924615	6.09E-07	KRT6A	-3.749526005	8.04E-07
SLC3A2	3.126964966	6.16E-07	ENPP2	-2.022096195	8.09E-07
SGK1	2.064430909	6.24E-07	ROR2	-2.421343951	8.38E-07
CAPZA2	1.912243926	6.29E-07	---	-1.813868049	8.40E-07
TPM3	1.885840588	6.66E-07	DAPK1	-2.588256778	8.52E-07
ALDH1A3	1.918824635	6.68E-07	SP140	-1.915543009	8.54E-07
TSC22D1	1.950202784	6.69E-07	IFIH1	-1.782771172	8.60E-07
PTTG1IP	2.554622836	6.75E-07	SP100	-2.027181436	8.74E-07
CD44	2.095594008	6.92E-07	C1orf21	-1.987986607	8.74E-07
FZD6	1.894773666	7.09E-07	SAA1	-1.957811738	8.89E-07
BZW2	1.865097168	7.19E-07	IL13RA2	-1.977132296	9.04E-07
SPARC	1.861666628	7.26E-07	RTP4	-2.058713763	9.08E-07
PICALM	2.037141995	7.44E-07	SAA1 /// SAA2 /// SAA2-SAA4	-1.981742981	9.19E-07
MTAP	1.950579908	7.56E-07	IFI44L	-1.936400278	9.31E-07
CSGALNACT1	1.996057992	7.85E-07	RRAGD	-2.679407882	9.61E-07
ACTB	1.875414455	8.00E-07	DMRT3	-1.894248192	9.69E-07
TMED3	1.852646595	8.24E-07	HLA-F	-1.749648164	9.72E-07

Appendix

INHBA	1.860552644	8.54E-07	ZBTB20	-1.978920898	9.87E-07
NR3C1	1.841979036	8.57E-07	HSD17B2	-1.69490211	1.03E-06
DIO2	2.208501703	8.58E-07	FXYD3	-2.798766626	1.06E-06
TAGLN2	1.785157807	8.59E-07	TMEM47	-2.080552331	1.07E-06
KIF22	2.016107962	8.62E-07	FAM134B	-1.71196242	1.07E-06
CXCL3	1.877167924	8.65E-07	LOC100130872 /// SPON2	-1.841420469	1.10E-06
EEF1G	1.954789763	8.75E-07	HLA-F	-1.765586572	1.10E-06
PTP4A1	2.580794	8.93E-07	SLAMF7	-1.870445277	1.11E-06
PHB2	1.931321259	8.96E-07	CDH1	-3.738623062	1.14E-06
SPARC	1.852945864	8.99E-07	SPP1	-1.663587862	1.15E-06
RHOA	2.01930362	9.13E-07	SP140	-2.023039193	1.16E-06
VCAN	1.975278032	9.34E-07	PLAGL1	-1.782718339	1.18E-06
YIPF5	1.821333407	9.37E-07	KIAA1211	-2.124527704	1.24E-06
ZFAND6	1.937946655	9.45E-07	CTSB	-1.635193823	1.25E-06
B3GNT2	1.922234199	9.47E-07	TMEM106B	-1.706389456	1.26E-06
CNBP	1.7858458	9.47E-07	IFI44L	-1.677832499	1.27E-06
TM9SF3	1.916014099	9.72E-07	RSAD2	-1.624734976	1.30E-06
DIO2	2.006654812	9.81E-07	TLR2	-1.677208468	1.31E-06
NELFCD	1.87632316	9.86E-07	HSD11B1	-1.649278129	1.31E-06
CCNG1	1.77705667	9.90E-07	NRG2	-1.613949238	1.32E-06
CIRBP	1.876593337	9.96E-07	CDH3	-1.667657753	1.33E-06
CLTC	1.735643257	1.01E-06	FAT2	-1.626978999	1.33E-06
HSPD1	1.7498367	1.02E-06	LAMA3	-2.21679514	1.35E-06
GPR183	3.003052025	1.04E-06	FAM134B	-1.645374601	1.36E-06
POLR2E	1.700728217	1.04E-06	SPP1	-1.683932589	1.39E-06
RUVBL2	1.907674785	1.05E-06	DKK3	-1.618759894	1.39E-06
PPIF	2.19390273	1.07E-06	MOXD1	-1.765023694	1.47E-06
NOP58	2.067679465	1.07E-06	GBP5	-2.638497548	1.48E-06
RHOA	2.924895962	1.08E-06	OAS3	-1.725336577	1.48E-06
HSPA5	2.527605329	1.08E-06	SORL1	-2.816511886	1.50E-06
BIRC5	2.246038647	1.08E-06	TLR2	-1.65959268	1.50E-06
ARL2BP	1.959725834	1.08E-06	PARP9	-1.583751311	1.56E-06
AP2M1	1.914633648	1.09E-06	HKDC1	-1.589103866	1.57E-06
IMPA1	1.974640531	1.10E-06	MAL2	-1.679941908	1.69E-06
TRA2A	1.804394973	1.10E-06	ISG20	-1.743733896	1.70E-06
RTN3	1.923714924	1.11E-06	DOCK9	-1.735307964	1.71E-06
CDK2AP2	2.123932887	1.14E-06	COBLL1	-1.989901127	1.73E-06
YIF1B	1.686443523	1.14E-06	PCDHGA1 /GA10 /GA11 /GA12 /GA2 /GA3 /GA4 /GA5 /GA6 /GA7 /GA8 /GA9 /GB1 /GB2 /GB3 /GB4 /GB5 /GB6 /GB7 /GC3 /GC4 /GC5	-1.70399725	1.74E-06
HES1	1.980532122	1.16E-06	AKIRIN1	-1.710744125	1.75E-06
ITM2C	1.945388933	1.16E-06	AKAP2 /// PALM2-AKAP2	-1.656878078	1.75E-06
NPTN	1.882855785	1.16E-06	OAS2	-1.689695753	1.76E-06
BZW2	1.682289726	1.16E-06	PRNP	-2.026946293	1.78E-06

Appendix

SNX3	1.668813329	1.16E-06	RARRES3	-1.791121287	1.78E-06
TMED3	1.744315454	1.17E-06	CD74	-1.727036718	1.78E-06
HNRNPA1	1.640366386	1.21E-06	AFF3	-1.513370967	1.78E-06
ALDH1A3	2.966379162	1.22E-06	WDR78	-1.518339827	1.79E-06
G3BP1	1.673557264	1.22E-06	CXorf57	-1.798255862	1.80E-06
SRSF1	1.816166535	1.23E-06	MX2	-1.577514762	1.80E-06
POLR2E	1.710793906	1.25E-06	SIRPA	-2.183738257	1.82E-06
HAS2	1.842671658	1.26E-06	TMEM144	-1.75963632	1.83E-06
TRA2A	1.741344672	1.26E-06	C1orf116	-1.900225843	1.85E-06
CXCL1 /// CXCL2	2.249025226	1.28E-06	CFH	-1.703678884	1.86E-06
RAB6A	2.194243448	1.30E-06	SPP1	-1.544978012	1.88E-06
ARL8B	2.12564978	1.30E-06	PPL	-1.992915582	1.89E-06
FOS	2.08830041	1.30E-06	RNF182	-1.500005432	1.90E-06
NEK2	2.071290961	1.33E-06	ST6GAL1	-1.826395372	1.92E-06
AKT2	1.925470379	1.35E-06	TMEM71	-1.548222656	1.93E-06
RTN3	1.6415898	1.35E-06	GPR124	-1.603764022	1.97E-06
HIF1A	3.198914373	1.36E-06	SYNE2	-1.792485075	1.98E-06
EEF2	1.60812899	1.36E-06	BST2	-1.524448736	1.98E-06
CD151	1.686245296	1.37E-06	FLRT3	-3.29041666	1.99E-06
DKFZp686K1684 /// RCN1	1.774119422	1.38E-06	SASH1	-1.49072366	2.02E-06
BMI1 /// COMMD3-BMI1	2.172708411	1.40E-06	NID1	-1.643563929	2.03E-06
AP4M1	1.798129441	1.40E-06	DDAH1	-1.6718106	2.14E-06
AP4M1	1.798129441	1.40E-06	---	-1.514764164	2.17E-06
TAGLN2	1.706544219	1.45E-06	SIMC1	-2.58310554	2.20E-06
COX7A2L	1.605321697	1.45E-06	ANO1	-4.37761476	2.22E-06
EGR1	1.619362924	1.46E-06	ABI3BP	-3.048136056	2.23E-06
PPP1CB	1.784267807	1.47E-06	MEGF9	-1.4808069	2.25E-06
CSE1L	1.602711336	1.49E-06	PCLO	-1.453419211	2.26E-06
C11orf96	1.575089854	1.49E-06	DKK3	-1.528156242	2.28E-06
POLR2E	1.781232865	1.51E-06	GBP4	-1.528264721	2.32E-06
TUBB	1.571379883	1.51E-06	IFNLR1	-1.504357249	2.32E-06
TNFRSF11B	1.967266361	1.52E-06	NFIA	-1.505153565	2.33E-06
SAE1	1.644135745	1.52E-06	RDH10	-1.7616131	2.34E-06
HIF1A	2.000377013	1.55E-06	ZNF549	-1.469335671	2.35E-06
IFT52	1.854639275	1.55E-06	MDM4	-1.717606254	2.42E-06
SMIM15	1.664215144	1.55E-06	TPD52L1	-1.687315029	2.42E-06
HSPA5	2.476775797	1.56E-06	PRKAA2	-1.800154615	2.48E-06
AK4 /// LOC100507855	2.349233464	1.59E-06	IGDCC4	-1.433193077	2.49E-06
PGAM1	1.893322481	1.62E-06	RORA	-1.709261739	2.50E-06
PLRG1	1.781178326	1.62E-06	ZBTB20	-2.030066288	2.51E-06
TRA2A	1.738846267	1.63E-06	SULT1C2	-1.443634936	2.56E-06
HSPA8 /// SNORD14C /// SNORD14D	1.575487393	1.63E-06	TTC28	-1.598572933	2.59E-06
ADIPOR1	2.254466065	1.65E-06	TSPAN2	-1.432989124	2.63E-06

Appendix

NUS1 /// NUS1P3	2.06005903	1.66E-06	OAS1	-1.548936891	2.64E-06
BIRC5	1.602644745	1.66E-06	IL7	-1.443055356	2.66E-06
SNAP23	1.562680761	1.67E-06	PLAGL1	-1.427085428	2.71E-06
CAPZB	1.705204949	1.69E-06	AIM2	-1.425350595	2.71E-06
SERPINB2	1.54100791	1.69E-06	PCDH7	-2.47344897	2.72E-06
IST1	1.909580075	1.70E-06	KRT6A	-6.890246076	2.75E-06
SLC14A1	1.59996507	1.71E-06	DRAM1	-1.842422307	2.75E-06
RTCB	1.570123097	1.72E-06	ZNF43	-1.702436865	2.81E-06
TOMM22	1.556898561	1.73E-06	IFIT1	-1.392286164	2.82E-06
VCAN	1.854182598	1.74E-06	CSAG2 /// CSAG3 /// LOC101060231	-2.13003505	2.84E-06
RPL15	1.615358772	1.74E-06	GJB2	-1.581245386	2.88E-06
FOS	1.562773096	1.74E-06	LEMD1	-1.587688917	2.89E-06
AAGAB	1.903138441	1.75E-06	GLUL	-2.146140382	2.91E-06
CCNC	1.820825848	1.77E-06	NMU	-1.766071316	2.98E-06
UTP6	1.556390648	1.77E-06	KRT5	-3.317781193	3.01E-06
IL11	2.012283238	1.78E-06	OAS2	-1.410376323	3.03E-06
CNN2	1.75767263	1.79E-06	WISP3	-1.521242008	3.05E-06
WNT5A	1.734296467	1.79E-06	EVI2A	-1.8402418	3.07E-06
ANKRD28	1.674845287	1.80E-06	KANK1	-1.543833049	3.07E-06
SLC7A2	1.57794537	1.80E-06	PNISR	-1.399028958	3.08E-06
RHOB	2.184353204	1.81E-06	USP18	-1.350778639	3.08E-06
NRG1	1.605186611	1.87E-06	LOC100505946	-1.66566141	3.10E-06
PHLDA2	1.586121937	1.91E-06	GRIP1	-2.204919956	3.11E-06
CCNG1	2.51590729	1.92E-06	APOL1 /// APOL2	-1.541609593	3.11E-06
KRT8	1.852846321	1.92E-06	DBT	-1.383678691	3.11E-06
PRPF31	1.641075827	1.92E-06	CPEB2	-1.389491956	3.13E-06
TMBIM6	1.926364951	1.94E-06	PLAGL1	-2.05168602	3.17E-06
KLF6	2.626564363	1.98E-06	KLK8 /// KLK9	-1.549538544	3.17E-06
SLC39A6	1.737513453	1.98E-06	STAT2	-1.386599924	3.18E-06
RND3	2.171428865	2.01E-06	ANXA11	-1.456944862	3.20E-06
BIRC5	1.594135223	2.06E-06	OAS2	-1.459364063	3.22E-06
ADRM1	1.681600609	2.10E-06	PVRL4	-1.348929828	3.22E-06
ATP8B5P /// ZFAND6	1.667698782	2.10E-06	PLCG2	-1.749206517	3.24E-06
ECT2	1.501667388	2.11E-06	CFH /// CFHR1	-1.672989867	3.27E-06
HSPD1	1.553776308	2.12E-06	UBE2D2	-1.375470387	3.27E-06
GNL3 /// SNORD19B	2.432253292	2.13E-06	CFH /// CFHR1	-1.849997252	3.28E-06
GMPPA	2.327078044	2.13E-06	SOX15	-1.430253352	3.28E-06
IL33	2.078154287	2.15E-06	SEL1L3	-1.728785089	3.36E-06
IL33	2.078154287	2.15E-06	CH25H	-2.199978388	3.37E-06
NFKBIA	1.614436462	2.15E-06	EBF1	-1.771172764	3.39E-06
HIF1A	1.812736097	2.16E-06	TMEM40	-1.573969312	3.39E-06
SDCBP	1.660593172	2.16E-06	NDRG4	-1.438422946	3.42E-06
EPHA3	1.796828689	2.18E-06	TCF7	-1.773163575	3.45E-06
COL1A1	1.587575793	2.21E-06	PAX6	-1.787602528	3.47E-06

Appendix

UBA2	1.452848454	2.21E-06	GPR124	-1.43065505	3.53E-06
SPTBN1	1.446414535	2.21E-06	INADL	-1.636412158	3.54E-06
CXCL6	1.85116454	2.22E-06	CLDN23	-1.360558979	3.54E-06
CIAPIN1	1.497003843	2.23E-06	PER2	-1.327718497	3.54E-06
SIRT2	1.474189059	2.26E-06	KLK8 /// KLK9	-1.53369094	3.56E-06
KRT8	1.668551794	2.30E-06	HCP5	-1.370099798	3.58E-06
OXA1L	1.972797637	2.32E-06	STEAP2	-1.635649236	3.59E-06
PPP4R1	1.519985111	2.32E-06	DICER1	-1.378170808	3.59E-06
SEC23A	2.254609191	2.33E-06	ARMCX3	-1.333820632	3.59E-06
FAM49B	1.596244672	2.33E-06	H1FO	-1.414187483	3.66E-06
VCAN	1.453262624	2.35E-06	LOXL4	-1.33088794	3.68E-06
MAD2L1	1.43720446	2.37E-06	KLK8 /// KLK9	-1.958175384	3.69E-06
POLM	1.432926092	2.37E-06	MME	-1.915454237	3.71E-06
RAB6A	2.206810041	2.39E-06	APOL1	-1.396132385	3.76E-06
ANLN	1.85326533	2.39E-06	TRIM6	-1.549448533	3.83E-06
BIRC5	1.514238452	2.43E-06	C5orf30	-1.376952842	3.84E-06
MAPK6	1.503084299	2.45E-06	ITPRIPL2	-1.441397453	3.85E-06
PLAU	1.632411841	2.46E-06	LAMA1	-1.336690923	3.85E-06
BMP2	1.451192233	2.47E-06	SMPX	-1.716452886	3.89E-06
ANXA8 /// ANXA8L1 /// ANXA8L2	1.44941554	2.47E-06	PTPRR	-2.25368355	3.91E-06
IMPDH2	1.413177448	2.47E-06	CTSL2	-1.427485749	3.91E-06
TWF1	2.548323552	2.49E-06	FAM171B	-1.424886407	3.92E-06
SEPW1	1.575458576	2.49E-06	AKIRIN1	-1.765358588	3.96E-06
PRDX3	1.436277518	2.49E-06	MYO6	-1.409067053	3.99E-06
FOSB	1.870920516	2.50E-06	DLG1	-1.338174213	4.00E-06
TMED3	1.687147403	2.50E-06	PPP1R12A	-1.27842033	4.03E-06
DCK	1.427332167	2.50E-06	KRT14	-4.50991358	4.05E-06
RNF11	1.719968263	2.51E-06	LOC100509445 /// LOC728715 /// OVOS2	-1.358891289	4.06E-06
MAGED2	1.612014244	2.51E-06	STRBP	-1.276579514	4.06E-06
TAF9B	2.150073275	2.54E-06	DOCK9	-1.496023767	4.18E-06
RAB5C	1.534085839	2.55E-06	CSAG2 /// CSAG3	-1.913739526	4.22E-06
PEF1	1.582739374	2.58E-06	FRMD4A	-1.455952291	4.22E-06
PERP	1.427455262	2.58E-06	TRIM22	-1.393855993	4.22E-06
SRSF3	1.413481987	2.59E-06	ICK	-1.463346532	4.25E-06
GABRA2	2.280806034	2.61E-06	CA12	-1.762929378	4.26E-06
FOXP1	1.572167116	2.62E-06	NEDD9	-1.346898851	4.34E-06
TFAP2C	1.7138763	2.64E-06	---	-1.345132095	4.37E-06
TUBB	1.500808975	2.65E-06	GSPT1	-1.267099471	4.37E-06
RAD21	1.709131668	2.66E-06	HDAC9	-1.746369156	4.38E-06
SLC25A11	1.532637783	2.70E-06	PBX3	-1.437059555	4.38E-06
ATP6V0D1	1.466747421	2.71E-06	ZNF518B	-1.501212611	4.39E-06
LOC101060363 /// PPIA	2.295781133	2.72E-06	MAP1B	-1.460345698	4.39E-06
NPTN	1.674870905	2.73E-06	SP110	-1.417839902	4.42E-06

Appendix

KRT8	2.0358338	2.74E-06	CLDN11	-1.295499277	4.43E-06
RIPK4	1.817332767	2.74E-06	TRIM2	-1.260043398	4.43E-06
ATP11B	1.533404207	2.75E-06	ATP11C	-1.386682791	4.46E-06
NDE1	1.565448241	2.76E-06	CDH11	-1.287865375	4.46E-06
EIF2B1	1.985819542	2.77E-06	USP6	-1.272092063	4.50E-06
GLO1	1.813983539	2.77E-06	XDH	-1.570417724	4.51E-06
PGK1	1.492889612	2.78E-06	DHX58	-1.269214323	4.55E-06
BZW1	1.424395168	2.78E-06	LRRC8A	-1.284323098	4.56E-06
GPR183	3.591729911	2.80E-06	ACSL3	-1.251924472	4.56E-06
ALDOC	1.647163165	2.80E-06	AK5	-1.572452183	4.58E-06
ALDOA	1.413962758	2.84E-06	DOPEY2	-1.585740709	4.59E-06
WRB	1.570231603	2.86E-06	ACTA2	-1.358188944	4.67E-06
PDGFC	2.414100739	2.90E-06	ANK2	-1.58128354	4.69E-06
BSG	1.466791058	2.90E-06	OSTM1	-1.249270807	4.71E-06
TMBIM1	1.485214953	2.91E-06	FAM83A	-1.280174156	4.73E-06
CALU	1.608344521	2.93E-06	CA12	-1.807917695	4.74E-06
PHLDB2	1.565827572	2.93E-06	SNX18	-1.238735179	4.74E-06
ATP5SL	1.514158804	2.93E-06	GRAMD3	-1.687648259	4.81E-06
NCKAP1	1.470928493	2.97E-06	DDX58	-1.53812833	4.84E-06
ARFIP2	1.386331645	2.97E-06	TMEM144	-1.490694076	4.84E-06
TPM1	1.435108812	2.98E-06	RARRES3	-1.738969358	4.86E-06
ATP6V0D1	1.359234846	2.99E-06	TEP1	-1.69960333	4.86E-06
PMEPA1	1.51782361	3.04E-06	BST2	-1.458664787	4.87E-06
F3	1.640964838	3.05E-06	MCTP1	-1.331976124	4.88E-06
AASDHPPT	1.789063902	3.07E-06	COL17A1	-3.305809671	4.89E-06
NAPA	1.925986079	3.12E-06	TMCC3	-1.363424361	4.91E-06
ARL8B	1.37160684	3.12E-06	DRAM1	-1.231353934	4.93E-06
PABPC4	1.563512591	3.13E-06	CFH	-1.493437315	4.97E-06
PGAM5 /// PXMP2	1.419030276	3.13E-06	AHNAK2	-1.310056303	4.97E-06
EIF5A /// EIF5AL1	1.405018882	3.14E-06	B3GAT2	-1.688633925	5.00E-06
POLE3	1.362667633	3.15E-06	CDH18	-1.491409992	5.02E-06
NRG1	1.602307031	3.18E-06	DOCK4	-1.269883085	5.02E-06
CTGF	1.376960602	3.20E-06	SPP1	-1.381228892	5.07E-06
---	1.429380481	3.21E-06	NUP43	-1.21672699	5.16E-06
CFL1	1.365816817	3.21E-06	CNEP1R1	-1.239909331	5.27E-06
THBS1	1.52893716	3.22E-06	MAF	-1.371169827	5.29E-06
PEF1	1.344142269	3.22E-06	HSD11B1	-1.60198229	5.32E-06
PRSS2 /// PRSS3	1.465923021	3.23E-06	RASGEF1A	-1.530531951	5.34E-06
ATP6V1G2- DDX39B /// DDX39B /// SNORD84	1.371896789	3.24E-06	CEP68	-1.277151805	5.36E-06
COPS7A	2.596817472	3.26E-06	---	-1.583790887	5.38E-06
TPM3	1.391439577	3.26E-06	RRAGD	-1.9463612	5.39E-06
NAP1L4	2.003465369	3.27E-06	OAS3	-1.702240941	5.42E-06
THOC1	2.162534589	3.29E-06	SPG20	-1.325264211	5.43E-06

Appendix

LAPTM4A	1.619287387	3.29E-06	MME	-1.894769116	5.44E-06
PTGS2	1.476235926	3.32E-06	VAV3	-1.464448833	5.44E-06
FYTTD1	1.369377929	3.35E-06	KCNJ2	-1.934693593	5.45E-06
SERP1	1.9952334	3.42E-06	NUDT7	-1.21314227	5.45E-06
PRKAR1A	1.420136165	3.43E-06	MAMDC2	-1.946564995	5.51E-06
CYB5B	1.372218153	3.45E-06	PAQR5	-1.218174789	5.52E-06
AP2M1	1.785721974	3.46E-06	FAS	-1.429008581	5.53E-06
UNC119	1.979885884	3.51E-06	NAPEPLD	-1.272254875	5.59E-06
CFL1	1.36058017	3.52E-06	XAF1	-1.277979939	5.61E-06
CNBP	1.347351241	3.57E-06	RREB1	-1.20700797	5.64E-06
KDELR2	1.31452928	3.57E-06	PROS1	-2.279416015	5.66E-06
CDC16	1.96848004	3.59E-06	HIAT1	-1.202324188	5.68E-06
HADHA	1.605856439	3.60E-06	SERPINB5	-1.913395958	5.73E-06
IL11	1.654018062	3.61E-06	FAM84B	-1.26998864	5.77E-06
CXCL1	1.50163619	3.62E-06	ZCCHC2	-1.449044666	5.80E-06
WRB	1.445746297	3.62E-06	GPNUMB	-1.24700339	5.84E-06
ZFAND6	1.33916668	3.65E-06	NHLRC3	-1.730727093	5.88E-06
EGR1	1.516784805	3.67E-06	KRT19	-1.653068938	5.90E-06
ANXA10	2.0002571	3.68E-06	MAF	-1.211445251	5.91E-06
ACADM	1.320870877	3.72E-06	LPIN1	-1.201404344	5.91E-06
MANBAL	1.567780269	3.75E-06	FOXRED2	-1.212274657	5.92E-06
CCDC130	1.720062255	3.77E-06	RFC5	-1.888905439	5.94E-06
TPD52L2	1.443669876	3.79E-06	WDR66	-1.177052794	5.95E-06
TPD52L2	1.396098378	3.80E-06	NLRC5	-1.285238493	5.97E-06
UBE2M	1.322617766	3.80E-06	ZFX	-1.208704356	6.02E-06
FAM98A	1.592179715	3.82E-06	CYSTM1	-1.23494271	6.03E-06
ASF1B	1.67223479	3.85E-06	TRIM22	-1.200619463	6.05E-06
NDUFA10	1.419092038	3.85E-06	FBXO11	-1.686552843	6.09E-06
TRIM16 /// TRIM16L	1.308484979	3.85E-06	GCNT3	-1.625148017	6.09E-06
MORF4L2	1.307302605	3.88E-06	CYSTM1	-1.173054298	6.10E-06
SLC16A1	2.28477554	3.89E-06	RPS6P6 /// TMEM150C	-1.230003883	6.11E-06
PRC1	1.414793986	3.89E-06	KRT222	-1.708702187	6.17E-06
COL1A1	1.646551677	3.92E-06	ABCC6 /// ABCC6P1 /// ABCC6P2	-1.201539194	6.19E-06
IL8	1.428429347	3.93E-06	SEPP1	-1.787266922	6.21E-06
PHLDB2	1.381149284	3.93E-06	CLVS1	-2.060006086	6.25E-06
DEK	1.330488411	3.93E-06	ZFHx4	-1.334565028	6.26E-06
PGK1	1.455260293	3.96E-06	TMTC3	-1.309992734	6.28E-06
PDIA6	1.533775018	3.97E-06	HERC5	-1.606905541	6.34E-06
EI24	1.366705597	3.97E-06	AQP11	-1.688046796	6.35E-06
SAFB	1.342273068	4.02E-06	REV3L	-1.530242343	6.36E-06
RRM1	1.684781946	4.04E-06	MOXD1	-1.30008197	6.39E-06
MAD1L1	1.35700424	4.04E-06	KCNT2	-2.698233192	6.42E-06
GART	1.582796677	4.10E-06	BST2	-1.583943679	6.47E-06
IFNGR1	3.616383024	4.13E-06	SAMD12	-2.104617542	6.48E-06
CIAPIN1	1.394621846	4.14E-06	XIAP	-1.331851071	6.51E-06

Appendix

PBX1	1.397678462	4.16E-06	SH3GL3	-1.221249133	6.51E-06
PRSS23	1.273867868	4.16E-06	FAM129A	-1.260194745	6.60E-06
MAEA	1.605098603	4.22E-06	ADCY1	-1.454178891	6.62E-06
PRDX2	1.444981638	4.28E-06	AHNAK2	-1.164825557	6.62E-06
C1orf43	1.272722639	4.28E-06	C5orf45	-1.442870547	6.65E-06
MRPL38	1.477755161	4.32E-06	SCIN	-2.781175017	6.67E-06
KYNU	1.418758695	4.33E-06	TMEM30B	-1.900036613	6.67E-06
ADSS	1.313861019	4.35E-06	NEXN	-1.216235157	6.75E-06
C6orf211	1.347102128	4.41E-06	FLRT2 /// LOC100506718	-1.159508119	6.76E-06
CTNNB1	1.306427669	4.41E-06	TTC28	-1.720225915	6.77E-06
TNFAIP3	1.361197069	4.46E-06	GPNMB	-1.180369595	6.77E-06
DIO2	1.446497872	4.47E-06	BNC2	-1.451639354	6.83E-06
MLLT11	1.535488491	4.48E-06	TSHZ3	-1.223857169	6.90E-06
TMED2	3.384652122	4.49E-06	TAP1	-1.142656279	6.92E-06
LOC101060363 /// PPIA	2.022071119	4.51E-06	PM20D2	-1.41333899	6.95E-06
PPT1	1.508465781	4.53E-06	APOBEC3F	-1.15289923	6.96E-06
STK25	1.93770889	4.54E-06	TENM2	-2.196847919	6.97E-06
MCM7	1.932111669	4.56E-06	RRAGD	-1.840279074	7.01E-06
MAEA	1.415103027	4.59E-06	SATB1	-1.577610211	7.04E-06
EPS8	1.254676822	4.61E-06	PDE5A	-1.147550899	7.06E-06
MAP1LC3B	1.376045822	4.62E-06	CELSR2	-1.206647891	7.11E-06
TMPRSS15	1.491674239	4.67E-06	NAV2	-1.266330896	7.16E-06
LYPD1	1.293070722	4.68E-06	GPNMB	-1.204422009	7.16E-06
VCAN	2.444005759	4.72E-06	MME	-2.423335299	7.18E-06
CCNC	1.467901477	4.72E-06	IDNK	-1.188571851	7.24E-06
PLK2	1.878094947	4.74E-06	GRB10	-1.149837931	7.25E-06
ADAM10	1.646630312	4.78E-06	FAT1	-1.376623284	7.26E-06
RBM3	1.311285261	4.79E-06	PLXDC1	-1.61464775	7.29E-06
PBX1	1.486547467	4.80E-06	NPHP3	-1.307035891	7.32E-06
G3BP1	1.369634832	4.80E-06	FAS	-1.265704742	7.32E-06
METTL17	1.675981079	4.86E-06	ZFP36L2	-1.160639707	7.33E-06
HIBADH	1.426898144	4.88E-06	ADCY9	-1.175055195	7.37E-06
JUNB	1.299766681	4.88E-06	LCP1	-1.245676705	7.38E-06
HDAC1	1.228316058	4.88E-06	APH1B	-1.166675189	7.38E-06
ARPC4	1.410465528	4.89E-06	CTSL2	-1.657947686	7.42E-06
FNDC3B	1.323965294	4.92E-06	PLSCR1	-1.304127531	7.42E-06
FAM98A	1.267004746	4.97E-06	IL31RA	-1.124624958	7.44E-06
KDELRL1	1.615861482	4.98E-06	TMEM170A	-1.145054925	7.48E-06
C17orf76-AS1 /// SNORD49A /// SNORD49B /// SNORD65	1.444290437	5.02E-06	STX17	-1.136112648	7.51E-06
CDK2AP2	1.472586427	5.03E-06	APOBEC3A /// APOBEC3A_B /// APOBEC3B	-1.275739716	7.52E-06
DIMT1	1.499796028	5.05E-06	NCF2	-2.316069186	7.54E-06
VCAN	2.040127866	5.11E-06	PHIP	-1.134909549	7.54E-06

Appendix

ITGAV	1.586353386	5.11E-06	PDPN	-1.276875047	7.57E-06
EEF1A1	1.418092973	5.11E-06	AK5	-1.297247897	7.58E-06
PSMD2	1.260755752	5.17E-06	TCEAL7	-1.699940661	7.62E-06
PHLDB2	1.569631628	5.18E-06	ATP10D	-1.32126518	7.67E-06
BMP2	1.499987341	5.22E-06	CRADD	-1.117312125	7.73E-06
C9orf3 /// LOC100507319	1.486394828	5.22E-06	XKR3	-1.805236652	7.78E-06
CD9	1.290047035	5.22E-06	C1orf56	-1.390395929	7.80E-06
ASNA1	1.253811994	5.22E-06	PLCB1	-1.76584663	7.84E-06
DLST	1.283090315	5.25E-06	SCN3A	-2.210323699	7.90E-06
P4HB	1.465371449	5.26E-06	COL24A1	-1.361381603	7.98E-06
SNX10	1.364877995	5.27E-06	NEXN	-1.19675381	8.01E-06
SLC25A6	1.290229239	5.27E-06	CXCL11	-1.585470853	8.03E-06
RHOA	1.778308883	5.29E-06	SOX7	-1.288013894	8.03E-06
LPCAT3	1.493867803	5.29E-06	ZNF528	-1.178807523	8.04E-06
ASNA1	1.282141902	5.29E-06	MAP2	-1.669341883	8.06E-06
PFN1	1.225390035	5.30E-06	IQCJ-SCHIP1 /// SCHIP1	-1.111427682	8.06E-06
PTGES3	2.064320812	5.31E-06	SH3BP5	-1.12841471	8.10E-06
DPYSL2	1.337443012	5.34E-06	ITPRIPL2	-1.841501893	8.13E-06
NUP85	1.383848864	5.40E-06	DAB2	-1.441565875	8.13E-06
EXOC5	1.453154216	5.41E-06	MANBA	-1.357185773	8.13E-06
ORC5	1.671040162	5.42E-06	DTX3L	-1.379162033	8.18E-06
TFDP1	2.033269252	5.47E-06	XIAP	-1.245884762	8.19E-06
CD99	1.242404087	5.47E-06	SEPSECS	-1.259287184	8.22E-06
NAP1L4	1.522409478	5.50E-06	SBSN	-1.462922758	8.28E-06
CFL1	1.327220993	5.52E-06	WDFY3	-1.246744965	8.30E-06
SEC13	1.256615509	5.52E-06	CARD6	-1.173674442	8.35E-06
MAD1L1	1.296072096	5.54E-06	ITGAX	-1.602294059	8.42E-06
MPDU1	1.332138278	5.55E-06	---	-1.567265195	8.52E-06
NT5DC2	1.467413397	5.60E-06	ANK1	-1.207526066	8.52E-06
CAPNS1	1.250467754	5.60E-06	RPS6KA2	-1.329702894	8.54E-06
VDAC3	1.246781226	5.63E-06	NMU	-1.898751375	8.66E-06
SHMT2	1.340441762	5.69E-06	CD24	-1.338888021	8.67E-06
COMT	1.595160428	5.72E-06	TNFSF13B	-1.89408781	8.71E-06
LOC101060567 /// PEX11B	1.404253279	5.73E-06	ASPH	-1.15861694	8.73E-06
PWP1	1.379243054	5.73E-06	OAS2	-1.559358395	8.75E-06
TGFBI	1.225641542	5.74E-06	MRPS25	-1.293578411	8.75E-06
ATP5SL	1.239115462	5.78E-06	PCMTD1	-1.144025674	8.79E-06
HNRNPA1 /// HNRNPA1P10 /// HNRNPA1P33	1.225112507	5.79E-06	ZNF117	-1.166588097	8.81E-06
F3	1.8639164	5.81E-06	GKAP1	-1.149341253	8.83E-06
C17orf76-AS1 /// SNORD49A /// SNORD49B /// SNORD65	1.352057727	5.81E-06	FOXO1	-1.414924181	8.84E-06

Appendix

UHRF1	1.77946648	5.82E-06	SGTB	-1.126813412	8.90E-06
ARMC1	1.391461372	5.88E-06	FYB	-1.17599226	8.93E-06
DNAJB6 /// TMEM135	1.281258538	5.90E-06	SLC17A5	-1.296492792	8.98E-06
RNPS1	1.236017542	5.91E-06	LOC100996668 /// ZEB1	-1.143028138	8.99E-06
DUSP1	2.333591707	5.92E-06	FXVD3	-1.991911754	9.00E-06
BSG	1.358081587	5.93E-06	APBB2	-1.516592	9.01E-06
GPRC5A	1.933645266	5.95E-06	MAL2	-1.895532523	9.06E-06
UQCRC1	1.176140591	5.96E-06	ZBTB1	-1.273597728	9.10E-06
PFN1	1.278109682	5.98E-06	PLCL2	-1.321239629	9.12E-06
DKC1 /// MIR644B /// SNORA56	1.31823344	5.99E-06	CREBRF	-1.461080206	9.20E-06
TNFAIP8	1.887137347	6.05E-06	DDX60	-1.115139936	9.26E-06
PSMF1	1.243101037	6.07E-06	TRIM59	-1.229548376	9.28E-06
CDC20	2.24063859	6.09E-06	SH3PXD2A	-1.38977797	9.34E-06
ANLN	1.378243089	6.12E-06	C14orf37	-1.247588892	9.41E-06
SCAMP2	1.250953427	6.12E-06	AKAP2 /// PALM2-AKAP2	-1.200707309	9.41E-06
CNOT6	1.358817167	6.13E-06	SRRM2	-1.100634265	9.42E-06
C5orf15	2.101143765	6.16E-06	LAMP3	-1.08451484	9.43E-06
AP1S1	1.380247201	6.19E-06	DKK2	-1.738572675	9.44E-06
RNF220	1.297243458	6.19E-06	ISG15	-1.128535876	9.49E-06
EIF5	1.214343648	6.22E-06	FRY	-1.220558521	9.53E-06
FAM195A	1.165036716	6.23E-06	NAV3	-1.136086088	9.55E-06
YWHAQ	1.29076988	6.24E-06	PODXL	-1.09061618	9.55E-06
OLA1	1.465635401	6.25E-06	ZNF557	-1.118365307	9.62E-06
MTERFD2	1.265543163	6.27E-06	EEA1	-1.116032699	9.67E-06
HMOX1	1.171514638	6.28E-06	CCL5	-1.158519017	9.71E-06
CFL1	1.214217214	6.32E-06	GBP4	-1.544698395	9.75E-06
PRSS23	1.21540562	6.33E-06	MKL2	-1.060676227	9.75E-06
NAP1L4	1.671731921	6.34E-06	TMEM171	-1.624610039	9.82E-06
DNAJB6	1.171516823	6.34E-06	MIR205HG	-2.579371143	9.84E-06
DNAJB6	1.171516823	6.34E-06	SLC6A6	-1.133232605	9.84E-06
DDX39A	1.632091025	6.35E-06	NFAT5	-1.060604576	9.85E-06
SYNGR2	1.162377688	6.37E-06	C12orf56	-1.236424655	9.86E-06
CAPN2	1.341042395	6.38E-06	CPA3	-1.360393979	9.87E-06
ELOVL5	2.686412715	6.39E-06	HLA-DMA	-1.212235418	9.92E-06
HTATIP2	1.376639275	6.40E-06	KRT15	-1.188695118	9.92E-06
ZMPSTE24	1.217698598	6.40E-06	TMEM60	-1.247131564	9.99E-06
PABPC1	1.176915088	6.40E-06	FKBP5	-1.136169902	9.99E-06
CSRP1	1.809512157	6.41E-06	PPP6C	-1.20256249	1.00E-05
BSG	1.459056277	6.41E-06	BDP1	-1.163449406	1.00E-05
FYTTD1	1.405975893	6.41E-06	ZNF264	-1.289241013	1.01E-05
TMX1	1.431889615	6.43E-06	CA12	-1.638781429	1.02E-05
CXCL3	2.393589847	6.46E-06	KLF3	-1.228608383	1.02E-05
TIMP3	1.640005945	6.47E-06	GTF2H1	-1.108893451	1.02E-05
THBS1	1.687823122	6.51E-06	VWA8	-1.316396483	1.03E-05

Appendix

NUSAP1	1.704248023	6.53E-06	ZNF281	-1.109636602	1.03E-05
VBP1	1.329196479	6.53E-06	PCDHGA1 /GA10 /GA11 /GA12 /GA2 /GA3 /GA4 /GA5 /GA6 /GA7 /GA8 /GA9 /GB1 /GB2 /GB3 /GB4 /GB5 /GB6 /GB7 /GC3 /GC4 /GC5	-1.384313219	1.04E-05
RPS6KB2	1.319554573	6.54E-06	KDSR	-1.135387043	1.04E-05
GLTSCR2 /// SNORD23	1.7059051	6.59E-06	BEX2	-1.131623887	1.04E-05
LYPLA1	1.524826671	6.59E-06	FNIP2	-1.055915856	1.04E-05
FN3KRP	1.249870851	6.64E-06	SH3D19	-1.07564952	1.05E-05
ANXA5	1.213579893	6.64E-06	PTPRB	-2.220990411	1.06E-05
DLST	1.293516498	6.68E-06	ZNF566	-1.443708506	1.06E-05
/// MIR1244-1 /// MIR1244-2 /// MIR1244-3 /// PTMA	1.351337849	6.69E-06	LOC100996782 /// MED18	-1.128091961	1.06E-05
IDI1	1.283665634	6.70E-06	CCDC88A	-1.106535965	1.06E-05
CCNG1	1.727418711	6.71E-06	LRP8	-1.088563643	1.06E-05
KDELR1	1.411539618	6.71E-06	KLF7	-1.350562901	1.07E-05
CLINT1	1.155202814	6.71E-06	TBC1D9	-1.108245147	1.07E-05
STX12	1.307810567	6.73E-06	RNF13	-1.068891928	1.07E-05
WDR45B	1.315736191	6.74E-06	SEL1L3	-1.054669889	1.07E-05
ITGB1	1.219227713	6.79E-06	XAF1	-1.244844713	1.08E-05
BTBD10	1.285231008	6.82E-06	KITLG	-1.132125288	1.08E-05
CSTF1	1.246401423	6.87E-06	FAM134A	-1.060433493	1.08E-05
PSMF1	1.193638845	6.95E-06	PLEKHM1	-1.04624054	1.08E-05
CDK11A /// CDK11B	1.229732946	6.97E-06	KRT6A	-3.972870381	1.09E-05
ITGAV	2.218130675	7.00E-06	CLDN12 /// GTPBP10	-1.121632832	1.09E-05
DAGLB	1.232378744	7.02E-06	SVIL	-1.115498638	1.09E-05
HDGF	1.254816422	7.09E-06	SCARB2	-1.091382049	1.09E-05
EIF3L	2.144840904	7.11E-06	MMP1	-1.041087823	1.10E-05
ELK1	1.963507701	7.11E-06	AKIRIN1	-1.839697875	1.11E-05
CMPK1	1.524109601	7.16E-06	TMTC1	-1.129207819	1.11E-05
RRN3	1.200866763	7.16E-06	MAP2	-2.578271336	1.12E-05
FST	1.403790049	7.18E-06	LRIG1	-1.352585206	1.12E-05
ABCG1	1.384180182	7.19E-06	VSNL1	-1.226431455	1.12E-05
ST13 /// ST13P4	1.506020224	7.22E-06	RNF141	-1.136293797	1.12E-05
CTNNB1	1.201072179	7.22E-06	LOC100996668 /// ZEB1	-1.105302799	1.12E-05
NMT1	1.318188288	7.23E-06	SAMD9	-1.044069723	1.12E-05
MYO1C	1.230552333	7.23E-06	TMEM98	-2.05395635	1.13E-05
ELL2	1.180653928	7.23E-06	RABL2B	-1.049921318	1.13E-05
USP3	1.817791774	7.26E-06	RAPH1	-1.031377432	1.13E-05
PKM	1.134240506	7.30E-06	RPL39L	-1.394342269	1.14E-05
CDK4	1.412632047	7.31E-06	BDH2 /// SLC9B2	-1.10762247	1.14E-05
APMAP	1.392115606	7.37E-06	ITGB1BP1	-1.050742483	1.14E-05
KIAA0895	1.326391501	7.37E-06	DNMT1	-1.353846991	1.15E-05

Appendix

KLF5	1.294119774	7.41E-06	CYFIP1	-1.275756615	1.15E-05
ADIPOR1	1.246730378	7.48E-06	AS3MT /// C10orf32- AS3MT	-1.646970079	1.16E-05
FADD	1.12892026	7.51E-06	KCTD4	-1.271696015	1.16E-05
LTBP1	1.128787817	7.61E-06	MDN1	-1.12981651	1.16E-05
SNRPB	1.128393979	7.61E-06	SVIL	-1.096460738	1.16E-05
SFRP1	1.366560531	7.64E-06	FLCN	-1.024606243	1.16E-05
B4GALT2	1.351268651	7.67E-06	SP110	-1.557638434	1.17E-05
SNX10	1.218144693	7.67E-06	SLC8A1	-1.238475715	1.18E-05
SNAP23	1.415553679	7.68E-06	POSTN	-1.110012221	1.18E-05
KRT7	1.557392579	7.71E-06	ZNF175	-1.101123462	1.18E-05
PTP4A1	1.612335198	7.76E-06	ERAP1	-1.073815667	1.18E-05
PKM	1.190965898	7.76E-06	HYAL1	-1.031882752	1.18E-05
MTRF1	1.138325487	7.77E-06	AP5M1	-1.024925331	1.18E-05
TRAPPC8	1.40399764	7.79E-06	ARHGAP15	-1.860149095	1.19E-05
DUSP1	1.185865893	7.79E-06	NIPBL	-1.218367025	1.19E-05
TNFRSF21	2.068119952	7.83E-06	UQCRB	-1.196944943	1.19E-05
SGPP1	1.291647697	7.84E-06	MCC	-1.186414201	1.19E-05
ATP6AP2	1.243101845	7.96E-06	CD68	-1.150345644	1.19E-05
LONP2	1.15323346	7.96E-06	MACF1	-1.141602799	1.19E-05
CRK	2.105380195	7.98E-06	SYT11	-1.213761893	1.20E-05
SRRM1	1.126587546	7.99E-06	SAMD9L	-1.102286645	1.20E-05
BSG	1.257514088	8.01E-06	CPEB1	-1.086514969	1.20E-05
ADAMTS1	1.539900051	8.02E-06	PLK1S1	-1.05845607	1.20E-05
LSM4	1.109333928	8.02E-06	IGDCC4	-1.24628966	1.21E-05
HIF1A	3.621251285	8.03E-06	ACOT13	-1.177091004	1.21E-05
PPIA	1.304212616	8.08E-06	FAM179B	-1.038590351	1.21E-05
SLC25A37	1.173337883	8.09E-06	PCOLCE2	-1.215414882	1.23E-05
PTPN12	1.228584618	8.14E-06	AFF1	-1.052417758	1.23E-05
NR2C2AP	1.102625794	8.25E-06	ZNF232	-1.009601864	1.23E-05
SPTLC1	1.757478302	8.26E-06	SLC17A5	-1.190606454	1.24E-05
RCN2	1.369847093	8.27E-06	USP48	-1.033289785	1.24E-05
TADA3	1.220780469	8.30E-06	SLCO1B3	-1.044153649	1.25E-05
GABARAPL1	1.200546518	8.31E-06	KAT2B	-1.038538214	1.25E-05
PLS3	1.251465899	8.32E-06	IFIT2	-1.813292922	1.26E-05
PRNP	1.250527006	8.32E-06	CCL5	-1.135884519	1.26E-05
NIT1	1.282360715	8.35E-06	ERO1LB	-1.121544676	1.26E-05
PRDX2	1.217274637	8.37E-06	PSMB9	-1.08739688	1.26E-05
IRF1	1.324428998	8.41E-06	ZNF527	-1.047012057	1.26E-05
UBE2I	1.139802634	8.41E-06	SYNC	-1.049048808	1.27E-05
Sep-07	1.651630469	8.43E-06	LRRC8B	-1.289927877	1.28E-05
HES4	1.106385983	8.43E-06	CAPRIN2	-1.10308849	1.29E-05
NMD3	1.137519447	8.45E-06	SPIN4	-1.081936522	1.29E-05
Sep-07	1.556268924	8.46E-06	POLK	-1.245697303	1.31E-05
SDCBP	1.510363119	8.49E-06	HS2ST1	-1.096840648	1.31E-05
ABHD11	1.358905036	8.49E-06	C2orf69	-1.221550402	1.32E-05
MEDAG	1.808727044	8.50E-06	MORC4	-1.18824277	1.32E-05

Appendix

GDI2	1.239512254	8.53E-06	GJB7	-1.092721333	1.32E-05
CD44	1.206596808	8.58E-06	SAMD9L	-1.361265216	1.33E-05
METRNL	1.113618903	8.60E-06	DPP4	-1.280803922	1.33E-05
RFTN1	1.326002077	8.61E-06	CSTA	-1.161595931	1.33E-05
PPIL1	1.352830034	8.62E-06	F8	-1.008112589	1.33E-05
PIP5K1A	1.202547501	8.63E-06	---	-1.003762778	1.33E-05
GID8	1.389963336	8.67E-06	ROR2	-1.579322301	1.34E-05
RIPK4	1.146943815	8.70E-06	FGF12	-1.478847776	1.34E-05
CDH12	1.493568757	8.72E-06	PTPRR	-1.538240274	1.35E-05
KLHL7	1.235830609	8.72E-06	ASAH1	-1.144895655	1.35E-05
UBE2I	1.157739105	8.73E-06	S1PR1	-1.1277996	1.35E-05
ARL6IP1	1.150131622	8.75E-06	SNTB2	-1.082425841	1.35E-05
PWP1	1.197023676	8.76E-06	SEC14L1	-1.060647459	1.35E-05
CAPNS1	1.425613958	8.77E-06	CHN2	-1.396169744	1.36E-05
RNF13	1.089062875	8.77E-06	SFN	-1.235120938	1.36E-05
SNAP23	1.739562443	8.79E-06	EIF5A2	-1.062822776	1.36E-05
MRPL12 /// SLC25A10	1.509943933	8.82E-06	PHLDA3	-1.001801094	1.36E-05
FLOT1	1.388166436	8.82E-06	UHRF1BP1	-1.008730245	1.37E-05
HNRNPF	1.306908901	8.83E-06	GM2A	-1.003508745	1.37E-05
MAPKAP1	1.285440074	8.87E-06	CXorf57	-2.563529085	1.38E-05
NCOA7	2.483656331	8.88E-06	PAPLN	-1.623064614	1.38E-05
IST1	1.32791922	8.90E-06	FAM129A	-1.589930263	1.38E-05
LOC100996620 /// ZNF644	1.183877749	8.90E-06	VSNL1	-1.306067209	1.38E-05
Sep-07	1.55769385	8.91E-06	SLC43A3	-1.141986242	1.38E-05
COL4A2	1.655899997	8.93E-06	RIT1	-1.082712379	1.38E-05
STRA6	1.187427336	8.93E-06	SNTB2	-1.062809475	1.38E-05
MON1B	1.160258321	8.94E-06	RAB38	-1.041747388	1.39E-05
SDHC	1.301149697	8.98E-06	RRAS2	-1.38391765	1.40E-05
SORBS2	1.150007436	8.99E-06	HSPA12A	-1.102967164	1.40E-05
CDC45	1.145701545	9.08E-06	OSTM1	-1.089081402	1.40E-05
RNF220	1.389255591	9.14E-06	EIF4E3	-1.470659499	1.42E-05
TWF1	1.611208996	9.16E-06	BTAF1	-1.084826205	1.42E-05
TAF9B	1.089919964	9.22E-06	CLEC2B	-1.035532473	1.42E-05
ANXA2	1.281541271	9.26E-06	XRN1	-1.290183398	1.43E-05
HMGB1	1.446343377	9.27E-06	WNT5B	-1.189361982	1.43E-05
UBE2S	1.094619498	9.28E-06	---	-1.157948908	1.43E-05
UBAC2	1.282665438	9.36E-06	GJB2	-1.939572896	1.44E-05
C5orf46	1.536038407	9.40E-06	HECW2	-1.483783609	1.44E-05
CSNK1A1	1.127075912	9.44E-06	TMEM154	-1.358632073	1.44E-05
LETMD1	1.549556642	9.46E-06	AGGF1	-1.053691544	1.44E-05
EIF2S3	1.515438487	9.48E-06	CTNND1 /// TMX2- CTNND1	-1.019478761	1.44E-05
TFDP1	1.910363851	9.54E-06	KLK5	-1.23588299	1.45E-05
PRDX2	1.178478792	9.57E-06	C11orf58	-1.073938059	1.45E-05
C1orf43	1.244197794	9.61E-06	TTC32	-1.017636533	1.46E-05

Appendix

LETMD1	1.101230833	9.65E-06	PLAGL1	-1.865172184	1.47E-05
BECN1	1.24392067	9.66E-06	PEAR1	-1.408435858	1.47E-05
TOP2A	1.328050024	9.71E-06	MX1	-1.031235618	1.47E-05
APMAP	1.300331878	9.72E-06	LONRF1	-1.214633096	1.48E-05
CDC5L	1.303607411	9.82E-06	NAP1L2	-1.1994882	1.48E-05
CNN2	1.117025104	9.86E-06	IFI44L	-1.049067028	1.49E-05
EIF4A2 /// MIR1248 /// SNORA4 /A63 /A81 / SNORD2	1.101548886	9.86E-06	FBXO36	-1.122435032	1.51E-05
EIF2AK1	1.085175239	9.87E-06	ZFHX3	-1.289746639	1.52E-05
PPT1	1.450872418	9.89E-06	ASAH1	-1.139502466	1.52E-05
EXOC5	1.072367164	9.90E-06	SPANXC /// SPANXE	-1.097591289	1.52E-05
COPE	1.097228147	9.93E-06	CACNA1C	-1.52446512	1.53E-05
ARFRP1	1.488145126	9.95E-06	SPIRE1	-1.093605794	1.53E-05
CAPZA2	1.192968936	9.95E-06	FBN2	-1.170725434	1.54E-05
RRP1	1.082799008	9.96E-06	FYCO1	-1.502215054	1.55E-05
NDUFAF7	1.245006548	9.97E-06	CREBBP	-1.230883703	1.55E-05
RAB5A	1.378959302	9.99E-06	IGSF10	-1.110228925	1.55E-05
TMEM189 /// TMEM189- UBE2V1 /// UBE2V1	1.141969438	1.00E-05	GM2A	-1.05126146	1.55E-05
PRDX6	1.100817113	1.00E-05	TRIM38	-1.047913455	1.56E-05
METTL3	2.128443844	1.01E-05	NT5C1B-RDH14 /// RDH14	-1.0090825	1.57E-05
PBX1	1.531775609	1.01E-05	CPED1	-1.298472623	1.58E-05
CTNNB1	1.396145719	1.01E-05	TNRC6B	-1.086505841	1.58E-05
PAFAH1B2	1.265608146	1.01E-05	GBA /// GBAP1	-1.018276895	1.58E-05
FAM195A	1.064723688	1.01E-05	ZNF573	-1.064710486	1.59E-05
WDR1	1.052840967	1.01E-05	NPAS2	-1.040086188	1.59E-05
SLC25A11	1.143022601	1.02E-05	INTS2	-1.030043211	1.60E-05
GPN1	1.141774023	1.02E-05	SCIN	-1.150827689	1.61E-05
GOLGA7	1.101196316	1.02E-05	KMT2E	-1.048855749	1.62E-05
UBALD2	1.081212423	1.02E-05	ARG2	-1.022877335	1.63E-05
RAB5A	2.656471288	1.03E-05	MAGI3	-1.015723093	1.63E-05
TXNRD1	2.011188507	1.03E-05	SIX4	-1.06884559	1.64E-05
RNPS1	1.45882292	1.04E-05	SH3RF2	-2.005816978	1.65E-05
RAB5C	1.225134607	1.04E-05	ZNF595	-1.295756362	1.66E-05
SLC25A6	1.101747642	1.04E-05	METTL15	-1.249532622	1.66E-05
RCN2	1.084497489	1.04E-05	TPP2	-1.161667975	1.66E-05
ITGA6	1.723636249	1.05E-05	LIN54	-1.148310503	1.66E-05
GORASP2	1.533424383	1.05E-05	SYNCRIP	-1.182120684	1.67E-05
NXT2	1.424940003	1.05E-05	PRRX1	-3.180761784	1.68E-05
MLF2	1.417801128	1.05E-05	ATG5	-1.289199291	1.68E-05
EXTL2	1.393845329	1.05E-05	MCC	-1.404125865	1.69E-05
UNG	1.215081007	1.05E-05	QKI	-1.106347443	1.69E-05
SIGMAR1	1.203358141	1.05E-05	ZNF226	-1.048939927	1.69E-05
CTNNB1	1.165373503	1.05E-05	PDCD1LG2	-1.762308888	1.70E-05

Appendix

ADAM9	2.044352099	1.06E-05	ZNF507	-1.140956603	1.70E-05
METTL21D	1.726811924	1.06E-05	MCCC1	-1.053695144	1.70E-05
FLNA	1.183889922	1.06E-05	GGA2	-1.068817442	1.73E-05
RAB5C	1.113018116	1.06E-05	NBEA	-1.166709513	1.75E-05
RBM17	1.079658884	1.06E-05	ENPP2	-1.149125436	1.75E-05
XBP1	1.1224191	1.07E-05	SPP1	-1.110105567	1.75E-05
PMEPA1	1.108235087	1.07E-05	RBM47	-1.080229734	1.75E-05
CLTC	1.072638241	1.07E-05	KRT5	-2.110533566	1.76E-05
CAPZA2	1.435044575	1.08E-05	TUBBP5	-1.485036138	1.76E-05
SERPINE2	1.314093757	1.08E-05	DMXL1	-1.429358413	1.76E-05
CSRP1	1.296133606	1.08E-05	SEMA3D	-1.35629121	1.76E-05
TMEM9	1.08111538	1.08E-05	ZNF706	-1.282195983	1.76E-05
PCNP	1.529041442	1.09E-05	C12orf56	-1.128457707	1.76E-05
COTL1	1.291079769	1.09E-05	LPGAT1	-1.031149581	1.76E-05
CRIM1	1.149092676	1.09E-05	APOBEC3F	-1.057386487	1.78E-05
CPA4	1.148994056	1.09E-05	FCHO2	-1.043149824	1.78E-05
NUDT22	1.100549967	1.09E-05	GUCY1B3	-1.219014954	1.79E-05
RIOK3	1.235824301	1.10E-05	SLC1A3	-1.520295131	1.82E-05
YIF1B	1.168441048	1.10E-05	LOC100996628 /// SHROOM3	-1.371654761	1.82E-05
SMAD3	1.133872766	1.10E-05	ZNF345	-1.251081276	1.83E-05
PLOD2	1.102346873	1.10E-05	KRTAP1-5	-1.177085098	1.83E-05
AIMP2	1.082669422	1.11E-05	TRIM8	-1.062669627	1.83E-05
KDM4C	1.348972671	1.12E-05	TMEM60	-1.019153251	1.84E-05
ABI1	1.343075753	1.12E-05	SOAT1	-1.080932014	1.87E-05
SIAH1	1.285362961	1.12E-05	ACVR1	-1.006188149	1.87E-05
PRDX2	1.183545363	1.12E-05	FEZ1	-1.511254244	1.88E-05
MAT2B	1.085903562	1.12E-05	NOM1	-1.238456481	1.88E-05
CLPTM1	1.031520614	1.12E-05	ZNF721	-1.179106291	1.89E-05
DNM1L	1.685359286	1.13E-05	ZNF92	-1.112634798	1.89E-05
CERS2	1.337240816	1.13E-05	ANKRD29	-1.210378094	1.91E-05
RABAC1	1.065056079	1.13E-05	HEATR5A	-1.048138539	1.91E-05
KDELR3	1.037537906	1.13E-05	PLK1S1	-1.035629443	1.91E-05
STAU1	2.116474428	1.14E-05	PIFO	-1.033756797	1.92E-05
NAP1L1	1.501340958	1.14E-05	RNF144A	-2.870381147	1.93E-05
GNAI3	1.029542464	1.14E-05	SDPR	-1.009904888	1.93E-05
DPP7	1.263760996	1.15E-05	TAF1B	-1.330940581	1.94E-05
NBN	1.224299009	1.15E-05	APOBEC3F	-1.13893321	1.94E-05
CCDC126	1.15338282	1.15E-05	TAF9	-1.101431083	1.94E-05
RASA1	1.145251011	1.15E-05	DYNC1LI2	-1.065638265	1.95E-05
PSAP	1.053692929	1.15E-05	ZFP36L2	-1.005726956	1.95E-05
UBXN1	1.032734525	1.15E-05	TAB3	-1.099191128	1.96E-05
MED27	1.030865376	1.15E-05	ZBTB8A	-1.278413624	1.97E-05
POLR2E	1.203881849	1.16E-05	GLUL	-1.076808872	1.97E-05
TRPM2	1.099645391	1.16E-05	TRAK1	-1.01641918	1.97E-05
RTN3	1.367999485	1.17E-05	TCF19	-1.049401489	1.99E-05
WNT5A	1.129049672	1.17E-05	SLC12A8	-1.035871821	1.99E-05

Appendix

CAPN2	1.068086534	1.17E-05	RSBN1	-1.048468581	2.00E-05
SNRPB	1.055580466	1.17E-05	IFI44	-1.017459376	2.01E-05
COG6	1.59721511	1.18E-05	IDO1	-1.618142421	2.02E-05
HMGNI	1.089537264	1.18E-05	HOXD10	-1.679821383	2.03E-05
SORBS2	1.148103721	1.19E-05	WISP1	-1.586561568	2.03E-05
EFEMP1	1.053541785	1.19E-05	DDIT4L	-2.736500585	2.05E-05
HADHB	1.048866038	1.19E-05	RNF213	-1.492786944	2.05E-05
NFKBIA	1.040542475	1.19E-05	CCDC88A	-1.240810119	2.05E-05
LPCAT3	1.498693733	1.20E-05	DTNA	-1.148192485	2.05E-05
ALCAM	1.226649604	1.20E-05	TRIM22	-1.194315378	2.06E-05
LOC101059993 /// RBM14	1.19167888	1.20E-05	PGAP1	-1.003281062	2.08E-05
SNRPB	1.06364976	1.20E-05	PCDH7	-1.871109752	2.09E-05
TCEA1	1.058764477	1.21E-05	MPP5	-1.021509052	2.09E-05
RNFT1	1.09655892	1.23E-05	ECM2	-1.190664592	2.10E-05
CD9	1.058091827	1.23E-05	SLC37A2	-1.233855231	2.11E-05
SRSF3	1.163205768	1.24E-05	IL17RD	-1.638106017	2.12E-05
RHEB	1.158789519	1.24E-05	CD74	-1.362765661	2.12E-05
MAGED1	1.452335181	1.25E-05	QRSL1	-1.334934088	2.12E-05
RSRC2	1.449176425	1.25E-05	KIAA1671 /// LOC100996283	-1.314271727	2.12E-05
GALNT1	1.241011219	1.25E-05	EPB41L2	-1.098833945	2.12E-05
USP10	1.208613761	1.25E-05	ENTPD3	-1.286894609	2.13E-05
CFL1	1.072980315	1.25E-05	SMAD1	-1.010031566	2.13E-05
TOX	1.227570529	1.26E-05	LRRCC1	-1.304157376	2.15E-05
MAGEA4	1.221778906	1.26E-05	FOXO3 /// FOXO3B	-1.008037328	2.17E-05
SRSF5	1.219647314	1.26E-05	WDFY3	-1.447016729	2.19E-05
PTTG1IP	1.227561553	1.27E-05	IMMP2L	-1.197677715	2.19E-05
GNB2	1.026716347	1.27E-05	KBTBD3	-1.21731801	2.20E-05
SUGP1	1.182364698	1.28E-05	PPP1R1C	-1.117518977	2.24E-05
BCLAF1	1.088110446	1.28E-05	RTP3	-1.160730546	2.25E-05
DRG2	1.075324832	1.28E-05	ZNF267	-1.120010997	2.25E-05
MAD1L1	1.275603084	1.29E-05	CNIH4	-1.020237476	2.25E-05
MBD2	1.047411646	1.30E-05	LYST	-1.379591129	2.26E-05
RHPN2	1.248870592	1.31E-05	ZNF254	-1.123531351	2.26E-05
PLAU	1.79300214	1.32E-05	SLC7A8	-1.144969225	2.30E-05
GLUD1 /// GLUD2	1.33963806	1.32E-05	GDPD1	-1.213122717	2.31E-05
WDR1	1.1728661	1.32E-05	GREB1	-1.240833808	2.33E-05
MDK	1.147904284	1.32E-05	TARDBP	-1.220464171	2.34E-05
KDM6A	1.033449997	1.32E-05	TMEM41B	-1.010402739	2.34E-05
TLCD1	1.026481569	1.33E-05	CACNA1A	-1.141610992	2.35E-05
CPNE1	1.003870132	1.33E-05	PSG9	-1.862715872	2.36E-05
HNRNPF	1.242404794	1.34E-05	KIAA0825	-1.492421856	2.36E-05
SLC25A32	1.176172727	1.34E-05	AGA	-1.129643283	2.36E-05
ALDH9A1	1.168170863	1.34E-05	VPS29	-1.063237299	2.37E-05
TBL1XR1	1.031315299	1.36E-05	GNE	-1.034191897	2.37E-05

Appendix

F2RL1	1.990063451	1.37E-05	LOX	-1.032354016	2.37E-05
ARFGAP3	1.435718569	1.37E-05	---	-1.467598726	2.38E-05
FAM60A	1.029121778	1.38E-05	Mar-01	-1.244865088	2.38E-05
ANPEP	1.65354489	1.39E-05	---	-1.020418676	2.38E-05
PROSC	1.48063357	1.39E-05	PROSER1	-1.035251947	2.39E-05
DKFZp686K1684 /// RCN1	1.301988459	1.39E-05	EPB41L4B	-1.691745791	2.41E-05
COQ6	1.101111777	1.39E-05	USP31	-1.143225599	2.44E-05
DDB1	1.062039663	1.39E-05	LINC00341	-1.202714955	2.45E-05
PRKCZ	1.041067307	1.39E-05	GNAQ	-1.121974523	2.46E-05
BIN3	1.016773795	1.39E-05	KRIT1	-1.098914086	2.46E-05
KLHL9	1.303883899	1.40E-05	ZNF281	-1.011547091	2.46E-05
SRRT	1.209473032	1.40E-05	ANK1	-1.186979503	2.48E-05
SNRPB	1.049222854	1.40E-05	ARHGAP26	-1.171092316	2.48E-05
PDXDC1	1.06586314	1.41E-05	ARHGAP24	-1.412621527	2.50E-05
ANXA8 /// ANXA8L1 /// ANXA8L2	1.166876116	1.43E-05	LTBP2	-1.289669521	2.51E-05
EIF4E	1.076376276	1.43E-05	ZNF883	-1.279239382	2.53E-05
EED	1.31382268	1.44E-05	PARP8	-1.128116852	2.53E-05
ID1	1.206353155	1.44E-05	PDLIM5	-1.095873525	2.56E-05
BIRC2	1.076600887	1.44E-05	CEP170	-1.18253134	2.57E-05
SLC25A11	1.046535842	1.44E-05	---	-1.095508357	2.58E-05
SOCS2	1.204561003	1.45E-05	PTPRM	-1.053386755	2.60E-05
MOSPD1	1.121516897	1.45E-05	KCNG3	-1.363734233	2.61E-05
TM9SF4	1.283683041	1.46E-05	APOBEC3B	-1.06807307	2.61E-05
PGK1	1.087298995	1.46E-05	EPCAM	-1.137066576	2.65E-05
EEF2	1.013814199	1.46E-05	LYPD5	-1.029688689	2.66E-05
XPO1	1.06191293	1.47E-05	ESF1	-1.01805607	2.66E-05
PAFAH1B2	1.097098157	1.48E-05	CSAG2 /// CSAG3 /// LOC101060231	-1.05412073	2.67E-05
CDC16	2.890525431	1.49E-05	MYO6	-1.296080029	2.69E-05
RSU1	1.161524559	1.49E-05	CACUL1	-1.219460497	2.70E-05
PRKCZ	1.131693639	1.49E-05	TAPT1	-1.142611447	2.72E-05
CAPZA2	1.103971099	1.49E-05	SMC2	-1.075944118	2.72E-05
BTBD1	1.100287137	1.49E-05	MFSD8	-1.061153777	2.72E-05
MSMO1	1.333909819	1.50E-05	USP1	-1.059903719	2.76E-05
C3orf17	1.287171805	1.50E-05	AS3MT /// C10orf32- AS3MT	-1.480237541	2.77E-05
ARGLU1	1.069606283	1.50E-05	PTGER2	-1.035171603	2.77E-05
SLC25A1	1.209789122	1.51E-05	IL1RN	-2.634736161	2.78E-05
PSAT1	1.701676964	1.52E-05	TNRC6A	-1.0040524	2.78E-05
TBL1XR1	1.022465671	1.53E-05	SLC5A3	-1.348318091	2.81E-05
PPP2R5C	1.056236489	1.54E-05	ZNF562	-1.165960534	2.81E-05
SDHD	1.037773714	1.54E-05	RAPGEF1	-1.112005606	2.82E-05
SDHD	1.037773714	1.54E-05	HERC6	-1.078287595	2.82E-05
LACTB	1.021228984	1.54E-05	CCL5	-1.155032195	2.83E-05
PRPSAP2	1.492258692	1.55E-05	APOL6	-1.096984867	2.85E-05

Appendix

ODC1	1.142956909	1.55E-05	FXYD3	-1.4046318	2.86E-05
WTAP	1.039377511	1.59E-05	SYNE1	-1.377649362	2.89E-05
KDM4C	1.035504754	1.60E-05	NEXN	-1.149808892	2.91E-05
PRSS3	1.006523157	1.60E-05	ARID1B	-1.12432976	2.91E-05
GLUD1	1.219489353	1.61E-05	WISP1	-1.690807444	2.92E-05
FDFT1	1.01562405	1.61E-05	CD36	-1.967596676	2.94E-05
NR4A1	1.297253643	1.62E-05	B4GALT6	-1.34475755	2.95E-05
EIF2B4	1.166639566	1.62E-05	LYPD5	-1.207788615	2.95E-05
HSPH1	1.097538964	1.62E-05	EFNA5	-1.097329466	2.95E-05
PDGFRA	1.052654344	1.63E-05	MED28	-1.045289392	2.97E-05
CD44	1.039537164	1.63E-05	TNFSF10	-1.052435159	2.99E-05
NRG1	1.28485877	1.64E-05	AFTPH	-1.191596351	3.00E-05
DERA	1.102423501	1.64E-05	SLC47A1	-1.155151432	3.01E-05
LOXL2	1.346033504	1.65E-05	FCF1	-1.027481933	3.01E-05
TSTA3	1.178858425	1.65E-05	RAB7L1	-1.127943695	3.05E-05
COPS7A	1.109109855	1.65E-05	TNRC6B	-1.147511128	3.07E-05
ZDHHC7	1.112570278	1.66E-05	ANK1	-1.057598248	3.12E-05
PPTC7	1.022881999	1.66E-05	ZNF552	-1.228801982	3.13E-05
DEK	1.145199988	1.67E-05	SNX30	-1.082678633	3.14E-05
LMAN2L	1.038633637	1.67E-05	MYO5C	-1.521900928	3.15E-05
MAP3K2	1.317603047	1.68E-05	KIAA1407	-1.011418203	3.15E-05
TMEM189 /// TMEM189- UBE2V1 /// UBE2V1	1.183081248	1.68E-05	SH3YL1	-1.134088103	3.18E-05
HPCAL1	1.495406958	1.69E-05	PLA2G4C	-1.381200903	3.20E-05
DIMT1	1.344153898	1.69E-05	SMIM13	-1.114612884	3.20E-05
UBL3	1.251559896	1.69E-05	DCLK1	-1.880298557	3.22E-05
ATF3	1.135682639	1.69E-05	SUCO	-1.007464591	3.25E-05
SLC25A4	1.294557638	1.70E-05	SATB1	-2.97733384	3.27E-05
IQGAP1	1.075407637	1.70E-05	FAM76A	-1.083310088	3.29E-05
PGM1	1.044905901	1.70E-05	DMRT1	-1.094156075	3.31E-05
MCM7	1.036806648	1.70E-05	CCDC113	-1.065777947	3.31E-05
ACADM	1.229789822	1.71E-05	HLA-E	-1.05522942	3.36E-05
YIPF5	1.013868703	1.71E-05	NFATC4	-1.324151834	3.37E-05
JAK1	1.649510101	1.72E-05	FAM46C	-1.63289949	3.38E-05
RSRC2	1.396673585	1.74E-05	ELOVL7	-1.117568972	3.41E-05
ATP6V1G2- DDX39B /// DDX39B /// SNORD84	1.132682721	1.74E-05	E2F8	-1.049847142	3.41E-05
ZNF410	1.120328864	1.74E-05	ACVR2A	-1.053365901	3.43E-05
PERP	1.02999649	1.74E-05	GFPT1	-1.002866095	3.43E-05
AGPAT4	1.623237492	1.75E-05	APBB2	-1.099050902	3.44E-05
NDEL1	1.637497014	1.76E-05	CCDC69	-1.413515482	3.45E-05
SDCBP	1.13401008	1.77E-05	PCDH1	-1.202521931	3.46E-05
FBXO3	1.442223107	1.79E-05	MEF2A	-1.085808328	3.48E-05
RHOF	1.146521372	1.79E-05	BTN3A3	-1.260277268	3.50E-05

Appendix

LOC101060439 /// RAP1B	1.13949395	1.79E-05	RAB27A	-1.143430103	3.50E-05
CTPS1	1.235541123	1.81E-05	APOL6	-1.11828997	3.50E-05
EIF4G2	1.020419967	1.81E-05	DAB2	-1.139399824	3.52E-05
LETMD1	1.014016542	1.82E-05	C6orf120	-1.000601819	3.52E-05
CSNK2B	1.223010883	1.83E-05	MCM9	-1.254090028	3.53E-05
PSEN1	1.999981068	1.84E-05	TMTC4	-1.486588254	3.55E-05
INSIG1	1.135329501	1.84E-05	LOC653501 /// ZNF658 /// ZNF658B	-1.138771243	3.57E-05
ACO1	1.117225546	1.84E-05	PDP2	-1.280732847	3.59E-05
PRMT3	1.059240166	1.84E-05	EFNA5	-1.559365313	3.64E-05
IBTK	2.089346105	1.85E-05	C17orf103	-1.006313666	3.64E-05
LUC7L2	1.134522466	1.85E-05	PLXNC1	-1.282466704	3.65E-05
TMEM134	1.06575266	1.85E-05	TRPV2	-1.030479227	3.65E-05
CSNK2B	1.205828002	1.87E-05	STRBP	-1.076364427	3.67E-05
CBX4	1.16785966	1.88E-05	DHRS7	-1.148940157	3.69E-05
EIF3G	1.107800245	1.88E-05	STRIP2	-1.512816216	3.72E-05
SMOX	1.249591953	1.90E-05	RMI1	-1.054176869	3.73E-05
SNX17	1.16979428	1.90E-05	ARMC4	-1.045445202	3.74E-05
POTEE /// POTEF /// POTEI /// POTEJ	1.576072984	1.91E-05	RSF1	-1.027335796	3.74E-05
CDH12	1.971606618	1.92E-05	CLCA2	-1.073293278	3.78E-05
UBE2Q2	1.762271176	1.92E-05	IREB2	-1.079328229	3.81E-05
MRPS27	1.197524566	1.92E-05	TDO2	-1.338387429	3.82E-05
AGPS	1.284755984	1.93E-05	PTPN13	-1.090078871	3.82E-05
MRPS27	1.739765984	1.94E-05	PTPN13	-1.090078871	3.82E-05
FOXA1	1.143830044	1.94E-05	TRIM29	-1.639515788	3.87E-05
SOX4	1.03950731	1.94E-05	DIXDC1	-1.203968955	3.88E-05
MTMR2	1.119717105	1.95E-05	KRT6A	-3.242395491	3.89E-05
MFAP2	1.079310305	1.95E-05	COA6	-1.07691789	3.91E-05
CYB5R1	1.00094039	1.95E-05	DICER1	-1.061185689	3.92E-05
SET /// SETP4	1.076698856	1.96E-05	ZBTB14	-1.141488305	3.96E-05
SSFA2	1.728143039	1.97E-05	PIK3R1	-1.16221045	3.97E-05
COPS7A	1.553339757	1.98E-05	CHST2	-1.21739987	4.01E-05
ATP6V1G2- DDX39B /// DDX39B /// SNORD84	1.379285904	1.99E-05	BNC2	-1.119461928	4.07E-05
UBAC2	1.056893226	1.99E-05	MDM4	-1.010680018	4.08E-05
SSFA2	1.168153734	2.02E-05	GAS1	-1.33969877	4.16E-05
GFPT2	1.009324874	2.02E-05	KIAA1211	-1.736752659	4.20E-05
SPAG9	1.177495134	2.03E-05	PAG1	-1.121122747	4.20E-05
E2F6	1.364458008	2.04E-05	NHLRC1	-1.220362989	4.21E-05
DR1	1.063405008	2.04E-05	PRPF4	-1.034733119	4.21E-05
CCNA1	1.252691181	2.06E-05	LRRC16A	-1.034381061	4.22E-05
RNFT1 /// TBC1D3P1- DHX40P1	2.020302898	2.07E-05	ZNF879	-1.000724319	4.26E-05

Appendix

MIR22 /// MIR22HG	1.024406127	2.09E-05		DACT1	-1.115329014	4.30E-05
RAB11A	1.26650758	2.10E-05		GBP6	-2.772420837	4.32E-05
RRAS	1.001320383	2.11E-05		PAQR8	-1.04613686	4.33E-05
TSPAN3	1.110256273	2.12E-05		XAF1	-1.061859861	4.34E-05
SORBS2	1.072956357	2.12E-05		RAD51L3-RFFL /// RFFL	-1.011617967	4.35E-05
PPP4C	1.14064265	2.15E-05		IFI16	-1.63768042	4.36E-05
AMACR /// C1QTNF3 /// C1QTNF3- AMACR	1.076188947	2.15E-05		CREBRF	-1.159031034	4.39E-05
NUCKS1	1.438891012	2.16E-05		FGF12	-2.452358911	4.42E-05
ATF3	2.065005156	2.17E-05		DOCK9	-1.540320432	4.42E-05
PAPOLA	1.64694714	2.17E-05		RBM47	-1.002124253	4.45E-05
HSPBP1	1.278492317	2.17E-05		OSGEPL1	-1.065663337	4.46E-05
FBXO22	1.196224132	2.17E-05		CRYM	-1.772666181	4.47E-05
SHISA5	1.158027613	2.17E-05		RHOU	-1.345365539	4.48E-05
PPP6R3	1.172605575	2.18E-05		MED13	-1.009650722	4.49E-05
RBMX /// SNORD61	1.12153324	2.18E-05		APOL3	-1.027179999	4.51E-05
CITED2	1.217623959	2.19E-05		GSR	-1.005932901	4.52E-05
RPL4 /// SNORD16 /// SNORD18A /// SNORD18B /// SNORD18C	1.246478674	2.22E-05		ZCCHC10	-1.103756222	4.53E-05
RPS28	1.123373628	2.22E-05		MIA3	-1.308060262	4.55E-05
MRPL37	1.18421747	2.24E-05		IL36RN	-1.127877817	4.55E-05
NREP	1.087010742	2.24E-05		TMPRSS11D	-1.206088863	4.56E-05
LOC128322 /// NUTF2	1.023509027	2.24E-05		RDH10	-1.59766289	4.59E-05
ARHGAP12	1.260594872	2.26E-05		JMJD1C	-1.01094944	4.61E-05
NECAP2	1.247263797	2.26E-05		MYO10	-1.283373384	4.62E-05
LSM4	1.016039983	2.26E-05		CELSR1	-1.030171888	4.63E-05
RPL41	1.29340324	2.27E-05		MSR1	-1.11410438	4.64E-05
JUN	1.012859108	2.27E-05		MRPS18C	-1.027971705	4.64E-05
HNRNPUL1	1.075134127	2.28E-05		SLITRK6	-1.224410524	4.65E-05
SRRM1	1.020333581	2.29E-05		SNTB1	-1.314385729	4.67E-05
SMARCE1	1.082017828	2.30E-05		WDR26	-1.059770016	4.68E-05
PRDM1	1.005036974	2.30E-05		USP54	-1.058582611	4.72E-05
PMP22	1.888496422	2.31E-05		PLAC8	-1.289358559	4.74E-05
SDCBP	1.035263578	2.32E-05		MAP3K7CL	-1.057964158	4.81E-05
ATP6V1G2- DDX39B /// DDX39B /// SNORD84	1.199241437	2.33E-05		CFI	-1.52588316	4.87E-05
ACTR3	1.032449233	2.35E-05		ARSD	-1.043081343	4.87E-05
SYTL2	1.36103749	2.36E-05		SPP1	-1.343823785	4.88E-05
ZC3H15	1.054719746	2.36E-05		IL24	-1.527792357	4.94E-05
AKTIP	1.002798261	2.37E-05		---	-1.588268642	4.96E-05

Appendix

DNAJB4	1.429421894	2.39E-05	FAM43A	-1.391443505	4.98E-05
RTN3	1.350326753	2.39E-05	SHROOM4	-1.063228968	4.99E-05
DPP7	1.032428554	2.39E-05	RBP7	-1.032265614	5.00E-05
SIN3A	1.195989897	2.40E-05	TRIM13	-1.107406002	5.01E-05
SRM	1.159505698	2.40E-05	LDB2	-2.028183836	5.02E-05
CYP1B1	1.116466796	2.44E-05	C1orf110	-1.506838842	5.05E-05
AHCYL1	1.09483164	2.44E-05	EMR1	-1.134282586	5.08E-05
ABI2	1.512278276	2.45E-05	SOX2	-1.389732564	5.19E-05
LAMP2	1.367759651	2.45E-05	PSG1 /// PSG3 /// PSG4	-1.198399849	5.23E-05
TMEM2	1.283182329	2.45E-05	SASH1	-1.320228911	5.24E-05
DBNL	1.070680679	2.45E-05	ST6GALNAC5	-1.098892484	5.42E-05
PRPF31	1.501428286	2.46E-05	SIX1	-1.071601503	5.42E-05
CNPY3	1.100649457	2.46E-05	SLFN5	-1.170046252	5.45E-05
CDIPT	1.399651719	2.47E-05	SNX25	-1.138792402	5.48E-05
EXOSC10	1.065560291	2.47E-05	ARMC9	-1.285350113	5.52E-05
ASPH	1.579833558	2.48E-05	OXTR	-1.360180576	5.58E-05
RSRC2	1.12426962	2.49E-05	Mar-02	-1.268361086	5.62E-05
CCNG2	1.463647605	2.51E-05	MREG	-1.119761374	5.67E-05
NCOA4	1.510709408	2.52E-05	ANKRD17	-1.135568542	5.68E-05
SHOC2	1.057637583	2.52E-05	ARHGEF7	-1.029956719	5.75E-05
AP2M1	1.335558459	2.53E-05	TMEM200B	-1.121412672	5.76E-05
MVB12A	1.115500941	2.55E-05	EDNRA	-1.034786042	5.78E-05
CNN2	1.058187643	2.55E-05	SDR16C5	-1.220343629	5.84E-05
CCNL1	1.064795694	2.58E-05	PTPRZ1	-2.37096436	5.87E-05
RIOK1	1.876167788	2.59E-05	TAF1B	-1.066464239	5.87E-05
KDM3B	1.843039164	2.59E-05	SYNE2	-1.262764474	5.95E-05
FN3KRP	1.573913579	2.59E-05	PROM2	-1.227428689	5.96E-05
PGK1	1.20984212	2.60E-05	ENPP5	-2.477660753	6.02E-05
GFM2	1.163348989	2.60E-05	CPE	-2.126761847	6.04E-05
DNAJB6	2.177733353	2.62E-05	IQSEC1	-1.120581738	6.08E-05
TIPARP	1.039522815	2.62E-05	STOX2	-1.155746757	6.15E-05
DNAAF2	1.011103402	2.62E-05	BCLAF1	-1.133297409	6.16E-05
SOCS2	1.66912096	2.63E-05	NECAB1	-1.047520936	6.27E-05
RAB5A	1.650519925	2.66E-05	RP2	-1.057200174	6.31E-05
MDK	1.015807307	2.66E-05	DDR2	-1.509400793	6.36E-05
P4HB	1.009141642	2.66E-05	FOLR3	-1.681260629	6.39E-05
LOC101060439 /// RAP1B	1.64186434	2.67E-05	RAB9B	-1.153307117	6.40E-05
MTFR1L	1.479201426	2.67E-05	PDPN	-1.603719739	6.46E-05
YWHAZ	1.416568894	2.67E-05	DIP2C	-1.004903307	6.58E-05
ELF1	1.604685859	2.72E-05	ARFGEF2	-1.055209979	6.61E-05
BIRC5	1.473886393	2.74E-05	LDB2	-1.208936757	6.64E-05
PRPS2	1.26710765	2.74E-05	CLN5	-1.009513764	6.64E-05
CAPNS1	1.152245762	2.76E-05	DAZAP2	-1.007562143	6.64E-05
TSG101	1.083741843	2.76E-05	MANSC1	-1.190195676	6.67E-05
WSB2	1.081607175	2.76E-05	SORT1	-1.147864922	6.69E-05
RNF24	1.08234876	2.78E-05	PSG5	-1.27042547	6.70E-05

Appendix

SP3	1.195195947	2.79E-05	RABL2A	-1.002624226	6.76E-05
FAM133B /// FAM133CP /// FAM133DP	1.549512173	2.80E-05	SYNM	-1.230512418	6.86E-05
POLR1E	1.089556214	2.80E-05	IGIP	-1.036519314	6.86E-05
ALG3	1.006147491	2.83E-05	VSNL1	-1.542965197	6.92E-05
TPD52	1.130680346	2.86E-05	DTX3L	-1.014943191	6.92E-05
SCYL2	1.097174644	2.86E-05	RECK	-1.685530581	6.93E-05
ATP6V1G2- DDX39B /// DDX39B /// SNORD84	1.093246934	2.87E-05	CREBRF	-1.123412326	6.94E-05
TSTA3	1.846640827	2.88E-05	FRK	-1.031118435	6.96E-05
PLK2	1.749186605	2.88E-05	GRIN2A	-1.541849182	7.02E-05
GDI2	1.557808322	2.88E-05	RALGAPA1	-1.252084364	7.05E-05
---	1.422449827	2.88E-05	MDM2	-1.7995947	7.06E-05
FOPNL	1.079444261	2.89E-05	JPH1	-1.270174309	7.06E-05
BMPR1A	1.228206504	2.90E-05	GJB6	-1.656969648	7.16E-05
SLC31A1	1.248541254	2.91E-05	ZNF43	-1.967703964	7.18E-05
UPRT	1.097155801	2.91E-05	DTNA	-1.235661116	7.18E-05
KRT81	1.12394971	2.93E-05	SLC38A9	-1.17441902	7.19E-05
ITM2C	1.215446829	2.96E-05	GDPD1	-1.131071974	7.33E-05
RBM27	1.062493072	2.97E-05	SETDB2	-1.163249068	7.39E-05
NREP	1.258997476	3.00E-05	OSBPL6	-1.006146157	7.63E-05
APPL2	1.065068885	3.00E-05	LOC100133299	-1.050865434	7.65E-05
MFSD1	1.760700257	3.01E-05	ZNF608	-1.021035093	7.65E-05
YIF1B	1.090240961	3.01E-05	VPS13D	-1.01798485	7.67E-05
FUCA1	1.195810569	3.02E-05	NEXN	-1.480814869	7.75E-05
QKI	1.546867308	3.06E-05	DISP1	-1.110219682	7.80E-05
AHCY	1.364546154	3.06E-05	ZNF571	-1.029133204	7.92E-05
ACADM	1.360121986	3.08E-05	CXCL10	-1.208981407	8.05E-05
PRDX2	1.132884547	3.11E-05	GNPTAB	-1.352266727	8.11E-05
CNN2	1.006277846	3.11E-05	NUDT12	-1.11048237	8.17E-05
NCBP2	1.438812973	3.19E-05	ZNF137P	-1.096968182	8.35E-05
STC1	1.15437157	3.19E-05	TRIM29	-1.292881729	8.37E-05
ATG4B	1.005371228	3.19E-05	ENPP2	-1.825606624	8.46E-05
NXF1	1.943247538	3.21E-05	FIBIN	-1.456716077	8.67E-05
PARVA	1.021649344	3.21E-05	IRF6	-1.388246727	8.78E-05
USP16	1.012710656	3.21E-05	CD74	-1.312658537	8.89E-05
WSB1	1.470401924	3.22E-05	DHRS7	-1.002007951	9.07E-05
SMNDC1	1.001243304	3.22E-05	CEP19	-1.125680943	9.16E-05
ILF3	1.472797268	3.24E-05	EBF1	-1.425311709	9.25E-05
COPE	1.065754292	3.24E-05	CD36	-1.438506298	9.28E-05
TPD52L2	1.700260016	3.29E-05	SORL1	-1.89484797	9.38E-05
ZFR	1.113735232	3.30E-05	ZNF445	-1.051676927	9.39E-05
CNN2	1.02667871	3.33E-05	TRAF5	-1.098987733	9.41E-05
NAPA	1.532700012	3.36E-05	GALNT12	-1.072938906	9.43E-05
SUN1	1.783264515	3.40E-05	CD36	-1.320883234	9.47E-05

Appendix

RAP1A	1.178536268	3.43E-05	ZNF136	-1.318799269	9.50E-05
SPATC1L	1.006811928	3.44E-05	EPCAM	-1.59235401	9.58E-05
ABHD3	1.073010777	3.45E-05	CCR3	-1.464517539	9.82E-05
SAE1	1.26298028	3.46E-05	GRAMD1C	-1.489259247	9.84E-05
HSPA9	1.074423876	3.47E-05	FOXN3	-1.073692877	9.88E-05
SERPINA1	1.151720074	3.48E-05	CXCL11	-1.11513615	9.98E-05
HAS2	2.699440593	3.49E-05	PSG9	-1.10452488	0.000100778
COL1A1	1.404716454	3.53E-05	PTPRB	-1.288147391	0.00010161
NMD3	1.139624952	3.58E-05	HLA-F	-1.444729729	0.000101837
OS9	1.041002402	3.58E-05	HLA-DMB	-1.276113894	0.000101874
PICALM	1.181407996	3.59E-05	WDR78	-1.168179834	0.000103314
AKT3	1.127136461	3.60E-05	RSPO3	-1.622442633	0.000103472
CST3	1.10575552	3.60E-05	NDRG4	-1.136375198	0.000103927
PSMD2	1.708892148	3.63E-05	PLXDC1	-1.424917655	0.000104265
ADIPOR1	1.177090725	3.64E-05	FRMD4B	-1.765680877	0.000104409
ADTRP	1.052236144	3.64E-05	DCDC2	-1.352697662	0.000104524
PSAT1	1.549556294	3.66E-05	C10orf32	-1.211358459	0.000105511
PSAT1	1.549556294	3.66E-05	PLSCR1	-1.086494737	0.000106436
SNX17	1.164068814	3.70E-05	---	-1.019206798	0.000107155
CERK	1.173215775	3.71E-05	ADAT2	-1.018290612	0.000107657
PTCD2	1.667608106	3.75E-05	UHMK1	-1.06199158	0.000107754
PCTP	1.185993146	3.77E-05	SNCA	-1.099784479	0.000108809
NOC3L	1.214893343	3.80E-05	TGFBR3	-1.134591572	0.000112324
NFIB	1.164163296	3.80E-05	CACNA1A	-1.045659108	0.000112981
COPG2	2.174180565	3.82E-05	ORAOV1	-1.202061456	0.000113563
LMAN1	1.072048785	3.87E-05	AKAP7	-1.135239346	0.000113624
AP1M1	1.004308966	3.93E-05	RAB12	-1.0077072	0.000114177
RNF145	1.065647919	3.97E-05	CEACAM1	-1.2155934	0.000116949
ITM2C	1.171636358	3.99E-05	EMB /// EMBP1	-1.622548539	0.00011698
FSTL5	1.342560891	4.00E-05	MGARP	-1.119350931	0.000117301
UBE2Q2	1.626185662	4.02E-05	PRUNE2	-1.079537018	0.000117429
PTGES2	1.525509496	4.02E-05	FABP3	-1.771164628	0.000118028
CHN1	1.200180885	4.02E-05	ADRBK2	-1.451805663	0.00011806
HSPH1	1.010520664	4.03E-05	ZNF680	-1.091261218	0.000118978
AK3	1.483258712	4.06E-05	KIT	-1.1314202	0.000120273
P4HB	1.021586955	4.06E-05	FNIP2	-1.142734933	0.000121331
FKBP10	1.005918011	4.07E-05	KIAA0040	-1.219269661	0.000121812
ARAF	1.249027126	4.08E-05	MARK1	-1.77123213	0.000122316
ANXA8 /// ANXA8L1 /// ANXA8L2	1.738994068	4.11E-05	---	-1.003336569	0.000122618
RAB23	1.071862158	4.11E-05	FOXQ1	-1.101026337	0.000122933
BIN1	1.01630425	4.13E-05	ARHGAP26	-1.121772577	0.000129729
TRMT10C	1.188957896	4.14E-05	ZNF415	-1.183731141	0.000130583
PTCD3	1.793101977	4.15E-05	MYO5C	-1.246231308	0.00013173
EIF4A2 /// MIR1248 /A4	1.068445439	4.16E-05	MTF1	-1.047822797	0.000131851

Appendix

/A63 /A81 / SNORD2					
POLE3	1.085804495	4.17E-05	SSX2IP	-1.072672536	0.00013408
HSPBP1	1.144646529	4.22E-05	ZNF204P	-1.448248169	0.000135017
ADIRF	1.005839689	4.26E-05	TRERF1	-1.001608572	0.000138988
RANGAP1	1.20164213	4.28E-05	MTDH	-1.010105515	0.000139072
POLR2D	1.368231834	4.29E-05	PSG1	-1.593325521	0.000139322
UGDH	1.37491484	4.30E-05	C9orf41	-1.032109812	0.000139618
PPP2R1A	1.009955386	4.30E-05	BMPER	-1.596919112	0.000139732
SETD8	1.127637106	4.31E-05	ZC3HAV1	-1.202337906	0.000142543
SLC25A46	1.073402156	4.35E-05	RNASEL	-1.141140707	0.000143398
ODF2	1.290559766	4.36E-05	KIAA0226L	-1.198774598	0.000145764
ACADM	1.356777101	4.37E-05	ZNF709	-1.048294012	0.00014583
ABI1	1.180239956	4.41E-05	SP110	-1.026442504	0.000148454
LIPA	1.336453592	4.42E-05	MCOLN3	-1.306938741	0.000149691
NR3C1	1.282843643	4.42E-05	C3AR1	-1.433164658	0.00015004
IDH3A	1.082498358	4.42E-05	AHCTF1	-1.039887133	0.000152099
DUSP1	1.184472181	4.43E-05	FAIM3	-1.233286495	0.000153326
SMARCB1	1.007760382	4.46E-05	TUB	-1.123635972	0.000155
NBPF1 /F10 / F11 /F12 /F14 /F15 / F16 /F24 /F7 /F8 /F9	1.206452718	4.48E-05	KLK8	-1.264234412	0.000157584
SERPINA1	2.174691116	4.49E-05	CD74	-1.243597654	0.000160119
SERPINH1	1.027673186	4.50E-05	FAM111B	-1.007158893	0.000160378
PPP2R1A	1.19289302	4.51E-05	TLR3	-1.231081315	0.00016161
ABHD14A-ACY1 /// ACY1	1.152546988	4.51E-05	ESRP1	-1.533756669	0.000162
UGGT2	1.145569005	4.51E-05	NRN1	-2.455802828	0.000162108
RHOB	1.058398332	4.51E-05	CCDC169-SOHLH2 ///	-1.121103509	0.000162708
UBE2W	1.368372096	4.59E-05	SOHLH2	-1.071115023	0.000163744
CASP3	1.125322346	4.59E-05	LPIN2	-1.932751429	0.000169378
DCK	1.448162832	4.62E-05	TMPRSS4	-1.073602849	0.000170206
CDC23	1.226344015	4.62E-05	GBP2	-1.110602074	0.000184464
PITHD1	1.025963401	4.71E-05	SNX16	-1.198589378	0.0001857
SETD3	1.168844969	4.72E-05	GAB1	-1.437011024	0.000186198
UBE2D3	1.269234788	4.73E-05	SHFM1	-1.153455927	0.000186794
STARD4	1.727753735	4.78E-05	LRRCC1	-1.195345095	0.000186949
FAM220A	1.521126163	4.79E-05	HYAL1	-1.108317432	0.000187908
RPL15	1.133869425	4.86E-05	EPCAM	-1.051262643	0.000189766
SLC3A2	1.030909559	4.90E-05	TAOK1	-1.491254254	0.000192995
IGFBP3	2.231955092	4.96E-05	SLC22A15	-1.842359663	0.000193114
WDR77	1.063176669	4.96E-05	SDPR	-1.12628299	0.000195259
PRDX6	1.012520794	4.96E-05	PDSS1	-1.200263179	0.000197749
PRADC1	1.122499063	4.97E-05	CREBRF	-1.097836119	0.000199704
CSNK1D	1.43826022	4.99E-05	HCAR2 /// HCAR3	-1.025222144	0.000208439
SPSB3	1.00174059	5.02E-05	---	-1.274764662	0.0002115
			PELI2		

Appendix

KBTBD2	1.18992014	5.05E-05	MFAP3L	-1.313295105	0.000215844
PPM1B	1.833967101	5.19E-05	MIR1304 /// SNORA1 /// SNORA18 /// SNORA25 /// SNORA32 /// SNORA40 /// SNORA8 /// SNORD5 /// TAF1D	-1.342032042	0.000229829
ERGIC1	1.076813807	5.22E-05	ZNF273	-1.090183604	0.000230037
SKIL	1.198037428	5.29E-05	SLITRK6	-1.53811655	0.000230452
IL33	2.230383534	5.32E-05	SLC6A15	-1.059106642	0.000236476
COL1A1	1.446253026	5.33E-05	SP100	-1.098001507	0.000237036
USP8	1.102718809	5.34E-05	SPCS1	-1.433872024	0.000239835
GABARAPL1	1.198229968	5.35E-05	ATP8B1	-1.002930337	0.000241003
FOXC2	1.177825269	5.36E-05	DNAJB14	-1.385344076	0.000248433
COQ6	1.214925619	5.44E-05	---	-1.383161687	0.000248806
SRI	1.056571471	5.44E-05	KLK8	-1.231593429	0.00024882
TCTN1	1.506859776	5.47E-05	FZD1	-1.065057452	0.000253367
MAGED2	1.210847129	5.48E-05	LGALS	-1.127494009	0.000254298
ORC5	1.314460393	5.50E-05	MTR	-1.125713615	0.000255788
ZFPL1	1.129713347	5.50E-05	PSG9	-1.292522703	0.000258337
MAPRE2	1.24233133	5.51E-05	CXCL11	-1.419520638	0.000261969
RNF145	1.017716275	5.51E-05	ADRB1	-1.314770553	0.000262472
TMPO	1.547244308	5.54E-05	CAPSL	-1.477650252	0.000265154
GOLT1B	1.017015255	5.58E-05	DNAJC21	-1.226966313	0.0002693
TSG101	1.145523332	5.63E-05	GLI2	-1.03725414	0.000271214
RARRES1	1.076779753	5.65E-05	ZBED2	-1.013939308	0.00027195
ADCY7	1.084240208	5.66E-05	ZNF23	-1.063810933	0.000272604
POLM	1.114774534	5.68E-05	NHLRC2	-1.310178249	0.000279701
MARCKS	1.100563707	5.71E-05	ZNF273	-1.102483463	0.000280978
RICTOR	1.622093004	5.73E-05	DCN	-1.024769394	0.000282386
REEP4	1.225175014	5.73E-05	JMY	-1.060436637	0.000282918
LMNB1	1.30911355	5.76E-05	ANK1	-1.37104677	0.000287281
RB1CC1	1.028011462	5.77E-05	---	-1.258002501	0.000292854
YTHDF3	1.462025784	5.78E-05	IL12A	-1.398427795	0.000293207
MRS2	1.07812385	5.78E-05	ZNF585A	-1.075751971	0.000320036
ABCD3	1.265556604	5.80E-05	ZNF136	-1.119645109	0.000322533
METAP1	1.261577779	5.83E-05	PGAP1	-1.014437835	0.000322932
GABRA2	1.571091447	5.91E-05	CXCR7	-1.065653996	0.000330135
PAPSS1	1.296235787	6.02E-05	KCNE4	-1.078499845	0.000341233
MAP4K3	1.334631481	6.04E-05	SPATS1 /// TMEM151B	-1.371732775	0.000341403
PDE4D	1.325529989	6.07E-05	MALAT1	-1.029545825	0.00034424
SETD8	1.126862402	6.11E-05	DSC3	-1.193786235	0.000356569
Mar-07	1.160001509	6.12E-05	GBP4	-1.216189686	0.000371621
COL12A1	1.062605817	6.21E-05	ESM1	-1.250221974	0.000372499
TFDP1	2.121584942	6.24E-05	LOC100128816	-1.179987289	0.000373584
ATG4B	1.200387545	6.28E-05	ESR2	-1.067007739	0.000374856
---	1.886099966	6.29E-05	PCDH18	-1.267852742	0.000378276
SH3KBP1	1.069699942	6.32E-05	SLC44A3	-1.105971134	0.000378294

Appendix

DLX2	1.832144939	6.39E-05	HLA-DRA	-2.298105908	0.000380287
WNT5A	1.064742801	6.40E-05	KIAA0232	-1.198548825	0.000381032
CPOX	1.014219961	6.41E-05	SLC46A3	-1.085950352	0.000387821
GNAI2	1.026330531	6.46E-05	C20orf197	-1.114191024	0.000388468
SIGMAR1	1.185232792	6.47E-05	PROS1	-1.458586541	0.00038928
LMAN1	1.811890698	6.50E-05	FMN1	-1.141723851	0.000392855
TXNRD1	1.202972972	6.50E-05	CLEC7A	-1.130077025	0.000404161
TRIM36	1.033639616	6.55E-05	SLC1A4	-1.033057669	0.000404764
KRCC1	1.061902325	6.63E-05	C1orf56	-1.004533618	0.000405241
HAS2	1.41352716	6.64E-05	GPD2	-1.011979771	0.000405455
DLST	1.11202263	6.67E-05	VANGL2	-1.187820017	0.000408208
NAPA	1.192602575	6.79E-05	TDRP	-1.019797293	0.000412269
PMEPA1	1.189117219	6.89E-05	RCAN2	-1.865407308	0.000420072
MFF	1.049878626	6.97E-05	CLCC1	-1.020576483	0.000426681
ALDH18A1	1.477716116	7.03E-05	ST6GALNAC5	-1.148362546	0.000435779
MPDU1	1.375353683	7.03E-05	S100A8	-1.11132599	0.000445586
CXCL12	1.023459282	7.11E-05	YTHDC1	-1.081465128	0.000455754
SERPINA1	1.243604351	7.13E-05	DYSF	-1.012019678	0.000459582
TEX10	1.151240931	7.16E-05	ESRP2	-1.124252551	0.000464455
DLAT	1.086826653	7.20E-05	TMOD2	-1.005981463	0.000470081
SIGMAR1	1.487767109	7.26E-05	GREM1	-1.14067359	0.000498175
FSCN1	1.061915032	7.31E-05	BNC2	-1.352513752	0.000511812
TMPRSS15	1.051652063	7.31E-05	RLN1	-1.242589399	0.000512721
GADD45B	1.862772541	7.37E-05	PRPF38B	-1.011243721	0.00052678
NEDD1	1.2522106	7.41E-05	PRKCO	-1.025516349	0.000542897
GPR37 /// SEL1L2	1.326028905	7.49E-05	NPAS3	-1.419957	0.000543885
AMD1	1.280770219	7.52E-05	ST6GAL1	-1.079966134	0.000547295
TMEM66	1.379184501	7.53E-05	IKZF2	-1.492042268	0.000570919
LYPD1	2.051909194	7.58E-05	---	-1.299396671	0.000573454
C3orf17	1.246036639	7.60E-05	ERICH2	-1.181841129	0.000614537
MFHAS1	1.108006898	7.64E-05	LOC441155 /// ZC3H11A	-1.055558129	0.000619704
UXS1	1.133086516	7.66E-05	FXYD3	-1.119526133	0.00063557
LRP11	1.188066321	7.70E-05	ZNF165	-1.19960071	0.000636767
E2F4	1.020771281	7.73E-05	CYP2U1	-1.033077248	0.000640932
EIF4A2 / MIR1248 / SNORA4 /A63 /A81 / SNORD2	1.504320774	7.76E-05	TNRC6B	-1.128619773	0.000645813
PDE4B	1.269698829	7.92E-05	CHN2	-1.131814119	0.000672967
CLIC3	1.109170568	8.01E-05	SEPP1	-1.201676959	0.000675541
GPR89A /// GPR89B	2.074464037	8.03E-05	RERG	-1.004794128	0.0006821
MID1	1.251183617	8.03E-05	SMPDL3A	-1.705207901	0.000682492
MAEA	1.38758168	8.05E-05	IL36G	-1.403153647	0.000697205
CDCA8	1.383232867	8.06E-05	CCDC58	-1.156295728	0.000710847
QARS	1.613705475	8.11E-05	PIK3AP1	-1.607460617	0.00071268
ASL	1.262132008	8.19E-05	DGKH	-1.129740119	0.000724398

Appendix

CALD1	1.405009611	8.20E-05	MDM4	-1.18903675	0.000727673
ABHD6	1.210741501	8.20E-05	KIAA1009	-1.184352804	0.000750249
ABI1	1.143644417	8.26E-05	ZNF681	-1.023084721	0.000783248
PRKAA1	1.646166116	8.31E-05	IL24	-1.458728575	0.000846922
SMAD4	1.440761462	8.45E-05	CDK18	-1.030906516	0.00084941
YWHAZ	1.380997856	8.45E-05	DMRT2	-1.101496012	0.000853608
CYB561A3	1.126087838	8.55E-05	KIAA0040	-1.262703864	0.000870497
CTNNB1	1.196757381	8.65E-05	SPDYA	-1.043577036	0.000899301
ABCD3	1.242394079	8.66E-05	CHRD1	-1.766718745	0.0009332
BTBD10	1.100862733	8.68E-05	NAP1L5	-1.568142115	0.000992907
POLR3D	1.056883486	8.74E-05	DCN	-1.11451146	0.000995515
ATP5SL	1.40949762	8.82E-05	FBLN1	-1.011138682	0.001036981
LRRFIP1	1.090649986	8.83E-05	CLEC7A	-1.268980982	0.001056103
CLPTM1	1.157069381	8.91E-05	PPP6R2	-1.025237722	0.001059016
ANXA8 /// ANXA8L1 /// ANXA8L2	1.391632883	9.03E-05	FMN1	-1.201066741	0.001070522
EIF4B	1.157776772	9.05E-05	FAM189A1	-1.280244059	0.001070671
MTFR1L	1.027054421	9.21E-05	C9orf84	-1.050614326	0.001096785
DLST	1.421284618	9.22E-05	MUM1L1	-1.476260354	0.001110655
NBPF1 /F10 /F11 /F12 /F14 /F16 /F24 /F7 /F8 /F9	1.399666828	9.25E-05	CERS6	-1.279430855	0.00122379
GABRB1	1.007554528	9.27E-05	TNFAIP8L3	-1.286650931	0.001363314
TSC22D3	1.057367532	9.51E-05	APBB1IP	-1.159941056	0.001381903
MMD	1.539953465	9.63E-05	CCL28	-1.152504422	0.001437668
WIPI2	1.083678034	9.67E-05	C8orf47	-1.156273988	0.001501439
PIAS2	1.150847856	9.72E-05	CLEC7A	-1.280391515	0.001590123
ATF3	1.981467297	9.80E-05	SULF1	-1.060686066	0.001598734
HSD17B12	1.585619618	9.87E-05	SP6	-1.112587915	0.001602445
MKRN1	1.110010153	9.90E-05	ZNF462	-1.151004244	0.001665129
SUMF2	1.108349239	9.94E-05	PSG1	-2.157720133	0.001681484
GFM2	1.186558524	9.96E-05	IFIH1	-1.307283594	0.001797601
FKBP14	1.070674547	9.98E-05	AKTIP	-1.152098742	0.002044052
COX11	1.14361272	0.000100744	CCDC169 /// CCDC169- SOHLH2 /// SOHLH2	-1.078973894	0.00218965
NARF	1.36600245	0.000101003	LOC101060141 /// TPRG1	-1.134482048	0.002279497
CDK2	1.039165711	0.000101626	ETV7	-1.207876313	0.002328607
EREG	1.110651692	0.00010165	TRA2A	-1.193111775	0.002362965
PTDSS1	1.236701219	0.000102769	FAM111B	-1.038751826	0.002641387
DEXI /// LOC100289656	1.254674814	0.000106949	HLA-DPA1	-1.141877867	0.002693246
DZIP3	1.035821292	0.000108736	TNFSF13B	-1.001684	0.002829658
ATF2	1.18778897	0.000109027	STK4	-1.112002058	0.003150485
WDR73	1.307080966	0.000109309	LPHN2	-1.086653073	0.003216784
MLLT10 /// PICALM	1.60248758	0.000109511	OTTHUMG00000164286 /// RP11-150O12.6	-1.197725823	0.003389064

Appendix

RRAD	1.180933443	0.000109616	ZNF440	-1.058913136	0.003870901
PICALM	1.142942838	0.000111528	PLXDC1	-1.243095579	0.004145398
TGDS	1.723467931	0.000111816	MAP7	-1.028465922	0.004178838
GPR89A / GPR89B	1.830790761	0.000111956	SAA1 /// SAA2 /// SAA2- SAA4	-1.118075177	0.004677102
LTV1	1.096107676	0.000112048	PKNOX2	-1.19750093	0.005064689
HNRNPDL	1.250237459	0.000114833	NCAM1	-1.312257503	0.00754148
GTSE1	1.196447095	0.000116394	H6PD	-1.140098068	0.009211409
CHMP6	1.09171659	0.000117019	GAD1	-1.015284205	0.009605829
PPM1B	1.008344862	0.000118078	HLA-F	-1.164948004	0.010128746
ARL6IP5	1.135129362	0.000118456	METTL20	-1.186217353	0.011920667
PARPBP	1.026606929	0.000119233	ST6GALNAC5	-1.063481513	0.012862716
MLEC	1.075501665	0.000119445	MACF1	-1.015626808	0.02897981
WSB2	1.138092918	0.000119744			
SLC2A1	1.165359763	0.00012025			
NARS	1.252567634	0.000120317			
GLS	1.631539873	0.000121306			
NR4A1	1.470497356	0.000122142			
CSNK1D	1.505115071	0.000123009			
FKBP10	1.504367984	0.000123209			
CD99	1.099921775	0.000124724			
C19orf48 /// SNORD88C	1.096988897	0.000128824			
C21orf33	1.258109578	0.000128946			
ASB8	1.154510983	0.000130909			
ZBTB11	1.105305615	0.000131334			
AHCYL1	1.02487661	0.000131357			
AP3M1	1.029306603	0.000131506			
CYP1A1	1.038525976	0.000131588			
ARFIP2	1.293979669	0.000131602			
REEP5	2.014773981	0.000131888			
MBNL2	1.783553344	0.000132085			
PGRMC1	1.319994443	0.000133			
MEI1	1.314429935	0.000134107			
ADAMTS5	1.240477438	0.000135501			
ABI1	1.810733434	0.000137398			
FMR1	1.190179152	0.000140733			
IGFBP5	1.014569937	0.0001435			
KIFC3	1.125377583	0.000144526			
PIP5K1A	1.009685718	0.000149895			
NET1	1.159616236	0.000152195			
ZNF277	1.012446535	0.00015502			
MGAT2	1.518841887	0.0001567			
LPXN	1.093589834	0.00015889			
CD9	1.051047392	0.000159111			
CLPTM1	1.083037428	0.000162582			
MSH6	1.06777255	0.000165774			

TMEM54	1.008713945	0.000168656			
PICALM	1.766653038	0.000169341			
MBOAT2	1.109000044	0.000169492			
EIF2AK3	1.168798072	0.000170091			
PGAP2	1.785438914	0.000170266			
SLC31A2	1.344524732	0.000172012			
MORC3	1.436959576	0.000172518			
ADPGK	1.044189428	0.000174065			
TOE1	1.019197633	0.000179289			
ASCC1	1.149782888	0.000181511			
BCL7B	1.344933096	0.000182315			
NEK4	1.259339361	0.000189795			
CEP57	1.313017407	0.000193309			
LOC100996620 /// ZNF644	1.072412334	0.000198766			
LETMD1	1.96503178	0.000200299			
RPS6KB2	1.265062656	0.000200532			
JARID2	1.181518283	0.000214692			
MYO1C	1.193481198	0.000227655			
TRA2B	1.222298168	0.000230629			
HYOU1	1.07193316	0.000231236			
SUB1	1.579434529	0.000231956			
MRPL4	1.049657554	0.00023424			
FARS2	1.088848744	0.000237644			
SLC30A9	1.002253624	0.000239236			
RPS6KB2	1.099317969	0.000240895			
UBE4A	1.068052428	0.000241113			
UBAC2	1.303255772	0.00024322			
BIVM-ERCC5 /// ERCC5	1.273075079	0.000246183			
PPP6R3	1.026805441	0.000248537			
MBOAT7	1.555722127	0.000251324			
RPP14	1.012275688	0.00025457			
DAPK3 /// MIR637	1.305447714	0.000256147			
MAX	1.374107684	0.000257416			
ASF1B	1.330413897	0.000262461			
PARG	1.079873979	0.000266154			
PUM2	1.018171944	0.00026674			
SPTAN1	1.419235097	0.000266864			
LRPPRC	1.221731916	0.000267556			
LEMD3	1.074597177	0.000268419			
GPR37 /// SEL1L2	1.222041114	0.000271491			
TUBGCP3	1.074719845	0.000274403			
CPSF4	1.251540057	0.000274706			
DEDD	1.215899209	0.000278492			
TMEM30A	1.022897905	0.000280502			

Appendix

ROCK1 /// ROCK1P1	1.31266247	0.00028356			
RRBP1	1.10426965	0.000288614			
ABCE1	1.643878651	0.000290053			
UBAC2	1.171943299	0.000294249			
CDC23	1.062484845	0.000296372			
TNFRSF9	1.394523533	0.00029982			
RING1	1.191663044	0.000302868			
VPS45	1.158997755	0.000303311			
ZNHIT6	1.377510498	0.000305843			
C9orf64	1.146560271	0.000308268			
NR4A1	1.101363009	0.000310801			
PIP5K1A	1.456794572	0.0003169			
WLS	1.102198376	0.000319706			
TMEM183A /// TMEM183B	1.058970385	0.000320826			
GPAM	1.122073308	0.00032356			
MAP2K4	1.03063525	0.000325857			
PITRM1	1.062622299	0.00033032			
MPP1	1.007791127	0.000330721			
TWISTNB	1.153238189	0.000339704			
PPM1B	1.377770553	0.000343926			
EREG	1.004166335	0.000347451			
SORBS2	1.132322521	0.000351128			
MAPRE2	1.081855057	0.000352126			
POSTN	1.006805522	0.000353561			
MAGEC2	1.589153762	0.000366343			
TTC8	1.284053747	0.00036837			
GULP1	1.46827525	0.000384212			
POGLUT1	1.156211216	0.000386631			
AGPAT4	1.675953728	0.000408081			
IGF2 /// INS- IGF2	2.007860215	0.000428449			
FUBP3	1.377020373	0.000436486			
STK25	1.558004657	0.000440071			
ACVR1	1.113010955	0.000448895			
MKRN2	1.026161009	0.00046884			
VAMP3	1.141767531	0.000477739			
WDR4	1.505030124	0.000479449			
C9orf16	1.016361343	0.00048012			
ATF7IP	1.041741884	0.000485058			
NUP153	1.256934092	0.000487264			
STARD4	1.141452682	0.000490505			
RPL28	1.559726191	0.000504306			
LOC729852	1.836101861	0.000506176			
SGK494 /// SPAG5	1.302461907	0.000509243			
COQ10B	1.418346062	0.000510152			

SCML1	1.155515964	0.000517388			
SORBS2	1.03949468	0.000527819			
TRIB1	1.107468823	0.000535389			
NDUFV3	1.067014161	0.000552705			
APH1A	1.078198384	0.000576778			
ALDH2	1.038412557	0.000584336			
ACAD9	1.104840244	0.000615976			
YWHAE	1.091665881	0.000617374			
PDGFC	1.74908577	0.000634513			
PTPN20A /// PTPN20B	1.112977278	0.000655723			
DCAF6	1.064336061	0.000659155			
CARKD	1.165717115	0.000664664			
TNKS2	1.171832696	0.000667156			
STT3B	1.020339936	0.000692386			
CAPN7	1.267873863	0.000693984			
SNAP25	1.115079825	0.000699004			
PGM2	1.538660512	0.000722604			
R3HDM1	1.160780798	0.000748977			
MAP2K4	1.049594108	0.000805414			
POLR3F	1.025847732	0.000809273			
CASP7	1.325663711	0.000820056			
RALB	1.071765234	0.000849609			
RB1	1.662896464	0.000855418			
DDX3X	1.006817871	0.000898457			
DBNL	1.28056042	0.000954221			
PTGER4	1.180328083	0.000957972			
ITM2C	1.718005786	0.000960789			
ARGLU1	1.071778107	0.000969913			
NBPF1 /// NBPF10	1.135010516	0.001016256			
SUCO	1.327744353	0.001025552			
PBX1	1.120204187	0.001029552			
FAM111A	1.191828985	0.001076966			
GABPB1	1.605442373	0.001112763			
UBAP1	1.170941588	0.001151347			
KANK4	1.19503744	0.001160896			
RCAN1	1.059452256	0.001169343			
ERI3	1.023534547	0.00123175			
ARID4B	1.380639436	0.001247432			
SPTBN1	1.25086587	0.001249942			
PGS1	1.124178724	0.001346807			
HIATL1	1.573128694	0.001419868			
CASP3	1.003094187	0.001482663			
RNF219	1.128983995	0.001496175			
C2orf15 /// MRPL30	1.029961157	0.001501726			

Appendix

LOC100996481 /// PRIM2	1.106956566	0.001585608			
CRIP2	1.069781327	0.001905939			
MRE11A	1.10978349	0.002032831			
MATN3	1.240204915	0.002117886			
CPOX	1.073082531	0.002429276			
POTEG /// POTEH /// POTEM	1.062374385	0.0024937			
TOP1 /// TOP1P1	1.590445322	0.002988184			
NECAP1	1.139848144	0.003078625			
CCM2	1.016236333	0.003133187			
BBS10	1.069915723	0.003133324			
TTC3 /// TTC3P1	1.197770452	0.003502426			
PBX1	1.226992197	0.003657086			
MCCC1	1.170263829	0.003703801			
PIGT	1.185700091	0.004129011			
TGS1	1.394533651	0.004408461			
LRRC28	1.177924568	0.004843123			
SMAD7	1.000513137	0.004913436			
PBX1	1.125860779	0.005357463			
IQGAP2	1.200655112	0.005692872			
C1orf112	1.017949038	0.00586257			
EPGN	1.010950199	0.007284345			
TIA1	1.059173398	0.007937777			
RNF19A	1.003022098	0.008054076			
PRKAG1	1.216890209	0.013815632			
RNF166	1.006177922	0.031665003			

Up & Down regulated gene list for AW13516/70Gy-AW13516 (≥ 2 fold, $p \leq 0.05$)

Upregulated			Downregulated		
Gene Symbol	Log FC	p Value	Gene Symbol	Log FC	p Value
CSF2	4.723829037	4.33E-10	LCMT2	-3.880875998	7.34E-09
SAA1 /// SAA2 /// SAA2-SAA4	4.430150294	6.48E-10	DIDO1	-3.746190331	8.30E-09
TNFAIP3	4.078259035	1.26E-09	ZNRF3	-2.746440902	2.56E-08
IL1B	3.789767457	2.09E-09	SUV420H1	-2.582554159	2.56E-08
EREG	4.349200386	2.49E-09	DSCAM	-2.466622809	3.72E-08
GBP2	3.664958859	3.50E-09	NCOA5	-2.402016206	5.42E-08
AKR1C1	4.032877802	3.54E-09	PANK1	-2.334654275	7.46E-08
CXCL3	3.453949037	4.13E-09	SUV420H1	-2.956362957	1.08E-07
MMP3	3.368372243	5.38E-09	TTC30A	-2.029806434	1.17E-07
DUSP10	3.382859903	5.99E-09	OLR1	-1.986856422	1.63E-07
AKR1C1	4.099973724	6.37E-09	C14orf169	-1.965212549	1.65E-07
SAA1	3.367715663	7.01E-09	ZN557	-1.919090828	1.73E-07
FBXO32	3.296772177	8.16E-09	PRMT6	-2.009340036	1.93E-07
CCL20	3.504462418	9.06E-09	DOLK	-1.906223947	2.18E-07
NFKBIZ	3.387319452	9.16E-09	ANO4	-1.919591156	2.43E-07
SAA1 /// SAA2 /// SAA2-SAA4	3.541063138	9.93E-09	CPSF6	-1.78941879	2.89E-07
DUSP10	3.187856267	1.09E-08	GDA	-2.50119156	3.01E-07
EDIL3	2.985350665	1.12E-08	CPSF6	-1.839696291	3.23E-07
LOC101060503 /// TXNIP	2.911708524	1.17E-08	ZN480	-2.101290775	3.26E-07
DDIT3	3.02549108	1.19E-08	POGLUT1	-1.76170187	3.37E-07
LOC101060503 /// TXNIP	2.95266519	1.25E-08	PHF23	-1.738096014	3.41E-07
TNFAIP3	3.123332244	1.39E-08	GABPB1	-1.746693117	3.52E-07
FOS	3.362351358	1.42E-08	BTBD7	-2.093916916	3.77E-07
DDIT3	3.083001136	1.47E-08	MOCS3	-1.961893352	3.92E-07
FOS	3.226388626	1.49E-08	LPAR1	-1.826313568	4.19E-07
C8orf4	2.784404038	1.53E-08	CREBBP	-1.955369568	4.23E-07
C15orf48	3.870598229	1.79E-08	SRSF1	-1.724800373	4.29E-07
IRF1	2.822748118	1.81E-08	DDX28	-1.891625518	4.38E-07
ZFP36	3.017025683	2.01E-08	SRSF1	-1.672304291	4.40E-07
HBE1	3.234298533	2.16E-08	ZC3H4	-2.018816942	4.64E-07
DUSP1	2.67129529	2.43E-08	TET2	-1.655277334	4.67E-07
BLZF1	3.219883826	2.60E-08	NANOS1	-1.673544217	4.71E-07
CXCL2	2.895477632	2.68E-08	CCL2	-1.663189354	5.03E-07
SAT1	2.56953348	2.69E-08	ZN879	-1.696525058	5.06E-07
IGF2 /// INS- IGF2	2.628441867	3.06E-08	SETMAR	-1.857815042	5.42E-07
KLRC1 /// KLRC2	2.597327498	3.08E-08	UMPS	-1.648739711	5.42E-07
RPL28	2.529639638	3.08E-08	LOC100996496 /// SFPO	-1.641582189	5.52E-07
IGF2 /// INS- IGF2	2.5711772	3.20E-08	LCMT2	-1.674604422	5.62E-07
ATF3	2.980779658	3.38E-08	CENPBD1	-1.61503387	5.70E-07
PTPRJ	2.64186228	3.41E-08	SRSF8	-1.641122378	5.73E-07

SEC24A	2.590532234	3.48E-08	GDA	-1.640755569	5.75E-07
SYTL2	2.498960791	3.65E-08	MKL2	-1.705117076	5.83E-07
ARRDC3	3.09604456	3.68E-08	BRI3BP	-1.8874604	5.86E-07
ANGPTL4	3.566148156	3.71E-08	CPSF6	-1.719370405	6.06E-07
LOC101060503 /// TXNIP	3.420453667	3.83E-08	NETO2	-1.649791535	6.11E-07
HIST2H2AA3 /// HIST2H2AA4	3.462437521	3.86E-08	AQP11	-1.608227802	6.13E-07
BCL2A1	3.743865183	3.98E-08	LOC100996496 /// SFPO	-1.619800634	6.24E-07
KLHL24	2.654895355	4.16E-08	BPTF	-1.6104782	6.55E-07
KLF3	2.787542846	4.20E-08	GIT2	-1.58982506	6.83E-07
CXCL1	2.726890833	4.31E-08	ZNF200	-1.991781993	7.10E-07
TSC22D3	2.413767204	4.31E-08	EIF5	-1.944100135	7.47E-07
CXCL3	3.887016506	4.35E-08	ERCC4	-2.057086368	7.71E-07
PIM1	2.525482796	4.39E-08	PIGM	-1.544807875	7.71E-07
HSD11B1	2.823784695	4.86E-08	POLR3B	-1.564235641	7.89E-07
FOS	2.786100885	4.91E-08	HDAC4	-2.159533029	8.10E-07
TNF	2.649272912	5.09E-08	POLE2	-1.643039117	8.14E-07
KLF10	2.288508837	5.31E-08	TTC30A	-1.517009233	8.30E-07
SULT1C2	2.31675635	5.35E-08	PAFAH1B1	-1.570615054	8.37E-07
CCRN4L	2.383903548	5.46E-08	PHF15	-1.654237549	8.87E-07
KYNU	2.532189991	5.51E-08	DACH1	-1.791910603	8.93E-07
KYNU	2.654516964	5.60E-08	AJAP1	-1.666360773	9.68E-07
GDF15	2.305165244	5.62E-08	CCNF	-1.533430012	9.91E-07
IL24	2.572930762	5.95E-08	ZAK	-1.76831792	1.02E-06
SFT2D3 /// WDR33	2.690066468	6.02E-08	PKD2	-1.836180779	1.04E-06
IRF1	2.31414875	6.14E-08	SRSF1	-1.598854729	1.07E-06
RPS18	2.302156546	6.19E-08	MESDC2	-1.448604409	1.13E-06
RND1	2.518086697	6.21E-08	CST7	-1.443280752	1.17E-06
CA12	2.582906262	6.38E-08	TET3	-1.764438098	1.20E-06
IL6	2.604643335	6.54E-08	ARMC8	-2.143349158	1.21E-06
ZC3HAV1	2.313659402	6.54E-08	SOGA2	-1.618660175	1.22E-06
C3	2.91356927	6.55E-08	SPRED2	-1.507846495	1.22E-06
DUSP1	2.878314889	6.86E-08	CPSF6	-1.76243014	1.23E-06
LOC100129518 /// SOD2	3.076161027	6.90E-08	SLC1A4	-1.587153827	1.24E-06
ICAM1	2.207918233	7.14E-08	STXBP5	-1.642553629	1.25E-06
HIST2H2AA3 /// HIST2H2AA4	3.564366914	7.21E-08	TUBGCP3	-1.73624082	1.26E-06
GBP1	2.255404767	7.24E-08	EXO5	-1.803320336	1.31E-06
DUSP5	2.540239844	7.25E-08	GATAD2A	-1.45063262	1.33E-06
HLA-B	2.21627986	7.28E-08	ALPK2	-1.41939331	1.35E-06
AKR1C1 /// AKR1C2 /// LOC101060798	3.842000973	7.45E-08	FDXACB1	-1.500579601	1.36E-06

CXCL1	2.430946828	7.51E-08	STARD7	-1.448448162	1.37E-06
CA12	2.577936969	7.60E-08	PRMT6	-1.699188142	1.38E-06
PDCD6	2.163105753	7.71E-08	PHLDB2	-1.443528825	1.39E-06
NDRG1	2.754023545	7.72E-08	BRCC3	-1.418072767	1.42E-06
PLAU	2.161566596	7.77E-08	EID2	-1.396334248	1.42E-06
RGS3	2.445673005	7.78E-08	POGLUT1	-1.568624517	1.45E-06
SRGN	3.210246595	7.88E-08	EIF5	-1.604674689	1.46E-06
FKBP1A- SDCBP2 /// SDCBP2	2.203832354	7.88E-08	AJUBA	-1.798587844	1.49E-06
TNFSF9	2.354292799	7.92E-08	BMPR2	-1.480869338	1.52E-06
PDE4DIP	2.303547674	8.08E-08	BPTF	-1.810629208	1.54E-06
GADD45A	2.3929669	8.18E-08	BRCC3	-1.436797018	1.54E-06
IRAK2	2.206611353	8.31E-08	EIF5	-1.433658107	1.54E-06
CXorf57	2.133818258	8.45E-08	HYLS1	-1.639821515	1.61E-06
FBN2	2.174530703	8.52E-08	MPHOSPH8	-1.53205543	1.65E-06
AKR1C3	2.194102251	8.89E-08	PHTF2	-1.385132559	1.73E-06
ICAM1	2.197776835	8.96E-08	KMT2A	-1.46903161	1.74E-06
SERPINE1	2.194733754	9.08E-08	EIF5	-1.379472081	1.76E-06
TBC1D8B	2.350770528	9.46E-08	GID8	-1.532999686	1.78E-06
MET	2.326197893	9.53E-08	MPHOSPH8	-1.519341454	1.79E-06
EGR2	2.253338292	9.61E-08	HNRNPM	-1.389923836	1.80E-06
PLA2G4A	2.279223123	9.67E-08	ZNF180	-1.97961595	1.81E-06
TTC39A	2.871058436	9.70E-08	ZAK	-1.940306144	1.81E-06
CDCP1	2.506724166	9.72E-08	EIF5	-1.826936597	1.81E-06
IFI27	2.18626984	9.73E-08	LOC101060460 /// POLR3C	-1.373259037	1.89E-06
GBP1	2.538699376	9.75E-08	ITPRIPL2	-1.502056851	1.91E-06
SIK1	2.252807403	9.83E-08	BRCC3	-1.434250337	1.91E-06
PIM1	2.51001658	9.84E-08	FAM178A	-1.355679373	1.91E-06
PIM1	2.068346549	1.03E-07	GIT2	-1.780162701	1.93E-06
SEMA7A	2.070001953	1.06E-07	ZNF544	-1.585209735	1.95E-06
LOC101060503 /// TXNIP	3.644191342	1.07E-07	GIT2	-1.706323736	1.99E-06
KLF10	2.191251934	1.07E-07	SUV420H1	-1.63474725	2.02E-06
CREB3L2	2.594422973	1.08E-07	PCF11	-1.71543162	2.03E-06
IRF1	2.266082238	1.10E-07	MALT1	-1.315121568	2.03E-06
ADRB2	2.201024157	1.12E-07	DHRS13	-1.735723503	2.04E-06
PER1	2.672688267	1.13E-07	REP15	-1.584203116	2.04E-06
LOC101060503 /// TXNIP	3.644652297	1.20E-07	PGBD2	-1.380373641	2.04E-06
GJA1	2.576854303	1.20E-07	JAGN1	-1.347316701	2.04E-06
IL23A	2.610430861	1.26E-07	KCTD15	-1.766658416	2.05E-06
LAMB3	2.252417338	1.26E-07	EIF5	-1.972574056	2.07E-06
FOSL2	2.228920471	1.26E-07	MAPK1IP1L	-1.438486478	2.08E-06
PDCD6	2.217353208	1.26E-07	LOC100507472 /// PCSK6	-1.519706716	2.15E-06
PTPRR	2.893208208	1.38E-07	CCDC71	-2.164901306	2.23E-06

BIRC3	2.522544188	1.38E-07	ZBTB1	-1.780425229	2.23E-06
UBE2L6	1.99771165	1.41E-07	TMEM185B	-1.40169298	2.24E-06
C10orf10	2.544253595	1.47E-07	SRSF3	-1.375076425	2.26E-06
LOC100129518 /// SOD2	1.963288473	1.47E-07	TUBGCP3	-1.587670138	2.28E-06
TSC22D3	2.341085838	1.49E-07	FADD	-1.315473506	2.35E-06
CXCL1 /// CXCL2	2.649271824	1.59E-07	CDK13	-1.586374969	2.40E-06
CNST	2.187219459	1.59E-07	SIPA1L2	-2.053974872	2.41E-06
MXD1	2.312159918	1.60E-07	LOC101060460 /// POLR3C	-1.366873416	2.41E-06
RGS3	2.254980191	1.60E-07	SOGA1	-1.347415109	2.41E-06
ZFC3H1	2.001195362	1.62E-07	TFDP1	-1.395162977	2.46E-06
C1orf63	2.654703529	1.63E-07	NEXN	-1.31137829	2.48E-06
SQSTM1	1.960228333	1.64E-07	PHF15	-1.568460561	2.51E-06
PDE4DIP	1.99253029	1.66E-07	FAM135A	-1.385815391	2.56E-06
DST	1.987082112	1.66E-07	STARD7	-1.383882454	2.62E-06
C1orf63	1.984900725	1.67E-07	PFAS	-1.27317076	2.65E-06
MET	2.073555362	1.70E-07	MIR1292 /// NOP56 /// SNORD110 /// SNORD57 /// SNORD86	-1.261326221	2.72E-06
C1orf63	2.015811082	1.70E-07	GDA	-1.49176924	2.74E-06
LAMC2	1.92228843	1.81E-07	MIR1292 /// NOP56 /// SNORD110 /// SNORD57 /// SNORD86	-1.261326221	2.74E-06
GBP2	2.746451416	1.83E-07	UMPS	-1.464965286	2.76E-06
PCP4	2.013336604	1.83E-07	ANKRD12	-1.645487447	2.81E-06
BEX5	1.987468068	1.83E-07	NDNF	-1.481020375	2.84E-06
STC1	2.046827815	1.84E-07	FOXRED2	-1.408506341	2.85E-06
SERAC1	1.92957117	1.84E-07	FAM208A	-1.281809921	2.87E-06
EGR1	1.969508376	1.86E-07	FADD	-1.471743146	2.90E-06
LOC100506403 /// RUNX1	2.709769306	1.88E-07	PGBD2	-1.292430404	2.93E-06
TSLP	3.020883449	1.91E-07	SCLY /// UBE2F- SCLY	-1.291093739	2.93E-06
NAV2	2.300537058	1.92E-07	SCD	-1.335718322	2.99E-06
SMEK2	2.580926953	1.93E-07	TRMT1L	-1.45994161	3.02E-06
VWA5A	3.058641794	1.95E-07	ALG10 /// ALG10B	-1.308978219	3.04E-06
EGR1	1.987015065	1.96E-07	KCNMA1	-1.347966776	3.05E-06
RND3	3.124117102	2.02E-07	HPS6	-1.806346976	3.06E-06
LTF	1.900707376	2.04E-07	IGFBP1	-1.241472408	3.12E-06
SMIM14	2.111611145	2.07E-07	FAIM	-1.873461353	3.17E-06
PTGS2	2.325708389	2.11E-07	FAIM	-1.873461353	3.17E-06
KRT12	2.151301442	2.11E-07	PHTF2	-1.351586082	3.20E-06
ICAM1	1.982625568	2.12E-07	BPTF	-1.935822579	3.21E-06

BCL6	2.162371767	2.16E-07	C7orf25 /// PSMA2	-1.570623669	3.33E-06
ZKSCAN1	2.028434714	2.22E-07	MMACHC	-1.248720386	3.33E-06
HIST1H2AB /// HIST1H2AE	2.120962585	2.23E-07	DENND5B	-1.609125675	3.34E-06
SMIM14	1.927857402	2.27E-07	---	-1.287934838	3.34E-06
JUN	1.842925105	2.27E-07	TRAK2	-1.530876215	3.36E-06
RGS2	3.092893854	2.28E-07	ANGEL2	-1.246941997	3.37E-06
CLEC2B	3.154773507	2.29E-07	MPHOSPH8	-1.336505766	3.41E-06
HDAC9	2.498604781	2.29E-07	AIMP2	-1.301885383	3.41E-06
HERPUD1	1.91528363	2.29E-07	LCMT2	-1.925248206	3.43E-06
VEPH1	2.766020254	2.30E-07	KLHL42	-1.240938863	3.43E-06
PLK3	2.013002493	2.31E-07	SLC35G1	-1.292421686	3.44E-06
RND3	2.508399668	2.35E-07	TOE1	-1.217142322	3.44E-06
MAP3K7CL	2.282362676	2.41E-07	RRP15	-1.335317173	3.46E-06
DEDD2	2.035453919	2.46E-07	SLC30A6	-1.436891568	3.51E-06
STK17B	1.827562081	2.49E-07	CREBBP	-1.386855086	3.52E-06
KLF9	1.965691617	2.50E-07	SCD	-1.336639588	3.52E-06
CREB3L2	2.517117763	2.51E-07	PPL	-1.965452889	3.53E-06
TMEM159	1.848874052	2.52E-07	BCDIN3D	-1.293256699	3.58E-06
CLK1	1.913768919	2.53E-07	COG2	-1.237091239	3.61E-06
STON1	1.806327117	2.59E-07	SIK2	-1.380009863	3.71E-06
NF1	2.164713889	2.67E-07	ADCY9	-1.232008504	3.73E-06
F11R	1.800424986	2.67E-07	ALG10 /// ALG10B	-1.336777376	3.78E-06
BCL6	2.141186722	2.68E-07	MIR1292 /// NOP56 /// SNORD110 /// SNORD57 /// SNORD86	-1.234812394	3.78E-06
CXCL2	3.056705225	2.74E-07	TOE1	-1.211126954	3.78E-06
KLRC3	1.840374456	2.74E-07	COG8 /// PDF	-1.284616279	3.82E-06
TMEM255A	1.781999844	2.75E-07	PHF17	-1.207906692	3.88E-06
HERPUD1	2.009691601	2.77E-07	PHF23	-1.289913016	3.91E-06
SLC25A37	1.924601675	2.80E-07	ARHGEF28	-1.211705816	3.92E-06
EYA3	1.884827324	2.80E-07	EXO5	-1.751919111	3.93E-06
MPZL2	1.859646641	2.89E-07	ZNF232	-1.338169273	3.93E-06
TFPI	1.972286782	2.91E-07	PHACTR2	-1.261214936	3.97E-06
FAM46C	2.151649471	2.93E-07	AIMP2	-1.207211709	3.99E-06
GBP1	1.805068385	2.93E-07	RHNO1	-1.316899009	4.04E-06
JUN	1.896043311	2.94E-07	TRERF1	-1.25283589	4.08E-06
HNRNPA1	1.820396341	2.95E-07	IKBIP	-1.307169334	4.09E-06
HERPUD1	2.051676622	3.09E-07	MIR1292 /// NOP56 /// SNORD110 /// SNORD57 /// SNORD86	-1.397979373	4.11E-06
ERMP1	2.180464106	3.10E-07	FAM217B	-2.183691119	4.14E-06
CFB	2.032298755	3.11E-07	B3GALT6	-1.59330917	4.16E-06

TGFA	4.279026068	3.18E-07	ADRA2C	-1.33642327	4.16E-06
DIS3L2	1.800660105	3.18E-07	ANP32A	-1.299856528	4.19E-06
DNAJB1	2.162353127	3.26E-07	METAP2	-1.34711872	4.26E-06
PKIB	2.421873699	3.33E-07	FAM111B	-1.620997195	4.29E-06
ABCC3	2.019206159	3.36E-07	FAM101B	-1.287577025	4.29E-06
GEM	3.081116344	3.38E-07	MFAP3	-1.245514564	4.31E-06
HBP1	1.794554562	3.38E-07	KCTD15	-1.416638588	4.32E-06
STC1	2.336481466	3.44E-07	AP1M2	-1.299541169	4.36E-06
ARRDC3	1.894379629	3.46E-07	SCD	-1.20748803	4.43E-06
MAFF	2.202484598	3.51E-07	C1orf131	-1.313823313	4.46E-06
PKIB	1.845559656	3.59E-07	HNRNPM	-1.243128002	4.47E-06
PIM1	1.819348836	3.60E-07	BMPR2	-1.283774924	4.55E-06
SERPINI1	2.06233237	3.69E-07	ZNF544	-1.653272428	4.57E-06
PKIB	2.051162326	3.70E-07	ST7L	-1.172507532	4.59E-06
LEMD1	1.982109365	3.78E-07	ZNF181 /// ZNF302 /// ZNF807	-1.20805269	4.64E-06
EGR1	1.95587564	3.78E-07	BEND3	-1.649298044	4.65E-06
CCNA1	2.378083356	3.82E-07	GABPB1	-1.29474469	4.66E-06
CREBRF	1.822212003	3.82E-07	RGMA	-1.184184086	4.69E-06
BEX2	1.848702883	3.96E-07	SRSF1	-1.548311308	4.70E-06
INHBA	1.886684764	4.08E-07	PHF17	-1.458828162	4.71E-06
TRIB1	1.676405489	4.21E-07	CCDC96	-1.350143722	4.74E-06
GPR98	2.141332316	4.39E-07	TTPAL	-1.16637482	4.84E-06
HSPA5	1.913917165	4.40E-07	FRY	-1.211289763	4.85E-06
RAB38	1.715267756	4.40E-07	KIAA0825	-1.164224713	4.87E-06
IFI44	1.688208812	4.40E-07	GLI2	-1.73237916	4.88E-06
BBC3 /// MIR3190 /// MIR3191	1.733254974	4.44E-07	ACADSB	-1.242410163	4.92E-06
GPR68	1.805555237	4.49E-07	RBBP6	-1.371685231	4.96E-06
CADPS2	1.674823689	4.52E-07	KLHL42	-1.310450743	4.96E-06
BIRC3	2.720599063	4.59E-07	IREB2	-1.183474264	4.97E-06
KLF7	2.383683398	4.64E-07	TMEM87A	-1.182488083	5.04E-06
PKIB	1.934395994	4.70E-07	PPP1R3D	-1.814934405	5.07E-06
LINC00839	1.872074022	4.76E-07	AMMECR1	-1.253102406	5.12E-06
C1orf213	1.866229429	4.80E-07	TM2D2	-1.228184928	5.18E-06
ZKSCAN1	1.962615077	4.84E-07	SOX18	-1.503683531	5.23E-06
PLAU	1.80671572	4.90E-07	DCAF6	-1.143418581	5.24E-06
ADM	1.704990179	4.91E-07	LARP4	-1.49301548	5.25E-06
C1R	1.656413555	4.94E-07	LOC100506403 /// RUNX1	-1.320000384	5.27E-06
BCHE	2.046651503	4.97E-07	ST6GALNAC5	-1.536135185	5.48E-06
CCNG2	1.654635244	5.05E-07	SRSF3	-1.166539726	5.53E-06
GNPMB	1.873535704	5.16E-07	C7orf25 /// PSMA2	-1.741271752	5.59E-06
EYA3	1.809029937	5.17E-07	LRR1	-1.15139927	5.62E-06
HES1	1.777010291	5.17E-07	TADA2B	-1.149897425	5.63E-06

GADD45B	2.096533303	5.22E-07	C12orf4	-1.41158649	5.71E-06
KLF6	1.621633266	5.25E-07	BCLAF1	-1.454102987	5.80E-06
MCTP1	1.761935268	5.28E-07	ZNF594	-1.512692254	5.87E-06
CLK4	1.633698571	5.29E-07	ZNF232	-1.216915994	5.88E-06
CKAP2	1.818090393	5.46E-07	CENPN	-1.280402449	6.03E-06
EYA3	1.750457302	5.51E-07	ZNF362	-1.313320137	6.08E-06
CREB3L2	1.697439558	5.61E-07	ZNF232	-1.589904026	6.12E-06
KLHL24	1.771695294	5.74E-07	UTP20	-1.11814126	6.16E-06
CFI	1.879988894	5.75E-07	FAM111B	-1.65538261	6.22E-06
DUSP6	1.690111536	5.81E-07	ACAT2	-1.159389924	6.26E-06
NELL2	2.649911517	5.86E-07	TTPAL	-1.1532528	6.29E-06
CPT1A	1.669298513	5.88E-07	FOXRED2	-1.717861001	6.30E-06
STC1	2.127333864	5.89E-07	ZNF490	-1.206483801	6.41E-06
LCP1	3.427124523	5.90E-07	C12orf43	-1.186860369	6.49E-06
NFIL3	1.710860887	5.93E-07	ELAC1	-1.266824831	6.55E-06
STC1	2.325407139	5.98E-07	TRAPPC12	-1.108065649	6.56E-06
CREBRF	1.712001516	5.99E-07	DDX17	-1.112105828	6.66E-06
DNAJB1	2.000802024	6.20E-07	ANO1	-1.13688173	6.67E-06
KMT2E	2.029636552	6.27E-07	TAF5L	-1.187192099	6.69E-06
AKIP1 /// NUAK2	1.869104122	6.30E-07	IREB2	-1.16379721	6.69E-06
ADM	1.684703981	6.41E-07	DDX39A	-1.15455247	6.69E-06
STEAP1	2.409221117	6.43E-07	NSL1	-1.181092334	6.70E-06
PLSCR1	1.679166246	6.47E-07	CAP2	-1.722857929	6.95E-06
KMT2E	2.021470092	6.49E-07	CNPY2	-1.10843574	6.96E-06
HSPA6	3.021775269	6.71E-07	RHOU	-1.219829123	6.97E-06
CLK4	1.934696307	6.90E-07	MTDH	-1.251784588	6.98E-06
TBX3	1.611281004	6.92E-07	ZNF302	-1.243305488	6.98E-06
HIST2H2BE	3.412140845	6.98E-07	MANSC1	-1.098051843	7.13E-06
TBC1D10A	1.723413554	7.04E-07	CTBP1-AS2	-1.088235927	7.13E-06
YPEL2	2.06351813	7.15E-07	MIR1257 /// TAF4	-1.087777891	7.37E-06
ARMCX3	1.711735164	7.23E-07	ZSCAN5A	-1.412783166	7.56E-06
PPM1K	1.964394779	7.41E-07	MANSC4	-1.246446252	7.60E-06
CD82	1.716841317	7.61E-07	DCAF6	-1.139211464	7.71E-06
CD82	1.716841317	7.61E-07	BIVM	-1.212223592	7.72E-06
ADAMTS16	1.636557246	7.79E-07	SIN3A	-1.129645634	7.74E-06
OGDH	1.792266236	7.90E-07	DIEXF	-1.093012679	7.77E-06
HSPA5	1.78740018	7.92E-07	SPDL1	-1.148014833	7.78E-06
DNAJB9	1.758228438	8.08E-07	ANKRD26	-1.23010033	7.79E-06
CDKN1A	1.586851784	8.16E-07	PBRM1	-1.068259435	7.83E-06
HSPA6 /// HSPA7	4.034251155	8.22E-07	GK5	-1.11022592	7.92E-06
CLK1	1.764332125	8.26E-07	PPP2R1B	-1.115209558	7.99E-06
GPC2	1.53090498	8.37E-07	NUP50	-1.066842088	8.01E-06
JUNB	1.506975598	8.52E-07	BRCC3	-1.487398712	8.04E-06
DDIT4	2.376675744	8.54E-07	TCAIM	-1.082229035	8.12E-06

HIST1H1C	1.781000732	8.55E-07	ATP13A5 /// C10orf54 /// HARS	-1.518046534	8.16E-06
ERP44	1.531620156	8.68E-07	ZMPSTE24	-1.118478862	8.17E-06
CEBPD	1.747027569	8.72E-07	RIPK1	-1.083202541	8.25E-06
TPM1	1.516742405	8.75E-07	ST6GALNAC5	-1.552187633	8.34E-06
ZFP36L1	1.540824164	8.79E-07	ANKRD12	-1.683911149	8.38E-06
C10orf10	1.754875702	8.80E-07	CENPN	-1.119757798	8.38E-06
ALOX5AP	1.692047854	8.88E-07	CSTF3	-1.459478471	8.41E-06
KRT15	1.879749386	8.94E-07	ST6GALNAC5	-1.672641988	8.43E-06
IL24	2.624797516	8.96E-07	RIMKLB	-1.40458958	8.43E-06
PPIF	1.502355699	9.00E-07	KLHL42	-1.302348194	8.52E-06
ADM	1.620387092	9.07E-07	ANKLE2	-1.097264339	8.52E-06
ARHGEF12	1.635251907	9.08E-07	DHCR24	-1.179229431	8.67E-06
DUSP6	1.79623016	9.14E-07	SRSF3	-1.233050259	8.69E-06
PTGS2	1.778523322	9.17E-07	YAE1D1	-1.249178417	8.72E-06
EFNA1	1.511198037	9.20E-07	BPTF	-1.86435628	8.73E-06
RDM1	1.659203373	9.21E-07	DCAF6	-1.238956889	8.73E-06
MKRN1	1.704806941	9.25E-07	KDSR	-1.077375844	8.73E-06
EPAS1	2.084266123	9.32E-07	GIN52	-1.052018393	8.73E-06
BIRC3	2.820626736	9.39E-07	GLI2	-1.547602343	8.74E-06
ADIRF	1.530255185	9.43E-07	SLC43A3	-1.072480119	8.76E-06
HSPA5	1.68469889	9.45E-07	ACAT2	-1.076622659	8.77E-06
LPXN	1.949512486	9.51E-07	COG8 /// PDF	-1.050278097	8.90E-06
IFI44	1.711487209	9.60E-07	B3GALT	-1.126153097	8.94E-06
PHF12	1.841150073	9.62E-07	FAM171A1	-1.072352143	9.01E-06
WHSC1	1.723202423	9.67E-07	CHAMP1	-1.200941011	9.07E-06
MYCT1	1.492243874	9.79E-07	LOC100128551 /// ZDHHC14	-1.092259469	9.11E-06
FA2H	2.083513315	9.83E-07	CALM1 /// CALM2 /// CALM3	-1.145122337	9.14E-06
LAMC2	1.573445006	9.91E-07	CREBBP	-1.534572481	9.18E-06
CEBPD	1.596161886	9.96E-07	METTL18	-1.352244902	9.18E-06
SERPINA1	2.078849655	1.00E-06	CUL4A	-1.075346253	9.24E-06
MYO6	1.504041757	1.01E-06	TNRC6C	-1.091780756	9.34E-06
PTN	1.568081381	1.02E-06	MSRB3	-1.26606963	9.47E-06
CA2	2.621365466	1.04E-06	SIK3	-1.052838983	9.53E-06
ZNF165	2.359998924	1.04E-06	ZNF789	-1.463916128	9.59E-06
HIST1H2BJ	1.724105248	1.05E-06	AP5M1	-1.167521827	9.66E-06
ATF7IP	2.446103819	1.07E-06	UBE2Q1	-1.164011731	9.90E-06
VNN1	1.766992403	1.07E-06	SFT2D3 /// WDR33	-1.10485099	9.90E-06
PARD6B	2.257529141	1.11E-06	ERCC6-PGBD3 /// PGBD3	-1.052468532	9.98E-06
BHLHE40	1.883229765	1.13E-06	ZNF518B	-1.276413274	1.00E-05
SQRDL	1.776339104	1.14E-06	ZSCAN31	-1.138337751	1.01E-05
NF1	1.823350634	1.15E-06	TRIM27	-1.096611015	1.01E-05

TBC1D10A	1.668594186	1.15E-06	TPM1	-1.068109416	1.01E-05
CDH11	1.649058881	1.15E-06	TOE1	-1.043812344	1.01E-05
KLF6	1.444430921	1.15E-06	C1orf131	-1.29724411	1.02E-05
GADD45B	1.586574292	1.17E-06	AJAP1	-1.344278984	1.03E-05
SMOX	1.486106311	1.18E-06	TPM1	-1.032423842	1.03E-05
GBP1	3.11458657	1.19E-06	REPS1	-1.17466079	1.05E-05
GOLGA7B	1.522810658	1.20E-06	CAP2	-1.165798468	1.05E-05
DDX60	1.773699454	1.21E-06	SPARC	-1.082452527	1.05E-05
DNAJB1	1.735933098	1.22E-06	SRGAP2 /// SRGAP2D	-1.055280221	1.05E-05
CREBRF	1.68224462	1.22E-06	C15orf37	-1.464916322	1.06E-05
PPIG	1.532618457	1.22E-06	CBX2	-1.289696035	1.06E-05
EPB41L4A-AS1	1.435246625	1.23E-06	EPHX4	-1.263040813	1.07E-05
CDKN2AIPNL	2.139277723	1.24E-06	ANKFY1	-1.25810136	1.07E-05
ZCCHC6	2.034526148	1.24E-06	PTPN21	-1.503846988	1.08E-05
SLC25A20	1.459211373	1.24E-06	CCNJL	-1.109609923	1.08E-05
BCL3	1.434443783	1.25E-06	SEPHS2	-1.226067294	1.09E-05
EHF	2.19148181	1.26E-06	TDG	-1.114189396	1.10E-05
CDKL3	1.505289922	1.27E-06	STXBP5	-1.617731016	1.11E-05
GKAP1	1.692289235	1.28E-06	MIR636 /// SRSF2	-1.013634377	1.11E-05
ZFAND5	1.680056672	1.29E-06	LOC100996657 /// SRSF10	-1.043090471	1.12E-05
FOS	2.442245594	1.30E-06	ANKRD13C	-1.163440557	1.14E-05
KLF6	1.473632917	1.31E-06	PRKCQ	-1.117351261	1.14E-05
DUSP6	1.745496332	1.32E-06	C8orf58	-1.046121347	1.14E-05
HMOX1	1.492224847	1.32E-06	TPM1	-1.028806862	1.14E-05
HES1	1.576666039	1.34E-06	ST7 /// ST7-OT3	-1.00798244	1.14E-05
ZNF836	1.427942012	1.34E-06	DARS2	-1.098500609	1.15E-05
IL8	2.344965564	1.35E-06	VANGL1	-1.235811206	1.16E-05
PTPRR	2.716894838	1.36E-06	FGFR1OP2	-1.190172685	1.16E-05
MAP3K7CL	2.516080336	1.36E-06	ANO1	-1.09544443	1.16E-05
NAV2	1.807717735	1.36E-06	ZNF780A	-1.016275477	1.16E-05
STX11	1.442294055	1.36E-06	MAT2A	-1.028224591	1.17E-05
MYLK	1.611348254	1.37E-06	SIPA1L2	-1.725797558	1.18E-05
ZNF697	1.511331392	1.38E-06	RBBP6	-1.231368906	1.18E-05
KLF4	1.396964589	1.38E-06	SOBP	-1.101105978	1.18E-05
FAM46A	1.462553563	1.45E-06	BCLAF1	-1.256595267	1.19E-05
TTC39B	1.450528245	1.47E-06	CHSY3	-1.181759585	1.19E-05
HLA-B	1.605593861	1.48E-06	NCAPG	-1.175106243	1.19E-05
HSD11B1	1.846474908	1.49E-06	CENPBD1	-1.395115698	1.20E-05
ARRDC4	1.645178459	1.49E-06	ZBTB1	-1.260884503	1.21E-05
IFI44	1.547865574	1.49E-06	PDSS1	-1.068123776	1.22E-05
HSPA5	2.041868658	1.50E-06	ARMC8	-1.529380702	1.23E-05
ELF3	2.735130689	1.54E-06	SOAT1	-1.184051201	1.23E-05
ABTB2	1.428895072	1.54E-06	CREB1	-1.204638318	1.25E-05
LOX	1.49173112	1.55E-06	PGBD1	-1.045405095	1.25E-05

NFYA	1.386182412	1.56E-06	ZFHX4	-1.083938162	1.27E-05
SYTL3	1.392842123	1.57E-06	MTMR12	-1.060464457	1.27E-05
CSTA	1.662413881	1.58E-06	TFDP1	-1.045962258	1.27E-05
LCN2	2.079815103	1.59E-06	DCAF6	-1.159979476	1.29E-05
NEDD4L	1.546496641	1.60E-06	SMIM12	-1.157156593	1.29E-05
CDKN1C	1.532441533	1.62E-06	SEPHS1	-1.00142061	1.29E-05
IFIH1	1.700201181	1.63E-06	ZNF287	-1.185292622	1.30E-05
MSMO1	2.18624772	1.64E-06	ZNF549	-1.410624854	1.31E-05
RPL31	1.766150226	1.65E-06	LDLRAD4	-1.405842344	1.31E-05
ADSSL1	1.512701287	1.66E-06	RAB23	-1.042410835	1.31E-05
GIMAP2	1.436509448	1.67E-06	C6orf120	-1.035974704	1.31E-05
TBX3	1.558595197	1.69E-06	GEMIN4	-1.109713846	1.32E-05
---	2.079272892	1.71E-06	RPRD2	-1.319873756	1.33E-05
HIST1H2BD	1.754765046	1.71E-06	SLC25A13	-1.094790404	1.33E-05
MPZL2	2.547291824	1.72E-06	PHLPP2	-1.092949636	1.33E-05
PHTF2	1.806142208	1.72E-06	STK38	-1.025159599	1.33E-05
PPP1R15B	1.559390003	1.74E-06	TENM2	-1.023503384	1.33E-05
LOX	1.488964388	1.76E-06	ESCO2	-1.281274088	1.34E-05
ATM	2.102542144	1.78E-06	CERK	-1.057586761	1.34E-05
PTN	1.499205882	1.78E-06	FEN1	-1.032392654	1.35E-05
UGGT2	1.48881154	1.78E-06	ZNF764	-1.235646488	1.36E-05
ADIRF	1.395689406	1.79E-06	PRKX	-1.013479198	1.36E-05
HLA-E	1.363419045	1.81E-06	SPATS2L	-1.191502353	1.37E-05
RGMB	1.411683174	1.84E-06	DICER1	-1.038623277	1.37E-05
AREG /// AREGB	1.531357406	1.85E-06	RBBP6	-1.260638691	1.38E-05
PTGES	1.414415963	1.85E-06	NEXN	-1.217570784	1.38E-05
NEDD4L	1.39789595	1.86E-06	SLC38A6	-1.158102919	1.39E-05
ATF3	1.514572604	1.88E-06	HNRNPA0	-1.029182495	1.39E-05
CLK4	1.94781948	1.89E-06	C1orf56	-1.016862053	1.40E-05
ZFAND2A	1.604981207	1.89E-06	SLC35F3	-1.009306856	1.40E-05
MALAT1	1.46241488	1.91E-06	DAPK1	-1.299842877	1.41E-05
SMAD3	1.375707979	1.91E-06	ADI1	-1.164661867	1.41E-05
VEGFA	2.18899089	1.93E-06	ZNF37A	-1.156968953	1.41E-05
CPD	1.329130533	1.93E-06	CUL4A	-1.116221598	1.41E-05
SERPINB2	2.618389241	1.94E-06	HELO	-1.034676152	1.42E-05
SEC31A	1.553851033	1.95E-06	KIAA0586	-1.018471251	1.42E-05
NTNG1	1.972306038	1.96E-06	SNX21	-1.185244788	1.43E-05
TCP11L2	1.431613917	1.96E-06	AP5M1	-1.37348794	1.44E-05
TOX2	1.340856969	1.96E-06	NANOS1	-1.021345786	1.44E-05
DUSP10	2.085872565	1.98E-06	PHF20L1	-1.124974398	1.45E-05
C11orf96	2.021999026	2.00E-06	SNRNP35	-1.124890268	1.45E-05
---	3.865748927	2.02E-06	LYRM7	-1.036574426	1.45E-05
IL1RAPL1	2.670494709	2.02E-06	SIPA1L2	-1.004902292	1.45E-05
BTG4	1.444748879	2.03E-06	C8orf48	-1.046680792	1.46E-05
FOSL1	1.363510435	2.04E-06	SFT2D2	-1.001850352	1.46E-05
ZNF226	1.671531292	2.06E-06	KLF3	-1.292127436	1.49E-05

AKAP13	1.526269281	2.06E-06	LOC100506403 /// RUNX1	-1.215274634	1.50E-05
RNASE4	1.442158454	2.06E-06	ZNF200	-1.132320105	1.50E-05
NRP1	1.953887451	2.07E-06	WDR73	-1.044204048	1.50E-05
RARRES3	1.530788084	2.07E-06	ADAT1	-1.035639051	1.50E-05
IL8	3.209178844	2.09E-06	ANAPC7	-1.008730525	1.50E-05
DUSP6	1.767913116	2.11E-06	UTP14A /// UTP14C	-1.092731226	1.51E-05
SEMA4B	1.410516424	2.11E-06	MAT2A	-1.250218955	1.52E-05
YPEL5	1.648966433	2.12E-06	ZNF512B	-1.188028633	1.52E-05
TMX3	1.829132034	2.13E-06	ZNF285	-1.171004806	1.53E-05
GALNT3	1.496068404	2.13E-06	ZXDC	-1.112285293	1.54E-05
FTH1	1.575834089	2.14E-06	SP5	-1.307182911	1.55E-05
RND1	1.866306333	2.15E-06	STC2	-1.008388577	1.55E-05
PMS1	1.321374162	2.15E-06	TADA2A	-1.058182601	1.56E-05
GPC2	1.385577598	2.16E-06	WSB1	-1.174065996	1.57E-05
IL15	1.625705714	2.17E-06	TMEM177	-1.101277246	1.57E-05
DHRS3	1.586929976	2.18E-06	ALG6	-1.064146012	1.57E-05
MAN1A1	1.438779098	2.19E-06	LYRM7	-1.321948535	1.59E-05
TNKS	1.505477772	2.23E-06	LDLOC1L	-1.027305233	1.59E-05
SAT1	2.24278872	2.27E-06	SCAF4	-1.123928715	1.60E-05
NR4A2	1.743427612	2.29E-06	TMEM209	-1.189569797	1.61E-05
FOSL1	1.442681859	2.30E-06	C7orf49 /// LOC653739	-1.024639988	1.61E-05
MMP1	1.323909354	2.30E-06	FAM65B	-1.757889658	1.62E-05
PTPN14	1.5847555	2.31E-06	TAGLN	-1.161950254	1.62E-05
PIM3	1.300539596	2.32E-06	PDPK1	-1.044919889	1.63E-05
GSN	1.439865924	2.33E-06	FASTKD3	-1.036688198	1.63E-05
CREBRF	1.909959985	2.34E-06	SIK2	-1.229856323	1.66E-05
MKRN1	1.621661851	2.36E-06	IMP3	-1.040118674	1.67E-05
ACTR3C	1.314519564	2.36E-06	PHF17	-1.364028061	1.69E-05
KRT7	1.382670072	2.39E-06	FMN1	-1.309519555	1.69E-05
CA12	1.750685068	2.41E-06	BTBD7	-1.215723796	1.69E-05
SERPINE1	1.836831121	2.43E-06	C9orf156	-1.021922919	1.70E-05
TNFSF9	1.71204037	2.45E-06	TIGD5	-1.335502626	1.71E-05
NEDD4L	1.328714328	2.47E-06	EED	-1.075765749	1.73E-05
IER5	1.745617096	2.51E-06	CCNJL	-1.083794782	1.74E-05
SAT1	1.457014443	2.52E-06	METTL25	-1.05105544	1.74E-05
OSMR	2.198801298	2.55E-06	KIAA1586	-1.045711983	1.74E-05
TNC	1.303529449	2.55E-06	XXYL1	-1.021310911	1.74E-05
SERPINA1	2.030923224	2.57E-06	ZNF226	-1.266140928	1.76E-05
MIR1304 /// SNORA1 /// SNORA18 /// SNORA32 /// SNORA40 /// SNORA8 /// SNORD5 /// TAF1D	1.62531715	2.57E-06	NSD1	-1.76377623	1.77E-05

BCL2L11	1.829716684	2.60E-06	GTF2H1	-1.305364303	1.77E-05
FAF2	1.312051771	2.63E-06	GPS2	-1.239563901	1.77E-05
HBP1	2.259262976	2.66E-06	STAG1	-1.017846227	1.77E-05
ESM1	1.918139061	2.67E-06	PIGM	-1.413556345	1.78E-05
NELL2	1.369553667	2.70E-06	ZNF546	-1.163057593	1.78E-05
CDKN1A	1.294639069	2.70E-06	PHF17	-1.455269034	1.79E-05
COL12A1	1.90553052	2.71E-06	LYRM7	-1.09191593	1.79E-05
CTSC	1.558608774	2.73E-06	FAM122A	-1.002464124	1.80E-05
HIST1H2BK	1.264405286	2.74E-06	ZNF827	-1.539049334	1.82E-05
POT1	1.828516515	2.76E-06	EP300	-1.212167291	1.83E-05
KLRC1	1.582824539	2.81E-06	MGAT2	-1.200484625	1.83E-05
PTX3	2.278187624	2.85E-06	LPAR1	-1.172707841	1.83E-05
SERPINB5	1.617581483	2.85E-06	FAM111B	-1.736631376	1.84E-05
KITLG	1.851359925	2.87E-06	DPH1 /// OVCA2	-1.022146014	1.84E-05
RIPK2	1.414116032	2.87E-06	TMEM97	-1.211865472	1.85E-05
SMAD3	1.461300655	2.88E-06	LOC101060460 /// POLR3C	-1.142218876	1.85E-05
SLC25A20	1.326721753	2.89E-06	DISC1 /// TSNAX-DISC1	-1.116561079	1.85E-05
METRNL	1.399003437	2.92E-06	MRPL1	-1.194336773	1.86E-05
VSNL1	1.260892549	2.93E-06	BIVM	-1.113763671	1.86E-05
YPEL5	1.303671823	2.95E-06	ZNF469	-1.561797992	1.87E-05
ELF3	2.768428299	2.98E-06	ZNF268	-1.219091354	1.87E-05
SYTL3	1.478466477	2.98E-06	TLE4	-1.089360194	1.87E-05
LARP6	1.30007667	3.04E-06	RAC1	-1.054358896	1.87E-05
HNRNPD	1.265418208	3.05E-06	MMAB	-1.062112678	1.88E-05
NEDD4L	1.497268926	3.06E-06	CSTF2T	-1.018341125	1.88E-05
UBR1	1.454396427	3.06E-06	ARID2	-1.055327587	1.89E-05
CLK1	1.5144226	3.07E-06	SURF2	-1.015338341	1.92E-05
CDKAL1	1.494359789	3.08E-06	TUBGCP3	-1.526594333	1.93E-05
SLC30A1	1.699951209	3.10E-06	FER	-1.1201163	1.93E-05
MTSS1	1.232333677	3.10E-06	OTTHUMG0000 0173400 /// RP11-401P9.4	-1.771994449	1.94E-05
HCP5	1.652009801	3.12E-06	NT5DC2	-1.299013343	1.95E-05
CA13 /// LOC100507258	1.396687841	3.13E-06	SIK2	-1.154599954	1.95E-05
RASA2	1.609991009	3.23E-06	CDC42EP3	-1.054415127	1.95E-05
EGR1	1.660739892	3.27E-06	SRSF3	-1.02663697	1.96E-05
IL8	3.176244147	3.28E-06	TFDP1	-1.026867591	1.97E-05
HIST1H2BD	2.405708095	3.33E-06	DENND1B	-1.269646901	1.99E-05
RBPMS	1.314655956	3.33E-06	ZNF189	-1.233855015	2.01E-05
KLF9	2.162570066	3.35E-06	MSX2	-1.218656825	2.01E-05
IL1A	2.408847774	3.36E-06	VANGL1	-1.056805594	2.03E-05
HMOX1	1.265837548	3.37E-06	TRPS1	-1.002599869	2.05E-05
ATP6V1G2	1.474456752	3.38E-06	TMEM45A	-1.174232567	2.06E-05
IFI27L2	1.513241245	3.40E-06	ZNF75A	-1.359569769	2.10E-05
EYA3	1.491891752	3.40E-06	BDH1	-1.326686044	2.10E-05

MIR1304 /// SNORA1 /// SNORA18 /// SNORA32 /// SNORA40 /// SNORA8 /// SNORD5 /// TAF1D	1.410705908	3.40E-06	PAGR1	-1.085091417	2.11E-05
HIST1H2BD	1.365372129	3.46E-06	ZNF189	-1.179447388	2.16E-05
CASP4	1.902698066	3.47E-06	IFNAR1	-1.01216976	2.16E-05
AVPI1	1.300289218	3.47E-06	B3GALT	-1.184706883	2.19E-05
SMOX	1.740284509	3.49E-06	DNAJC28	-1.121720326	2.19E-05
TNC	1.288556664	3.50E-06	PBRM1	-1.292812204	2.21E-05
CAPG	1.359446825	3.51E-06	RBM4B	-1.042383906	2.22E-05
NOTCH2	1.308761779	3.51E-06	ZMYND11	-1.287876347	2.23E-05
TNC	1.215975619	3.52E-06	ARHGEF28	-1.217211979	2.23E-05
DNAJB9	1.634610893	3.55E-06	DNAJB12	-1.040632288	2.23E-05
MCTP2	1.444266316	3.56E-06	TBCCD1	-1.023707355	2.24E-05
KCNK6	1.246495444	3.57E-06	AP4S1	-1.031747593	2.25E-05
PHTF2	1.226318116	3.57E-06	SLC12A2	-1.026213003	2.26E-05
BDKRB1	1.260374949	3.60E-06	BCLAF1	-1.34639759	2.27E-05
NLRP3	1.244480115	3.63E-06	RRP15	-1.035726011	2.29E-05
RUFY3	1.616876604	3.68E-06	ZNF652	-1.132663754	2.30E-05
KIAA0907	1.469072704	3.69E-06	BAZ1A	-1.077494994	2.30E-05
RDM1	1.386729443	3.71E-06	ZNF786	-1.083954182	2.32E-05
AKR1C2 /// LOC101060798	2.427669908	3.73E-06	PLAGL2	-1.0113457	2.32E-05
OASL	1.459591228	3.78E-06	ABCB10	-1.174319124	2.33E-05
FAM46A	1.199199289	3.78E-06	DACH1	-1.259720755	2.34E-05
FAM46A	1.195821993	3.83E-06	CCNYL1	-1.268647516	2.36E-05
C1S	1.398801978	3.84E-06	SETD1B	-1.128564308	2.36E-05
SCNN1A	1.573617374	3.85E-06	MCM10	-1.088200563	2.36E-05
LOC101060235 /// TMSB15A /// TMSB15B	1.296956796	3.87E-06	ST7L	-1.265407151	2.39E-05
GBP1	2.542451278	3.89E-06	GLI3	-1.320360531	2.42E-05
SLC25A37	1.264125313	3.96E-06	ARID1A	-1.035955474	2.44E-05
PLAUR	1.245789325	3.97E-06	ATMIN	-1.023344264	2.46E-05
RBKS	1.239968405	3.98E-06	L3HYPDH	-1.422059196	2.47E-05
SORBS1	1.214371009	4.00E-06	BRCC3	-1.391976772	2.47E-05
LOC101060315 /// LOC101060683 /// NOTCH2 /// NOTCH2NL	1.306978046	4.03E-06	GAS1	-1.332279289	2.47E-05
LINC00478	1.273805969	4.03E-06	NSUN2	-1.093600682	2.47E-05
JUN	1.322018855	4.05E-06	TUBGCP3	-1.102622424	2.52E-05
TNIP1	1.251482781	4.05E-06	MALT1	-1.275960813	2.55E-05
PPP1R15B	1.436607398	4.09E-06	TRPM7	-1.032725807	2.56E-05

LOC100506548 /// RPL37	1.252073319	4.09E-06	SKA3	-1.047068383	2.57E-05
PXK	1.190910533	4.10E-06	BIVM	-1.232699492	2.61E-05
EGR1	1.30876049	4.12E-06	DHFRL1	-1.103611435	2.61E-05
IL18	1.259678245	4.12E-06	LINC00341	-1.15345455	2.63E-05
THBD	1.399642213	4.14E-06	NSUN2	-1.005620826	2.63E-05
GKAP1	1.839331406	4.15E-06	EPC2	-1.232848462	2.65E-05
LCORL	1.490154185	4.15E-06	FMN1	-1.179372485	2.65E-05
MXI1	1.239006497	4.17E-06	CCDC18	-1.225324069	2.66E-05
ADTRP	1.216695457	4.24E-06	FAM171A1	-1.063164562	2.68E-05
NRIP3	1.225671771	4.25E-06	FUS	-1.017135217	2.68E-05
RPL4	1.700212805	4.26E-06	SLC38A1	-1.063421348	2.71E-05
EIF4A2 /// MIR1248 /// SNORA4 /// SNORA63 /// SNORA81 /// SNORD2	1.278712741	4.26E-06	SRSF3	-1.187508555	2.72E-05
CAPG	1.364742247	4.27E-06	UBE3B	-1.047816737	2.72E-05
RBPJ	1.724202891	4.28E-06	IFNAR1	-1.391683131	2.73E-05
PSMB9	1.359565649	4.28E-06	MRPL1	-1.063843406	2.78E-05
CDKN1C	1.45939271	4.29E-06	MPDU1	-1.013770689	2.79E-05
C3orf52	1.279797223	4.29E-06	ZNF181 /// ZNF302	-1.174144793	2.83E-05
HSPA1A /// HSPA1B	1.314412703	4.30E-06	KIAA2026	-1.574654895	2.87E-05
LIF	1.450522887	4.31E-06	AXIN2	-1.098526268	2.88E-05
ISG20	1.654586735	4.32E-06	EPHA4	-1.093509394	2.90E-05
LST1	1.612645695	4.32E-06	RUNX3	-1.110151105	2.92E-05
TTC39B	1.368576648	4.34E-06	ZCCHC14	-1.024853069	2.93E-05
LIF	1.280541188	4.34E-06	RFX7	-1.921889849	2.97E-05
TNFRSF10B	1.219494495	4.35E-06	MED11	-1.007998829	3.01E-05
RFX3	1.690954465	4.44E-06	KCTD20	-1.291575169	3.03E-05
HS3ST3A1 /// HS3ST3B1	1.25513005	4.44E-06	ZNF470	-1.147546546	3.03E-05
SEL1L3	1.298710366	4.45E-06	COX3	-1.133925068	3.06E-05
SCG5	1.954012209	4.48E-06	PPP1R10	-1.425491639	3.14E-05
CDKN2D	1.280133894	4.54E-06	TRIM32	-1.025886508	3.19E-05
CLDN4 /// LOC100996451	1.326128025	4.56E-06	TMEM2	-1.086926105	3.21E-05
SERTAD1	1.400913798	4.59E-06	ZNF804A	-1.060953036	3.29E-05
TRIO	1.182324034	4.61E-06	ZFP112	-1.046411144	3.31E-05
RC3H2	1.232640222	4.62E-06	ZNF613	-1.335962269	3.32E-05
TIA1	1.380371432	4.63E-06	FER	-1.293980951	3.37E-05
BCL2L11	1.619171398	4.66E-06	KRT80	-1.00644182	3.38E-05
WDR26	1.209045359	4.71E-06	HNRNPU	-1.021956957	3.40E-05
FAM72A /// FAM72B /// FAM72C /// FAM72D ///	1.320851901	4.73E-06	CEP128	-1.130744334	3.41E-05

LOC101060656					
NFKBIE	1.196951567	4.76E-06	CGRRF1	-1.100899575	3.43E-05
FAS	1.32746897	4.82E-06	RABEP1	-1.073479877	3.43E-05
SORBS1	1.180775238	4.84E-06	MFAP3	-1.099165224	3.44E-05
IL15	1.551457357	4.89E-06	BTRC	-1.250371977	3.49E-05
TRHDE	2.034815095	4.92E-06	ANKRD32	-1.006620425	3.49E-05
VWA5A	2.226883798	4.95E-06	CHD6	-1.200568759	3.52E-05
ZNF789	1.661802042	4.96E-06	NEXN	-1.06690027	3.65E-05
TRAPPC6A	1.172568941	4.96E-06	PHACTR2	-1.144124098	3.69E-05
SLC35D2	1.189345601	4.97E-06	HOXA7	-1.066219475	3.69E-05
TAB2	1.435647543	4.99E-06	GRIP1	-1.569056257	3.71E-05
DDR1 /// MIR4640	1.380785525	4.99E-06	SYNM	-1.178021351	3.73E-05
PIK3R1	1.325499297	5.10E-06	CXCR7	-1.427130168	3.75E-05
SRPX	1.246346948	5.16E-06	PPM1D	-1.098934494	3.82E-05
BET1	1.423913489	5.17E-06	NUP50	-1.087153549	3.82E-05
CDKN1C	1.884852719	5.21E-06	BAZ1A	-1.199768969	3.86E-05
TGM2	1.156636425	5.22E-06	SDC2	-1.080107076	3.99E-05
ARRDC4	1.323419486	5.26E-06	ZC3H12C	-1.070361599	4.01E-05
TNFAIP2	1.233116494	5.27E-06	APC	-1.006439761	4.11E-05
TNFRSF10B	1.30811898	5.28E-06	SOS2	-1.288658667	4.14E-05
CPT1A	1.296912936	5.31E-06	PHTF2	-1.181994842	4.14E-05
NBR1	1.204930366	5.33E-06	KIAA2018	-1.190943407	4.18E-05
GJB2	1.133295149	5.34E-06	HMGA2	-1.028384338	4.20E-05
MAN1A1	1.298416892	5.37E-06	EED	-1.076223077	4.23E-05
CD109	1.33355657	5.46E-06	FER	-1.185675141	4.27E-05
LAPTM5	1.308787767	5.47E-06	ZNF268	-1.218126461	4.33E-05
SEL1L3	1.248967675	5.57E-06	COG2	-1.194518987	4.37E-05
EYA4	1.237399134	5.58E-06	COMT	-1.007458721	4.37E-05
CXorf57	1.98000229	5.60E-06	SMARCA1	-1.152282333	4.45E-05
LOC100129518 /// SOD2	1.243527341	5.67E-06	GEN1	-1.654225123	4.52E-05
SDC4	1.191408318	5.71E-06	TFDP1	-1.127019154	4.52E-05
RIPK2	1.479173886	5.79E-06	ACP2	-1.037810997	4.53E-05
SERPINA1	2.201204685	5.84E-06	PTCH1	-1.050646968	4.57E-05
TET2	1.567307675	5.85E-06	CCDC138	-1.193800551	4.65E-05
MGAT4A	1.137079436	5.86E-06	MBLAC2	-1.359025252	4.67E-05
ITPRIP	1.298100346	5.87E-06	BIVM	-1.342333015	4.67E-05
SDC4	1.17582538	5.92E-06	CCDC82	-1.081257562	4.73E-05
LOC101060315 /// LOC101060683 /// NOTCH2 /// NOTCH2NL	1.310600499	5.99E-06	CAP2	-1.343309256	4.75E-05
RTKN2	1.202185483	6.03E-06	C12orf4	-1.202073354	4.79E-05
LOC100506548 /// RPL37	1.323065939	6.04E-06	FOXRED2	-1.267910441	4.90E-05
PHLDB2	1.675090648	6.09E-06	C1orf131	-1.525749362	4.93E-05

ZFAND5	1.45187018	6.16E-06	TSEN2	-1.148681626	5.10E-05
HS3ST1	1.323650267	6.17E-06	CENPN	-1.172489847	5.14E-05
PHLDA1	1.127854509	6.24E-06	ZNF235	-1.400979554	5.15E-05
HYPK /// MIR1282 /// SERF2 /// SERF2- C15ORF63	1.328255971	6.27E-06	SLC8A1	-1.193231857	5.16E-05
UQCRO	1.437683962	6.28E-06	VANGL1	-1.133442905	5.19E-05
PLAUR	1.162607838	6.29E-06	SCLY /// UBE2F- SCLY	-1.101779754	5.45E-05
RHOB	1.404428461	6.32E-06	NUP214	-1.107437994	5.47E-05
RRAD	1.192953223	6.32E-06	BCLAF1	-1.229911066	5.59E-05
ECE1	1.125835103	6.32E-06	BRI3BP	-1.409169117	5.63E-05
RSRC2	1.448294795	6.33E-06	LBH	-1.022329625	5.65E-05
KIAA0907	1.52553214	6.36E-06	PDPK1	-1.09345561	5.66E-05
TMEM71	2.238459836	6.37E-06	IREB2	-1.062279912	5.76E-05
HIST1H2BC /// HIST1H2BE /// HIST1H2BF /// HIST1H2BG /// HIST1H2BI	1.117278	6.37E-06	TMEM177	-1.083293341	5.80E-05
LIMS1 /// LIMS3 /// LIMS3L	1.559163442	6.40E-06	SFXN2	-1.032704201	5.80E-05
LARP6	1.253378567	6.44E-06	TTC30B	-1.380686042	5.91E-05
RPS29	1.298125924	6.45E-06	LIN9	-1.103625063	5.95E-05
C17orf103	1.111674212	6.45E-06	HEATR3	-1.214430922	6.14E-05
WWP2	1.334502176	6.51E-06	PPM1F	-1.05017077	6.14E-05
CCNL1	1.13555365	6.52E-06	ZNF268	-1.123266582	6.19E-05
SPANXA1 /// SPANXA2 /// SPANXC /// SPANXD /// SPANXE	1.113019536	6.55E-06	ZNF790	-1.301502234	6.21E-05
SPRY4	2.199324051	6.63E-06	MOCS3	-1.20652036	6.24E-05
SLC6A6	1.432249198	6.67E-06	SLC26A2	-1.011882519	6.27E-05
RASA4 /// RASA4B	1.29526514	6.69E-06	FAM122A	-1.072620238	6.39E-05
CLDND2	1.237894328	6.76E-06	NPIPA2 /// NPIPA3 /// NPIPA5 /// PKD1P1	-1.078969992	6.43E-05
TMEM200A	1.487498591	6.79E-06	USP31	-1.10751685	6.48E-05
CSRNP1	1.251907969	6.85E-06	ZNF544	-1.334006998	6.52E-05
KYNU	2.349931656	6.88E-06	MCM9	-1.152718715	6.59E-05
CD96	1.211241966	6.91E-06	PRDM1	-1.358703816	6.69E-05
NEFL	1.400660742	6.98E-06	CREB1	-1.232055303	6.71E-05
PDGFRL	1.148667999	7.02E-06	ZNF181	-1.236016877	6.75E-05
TMX3	1.604662234	7.10E-06	MGAT2	-1.023616081	6.76E-05
SQSTM1	1.210015656	7.13E-06	PRR14L	-1.210447842	6.80E-05

PHLDA1	1.123471536	7.18E-06	BAG2	-1.055537996	6.80E-05
FZR1	1.18826156	7.20E-06	ZNF189	-1.133499198	6.97E-05
NCOA7	1.65047067	7.27E-06	RPL27A /// SNORA3	-1.150780544	7.04E-05
TBC1D14	1.181997104	7.37E-06	TLR4	-1.083756638	7.05E-05
OCIAD2	1.127301347	7.37E-06	SMURF2	-1.154567309	7.38E-05
TNFRSF9	1.214225971	7.41E-06	FRMD4A	-1.066023406	7.50E-05
GPR126	1.175135721	7.41E-06	CTNS	-1.079019748	7.69E-05
OPTN	1.345536824	7.42E-06	ATP11A	-1.108772388	7.99E-05
FOSL1	1.434556428	7.52E-06	LOC100996628 /// SHROOM3	-1.345580541	8.11E-05
TFAP2A	1.62687686	7.59E-06	CREB1	-1.017374942	8.18E-05
RIPK4	1.154753384	7.63E-06	ZBTB45	-1.09480262	8.20E-05
CD96	1.37382935	7.65E-06	TRIM13	-1.471490317	8.32E-05
NFYA	1.295669287	7.69E-06	RNASEL	-1.136461155	8.37E-05
ETS2	1.13270033	7.69E-06	LOC728819	-1.151118618	8.39E-05
LUC7L3	1.258365672	7.71E-06	ZSCAN29	-1.051217492	8.39E-05
LRIG2	1.220710249	7.82E-06	COL5A1	-1.091420801	8.41E-05
MAP4K4	1.270134719	7.90E-06	MALT1	-1.304287442	8.45E-05
AEBP2	1.122768068	7.91E-06	LOC100996628 /// SHROOM3	-1.223992001	8.49E-05
RARA	1.095305121	7.91E-06	BTBD7	-1.410203119	8.59E-05
CD70	1.606542063	7.92E-06	AFAP1L2	-1.10194778	8.66E-05
SRGAP2 /// SRGAP2D	1.218033079	7.92E-06	MEIS2	-1.083774308	8.83E-05
PHTF2	1.946444072	7.97E-06	ERCC4	-1.506261887	9.23E-05
GPNMB	1.304429841	7.98E-06	LOC653501 /// ZNF658 /// ZNF658B	-1.386228954	9.30E-05
OGDH	1.237572057	8.00E-06	PBRM1	-1.095701565	9.56E-05
KCNK6	1.193932323	8.02E-06	CCDC8	-1.425731558	9.72E-05
NEDD4L	1.445233595	8.07E-06	SLC25A13	-1.126497097	9.77E-05
EXOC4	1.096391533	8.11E-06	ASTE1	-1.127685233	9.82E-05
FEZ1	2.158418532	8.14E-06	APPBP2	-1.153741935	9.88E-05
HSPA1A /// HSPA1B	1.094205902	8.14E-06	ZBTB9	-1.325698174	9.89E-05
DUSP16	1.560606027	8.15E-06	ATAD2B	-1.043916669	0.00010 1543
RNF144B	1.50913178	8.15E-06	ZSCAN26	-1.104049224	0.00010 4039
GCNT1	1.133135829	8.16E-06	LANCL1	-1.089213736	0.00010 8322
SRP19	1.63738128	8.18E-06	ICK	-1.244663467	0.00010 95
SLC1A3	1.27960709	8.22E-06	L3HYPDH	-1.391235839	0.00011 0485
BCL2L11	1.169455281	8.23E-06	CSRNP2	-1.135281438	0.00011 1509
TMEM178A	1.675156335	8.26E-06	LYRM2	-1.048241381	0.00011 2122
HIST1H2BJ	1.235590365	8.31E-06	ZNF148	-1.085228839	0.00011 4896

JARID2	1.112959143	8.31E-06	FBXO9	-1.118137097	0.00012 1362
KLHL13	1.07512337	8.33E-06	CEP19	-1.064561971	0.00012 1514
CAPG	1.315870074	8.41E-06	ITPRIPL2	-1.157545159	0.00012 4065
MYEOV	1.172379735	8.46E-06	ZBTB24	-1.073785004	0.00012 6982
TMEM159	1.286367526	8.48E-06	LOC653501 /// ZNF658 /// ZNF658B	-1.066931959	0.00012 9254
ZAK	1.687226911	8.49E-06	HOMEZ	-1.092301359	0.00013 39
OPTN	1.067653491	8.49E-06	DNAAF2	-1.012736613	0.00013 5958
GPR126	1.125495969	8.51E-06	STARD7	-1.485787853	0.00014 5205
EIF4A2 /// MIR1248 /// SNORA4 /// SNORA63 /// SNORA81 /// SNORD2	1.300833881	8.53E-06	ZNF302	-1.113665183	0.00014 5299
PSMB9	1.382922646	8.62E-06	ERCC6	-1.050119274	0.00014 5779
CTSB	1.197253462	8.62E-06	ZNF17	-1.188157314	0.00014 6448
CAT	1.167687628	8.63E-06	GPATCH4	-1.112820292	0.00014 718
CLK4	1.57702981	8.65E-06	ARID1A	-1.305465517	0.00014 7825
HIVEP2	1.273951313	8.66E-06	ZIC5	-1.077996968	0.00014 9832
CAPG	1.27194135	8.72E-06	TAGLN	-1.037453649	0.00015 0795
TRPS1	1.11932433	8.72E-06	IKBIP	-1.300982417	0.00015 0915
BTN3A3	1.056864772	8.77E-06	FGFR1OP2	-1.06819856	0.00015 1127
NUP62CL	1.054250371	8.78E-06	KIAA0232	-1.291429599	0.00015 3743
RASSF1	1.437736615	8.86E-06	NEXN	-1.135972768	0.00015 5777
PPAP2B	1.063395996	8.90E-06	PRKX	-1.216444604	0.00015 8346
OBFC1	1.439203059	8.92E-06	ZNF624	-1.206873067	0.00015 8492
AFF3	1.106197854	8.92E-06	NIN	-1.21672248	0.00016 0979
PDZK1IP1	1.046834144	8.96E-06	ATP6V1G2- DDX39B /// DDX39B /// SNORD84	-1.057174692	0.00018 2253
SLC25A20	1.169529436	8.99E-06	HAUS3	-1.327395898	0.00018 3276
FAS	1.095378544	9.13E-06	CAP2	-1.456361486	0.00018 7068
ANKHD1 ///	1.086849747	9.24E-06	CDC27	-1.028244766	0.00019

ANKHD1- EIF4EBP3					8031
KLF11	1.468832167	9.25E-06	SYNJ2	-1.136546229	0.00020 4978
CSTF3	1.126151537	9.37E-06	HECTD2	-1.008053395	0.00020 7826
CDK14	2.76328604	9.39E-06	FER	-1.216661892	0.00020 8727
IFRD1	1.066743342	9.44E-06	SLC25A13	-1.031206192	0.00023 0663
MT1F	1.044733561	9.50E-06	SKIDA1	-1.260021018	0.00024 0272
RASSF1	1.168246916	9.59E-06	FDXACB1	-1.019650708	0.00024 1151
MCTP1	1.311167382	9.65E-06	CAP2	-1.459659226	0.00024 1991
TRIM34 /// TRIM6-TRIM34	1.386461118	9.66E-06	TMEM170B	-1.02053955	0.00025 97
CXorf38	1.536165554	9.84E-06	TRPC4	-1.02635857	0.00026 4467
LAMC2	1.539716446	9.88E-06	SRSF6	-1.158433217	0.00026 9349
TNIP1	1.189959669	9.88E-06	POGLUT1	-1.064150794	0.00027 1553
MICAL3	2.092654411	1.00E-05	AP5M1	-1.021868735	0.00028 6375
NDUFS2	1.55181741	1.00E-05	ARID1A	-1.073528406	0.00029 6208
BTN2A2	1.064956661	1.01E-05	ACTRT3	-1.320902705	0.00030 2081
OPTN	1.039431674	1.01E-05	TEFM	-1.015502496	0.00030 7824
PAPOLA	1.915111533	1.03E-05	ZNF543	-1.024680754	0.00030 808
GCOM1 /// MYZAP	1.117518345	1.03E-05	ATP6V1G2- DDX39B /// DDX39B /// SNORD84	-1.030561121	0.00032 8427
GLRX	1.095034694	1.03E-05	NEXN	-1.019538169	0.00032 9205
HBP1	1.02792472	1.03E-05	CAP2	-1.435906496	0.00035 1705
GLG1	1.258486836	1.04E-05	ITFG2 /// LOC100507424	-1.176788502	0.00036 3676
BLZF1	1.070116982	1.04E-05	ZNF239	-1.079225792	0.00038 9823
PMEPA1	1.064200316	1.04E-05	ARID2	-1.310889324	0.00040 6969
GABBR1 /// UBD	2.040931342	1.05E-05	CAP2	-1.429682391	0.00040 8356
IDS	1.127201905	1.05E-05	ITGBL1	-1.11157842	0.00044 2043
ADD2	1.071925429	1.05E-05	TAGLN	-1.099497461	0.00044 9092
BTG1	1.067691698	1.05E-05	DGCR8 /// MIR1306	-1.126148066	0.00055 1185
LAMC2	1.474876206	1.06E-05	TMEM131	-1.00520783	0.00058 3739

PELI2	1.221699332	1.06E-05	SLC26A2	-1.081976377	0.00061 2514
CAT	1.171894271	1.06E-05	TMEM131	-1.00520783	0.00062 9634
GJB2	1.154561638	1.06E-05	RIPK1	-1.121147883	0.00063 6756
HLA-F	1.560071492	1.07E-05	ALG2	-1.048508667	0.00065 8141
SERPINE1	1.446082398	1.07E-05	ATP6V1G2- DDX39B /// DDX39B /// SNORD84	-1.050051726	0.00067 1189
SLC25A27	1.443275996	1.07E-05	TIGD6	-1.144481082	0.00067 3685
GALNT11	1.214183234	1.08E-05	ANKRD13C	-1.165414847	0.00068 5133
RIOK3	1.201339386	1.08E-05	PPL	-1.158139161	0.00071 3541
LPXN	1.26946505	1.09E-05	ZNF22	-1.079776958	0.00072 8591
TNIP1	1.169321296	1.09E-05	MTDH	-1.092421953	0.00084 0688
PAIP2B	1.085644107	1.09E-05	ZNF708	-1.006913998	0.00085 347
RAB33B	1.073384679	1.09E-05	FER	-1.097728552	0.00088 6608
FNIP1	2.316666919	1.10E-05	DICER1	-1.026714833	0.00090 3876
HIST1H2BC /// HIST1H2BE /// HIST1H2BF /// HIST1H2BG /// HIST1H2BI /// NCALD	1.360798379	1.10E-05	BRCC3	-1.017320286	0.00107 0312
PDLIM4	1.028572913	1.10E-05	BICD1	-1.181953745	0.00108 0606
BACH1 /// GRIK1-AS2	1.753161746	1.11E-05	BCLAF1	-1.089197764	0.00109 1285
AXIN2	1.399377816	1.11E-05	ZNF549	-1.258944337	0.00124 4759
EGFR	1.162672941	1.11E-05	KLHL23 /// PHOSPHO2- KLHL23	-1.132744037	0.00143 6494
ZNF451	1.112847516	1.11E-05	NEXN	-1.005784515	0.00144 0711
IFIT3	1.091058598	1.11E-05	ZNF37A	-1.01488908	0.00280 7125
DCAF5	1.054874617	1.11E-05	ZNF37A	-1.083499784	0.00293 6472
HLA-F	1.316309712	1.12E-05	CEP19	-1.010491936	0.00399 7652
IGFBP6	1.196624327	1.12E-05	LINC00273	-1.036255718	0.01039 2399
AIG1	1.05913418	1.12E-05	---	-1.041032182	0.02474 2846
ADAM15	1.156676329	1.13E-05			
HIPK2	1.150546397	1.14E-05			

GOLGA2	1.090773141	1.14E-05			
CCDC69	1.053563078	1.14E-05			
EHD1	1.128246157	1.15E-05			
RIMBP2	1.033921623	1.15E-05			
B3GNT5	1.060975352	1.16E-05			
CRYL1	1.05769427	1.16E-05			
CDKN1C	1.342582038	1.19E-05			
UBE2H	1.133318436	1.19E-05			
RORA	1.239680869	1.20E-05			
SEC24A	1.074124704	1.20E-05			
MEF2C	1.485513178	1.21E-05			
C6orf57	1.456438625	1.21E-05			
SP140L	1.353017003	1.21E-05			
P4HA2	1.015983354	1.21E-05			
MXD1	1.059551068	1.22E-05			
PRPF4B	1.039873942	1.22E-05			
ANKRD44	1.017859193	1.22E-05			
ZNF277	1.120246163	1.24E-05			
MIR4680 /// PDCD4	1.04836537	1.25E-05			
DUSP10	1.653206829	1.26E-05			
DNAJB4	1.440054963	1.26E-05			
C12orf39	1.123012012	1.26E-05			
EHD1	1.09425572	1.26E-05			
HIST1H2BC /// HIST1H2BE /// HIST1H2BF /// HIST1H2BG /// HIST1H2BI	2.463084216	1.27E-05			
NR4A1	1.750353807	1.27E-05			
STK17B	1.706922506	1.27E-05			
GNB5	1.075220787	1.27E-05			
LAMC2	1.439886204	1.28E-05			
HOXB8	1.055809708	1.28E-05			
HBEGF	1.493965805	1.29E-05			
CRYZL1	1.195408883	1.29E-05			
PROS1	1.057674287	1.29E-05			
GTF2E1	1.440052103	1.30E-05			
MYLK	1.390528591	1.30E-05			
NAMPT	1.094514454	1.30E-05			
HSD11B1	2.00662621	1.31E-05			
PDE4DIP	1.612096208	1.31E-05			
PMAIP1	1.138065965	1.32E-05			
RHCE /// RHD	1.091941059	1.32E-05			
PSAP	1.063253642	1.32E-05			
MYEOV	1.005916893	1.32E-05			
LATS1	1.357822747	1.34E-05			
ARRDC3	1.355366728	1.34E-05			

NFKBIA	1.251759914	1.34E-05				
APOL1 /// APOL2	1.247848586	1.34E-05				
SEC24A	1.010749347	1.34E-05				
VEPH1	1.292935325	1.36E-05				
TFPI	1.269823146	1.36E-05				
PSAP	1.053082429	1.36E-05				
CLK4	1.490368006	1.37E-05				
SAA2-SAA4 /// SAA4	2.296591454	1.38E-05				
EIF4A2 /// MIR1248 /// SNORA4 /// SNORA63 /// SNORA81 /// SNORD2	1.55898269	1.38E-05				
HLA-C	1.186097305	1.38E-05				
CREBRF	1.734397452	1.39E-05				
CD47	1.244528776	1.39E-05				
DDX58	1.21529811	1.39E-05				
SORBS1	1.186848815	1.39E-05				
MAN1A1	1.356070212	1.41E-05				
SERPINB3 /// SERPINB4	1.364762496	1.42E-05				
BACH1 /// GRIK1-AS2	1.89386708	1.43E-05				
PCDHB16	1.268942499	1.43E-05				
YIPF2	1.130445807	1.43E-05				
LHFPL2	1.063654133	1.43E-05				
POFUT2	1.0123268	1.43E-05				
RGS16	1.675494946	1.44E-05				
SMAD3	1.175681088	1.44E-05				
GRPEL2	1.104127543	1.44E-05				
DMXL1	1.056059481	1.44E-05				
CEBPD	1.542128599	1.45E-05				
TSC22D1	1.056653589	1.45E-05				
HLA-F	1.009798089	1.48E-05				
IL1RAP	1.410479979	1.49E-05				
TFPI	1.191298832	1.49E-05				
PIK3R1	1.264176515	1.52E-05				
DSE	1.083678479	1.52E-05				
DSE	1.083678479	1.52E-05				
RHCE /// RHD	1.02622946	1.53E-05				
ARHGAP11A	1.222957381	1.54E-05				
SERPINB1	1.20962906	1.54E-05				
ERP44	1.121574911	1.54E-05				
H3F3A /// H3F3B /// MIR4738	1.001625895	1.54E-05				

ABAT	1.018133397	1.55E-05				
Mar-02	1.000744007	1.56E-05				
GAD1	1.364281781	1.58E-05				
ANKHD1 /// ANKHD1- EIF4EBP3	1.051895962	1.58E-05				
LOX	1.055653718	1.59E-05				
JMY	1.941967177	1.60E-05				
---	1.596510183	1.60E-05				
SLCO1B3	1.077505695	1.61E-05				
VEGFA	1.131050434	1.62E-05				
ARHGAP26	1.433637352	1.64E-05				
EHD1	1.1636738	1.64E-05				
DGKE	1.299135613	1.65E-05				
PPP4R1L	1.246371006	1.67E-05				
ZNF226	1.701047891	1.68E-05				
EIF5A2	1.047904546	1.68E-05				
CSTF3	1.00182747	1.68E-05				
SHB	1.108554387	1.70E-05				
PALM2	1.338134015	1.71E-05				
CCNL1	1.149482158	1.73E-05				
N4BP2L1	1.415004226	1.74E-05				
ACSF2	1.109643438	1.74E-05				
BCL6	1.793658281	1.75E-05				
CSTF3	1.10468493	1.77E-05				
STK4	1.086833748	1.77E-05				
OTUD1	1.219794709	1.78E-05				
KCNMB4	1.11909941	1.78E-05				
SSH1	1.005158184	1.78E-05				
IFI27	1.153424574	1.80E-05				
LOC100505946	1.129370057	1.80E-05				
PDIA5	1.124311702	1.80E-05				
LEPR	1.057715222	1.81E-05				
SQSTM1	1.001283256	1.81E-05				
CAPS2	1.259810324	1.82E-05				
LAMB3	1.127645256	1.82E-05				
CPEB2	1.065597868	1.82E-05				
RGS16	1.716415503	1.83E-05				
CEBPB	1.151884801	1.83E-05				
MEF2D	1.121390742	1.84E-05				
TANK	1.491625219	1.85E-05				
HLA-F	1.401716346	1.86E-05				
SMARCA1	1.042509245	1.86E-05				
MYC	1.02901466	1.86E-05				
THADA	1.016278836	1.86E-05				
FAM72A /// FAM72B ///	1.2747001	1.87E-05				

FAM72C /// FAM72D /// LOC101060656						
MMD	1.187101474	1.87E-05				
ARHGDIB	1.122044403	1.87E-05				
KLF4	1.092207766	1.87E-05				
NFKBIA	1.316398317	1.88E-05				
INADL	1.378987153	1.89E-05				
KRTAP1-5	1.376052602	1.89E-05				
LAMA3	1.10797911	1.92E-05				
FAF2	1.077898629	1.92E-05				
GADD45B	1.001241134	1.93E-05				
PPP4R4	1.556071133	1.95E-05				
GSAP	1.538353145	1.95E-05				
EGFR	1.196436697	1.98E-05				
NBEAL1	1.223948374	2.01E-05				
WLS	1.025702764	2.01E-05				
ZNF267	1.100597244	2.02E-05				
STARD13	1.034234592	2.03E-05				
KLF7	1.347856723	2.04E-05				
TRIM6	1.416077872	2.05E-05				
HSPA1A /// HSPA1B	1.217095842	2.05E-05				
PSAP	1.127308001	2.05E-05				
BTN2A2	1.444541602	2.06E-05				
PLAUR	1.155312777	2.06E-05				
PLAT	1.004452647	2.06E-05				
SLC25A37	1.508331503	2.10E-05				
ZFP36L1	1.079297605	2.10E-05				
ARHGEF12	1.27934481	2.11E-05				
PCSK5	1.108516607	2.15E-05				
TNIP1	1.097482085	2.15E-05				
CD109	1.249215225	2.16E-05				
TESK2	1.075135167	2.16E-05				
RCAN2	1.333975212	2.17E-05				
PMAIP1	1.40391184	2.19E-05				
IREB2	1.172889693	2.19E-05				
C9orf72	1.140574574	2.21E-05				
REPS2	1.053447794	2.22E-05				
HILPDA	1.19899842	2.23E-05				
PML	1.037378504	2.25E-05				
IMMP2L	1.269196502	2.26E-05				
CSTF3	1.190401529	2.26E-05				
BIK	1.000335637	2.26E-05				
TICAM2 /// TMED7- TICAM2	1.405295033	2.28E-05				
SLC25A51	1.047525873	2.28E-05				

SH2D3A	1.09142959	2.29E-05			
PSAP	1.157210111	2.30E-05			
SH3RF2	1.059241833	2.30E-05			
HIST1H2AC	1.443263468	2.31E-05			
XRCC4	1.348128627	2.33E-05			
CLDN4 /// LOC100996451	1.210368771	2.33E-05			
CD59	1.066745014	2.35E-05			
ANKHD1 /// ANKHD1- EIF4EBP3	1.052197334	2.39E-05			
CCDC113	1.429096474	2.40E-05			
GLRX	1.106625051	2.40E-05			
RND3	1.032994953	2.43E-05			
TLE3	1.016605581	2.46E-05			
DIDO1	1.004631012	2.47E-05			
DIDO1	1.004631012	2.47E-05			
DNAJB4	1.290162599	2.48E-05			
EML2	1.146826058	2.48E-05			
C1orf213	1.33249382	2.49E-05			
NCOA7	1.085465924	2.49E-05			
PPP2R2C	1.081736539	2.50E-05			
GLRX	1.186162852	2.51E-05			
CFB	1.180257586	2.51E-05			
C10orf118	1.529654981	2.52E-05			
NEFL	1.156040021	2.52E-05			
ZBTB24	1.106302007	2.54E-05			
ACSL5	1.654556323	2.55E-05			
DYRK2	1.001089456	2.55E-05			
TMX3	1.56205039	2.57E-05			
ETS1	1.000742302	2.57E-05			
GDF15	2.104578193	2.59E-05			
VEGFA	1.178639169	2.61E-05			
HBG1	1.026548459	2.63E-05			
NCALD	1.492218051	2.64E-05			
TNIP1	1.11192327	2.71E-05			
NFKBIA	1.19912719	2.72E-05			
ST3GAL1	1.215887585	2.74E-05			
GIT2	1.110629545	2.77E-05			
ARC	1.051458173	2.79E-05			
SNHG12 /// SNORA16A /// SNORA44 /// SNORA61	1.226543425	2.81E-05			
BMP6	1.219769722	2.81E-05			
IFI16	1.095374685	2.81E-05			
HAUS6	1.125335629	2.83E-05			
NR1D2	1.415641057	2.84E-05			

TMEM156	1.222349658	2.87E-05				
GPR126	1.168470884	2.88E-05				
SPTY2D1	1.238069184	2.91E-05				
TMEM41B	1.194564499	2.92E-05				
COLEC10	1.133345807	2.93E-05				
CCNL1	1.527075143	2.96E-05				
PTGR2	1.145378277	2.97E-05				
WNT10A	1.625354215	3.00E-05				
CYR61	1.050366951	3.00E-05				
EXD3	1.179967653	3.01E-05				
EFNA1	1.105947833	3.02E-05				
SNHG12 /// SNORA16A /// SNORA44 /// SNORA61	1.267006801	3.04E-05				
DST	1.407434552	3.06E-05				
MALAT1	1.309839876	3.07E-05				
SOCS3	1.096815334	3.07E-05				
PLAT	1.028066537	3.10E-05				
CYFIP2	1.038590026	3.11E-05				
LSMEM1	1.325666759	3.15E-05				
HNRNPDL	1.466461706	3.16E-05				
CAMK2D	1.355180752	3.17E-05				
CACNB4	1.087681779	3.21E-05				
GHR	1.080920501	3.21E-05				
PXK	1.097498631	3.26E-05				
EIF3M	1.070347677	3.30E-05				
SNORA72	1.317522591	3.32E-05				
NR1D1 /// THRA	1.284116095	3.39E-05				
TIA1	1.035058925	3.39E-05				
RASSF4	1.130106536	3.40E-05				
PLAU	1.006620429	3.43E-05				
EYA4	1.138562156	3.44E-05				
BHLHE41	1.609398424	3.45E-05				
TNIP1	1.102204681	3.48E-05				
SCLT1	1.04460959	3.48E-05				
MLLT3	1.477178907	3.55E-05				
BIK	1.064801881	3.57E-05				
TRIO	1.043777707	3.57E-05				
GAL	1.465466419	3.58E-05				
ZBTB21	1.165362773	3.59E-05				
GADD45B	1.414350307	3.61E-05				
PROS1	1.064414755	3.62E-05				
TPD52L1	1.033427408	3.65E-05				
SDC4	1.217878371	3.66E-05				
EMP1	1.133742477	3.73E-05				

AHNAK	1.026473179	3.77E-05				
SNHG12 /// SNORA16A /// SNORA44 /// SNORA61	1.10214813	3.84E-05				
NAMPT	1.005356579	3.85E-05				
HLA-C	1.163021802	3.89E-05				
TRIQK	1.267509051	3.95E-05				
SH2D2A	1.562581759	3.96E-05				
YME1L1	1.04958991	4.01E-05				
OAS1	1.007308886	4.05E-05				
SUSD1	1.018521041	4.06E-05				
GPR155	1.141849944	4.07E-05				
GJC1	1.055681676	4.08E-05				
AVL9	1.016898095	4.12E-05				
SGPP2	1.300196503	4.19E-05				
ZNF267	1.17846034	4.23E-05				
SERPINB3	1.150059142	4.26E-05				
PPAP2B	1.097990996	4.29E-05				
RAB11FIP4	1.084343055	4.29E-05				
PALM2	1.406837534	4.30E-05				
SATB1	1.478336169	4.32E-05				
STMN1	1.019230977	4.33E-05				
CD274	1.255672214	4.37E-05				
FGF5	1.121544911	4.41E-05				
PIK3R1	1.04783201	4.45E-05				
IFI44L	1.196076441	4.48E-05				
---	1.067265521	4.48E-05				
PNPLA8	1.004449636	4.53E-05				
FGGY	1.060431478	4.55E-05				
MALAT1	1.872521166	4.56E-05				
CTSS	1.196381408	4.56E-05				
GNA15	1.450083965	4.58E-05				
ING1	1.005968091	4.66E-05				
EIF5 /// SNORA28	1.725488569	4.67E-05				
PAQR5	1.256190628	4.74E-05				
TRIO	1.308978539	4.79E-05				
CKAP2	1.108543825	4.81E-05				
GNPDA2	1.062681022	4.97E-05				
F11R	1.378114247	5.09E-05				
ZNF280D	1.007357572	5.09E-05				
PDLIM5	1.402638737	5.13E-05				
VEGFA	1.02232676	5.14E-05				
INSIG1	1.033551386	5.16E-05				
MAP3K7CL	1.660210807	5.20E-05				
ADD2	1.0675146	5.23E-05				

IFI16	1.093919034	5.28E-05				
TGFB2	1.181305237	5.31E-05				
LOC100509445 /// OVOS2	1.012764001	5.31E-05				
RGS17	1.138257281	5.37E-05				
CEBPD	1.318892689	5.42E-05				
GAB2	1.004681323	5.46E-05				
PPIF	1.024883396	5.48E-05				
DGKE	1.516833222	5.59E-05				
CXorf38	1.43022249	5.62E-05				
PPFIBP1	1.193109921	5.64E-05				
HMGCS1	1.050048468	5.64E-05				
DNAJB5	1.058885301	5.70E-05				
HECTD2	1.272899692	5.77E-05				
KRTAP4-9	1.228707004	5.77E-05				
TMX3	1.512443614	5.81E-05				
---	2.33620292	5.87E-05				
CEBPD	1.290287771	5.87E-05				
C5orf34	1.152320611	5.91E-05				
BCL6	1.373125658	5.94E-05				
GALNT3	1.153141351	6.03E-05				
RELB	1.073045227	6.07E-05				
RUFY3	1.058691974	6.07E-05				
BCHE	1.070908975	6.09E-05				
TPK1	1.304383855	6.16E-05				
HSPA13	1.374546898	6.20E-05				
RNF128	1.263400734	6.21E-05				
HAUS6	1.127419156	6.26E-05				
PKIB	1.530945452	6.30E-05				
C5orf45	1.325272346	6.32E-05				
SLC4A8	1.068452598	6.39E-05				
PKIA	1.2107626	6.46E-05				
PDE4DIP	1.21285223	6.51E-05				
ARHGAP11A	1.150969186	6.61E-05				
CREBRF	2.359506645	6.62E-05				
IL7	1.270482171	6.68E-05				
GBP3	1.189109672	6.69E-05				
SATB1	1.01616666	6.74E-05				
NDRG4	1.036047126	6.78E-05				
SH3GL2	1.083496728	6.84E-05				
ATF3	1.051594427	6.93E-05				
SLC11A2	1.025281447	7.06E-05				
SOX9	1.304648231	7.10E-05				
KLRC3	1.208251269	7.13E-05				
NDRG4	1.073213541	7.15E-05				
RHCE /// RHD	1.090475227	7.32E-05				
ZNF267	1.094847286	7.34E-05				

H6PD	1.020319498	7.47E-05			
RARRES3	1.1360923	7.53E-05			
ESM1	1.437122974	7.69E-05			
RTN4	1.011674182	7.69E-05			
TADA3	1.021631667	7.73E-05			
VWA5A	1.058858612	7.75E-05			
RUNDC3B	1.074414757	7.79E-05			
KLRC3	1.833435524	7.99E-05			
RPS6	1.163845753	7.99E-05			
HIST3H2A	1.004978494	8.09E-05			
PROCR	1.065074076	8.16E-05			
ECSCR	1.054991145	8.39E-05			
RICTOR	1.061654077	8.60E-05			
IPO11 /// LRRC70	1.389943311	8.65E-05			
C6orf57	1.140610739	8.70E-05			
TRAF3IP2	1.000474221	8.83E-05			
LY96	1.251802604	8.94E-05			
CCNL1	1.01395665	9.04E-05			
PTPRR	1.121287574	9.27E-05			
ZNF277	1.264385413	9.46E-05			
DLG4	1.03178504	9.75E-05			
GSAP	1.566228066	9.76E-05			
BTG4	1.421550107	0.000100333			
GNPDA2	1.137007095	0.000105366			
SDR16C5	1.152865543	0.000105492			
GALNT12	1.099605908	0.000109602			
IFI16	1.306771038	0.000113832			
IER5	1.47822647	0.000115176			
PAPOLA	1.09587588	0.000115457			
RRAGD	1.074118359	0.00011549			
RTKN2	1.305080758	0.000116919			
IGFBP3	1.139659821	0.000117944			
LOC100509445 /// LOC728715 /// OVOS2	1.094002677	0.000118204			
PIK3R1	1.222124652	0.000120018			
OTUD4	1.609815998	0.000121889			
PSD3	1.158901453	0.000125629			
SLMAP	1.310325901	0.000126763			
ABCC9	1.008721209	0.000127626			
CCSER2	1.076644673	0.000127937			
EHD1	1.048738367	0.000129318			
HIVEP2	1.020625479	0.000135302			
HILPDA	1.040282802	0.000136054			
LOC101060541 /// RBM8A	1.359816905	0.000136883			

SAA2	1.828177696	0.000139212				
EIF4G3	1.493034934	0.000139488				
FSBP /// RAD54B	1.045760019	0.000140629				
UBXN1	1.138504063	0.000140886				
TIPARP	1.256833168	0.000141216				
DNAJB4	1.0283838	0.000147686				
CYP11A1	1.242400151	0.000150789				
PLA2G16	1.071660159	0.000155545				
HUWE1	1.083788926	0.000160404				
CHRD1	1.335310716	0.000161818				
SLC16A9	1.270492474	0.00016403				
RPL31	1.236005716	0.000164536				
AFF3	1.158222187	0.000165747				
SYTL2	1.595291972	0.000165938				
ROR1	1.38270887	0.000167704				
KLRC3	1.875002452	0.000171659				
SYBU	1.740683826	0.000172944				
PARPBP	1.691976429	0.000174389				
PXK	1.070723908	0.000174803				
Sep-08	1.021569064	0.000176466				
ANKRD37	1.059995387	0.000176814				
ACSM3	1.035318428	0.00017983				
ENC1	1.094588768	0.000184469				
PRDM1	1.027760943	0.000189378				
IER5L	1.045838865	0.000193864				
MBD4	1.034322991	0.000193947				
C6orf141	1.298395926	0.000194066				
HSPA8 /// SNORD14C /// SNORD14D	2.344994793	0.000194343				
ZBTB10	1.300646378	0.000204948				
PLSCR4	1.21499002	0.000210501				
RAB30	1.088561586	0.000211844				
ZC3H12A	1.160964921	0.000217425				
ELOVL4	1.415162641	0.000218767				
NEFL	1.331207496	0.000221714				
LOX	1.019948621	0.000237838				
MLLT11	1.039752315	0.000239504				
HHIPL2	1.096065358	0.000239849				
CEP57	1.047744654	0.00024158				
SLC25A27	1.010710013	0.000247236				
TAPBP	1.153787516	0.000262817				
MIR1304 /// SNORA1 /// SNORA18 /// SNORA25 /// SNORA32 ///	1.315508248	0.000264009				

SNORA40 /// SNORA8 /// SNORD5 /// TAF1D						
IER5L	1.073620698	0.000282191				
PLLP	1.0029813	0.000296666				
SNORA13	1.061993906	0.000313135				
KAL1	1.121403222	0.000317099				
FAM209A /// FAM209B	1.071278568	0.000317508				
DHX58	1.173024152	0.000337687				
MMP1	1.102763965	0.000345105				
MED6	1.018657908	0.000346243				
NCAM1	1.003867401	0.000349107				
ACSL5	1.04997998	0.000368359				
KMT2A	1.000902099	0.000376639				
FN1	1.000633218	0.000391527				
HSPA8 /// SNORD14C /// SNORD14D	1.468550161	0.000398934				
GDF15	1.180090902	0.000403207				
FAM46C	1.323102351	0.000406967				
LYPD3	1.232787859	0.00042414				
GPR155	1.0555431	0.00043195				
CDC37L1	1.042444599	0.000436525				
FGF5	1.05158937	0.000449817				
CEP85L	1.089370652	0.000463257				
RAB38	1.101573487	0.000463561				
GCNT1	1.225881873	0.000479406				
SEMA7A	1.074336246	0.000512655				
SNHG12 /// SNORA16A /// SNORA44 /// SNORA61	1.011990397	0.000521334				
PTGS2	1.193692466	0.000563858				
INSIG1	1.046571848	0.000658464				
CTBS	1.206952402	0.000659636				
BCL6	1.064425997	0.000719362				
SEMA7A	1.223708937	0.000720289				
IL12A	1.194995721	0.000765349				
ELL2	1.018413979	0.000804229				
SLC25A27	1.06602603	0.00082183				
AP4E1	1.017045475	0.000822739				
ZNF429	1.092062805	0.0008236				
EHF	1.789156988	0.000880307				
ELL2	1.183711408	0.000884427				
WWC1	1.109287377	0.000945636				
RIOK3	1.012827329	0.000952047				
HSPA8 ///	1.018455455	0.000985072				

SNORD14C /// SNORD14D						
TRA2A	1.221733708	0.001120129				
N4BP2L1	1.088189751	0.001398107				
PGM3	1.050087887	0.001561197				
HERPUD1	1.111292226	0.001574957				
CA9	1.064663852	0.00157878				
TBC1D23	1.040880106	0.001891876				
PHC3	1.017975028	0.001955994				
---	1.368144568	0.002723023				
---	1.241298491	0.003161807				
---	1.195415672	0.003178671				
HSPA8 /// SNORD14C /// SNORD14D	1.564207339	0.003567988				
---	1.150697195	0.004045257				
---	1.362878087	0.004186667				
MSMO1	1.10611808	0.004220771				
---	1.061586332	0.004245628				
ARHGAP24	1.583088023	0.004792717				
STK3	1.003874484	0.004877002				
---	1.207540511	0.00519097				
---	1.199343233	0.005386741				
---	1.275967504	0.005425272				
---	1.02590189	0.005561549				
NRP2	1.049546605	0.00582824				
---	1.315299187	0.005914881				
---	1.210667857	0.00636832				
---	1.080730374	0.00731582				
---	1.370709071	0.007417625				
---	1.283876951	0.007525705				
---	1.23731884	0.007593536				
---	1.017695171	0.007679367				
---	1.133225298	0.00784318				
---	1.055560797	0.009160947				
---	1.459513376	0.009335727				
---	1.099438759	0.011769916				

Chapter 10

Publication

Raman Spectroscopic Study of Radioresistant Oral Cancer Sublines Established by Fractionated Ionizing Radiation

Mohd Yasser¹, Rubina Shaikh², Murali Krishna Chilakapati^{2*}, Tanuja Teni^{1*}

¹ KS-121, Teni Laboratory, ACTREC, Tata Memorial Centre, Kharghar-Node, Navi Mumbai, India, ² KS-04, Chilakapati Laboratory, ACTREC, Tata Memorial Centre, Kharghar-Node, Navi Mumbai, India

Abstract

Radiotherapy is an important treatment modality for oral cancer. However, development of radioresistance is a major hurdle in the efficacy of radiotherapy in oral cancer patients. Identifying predictors of radioresistance is a challenging task and has met with little success. The aim of the present study was to explore the differential spectral profiles of the established radioresistant sublines and parental oral cancer cell lines by Raman spectroscopy. We have established radioresistant sublines namely, 50Gy-UPCI:SCC029B and 70Gy-UPCI:SCC029B from its parental UPCI:SCC029B cell line, by using clinically admissible 2Gy fractionated ionizing radiation (FIR). The developed radioresistant character was validated by clonogenic cell survival assay and known radioresistance-related protein markers like Mcl-1, Bcl-2, Cox-2 and Survivin. Altered cellular morphology with significant increase ($p < 0.001$) in the number of filopodia in radioresistant cells with respect to parental cells was observed. The Raman spectra of parental UPCI:SCC029B, 50Gy-UPCI:SCC029B and 70Gy-UPCI:SCC029B cells were acquired and spectral features indicate possible differences in biomolecules like proteins, lipids and nucleic acids. Principal component analysis (PCA) provided three clusters corresponding to radioresistant 50Gy, 70Gy-UPCI:SCC029B sublines and parental UPCI:SCC029B cell line with minor overlap, which suggest altered molecular profile acquired by the radioresistant cells due to multiple doses of irradiation. The findings of this study support the potential of Raman spectroscopy in prediction of radioresistance and possibly contribute to better prognosis of oral cancer.

Citation: Yasser M, Shaikh R, Chilakapati MK, Teni T (2014) Raman Spectroscopic Study of Radioresistant Oral Cancer Sublines Established by Fractionated Ionizing Radiation. *PLoS ONE* 9(5): e97777. doi:10.1371/journal.pone.0097777

Editor: Gabriele Multhoff, Technische Universitaet Muenchen, Germany

Received February 7, 2014; Accepted April 23, 2014; Published May 19, 2014

Copyright: © 2014 Yasser et al. This is an open-access article distributed under the terms of the Creative Commons Attribution License, which permits unrestricted use, distribution, and reproduction in any medium, provided the original author and source are credited.

Funding: The Raman spectrometer employed in the study was procured from DBT project BT/PRI11282/MED/32/83/2008, entitled "Development of in vivo laser Raman spectroscopy methods for diagnosis of oral precancerous and cancerous conditions," Department of Biotechnology, Government of India. Mohd Yasser is funded by a fellowship from the University Grants Commission (UGC) - India. The funders had no role in study design, data collection and analysis, decision to publish, or preparation of the manuscript.

Competing Interests: The authors have declared that no competing interests exist.

* E-mail: mchilakapati@actrec.gov.in (MKC); tteni@actrec.gov.in (TT)

Introduction

Oral cancer is the sixth most common cancer worldwide [1]. In India, extensive tobacco usage in various forms makes it the leading type of cancer in males and third most common cancer in females [2,3]. Also, prevalence of oral buccal mucosa cancer type is high in the Indian subcontinent [4]. The treatment modalities of oral cancer are based on various factors including disease stage, access to the oral site, age and physical status of patient. Although surgery is choice of treatment in early stages; radiotherapy holds an important place either alone or as an adjuvant with chemotherapy [5,6]. Standard radiotherapy protocol involves daily exposure of 2Gy fraction dose for few weeks, where patients receive a cumulative dose of 50Gy to 70Gy during the radiotherapy course [7,8,9]. Fractionated radiotherapy kills fast dividing tumour cell population with decreased effects on surrounding normal tissues. Thus this method provides time for normal cells to repopulate and recover while diminishing tumour cells that have aberrantly activated signal transduction pathways [10,11]. However, sometimes tumour recurs with an acquired radioresistant phenotype posing as an obstruction towards the efficacy of radiotherapy. In order to make radiotherapy more

effective; it is important to explore the radioresistant phenotype in cancer cells. Association of several proteins such as p53 [12], Cox-2 [13], Ras [14], pAKT [15], MDM2 [16], Clusterin [17], Survivin [18], Bcl-2 [19] and Mcl-1 [20] with radioresistance have been reported earlier. However, so far there is no available tool that can predict radiotherapy response in oral cancer patients leading towards better treatment.

Biomedical application of optical spectroscopic techniques like Fluorescence, Fourier transfer infra-red (FTIR), Diffused reflectance and Raman spectroscopy (RS) for classification of different pathological conditions and cancer detection has already been reported [21–24]. Among these techniques, RS has added advantages like it is label free, sensitive to biochemical variations, applicable to in vitro and in vivo conditions, has minimum interference from water and provides molecular fingerprints [25–27]. Our previous studies have demonstrated the efficacy of RS in classifying healthy, premalignant and malignant lesions of oral submucosa [28–29]; classification of the normal and abnormal exfoliated cells [30] and in the prediction of tumour response towards concurrent chemo-radiotherapy in cervical cancers [31]. We have shown the potential of RS in identifying early transformation changes in oral buccal mucosa [32], its feasibility

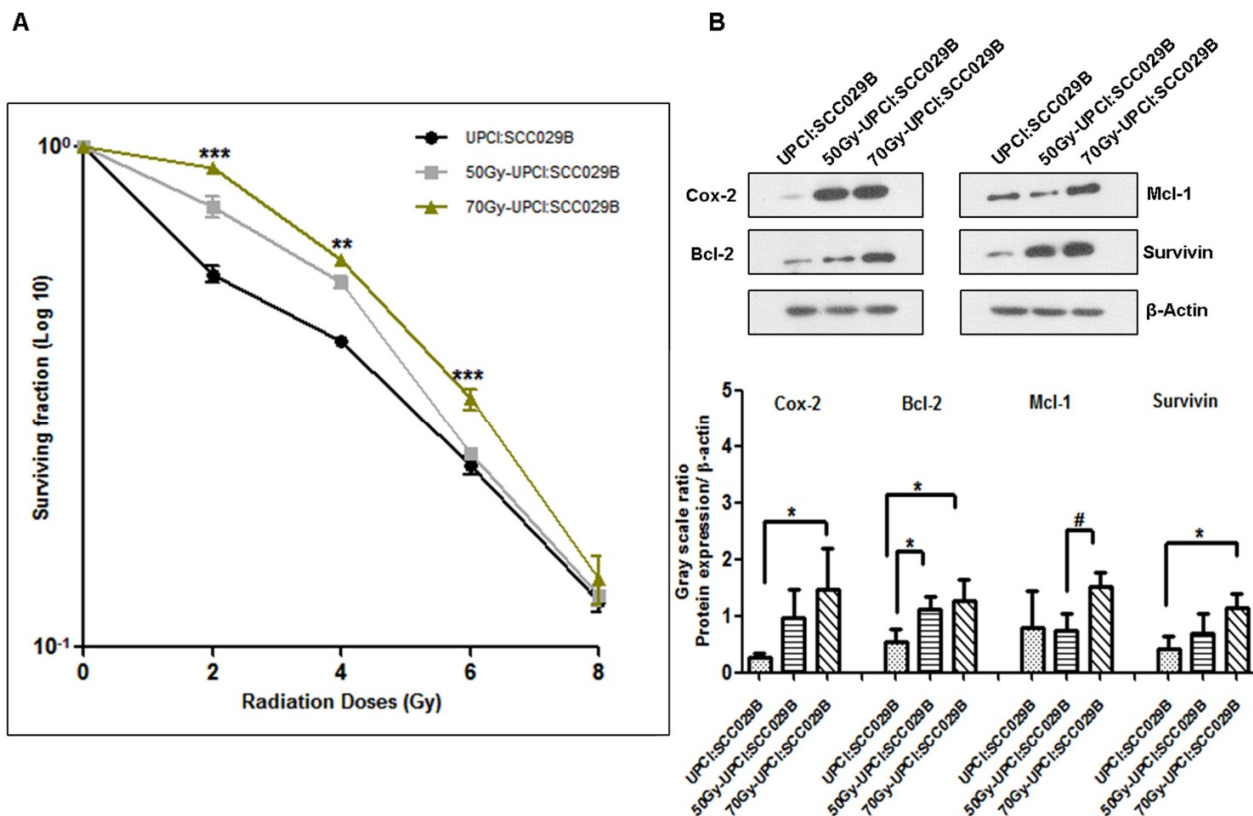


Figure 1. Radiosensitivity of parental and established radioresistant sublines. (A) Clonogenic cell survival curve. UPCI:SCC029B parental cells, 50Gy-UPCI:SCC029B intermediate radioresistant cells and 70Gy-UPCI:SCC029B final radioresistant cells. Data is represented as percentage survival of cells with mean (SD) of three independent experiments. One-way ANOVA statistical analysis was performed on surviving fractions at the given doses, $p < 0.01$ & 0.001 . (B) Expression of radioresistance markers in radioresistant oral sublines. Western blotting for Cox-2, Bcl-2, Mcl-1 and Survivin proteins; β -Actin is used as loading control. Densitometry analysis of western blots from three separate experiments is shown below, bars represent mean \pm s.d. * represent protein expression compared to parental cell line, while # represent protein expression compared between 50Gy-UPCI:SCC029B and 70Gy-UPCI:SCC029B sublines ($p > 0.05$).

doi:10.1371/journal.pone.0097777.g001

in detecting asthma and determining treatment response through serum in asthma patients [33], in classifying normal and oral cancer serum [34] and in identifying multidrug resistance phenotype in human leukemia [35] and uterine sarcoma cell lines [36].

RS studies related to radiation induced biochemical changes in prostate, lung and breast cancer cell lines irradiated with radiation doses between 15 and 50Gy are reported [37,38]. These studies were carried out at single doses of radiation that aimed to investigate the in vitro radiation response on human cancer cell lines. On the other hand, we carried out the present study, taking advantage of continuous low dose fractionated irradiation routinely used as standard radiotherapy protocol in clinics for oral cancer treatment. Our aim was to develop in vitro radioresistance character in the cell line over a period of time and then explore the feasibility of Raman spectroscopy to categorize the acquired trait from its parental untreated cells. We have established radioresistant oral cancer sublines of buccal mucosa origin by clinical implementable 2Gy fractionated radiation dose. After establishing the sublines, their radioresistant character was evaluated by clonogenic cell survival assay and Raman spectral profiles were obtained by RS. To the best of our knowledge, we are first to report the utility of RS in acquired radioresistant oral

cancer sublines established from parental oral cancer cell line by clinically administered fractionated ionizing radiation.

Materials and Methods

Establishment and Characterization of Radioresistant Cell Lines

a) Cell culture and establishment of radioresistant sublines by gamma radiation treatment. UPCI:SCC029B, human oral buccal mucosa carcinoma cell line was kindly provided by Dr. Susanne M. Gollin, University of Pittsburgh, USA [39]. Cells were maintained in Dulbecco's Modified Eagle Medium (DMEM, Gibco) supplemented with 10% heat inactivated fetal bovine serum (FBS, Sigma-Aldrich) and antibiotics (100 U/ml penicillin and 100 mg/ml streptomycin). Cells were maintained at 37°C in 5% CO₂ humidified atmosphere.

To generate radioresistant sublines, UPCI:SCC029B cells (1×10^6 cells) were seeded in 100 mm culture plates (BD-Biosciences) containing complete media. Cells were grown in standard condition and were irradiated with 2Gy of ionizing radiation using ⁶⁰Co-c Linear Accelerator (Bhabhatron-2, AC-TREC, Tata Memorial Centre) at 60% confluency. Immediately after irradiation the culture medium was renewed and cells were placed in incubator till they reached 90% confluency. Cells were

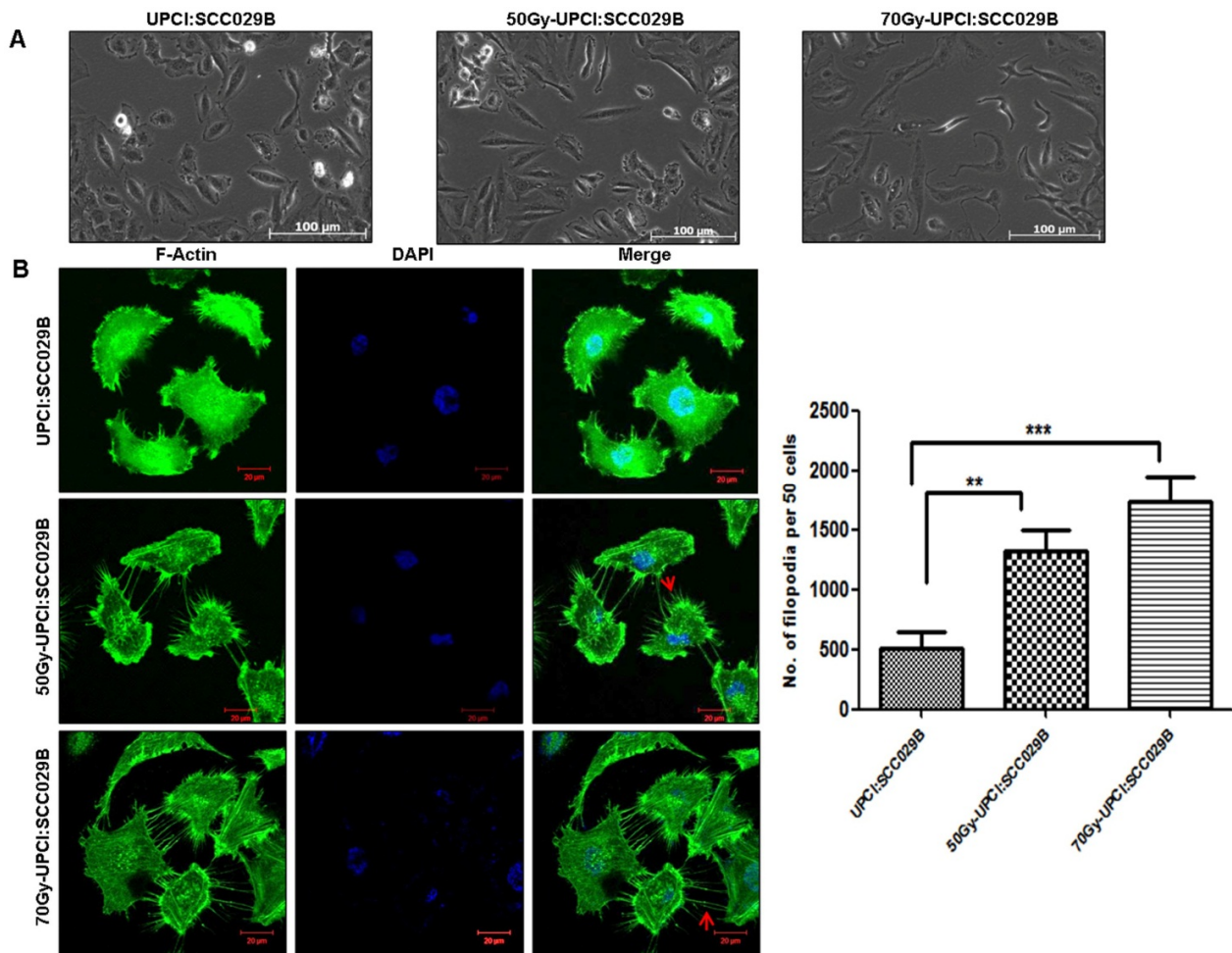


Figure 2. Fractionated irradiation leads to change in cell morphology. (A) Cell morphology analysis. Parental UPCI:SCC029B cells, radioresistant 50Gy-UPCI:SCC029B and 70Gy-UPCI:SCC029B cells. Scale bars: 100 µm. (B) Confocal images of filamentous-Actin stained with Alexa Fluor-488 phalloidin, cells were counter stained with DAPI. Scale bars: 20 µm. Arrow indicates filopodia as fine cell surface extensions. Analysis based on 50 cells per population with mean and standard deviation of three independent experiments, plotted at below right side ($p < 0.01, 0.001$). doi:10.1371/journal.pone.0097777.g002

then trypsinized, counted and passage into new culture plates. The cells were treated again with 2Gy of ionizing radiation at about 60% confluency. This procedure was repeated 25 times for generation of intermediate 50Gy-UPCI:SCC029B radioresistant subline and further continued upto 35 times over a period of 5 to 6 months till generation of final 70Gy-UPCI:SCC029B radioresistant subline.

b) Clonogenic cell survival assay. Briefly, known number of both the parental and radioresistant cells of UPCI:SCC029B were seeded in 100 mm culture plates and kept in CO₂ incubator overnight for adherence to the plates. Next day, cells were irradiated with even doses from 2Gy to 8Gy and incubated at 37°C for colony formation. After 14 days, colonies were fixed with absolute ethanol and stained with 0.1% crystal violet. Colonies consisting of 50 or more cells were counted as clonogenic survivors. The percent plating efficiency, D0 value (radiation dose at which 37% population survives) and surviving fraction at a given radiation dose were calculated on the basis of survival of non-irradiated cells as described earlier [40]. Three independent experiments were performed, each time in duplicates with parental and radioresistant sublines and cell survival curve was plotted after

calculating surviving fraction at each dose. Further, One-way ANOVA statistical analysis was performed to find the significant difference in survival at different doses of radiation.

c) Western blotting. Cells were lysed in mammalian cell lysis buffer containing 1% protease inhibitor (Thermo scientific, USA). The cell lysate was centrifuged at 13,000 rpm for 10 min at 4°C and supernatant containing total cellular protein was collected. The protein concentration was quantified by colorimetric assay [41]. Samples containing 40 µg total proteins were separated by 12% SDS-PAGE and transferred to a PVDF membrane (PALL laboratory, USA). The membranes were blocked at room temperature for 1 hour by incubation in TBS containing 0.1% Tween (TBST, pH 7.4) and 5% (w/v) low fat milk. After blocking, membranes were incubated with rabbit polyclonal IgG human anti-Mcl-1 (1:1000, sc-20679); Bcl-2 (1:500, sc-492), Survivin (1:1000, sc-10811), goat polyclonal IgG anti-Cox-2 (1:500, sc-1747) and housekeeping rabbit polyclonal IgG anti-β Actin (1:3000, sc-1616); (Santa Cruz Biotech., USA) overnight in blocking buffer. After washing six times in TBST, the membranes were incubated with an HRP-conjugated anti-rabbit IgG antibody (1:2800) or anti-goat IgG antibody (1:2500, Santa Cruz Biotech-

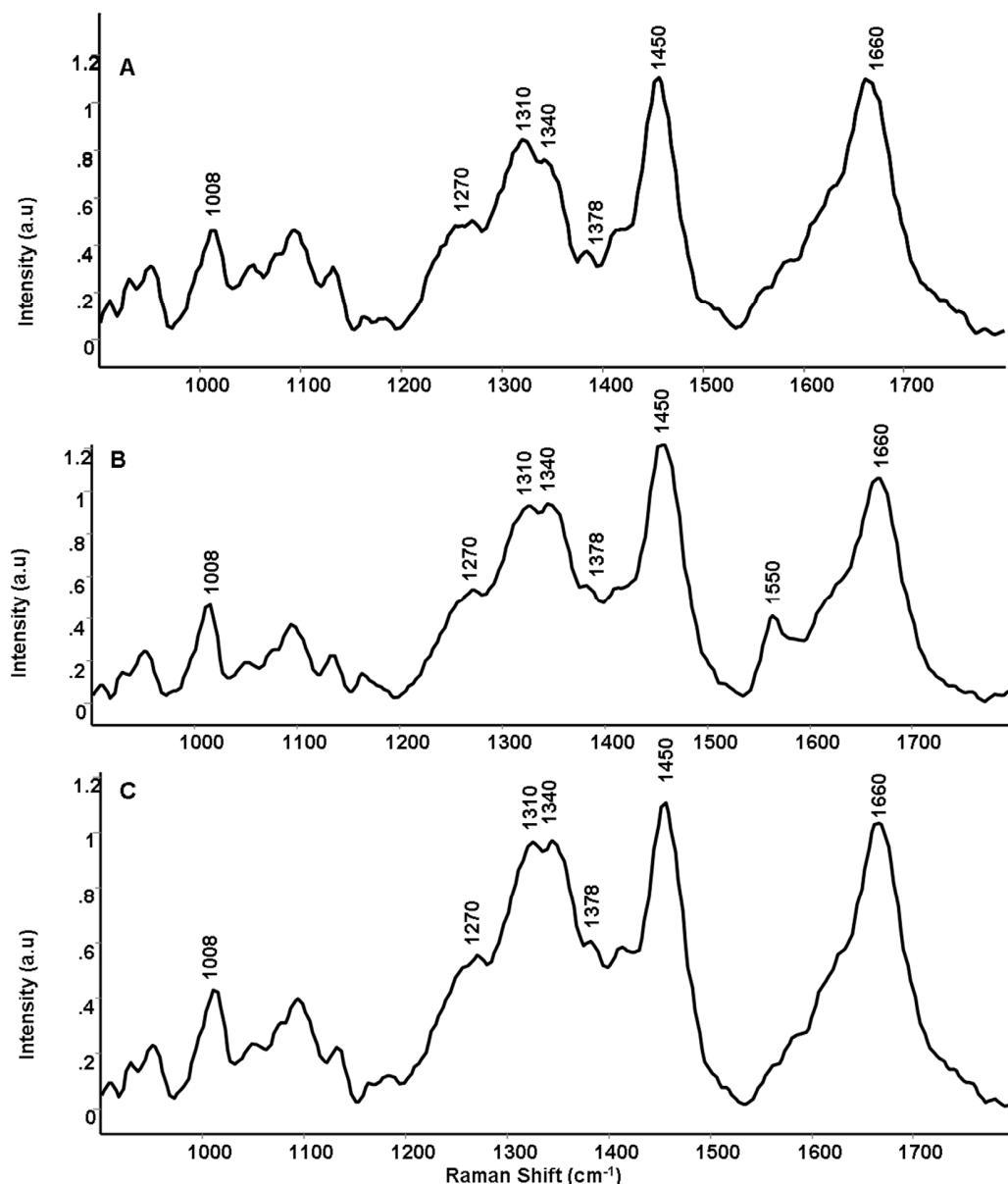


Figure 3. Mean Raman spectra of parental and radioresistant sublines. (A) Parental UPCI:SCC029B cell line (B) 50Gy-UPCI:SCC029B subline (C) 70Gy-UPCI:SCC029B subline.

doi:10.1371/journal.pone.0097777.g003

nology) in blocking buffer for 1 hour. After washing six times in TBST and two times in TBS, primary antibody binding was visualized by enhanced chemiluminescence substrate system (GE healthcare, USA). The western blotting was performed on three independent cell lysates of parental, 50Gy and 70Gy cells. The densitometry analysis was performed by Image J software (NIH, USA) against b-Actin housekeeping protein expression.

d) Morphological evaluation and F-Actin staining. Morphological changes observed during fractionated ionizing radiation were photographed by using the inverted microscope (Axiovert-200M, Zeiss) coupled with digital camera. Representative images of parental UPCI:SCC029B cell line, 50Gy-UPCI:SCC029B and 70Gy-UPCI:SCC029B sublines were processed by using Axiovision software (release 4.7, Carl Zeiss).

For filamentous Actin staining, cells were grown on coverslips, fixed with paraformaldehyde (4%) for 15 minutes and permeabilized in 0.7% Triton-X. A high affinity filamentous Actin (F-Actin) probe Alexa Fluor-488 phalloidin (Life technologies, USA) was diluted 1:20 (in 1X PBS) and incubated with cells on coverslips for

30 minutes at room temperature in dark. After incubation, the coverslips were washed two times with 1X PBS for 10 minutes. DAPI (1:20 diluted in 1X PBS) staining was done for approximately 1 minute and coverslips were then mounted in anti-quenching mounting agent (Vectashield, Vector labs, USA) on a clean glass slide and examined with LSM 510 Meta Carl Zeiss confocal system (Carl Zeiss Micro Imaging GmbH, Germany). Each of the parental, 50Gy and 70Gy cells were grown in duplicates on coverslips and random images for 50 cells were

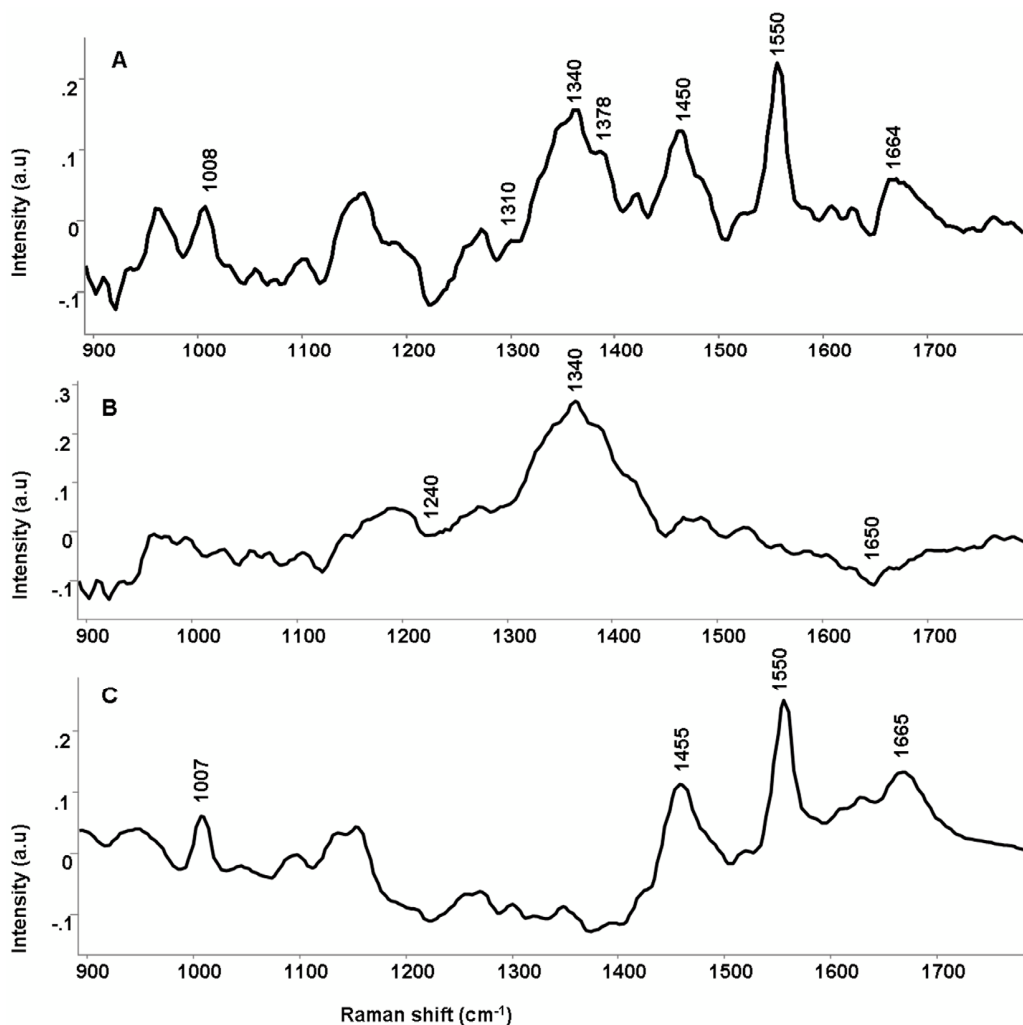


Figure 4. Difference Raman spectra of parental and radioresistant sublines. (A) 50Gy-UPCI:SCC029B subline – parental UPCI:SCC029B cell line (B) 70Gy-UPCI:SCC029B subline – parental UPCI:SCC029B cell line (C) 50Gy-UPCI:SCC029B subline – 70Gy-UPCI:SCC029B subline. doi:10.1371/journal.pone.0097777.g004

acquired. In this way, the staining was performed three times independently and 50 cells were analysed each time from all the cell population types for filopodia counting.

Raman Spectroscopy

a) Sample preparation and spectral acquisition. Parental UPCI:SCC029B, 50Gy-UPCI:SCC029B and 70Gy-UPCI:SCC029B cells were cultured in 100 mm culture plates. Exponentially growing cells (3.6×10^6 cells) from 6 independent cultures of each of the parental, 50Gy and 70Gy cells were harvested and phosphate buffer saline (PBS) wash was given to the cell pellets prior to spectra recording. Approximately 7 spectra were acquired from each cell pellet by using fibre-optic Raman microprobe system as described earlier [33]. Thus a total of ~ 40 spectra per group were acquired for each of the parental, 50Gy and 70Gy cells.

As mentioned above, Raman system utilized for study consists of a diode laser (Process Instruments) of 785 nm wavelength as excitation source and a high efficiency (HE-785, Horiba-Jobin-Yvon, France) spectrograph coupled with a CCD (Synapse, Horiba-Jobin-Yvon, France) as detection element. Optical filtering

of unwanted noise including Rayleigh signals are accomplished through 'Superhead' the auxiliary component of the system. Super head coupled with a 40 \times microscopic objective (Nikon, NA 0.65) was used to deliver laser light as well as to collect Raman signals. The spectrograph has no movable parts with fixed 950 gr/mm grating and spectral resolution as per manufacturer's specification is $\sim 4 \text{ cm}^{-1}$. Estimated laser spot size at the cell pellet sample was 5–10 mm. Spectra were integrated for 6 seconds and averaged over 3 accumulations. Typical laser power at the specimen was 40 \pm 0.05 mW.

b) Spectral pre-processing and data analysis. Raman spectra were pre-processed by correcting charged couple device (CCD) response by a National Institute of Standards and Technology (NIST) certified standard reference material 2241 (SRM 2241) followed by subtraction of background signals from optical elements and CaF_2 window. To remove interference of the slow moving background, first derivatives of spectra (Savitzky - Golay method) were used for data analysis [42,43]. Then spectra were interpolated in the 900–1800 cm^{-1} range and vector normalized. Analysis of the pre-processed spectra was carried out using PCA (principal component analysis)

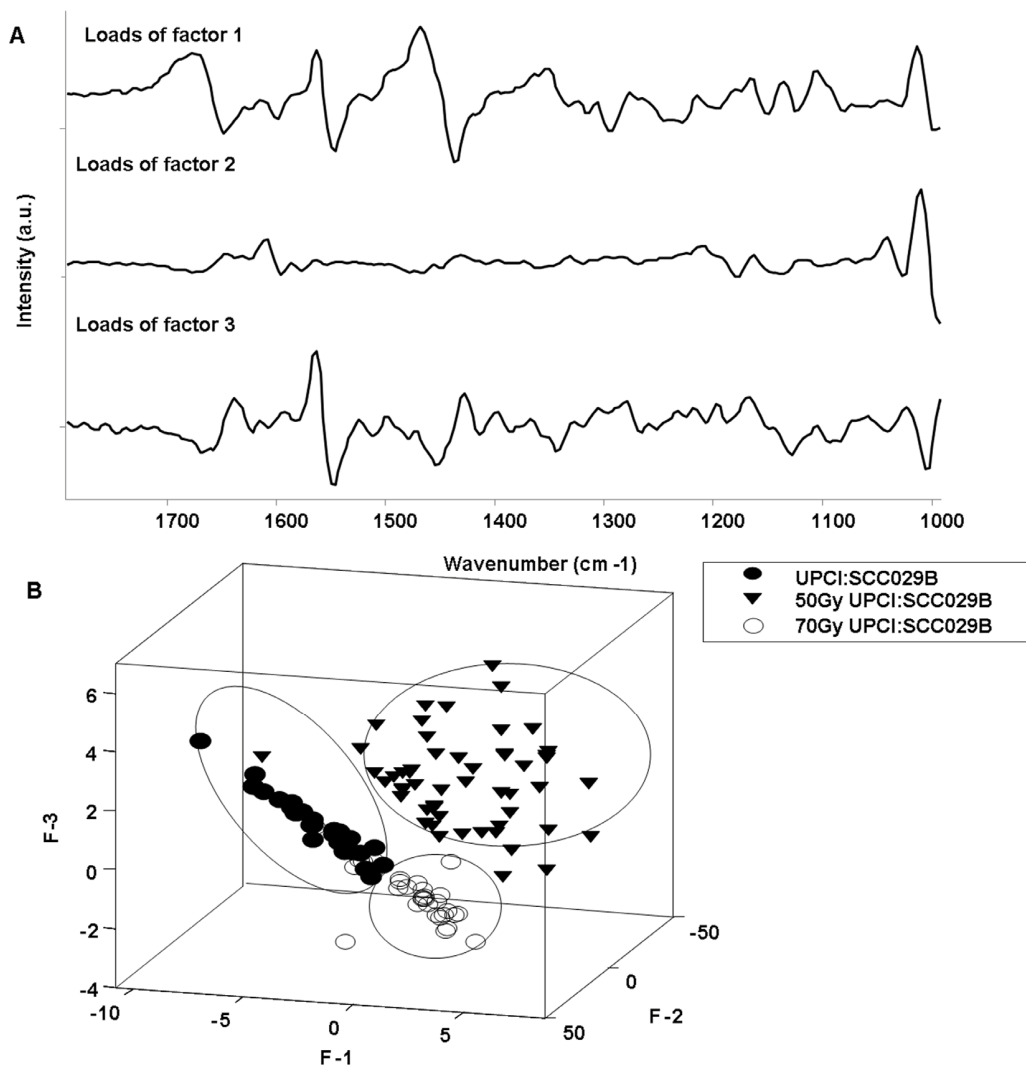


Figure 5. PCA analysis for parental and radioresistant sublines. (A) Loads of factor 1, 2 and 3 (B) 3-D scatter plot for parental UPCI:SCC029B cell line, radioresistant 50Gy-UPCI:SCC029B and 70Gy-UPCI:SCC029B sublines.
doi:10.1371/journal.pone.0097777.g005

algorithms implemented in MATLAB (Mathwork Inc.) based in-house software [44]. PCA is unsupervised data overview tool used to look at the differences and similarities among the spectra. This method reveals outliers, groups and trends in the data. It describes data variance by identifying a new set of orthogonal features, these are known as loads of factor or principal components (PCs) ($p < 0.05$). Principal components are linear combinations of original data variables. As the present study is an exploratory study therefore we have carried out PCA method of analysis and also used this method in our earlier *in vitro* studies on cell lines [35,36].

Mean and difference spectra were calculated for different cell populations and were used for spectral comparison. The mean spectra were computed from the background subtracted spectra prior to derivatization by averaging Y-axis variations and keeping the X-axis constant for each class. The baseline correction was performed by fitting a 5th order polynomial function. These baseline corrected spectra were used for spectral comparisons across all groups. Difference spectra were generated by subtracting the mean spectra of radioresistant cells (50Gy-UPCI:SCC029B &

70Gy-UPCI:SCC029B) with parental cells (UPCI:SCC029B) as well as by subtracting spectra of 50Gy-UPCI:SCC029B from 70Gy-UPCI:SCC029B cells.

Statistical Analysis

Data were statistically analysed by One-way ANOVA and Student's t-test, using Graph Pad Prism 5 software (version 5.01). A p value less than 0.05 was considered statistically significant. The statistical analysis used for Raman spectra processing are described under the respective section.

Results and Discussion

a) Development and Validation of Radioresistant Sublines

The radiotherapy protocols for oral cancer treatment consist of a total 50Gy to 70Gy radiation dose vide low dose fractionated radiation of 2Gy. Hence, two radioresistant sublines i.e. 50Gy-UPCI:SCC029B and 70Gy-UPCI:SCC029B were established by total 25 and 35 fractions of 2Gy respectively over a period of 5–6 months. The radioresistant character of sublines was demonstrated

by clonogenic cell survival assay. We have observed significant increase in cell survival for both of the radioresistant sublines as compared to its parental cell line by clonogenic assay [Fig-1(A)]. D0 doses for the parental, 50Gy and 70Gy subline were calculated and found to be 4.5Gy, 5.1Gy and 5.6Gy respectively. An increase in the D0 value for the radioresistant sublines from its parental cell line indicates their acquired radioresistance character. We also determined the status of known radioresistant and anti-apoptotic protein markers like Bcl-2 (B cell lymphoma-2), Mcl-1 (myeloid cell leukemia-1), Survivin & Cox-2 (cyclooxygenase-2) by western blotting. As illustrated in Fig-1(B) an increase in the levels of these proteins was observed in radioresistant sublines (except Mcl-1 in 50Gy-UPCI:SCC029B) as compared to parental cell line. The Mcl-1 levels in the intermediate 50Gy-UPCI:SCC029B subline were although comparable (densitometry analysis, Figure-1B, lower) to that of parental cell line and was found to be further significantly upregulated in the radioresistant 70Gy:UPCI:SCC029B subline. It is noteworthy that Mcl-1 has short half-life due to its rapid turnover through ubiquitination [45] and although Mcl-1 cellular stability against various stress factors has been studied but little is known about its regulatory mechanism on account of radiation treatment. Our result possibly implies that pathways including Bcl-2, Survivin and Cox-2 may contribute to the increased survival for radioresistant cells at early stages of acquired radioresistance development while Mcl-1 may have a role in later stage. Moreover, as mentioned in clonogenic cell survival assay, the 50Gy-UPCI:SCC029B cells acquired the radioresistance character and higher levels of other radioresistance related proteins in comparison to the parental cells. Therefore, development of radioresistance is a complex phenomenon that cannot be associated with a single marker or protein within the cell. The significant increase in the expression of these markers corroborates with earlier reports, including those from our laboratory on their association with radioresistance in oral squamous cell carcinomas [13,18–20,46–47].

b) Morphological Characterization of Radioresistant Sublines

We have observed altered morphology of radioresistant sublines in comparison to its parental cell line. The 50Gy-UPCI:SCC029B cells exhibited spindle shaped morphology while 70Gy-UPCI:SCC029B cells were found to be more elongated and irregular in shape [Fig-2(A)]. The gain of these morphological features in radioresistant sublines might hint towards its transformed characteristic related to the migration and invasion. Further, in order to get an insight in their actin reorganization; we have performed filamentous Actin (F-Actin) staining in the parental, 50Gy and 70Gy UPCI:SCC029B cells. F-Actin staining showed significant increase [Fig-2(B)] in the number of filopodia in 50Gy ($p > 0.01$) and 70Gy-UPCI:SCC029B ($p > 0.001$) cells in comparison to parental UPCI:SCC029B cells. The morphological changes exhibited by the radioresistant cells can be an additional phenotype acquired due to the continuous fractionated radiation treatment.

c) Raman Spectroscopy of Parental and Radioresistant Sublines

The mean normalized spectra for parental UPCI:SCC029B cell line, radioresistant 50Gy and 70Gy-UPCI:SCC029B sublines were computed and depicted in Figure-3. Mean spectrum has been used as a representative spectrum for the respective cell lines in the spectral analysis. As, illustrated in Figure-3, the spectral features were dominated by bands around 1008 (phenylalanine), 1270

(amide III), 1450 (d CH₂) and 1660 (amide I) cm⁻¹ and may be attributed to cellular proteins. Whereas, bands at 1310 (CH₃/CH₂) twisting or bending modes of lipid), 1340 (ring structure of adenine) and 1378 cm⁻¹ (ring breathing modes of nucleic acid) suggest presence of cellular nucleic acid and lipids. The mean spectra for 50Gy-UPCI:SCC029B cells [Fig-3(B)] showed shift around 1310, 1450 and 1660 cm⁻¹; while a prominent peak was observed at 1550 cm⁻¹ (tryptophan). Similarly, in mean spectra of radioresistant 70Gy-UPCI:SCC029B cells [Fig-3(C)] intensity related variations at 1270, 1310, 1340 and 1660 cm⁻¹ whereas a shift at 1450 cm⁻¹ was observed. Thus, it can be observed that overall differences in the form of shifts in Raman bands and intensity variations were observed in the average spectra of both the 50Gy and 70Gy groups.

In order to bring out spectral differences among groups; the difference spectra were calculated from mean spectra. The difference spectra provide a more clear illustration for the differences among groups. As shown in Figure-4, the difference spectra were computed for 50Gy-UPCI:SCC029B and 70Gy-UPCI:SCC029B cells by subtracting them from parental UPCI:SCC029B cells [Fig-4(A,B)] and between the two radioresistant cells [Fig-4 (C)]. The difference spectrum (50Gy - parental) exhibited positive peaks at 1008, 1340, 1378, 1450, 1550, 1664 cm⁻¹ and negative peaks at 1240 and 1310 cm⁻¹; suggesting changes in proteins and nucleic acids, possibly due to altered cell signalling cascades caused by irradiation [48]. The noticeable change at 1550 cm⁻¹ in 50Gy cells is indicative of freely accessible tryptophan possibly as a result of protein folding/misfolding by activated chaperones due to radiation stress. Similarly, in difference spectrum (70Gy - parental) positive peaks were observed at 1340 and 1378 cm⁻¹ which is associated with DNA, whereas negative peak was observed at 1240, 1450 and 1650 cm⁻¹ associated with protein change.

As shown by clonogenic assay, both the 50Gy-UPCI:SCC029B and 70Gy-UPCI:SCC029B cells have acquired radioresistant character in comparison to parental cells. Also, 70Gy cells are relatively more radioresistant than 50Gy cells and exhibit distinct difference spectra, which may be due to different properties acquired by them. Moreover, the (50Gy-70Gy) difference spectrum show positive peaks at 1008, 1450, 1550 and 1664 cm⁻¹ all related to proteins while DNA related negative peak was observed at 1378 cm⁻¹. The presence of prominent positive tryptophan peak (1550cm⁻¹) in 50Gy radioresistant subline hint towards the enriched tryptophan moieties that may have anti-oxidative property because of the indolic group which serves as hydrogen radical donor [49]. Since, ionizing radiation can induce reactive oxygen species (ROS) production that can cause endogenous attack on the deoxyribosyl backbone of DNA [50,51]. To counteract the effect of ROS, cells have several antioxidant factors that can scavenge ROS and protect against radiation [52]. The distinct tryptophan residue peak in 50Gy radioresistant cells might correlate with such factors that are rich in these residue types which shields the cell against oxidative stress. The upregulation of these factors have also been reported in the context of radioresistance [53–55]. Moreover, the recorded spectrum may result in an average and representative spectrum of the given cell line that reflects an overall information of the cell status; because in a cell pellet, the probing beam encounters a stack of cells and scattering can be expected from different organelles like nucleus, mitochondria and other cellular compartments.

d) Multivariate Analysis

As mentioned above, PCA was used to explore the feasibility of classification among radioresistant 50Gy and 70Gy sublines from the parental cell line. PCA is frequently used method for data compression and visualization to observe the pattern in the data. It is a mathematical analysis by which the features in the whole data set of thousands of points are resolved into a few significant eigenvectors that can express the entire data set with their scores for each spectrum. This can provide imperative clues on biochemical variations among different groups, in our case different classes of macromolecules. Further, the profiles of principal components also known as factor loadings can provide vital clues on biochemical variations among different classes. Loading of factors 1, 2 and 3 that lead to demarcation among groups are presented in Figure-5(A). Conforming spectral variability as suggested by difference spectra; the loading plots also indicate differences in DNA content, amino acids and protein profiles of parental and radioresistant groups. For visual discrimination, we project each of the spectra in the newly formed co-ordinate space of selected PCs. First three significant discriminating PCs were selected for three-dimensional visualization of the data. Three clusters belonging to parental UPCI:SCC029B cells and radioresistant 50Gy- UPCI:SCC029B, 70Gy-UPCI:SCC029B cells was observed [Fig-5(B)]. While 50Gy-UPCI:SCC029B cells formed a separate cluster but slight overlap between the clusters of 70Gy-UPCI:SCC029B and parental cells was observed. These pattern clustering may be due to overall different biochemical profile acquired by the cell types. Taking in view that PCA will reveal an overall change including the various cellular profiles, it indicates that radioresistant cells have acquired an altered molecular profile different from its parental cells with subtle variations.

Conclusion

In the present work, we have established radioresistant sublines from the parental oral buccal mucosa cell line using clinically admissible fractionated radiation dose. The acquired resistant character was determined by the standard clonogenic cell survival assay. The 50Gy-UPCI:SCC029B and 70Gy-UPCI:SCC029B established radioresistant sublines were found to be more

radioresistant in comparison to its parental UPCI:SCC029B cell line. The sublines were also characterized by assessing expression of radioresistance related protein markers like Mcl-1, Bcl-2, Cox-2 and Survivin that support their acquired radioresistant phenotype. Altered morphological features were observed in these long term irradiated cells that were different from the parental cells, including significant increase in filopodia numbers in 50Gy-UPCI:SCC029B cells and 70Gy-UPCI:SCC029B radioresistant cells. Further, Raman spectroscopy was performed on these radioresistant cells and parental cells to study their differential spectral profile. This study is first of its kind regarding utility of RS in characterization of acquired radioresistant sublines. The observed differential spectra between parental and both the radioresistant cells were majorly due to changes in DNA, lipid and protein profile of cells. Alterations in DNA content of these cells may be because of numerous genetic insults occurring through multiple fractions of radiation by FIR and change in lipids may be predominantly due to the altered morphology of these cells as shown above. The multivariate analysis using PCA revealed that the radioresistant 50Gy-UPCI:SCC029B and 70Gy-UPCI:SCC029B cells can be categorized from its parental UPCI:SCC029B cells. Taken together, the results of our work are quite promising and suggest the feasibility of RS as a potential non-invasive tool for oral cancer patients in predicting radiation response through spectral markers. It may improve the patient survival rates by virtue of optical diagnosis to categorize them in radiosensitive and resistant types; thereby help in selecting better treatment regimens.

Acknowledgments

The authors acknowledge Mr. Yashwant S. Temkar, Teni laboratory - ACTREC for his help in tissue culture; Mr. S.M Sawant, photography section ACTREC for his technical assistance and Dr. Susanne M. Gollin, University of Pittsburgh for providing the UPCI:SCC029B cell line.

Author Contributions

Conceived and designed the experiments: MY TT MKC. Performed the experiments: MY RS. Analyzed the data: TT MKC MY RS. Contributed reagents/materials/analysis tools: TT MKC. Wrote the paper: MY RS TT MKC.

References

1. Ferlay J, Shin HR, Bray D, Forman D, Mathers C, et al. (2010) Estimates of worldwide burden of cancer in 2008. *Int J Cancer* 127: 2893–2917.
2. Dikshit R, Gupta PC, Ramasundarahettige C, Gajalakshmi V, Aleksandrowicz L, et al. (2012) Cancer mortality in India: a nationally representative survey. *The Lancet*. doi: 10.1016/S0140-6736(12)60358-4.
3. Rajendran R, Shivapathasundharam B (2009) *Shafers Textbook of Oral Pathology*. Elseviers, New York, 6th edition.
4. Singh AD, Von Essen CF (1966) Buccal mucosa cancer in south India; etiologic and clinical aspects. *Am J Roentgenol* 96: 1.
5. Bessell A, Glenn AM, Furness S, Clarkson JE, Oliver R, et al. (2011) Interventions for the treatment of oral and oropharyngeal cancers: surgical treatment. *Cochrane Database System Rev* 9:CD006205.
6. Huang SH, Sullivan BO (2013) Current role of radiotherapy and chemotherapy. *Med Oral Patol Oral Cir Bucal* 18(2):e233–40.
7. John-Aryankalayil M, Palayoor ST, Cema D, Simone CB 2nd, Falduto MT, et al. (2010) Fractionated radiation therapy can induce a molecular profile for therapeutic targeting. *Radiat Res* 174: 446–458.
8. Martínez Carrillo M, Tovar Martín I, Martínez Lara I, Ruiz de Almodóvar Rivera JM, Del Moral Ávila R (2013) Selective use of postoperative neck radiotherapy in oral cavity and oropharynx cancer: a prospective clinical study. *Radiat Oncol* 8: 103. doi: 10.1186/1748-717X-8-103.
9. Bonner JA, Harari PM, Giralt J, Azarnia N, Shin DM, et al. (2006) Radiotherapy plus cetuximab for squamous-cell carcinoma of the head and neck. *N Engl J Med* 9; 354(6): 567–78.
10. Bucci B, Misiti S, Cannizzaro A, Marchese R, Raza GH, et al. (2006) Fractionated ionizing radiation exposure induces apoptosis through caspase-3 activation and reactive oxygen species generation. *Anticancer Res* 26: 4549–4558.
11. Fenton RG, Longo DL (2011) Cancer cell biology and angiogenesis. *Harrison's Principles of Internal Medicine*, 18th Edition, p. 294–317.
12. Bates S, Vousden KH (1996) p53 in signalling checkpoint arrest or apoptosis. *Curr Opin Genet Dev* 6: 12–18.
13. Terakado N, Shintani S, Yano J, Chunnan L, Mihara M, et al. (2004) Overexpression of cyclooxygenase-2 is associated with radioresistance in oral squamous cell carcinoma. *Oral Oncol* 40: 383–9.
14. Sklar MD, Thompson E, Welsh MJ, Liebert M, Harney J, et al. (1991) Depletion of c-myc with specific antisense sequences reverses the transformed phenotype in ras oncogene-transformed NIH 3T3 cells. *Mol Cell Biol* 11(7): 3699.
15. Osaki M, Oshimura M, Ito H (2004) PI3K-Akt pathway: its functions and alterations in human cancer. *Apoptosis* 9(6): 667–76.
16. Chen J, Lin J, Levine AJ (1995) Regulation of transcription functions of the p53 tumor suppressor by the mdm-2 oncogene. *Mol Med* 1: 142–152.
17. Shannan B, Seifert M, Boothman DA, Tilgen W, Reichrath J (2006) Clusterin and DNA repair: a new function in cancer for a key player in apoptosis and cell cycle control. *J Mol Histol* 37(5–7): 183–188.
18. Ambrosini G, Adida C, Altieri DC (1997) A novel anti-apoptosis gene, survivin, expressed in cancer and lymphoma. *Nat Med* 3: 917–921.
19. Kitada S, Miyashita T, Tanaka S, Reed JC (1993) Investigations of antisense oligonucleotides targeted against bcl-2 RNAs. *Antisense Res & Develop* 3: 157–169.
20. Skvara H, Thallinger C, Wacheck V, Monia BP, Pehamberger H, et al. (2005) Mcl-1 Blocks Radiation-induced Apoptosis and Inhibits Clonogenic Cell Death. *Anticancer Res* 25: 2697–2704.

21. De Veld DC, Witjes MJ, Sterenborg HJ, Roodenburg JL (2005) The status of in vivo autofluorescence spectroscopy and imaging for oral oncology. *Oral Oncol* 41(2): 117–131.
22. Wu JG, Xu YZ, Sun CW, Soloway RD, Xu DF, et al. (2001) Distinguishing malignant from normal oral tissues using FTIR fiber-optic techniques. *Biopolymers* 62(4): 185–192.
23. Ferreira DS, Coutinho PG, Castanheira ES, Correia JH, Minas G (2010) Fluorescence and diffuse reflectance spectroscopy for early cancer detection using a new strategy towards the development of a miniaturized system. *Conf Proc IEEE Eng Med Biol Soc* 1210(3). doi: 10.1109/IEMBS.2010.5626448.
24. Venkatakrishna K, Kurien J, Pai KM, Murali Krishna C, Ullas G, et al. (2001) Optical pathology of oral tissue: A Raman spectroscopy diagnostic method. *Curr Sci* 80(1): 665–669.
25. Krishna CM, Sockalingum GD, Kurien J, Rao L, Vento L, et al. (2004) Micro-Raman spectroscopy for optical pathology of oral squamous cell carcinoma. *Appl Spectrosc* 58(9): 1128–1135.
26. Malini R, Venkatakrishna K, Kurien J, Pai KM, Rao L, et al. (2006) Discrimination of normal, inflammatory premalignant, and malignant oral tissue: a Raman spectroscopy study. *Biopolymers* 81(3): 179–193.
27. Nijssen A, Koljenovic S, Schut TCB, Caspers PJ, Pupples GJ (2009) Towards oncological application of Raman spectroscopy. *J Biophoton* 2(1–2): 29–36.
28. Singh SP, Deshmukh A, Chaturvedi P, Krishna CM (2012) Raman spectroscopy in head and neck cancers: Toward oncological applications. *J Cancer Res Ther* 8(6): 126–132.
29. Singh SP, Deshmukh A, Chaturvedi P, Krishna CM (2012) In vivo Raman spectroscopic identification of premalignant lesions in oral buccal mucosa. *J Biomed Opt* 17(10): 105002. doi:10.1117/1.jbo.17.10.105002.
30. Rubina S, Maheswari A, Deodhar KK, Bharat R, Krishna CM (2013) Raman spectroscopic study on classification of cervical cell specimens. *Vib Spectrosc* 68: 115–121.
31. Rubina S, Vidyasagar MS, Krishna CM (2013) Raman spectroscopic study on prediction of treatment response in cervical cancers. *J Innov Opt Health Sci* 6(2): 1350014.
32. Singh SP, Sahu A, Deshmukh A, Chaturvedi P, Krishna CM (2013) In vivo Raman spectroscopy of oral buccal mucosa: a study on malignancy associated changes (MAC)/cancer field effects (CFE). *Analyst* 138: 4175–4182. doi: 10.1039/c3an36761d.
33. Sahu A, Dalal K, Naglot S, Aggarwal P, Krishna CM (2013) Serum Based Diagnosis of Asthma Using Raman Spectroscopy: An Early Phase Pilot Study. *Plos one* 8(11): e78921. doi:10.1371/journal.pone.0078921.
34. Sahu A, Sawant S, Mangain H, Krishna CM (2013) Raman spectroscopy of serum: an exploratory study for detection of oral cancers. *Analyst*. doi: 10.1039/c3an00308f.
35. Krishna CM, Kegelaer G, Adt I, Rubin S, Kartha VB, et al. (2006) Combined Fourier transform infrared and Raman spectroscopic approach for identification of multidrug resistance phenotype in cancer cell lines. *Biopolymers* 82(5): 462–70.
36. Krishna CM, Kegelaer G, Adt I, Rubin S, Kartha VB, et al. (2005) Characterisation of uterine sarcoma cell lines exhibiting MDR phenotype by vibrational spectroscopy. *Biochim Biophys Acta* 1726(2): 160–7.
37. Matthews Q, Brolo A, Lum J, Duan X, Jirasek A (2011) Raman spectroscopy of single human tumour cells exposed to ionizing radiation in vitro. *Phys Med Biol* 56(1): 19–38.
38. Matthews Q, Jirasek A, Lum JJ, Brolo AG (2011) Biochemical signatures of in vitro radiation response in human lung, breast and prostate tumour cells observed with Raman spectroscopy. *Phys Med Biol* 56(21): 6839–55.
39. Martin CL, Reshmi SC, Ried T, Gottberg W, Wilson JW, et al. (2008) Chromosomal imbalances in oral squamous cell carcinoma. Examination of 31 cell lines and review of the literature. *Oral Oncol* 44(4): 369–382.
40. Franken NA, Rodermond HM, Stap J, Haveman J, Van Bree C (2006) Clonogenic assay of cells in vitro. *Nat Protocol* 1(5): 2315–9.
41. Lowry OH, Rosenborough NJ, Farr AL, Randall RJ (1951) Protein measurement with Folin phenol reagent. *J Biol Chem* 193: 65–75.
42. Nijssen A, Maquelin K, Caspers PJ, Schut TCB, Neumann MHA, et al. (2007) Discriminating basal cell carcinoma from perilesional skin using high wave-number Raman spectroscopy. *J Biomed Opt* 12(3): 034004–1.
43. Koljenovic S, Choo-Smith LP, Schut TCB, Kros JM, Berge HJ, et al. (2002) Discriminating vital tumor from necrotic tissue in human glioblastoma tissue samples by Raman spectroscopy. *Lab Invest* 82(10): 1265–1277.
44. Ghanate AD, Kothiwale S, Singh SP, Bertrand D, Krishna CM (2011) Comparative evaluation of spectroscopic models using different multivariate statistical tools in a multicancer scenario. *J Biomed Opt* 16: 025003.
45. Wang B, Xie M, Li R, Owonikoko TK, Ramalingam SS, et al. (2014) Role of Ku70 in deubiquitination of Mcl-1 and suppression of apoptosis. *Cell Death Differ*. doi: 10.1038/cdd.2014.42.
46. Mallick S, Patil R, Gyanchandani R, Pawar S, Palve V, et al. (2009) Human oral cancers have altered expression of Bcl-2 family members and increased expression of the anti-apoptotic splice variant of Mcl-1. *J Pathol* 217: 398–407.
47. Palve V, Teni TR (2012) Association of anti-apoptotic Mcl-1L isoform expression with radioresistance of oral squamous carcinoma cells. *Radiation Oncology* 7: 135–146.
48. Ishigami T, Uzawa K, Higo M, Nomura H, Saito K, et al. (2007) Genes and molecular pathways related to radioresistance of oral squamous cell carcinoma cells. *Int J Cancer* 120: 2262–2270.
49. Moosmann B, Behl C (2000) Cytoprotective antioxidant function of tyrosine and tryptophan residues in transmembrane proteins. *Eur J Biochem* 267(18): 5687–5692.
50. Yamamori T, Yasui H, Yamazumi M, Wada Y, Nakamura Y (2012) Ionizing radiation induces mitochondrial reactive oxygen species production accompanied by upregulation of mitochondrial electron transport chain function and mitochondrial content under control of the cell cycle checkpoint. *Free Radic Biol Med* 53(2): 260–70.
51. Valko M, Izakovic M, Mazur M, Rhodes CJ, Telser J (2004) Role of oxygen radicals in DNA damage and cancer incidence. *Molecular and Cellular Biochemistry* 266 (1–2): 37–56.
52. Sun J, Chen Y, Li M, Ge Z (1998) Role of antioxidant enzymes on ionizing radiation resistance. *Free Radic Biol Med* 24(4): 586–593.
53. Yasuda H (2008) Solid tumor physiology and hypoxia-induced chemo/radio-resistance: Novel strategy for cancer therapy: Nitric oxide donor as a therapeutic enhancer. *Nitric Oxide* 19(2): 205–216.
54. Chapman JD, Engelhardt EL, Stobbe CC, Schneider RF, Hanks GE (1998) Measuring hypoxia and predicting tumor radioresistance with nuclear medicine assays. *Radiother Oncol* 46: 229–237.
55. Lee HC, Kim DW, Jung KY, Park IC, Park MJ, et al. (2004) Increased expression of antioxidant enzymes in radioresistant variant from U251 human glioblastoma cell line. *Int J Mol Med* 13(6): 883–887.